NOTTINGHAM POLYTECHNIC
CLIFTON CAMPUS
CLIFTON LANE
NOTTINGHAM NG11 8NS

NOTTINGHAM POLYTECHNIC
CLIFTON CAMPUS
CLIFTON LANE
NOTTINGHAM NG11 8NS

IDENTIFICATION OF THE LOW TEMPERATURE COMBUSTION PRODUCTS FROM COAL AND A STUDY OF THEIR EFFECT ON METAL OXIDE SEMICONDUCTORS

Presented by

S. GIBSON

A thesis submitted to the Council for National Academic Awards in partial fulfilment for the degree of Doctor of Philosophy, December 1988

Department of Physical Sciences,
Trent Polytechnic
Clifton Lane
Nottingham

Collaborating Establishment
British Coal
HQ Technical Department
Bretby, Staffordshire

A B S T R A C T

A large number of the gaseous products evolved from coal heated in the laboratory have been identified using a wide range of analytical procedures. Typical first appearance temperatures and concentration versus temperature profiles of the products were established under well defined experimental conditions in air and nitrogen. Three distinct patterns of evolution were observed and several products not previously considered to be present in the temperature range studied were identified. Carbon monoxide is currently used to indicate the onset of spontaneous combustion of coal. A number of other products were identified which appeared to have potential as alternative indicators including unsaturated hydrocarbons, benzene and toluene, methylcyclohexene, sulphur containing compounds, carbonyl species, hydrogen chloride and hydrogen.

The presence underground of many of these products was confirmed and their evolution patterns in relation to carbon monoxide during incidents of spontaneous combustion were studied in detail. Whilst carbonyl sulphide appeared to be the only definitive indicator of spontaneous combustion it was demonstrated that the ratio of different products to carbon monoxide may reveal a greater understanding of the degree and extent of activity of an incident of spontaneous combustion. The presence of methane in association with low aliphatic hydrocarbons underground was largely unaffected during the development of incidents of spontaneous combustion, any variations being due to a greater extent to other factors.

Three commercially available tin oxide based semiconductor gas sensors, namely, the TGS 711, 812 and 813 were selected for the detection of the products evolved from heated coal. The type 711 and 812 gas sensors were investigated for the detection of spontaneous combustion and the type 813 sensor for the measurement of methane concentrations. The basic operating characteristics of the sensors were investigated, including composition, surface morphology, working temperature, ambient atmosphere dependence and effect of varying oxygen concentration. It was demonstrated that if measurements were performed under well defined operating conditions the sensors exhibited consistent behaviour.

The effect of the products evolved from heated coal, both as individual species and collectively on the response of the gas sensors was investigated. This approach made it possible to identify the range of products which made significant contributions to the total sensor responses. Whilst the sensors lacked sufficient selectivity to be used as specific gas detectors, it was demonstrated that for the detection of spontaneous combustion the type 711 and 812 sensors have the potential to form the basis of a highly sensitive practical underground monitoring system indicating the presence of the products evolved during the low temperature heating of coal. However, the response characteristics of the 813 sensor were less amenable to the design of a single instrument for the direct measurement of methane concentrations.

A C K N O W L E D G E M E N T S

The author wishes to express his sincere thanks and gratitude to the following:

Dr. A. Braithwaite, as supervisor, for encouragement and guidance throughout the course of this thesis.

Mr. N. Wood, Scientific Services Manager South, as mentor, who has shown unfailing patience over many years, and who made a number of helpful suggestions concerning the thesis.

To colleagues at Headquarters Technical Department, particularly Mrs. S. Elliott for examining the semiconductor gas sensors using the scanning electron microscope.

To British Coal for providing the necessary support.

Finally, the skill and endless patience demonstrated by Miss J. Norman and Mrs. H. Greensmith in transforming the original script to the final text cannot be overestimated.

I N D E X

CHAPTER 1

I N T R O D U C T I O N

1.1 The Importance of Coal[1-3]

The potential of coal as a form of energy was recognised many centuries ago by the Chinese (Ghengei mines). The Greek philosopher Thesphastos, a pupil of Aristotle, knew of coal and called it anthrax, a name from which our word anthracite has been derived. Much later in 1280 Marco Polo mentioned coal as one of the curiosities he met with on his travels in China. When Gaul was invaded by the Romans they were surprised to see the excavation of coal in the vicinity of St. Etienne. In the middle ages, however, coal had to be rediscovered in Europe. The traffic of coal in Britain was well established by the 13th century and continued to grow through the industrial revolution and in 1947 led to the formation of the National Coal Board. Coal was used by the early colonists of North America and mines were important from the beginning of the 18th century in the development of the United States as a major industrial nation. Over the last century or two the world output of coal has increased manyfold and can be closely linked with industrial and economic growth (Fig.1). Current consumption of coal in this country amounts to some eighty million tonnes annually with technically recoverable resources estimated as being approximately 45×10^9 tonnes.[4,5] Thus, it can be seen that coal has a long history and that established reserves are large enough to sustain production for many years into the future.

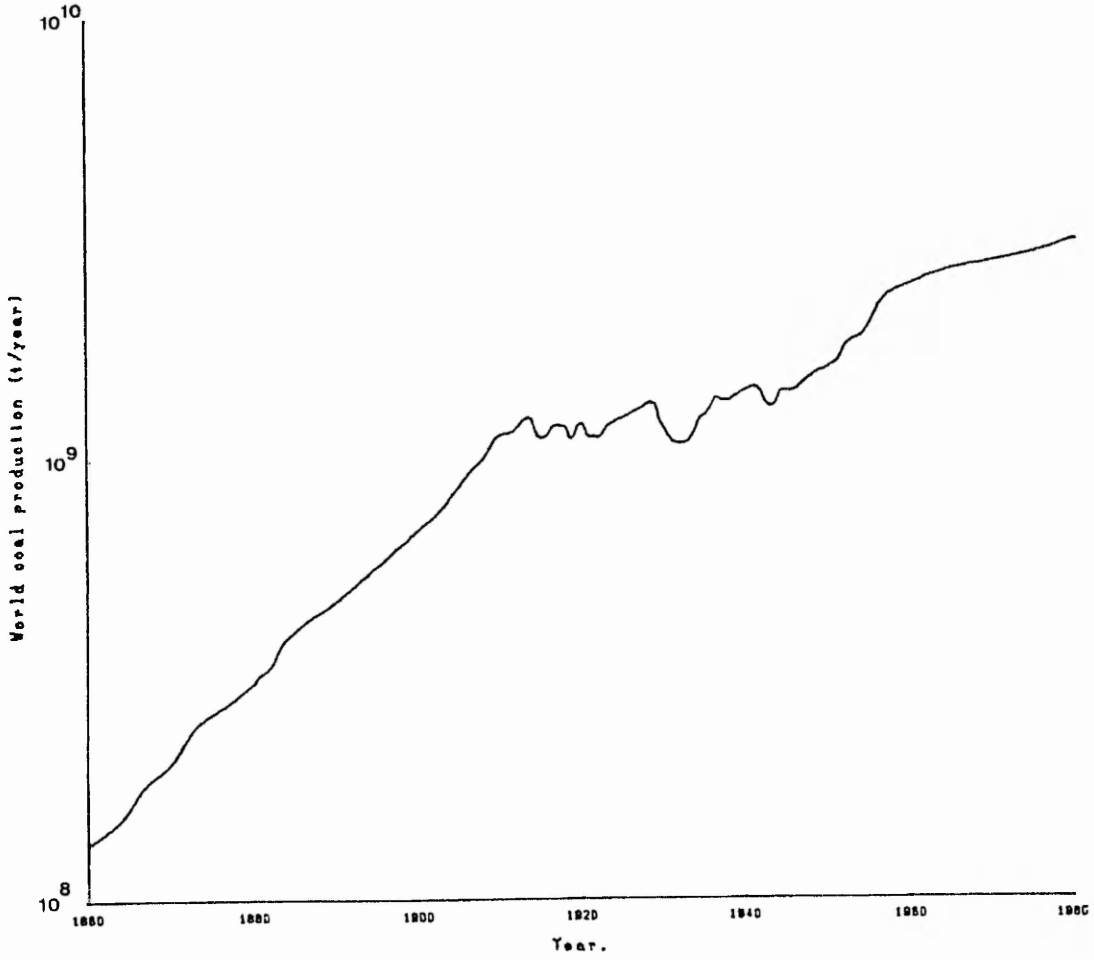

(1)

FIGURE 1 WORLD PRODUCTION OF COAL(SEMILOGARITHMIC SCALE).

1.2 The Origin and Composition of Coal[6-8]

Coal was formed from a series of biochemical and geochemical reactions in which plant materials were transformed into a readily combustible rock. Essentially, coal consists of carbon with smaller amounts of hydrogen, oxygen, nitrogen, sulphur, chlorine and numerous trace elements. The degree of coalification, or rank,[9] of the coal increases progressively throughout the series from lignite (containing 65% carbon), brown coal, high-, medium-, low-volatile bituminous coal to anthracite (containing approximately 94% carbon). This series is roughly equivalent to different stages in a sequential transformation from low to high rank coals. Coalification began with a biochemical stage, during which vegetable matter was partially decomposed, humic materials formed, and peat accumulated. For the successful formation of peat abundant plant materials, a suitable climate and areas for deposits to accumulate were required. Eventually inundation by water and the deposition of inorganic sediments terminated development of peat formation and initiated the geochemical stage of coalification.

The geochemical stage was accompanied by overburden pressure and heating. This compressed the peat and produced a series of chemical reactions which modified its chemical composition giving rise to a progressive increase in rank. The increase in rank is reflected by an increase in the aromatic character of coal, a continuous decrease in oxygen and hydrogen content and a corresponding increase in the proportion of carbon.[10,11] It has been estimated that between 10 and 20 feet of peat are eventually compressed to 1 foot of coal.[12]

Moisture content decreases from between 80 to 90% for peat to 30% for lignite,[13] with a corresponding increase in the concentration of humic acids. The humic acids are a group of polycondensed aromatic compounds with side chains containing active methoxyl, carboxyl and carbonyl groups. During coalification removal or closing of the side chains leads to an increase in aromatic content. The concentration of humic acids decreases in more mature coal and becomes negligible in bituminous coals since they are oxidised to neutral compounds.[14] The progression from lignite to bituminous coals involves the removal of aliphatic side chains containing oxygen. It has been shown that during transition from brown coal and lignite to low rank coal methoxyl groups are firstly removed, followed by carboxyl groups; the content of carbonyl groups is also decreased considerably. The percentage of hydroxyl groups remains almost constant during this transition. However, in the coalification range 81-89% carbon, the content of hydroxyl groups falls rapidly.[15] At carbon contents greater than 92% practically all oxygen is present in exceedingly stable non-reactive ether and heterocyclic ring systems.[16] The progression from high volatile to medium volatile bituminous coals is characterised by the removal of methyl and methylene groups. Aromatic clusters grow[17,18] larger and form lamellae orientated parallel to the bedding planes.[19] During digenesis to the low volatile stage, waxy and resinous materials are incorporated into the coal. The formation of anthracite involves ring condensation and the growth of large aromatic clusters with a graphite like structure. At this stage, the coal is composed of very large micelles in a more or less ordered arrangement.[20]

Very little appears to have been reported on the forms of organic nitrogen present in coal, there appears to be no correlation with rank, with about 1% weight present in all coals. The presence of nitrogen heterocyclic ring systems has been proven and the relative abundance of acridine/benzo-quinoline units in anthracite has been shown.[21,22]

Sulphur is known to exist in coal in three distinct forms. Firstly it can occur in an organic form as heterocyclic sulphur compounds.[23,24] However, there have been very few studies which have concentrated on the organic functional groups, but one study has shown that the presence of thiols is substantially larger in lignite and high volatile bituminous coals than in low volatile bituminous coals.[25] The fraction of aliphatic sulphides remains approximately constant at 18-25% of the total sulphur. The data indicates that larger fractions of the organic sulphur are present as thiophenic sulphur in higher rank coals than in lower ones. Studies on thiols, aliphatic sulphides and thiophenic sulphur have suggested that the coalification process has caused the organic sulphur to change from thiols through aliphatic sulphides to thiophenes in condensation reactions. Secondly, sulphur is present in inorganic forms of iron sulphides, principally as cubic pyrites with lesser amounts of orthorhombic marcasite and iron sulphates,[24] and is normally found as particles or globules. Finally, there is sulphate sulphur which occurs in weathered coals and normally exists as calcium sulphate. The sulphur content of coals may vary from below 1% to more than 10%.

In general coals formed under freshwater conditions have a low total sulphur content, whilst those formed under marine or estuarine conditions contain a higher percentage.[24]

Almost all coals contain chlorine in proportions varying from 0.05 to 1.0%. Opinions differ on its combination and mode of occurrence. The original view was that all chlorine was present as sodium and potassium chloride with smaller amounts of calcium and magnesium chlorides. This conclusion was based on the analysis of water soluble chlorine in coal obtained from extraction of powdered coal. However, it was later found that the chlorine in coal could only partially be extracted by water, which indicated that only a part was present as sodium chloride.[25,26] Other workers were of the opinion that a proportion of chlorine was present not as metal chlorides but as chloride ions attached to the coal substance by ion-exchange properties. The existence of chlorine as organic chlorine has also been established and in some coals the proportion of organic chlorine was found to be as high as 30-36% of the total chlorine content.[28]

The most widely held view of coal structure pictures coal as groups of fused aromatic and hydroaromatic ring clusters linked by relatively weak aliphatic bridges. The ring clusters contain the heteroatoms (oxygen, sulphur and nitrogen) and have a variety of attached functional groups. One of the most well known structures was suggested by Given on the basis of X-ray data.[29] Other models which propose different views of the structure have been presented by Pitt,[30] Chakrabarty and Berkowitz[31] and Hill and Lyon.[32] Figure 2 shows a coal structure as suggested by Solomon[33] for a Pittsburgh coal.

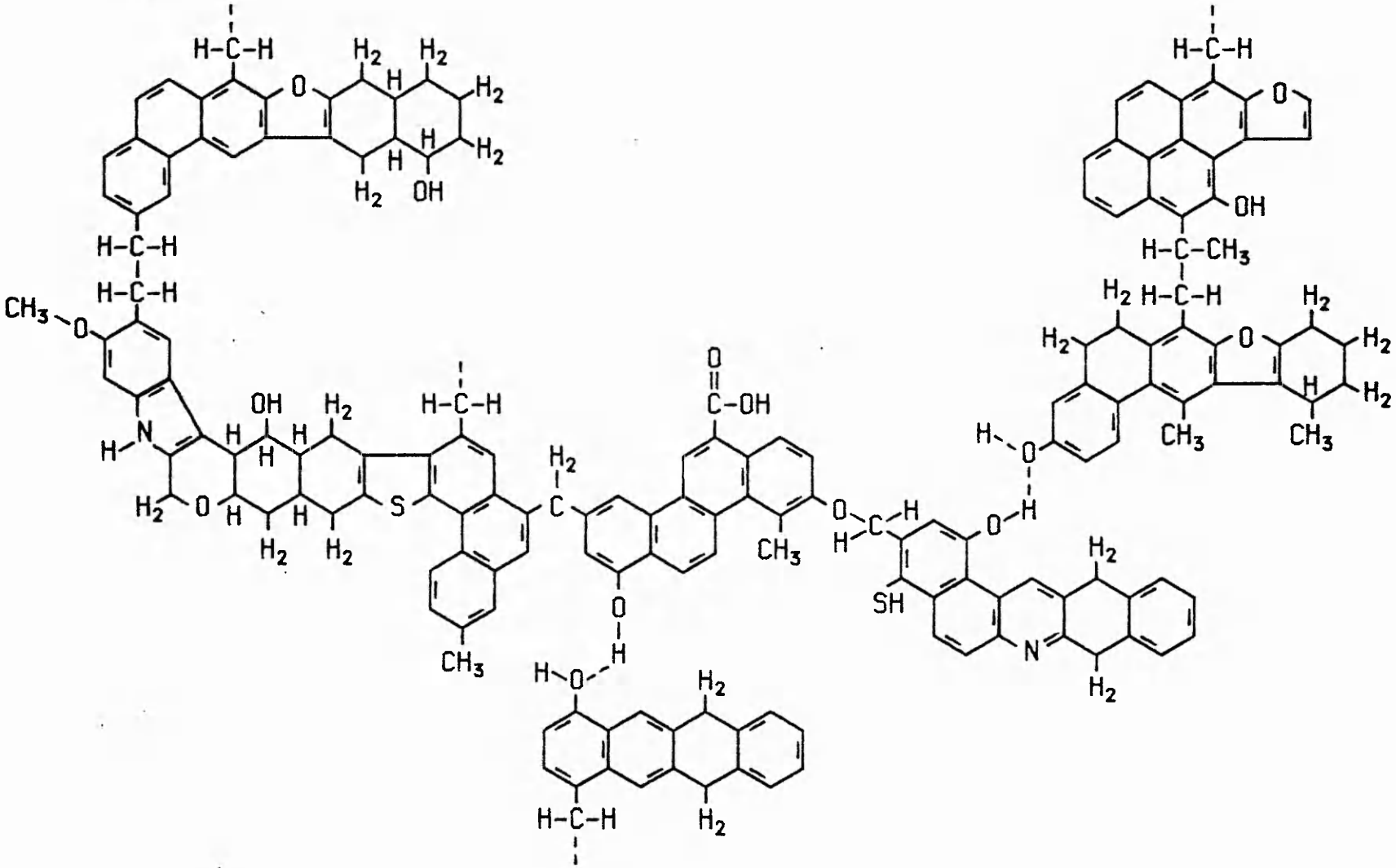

Figure 2. Summary of coal structure information in a hypothetical coal molecule. (33)

The structural parameters for the suggested model, the determined values and the source of data are summarised in Table 1.

Physically, coal is described as a solid colloid[46] which contains two distinct pore systems. The first is the macropore system which consists of cracks and fissures, the second is the micropore system which is similar to a molecular sieve structure. The micropores have an average diameter of 5 to 20 Angstroms and form a large internal surface area which for bituminous coals is of the order of 100-200$m^2 g^{-1}$.[47] The most abundant gaseous inclusion is methane, but other hydrocarbon gases, nitrogen and carbon dioxide can also exist in substantial quantities, either adsorbed on the internal surface of the micropores, or as free gases in the cracks and fissures. At extreme pressures bituminous coals have the potential to adsorb approximately 20m^3 tonne^{-1} of methane, 10m^3 tonne^{-1} of nitrogen or 30m^3 tonne^{-1} of carbon dioxide.[48] The amount of gas emanating from coal depends upon the temperature, pressure, degree of fracture, permeability of the coal and permeability of the adjacent strata.

The gases were undoubtedly formed during the biochemical stage of coalification and several proposals have been suggested to account for their existence even though no definitive experimental evidence exists. Methane may be produced by cleavage of alkyl side chains from aromatic molecules or from the decomposition of large straight chain molecules. It could also form as a by-product in the condensation of straight chain molecules to ring structures. These mechanisms would account for observed increases in aromatic character with rank.[49,50]

Table 1

Determination of coal structure

Parameter	Model	Coal	Source
Carbon	0.81	0.82	CHN Analyser[34]
Hydrogen	.055	.054	CHN Analyser[34]
Oxygen	.098	.094	Difference
Nitrogen	.011	.014	CHN Analyser[34]
Sulphur	.026	.019	Scanning electron microprobe[34]
$C_{aliphatic}$	.60	.60	N.M.R. and F.T.I.R[38,36]
$C_{aromatic}$	.20	.22	N.M.R. and F.I.I.R[35,36]
C_{methyl}	.03	.03	Average literature value[37-43]
$C_{ar}/C_{aliphatic}$	.74	.73	N.M.R. and F.T.I.R.[34,36]
$H_{aliphatic}$	.033	.033	F.T.I.R.[34]
$H_{aromatic}$	.018	.018	F.T.I.R.[34]
H_{OH}	.0029	.0027	F.T.I.R[34]
H_{methyl}	.0074	.0075	Average literature value[37-43]
H_{ar-1} adjacent	.006	.006	F.T.I.R.
H_{ar-2} adjacent	.008	.007	F.T.I.R
H_{ar-3} or $_4$ adjacent	.004	.005	F.T.I.R
O_{OH}	.046	.043	F.T.I.R[35]
O_{COOH}	.013	.009	Thermal decomposition[34]
O_{CO}	.039	.041	Thermal decomposition[34]
N_{ring}	.011	.014	Thermal decomposition[44,45]
S_{ring}	.013	.01	Thermal decomposition[44]
$S_{mercaptan}$	.013	.01	Thermal decomposition[44]
12 H_{al}/C_{al}	1.9	1.8	Average literature value[35]
Molecular weight of ring cluster	350	400	Gel permeation chromatography and vapour phase osmometry

It has also been suggested that methane could have formed at a later stage, with ethane, ethene and hydrogen as the major decomposition products. Methane would then be produced by a secondary reaction of these gases. If higher hydrocarbons are also produced they could decompose further to methane, with the coal acting as a catalytic surface. It is thought that carbon dioxide was also formed early in the coalification process, probably by oxidation in the presence of occluded oxygen or by removal of carboxyl groups from low rank bituminous coals. With increased rank, the CO_2/CH_4 ratio decreases.[51] Generally the ratio of carbon dioxide to hydrocarbon gases decreases with increasing rank, and the percentage of higher hydrocarbons decreases.[52]

It is evident, therefore, that coal has a complex macro molecular structure, and has the capacity to adsorb large volumes of gases. During normal mining operations there is the inevitable release of these gases into the mining environment. Further emissions of gases and volatiles occur as coal is heated. The net effect is to present a potential gaseous pollution and fire hazard, the nature of which forms the basis of this study.

1.3 Underground Fires and Spontaneous Combustion of Coal

Examination of recent Annual Reports by HM Chief Inspector of Mines[53-66] shows that there are about 50 reported incidents per year involving fire in British Coal Mines. Table 2 shows the different causes of fire in detail for the period 1970-1983.

Table 2

Statistical data from Annual Reports of H.M. Inspector of Mines and Quarries[53-66]

Cause of fire	1970	1971	1972	1973	1974	1975	1976	1977	1978	1979	1980	1981	1982	1983	Total
Spontaneous Combustion	7	7	1	2	3	3	1	0	2	0	1	5	3	2	37
Electricity	8	7	10	12	4	18	15	17	22	18	12	9	13	12	177
Mechanical Friction															
(a) Belt Conveyors	32	16	16	24	21	22	18	22	25	17	28	20	30	24	315
(b) Frictional Sparking	0	1	0	0	0	0	1	1	1	0	0	0	0	1	5
(c) Others	3	5	2	3	5	10	8	10	6	10	11	11	10	7	101
Locomotives	2	4	3	5	6	6	4	2	5	7	5	4	5	3	61
Burning Appliances	0	1	1	1	0	1	0	2	0	0	0	0	0	0	6
Shotfiring	1	0	0	2	2	1	0	1	0	1	0	0	0	0	8
Contraband	0	2	2	0	0	0	3	0	0	1	0	0	0	0	8
Unknown	1	3	0	2	2	1	0	2	2	1	0	0	0	1	15
TOTAL	54	46	35	51	43	62	50	57	63	55	57	49	61	50	733

It can be seen that during this period the spontaneous combustion of coal accounted for thirty seven incidents of underground fire. At first this figure may not appear to constitute a major problem within the mining industry, but since the earliest records of coal mining the liability of coal to undergo self heating has proven to be a widespread and persistent problem. In its earliest stages of development it is relatively unimportant but it is the precursor to further stages of intensity when it is known as a "heating" and finally, if left unchecked, can result in open fire. A number of combative measures including sand blanketing, flooding, digging, inert gases, chemical treatment and degasification[67-72] have all been employed to control spontaneous combustion with varying degrees of success. As yet no single long term solution has been found and many of the areas affected have been abandoned before open fire resulted. Today the abandonment of an area of coal from an incident of spontaneous combustion is much more series than in the past when it was hand worked. There is now a very high capital investment, so that in addition to sterilisation of reserves, the loss of mining equipment alone can cost up to five million pounds. As a consequence there are fewer coal faces at a colliery producing higher tonnage outputs; therefore, even short interruptions in production can give cause for concern. The spontaneous combustion of coal has been shown to be a problem in other mining countries. For example, it has been estimated that the total amount of coal lost to this cause in Indian coalfields since 1942 is approximately 34 million tonnes.[73]

It is not difficult to imagine the effects on the workforce of a serious incident of spontaneous combustion where the escape to the surface may be up to 10 Kilometres. The gases released from the heated coal may be toxic, flammable and/or asphyxiating which could lead to poisoning or suffocation of workmen whose escape might also be hindered by the presence of smoke. If an open fire were to break out there would then be an additional danger due to the ignition of methane which is normally present underground, being released from the coal during normal mining operations, as described in Section 1.2.

Thus it can be seen that the spontaneous combustion of coal does present a major problem within the mining industry and its detection at an early stage is of prime importance to prevent a serious incident developing.

The remaining fires which occur underground result mainly from the ignition of coal dust caused by mechanical friction in conveyor belt systems due to roller bearing failures, overheating of brakes or belt friction on driving drums. Many of these types of fires have been discovered at an early stage by workmen whose duties include the patrolling of the conveyor and extinguished quickly and effectively. However, it must be emphasised that every underground fire should be regarded as a source of potential disaster due to the possible ignition of methane and thus continuous fire detection is essential to achieve safe working conditions.

This section has shown the extent of the problem from the spontaneous combustion of coal and underground fires in the coal mining environment, and it is clear that their detection at an early stage is imperative if safer and more effective

working conditions are to be achieved. It has also been shown that the existence of methane underground presents an additional danger and thus requires careful monitoring to prevent dangerous accumulations occurring which could be ignited by the outbreak of fire.

1.4 Spontaneous Combustion of Coal

A number of theories and mechanisms have been postulated to explain this phenomenon, the main ones of which are outlined below:

1.4.1 The Pyrites Theory

One of the first papers covering spontaneous combustion was published by Dr. Plot, Professor of Chemistry at Oxford, in his book on the History of Staffordshire (1686).[74] He described the occurrences of fires in coal heaps and after experimental work attributed them to the oxidation of pyrites. Although differences in opinion have since existed about the role of pyrites,[75,76] it is now generally considered that it only plays a secondary role in the initiation of spontaneous combustion as follows:-

a) The heat of oxidation of pyrites contributing to the heat oxidation of coal

b) The oxidation of pyrites results in a volumetric change causing disintegration of coal, thus providing a greater surface area of coal for further oxidation.

1.4.2 The Coal Oxygen Complex Theory

Several papers appeared between 1848 and 1880 which described the changes that occurred in stored coal, including changes of weight, and suggested that the physical

absorption of oxygen by coal was an important factor. Russel[77] in 1898 showed that oxidising coal possessed the ability to affect a photographic plate (the "Russel Effect") and it was later shown in 1928 by Haslam that formaldehyde vapour was responsible for this phenomenon.[78] By the end of the 19th Century the capacity of coal to react with oxygen at ordinary temperatures and at an increasing rate at higher temperatures had been established.[79]

In order to explain this, the formation of a coal-oxygen complex was postulated by a number of investigators including Wheeler,[80] Davis and Byrne[81] and Schmidt.[82] Oplinski and others in 1953,[83] studied the reversibility of the oxygen adsorption processes and found that above 50°C the amount of oxygen which could be recovered was negligible. The oxidising power of coal was first measured by Yohe and Harman,[84] and later by Jones and Townsend[85] and Chalizhazar and Spooner.[86] In each of these methods the coal containing the active oxygen was treated with a solution of a suitable reducing agent. The amount of reducing agent oxidised by the coal was then determined by titration. Yohe[87] claimed that by using solutions of reducing agents, physically bound oxygen molecules, as well as those chemically bound, were determined together. It was therefore not possible to distinguish between the two types. Sevenster (1961)[88] indicated that the first reaction between oxygen and coal at low temperatures was predominantly chemisorption and not physical adsorption. Hence, from these findings, it would appear that there are very few physically adsorbed oxygen molecules on the coal surface to interfere in the manner

suggested earlier by Yohe.[87]

Van Krevelen and Schuyer[89] summarised the data on the reaction kinetics of coal and concluded that the primary reaction between coal and oxygen proceeds with a low activation energy (12-16KJ per mole) and results in the formation of a primary chemisorption complex.

1.4.3 The Humidity Theory

The importance of humidity in relation to spontaneous combustion was shown by Graham.[90] He compared the rate of oxidation of coal in a stream of 'dry air' with that of coal oxidised by water saturated air and found that below 55 °C the presence of moisture increased the oxidation rate by about 50%. Frey[91] has also reported that the presence of moisture increased the rate of oxidation. Guney,[92] who studied the effect of different humidity levels on coal oxidation found that the highest rates of temperature increase were obtained when moist air was passed over dry coal and the lowest were observed with saturated coal and moist air. Decreases in temperature were noted whenever drying took place.

From the various results obtained it would appear that the role of moisture is not the prime initiator of spontaneous combustion but can cause a more rapid rise in temperature than oxidation alone.

1.4.4 The Bacteria Theory

Many early workers examined the role of bacteria in the spontaneous combustion of coal. Cowards[93] review of this subject includes references to six investigations by different workers between 1908 and 1927.

In four of these investigations, definite evidence was presented to show that bacteria were capable of living on coal. However, Graham[90] found that a sterilised coal oxidised at the same rate as unsterilised coal and concluded the bacterial activity did not play a role in spontaneous combustion. A similar conclusion was also drawn by Windmill.[94]

1.4.5 The Mechanism of Spontaneous Combustion

It is now known that whenever coal is exposed to oxygen, adsorption occurs which results in the formation of a chemisorption complex and an increase in coal temperature. The temperature will then rise at a rate dependent upon how successfully the heat is dissipated. Any rise in temperature, will cause increased oxidation rates, a process which is self-accelerating. The conditions which determine whether or not low temperature oxidation will develop further in a coal mine are finely balanced. For example, if the air flow rate is small then the rate of oxidation will be low and a state of equilibrium will be attained whereby the heat is dissipated as quickly as it is generated. Alternatively if the air flow rate is large enough, the cooling effect may be so great as to prevent any significant increase in temperature. Should both the rate of oxygen supply and heat dissipation lie between these two limits then conditions would be favourable for oxidation to proceed at an increasing rate, and unless this process is interrupted, open fire may result. Controlled laboratory experiments have been used to study the effects of temperature,[82,95] oxygen partial pressure,[96] coal rank,[81]

particle size,[97] and previous oxidation,[96,98] on oxidation rate to help provide insights into the fundamentals of spontaneous combustion in coal.

1.5 Possible Means of Detecting Spontaneous Combustion in its Early Stages

1.5.1 Physical Means

It is generally agreed that the development of spontaneous combustion is accompanied by the progressive appearance of sweating of the strata, 'gob stink', 'fire stink', haze and eventually smoke and flame. Unfortunately some of these indications are not always observed and if present are not absolute evidence of an incident.

For example, the sweating of strata near a heating depends upon the humidity of the underground air and the strata temperature on which the moisture may be deposited. 'Gob stink' and 'fire stink' are old mining terms used to describe the odour produced from a heating at different stages of its development. Many descriptions of gob stink have been given by workers involved with different incidents including:

a) a musty smell

b) a petrol or paraffin like smell

c) an aromatic smell

d) a mercaptan smell

Although gob stink is a reliable indication of an abnormal condition, it requires trained and experienced personnel to recognise it with any degree of confidence.

1.5.2 The Carbon Monoxide/Oxygen Deficiency Ratio

Haldane and Meachem[79] first recognised that coal exposed to air at ambient temperature produced carbon monoxide. From this followed work by Graham[90] on the oxidation of coal in the temperature range 100 °C to 140 °C, whereby he utilised the increasing evolution of carbon monoxide and rate of oxygen consumption with rising coal temperature and produced a scheme whereby the ratio of carbon monoxide produced to the oxygen consumed served as an index of spontaneous combustion.

The ratio depends upon the constant proportions of oxygen and nitrogen in fresh air taken as being 20.93% and 79.04% respectively. An example of calculation of the ratio is as follows:

Laboratory analysis:

Carbon dioxide	0.80%
Methane	0.42%
Oxygen	19.95%
Nitrogen	78.83%
Carbon monoxide	0.005%

Oxygen associated with nitrogen in the sample

$$= 78.83 \times \left(\frac{20.93}{79.04}\right) = 20.87\% \quad \text{.....(a)}$$

Oxygen found in sample = 19.95% .....(b)

Oxygen deficiency = (a) - (b) = 0.92%

Carbon monoxide found in the sample = 0.005% ...(c)

$$\frac{\text{Carbon monoxide}}{\text{Oxygen deficiency}} \text{ ratio} = \frac{(c)}{(a) - (b)} 100$$

$$= \left(\frac{0.005}{0.92}\right) \times 100$$

$$= 0.54$$

In practice, it was later shown mathematically by Criddle[99] that this ratio in a heated area was greatly affected by a small degree of dilution unless the diluent air contained no carbon monoxide and was not deficient in oxygen.

However, he affirmed that a rise in the trend of this ratio showed that some abnormal condition was developing; although it was not strictly correct to judge the severity of an incident with an increase in the ratio. Graham's ratio has been used successfully over many years in the coal mining industry and is regarded as a reliable indicator of the presence and status of spontaneous combustion. It does suffer from one drawback in that it is affected by carbon monoxide produced from other legitimate mining activities such as shot-firing and diesel exhaust fumes, which can lead to false alarms when carbon monoxide fire detectors are used.

1.5.3 Products of Combustion

1.5.3.1 Laboratory Studies

With the development of improved analytical techniques, particularly gas chromatography and infra-red detection in the late 1950's and early 60's there followed a resurgence of interest in the gases evolved from heated coal.

The main efforts in this area were directed towards the kinetics of coal carbonisation and improving the knowledge and understanding of the mechanisms that lead to the products of coal combustion. Subsequently a vast number of papers appeared in the literature.[100-114]

On examination of these it soon becomes clear that the data is lacking in a number of areas; the range of products studied, particularly under oxidising conditions, was too restricted; the upper temperature limit of many studies was too excessive, being greater than 300 °C; the information on rates of evolution of products as a function of temperature was limited, and finally the correlation between work of different authors was not always good. Even so, attempts have been made to collate this dispersed information with particular reference to the range of volatile products evolved, the temperatures of evolution and the effect of different ambient conditions (e.g. oxidising or inert conditions). Probably the most comprehensive study undertaken was by Chamberlain et al, in 1970[100] who examined the relative rates of evolution of gaseous combustion products from seventeen British coals of differing rank, heated in air and nitrogen. The main experiments were carried out using 50g of 30-60 BS mesh coal heated at 35°C hr^{-1} in 80 ml min^{-1} air or nitrogen. The effect of varying the flow rate, humidity, heating rate, and coal size were also studied and the main findings are summarised below:

a) Experimental Parameters

i) Using different air flow rates indicated that the composition of product gases remained unaffected provided the combustion gas contained sufficient oxygen to satisfy the absorbent characteristics of the coal.

ii) The pattern and order of gaseous products were unaffected by different heating rates.

iii) There was no significant difference between results obtained using either water saturated air or dry air.

iv) Experiments using different size fractions of coal did not produce major differences in the rate or pattern of evolution of products.

v) Sample storage did not produce any significant effects on the products evolved above 100°C.

vi) At temperatures above 200°C, the more reactive coals (low rank) showed little or no residual air in the effluent, whereas high rank coals showed 30-50% residual air.

vii) The more reactive coals produced an oxygen deficiency of 1% below 95°C and above this temperature the oxygen deficiency increased by approximately 1% for each 7.5°C increase in temperature.

Products of Combustion

i) Carbon dioxide:- production from the test coals was variable and therefore gave no useful indications.

ii) Methane, ethane, propane:- evolution of methane was highest from fresh samples of coal. Methane was also shown to be an oxidation product from a low rank coal, but not from a high rank coal. Generally, as the temperature increased the proportion of methane decreased being

first replaced by ethane and later by propane.

iii) Butanes and butenes:- normal butane and butenes were detected at temperatures above 170°C.

iv) Ethene and propene:- when present ethene and propene were invariably detected at similar temperatures and increased in concentration at similar rates from coals heated in air. In nitrogen the production of these gases was insignificant. Acetylene was not detected at any temperature.

v) Carbon monoxide:- when heated in air, low rank coals showed rapid increases in carbon monoxide formation producing greater than 100 ppm by 90°C Medium rank coals gave slower rates of production of carbon monoxide initially but after 100°C increased to give similar rates to the lower rank coals. High rank coals gave the slowest rates of increase. In tests using nitrogen, carbon monoxide was detected in the effluent gases from each coal, but the concentrations were much lower than those found under oxidising conditions.

vi) Hydrogen:- at temperatures reater than 100°C hydrogen production increased with increasing temperature providing there was more than 1% residual oxygen in the effluent gas.
Tests using nitrogen produced insignificant quantities of hydrogen up to the maximum temperature studied.

The results shown in Table 3 are typical of those found by Chamberlain from a medium rank coal.

More recently Hurst[101] and co-workers using gas chromatography and gas chromatography linked mass spectroscopy (GC/MS) analysed the products evolved from a medium rank coal as a function of coal temperatures. Their results are summarised in Tables 4 and 5. The apparent disappearance of some products shown in these tables with increasing temperature, may be due to exhaustion of the original sample as much as to a change in the pattern of decomposition. In addition to those compounds listed, cyclohexane, methylcyclohexane, octane, nonane, unsaturated substituted benzenes, naphthalene and substituted naphthalenes were qualitatively identified at coal temperatures between 180-210°C using GC/MS. Tashiro[102] in Japan studied the evolution of carbon monoxide, carbon dioxide, methane, ethane, ethene, propane, propene and butane, and suggested that the spontaneous combustion of coal could be detected by monitoring the ratio of alkanes.

Whilst working for the CEGB, Street[103] carried out investigations into the evolution of hydrogen from coals of different rank, using a similar experimental arrangement to that of Chamberlain, to assess its feasibility as an indicator of spontaneous combustion in coal milling plants. The results obtained by Street for a coal of rank 902 are contrasted with those of Chamberlain[100] for a coal of rank 502 in Table 6.

Table 3

Results of Dynamic Heating Tests

Sample No. 8 Westoe Colliery Five Quarter Seam - Dry Air

Coal Temperature °C	Carbon Dioxide %	Oxygen %	Nitrogen %	Carbon Monoxide %	Hydrogen %	Helium %	Methane %	Ethane %	Propane %	Ethylene %	Propylene %	iso Butane %	n-Butane %	Butenes %
16	0.02	20.83	79.03	0.0008		0.0005	0.1188	0.0046						
29	0.01	20.91	78.92			0.0005	0.1539	0.0056						
35	0.02	20.81	78.84	0.0001		0.0005	0.3132	0.0112	0.0001					
48	0.02	20.75	78.81	0.0002		0.0005	0.4050	0.0186	0.0003					
59	0.03	20.57	78.82	0.0005		0.0005	0.5400	0.0354	0.0006					
73	0.02	20.39	79.05	0.0013		0.0005	0.5400	Missed	0.0009					
85	0.01	20.48	79.18	0.0030	0.0003	0.0005	0.2916	0.0385	0.0008					
97	0.01	20.25	79.52	0.0050	0.0003	0.0005	0.1809	0.0329	0.0008					
108	0.02	19.88	79.95	0.0125	0.0004	0.0005	0.1080	0.0294	0.0007					
121	0.06	19.23	80.58	0.0265	0.0009	0.0005	0.0709	0.0287	0.0010					
137	0.17	17.76	81.94	0.0590	0.0028	0.0005	0.0385	0.0280	0.0012		0.0002			
155	0.44	14.75	84.64	0.1100	0.0058	0.0005	0.0223	0.0273	0.0020	0.0012	0.0005			
173	0.84	10.72	88.03	0.3500	0.0096		0.0132	0.0252	0.0036	0.0018	0.0013	0.0005	0.0012	
191	1.40	5.68	92.21	0.6500	0.0119		0.0138	0.0217	0.0050	0.0037	0.0025	0.0005	0.0017	
212	2.30	1.62	95.01	1.0000	0.0116		0.0162	0.0172	0.0059	0.0058	0.0042	0.0007	0.0029	0.0016
233	3.25	0.09	95.10	1.5000	0.0099		0.0169	0.0116	0.0061	0.0077	0.0064	0.0012	0.0032	
248	4.20	0.03	93.77	1.9500	0.0084		0.0169	0.0084	0.0027	0.0098	0.0036	0.0009	0.0035	
Sample No. 8 - Oxygen Free Nitrogen														
23	0.02	0.14		0	0	0	0.0324	0.0042	0	0	0	0		0
24	0.02	0.04		0	0	0	0.0412	0.0033	0	0	0	0		0
38	0.02	0.04		0	0	0	0.0655	0.0077	0.0001	0	0	0		0
49	0.01	0.04		0	0	0	0.1242	0.0168	0.0002	0	0	0		0
61	0.01	0.03		0	0.0001	0	0.1175	0.0182	0.0002	0	0	0		0
73	0.005	0.03		0	0	0	0.1283	0.0280	0.0007	0	0	0		0
86	0	0.03		0	0	0	0.1040	0.0308	0.0007	0	0	0		0
99	0	0.02		0	0	0	0.0729	0.0280	0.0007	0	0	0		0
111	0	0.02		0	0	0	0.0500	0.0252	0.0008	0	0	0		0
112	0	0.03		0	0	0	0.0358	0.0245	0.0009	0	0	0		0
134	0.005	0.03		0.0001	0.0001	0	0.0189	0.0217	0.0010	0	0	0		0
153	0.01	0.05		0.0001	0.0001	0	0.0118	0.0256	0.0014	0	0	0		0
169	0.01	0.07		0.0001	0.0003	0	0.0047	0.0235	0.0016	0	0	0		0
185	0.01	0.07		0.0002	0.0004	0	0.0020	0.0154	0.0014	0	0	0		0
201	0.01	0.07		0.0002	0.0005	0	0.0015	0.0092	0.0014	0	0	0		0
216	0.01	0.06		0.0002	0.0007	0	0.0009	0.0042	0.0011	0.0001	0	0.0002	0.0006	0

Experimental Conditions - As described earlier

Table 4

Analysis results for coal dust heated in air

Temp. (°C)	Methane	Ethane	Propane	n-butane	n-pentane	n-hexane	2-methyl butane	2-methyl pentane	Ethene	Propene	Benzene	Toluene	Xylene	Hydrogen Sulphide	Sulphur Dioxide	Hydrogen	Carbon Monoxide
100																	2
110											2.0						3
120					1.0	1.0						4.0					5
130					1.0	0.5					2.0	6.0	3.5				9
140											2.0[a]	16	3.5[a]			2	13
150			0.1	0.5	2.0	1.5	2.0	2.0			3.5					4	23
160				1.0	2.5	2.0	2.5	2.0			4.0	16				5	41
170											4.0[a]	17.5	12			5	65
180		1.0	1.0	1.0												5	90
190	2.5		0.5	1.5	3.0	2.5	4.0	5.0			5.0	13	13[a]			5	150
200	5.0			2.5	3.0	3.0	5.0		0.5							7	500
210	5.0										5.0	15	14			8	900
220	100		4.0	2.0	2.0	3.0	9.0	10	2.0[a]		5.0[a]	13[a]	14[a]			10	980
230	75										4.0[a]	12	14			80	800
240	15	5.0							5.0							120	500
250	5.0						4.0				3.0	3[a]	3[a]		60	90	540
260			0.5	0.5	0.5	0.5	1.0	0.5				3.5				80	660
270											0.5	2.0	0.5			40	760
280		7.0						20	20						13	4	82
290														5.0	100	0	850
300										1.5				15[a]		3	900
310	5.0													25[a]		5	900
320	25	3.0												30	100	32	3900
330	70													40[a]		57	3600
340	25									1.5				65		80	3400
350	35								10					90[a]		25	3100
360	15													115[a]		20	2000
370	50													140[a]		15	4000
380	10													200	140	10	1440
390									5.0	1.5				195[a]		5	1900
400		10												190[a]		0	2280
410														180			2220
420														175[a]			2220
430														165[a]			2000
440		17							2.0					160[a]			1450
450														155[a]			1000
460														150	80		840
470														75[a]			700
480		30							2.0					20	50		
490																	
500																	
510									2.0								
520																	

Experimental conditions 0.7g of <240 BS mesh coal heated at 2°C min^{-1} in 100 $cm^3 min^{-1}$ air, followed by addition of 200 $cm^3 min^{-1}$ air

Concentration in ppm of component

a Interpolated value

Table 5

Analysis results for coal dust heated in nitrogen

Temp (°C)	Methane	Ethane	Propane	n-butane	n-pentane	n-hexane	2-methyl butane	2-methyl pentane	Ethene	Propene
100										
110					0.5	0.5				
120										
130							2.5			
140				1.0	2.0	1.0				
150										
160				2.5		5.0	5.0			
170				2.0				5.0		
180				2.0	3.0	3.0	4.0			
190								3.5		
200										
210										
220						2.0	4.0			
230				1.0	2.0			5.0		
240				0.5	0.5		1.5	1.0		
250										
260										
270										
280										
290										
300										
310										
320		2.0	1.0	0.5						
330	5.0									
340	10								1.0	1.0
350	20									
360	30				0.5					
370	50					0.5				
380	75			8.0	6.0					
390	100					5.0			35	50
400	200	100	60							
410	250					15	2.5			
420	300									
430	300			1.0	1.0					
440	300									
450	300					4.0	8.5	1.0	22[a]	22[a]
460									22[a]	22[a]
470									20	25
480							2.5			
490										
500										

Table 5 (continued)

Temp (°C)	2-hexene	2-methyl butene	2-methyl propene	Benzene	Toluene	Xylene	Hydrogen Sulphide	Sulphur Dioxide	Hydrogen	Carbon Monoxide
100										
110				2.0	6.0					
120										
130					12.0	4.0				
140				3.0	11.0	7.0				
150										
160										
170				6.0	19.0	12.0				
180										
190				3.5	13.0	12.0				
200										
210										
220				2.0	5.0	7.0				
230				5.0	11	5.0				
240										
250										10
260				1.0	3.0					10
270										10
280				3.0	1.0					10
290							5.0			10
300										14
310										14
320										16
330							6.0			20
340				1.0	4.0					24
350							8.0			26
360	1.0									28
370										30
380	5.0	2.0	5.5	4.0	13	13			2	36
390							10		6	36
400									13	44
410	5.5								21	45
420				19					36	45
430	19	14	20		30	36	60		82	70
440							70[a]		110	90
450	1.0[a]	1.0[a]	1.0[a]	10	10	10			160	120
460	1.0	1.0	1.0	2	2	2	100		240	200
470							75a		240	200
480										
490							30	100		
500										

Experimental conditions - as Table 4

Table 6

Comparison of data for hydrogen production from coals heated in air

Experimental parameter	Chamberlain et al	Street
Temperature for maximum hydrogen concentration	200°C	280°C
Hydrogen concentration after maximum reached	Falls with increasing temperature. Residual oxygen 0.5%	Remains constant with increasing temperature. Residual oxygen 0.1%
Coal temperature at:-		
10ppm hydrogen	130°C	240°C
30ppm hydrogen	140°C	260°C
60ppm hydrogen	155°C	265°C
Maximum hydrogen concentration (ppm)	120	130
Temperature range of hydrogen evolution (10ppm to maximum)	70°C	40°C

Experimental conditions

1. Chamberlain - as described earlier

2. Street - 140g of 72-150 BS mesh coal heated at $1.5°C\ min^{-1}$ in $250cm^3\ min^{-1}$ air.

According to Street the discrepancies between results are not easy to resolve and he concluded that they are either due to differences in the coal properties or the variation due to the different experimental techniques must be considered. This statement highlights the discrepancies between the results obtained by different workers even when using similar experimental arrangements.

To date, this section has covered work performed under both oxidising and non-oxidising conditions, the remaining text reviews data obtained under inert conditions only. Although the compounds produced from coal distillation had been investigated over many years[104,105] it was not until 1962 that Girling[106] heated small amounts of bituminous coals from ambient up to 700°C and examined in detail the rate of evolution of C_4-C_{10} hydrocarbons. He concluded that alkanes and aromatic hydrocarbons were produced in two coal temperature regions producing maximum rates of evolution around 200°C and 400°C whilst alkanes were only produced between 300-400°C. This pattern of evolution for alkyl benzenes was also confirmed by Holden and Robb[107] and alkyl phenols and alkyl naphthalenes were found to be released at the higher temperature only. Investigations into the kinetics of coal carbonisation have shown that at temperatures between 400°C and 700°C a number of alkanes and alkenes are produced giving maximum rates of evolution between 400°C and 500°C.[108] Hydrogen, carbon monoxide and methane were also evolved with increasing rates of evolution at

higher temperatures. The change in composition of hydrocarbons released from heating a low rank coal from the United States, has been studied by Kim.[109] She concluded that at 35 °C the evolved gas was predominantly methane, but at 125 °C methane comprised less than 50% of the hydrocarbons produced. Compounds present in the effluent, in order of decreasing concentration, were methane, pentane, methyl propane, propane, propene, ethane, ethene and trace amounts of butene. When the coal temperature was increased to 150 °C methane, butane and pentane showed the largest increases in concentration. A similar study has been carried out into spontaneous combustion of lignite from the North Czechoslavakian brown coal basin.[110] The author found that an increase in coal temperature was accompanied by the formation of several characteristic hydrocarbons including ethene, propene, butanes and butenes. Vahrman[111] showed that whilst incrementally heating thin layers of a weakly coking coal from Thoresby Colliery, hydrocarbons were evolved in two stages, at up to 250 °C for aliphatics and up to 300 °C for aromatics, in a sequence approximately to their boiling points. Above these temperatures a wider range of hydrocarbons appeared. The range of products identified by the author is wider than might be expected, particularly at low temperatures. For example, in the 100-150°C temperature interval aliphatics in the range hexane up to hexadecane and aromatics from benzene to dimethylnaphthalene were

identified. Recently, a thermogravimetric coupled gas chromatography/mass spectrometry system has been used to investigate the products evolved from a United States bituminous coal.[112] In the temperature range 0-260 C, carbon dioxide, methylcyclohexane xylenes, napthalene, methylnaphthalene, and substituted naphthalenes were identified as major products.

Herod and co-workers[113,114] used single ion monitoring MS to study the evolution of sulphur, oxygen and chlorine containing compounds from six coals heated up to 300°C. Hydrogen chloride was the only chlorine containing compound identified being evolved over the range 50-270°C the actual temperature of appearance being dependent upon the coal. Small quantities of carboxylic acids, indanols, phenols, dibenzothiophanes, and aza-dibenzothiophenes, were also evolved in the temperature range 150-300 °C.

1.5.3.2 Underground Studies

Only a very limited amount of work has been undertaken to determine the combustion products, other than carbon monoxide, evolved from actual incidents of spontaneous combustion. Pursall and Gosh showed the relationship between the formation of various gases peculiar to spontaneous combustion during its progression through different stages.[115] They found that unsaturated hydrocarbons were always associated with areas undergoing spontaneous combustion, but were absent from areas not affected. The unsaturated hydrocarbons detected were

ethene, propene and ethyne, this being the order in which they appeared as the heating activity increased. Alkanes up to butane were found in association with methane, but appeared to occur in larger quantities during abnormal conditions, however, no detailed studies of these gases were made. Kitagawa[116] used stain tubes to determine the presence of carbon monoxide and ethene from a number of sealed areas undergoing spontaneous combustion, in selected coal mines in Japan. He found that both gases existed together in a specific ratio and that the concentration of both increased as the intensity of activity increased.

Samples taken from a sealed chamber in the Pluto-2 mine, Czechoslavakia showed the presence of C1-C5 saturated and unsaturated hydrocarbons.[110] It was concluded that the formation of these products was characteristic of an area undergoing spontaneous combustion. It has been found from samples collected underground from collieries in South Nottinghamshire, that the simpler aromatic hydrocarbons benzene, toluene and xylenes increased markedly during incidents of spontaneous combustion.[117]

Chamberlain et al,[118] in a separate publication, carried out exploratory work on the production of acetaldehyde from sealed areas underground, and concluded that further underground investigations were necessary to establish the true value of this gas for predicting spontaneous combustion.

1.5.3.3 Additional Detection Methods

Hertsberg et al[119] compared the analysis of carbon monoxide and submicron particles as indicators of incipient combustion of coal, wood, polyvinyl chloride electrical insulation, and neoprene conveyor belting. In all cases submicron particles were detected before any perceivable changes in carbon monoxide were noted. Infra-red emissivities for underground strata are fairly consistent. Thus an infra-red measurement device can be used to detect areas of thermal emission higher than the surround strata.

Stateham[120] has reported that localised hot spots in coal mines could be detected by infra-red imaging techniques. Fauconnier[121] investigated the humidity patterns preceding the detection of spontaneous combustion at the Springfield coal mine, South Africa. He noted that the relative humidity, prior to the incident showed a general downward trend and concluded that some form of equilibrium had been established between the relative humidities of coal and air during the moist summer conditions. The sudden drop in the relative humidity of air with the onset of winter conditions would therefore cause a difference to be developed between the equilibrium humidity of coal, which was still high, and the relative humidity of the air, which had dropped. Using the results of Guney[92], which were summarised earlier, the author concluded that the differences in humidity were sufficient to cause an increase in coal temperature. The small random

temperature variations in thermal noise that occur in underground roadways are normally less than $\pm$ 0.1 °C, but if heat is being generated these variations increase in magnitude. This additional increase can be measured using thermistors, and is reported to provide an elegant method of fire detection.[122]

1.6 Methods of Spontaneous Combustion Detection currently in use in British Coal Mines

The detection of spontaneous combustion in the working of a coal mine is a complex and demanding problem. For example, the presence of ventilation not only leads to substantial dilution of the material products of combustion, such as gases and smoke and the dissipation of heat energy, but it can also enhance the development of the incident by a fanning effect. To cater for such conditions the 'ideal' detector must not only be highly sensitive and have a rapid response to one or more of the environmental changes produced, but must also be robust, immune to humid and dusty conditions and ultimately it must be able to fulfil the appropriate requirements of intrinsic safety for use underground. The systems described below are currently in use for the detection of spontaneous combustion of coal or open fires.

1.6.1 Systems based on Carbon Monoxide monitoring

1.6.1.1 Tube Bundle System[123,124]

This system was originally based on the philosophy of monitoring the carbon monoxide content of the

ventilating air passing critical underground locations in order to detect spontaneous combustion in its very early stages of development.

The main components of the system are:- the tube bundle which consists of a number of small bore poly-vinylchloride plastic tubes, bound together by an outer sheath, which conveys gas samples to the surface drawn by a pump to a selection unit and an infra-red analyser. Air is drawn continuously from strategic underground locations through the tubes to the surface where individual tubes are selected sequentially and the gas samples directed to the analyser unit.

The output from the analyser is recorded on either a simple chart display or computer based data processing display module. The latter permits the use of pre-set alarm programmes, data presentation and a rapid and accurate review of previous gas analyses. The advantages of the system are the relatively simple underground installation, the low cost involved in the instrumentation, and the ability to continue operating with underground power disconnected. The major disadvantages of the system results from the length of time from sampling to the time when analysis on the surface takes place. This may only be ten or twenty minutes when sampling from quite a short distance, but from ten kilometres the time of travel is 120 minutes. In the 1981 Annual Report from H.M. Chief Inspector of Mines the following incident was cited. "In an incident of spontaneous combustion, a deputy in the

course of a routine inspection during the holiday period, found open flame in the coal roof. The fire, which was extinguished six hours later by water jets, affected 8 metres of the roadway but was not detected by the tube bundle system until almost two hours after its discovery, due mainly to the long distances involved."

1.6.1.2 Shaft Monitors[125,126]

The shaft monitor was a development of the tube bundle system designed to detect any type of fire which might break out underground by analysing samples taken from the main ventilating air in the upcast shaft. The major source of delay in the tube bundle system is avoided because the analyser unit can be sited near the sampling point and since there is only one sampling point, there is no delay due to the cycle time. This method of monitoring has the advantages of covering the whole ventilated workings and is useful for providing an early warning of an incident at times when few men are working, such as weekends and holidays. Since the main ventilating air is being sampled this system will not identify the actual location of the fire and the response of the shaft monitor to a small incident during normal working tends to be masked by the usual fluctuations in carbon monoxide levels associated with normal mining practice.

For this application an increased sensitivity of detection for carbon monoxide is required (sub ppm).

1.6.1.3 Gas Detection Instruments[127,128]

A number of portable and fixed-site instruments are presently in use underground which are based on electrochemical methods of detection, giving either a meter or digital presentation of the carbon monoxide concentration being measured. The output from the instrument or monitor can give an audible or visual alarm, or be telemetered to the surface for data processing and control. Although a near instantaneous measurement is obtained, this type of instrument requires considerable maintenance and calibration against known gas concentrations and its use is limited to the life of the batteries. It has also been shown in practice that during an incident of spontaneous combustion high or "overreadings" are obtained due to the presence of interfering gases with similar redox potentials to carbon monoxide, especially hydrogen and unsaturated hydrocarbons.

1.6.1.4 Chemical Stain Tubes[129]

Until recently the most common in situ detection method used was the chemical stain tube, which operates on the principle of a colour change in a chemical reagent caused by the presence of a particular gas. For carbon monoxide the reagents used are iodine pentoxide, selenium dioxide and fuming sulphuric acid, which produces a colour change from white to brownish green. These tubes are normally used by colliery personnel on a routine basis to give an 'on the spot' indication of the carbon monoxide concentration.

1.6.2 Thermal Detection [130]

The Probeye instrument manufactured by Hughes Aircraft Corporation, America, has been used successfully underground to detect localised hot spots and roadside heatings by producing a thermal picture of the area in view. The instrument which is hand-held suffers from a number of limitations, for example, the need for argon gas cooling from a small cylinder at a pressure of 5000 pounds per square inch, limited usage time, and gradual deterioration of performance. In addition, the instrument is not certified for general use underground being restricted by the codes of practice to comply with the National Coal Board's, Production Department Instruction PI/1975/2 which covers "the use of Non-certified Electrical Apparatus Underground". An instrument based on the concept of "thermal noise" has been installed in underground roadways to protect specific locations from flash fires. This type of instrument requires to be accurately sited within the expected heat plume because the heat generated from a fire is rapidly dissipated by ventilating air. Two types of thermally operated links controlling water spray devices are presently installed underground. One type is a fusible link held by a low melting eutectic alloy, and the other a quartzoid bulb which collapses with the thermal expansion of the liquid. Both types of detector are able to respond at specific temperatures in the range 60 °C-250 °C, but those used underground operate at 60 °C. The actual effectiveness of

these sensors have been shown by Kennedy to be exceptionally limited.[131] He reported that, at a wind speed of 2 m sec^{-1} the maximum height of the 60°C contour from a fire producing 27kw to be only 14 inches and this was reached three feet downwind of the fire. The sensors are usually installed near the roof of a roadway and are regarded to be more of a strategic defence against open fire than a spontaneous combustion detection system.

1.6.3 Smoke Detection[132,133]

The first smoke detectors were introduced underground in 1962, their method of operation is as follows:

The detector consists of two electrodes connected to a D.C. source. The air between the electrodes is ionised by alpha particles emitted from an Americium radioactive source, (Am 241). The ions thus produced travel towards their respective electrodes with a velocity determined by their mass and the electrostatic field present. When particulate combustion products enter the detector they collide with the ions to produce a heavier charged species, their drift velocity is reduced and thus the ionisation current decreases.

The early detectors were found in practice to be very sensitive to high humidity and dusty atmospheres which resulted in instability and false alarms. Design modifications to improve performance resulted in the introduction of a new model in 1975. This overcame many of the earlier problems but it was shown to be unreliable under certain conditions and has therefore been used mainly as a warning type device.

To summarise, in this section it has been shown that during the last few years advances in technology have led to the development of a number of different systems for the monitoring of spontaneous combustion and open fires. Even so the number of incidents which involve open fire remain at a reasonably constant level and the financial consequences resulting from these and from spontaneous combustion causes concern. Therefore, the need for continuing research into producing more effective monitoring, alarm and reporting systems assumes a vital role if safer underground working conditions are to be achieved in the future.

1.7 The Occurrence and Dangers of Methane[134,135]

Methane is flammable and explosive between a lower limit of 5% and an upper limit of 15% when mixed with air at atmospheric pressure. It is the principal constituent of firedamp and occurs naturally in coal mines being evolved from coal seams during mining. The lower hydrocarbons ethane, propane, butanes and pentanes are also present as minor constituents normally accounting for five percent of the evolved gases.

It is not known when the first explosion of firedamp claimed human lives, but the earliest recorded instance was probably the death of "Richard Barkas , burned in a pit", noted in the burial registers of St. Mary's, Gateshead, in October 1621.[136] In 1675 at Wingerworth, near Chesterfield, a colliery is reported to have exploded no fewer than four times within five weeks. Certainly by this time firedamp was

a recognised adversary of the miner and the normal method of dealing with small accumulations in the roof area of a mine was by a person (the fireman) who crept along the floor covered in a wet cloth and ignited the accumulation with a long pole and candle. The first state legislation covering safety in British coal mines was passed in 1850[137] and in subsequent years further laws have been enforced in an effort to reduce the frequency and severity of colliery explosions. Current legislation included in the Mines and Quarries Act, 1954,[138] places responsibility on the Mine Manager for ensuring that all parts of the mine, not closed by specially constructed stoppings are adequately ventilated. To be 'adequate', ventilation must dilute and remove flammable and noxious gases. Measures designed primarily to regulate levels of flammable gas in the mine but which also may offer wider benefits, may be categorised under the term firedamp control as follows:

1) Improvements to the ventilation network
2) Efficient use of firedamp drainage techniques
3) Special treatments in areas prone to outburst problems
4) Firedamp monitoring

1.7.1 Improvements to the Ventilation

Improvements due to ventilation network may be achieved by enlarging the cross-sectional area of underground airways. Alternatively, improvements to the ventilation system may be realised through maintenance of airway cross-sections using roadway preservation techniques; reducing frictional

losses by providing smooth linings; or by increasing air flow through application of more efficient fans. The increase in air flow that can be achieved is limited by the resulting dust levels which must remain below current statutory limits. For practical purposes air velocities in the range 1.5 to 3.5 $m s^{-1}$ are acceptable.

1.7.2 Firedamp Drainage

Firedamp drainage involves drilling cross measure boreholes into the roof, and often also the floor, of a working area to capture gas released from adjacent seams progressively disturbed by the workings; this gas would otherwise enter and pollute the environment. The boreholes are connected by a series or 'range' of steel pipes to an extraction plant which is usually sited on the surface. Suction applied to the pipes draws firedamp from the surrounding strata to the surface where it can then be utilised. Careful sealing of stand pipes through which boreholes are connected to the range together with control of the pumping rate are essential to minimise the induction of mine air through the strata which may inadvertently create an incident of spontaneous combustion.

1.7.3 Special Treatments in areas prone to Outbursts

In the UK, outbursts of gas and coal from worked seams are a problem restricted to the anthracite mines of the Gwendraeth Valley, West Wales. Outbursts of up to 1000 tonnes of coal and approximately 0.1 million cubic metres firedamp have been recorded.[140] To alleviate this problem, special precautions have been adopted, such as a

volley firing to trigger impending outbursts from a safe distance. Other monitoring procedures including physical examination of the coal, microseismic studies, gas emission and gas content measurements have been adopted in an effort to develop an efficient early warning system.

1.7.4 Firedamp Monitoring

Comprehensive monitoring of the mine environment and the firedamp drainage system is necessary to ensure that ventilation requirements are sufficient to prevent dangerous accumulations forming, which could result in an explosion from a coincident source of ignition. References to specific concentrations of firedamp which require monitoring to comply with legislation are presented in the Mines and Quarries Act, 1954,[138] and a summary of these is shown in Table 7.

1.8 Current Methods of Detecting Methane

Two main methods of detecting the concentration of methane are used in British coal mines. The first involves taking discrete samples underground into pressure capsules. These are then returned to the laboratory for analysis using infra-red methods of detection. The second method provides an instantaneous measurement of the methane concentration by using an approved type of apparatus, known as a methanometer. In 1970 the Ministry of Technology (now Health and Safety Executive) issued Testing Memorandum No. 7[141] defining a methanometer as an approved instrument which is

a) Designed to detect and/or measure methane

b) Normally operated independently of any mine

Table 7

References in Legislation to Specific Concentration of Firedamp

Authority	Amount of Gas	Requirement
Ventilation Reg. 2	0-0.25% firedamp	Every intake airway the air of which has not ventilated another working place shall normally be kept free from inflammable gas up to within 300 feet of the first working place.
Loco. Reg. 14(1) (b) (i)	0.2% firedamp	Locomotive roadways ventilated with fresh air and containing not more than 0.2% firedamp over a period of thirty consecutive days need only be sampled at intervals not exceeding thirty days.
Vent. Reg. 2(2)	0.25% firedamp	If six samples taken by an inspector at not less than fortnightly intervals in the general body of the air in an intake airway up to 300 feet from the first working place average not more than 0.25% firedamp the roadway may be classified "free from inflammable gas".
Vent. Reg.13	0.5% firedamp	If the last six statutory determinations in a return airway 30 feet from the face exceed this level, a specified proportion of the firedamp detectors required by Ventilation Reg. 12(1) must be automatic detectors.
Loco. Reg. 14(1) (b) (ii) Vent. Reg. 7(1) (b)	0.6% firedamp	Locomotive roadways (other than those ventilated with fresh air), and also places sampled because either electricity is in use or because shots are fired, need be sampled only every thirty days if every result obtained in the previous thirty days is not more than 0.6%. Weekly sampling must be recommenced when any figure exceeds 0.6%.
Loco. Reg.14(1) (a) Vent. Reg. 7(1) (a)	0.8% firedamp	If any sample taken by virtue of the Locomotive Regulations or of the Ventilation Regulations relating to the use of either shot firing or electricity shows more than 0.8% samples must be taken at intervals not exceeding 24 hours for the next seven following working days.
Vent. Reg. 8(2)	1.0% firedamp	The Manager must inform the Inspector of any occasion other than when determinations are made at junctions in return airways in accordance with Vent. Reg. 7(A), when this concentration of firedamp if found to be exceeded unless the Inspector has otherwise directed or the excess was due to a temporary derangement of the ventilation.
Section 68(1) Elec. Reg. 6(1) and (3) (as amended 1967) Exp. Reg. 47(1) to (5) Loco. Reg. 16 Section 79(1) and (5)(b)	1.25% firedamp	(i) This is the upper limit that Regulations may prescribe as the concentration above which electricity must be cut off. (ii) Above 1.25% a person must either cut off the electricity from all electrical apparatus (other than telephone or signalling or any apparatus for detecting inflammable gas, including ancillary apparatus) or report to someone who is empowered to do so. Also, when the concentration falls to this level, the senior official on duty may restore the electricity supply. (iii) Shotfiring is prohibited on the return side of any point showing a greater firedamp content. (iv) Locomotive running must be discontinued if any determination of firedamp exceeds 1.25% until the Manager so directs. (v) In mines other than safety lamp mines men must be withdrawn from the affected area.
Section 79(5) (a) Firedamp drainage Reg. 13 (e)	2.0% firedamp	(i) In a safety lamp mine 2.0% is deemed to be "excessive concentration" and men must be withdrawn from the area. (ii) In an area where firedamp is vented from a drainage system into an underground roadway must be fenced.
Firedamp drainage Reg. 13 (c)	40.0% firedamp	Firedamp must not be discharged to a utilisation plant if it contains less than 40% flammable gas.

power services

c) Able to include any accessories e.g. sampling device, recorder, to form a self contained system.

All approved instruments are classified according to their function by a number and their accuracy by a letter. Apparatus in Category A are more accurate than those in Category B. There are also firedamp detectors which are classified as methanometers of Accuracy B. In addition certain instruments are approved as "electrical apparatus for measuring or detecting inflammable gases". A summary of the different classes of instruments and their accuracy is given in Table 8.

Generally, the detection method used in methanometers utilises the pellistor bead, although a number of instruments for the measurement of high concentrations incorporate thermal conductivity elements. The pellistor bead was developed in the 1950's at the Safety in Mines Research Establishment, and has been in use since 1960. The bead is approximately 1 mm in diameter and comprises a finely wound platinum coil on to which is deposited a porous oxide material, usually alumina. The alumina bead is formed by dipping the coil into a solution of aluminium nitrate followed by repeated flash firing. The material is catalytically activated either during or after formation of the porous oxide, by formation of surface coating of platinum/thorium oxide. Two thermally matched beads are incorporated in a typical detector head with one of the beads having catalytic activity. The passive bead being formed

Table 8

Summary of instrument category and accuracy

Category	Permitted Range %	Errors*
Class 1A : Methane indicators and recorders up to 5%	0-1.25 1.25+	± 0.1% CH_4 ± 8% of true value
Class 1B : Methane indicators and recorders up to 5%	0-1.25 1.25+	± 0.2% CH_4 ± 16% of true value
Class 2A : Methane indicators and recorders up to 100%	5-25 25-100	± 2% CH_4 ± 8% of true value
Class 2B : Methane indicators and recorders up to 100%	5-25 25-100	± 4% CH_4 ± 16% of true value
Class 3A : Methane alarms	0-100	± 8% of true value
Class 3B : Methane alarms	0-100	± 16% of true value

* Allowable errors (80% probability) of instruments

from alumina poisoned by boiling in potassium hydroxide. Both beads are heated to approximately 550 °C by passing a small current through each and when the catalytically active bead comes into contact with firedamp in the presence of oxygen an exothermic oxidation reaction takes place. The two beads are arranged as two arms of a Wheatstone bridge and the changing resistance of the catalytically active bead causes an imbalance in the bridge. The resulting detector signal is approximately proportional to the percentage of combustible gases present up to approximately 5%. Although these devices have been used underground for many years, they suffer a number of drawbacks. Such devices do not, as yet, differentiate between combustible gases, they are dependent upon the presence of oxygen and above 10% combustibles ambiguous results can arise. They are also subject to poisoning resulting in a loss of sensitivity.[142] The loss of sensitivity which may be temporary or permanent, varies depending on the form of poisoning and may be from a few percent to total failure. Furthermore, a sensor may be severely poisoned for one oxidation reaction but not for another. For example, after exposure to silicone vapour, a sensor may be completely insensitive to methane but readily detect propene or hydrogen.[143] Instruments based on the pellistor bead normally operate in areas where the concentration of methane is not likely to exceed 5%. In places subject to exceptionally high levels of methane, for example, where gas outbursts are encountered or monitoring of firedamp drainage systems are required, instruments based on thermal conductivity type detectors are utilised to measure

the actual concentration present. All instruments approved for use underground are shown in Table 9.

In conclusion, it is recognised that firedamp cannot be totally excluded from the underground environment, and so research into alternative detection systems must continue to complement existing methods in an effort to pre-empt accidents by maintaining a high degree of control over the mine environment. In the future this control may become even more essential with higher production and the mining of deeper seams that may be more 'gassy'. Legislation may also require more stringent knowledge of the actual composition and concentration of firedamp. Even now, a concentration of greater than 70 ppm methane in return air has been suggested as sufficient cause for assuming a potential methane hazard in United States non-coal mines.

1.9 Alternative Detection Devices

Over the last few years a number of gas sensitive devices have been developed which show potential to complement or possibly replace existing systems for the detection of spontaneous combustion and open fires or monitoring of methane in the underground environment. Their operating principles and possible applications are outlined below:

1.9.1 Mass Sensitive Devices

The first analytical application of the quartz crystal microbalance (QMB) was reported by King in 1961.[144] Subsequently this type of device has been widely studied for the environmental monitoring of gaseous vapours. A

Table 9

Approved methane monitors for use underground

Parameter	Type	Measuring range	Class or Approval Number	Principle of detection
A. Hand-held Monitors				
Methanometers	M.S.A D6D	0 - 5%	Class 1A	Pellistor
	M.S.A D6	0 - 5%	Class 1A	Pellistor
	M.S.A C4	0 - 5%	Class 1A	Pellistor
	Seiger SM1	0 - 5%	Class 1A	Pellistor
Methane Testers	M.S.A HC111	0 - 100%	O.G.D./29	Thermal conductivity
	M.S.A HC11	0 - 100%	E.R.21A/1	Thermal conductivity
Automatic Firedamp Detectors	M.S.A AFD1	0 - 3%	Class 1A 3A	Pellistor
	M.S.A AFD11	0 - 3%	Class 1A 3A	Pellistor
	Seiger AFD1	0 - 3%	Class 1A 3A	Pellistor
	Seiger AFD2	0 - 5%	Class 1A 3A	Pellistor
B. Fixed Monitors				
Methane (General atmosphere)	Seiger BM1	0 - 3%	Class 1A 2A	Pellistor
	Seiger BM1	0 - 50%	E.R.21A/30	Thermal conductivity
		0 - 100%		
Methane (Enclosed atmosphere)	Seiger BM2H	0 - 100%	E.R.21A/26	Thermal conductivity

M.S.A	Mine Safety Appliance
Class 1A, 3A	As described earlier
E.R.21A	Electricity Regulation 21A of the Coal and Other Mines 1956. "Apparatus for detecting or measuring inflammable gas". No electrical apparatus for detecting or measuring inflammable gas including ancillary apparatus operated by such apparatus, other than apparatus of a type approved by the Minister for the purpose of this regulation, shall be installed or used below ground in any part of a mine.
O.G.D	Other gas detectors.

comprehensive review of this subject containing 113 references was published in 1983 by Alder.[145] Briefly, these devices operate on the following principle.[146] When gas molecules absorb in the thin layer of a chemically selective material (1000 Å) applied as a coating on a quartz crystal surface, the resonance frequency of the crystal decreases in proportion to the quantity of absorbed molecules, that is:-

$$fm = -K \; m_{gas} \qquad \ldots\ldots\ldots\ldots\ldots\ldots \; 1.1$$

where fm is the frequency change caused by the mass of gas adsorbed, m_{gas} , K is a constant, which depends upon the crystal used.

Table 10 provides a list of applications and provides a scope for the wide versatility of the QMB as a chemical sensor. The main advantages of QMB devices are their simplicity, reliability and the frequency output which is simple to measure. Interferences, especially water vapour, present the major drawback in many of the systems, but these[147,148,150] can usually be overcome or reduced by physical means using filters, membranes or by compensation using a second crystal.[153]

A similar device which resembles the QMB device is the surface acoustic wave (SAW) sensor. Devices using this principle were first reported by Wohltjen and Dessy in 1979[154] and consist of a piezoelectric substrate that has interdigital electrode arrays microfabricated at each end. When excited by a radio frequency voltage of an appropriate frequency, a synchronous mechanical wave is created in the piezoelectric substrate. This Rayleigh

Table 10

Summary of applications using QMB devices

Date	Application	Sensor	Dynamic range	Interference	Ref
1980	Detection of carbon monoxide concentrations in the ppb and ppm range	Gold plated quartz crystal Reaction of carbon monoxide with Hg(11)O cell at 210°C to produce Hg vapour which is adsorbed on gold electrodes.	5-150 ppb 1-400 ppm	Formaldehyde olefines Sulphur dioxide, Hydrogen, Methane.	147
1980	Detection of toluene concentrations in the ppm range	Carbowax 550 coated crystal	30-300 ppm	Organics, Benzene	148
1970	Determination of methane and other hydrocarbon gases with a detection limit of 10 ppb	A coated crystal was used to detect moisture from the combustion of methane and other hydrocarbons	10 ppb	Other combustibles	149
1978	Detection of Hydrogen chloride concentrations in the ppb and ppm range	Triphenylamine (HCL) or triphenylamine coated crystal	10-100ppb or 100 ppb - 1 ppm 1-100 ppm	Ammonia None	150
1964	Determination of hydrogen sulphide in the low ppm range	Silver, copper or lead acetate coated crystals.	1-60 ppm		151
1976	Detection of sulphur dioxide concentrations in the ppm range	N.N.N. N. - tetrabis (2-hydroxyl-propyl) ethylenediamine or a Quadrol coated crystal.	10 ppb - 30 ppm	Nitrogen dioxide, water	152

surface wave then propagates from the transmitting electrode array across the surface to an identical receiving electrode where the mechanical energy is converted back into an electrical radio frequency voltage. Since Rayleigh wave energy is confined to about one acoustic wavelength (100 μm or less) of the surface, any material present on the surface will produce large changes in the wave characteristics (e.g. amplitude, velocity). The most sensitive response is obtained when the device is used as a delay line oscillator. Here the input and output transducers are connected to each other through a radio frequency amplifier.

In this configuration the device oscillates at a characteristic frequency determined by the electrode geometry and Rayleigh wave velocity. Small perturbations in the mass or elastic modules of a thin selective coating on the device surface will produce substantial shifts in the devices' resonant frequency. Thus, in this mode it behaves in a fashion similar to the QMB devices, although it has several fundamental differences including smaller size, more sensitive response, and can be microfabricated. Practical devices normally have two channels, one coated, the other not, and the difference in response is measured. This allows for some compensation for other atmospheric variables. Even so use of this device has been limited to the detection of sulphur dioxide, nitrogen dioxide and hydrogen due to the cost of specifically designed sensors.(155-158)

1.9.2 Micro-Gas Chromatography

A micro-gas chromatographic system suggested by Karas in 1970 [159] was further developed by Terry and co-workers [160] at Stanford University using microfabricated components as follows. The chromatographic column was produced by etching a lithographically defined spiral groove into a silicon wafer which was covered with an electrostatically bonded glass plate. This resulted in a 1.5 metre long capillary tube with a rectangular cross section approximately 30 μm deep and 20 μm wide. Coupled to the column on the same wafer was a solenoid actuated diaphragm injection valve. The valve seat was etched into the silicon wafer and covered with a flexible nickel diaphragm. Normally the diaphragm is pressed against the valve seat. In operation energising the solenoid releases pressure on the diaphragm, allowing higher pressure gas from a sampling loop to flow into the column. It is claimed that reproducible injections of nanolitre size samples can be readily achieved. The actual detector based on thermal conductivity was formed by etching an interdigital thin film (1000 Å) of nickel on to a thin slice of silicon which was clamped over the gas channel at the outlet of the capillary column. Detection of air contaminants in the ppm concentration range has been demonstrated, and analysis times of less than sixty seconds for many organic vapours are typical. A portable instrument consisting of five miniature chromatographs and a micromputer is currently being developed by Microsensor Technology Inc. However, considerable practical

difficulties have been reported, particularly with the microbore chromatographic column and at present a fully working system is not available. Such an instrument should have the capability to monitor and control the quality of a mine environment.

1.9.3 Semiconductor Junction Devices[161,162]

1.9.3.1 Schottky Devices[163-165]

A device that has shown considerable sensitivity as a gas sensor is the Schottky diode. In its simplest form a Schottky diode consists of a small area of metal in contact with a semiconductor. Here a barrier layer is formed from which charge carries are severely depleted. The reverse current through the diode is an exponential function of the barrier height. It is this barrier height which is the gas sensitive parameter which is probed by the variation of reverse current through the diode structure. It is commonly believed that the barrier height is affected by adsorption and electron exchange of gases with the metal resulting in changes in the work function of the metal. In order to achieve this the metal layer has to be extremely thin, since the charge exchanged with the adsorbate needs to be a significant fraction of the population of conducting electrons. Alternatively, adsorption at the metal/semiconductor interface could provide electronic surface states and thus affect the barrier height by changing the charge distribution in the semiconductor. Such adsorption could be brought about by having a

porous metal contact or by the gas dissociating on the metal to form a species such as H atoms which could diffuse through the metal to the junction. To date PbS/Si,[165] Pd/CdS,[166] Pd/TiO_2[167] diode structures have been investigated and have shown usable sensitivity to hydrogen.

A three layer structure, Pd/SiO_2 /Si, in which the intermediate layer of SiO_2 is 15-30 Å has also shown considerable sensitivity to hydrogen.[163] Formation of the oxide layer prevents the reaction between palladium and silicon to form palladium silicide. Three factors appear to be involved in the hydrogen sensitivity of the device, namely a change in metal work function, the formation of a dipole layer at the Pd/SiO_2 interface, and the appearance and removal of surface states at the Si/SiO_2 interface.

1.9.3.2 MOS Capacitors and Transistors[168]

In these devices a modulation of the thickness of a space charge layer in the surface of a semiconductor is measured. Responses have been obtained from Pd/SiO_2/Si structures with SiO_2 layer 100-1000 Å thick, which is much thicker than in the Schottky diodes described above. According to Lundstrom[169] the principle of operation for the detection of hydrogen depends upon the dissociation of hydrogen molecules on the catalytic palladium surface.

Some of the hydrogen atoms so formed diffuse through the thin metal film and are adsorbed at the metal insulator interface, where an equilibrium is reached

between hydrogen atoms at the gas and insulator interfaces.

The hydrogen atoms adsorbed at the metal insulator interface are electrically polarised and thus give rise to an electric field which can be measured as a change in the threshold voltage of an MOS transistor or as a shift of the flatband voltage of an MOS capacitor. The response is slow at ambient temperature due to the slow rate of catalytic reactions on the palladium surface. The devices are therefore heated to approximately 150°C to obtain increased response times and also to prevent water molecules adhering to the metal surface. If the palladium film is non-porous, the devices respond, but only to hydrogen or to gases which can dissociate to hydrogen atoms such as hydrogen sulphide[170] and ammonia.[171] If the metal layer is made porous the devices become sensitive to any gas which will adsorb on the palladium/gas interface and create a dipole there, such as carbon monoxide.[172]

1.10 Metal Oxide Semiconductors[173-176]

Although it has been known for many years that adsorption of a gas on the surface of a semiconductor will produce a measurable change in the electrical conductivity of the solid, it was Seiyama[178] who first applied the electrical conductivity changes of zinc oxide when exposed to reducing gases to gas detection. Over recent years there has been considerable interest in exploiting the electrical conductivity changes in a number of n and p type metal oxide

semiconductors when exposed to reducing gases. To date the most extensively studied solids have been the oxides of tin and zinc. As noted by Firth the oxides studied are semiconductors because of the ability of the metal to exist in different oxidation states. These oxides are either non-stoichiometric; n-type semiconductors, containing a slight excess of metal or p-type semiconductors having a slight deficiency of metal within the lattice. In order to preserve electrostatic neutrality of the oxide the excess metal in n-type semiconductors is present, as ions with a charge lower than that of the parent metal ion in the oxide lattice, for instance Zn^{o} in ZnO. Such impurity ions can be represented as having localised energy levels just below those of the conduction band of the oxide; the resulting localised electrons can be thermally excited into the conduction band and cause the oxide to have electrical conductivity. For example, tin oxide has a band gap of 3.6eV which would normally make it an insulator but the impurity ions give rise to energy levels only 0.03 to 0.15eVs below the conduction band.[180]

1.10.1 The Mechanism of Gas Sensitivity[177,181,182]

The variation in conductivity of metal oxide semiconductors when exposed to gases can be explained in terms of surface electronic properties.

1.10.1.1 Interaction of Oxygen

When an n-type semiconductor material such as tin oxide is heated to elevated temperature in air, physically bound molecular oxygen becomes adsorbed to form a

surface state by drawing electrons out of the bulk donors below the surface. Several adsorbed oxygen species have been suggested but it is now generally accepted that O_2^- ions dominate at temperatures below 200 °C which dissociate to O^- on heating. Above approximately 350 °C the oxygen coverage diminishes and the dominant species becomes O^{2-}.[173,183] As the process of oxygen adsorption proceeds, irrespective of its state, a positive space charge layer develops in the surface layer of the solid and a negative charge accumulates at the surface.[173,184] An electric field exists in this boundary layer which repels electrons away from the surface into the solid. This field decreases with distance into the semiconductor and at a short distance in the bulk (1-110 μm)[177] the distribution of electrons in the conduction band and in the donor levels has returned to normal. There is thus a boundary layer of decreasing electron concentration towards the surface of the semiconductor from the inner edge of the layer. As the space charge layer accumulates with continued adsorption, it becomes progressively more difficult to transfer electrons from the conduction band to the adsorbing oxygen. Chemisorption would therefore cease far short of a monolayer.[173] This process of oxygen adsorption on an n-type semiconductor material results in a decrease in charge carrier density and hence a decrease in surface conductivity of the solid.

A number of models have been described by different authors to account for surface conductivity changes in

devices fabricated not only from thin films and whiskers, but also from conglomerates produced from sintered grains formed into pellets, or grains pressed into pellets.[177,182,185,187] In thin films and whiskers, the withdrawal of electrons by adsorbed oxygen produces a space charge layer that extends throughout the whole material creating a marked decrease in charge carrier density and resultant decrease in conductivity of the material.[180,185,186] Morrison[182] has illustrated this effect numerically, using a 100 micron thick film, oxygen adsorption would produce little change in conductivity whereas a 10^{-2} micron film would produce a 10 fold change in conductivity.

The decrease in conductivity of conglomerates in the presence of oxygen can still be a function of a surface layer since the conduction may be dominated by 'necks' or intergrain boundaries. If one considers a pressed pellet consisting of grains sintered together to form thin 'neck' regions as shown below.

Figure 3

Schematic representation of the necking model for conduction.[182]

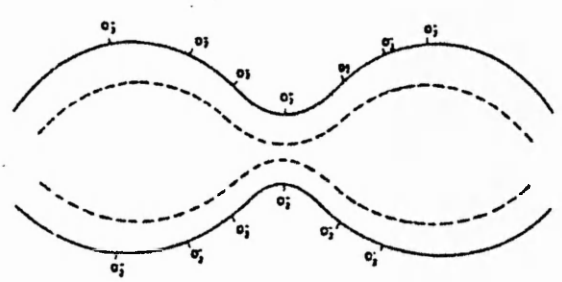

Then the necks are the resistance controlling feature of the pellet because they are regions where the withdrawal of electrons by surface adsorbed oxygen is most effective in reducing the charge carrier density. The essential feature of this model is that the current is controlled by a charge transfer mechanism operating normal to the direction of current flow as in the thin film devices. Finally, if the grains touch, as in a pressed pellet, but are not sintered together, then charge carriers must overcome the surface potential barrier formed by oxygen adsorption between the grains, as shown below:

Figure 4

Schematic representation of the Schottky barrier conduction model.[182,187]

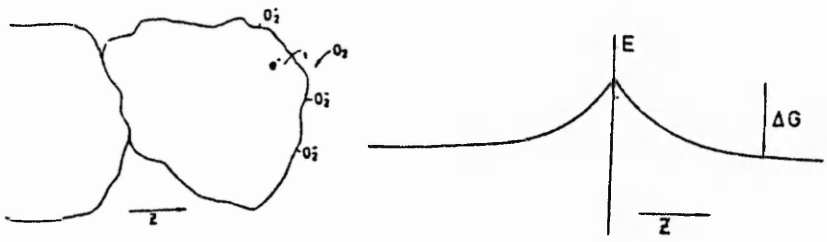

In this case the surface barrier potential, V_S, is a function of the concentration of adsorbed oxygen, Nt, and is given by the Schottky equation,[173]

$$V_S = \frac{eNt^2}{2K\epsilon_o N_D} \quad \text{.....1.2}$$

where $K\epsilon_o$ is the semiconductor permittivity and N_D is the volumetric density of electron donors. The conductivity is then given by:

$$\sigma = \text{Const. exp. } (-eV_S/KT) \text{.....1.3}$$

and is extremely sensitive to changes in V_S.

Finally, we can have a mixed case where the necks are thin enough for all the carriers in the neck region to be extracted by adsorbed oxygen. Then again, the carriers must overcome a potential barrier to traverse the neck, but according to Morrison the potential barrier is not as high as the V_S calculated from Equation 1.3.[182]

Thus, it can be seen that when n-type semiconductor materials are heated to elevated temperatures in air, they exhibit decreased conductivity, due to the presence of adsorbed oxygen.

1.10.1.2 Interaction of a reducing gas

In the case of a mixture of a reducing gas in air, an equilibrium concentration of adsorbed oxygen ions and reducing gas is present on the surface of the oxide, and hence the conductivity will be determined by the partial pressure of each gas. However, since in general, oxygen is strongly adsorbed on most oxides,

large changes in the gas phase oxygen concentrations (1.50% v/v) produce only small changes in the conductivity of the oxide. Most reducing gases, however, are generally weakly adsorbed so that relatively large changes in the conductivity of the oxide are produced by changing the reducing gas concentrations.

It is generally agreed that in order for a reducing gas to be detected by an n-type metal oxide semiconductor, it must participate in one of the following reactions.[177,179,182,185,188,189] The first involves a chemical reaction between the reducing gas and a surface state, usually oxygen ions, which produces a product gas which subsequently desorbs. The overall reaction involves the removal of oxygen ions in a neutral form and hence the electrons trapped on the ions will be donated back to the conduction band of the solid resulting in an increase in conductivity.

$$G_{gas} + O^-_{surf} \longrightarrow P_{gas} + e^-_{bulk} \quad \text{.....1.4}$$

Secondly,[177,182,190] a reducing gas itself can act as an electron donor. On adsorption it injects electrons into the sensor material conduction band and increases the conductivity.

$$G_{gas} \longrightarrow G^+_{surf} + e^-_{bulk} \quad \text{.....1.5}$$

Thirdly,[177,182,191] by way of oxidation reduction reactions, whereby reducing gases participate in a defect reaction which affects the bulk stoichiometry of the

semiconductor. Because the dominant electronic donor is a stoichiometric defect, the bulk conduction based electron concentration reflects the reducing gas concentration.

$$G_{gas} + MO_{2bulk} \longrightarrow P_{gas} + (MO)^{++}_{bulk} + 2e^-_{bulk} \quad \text{.....1.6}$$

Each of the above reactions occurs under suitable conditions and result in an increase in conductivity of the material. In particular, the reaction of gases with adsorbed oxygen ions, Equation 1.4 above, is the most frequently cited as being responsible for the detection response and is widely considered to be the fundamental reaction of gas detection with metal oxide semiconductors.

Even so, a further reaction model has been proposed by Clifford[192] in which it is suggested that reducing gases do not directly interact electrically with the semiconductor material. Instead they react with physically adsorbed oxygen and these non-equilibrium reactions catalysed by the metal oxide surface, result in a steady state concentration of physically adsorbed oxygen molecules which is far less than would result with no gas present. The physically adsorbed oxygen concentration determines the amount of oxygen adsorbed in a charged state as oxygen ions.

Consequently, the presence of a reducing gas decreases the amount of oxygen ions, and ultimately the conductivity of the material. Essentially only oxygen interacts with the electronic structure of the

semiconductor, contributions to the conductivity by reducing gases must be mediated by reactive desorption of physically adsorbed oxygen.

Morrison [182] whilst reflecting on the many possible reaction mechanisms by which the conductivity of a metal oxide semiconductor may be governed by a reducing gas concluded that in many of the proposed devices it is not clear which of the reactions described above dominates, but it is well to be aware of the various possibilities.

1.10.2 Gas detection using Metal Oxide Semiconductors

The previous sections have shown how the presence of a reducing gas in air can interact with an n-type semiconductor oxide and produce an increase in conductivity. It therefore follows that with a mixture of reducing gases in air the resultant change in conductivity will be due to a combination of reactions. The majority of research effort to date has been devoted to producing both a selective and sensitive device. Several approaches have been investigated, including the introduction of additives, varying the oxide temperature, and altering the physical form of the oxide.

Improvements in selectivity have been achieved by doping the metal oxide with an additive which is either active towards a particular gas or induces the formation of ions which are similarly active. For example, additions are deposited on to metal oxides to promote a chemical effect. Here catalytic materials are used to enhance activity

towards the species of interest and to suppress it towards other species. These additions are normally catalytically active metals or metal salts, such as palladium, platinum, rhenium or iridium and are deposited on to the surface of the oxide. This results in 'islands' of catalyst materials which provides active sites for the gases of interest. A recent review article by Gentry and Jones highlights the role of catalysis in metal oxide sensors.[193] Additives are also incorporated into the oxide to produce a purely physical electronic effect by changing the conductivity of the oxide. Jones[194] has shown that the conductivity of an n-type material can be increased by introducing into the oxide lattice an ion species in a higher valency state than the parent cation, for instance, introducing Ga^{3+} into zinc oxide increases its conductivity by promoting the formation Zn^{o}. Conversely introducing a lower valency ion such as Li^{+} into zinc oxide decreases conductivity. This effect was only observed when the ionic radii of the additive was similar to that of the parent cation. Table 11 illustrates the effect of different additives on the selectivity of a number of metal oxide semiconductors. Table 11 presents a summary of the numerous attempts to overcome the problem of selectivity, although with rather limited success. However, the processes involved are not well understood and to date the main advances have been made very much on an intuitive basis. The most popular additives studied have been platinum and palladium. It appears that increasing the concentration of palladium in tin oxide

Table 11

Effect of additives on selectivity

Basic material	Additive	Gas detected	Sensor type	Ref
Nickel oxide	3% Platinum	Hydrocarbons	Sintered bead	206
Tin oxide	15% w/w Bismuth oxide	Carbon monoxide	Sintered thick film	195
Tin oxide	5% Thorium oxide	Carbon monoxide	Sintered thick film	196
Tin oxide	4 molar ratio of Antimony and Platinum	Carbon monoxide	Sintered thick film	197
Tin oxide	0.2% w/w Palladium	Carbon monoxide	Sintered bead	198
Tin oxide	0.7% w/w Rubidium chloride	Carbon monoxide	Sintered thick film	199
Tin oxide	1.5% w/w Palladium	Methane	Sintered bead	198
Tin oxide	1.0% Palladium	Methane	Sintered bead	190
Tin oxide	Palladium and indium	Methane	Sintered bead	200
Tin oxide	1.5% w/w Palladium	Methane	Sintered thick film	195
Tin oxide	1.5% w/w Silver	Hydrogen	Sintered thick film	201
Tin oxide	Sulphur dioxide	Benzene/Hydrogen sulphide	Sintered pellet	202
Tin oxide	5-20% w/w	Propane	Sintered thick film	203
Uranium oxide	1% Palladium	Carbon monoxide	Sintered bead	206
Uranium oxide	0.5% Palladium/ 1% Cerium	Carbon monoxide	Sintered bead	204
Uranium oxide	0.5% Platinum	Methane	Sintered bead	204
Zinc oxide	3% Platinum	Hydrocarbons	Sintered bead	204
Zinc oxide	Vanadium/Molyb-denum/Alumina	Halogenated hydrocarbons	Sintered thick film	205

alters the selectivity of the material from carbon monoxide to methane. Due to the complexity of reactions that can occur on catalytically active materials, even with simple molecules, a thorough explanation of this enhanced selectivity has not been generally agreed. It has been noted that the influence of humidity plays an important role on the sensitivity to carbon monoxide.[179,207-209]

Studies using infra-red spectroscopy by Thornton and Harrison[210] show that water desorbs from polycrystalline discs of tin oxide in vacuum at 150 °C, whereas hydroxyl groups stick to the surface up to about 500 °C and it is these hydroxyl groups which play an important role in promoting the detection of carbon monoxide.

Considerable improvements in selectivity to carbon monoxide have been achieved by the use of additives which are claimed to operate by reducing surface moisture.[196] The dependence of the carbon monoxide response on water vapour has also been formulated by Clifford and Tuma.[211] They suggest that further investigations into the effect of water vapour on the response to other gases are necessary to gain an improved understanding of its role.

Apart from the correct type of additive it has been shown that further improvements in selectivity of metal oxide sensors can be achieved by choosing an appropriate operating temperature, normally in the temperature range 200-500 °C.[174,177,185,190] The processes of adsorption, reaction and desorption on the oxide depend on surface reactions, and Windischmann and Mark[185] have proposed a theoretical model which predicts that there should be a

temperature window at which the response to a particular gas is at a maximum. It has been found in practice that the change in conductivity produced by a reducing gas of a given concentration increases with the temperature of the oxide up to a maximum, thereafter decreasing with further temperature rise. Thus an optimum operating temperature exists for preferential response to different gases and this leads to improvements in selectivity.

The response of sensors which function by means of a surface reaction should be influenced by changes in surface microstructure. Thus increasing attention is being paid to studies on various methods of preparation of metal oxide sensors and evaluation of their electrical properties for gas detection. Windischmann and Mark[185] fabricated thin film tin oxide sensors by radio frequency sputtering deposition in a diode sputtering system at a pressure of 2 Pascals from a target of 99.99% pure tin oxide. A film thickness of 500 Å was deposited on to alumina substrates maintained at 300° C during deposition. When the films were operated at temperatures between 200-500 °C, they were shown to selectively detect 1-100 ppm carbon monoxide in a background gas comprising of 10% oxygen, 9% carbon dioxide, 3% water, 150 ppm sulphur dioxide, 150 ppm nitric oxide and balance nitrogen. The authors suggested two possible areas where the specificity of such thin films might be determined. First it is possible that an 'interfering' background gas constituent does not react with the chemisorbed oxygen and second even if such a reaction occurs, the reaction energy may not be

sufficient to transfer the electron from the product chemisorbed ion to the sensor conduction band.

In two separate publications, Oyabu[212,213] compared the response characteristics of thin and thick film palladium doped tin oxide sensors when exposed to carbon monoxide, hydrogen, isobutane and ethanol vapour. In both papers only limited experimental details are given regarding sensor preparation. Accordingly, the thin film sensors were fabricated by vacuum deposition on to a silicon oxide precoated ferrite substrate. The source material contained a powder mixed in the ratio of 99.8% tin oxide and 0.2% palladium by weight and the method produced a film thickness of 0.3-0.35 μm. Prior to characterization, the films were oxidised in air at 500-530 °C for 30-60 minutes. On exposure to the test gases these devices exhibited preferential detection of carbon monoxide and hydrogen. In the preparation of thick film sensors Oyabu[213] suggested that in order to obtain uniform gas sensitivity the tin oxide powder should be homogenous in particle size and quality. Preparation of the tin oxide resulted in a material with a particle size of approximately 0.5 μm in diameter. This powder was mixed with glass frit as a binder and 0.01% palladium. The mixture was formed into a paste for screen printing on to a silicon oxide precoated ferrite structure. Finally, sensors were heated to 830°C in air for 10 minutes. In contrast to the thin film sensors, these thick film devices exhibited selective detection of ethanol vapour and hydrogen. A highly reproducible procedure for preparing films from ultra fine

particles of tin oxide have been developed by Ogawa et al.[214] The ultra fine particles were grown by evaporation of the metal in low oxygen gas pressure. High purity tin was placed in the evaporator boat. The vacuum deposition chamber was pumped down to approximately 2 x 10^{-6} Torr and then oxygen was introduced into the chamber. A glow discharge in the oxygen was produced by applying a radio-frequency power input of 150W. Heating power was applied to the evaporator boat and after the growth rate of tin oxide particles in the glow discharge reached a stable condition the shutter was opened to deposit the particles on to a silica glass substrate. Finally, the deposit was heated at 250 °C in air for 30 minutes. The tin oxide ultra fine particle films fabricated using this procedure had a mean particle size of several tens of angstroms and showed either a columnar, porous columnar or spongy structure using an oxygen pressure of 0.05, 0.5 and 5 Torr respectively at the time of deposition. Films having porous columnar or spongy structures were found to display both high selectivity and sensitivity, for example, such sensors had high sensitivity to humidity when operated at 50 °C, to ethanol vapour between 200-300 °C and to isobutane between 350 °C and 400 °C. Therefore, selective detection of ethanol vapour or isobutane could be readily obtained by operating the sensors at the appropriate temperature. The high sensitivity was considered to originate from either, a large homogenous surface area or the porous surface structure enabling gas molecules to readily enter into the film and to be adsorbed on to the surface. One

report has studied the gas sensing characteristics of tin oxide whiskers.[186] Here whiskers were grown by oxidation of metallic tin at 1100°C in a mullite reactor tube. The source material placed in a mullite boat was pushed into the reactor tube with nitrogen flowing at 30 ml min^{-1}. A small amount of oxygen was allowed to migrate back into the reactor zone by removing the outlet from the reactor tube.

This procedure yielded ribbon like whiskers which were subsequently mounted on to alumina substrates. Using hydrogen, carbon monoxide and methane as test gases it was shown that individual whiskers exhibited different temperature dependencies in relation to gas sensitivity and selectivity. The authors concluded that although details of the differences in gas sensing characteristics from one whisker to another were not clear they did appear to be related to whisker size and surface reactivity. A study of the relationship between gas sensitivity and sintering temperature in the range 500-1000°C on palladium doped tin oxide polycrystalline gas sensors was carried out by Murakami et al.[215] Experimental details of sample preparation are outlined briefly as follows.

Sensors were formed by preparing stannic acid from a solution of stannic chloride by the addition of aqueous ammonia. The resulting stannic acid was then washed and dried, heated in air, and then a palladium catalyst in the form of palladium chloride added. After further heating and grinding the material was mixed with an equal proportion of alumina and water added to form a paste.

The paste was coated on to alumina substrates prior to sintering at different temperatures. When carbon monoxide, ethyl alcohol vapour, methane, isobutane and hydrogen were used as test gases it was found that increasing sintering temperatures resulted in enhanced sensitivity. The authors concluded that this affect resulted from the closeness of contact between grains sintered at high temperatures. It has also been claimed in a European Patent[216] that the surface area of a sensor material is important for selectivity. High surface area devices have the effect of discriminating against gases such as carbon monoxide, ethyl alcohol and benzene in favour of stable gases such as methane. Finally, the most extreme example of altering the physical oxide form has been afforded by Jones[217] who compared the behaviour of polycrystalline and single crystal zinc oxide sensors. Polycrystalline sensors were obtained by decomposition of zinc salts from a solution of zinc oxide in ammonium nitrate according to the British Patent in the name of Bott.[218] Single crystal sensors were grown from a melt in potassium hydroxide at 400 °C following the method described by Kashyap.[219] Using methane, carbon monoxide and water vapour as test gases it was shown that methane and water vapour had greater affects on the conductivity of polycrystalline zinc oxide, with the single crystal sensors being almost entirely selective towards carbon monoxide. The lack of selectivity of the polycrystalline sensors was attributed to the presence of a higher concentration of physical imperfections such as

dislocations, crystal edges and crystal corners which it was suggested may well form sites for methane to react.

The essential gas sensing characteristics of metal oxide gas sensors can thus be summarised as follows:

The detection characteristics show dependency upon sample preparation, composition and additives. Gases detected simultaneously show enhancement phenomena, with the effect of water vapour on carbon monoxide being well documented. The adsorption of a reducing gas will be temperature dependent and different gases will absorb at different temperatures. Generally it is found that the response to a reducing gas follows a power law relationship.

The aim of this project is to investigate the performance of metal oxide sensors to enable a thorough study of gas sensing properties to be carried out. A range of commercially available tin oxide gas sensors were chosen for the study, for example, the Taguchi Gas Sensor (TGS), to determine their potential as devices for the detection of spontaneous combustion and open fires or the monitoring of methane underground. The behaviour of this type of sensor is considered to be characteristic of state-of-the-art semiconductor gas sensors and they are readily available with a reliable production source. This study forms the remaining part of this work.

1.10.3 Taguchi Gas Sensors (TGS)

Taguchi Gas Sensors were developed in Japan by Naoyashi Taguchi of Figaro Engineering Inc.[220] and were first marketed in the United Kingdom in 1969. Subsequently the range of sensors has been increased and details of sensors

currently available are given in Table 12. Very little can be found from the literature about the precise method of individual sensor preparation, processes and composition although Ihokura of Figaro has given a brief description of the procedure.[198]

A schematic diagram of the general method outlined by Ihokura is given in Figure 5. Figaro hold many patents in the name of N. Taguchi covering inventions relating to their sensors. It was considered that a review of six patents held in the United Kingdom[221-226] may give a clearer understanding of oxide preparation and how differences in gas sensing characteristics are obtained. Of these six patents the first application was filed in January 1970 and published in December 1971. The remaining patents were all filed later in 1970 and subsequently published throughout 1972. Many of the specific claims made appear to be repeated not only within a given patent but also between different patents. In the first patent the invention relates to a gas detecting element including a semiconductor material which changes its electrical conductivity when a gas is absorbed, and a method of manufacturing the same. Three of the patents[221,223,225] describe methods aimed at improving sensitivity and mechanical strength of the sensors. In general, the mechanical strength of a sensor is required to be as high as possible and therefore the semiconductor material is normally sintered at high temperatures. However, since the mechanical strength obtained by this action is related to a reduction in the adsorption area due to partial fusion

Table 12

Taguchi Semiconductor Gas Sensors

Sensor type	Application and features
T.G.S. 109	Combustible gases such as propane, butane and methane. Large output signal to drive a buzzer directly.
T.G.S. 109M	City gas; suited for Japanese regulations.
T.G.S. 711	Carbon monoxide.
T.G.S. 712D	Carbon monoxide with low sensitivity to hydrogen.
T.G.S. 812	Organic solvent vapours, for example, alcohol, benzene. Toxic gases like carbon monoxide, ammonia, sulphur dioxide.
T.G.S. 813	General combustible gases like propane, butane, methane.
T.G.S. 813C	General combustible gases. Prepared for making a domestic gas detector.
T.G.S. 814D	Ammonia gas.
T.G.S. 816	T.G.S. 813 suited for high temperature circumstances with ceramic body.
T.G.S. 911	T.G.S. 813 suited for corrosive atmospheres with noble metal heated.
C.M.S. 102D	Control of monitor of combustion.

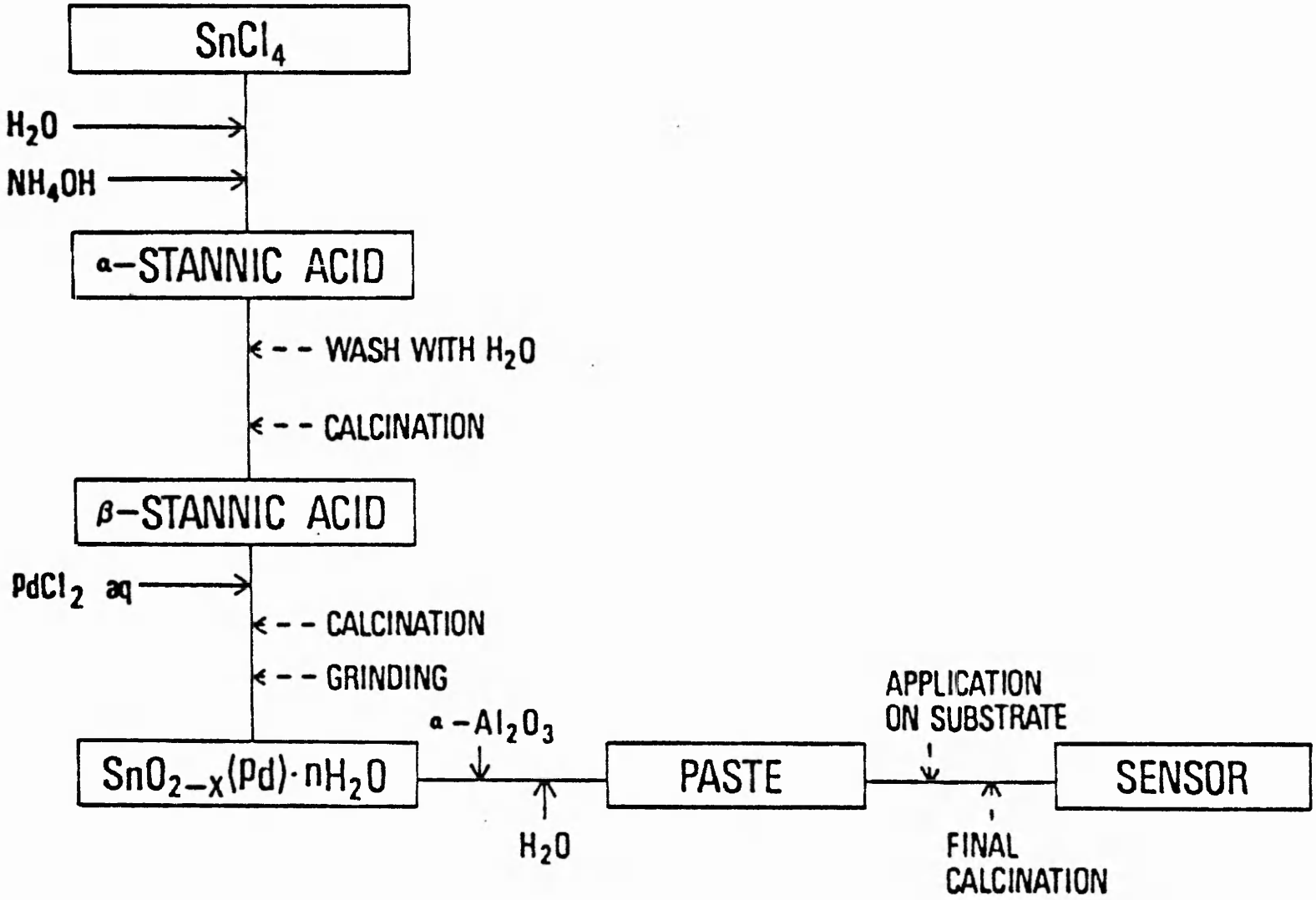

Figure 5 Block diagram for the preparation of Tin-oxide Gas Sensor

from sintering, the higher the mechanical strength the lower the sensitivity. To overcome this problem, one patent[223] suggests incorporating a substance such as silicate hydrosol which yields silica gel on heating to 600 °C. It is claimed that this treatment produces a sensor with high gas permeability and serves to improve its mechanical strength. Additionally, finely powdered alumina or quartz is added to help prevent crack formation of the main semiconducting material. Other methods of increasing gas sensitivity are also given.[225] One technique involves incorporating particles of quartz which are coarser than the oxide powder, to improve the effective surface area of the material. Sensors are then formed by press-shaping the material at a temperature where the mixture is neither fused or sintered to form a porous and gas-permeable block. In the same patent an alternative method of increasing gas sensitivity is given. Here, either flour, crushed rice, dog tooth violet starch, stearic acid, wax, sugar, polyvinyl alcohol or acrylic resin is mixed with the oxide. The material is then heated to a temperature that is sufficient to evaporate the organic additive and produce a number of pores in the oxide without producing sintering or fusing. To reinforce the mechanical strength of a sensor, one patent[221] proposes a procedure whereby a porous material such as asbestos, glass fibres or cement is mixed with an equal volume of aluminium hydroxide and formed into a paste with water. This is applied to the oxide surface of a sensor which is then heated to a temperature that converts the aluminium

hydroxide into aluminium oxide to harden the coating. Methods of applying the oxide material to various forms of support are described in a number of patents.[221,223,225] One of these patents[225] describes three different procedures. The first consists of a cylindrical metal case into which the oxide material is pressed. Gas permeable covers are placed at each end to give increased mechanical strength. The second configuration involves an insulating base on to which an oxide layer is formed on one surface by depositing of a slurry in the form of a spray or paste. Finally, the oxide powder is simply compressed into an open ended metal case.[221,224,225] In the remaining patents different methods of applying the oxide are described and repeated. Here, either the oxide material is pasted in the form of a slurry on to a small rectangular ceramic substrate and heated to 600 °C in air to form a spherical bead, or a drop of the slurry is deposited between two fine gold electrodes, followed by heating to 600 °C. The later method is claimed to produce a sensor less than 1 mm diameter. Two patents[221,223] describe methods of improving the sensitivity of a sensor to a particular gas. They suggest that the addition of 0.3% (w/w) palladium or 0.1% (w/w) gold gives an enhanced response towards butane compared with pure tin oxide.

Methods of improving performance characteristics of sensors are also described in two patents.[222,226] A period of time is required for a sensor to become stable at its pre-set operating temperature (usually between 170-230 °C) and an impedance circuit is proposed[222] which can be matched to

an alarm circuit, when one is used, and for which it may be substituted until the sensor has become stable. In order to overcome the effect of atmospheric temperature fluctuations on the stability of sensors an improved method of temperature compensation is suggested.[226] Although the six patents studied make numerous claims, many of which are repeated, they do not help to give a clearer understanding of oxide preparation or discuss in any detail the effect of additives on gas sensing characteristics.

1.10.3.1 Studies and applications of the TGS

Although the response data provided by the manufacturer in their general catalogue gives an indication of the sensitivity of a particular sensor to a number of gases, it is insufficient to provide a clear understanding of the gas sensing characteristics of each type of sensor. A general overview of the operation and applications of the TGS have been reported by Watson,[208,227,228] Department of Electrical and Electronic Engineering, University of Swansea. In an early paper published in 1974 the author clearly recognised the sensors potential as an inexpensive, sensitive sensor for gas concentration measurement. The characteristics and basic circuit design concepts for sensor operation were outlined. In a later paper, the performance of different sensors in particular the TGS 711, 812 and 813, were studied in respect of their sensitivity and selectivity to carbon monoxide and

methane. The problems associated by the sensors response to changes in ambient temperature and humidity were also presented. In conclusion the author suggested that a gas concentration monitor based on this range of sensors was feasible provided it is recognised that no sensor is highly selective. In the last of these papers the author discusses how such devices could be incorporated into a variety of electronic circuitry to produce systems for alarm devices, battery powered units, and gas concentration monitors. A qualitative study of the effect of carbon monoxide, water vapour and sensor temperature on the conductivity of a single TGS by Boyle,[207] showed that the TGS was more effective as a carbon monoxide sensor when the ambient relative humidity was greater than 25% because the response to carbon monoxide was almost independent of water vapour concentration above 25% relative humidity. Perhaps the most novel application of this type of device has been in the analysis of discrimination mechanisms on the mammalian olfactory system using a model nose.[229] Here the different responses obtained from the TGS 711, 812 and 813 to individual substances were studied. The sensors were arranged so that the ratio of their outputs could be derived. The ratio signal was passed to a window comparator and associated memory circuits which activated a designated light emitting diode. It was suggested that a system based on this principle could be of interest as a quality control device in

industries concerned with flavours, perfumes and smells. A study of particular interest to this work was undertaken by the Gillette Research Institute under contract to United States Bureau of Mines.[230] Their remit was to study the response characteristics of the TGS 109 sensor when exposed to a number of important mine fuels under pyrolytic, flaming and smouldering conditions. The materials chosen included, polyvinyl-chloride, polyurethane, polystyrene, polyethylene, wood, cardboard and isopropanol, but strangely enough not coal. The authors found that the sensor exhibited a good response to all the materials under pyrolytic and smouldering conditions. A resistance to irreversible poisoning from hydrogen chloride, a major product from polyvinylchloride, was also noted. In addition the sensor was shown to be insensitive to two major important mine contaminants, namely water mists and rock dust clouds. The authors recommended the need for additional studies on other TGS sensors in order to compare overall detector performances. All the investigations reported to date have been based on a non-theoretical foundation. However, Clifford and Tuma undertook a comprehensive experimental and theoretical study of the steady state gas sensing characteristics of the TGS 812.[211] The proposed theoretical model supplies the framework for comparisons of sensor performance and gas sensitivities. In addition it provides for the sensors intrinsic power law response and places emphasis on

multiple gas interactions. The authors measured the resistance responses of ten TGS 812 sensors when exposed to combinations of oxygen, nitrogen, methane, water vapour, carbon monoxide and hydrogen at different concentrations. Initially the sensors were exposed to a wide range of oxygen concentrations up to a maximum of 10%. When log-log plots of the sensor resistances against oxygen concentrations were made it was shown that at high concentrations the responses conformed to a power law relationship as follows:

$$R = R_0 P_{O_2} \quad \text{.....1.7}$$

where R_0 is the sensor resistance in air P_{O_2} is the relative oxygen partial pressure (P_{O_2} takes the value one for air and five for pure oxygen) and β is the power law exponent which was shown to vary from 0.25-0.55.

In the presence of methane concentrations up to a maximum of 1%, in dry air, the significant features of the sensors responses were an asymptotic approach to constant resistance at low concentrations and an asymptotic approach to a power law relationship at high concentrations. The essential forms of the response curve were expressed as follows:

$$R = R_0 \quad (1 + K_{CH_4} \quad [CH_4]^{-\beta} \quad \text{.....1.8}$$

where $[CH_4]$ is the concentration of methane expressed in parts per million (ppm) and K_{CH_4} is a constant of dimension, (ppm^{-1}). The mean values of R_0, K_{CH_4} and β

were determined to be 27.4KΩ 4.37 x 10^{-3} ppm^{-1} and 0.34 respectively. Since the power law exponent was of the same magnitude for methane as it was for oxygen, but of the opposite sign, the authors termed the methane response as first order with respect to oxygen. Zero order response was defined by a constant sensor resistance response independent of methane concentrations for instance, at lower concentrations. Therefore the threshold of detection was defined by the methane concentration at which the response changed from zero order to first order. This occurs when $[CH_4] = K^1\ CH_4$. It is this transition which identifies the parameter K_{CH_4}, as the sensitivity coefficient for methane. This definition allows comparisons of sensor performance and largely determines the devices usefulness as a gas sensor. When the response of the sensors to methane in pure oxygen were measured the difference in resistance was attributed solely to the term in oxygen pressure, P_{O_2} as follows:

$$R = R_0 P_{O_2}^{\beta} \quad (1 + K_{CH_4} [CH_4]^{-\beta} \quad \text{.....1.9}$$

The form of this equation suggests that the sensor resistance at high methane concentrations is determined by the ratio of oxygen to methane concentrations:

$$R^{1/\beta} \sim [O_2] / [CH_4] \quad \text{.....1.10}$$

It is this suggestion of a mass action law that the authors justified, referring to the methane response as 'first order with respect to oxygen'. Similar

expressions were used to describe the response of the sensors to water vapour. In the presence of carbon monoxide at concentrations below 3000 ppm the response was also shown to be first order with respect to oxygen but the sensitivity coefficient was shown to be dependent upon the water content of the ambient air. A single expression was found to describe the response:

$$R = R_0 P_{O_2} \quad (1 + K_{CO} \ [H_2O][CO])^{-\beta} \quad \ldots\ldots\ldots 1.11$$

In later experiments it was shown that the sensor resistance response to some gases, particularly hydrogen and carbon monoxide at concentrations greater than 3000 ppm, were characterised by a calibration graph with a power law slope which was twice that of the response to methane. The equation for this response was found to be similar to that for methane:

$$R = R_0 P_{O_2}^{\beta} \ (K_0 + K_{H_2} \ [H_2]^2)^{-\beta} \quad \ldots\ldots\ldots\ldots 1.12$$

The term K_0 was included to account for small differences in the impurity contents of the gas mixtures used. For high concentrations of hydrogen, this expression reduces to:

$$R^{1/\beta} = [O_2] \ / \ [H_2]^2 \quad \ldots\ldots\ldots\ldots\ldots\ldots 1.13$$

From this equation the resistance response is first order in oxygen pressure and second order in hydrogen pressure. The influence of the simultaneous presence of various gases on the detection properties was also

investigated and was found to conform to the following formulation:

$$R = R_0 P_{O_2}^{\beta} (1 + K_{CH_4}[CH_4] + K_{H_2O}[H_2O] + K_{CO}[H_2O][CO] + K_{H_2}[H_2]^2)^{\beta} \quad \ldots\ldots\ldots\ldots 1.14$$

This response illustrates the possibilities for complex gas interactions. Since the resistance response depends on the sum of individual reaction terms, the effect of one gas can be masked by the effects of others.

In conclusion the authors noted that some idiosyncratic behaviour in the response of these sensors have caused many researchers to consider metal oxide devices as non-reproducible sensors. However the above work indicates the long term stability of gas response irrespective of the sensors history, which suggests great metallurgical and chemical stability of the sensing material.

1.11 Introduction to and Aims of the Project

It is expected that coal will continue to be mined for many years and will remain an important and reliable form of energy, making a major contribution to future energy demands.

By its very nature, coal mining has always been recognised as a hazardous occupation and, notwithstanding technological advances in mining systems and fire detection, the dangers to life and financial consequences resulting from spontaneous combustion and underground fires remain at a disturbingly high level which cannot be over emphasised. The

presence of methane, a recognised adversary of the miner, requires particular attention to prevent dangerous accumulations forming which could result in an explosion from a source of ignition. Therefore, the early and reliable detection of these situations is of paramount importance if safer and more effective working conditions are to be achieved in the future. At present, systems based on the accurate monitoring of carbon monoxide concentrations and the carbon monoxide/oxygen deficiency ratio are primarily used to determine the presence and status of spontaneous combustion and underground fires. Instruments based on pellistor sensors are used in the general body of air underground for the detection of methane concentrations below five per cent. In situations where higher concentrations exist (methane drainage), instruments based on thermal conductivity detectors are operated.

The last major investigation into gases evolved during the low temperature heating of coal was undertaken by Chamberlain et al in 1970[100] (Section 1.5.3.1) and from Tables 3 and 4 it can be seen that the products identified were restricted to permanent gases and simple hydrocarbons. From this work the authors concluded that carbon monoxide was superior to any other detectable gas for predicting the onset of spontaneous combustion. It has been shown that investigations into the identification of products evolved from incidents of spontaneous combustion occurring underground, except for carbon monoxide, have been even less well studied (Section 1.5.3.2). This has probably resulted from difficulties encountered with sample collection and the

stability of the components during transport from underground to the laboratory.

In recent years significant advances have been made in gas sampling techniques, particularly in respect of sample enrichment and these are considered for application to an underground sampling - surface analysis regime.

i. Cryogenic trapping from a gas stream using liquid nitrogen, oxygen or dry ice followed by flash heating of the collected material. Although used successfully by other workers[231-236] it was considered that liquid oxygen was too hazardous for routine use and if liquid nitrogen was used then oxygen and water may condense in the trap and lead to problems. Also the use of coolants underground was regarded as not practicable.

ii. Adsorption on activated charcoal followed by solvent extraction and subsequent analysis. Although this sampling method is convenient and well documented,[237,238] it does suffer from a number of disadvantages, such as incomplete recovery with certain classes of compounds, a lack of sensitivity due to dilution of the sample with excess solvent, interferences from the solvent and its impurities during analysis, toxic flammable solvents are normally involved, and finally the sampling tubes cannot be re-used.

iii. The method chosen for this work evolved from gas adsorption on chromatographic support coated packing and involves collecting a known sample volume on to a suitable adsorbent packed in a glass or metal tube

followed by direct thermal desorption into either a gas chromatograph or gas chromatograph linked mass spectrometer for analysis.[240-246] This technique has the advantages of high sensitivity and the absence of a solvent, furthermore the sampling tubes are ready for re-use after analysis. The type of adsorbent used in the sampling tube is dependent upon the nature of the substances to be sampled. Ideally a sampling tube should meet the following requirements:

a) allow sufficient volume of air to be sampled without the loss of compounds of interest;
b) allow desorption of the vapour in a volume small enough to give a good chromatographic analysis;
c) give complete sample recovery without degradation;
d) have a high loading capacity to cope with maximum vapour concentrations likely to be sampled;
e) be unaffected by atmospheric moisture;
f) retain the sample during storage without loss or degradation;

Materials generally employed for sample collection by adsorption include the Chromosorb Century series, Porapaks , Tenax T.A. and Ambersorb XE340.

Where applicable, the method of sample enrichment has been developed in this work for the collection of the following classes of compounds. Subsequent analysis has been performed using several chromatographic techniques.

i. Initially, studies were carried out to determine the production of hydrocarbon gases since their existence

in the mining environment is well known.

ii. It was considered that sulphur containing compounds, because of their odorous nature, might be important components of gob stink, used traditionally as the subjective detector of spontaneous combustion.

iii. Aldehydes and ketones were a further class of compounds studied, because recent work on the thermal and oxidation chemistry of coal concluded that when a test coal was oxidised at 100°C, a wide variety of carbonyl containing species formed on the coal surface.(247)

iv. Other products studied during the course of this work included, hydrogen, hydrogen chloride and oxides of nitrogen.

v. A comprehensive study of evolved products was also undertaken using gas chromatography linked mass spectrometry.

vi. Additionally the evolution of simple gaseous products has been investigated using infra-red and paramagnetic monitoring equipment.

This part of the investigation has been based on the development of methods for the quantitative collection and analysis of a wide range of products and will enable a detailed examination of the products evolved from coal heated in the laboratory, and where appropriate, from underground sites during 'normal' and 'abnormal' conditions to be performed. From the laboratory studies, appearance temperatures and rates of production of combustion products evolved from heated coal can be ascertained. Results from

the underground studies will extend knowledge concerning the existence of combustion products in the mining environment and it will enable an assessment of their usefulness as indicators of spontaneous combustion. In conjunction with this work, a study of gases produced during shotfiring and from diesel locomotive exhausts has also been conducted.

The main purpose of this work has been to determine whether any gaseous product or class of products evolved from heated coal can be identified which is superior or complementary to carbon monoxide as an early and unambiguous indicator of spontaneous combustion.

In the second part of this project, three different types of TGS devices, the 711, 812 and 813 have been investigated to determine their basic operating characteristics and to explore their potential as alternative sensors for either the early detection of spontaneous combustion or the monitoring of methane concentrations. The types 711 and 812 have been considered primarily for the former application and type 813 for the latter.

1. Initially, basic sensor characteristics were determined as follows:

   a) At the moment, unfortunately the additives incorporated into different sensors, and the role they place in differing gas sensing characteristics (Section 1.10.3) are not known. An attempt to obtain information concerning the chemical composition of each type of sensor has been undertaken.

   b) The effect of sensor temperature on gas

selectivity and sensitivity characteristics has been described earlier (Section 1.10.2). Therefore, an assessment of the operating temperature range of each type of sensor has been undertaken to determine whether this plays any role in gas sensing characteristics.

c) To determine whether nitrogen plays any part in the sensors behaviour, the effect of argon as the inert constituent in air has been investigated. Additionally the effect of varying the oxygen concentration, using oxygen/nitrogen mixtures, on the response characteristics of each sensor has been performed.

2. The potential of each sensor for the detection of products evolved from heated coal has been evaluated as follows:

a) Any system based on the detection of combustion products released from the decomposition of heated coal must have a rapid response and high selectivity to one or more of the evolved products and must not be poisoned by other compounds present. The magnitude of response of each TGS sensor to the products evolved from heated coal has been examined in detail with respect to device sensitivity at different sensor operating temperatures.

b) The overall response of a particular sensor to the evolved products has been determined from its respective sensitivity to individual components.

To identify the products responsible, the effect of exposure to individual products, identified earlier in this work, on the response of each sensor has been carefully examined under controlled operating conditions.

Therefore, from this study and information established earlier in this work, it should be possible to explain the main features of response for each sensor to the products evolved from heated coal.

3. A further study has been conducted to examine the potential of the TGS 813 for the monitoring of methane.

a) The formation and presence of methane in underground coal mines was discussed in Section 1.7 with the lower hydrocarbons, (ethane, propane, butanes and pentanes) present as minor constituents totalling approximately five per cent of the methane, as firedamp. From this knowledge and that gained in this work concerning the gaseous constituents present in the mining environment, a study of the potential of the TGS 813 as a methane detector has been conducted. The response to individual gases and mixed synthetic mine atmospheres has been carefully investigated to determine the synergistic effects on the total response of the sensor.

To summarise, the complete project forms a comprehensive study of the low temperature combustion products evolved from heated coal and reveals potential techniques for monitoring their presence in coal mine atmospheres. Additionally, a possible alternative sensor to the pellistor bead has been examined in detail and its suitability for the detection of methane assessed.

CHAPTER 2

DEVELOPMENT OF METHODS FOR THE SAMPLING AND ANALYSIS OF PRODUCTS EVOLVED FROM HEATED COAL

This part of the experimental work was conducted in the manner described, the range of gases of interest specified and suitable chromatographic system developed. Only when this had been established could a suitable sampling system be developed and evaluated. Where appropriate the experimental work followed this pattern.

2.1 Experimental

2.1.1 Chromatographic Analysis of Low Molecular Weight Hydrocarbons

a) Apparatus

The gas chromatographic system consisted of an Intersmat Instruments , series 120 gas chromatograph with single channel flame ionisation detector (F.I.D). For direct gaseous injections a Pye Unicam six-way injection valve, 2ml sample loop and 6mm injector inlet were fitted to the chromatographic oven. Output from the detector was linked to a Perkin Elmer series 100 computing integrator for retention times and peak area measurements. Molecular sieve 5A and activated charcoal purification traps (Phase Separation Ltd.) were fitted to the gas lines to remove residual moisture and organic contaminants from the hydrogen and air (British Oxygen Company B.O.C)* which

Note:

* All pure gases and mixtures were obtained from British Oxygen Company.

supplied the F.I.D. flame at 25 and 400ml min^{-1} respectively, and from the oxygen free nitrogen carrier gas supply.

b) Chromatographic Columns

Three chromatographic packings were chosen from a literature survey[248-252] as possible materials for the separation of low molecular weight saturated and unsaturated hydrocarbons using gas solid chromatography and are shown in conjunction with their recommended operating conditions in Table 13. Two of the packing materials, Porapak Q and alumina F-1, were obtained commercially (Phase Separation Ltd). The alkali halide modified alumina (blocked alumina) was prepared according to Scott as follows: 10g of 80/100 BS mesh alumina F-1 was placed in a muffle furnace at 300°C overnight and then allowed to cool in a dessicator.

A fresh solution of 40% weight/volume (w/v) sodium iodide was prepared in distilled water, mixed with the alumina to form a slurry and allowed to stand for 48 hours with occasional stirring. The resultant sediment was filtered under suction and finally heated in a muffle furnace at 300°C. Three columns were prepared from chromatographic grade stainless steel tubing (Phase Separation Ltd.) cut to the appropriate length and a 10cm long x 6mm o.d. injector adaptor brazed on to each column to fit a Pye chromatographic inlet connector. Before packing, each length of tubing was coiled to fit into the chromatographic oven. The columns were packed under suction with the material held in place with silanised

glass wool plugs.

c) Evaluation Procedure

Each column was connected into the chromatographic oven, checked for leaks (Galutec leak detection spray) and conditioned overnight at 200 °C with oxygen free nitrogen flowing at 20ml min^{-1} . Carrier gas flow rates were measured at the column outlet via a soap bubble flowmeter against a stopwatch. For column evaluation a certified standard gas mixture containing C_1-C_4 hydrocarbons in air at high pressure in a steel cylinder was obtained from B.O.C. Special Gases.

The cylinder was connected to a two stage regulator (B.O.C., 0-276/0-2 bar) and the low pressure outlet linked to the Pye injection valve. Samples, at atmospheric pressure, were injected on to the chromatographic column after the 2ml sample loop and associated pipework had been continuously flushed with the standard mixture.

Evaluation of the Porapak Q and untreated alumina F-1 columns was initially undertaken using the manufacturers recommended operating conditions (shown in Table 13). The effect of varying the mean carrier gas velocity at different column temperatures on column efficiency was also studied using the alumina F-1 column, to obtain the Van-Deemter plot.[254] Separation of the standard gas mixture on the NaI blocked alumina column was examined at temperatures of 50°, 60° and 70 °C over a range of mean carrier gas velocities to determine optimum column

efficiencies. Further studies were also performed on the blocked alumina column to identify its useful operating range with a standard gas mixture containing C_2-C_7 hydrocarbons.

2.1.2 Adsorbents for Sampling Low Molecular Weight Hydrocarbons with Subsequent Thermal Desorption

a) Sampling Tube Preparation

The sampling tubes were constructed of pyrex glass tubing (Fisons Ltd.) 10cm long, 6mm o.d. 4mm i.d. containing the following adsorbents:

300 ± 10 mg. of Porapak Q, 30-60 B.S mesh (Phase Separation Ltd.)

350 ± 10 mg. of charcoal type 208C, 30-60 mesh (Sutcliffe and Speakman Ltd.)

300 ± 10 mg. of charcoal type NIOSH, 20-40 mesh (Standard NIOSH tubes containing 150 mg of coconut charcoal, from S.K.C. Ltd.)

Equipment free of organic vapours and residues was found to be crucial to avoid false analytical results. The following procedure was adopted to prepare a batch of sampling tubes:

A piece of pyrex glass tubing was cut into appropriate lengths and the ends polished in a "red hot" gas flame. Batches of up to 20 tubes were soaked in a 5% solution of Decon 90 in distilled water for 24 hours to remove grease.

The tubes were removed from the solution using clean PVC

gloves and rinsed four times with distilled water. The tubes were then placed in a clean dry beaker and allowed to air dry with a perspex lid cover to keep out dust.

Glass wool (Phase Separation Ltd.) used to hold the adsorbent in place in the tubes was Soxhlet extracted with acetone for 2 hours. After extraction the glass wool was dried in a vacuum oven for 1 hour at 110°C and transferred using tweezers into a ground glass stoppered bottle.

Gross contamination of the charcoal type 208C and Porapak Q adsorbents was removed by heating overnight at 250°C and 200°C respectively in a stream of purified oxygen free nitrogen flowing at 50ml min^{-1}. A number of NIOSH tubes were broken open and the charcoal emptied out to give sufficient packing material to fill the sampling tubes. A plug of glass wool was first inserted 1cm into one end of an empty pyrex glass tube using tweezers and the appropriate adsorbent added to a bed length of 6cm using a glass funnel. A second plug of glass wool was then inserted into the opposite end of the tube. Two short lengths of tempered steel previously cleaned in a hot flame were fixed into each end of the tube to hold the adsorbent in place. It was anticipated that during sampling underground fine coal dust could be drawn on to the glass wool plug on the tube inlet and may lead to erroneous results during analysis. To overcome this problem a second glass wool plug was inserted into the tube which could be removed

prior to analysis. Prior to sampling each tube was again heated overnight at either 200°C or 250°C in a stream of oxygen free purified nitrogen at 50ml min^{-1}.

The prepared tubes were stored separately in marked brass holders, (10.5cm long, 9.5mm o.d. 7mm i.d.) closed by air tight screw-on brass caps to prevent contamination, and to provide protection in transit. The holders were prepared from a solid brass rod cut into appropriate lengths. Each length was drilled-out to the required depth and the top threaded using an 1/8" B.S.P. die. Caps to fit the holders were fabricated from 3.2mm Wade coupling nuts by infilling the outlet hole with 60/40% lead tin solder. The holders and caps were degreased and cleaned using 5% Decon 90 solution as described earlier and finally heated to 150°C in an oven overnight.

b) Thermal Desorption System

The chromatographic system described in Section 2.1.1.a was modified to enable sampling tubes to be thermally desorbed directly on to the blocked alumina analytical column. A schematic diagram of the arrangement is shown in Figure 6. The normal carrier gas inlet union to the analytical column was adapted by fixing an additional carrier gas inlet connector into a 3mm hole drilled into the union. A sampling tube fitted into the system with two Pye 6mm 'O' compression couplings and 1.5mm o.d. stainless steel tube was used for all the interconnections. To help prevent cold spots developing between the sampling tube outlet and injector heater, the

transfer line was kept to a minimum length and wrapped in glass fibre insulation. The sequence of operations for sample desorption on to the analytical column were as follows:

The protective glass wool plug was removed from the sampling tube and discarded. With the Pye injection valve placed in the central position carrier gas flow was stopped and the sampling tube connected into the system so that flow through the tube was in the opposite direction to that during sampling, i.e. tube should be back flushed (See Section 2.1.2 c). Gas tight seals were made on to the tube by hand tightening the 0 ring compression couplings. The Pye injection valve was then placed into the inject position with the two way valve in position A for 60 seconds, thus allowing carrier gas to sweep residual air from the sampling tube. (Figure 6). Subsequently the two way valve was switched to position B, to isolate the sampling tube, whilst maintaining carrier gas flow to the chromatographic column. The sampling tube was then heated for a pre-determined time (heating period) by surrounding it with an axially bisected aluminium block, 7.5cm long and 4.5cm diameter. A 2kW variable temperature hot plate (Fisons Ltd.) maintained the block at the appropriate temperature prior to heating the sample tube.

The block temperature was easily and accurately measured using a 0-500°C thermometer fitted into a hole drilled into the block. After the required heating period the two way valve was switched to position A, carrier gas

redirected through the sampling tube and the desorbed sample flushed on to the chromatographic column for analysis. The heater block was left in place throughout the analysis.

The actual temperature of adsorbent within the sampling tube was determined at different heater block temperatures by inserting a Chrome/Alumel thermocouple (R.S. Components Radio Spares Ltd.) into the centre of the packing and monitoring the output on a Chessel series 3000 chart recorder. This procedure was repeated on five separate sampling tubes for each adsorbent.

c) Evaluation Procedure

The efficiency of each adsorbent for the collection and subsequent thermal desorption of low molecular weight hydrocarbons has been studied using the standard gas mixture containing C_2-C_7 hydrocarbons. The following parameters were investigated for sampling tube evaluation.

i. Optimum desorption temperature

ii. Safe sampling volume

iii. Standardisation

iv. Sampling storage

i. Optimum desorption temperature

The optimum desorption temperature of each type of adsorbent packed sampling tube was measured as follows.

The low pressure outlet from the two stage regulator (0-276/0-2 bar) fitted to the standard gas mixture cylinder was connected to a length of 6mm o.d high quality

stainless steel tubing using compression fittings (Wade couplings). A short piece of silicone tubing attached a freshly conditioned sampling tube to the stainless steel tubing. Care was taken to ensure that the end of the two tubes met inside the silicone tubing connector. In each experiment the end of the sampling tube containing the protective glass wool plug was connected to the stainless steel tube outlet. Sampling loading in this manner was adopted in the remaining part of this work. The sampling tube outlet was then connected to a fine needle valve controlled flowmeter (Platon gapmeter, GTV 10-250ml min^{-1}). A pressure of 0.2 bar was set at the gas cylinder regulator and the fine needle valve opened to allow a flow of 200ml min^{-1} through the sampling tube for 30 seconds. Flow was then discontinued and the sampling tube removed. The collected sample was immediately desorbed on to the chromatographic column following the sequence of operations described in Section 2.1.2 b). This procedure was performed in duplicate for each adsorbent. Tubes that could not be analysed immediately were stored in the brass holders closed by air-tight caps. Standardisation of the sample collection and desorption procedure has allowed the optimum desorption temperature of each adsorbent to be measured by studying the effect of different temperatures on sample recovery.

ii. Safe sampling volume

This is the volume of air containing particular contaminants that may be sampled over a range of

circumstances without significant breakthrough or loss of any component. The maximum sample volume that may be drawn through each sampling tube for quantitative collection of the components present in the standard mixture was determined under the most adverse conditions that might be expected to be encountered underground, namely 95% relative humidity at an ambient temperature of 35°C.

Since humidity varies significantly with changes in ambient temperatures (vapour pressure values of 12.788 and 42.175mm Hg are obtained at temperatures of 15°C and 35°C respectively) the experimental arrangement and gas flow was thermostatically controlled. The standard gas mixture containing C_2-C_7 hydrocarbons fitted with the two stage regulator was connected to a fine needle valve controlled flowmeter (Platon gapmeter, GTV 60-500ml min^{-1}) using high quality, clean 6mm o.d. stainless steel tubing. The outlet from the flowmeter passed through an 8mm hole drilled through the side of a Pye Unicam 104 chromatographic oven, maintained at 35± 1°C, and connected inside the oven to a two metre coil of stainless steel tubing. The coil was used to help equilibriate the gas to the oven temperature before passing through two Dreschel bottles (250ml capacity, size 1 frit) in series, each containing approximately 100ml of deionized water.

The final arrangement is shown in Figure 7. The standard procedure now used to determine the safe sampling volume of each adsorbent was as follows.

A pressure of 0.5 bar was set at the cylinder head and the fine needle valve opened to allow a flow of 500ml min^{-1} through the water bubblers and associated tubing. After completely flushing the system for 5 minutes the needle valve was adjusted to give a flow of 200ml min^{-1} and two sampling tubes, preheated to 35° C, connected in series with silicone rubber tubing to the bubbler outlet The second sampling tube served as an indicator that the collection tube had not suffered any losses. After a known volume had been collected both tubes were disconnected and desorbed separately as described earlier. A blank analysis of the 'back-up' sampling tube showed that the safe sampling volume of the collection tube had not been exceeded. The standard procedure for sample collection was repeated using larger sample volumes until the back-up tube gave a positive analysis. Duplicate determinations were made at each sample volume. At this stage in the investigation consideration was given to the type of pump that could be used underground with the sampling tubes. To overcome any problems associated with using electrically powered sampling pumps a Draeger hand bellows pump (Draegerwerk AG Lubeck) was examined for sample collection. One pump stroke gives a 100ml volume and with a sampling tube connected to the pump inlet a flow of 600ml min^{-1} was measured. High and low sampling flow rates are not recommended for adsorbent collection techniques.[256] This is because during sampling the tube acts as a small chromatographic column and in accordance

with the Van-Deemter equation will be less efficient under these conditions. Additionally at flowrates lower than 10ml min^{-1} passive sampling may become significant.[257] Therefore a crimped orifice was placed in the Draeger pump inlet to give a measured flow of approximately 200ml min^{-1} through the sampling tubes. Sampling loading has been carried out with the Draeger pump in the remaining part of the evaluation procedure.

A number of workers have observed that when sampling in the presence of a high concentration of a component of secondary interest overloading of the sampling tube adsorbent can occur resulting in non quantitative collection of the components of interest.[256,257] The effect of a high concentration of methane on sampling tube collection efficiency was studied as follows:

Chemically pure grade methane. 99.0% was added to the standard mixture in a five litre Tedlar gas sampling bag (S.K.C.Ltd). A sampling tube was connected with silicone rubber tubing to the Tedlar bag outlet and the Draeger pump inlet and a 100ml aliquot of the mixture (one pump stroke) drawn through the tube at 200ml min^{-1}. Care must be taken to allow at least five seconds at the end of the pump stroke for passage of the full volume. Desorption and analysis were performed in the normal manner.

iii. Standardisation

Calibration of the method and the reproducibility of sampling, desorption and analysis procedures were determined as follows:

A cylinder of purified compressed air and a certified gas mixture containing 1% (v/v) carbon monoxide in air were connected via lengths of clean high quality stainless steel tubing to a Signal series 850 gas blender at the recommended inlet pressure of 2 bar. The preset outlet flow of 600ml min^{-1} was fed to the experimental arrangement used in the preceding work. Confirmation of the blender calibration graph was achieved by varying the blender control setting in the range 1-19. At each dilution stage the concentration of carbon monoxide produced was determined to an accuracy of $\pm$ 1.0% using a pre-calibrated infra-red analyser (Analytical Development Co. Ltd). The certified gas mixture was then disconnected and the C_2-C_7 hydrocarbon standard mixture connected to the blender inlet. From the calibration graph, shown in Figure 8, known concentrations of the standard mixture could be generated. At each dilution stage the total flow was collected at the water bubbler outlet into a five litre Tedlar bag. Using a Draeger gas sampling pump duplicate 100ml samples were loaded on to separate sampling tubes at approximately 200ml min^{-1}. Desorption and analysis were performed in the normal manner.

To study the reproducibility of the method the blender controller was set to 1.0 (Figure 8) and the undiluted standard mixture produced was collected at the water bubbler outlet into a five litre Tedlar bag. With the Draeger hand pump 100ml samples were loaded on to ten sampling tubes chosen at random. Desorption and

analysis were performed as normal.

iv. Storage

Sample storage experiments were conducted to test the feasibility of collecting samples underground and returning them to the laboratory at a later date for analysis. 100ml samples of the undiluted standard mixture were collected on to ten sampling tubes. The tubes were then placed into brass holders and closed with the air tight screw-on caps. Five of the tubes were left on the laboratory bench at an ambient temperature of approximately 22°C and the remainder placed into a refrigerator. A sampling tube from each storage condition was desorbed and analysed after 8, 24, 36, 48 and 72 hours. Additionally, an unsampled tube contained in a brass holder was placed on the laboratory bench for 72 hours prior to desorption and analysis.

2.1.3 Chromatographic Analysis of Aromatic Hydrocarbons

a) Apparatus

The analytical system comprised a Pye Unicam Series 104 gas chromatograph and single channel flame ionisation detector with the signal output connected to a Perkin Elmer series 100 computing integrator. A Pye Unicam six way injection valve and 1.0ml sample loop were used for direct injection of gaseous samples. All gas lines were fitted with Molecular sieve 5A and activated charcoal purification traps. Hydrogen and air were used to feed the detector flame at 35 and 550ml min^{-1} respectively.

b) Chromatographic Columns

A mixture of aliphatic and aromatic hydrocarbons were expected as products of decomposition from heated coal, therefore, for ease of identification a column capable of completely separating the two classes of compounds was sought. Examination of the literature [248-250] showed a number of column materials with the selectivity to separate such a mixture. Two materials were chosen for evaluation and are shown with their appropriate operating conditions in Table 14. Each material was packed under suction into chromatographic grade stainless steel tubes and held in place with silanised glass wool plugs.

c) Evaluation Procedure

The Tenax GC and 1, 2 and 3 tris (2-cyanoethoxy) propane (TCEP) packed columns were connected into the chromatographic oven, checked for leaks and conditioned overnight at 175°C and 120°C respectively with oxygen free nitrogen at a flowrate of 20ml min^{-1}. Evaluation of each column was undertaken using a standard mixture of aliphatic and aromatic hydrocarbons in air contained in a high pressure steel cylinder (B.O.C Special Gases).

Separation of this mixture was examined on each column under isothermal conditions using 1.0ml direct injections. A further study was undertaken with the TCEP column to obtain the Van-Deemter plot by varying the mean carrier gas velocity at a column temperature of 80°C.

2.1.4 Adsorbents for sampling Aromatic Hydrocarbons with subsequent Thermal Desorption

A number of adsorbents including the Chromosorb[258] and Porapak Series[259] have been used for the collection and analysis of aromatic hydrocarbons. However, the most widely used material has been Tenax GC,[256,260,261] which is based on a polymer of 2,6 diphenyl-p-phenylene oxide. Its main advantages over other adsorbents are its high thermal stability, hence low bleed on thermal desorption, and its relative insensitivity to the effects of water vapour. Tenax GC was selected as the most suitable adsorbent for evaluation and has been examined in this study for the quantitative collection and analysis of aromatic hydrocarbons.

a) Sampling Tube Preparation and Desorption System

The sampling tubes were pyrex glass with identical dimensions to the charcoal tubes used previously. The same methods of tube cleaning, packing, handling and protection in transit have also been applied. Each tube was packed with 130 ± 10 mg. of 60-80 B.S mesh Tenax GC (Phase Separation Ltd.) that had previously been conditioned at 350° C overnight in a stream of purified nitrogen, flowing at 50ml min^{-1} . A thermal desorption system identical to that described in Section 2.1.2 b) and shown in Figure 6 was constructed and connected into the TCEP column inlet.

b) Evaluation Procedure

The efficiency of the Tenax GC sampling tubes for the collection, subsequent thermal desorption and analysis of

aromatic hydrocarbons has been examined using the standard gas mixture containing aliphatic and aromatic hydrocarbons, following the evaluation procedure adopted with the charcoal tubes.

2.1.5 Chromatographic Analysis of Low Molecular Weight Sulphur Compounds

a) Apparatus

A Pye Unicam Series 304 gas chromatograph with linearis flame photometric detector (FPD) and sulphur narrow band pass filter at 394 nm was used in this investigation. Direct injection of gaseous samples was made via a Pye polytetraflouroethylene, (PTFE) lined six way injection valve and 2.5ml PTFE sample loop. The detector output was initially connected to a LTTICAP5 integrator whi s later replaced by a Perkin Elmer series 100 c utin integrator. The carrier gas was oxygen free nit gen and hydrogen and air each at 30 ml min^{-1} were use for flame gases. All gases were purified by passing through activated charcoal and Molecular sieve 5A traps.

b) Chromatographic Columns

A number of column packing materials have been reported (248,262-264) for the chromatographic separation of low molecular weight sulphur compounds. Two materials were chosen for evaluation, Porapak QS and Tenax GC and are shown with their respective operating conditions in Table 15. These materials were obtained commercially (Phase Separation Ltd.) however, the Porapak QS, a porous polymer composed of ethylvinyl benzene cross linked with divinyl benzene, was used, as received, and following the method of

treatment described by de-Souza.[263] The treatment procedure was as follows:

4g of 80/100 B.S mesh Porapak QS was placed in a fine sintered glass funnel (B.D.H. pore size 40 microns) and washed under suction with jets of Aristar grade acetone for five minutes. The material was dried by continuously drawing air through the funnel until the polymer particles were loose and fine flowing.

A 45cm long, 3mm o.d. acetone washed and dried PTFE tube was then lightly packed with the treated Porapak QS using the vibration technique to an effective packed length of 30cm and held in place with silanised glass wool plugs. The untreated Porapak QS was packed into a PTFE column of the same dimensions in an identical manner. The Tenax GC was packed into a PTFE column under suction in the manner described earlier (2.1.1 b).

c) Evaluation Procedure

The packed columns were connected into the chromatographic oven, checked for leaks, and conditioned overnight, at 240°C for the Porapak QS and 100°C for the Tenax, with oxygen free nitrogen carrier gas flowing at 20ml min^{-1}. Swagelok PTFE couplings, nuts and ferrules were used for both column inlet and detector connections. Column evaluation was undertaken using four separate standard mixtures, each containing a nominal 20 ppm concentration of one of the following components.

Hydrogen sulphide in nitrogen

Carbonyl sulphide in nitrogen

Sulphur dioxide in air

Carbon disulphide in nitrogen

Additional concentrations were prepared into five litre Tedlar gas sampling bags by dilution with oxygen free nitrogen using a range of calibrated needle valve controlled flowmeters (Platon gapmeters GTV 10-250, 200-2000 and 600-500ml min^{-1}). The selectivity of each column to separate a mixture of the standard gases, the extent of losses on the system and linearity of response were investigated using direct injections of known concentrations of one or more of the sulphur gases. A further study was undertaken with the treated Porapak QS column to obtain the Van-Deemter plot by varying the mean carrier gas velocity at a column temperature of 40° C.

2.1.6 Adsorbents for Sampling Low Molecular Weight Sulphur Compounds with Subsequent Thermal Desorption

Several adsorbent based collection techniques have been investigated for sampling sulphur containing compounds. The literature indicated that the most promising materials were Molecular sieve 5A and Porapak Q.[265-267] Additionally, the treated Porapak QS, used for packing the analytical column, was further investigated as a collection material.

a) Sampling Tube Preparation and Desorption System

Identical pyrex glass sampling tubes cleaned as described earlier (Section 2.1.2 a) were additionally heated to 200° C for two hours in a flow of 25ml min^{-1} purified oxygen free nitrogen, as suggested by Bruner,[268] to increase their inertness towards sulphur compounds. After heat treatment the tubes were packed with the following

materials as described earlier, (Section 2.1.2 a).

620 ± 10 mg of Molecular sieve 5A, 60-80 B.S mesh (Phase Separation Ltd)

300 ± 10 mg of Porapak Q, 60-80 B.S mesh (Phase Separation Ltd)

300 ± 10 mg of Porapak QS, 60-80 B.S mesh (Phase Separation Ltd)

To remove contamination prior to packing, the Molecular sieve 5A and Porapak materials were heated overnight to 250°C in a stream of purified oxygen free nitrogen at 50ml min^{-1} . When not in use the sampling tubes were capped with 6mm Swagelok end caps fitted with PTFE ferrules (Phase Separation Ltd).

All tubes were conditioned prior to use by heating at 250° C for at least 12 hours with purified oxygen free nitrogen at 50ml min^{-1} . A thermal desorption system similar to that shown in Figure 6 was constructed and connected to the analytical column inlet. Modifications to the system were made by replacing the stainless steel tubing with 1.5mm o.d PTFE tubing, connections to the sampling tube being achieved by 6mm - 1.5mm reducing unions and PTFE ferrules.

b) Evaluation Procedure

The effectiveness of each adsorbent packed sampling tube has been evaluated for the quantitative collection, thermal desorption and analysis of low molecular weight sulphur compounds. Because of the high reactivity of sulphur compounds the experimental procedures used previously were modified to minimise component losses on equipment.

The optimum desorption conditions for each sampling tube were determined with hydrogen sulphide as the test compound. The standard mixture and purified oxygen free nitrogen were blended at a ratio of 1:20 using two fine needle valve controlled flowmeters (Platon GTV 5-100, 200-2000ml min^{-1}). PTFE 6.0mm tubing was used throughout the arrangement with silicone rubber connections.

The standard mixture regulator and associated pipework were flushed at 50ml min^{-1} for ten minutes prior to blending. A total flow of 500ml min^{-1} was then established (25ml min^{-1} hydrogen sulphide, 475 ml min^{-1} nitrogen) and the system left to stabilise for a further ten minutes. The resultant mixture was collected into a five litre Tedlar bag. Immediately after collection 100ml aliquots were drawn through each sampling tube with a Draeger gas sampling pump. Desorption and analysis were performed without delay.

The optimum temperature and heating period for quantitative desorption of hydrogen sulphide from each adsorbent were determined by studying the effect of a range of heater block temperatures and different heating periods on percentage sample recovery. The true bed temperature of each adsorbent at different heater block temperatures was determined as described in Section 2.1.2 b).

The water bubbler arrangement (Figure 7) used previously in the safe sampling volume experiments was considered unsuitable for the range of sulphur compounds being studied. Alternative methods of sample collection were

developed as follows:

The first method was similar to that described in the previous experiment and used two fine needle valve controlled flowmeters (GTV 5-100, 60-500ml min^{-1}) to give a blend ratio of 1:200 with the resultant mixture collected into a five litre Tedlar bag. Increasingly larger volumes of hydrogen sulphide in the range 100-1000ml were introduced on to two sampling tubes in series using the Draeger pump. The front and back-up tubes were desorbed immediately. This procedure was repeated with carbonyl sulphide, sulphur dioxide and carbon disulphide.

In the second method a mixture of hydrogen sulphide, carbonyl sulphide and sulphur dioxide was prepared into a five litre Tedlar bag. Initially a 100ml aliquot of the mixture was drawn through two sampling tubes in series using the Draeger pump, followed by the addition of an identical quantity of clean laboratory air. This procedure was repeated using increasingly larger volumes of clean laboratory air up to a maximum diluent volume of 900ml. Desorption of the front and back-up tubes was performed immediately. This procedure was repeated with carbon disulphide because of the different chromatographic conditions required for its analysis.

Studies were again undertaken to examine the effect of a high concentration of methane on the sampling tube collection efficiency. A mixture containing a nominal 0.1 ppm hydrogen sulphide, carbonyl sulphide and sulphur dioxide was prepared in nitrogen into a five litre Tedlar bag with methane added to give a concentration of

approximately 5%. Sampling tubes were loaded with one litre aliquots of the mixture using the Draeger pump and were desorbed immediately. Additionally experiments were performed to establish whether the presence of methane created any response on the flame photometric detector. The desorption system was dismantled and 2.5ml samples of a mixture containing 5% methane in nitrogen injected directly on to the analytical column.

The flowmeter arrangement was used again to generate known calibration mixtures. Each standard mixture and purified oxygen free nitrogen were blended at different ratios in the range 1:100 (Platon GTV 5-100, 200-2000ml min^{-1}). Further dilutions were prepared by directing part of the total flow from the flowmeters to a second dilution stage consisting of an identical flowmeter arrangement to give an overall dilution ratio in the range 1:10000. At each dilution stage the resultant mixture was collected into a five litre Tedlar bag. Sampling tubes were loaded with known volumes of the mixture using the Draeger hand pump and were desorbed immediately.

The reproducibility of the method and sample storage stability were examined with a mixture containing 0.1ppm hydrogen sulphide, carbonyl sulphide and sulphur dioxide prepared in nitrogen into Tedlar bags. A Draeger hand pump was used to load sampling tubes with one litre aliquots of the mixture. Ten tubes were desorbed and analysed immediately to determine reproducibility and the remainder stored under identical conditions and times to those described earlier for the charcoal tubes (Section 2.1.2 c).

Carbon disulphide was again studied separately.

2.1.7 Chromatographic Analysis of Aldehydes and Ketones as their 2,4 Dinitrophenylhydrazine Derivatives

a) Apparatus

High performance liquid chromatography (HPLC) was performed on a Waters Associates Model 6000 liquid chromatograph equipped with dual U.V detectors operated at 254 and 350 nm. A rheodyne injection valve was fitted to inject 10 microlitre samples on to a 25cm long, 4.6mm i.d. C_{18} bonded silica column operated at ambient temperature. Methanol/water, 65/35% was used as the eluent at a flowrate of 1.0ml min^{-1}. For quantitative work retention times and peak areas were measured using a Spectra Physics model 4100 computing integrator.

b) Preparation of Derivatives

2,4 Dinitrophenylhydrazine (2,4 DNPH) derivatives of formaldehyde, acetaldehyde, propionaldehyde, acrolein, crotonaldehyde and acetone (Aldrich Chemical Co. Ltd) were prepared as follows:

0.2g of 2,4 DNPH was placed in a clean boiling tube with 0.5ml of concentrated sulphuric acid, followed by the careful addition of 10ml of ethanol. After warming and formation of a clear solution, 0.5ml of the sample was added. The solution was boiled for two minutes, cooled, and the precipitate filtered. Each derivative was recrystallised from ethanol and its purity checked by melting point determination, shown in Table 16.

c) Evaluation Procedure

The HPLC operating conditions were similar to those used by Muller and co-workers[269] who determined the presence of formaldehyde and acetaldehyde in the thermal decomposition products of rosin. Evaluation of the chromatographic system for the separation and detection of the prepared derivatives was undertaken as follows:

A mixture containing each derivative was prepared in acetonitrile at the following concentrations:

2,4 DNPH derivative	Concentration (µg/10ml)
formaldehyde	125
acetaldehyde	210
propionaldehyde	140
acrolein	153
crotonaldehyde	110
acetone	170

Prior to studying this synthetic mixture, retention times of individual derivatives were determined for positive identification purposes. Calibration curves of detector response versus concentrations were determined over the range 2.5-800 µg/10ml acetonitrile using known quantities of each derivative obtained from their respective carbonyl compound.

Optimization of the chromatographic conditions was not undertaken due to lack of time resulting from instrument demand.

2.1.8 Adsorbents for Sampling Aldehydes and Ketones with subsequent Solvent Desorption

a) Sampling Tubes

The sampling tubes were based on those suggested by Muller,[269] who used silica gel impregnated with approximately 1% DNPH (w/w) as the collection medium. Details given in the experimental section of Muller's work covering sampling tube preparation are minimal, therefore, sampling tubes were prepared as follows:

Batches of up to twenty sampling tubes made from Pyrex glass 15cm long, 10mm o.d. were prepared and cleaned as described earlier with the charcoal tubes. To prevent interference during analysis it was found essential that all glassware should be scrupulously clean. The tube packing material was initially prepared by adding 2ml of 12M hydrochloric acid to 0.5g of 2,4 DNPH dissolved in 200ml of HPLC acetonitrile (BDH Ltd). The addition of 10ml of distilled water was found necessary to completely dissolve the 2,4 dinitrophenylhydrazine hydrochloride. After dissolution was complete, 50g of silica gel 30-70 B.S mesh (Fisons Ltd.) was added. The solvents were then removed using a rotary evaporator at 50° C and 15mm Hg (Gallenkamp Ltd). It was later found important to give the 2,4 dinitrophenylhydrazine hydrochloride adsorbed on silica gel a final washing with dichloromethane. The empty pyrex tubes were filled with 1.5g ± 10mg of the impregnated support and packed to a length of 5cm. The packing material was held in place with clean glass wool plugs, and the tube ends sealed by drawing out in a red

hot flame. The tube ends were broken open prior to sampling and on completion were sealed with 3mm plastic caps.

b) Sampling Tube Evaluation Procedure

Ultrasonic desorption of the impregnated support was performed in 10ml acetonitrile for ten minutes as suggested by Muller.[269] Using this procedure an unsampled tube was desorbed into acetonitrile and a 10 µl aliquot injected on to the HPLC column. The resulting chromatogram indicated the extent of interferences present on the support material. Once a blank analysis had been established the desorption efficiency of each derivative except formaldehyde, was established. For acetaldehyde, which was assumed to be gaseous at 25°C, known volumes were injected into a twin necked glass flask having a sampling tube connected at the outlet. The vessel was then swept with purified compressed air passing through the sampling tube at a flowrate of 600ml min^{-1} for ten minutes. The remaining carbonyl compounds were introduced separately on to the impregnated support by direct liquid injection followed by addition of the same volume of air as above. Triplicate runs were performed on each compound to give an assessment of the reproducibility of desorption. It was noted that during sample collection the colour of the coated silica gel changed from yellow to orange over the first few centimetres of the packing material. Each sampling tube was immediately desorbed and analysed and the desorption efficiency of each compound determined by comparison with standard calibration graphs

prepared earlier for the respective DNPH derivative.

To determine the safe sampling volume of the impregnated support a number of tubes were prepared with the material divided 1.0:0.5g, separated by a glass wool plug. A known quantity of carbonyl compound was loaded directly on to the major portion of the support. The sampling tube was then connected to a clean air supply and a known volume passed through the major and minor portion in turn at a flowrate of 600 ml min^{-1}. This procedure was repeated using different volumes of air up to a maximum of 30 litres. Each portion was desorbed and analysed separately with a negative result from the back-up portion confirming breakthrough had not occurred. The sampling tube collection efficiency for each carbonyl compound was determined in this manner.

Because of the limited time available for HPLC analysis sample storage stability experiments were only performed for acetaldehyde and acetone. Known quantities of each compound and clean air were loaded on to separate sampling tubes as described in the desorption efficiency experiments. Immediately after sampling, the tubes were sealed with plastic caps and stored either on the laboratory bench or in a refrigerator. Desorption on analysis were performed after 8, 24, 36, 48 and 72 hours. An unsampled tube was also broken-open, sealed and left on the laboratory bench for 72 hours prior to desorption and analysis.

2.1.9 Measurement of Other Gases of Interest

a) Permanent gases

This range of gases included carbon dioxide, carbon monoxide, methane and oxygen. The first three gases were measured on Analytical Development Company, series 100, non dispersive and double beam infra-red instruments, connected in series with 3.0mm nylon tubing to a Servomax paramagnetic oxygen analyser. Manufacturers specifications for each instrument are given in Table 17. Calibration was undertaken before and after each experiment using certified gas mixtures (B.O.C Ltd). Samples for analysis were collected into metal sample tubes using a hand pump as adopted by the National Coal Board for routine sampling of mine atmospheres.[270] Sample tubes are 19.5cm long 2.2cm o.d. constructed from impact extruded aluminium alloy with a brass screwed cap fitted with a high pressure Schrader valve (Gresham Engineering Company). The sampling pump consists essentially of a stainless steel barrel and piston shaft, a non-return inlet valve, and an outlet bayonet coupling to which the sample tube is fitted. Samples were collected by filling the tube to approximately 180 psi using twenty strokes of the pump. Samples were analysed by connecting the tube to a pressure reducing valve (0-500 psi) and the sample passed at 300ml min^{-1} through each instrument. Plate 1 shows the sampling equipment and instrument arrangement.

b) Hydrogen

The analytical system consisted of a Pye Unicam 104 chromatographic oven fitted with a 2.0m long x 6mm o.d.

stainless steel column packed with Molecular Sieve 13 X, 40-60 B.S mesh, operated at 50 °C. Purified argon carrier gas was used at a flowrate of 40ml min^{-1} . The column effluent was fed to a Pye Unicam katharometer set at bridge current of 100mA with the output connected to a 10 mV potentiometric recorder (Omniscribe Series B-500). Standard mixtures containing hydrogen in air, and helium and hydrogen in air were used for calibration purposes and injections were performed via a 5ml sample loop. Figure 9 shows duplicate chromatograms resulting from injection of 1260 ppm and 95 ppm hydrogen. Samples were initially collected into the aluminium tubes, however, during the underground investigations it was found important to use tubes manufactured from stainless steel. An explanation is given in Appendix 1.

c) Oxides of nitrogen

Nitrogen dioxide and nitric oxide were measured in the laboratory on an Ecolyser 7000 series analyser (Analysis Automation Ltd). The instrument is based on electrochemical detection with range for nitrogen dioxide covering 0-5ppm and 0-20ppm and 0-20 and 0-100ppm for nitric oxide. Calibration was undertaken with BOC spectra seal mixtures containing 18 ppm nitrogen dioxide in air and 70 ppm nitric oxide in nitrogen. To prevent component losses sample transfer lines and connections were made from PTFE. During operation samples were drawn directly to each sensor at approximately 500ml min^{-1} by an internal pump. This instrument failed to satisfy the electrical regulations for use in coal mines, therefore, Draeger

stain tubes types 0.5/a and 2/a were employed for the measurement of nitrous fumes ($NO+NO_2$) underground covering the ranges 0.5-10 ppm and 5-100 ppm.

d) Hydrogen chloride

Draeger stain tubes were again utilised for the semi-quantitative measurement of hydrogen chloride in the laboratory and underground. The stain tubes covered the range 0.1-100 ppm hydrogen chloride.

e) Extended analysis using gas chromatography linked mass spectrometry (GC/MS)

To complement the analysis techniques developed in this part of the work GC/MS facilities have been employed to provide additional information. This system was made available by kind permission of the Health and Safety Executive Laboratories, Cricklewood, London. The analytical system was fully automated and consisted of a Perkin Elmer automatic thermal desorption unit ATD50, coupled to a Sigma 3 gas chromatograph whose effluent was fed into a Finnegan 1020 quadrupole mass spectrometer. The chromatograph and mass spectrometer operating conditions were fully controlled by a Nova 3 minicomputer. Stainless steel sampling tubes packed with 130 mg Tenax GC manufactured by Perkin Elmer were used to collect samples prior to thermal desorption and analysis. The systems operating conditions are summarised below:

Automatic thermal desorber ATD50	
Sampling tube sample volume	100 ml
Primary desorption temperature	220°C
Primary desorption time	10 mins.

Cold trap packing	Porapak Q
Cold trap low temperature	-30 °C
Cold trap high temperature	220 °C
Transfer line temperature	150 °C

Sigma 3 chromatograph

Chromatographic column	25m long x 0.42 mm o.d. across linked methyl silicone, B.P.1 (SGE Ltd.)
Carrier gas flow rate	1ml min^{-1} helium
Split ratio	50:1
Temperature programme	40-250 °C at 10° C min^{-1} , hold for 15 minutes.

Finnegan 1020 mass spectrometer

Mass range	33-300 amu
Scan time	1 second
Resolution	1200
Mass stability	$\pm$ 0.1 amu per day

2.2 Results and Discussion

The experimental work presented herein has involved a wide ranging study of analytical procedures for the quantitative collection and analysis of selected groups of gases and vapours that are of interest in coal mine atmospheres. The main part of this work falls into two areas; the separation and measurement of the compounds of interest using chromatographic techniques, where applicable, and the development of methods for sample collection and

transference to the analytical system. Four main groups of gases and vapours were studied, namely, low molecular weight hydrocarbons, aromatic hydrocarbons, low molecular weight sulphur compounds and carbonyl compounds. Chromatographic column packing materials were evaluated for the separation of a number of compounds from each group and adsorption tube sampling techniques were studied for their quantitative collection and desorption. Plate 2 shows the different sampling tubes used for the collection of each group of compounds.

For quantitative analysis it is essential that collected samples be completely released from the adsorbent during desorption, directly on to the analytical chromatographic column for their separation and measurement. The optimum desorption conditions of each sampling tube were determined for the particular range of gases and vapours collected. Additionally the safe sampling volume of each sampling tube has been determined. This is the maximum volume of air containing a number of gases and vapours that may be drawn through a sampling tube without significant loss from the adsorbent of any of the compounds of interest. A number of workers[256,271] have derived this volume from either knowledge of retention volume of a particular component on a chosen adsorbent, then the safe sampling volume is normally taken as 50% of the retention volume, or by evaluation of the components breakthrough volume on the adsorbent. The breakthrough volume is taken as the point at which a continuous atmosphere drawn through the sampling tube appears in the tube effluent. It is normally measured by

drawing a standard atmosphere through a sampling tube and monitoring the tube effluent continuously for the appearance of any compounds of interest. Alternatively, a known volume of a standard atmosphere may be drawn through two sampling tubes connected in series with the front and back-up tube being desorbed and analysed separately. This procedure is repeated with progressively larger samples until the back-up tube gives a positive result on analysis. The latter method, which is essentially frontal chromatography, has been adopted here for evaluation of the safe sampling volume of each sampling tube for the particular range of compounds collected. The preferred collection and analysis methods have been validated and sample storage stability examined.

Techniques for the measurement of other gases of interest including methane, carbon monoxide, carbon dioxide, oxygen, oxides of nitrogen and hydrogen chloride have also been studied. Finally, GC/MS facilities have been utilized to provide an extended analysis. The following part of this section aims to collate results from work carried out in the experimental section and discusses the observations.

2.2.1 Low Molecular Weight Hydrocarbons

a) Chromatographic analysis

Three gas-solid chromatographic packing materials were examined for the separation of this range of gases. Using the Porapak Q column operated at the manufacturers recommended conditions (column temperature 30 °C carrier gas flow rate 23ml min^{-1}) methane, ethene and ethane eluted in 10.3 mins, although the remaining components in the C_1-C_4 standard mixture

had not eluted after 60 minutes. Baseline separation of the mixture could not be achieved by varying either the carrier gas flow or column temperature. Figure 10 shows a chromatogram obtained by increasing the column temperature to 100°C, at a carrier gas flow rate of 25ml min^{-1}. Under these conditions the elution order was estimated to be methane, ethene, ethane, propene/propane, 2-methyl propane, n-butane. Resolution between two components has been taken as being equal to twice the difference between the retention times for two components divided by the sum of the peak widths for the two components. When the resolution is equal to or greater than 1.5 complete separation is obtained.(272)

$$\text{Resolution} = \frac{2(t_{R2} - t_{R1})}{W_1 + W_2} = 1.5 \text{ for baseline separation} \quad \ldots\ldots 2.1$$

An acceptable separation of the standard mixture could not be achieved by varying the chromatographic conditions and further work on this column was discontinued.

When the untreated alumina F-1 column was operated at the manufacturers recommended conditions (column temperature 100°C, carrier gas flow rate 12.5ml min^{-1}) all components in the C_1-C_4 standard mixture were completely resolved to baseline separation. The elution order was identical to the Porapak Q column except for ethane which eluted prior to ethene.

The efficiency of a chromatographic column may be determined from the number of theoretical plates it possesses which is calculated using the expression:

$$N = 16 \left(\frac{t_r}{W_b} \right)^2 \quad \ldots\ldots 2.2$$

where t_r = the unadjusted, observed retention time taken as the time from sample injection to peak apex and W_b is the time corresponding to the peak width at base, where the base is defined as the distance between intercepts of the peak tangents with the interpolated baseline.

The efficiency of a chromatographic column can then be expressed by equation 2.3 below which shows the height equivalent to a theoretical plate (HETP), being equal to the column length divided by the number of plates.

$$HETP = L/N \quad \ldots\ldots\ldots\ldots\ldots\ldots \quad 2.3$$

where the HETP value is expressed in millimetres.

Factors which affect the efficiency of a column can be expressed by a simplified form of the Van-Deemter equation (254)

$$HETP = A + \frac{B}{\bar{\mu}} + C\bar{\mu} \quad \ldots\ldots\ldots\ldots\ldots\ldots \quad 2.4$$

where A = the eddy diffusion or multiple path term, B is the molecular diffusion term, C is the resistance to mass transfer and $\bar{\mu}$ is mean linear carrier gas velocity.

A plot of HETP versus $\bar{\mu}$ is an expression of the Van Deemter equation which produces a hyperbolic curve with a minimum in HETP, hence maximum number of theoretical plates, at the optimum carrier gas velocity.

The optimum carrier gas flow rate determined from a plot of height equivalent to a theoretical plate (HETP) against mean linear gas velocity ($\bar{\mu}$) was found to be 8.5ml min^{-1}. This gave a corresponding number of theoretical plates for the column equivalent to 3175 and 3330 for 2-methyl propane and n-butane respectively with a resolution greater than 1.5 in a complete analysis time of 16.5 mins. A chromatogram of the separation is given in Figure 11a

and the Van-Deemter plot of HETP versus $\bar{u}$ for 2-methyl propane, is shown in Figure 11b. Increasing the optimum gas velocity to the optimum practical gas velocity, normally taken as a two fold increase,[273] resulted in a decrease in analysis time but no improvement in separation. Operating the column at lower temperatures gave no significant improvement in separation. Figure 12a shows the chromatogram obtained at 80°C at the optimum gas velocity, with a plot of HETP versus $\bar{u}$ for 2-methyl propane shown in Figure 12b. Under optimum conditions the column exhibited 3510 and 3550 theoretical plates for 2-methyl propane and n-butane respectively with an analysis time of 26.5 minutes.

The NaI blocked alumina column operated at either 50°, 60° or 70° C under optimum carrier gas conditions resolved all the components in the C_1-C_4 standard mixture almost to baseline separation. A chromatogram obtained at 60°C is given in Figure 13a and a plot of HETP versus $\bar{u}$ for 2-methyl propane is shown in Figure 13b. The optimum flow rate, number of theoretical plates, resolution and analysis time at each temperature examined are summarised below:

Column temp °C	Optimum flow rate ml min^{-1}	Number of theoretical plates		Resolution	Analysis time minutes
		2-methyl propane	n-butane		
50	9.2	3560	3620	1.58	18.2
60	8.5	3300	3410	1.52	13.6
70	7.7	3120	3320	1.47	9.9

The lower operating temperature and shorter analysis time of this column compared with the untreated alumina F.1 alumina F.1 column suggested that its useful working range range could be extended to cover a wider range of hydrocarbons. A new standard gas cylinder mixture containing C_2-C_7 hydrocarbons was obtained.

Figure 14 shows a chromatogram obtained from the NaI modified alumina column using the operating conditions as follows:

Column temperature programme 50-200°C at 8 °C min^{-1}

Injector temperature 110°C

Detector temperature 250°C

Carrier gas flow rate 15ml min^{-1}

The chromatogram demonstrates the typical symmetry and sharpness of the peaks obtainable with this column. The exact nature of the modified surface is unknown but it is possible that the original alumina surface has been completely covered by one or more layers of the modifier so that an absorbent surface is formed with an active area somewhat less than that of the supporting surface which would lead to shorter analysis times.

Further work on this column indicated that cyclopentane and cyclohexane co-eluted with their respective methyl substituted isomers whilst ethyne eluted after 11.4 mins. The chromatographic conditions shown above have been adopted for the separation and analysis of C_2-C_7 hydrocarbons in the remaining part of this work.

b) Sampling tube evaluation

Sampling tubes packed with Porapak Q, charcoal 208C and NIOSH charcoal were examined for the quantitative collection and desorption of low molecular weight hydrocarbons using the C_2-C_7 standard mixture. Initially the optimum desorption conditions for each type of sampling tube were determined. The desorption temperature must be sufficient to quantitatively release all the collected compounds in such a manner as to prevent peak broadening during analysis, but not so high as to cause packing material or sample component decomposition. To ensure that desorption conditions were reproducible it was considered important to determine the time dependence of the temperature of each adsorbent at various heater block temperatures. Measurements at six different heater block temperatures showed the temperature at the sampling tube centre to be almost independent of the type of packing material. The results obtained are shown in Figure 15. It has been suggested[274] that a longer heating period normally plays a more important role in the possibility of decomposition, than a higher sample tube temperature.

The effect of different heater block temperatures on the desorption efficiency of 100ml aliquots of the standard mixture collected on to each adsorbent was studied and the results obtained are shown in Tables 18-20. The sampling tubes were heated for 60 seconds prior to injection on to the chromatographic column. Percentage recoveries of desorbed compounds were determined from their peak area measurements compared with 2ml direct injections of the

standard mixture.

At heater block temperatures of 250° C and 300° C the Porapak Q sampling tubes gave good recoveries for all the desorbed components in the standard mixture, except ethane, ethene, propane and propene. Figure 14 shows these heater block temperatures correspond to adsorbent bed temperatures of 155° and 200° C respectively. The low recoveries found most probably result from the safe sampling volume of the tube being exceeded, which is discussed later, and not to be the desorption conditions employed.

Compared with the Porapak Q sampling tubes the stronger adsorptive properties of both types of charcoal studied can be seen from Tables 18 and 19 with higher heater block temperatures required to quantitatively desorb all the compounds under test. Analysis showed that at heater block temperatures below 300 °C the higher boiling compounds in the standard mixture exhibited severe peak broadening. This would result from slow release of strongly adsorbed compounds from the adsorbent on to the analytical chromatographic column. Coker [275] found that thermal desorption of a sampling tube packed with 550mg of NIOSH type charcoal gave broadened peaks for vapours more strongly retained than pentane. We have found that using heater block temperatures of either 350° C or 400°C, with a heating period of 60 seconds prior to desorption that only slight peak broadening of the higher boiling point components occurred and using peak area measurements a reproducible quantitative analysis of all the tubes under

test could be made. Figure 14 shows that heater block temperatures of 350 °C and 400 °C correspond to adsorbent bed temperatures of 275 °C and 348 °C respectively after a 60 second heating period. At the higher temperature benzene was found to give a consistently high recovery and further tests to determine the temperature gradient across the adsorbent bed, using a Chrome/Alumel thermocouple, showed that the bed periphery attained a temperature of 390° C after 60 seconds. This temperature gradient could result in decomposition and re-arrangement of one or more of the components present. At a heater block temperature of 350 °C the temperature gradient across the adsorbent bed was found to be more homogeneous with only a 15 °C increase from bed centre to periphery.

This series of experiments have shown that all the gases of interest can be completely desorbed from the Porapak and charcoal sampling tubes at heater block temperatures of 250 °C and 350° C respectively using a heating period of 60 seconds prior to sample injection. These conditions resulted in no sample or packing material decomposition.

The maximum sample volume of standard mixture that could be drawn through each sampling tube for quantitative collection of the components of interest was determined using known volumes in the range 50-500ml. The results shown in Tables 21-23 were obtained at a flow rate of 200ml min^{-1} using the desorption conditions as determined for each adsorbent. The Porapak Q sampling tubes were found to have a low adsorptive capacity for quantitative collection of the test compounds giving a safe sampling

volume of less than 50ml for ethane and ethene. At the highest sample volume examined all components in the standard mixture up to 2 methyl butane exceeded the safe sampling volume of the tube. Coker[275] has derived an expression based on Kovats retention indices[276] to predict the safe sampling volume of a tube packed with 330mg of Porapak Q. At an ambient temperature of 35° C calculations using this expression gave safe sampling volumes of 68, 172 and 434ml for ethane, propane and n-butane respectively. These figures are in reasonable agreement with the values found experimentally in this work. Since the Porapak Q sampling tubes have shown insufficient capacity to quantitatively collect the full range of compounds, even at the minimum sampling volume examined, further work with this material was discontinued.

Examination of Tables 22 and 23 shows that both types of charcoal packed sampling tubes exhibited higher collection capacities. However, for collection efficiencies better than 95% the maximum sample volume was found to be limited to 150ml. At increasingly larger sample volumes the percentage recoveries of ethane and ethene decreased being less than 85% at the maximum volume examined. Desorption and analysis of the back-up tubes confirmed that above 150ml breakthrough of ethane and ethene occurred from the collection tube. To remain well within the maximum sampling volume the safe sampling volume has been limited to 100ml.

The collection efficiencies of the charcoal sampling tubes were further examined in the presence of a high

concentration of methane since its occurrence in the underground environment is well known. The presence of a high concentration of methane loaded on to the tubes was found to have no effect on the collection efficiencies of either form of charcoal adsorbent with the components of interest giving recoveries better than 95% on analysis. The labile nature of methane and the limited sample volume drawn through the adsorbents means that its effect on blocking active sites is likely to be negligible, hence the collection efficiencies of the remaining components are unaffected.

Although the Porapak Q sampling tubes have been found to be unsatisfactory for the quantitative collection of low molecular weight hydrocarbons, both types of charcoal packed sampling tubes have proved suitable exhibiting similar collection and desorption efficiencies. However, preparation of sampling tubes packed with the NIOSH type charcoal (Section 2.1.2 a) was time consuming and relatively expensive compared with the Sutcliffe and Speakman 208C charcoal which was obtained in bulk quantities and therefore resulted in a lower unit cost per tube. Further work has continued with the latter material only.

Calibration curves were constructed for each component by serial dilution of the standard mixture. Desorption and analysis of duplicate sampling tubes taken at each dilution stage resulted in a linear response from the flame ionisation detector for each component with a limit of detection of approximately 0.005 ppm.

The limit of detection is defined as the minimum component concentration required to achieve a detector response twice the average base line noise. The linear response confirms that in the region of low concentrations when the adsorbent may not be coated by a monolayer of sample and, as a consequence, the molecules are adsorbed mainly on the active sites of higher energy, thermal desorption occurs completely.

The reproducibility of the method is shown in Table 24 where the mean recovery and relative standard deviation of each components are given. Using standardised collection, desorption and analysis procedures mean recoveries varying in the range 94.1-96.9% were obtained with ethane showing the highest relative standard deviation at $\pm$ 2.99%. A typical chromatogram resulting from desorption and analysis of a 100ml sample of the standard mixture is shown in Figure 16. The major source of error in the determination of air pollutants normally results during sample collection due to the volume measurement associated with the use of flow counters on electrically operated pumps arising from the different permeabilities of each sampling tube. Here this error has been eliminated because the sample volume is fixed by the Draeger hand pump and the flow rate is controlled by a crimped orifice and not the adsorbent packing density or glass wool plugs.

Storage experiments were conducted to test the feasibility of collecting samples underground and returning them to the laboratory for desorption and analysis. The sampling

tubes stored on the bench showed no significant losses up to 36 hours. After 48 hours the recoveries of ethane and ethene had decreased to 82% and 78% respectively, and after 72 hours to 73% and 69% with the remaining components giving complete recoveries. No losses were observed from the sampling tubes stored in the refrigerator up to the maximum period studied. It was considered that 36 hours was sufficient to return sampled tubes from any location back to the laboratory for analysis. As a precaution all sampled tubes returned to the laboratory were immediately placed in the refrigerator prior to analysis. The design of the brass holder and cap to prevent external contamination was confirmed by analysis of an unsampled tube after 72 hours storage.

On analysis no background levels of low molecular weight hydrocarbons were observed above the limit of detection of the system (0.005 ppm).

2.2.2 Aromatic Hydrocarbons

a) Chromatographic analysis

Two chromatographic column packings, Tenax GC and 1,2,3 tris (2-cyanoethoxy) propane (TCEP), were evaluated for the separation of a range of aliphatic and aromatic hydrocarbons. Figure 17 shows the separation with the Tenax GC column operated at its recommended operating conditions (column temperature 150° C carrier gas flow rate 15ml min^{-1}). No significant improvements in this separation could be achieved by varying the carrier gas flow rate or column temperature and further work with this column was abandoned. No attempt was made to identify

peaks present in the chromatogram. When the TCEP column was operated at 80°C, over the range of carrier gas flow rates studied (5-40ml min^{-1}), all components in the standard mixture were well separated except ethyl benzene and meta-xylene. A chromatogram of the separation obtained at the optimum carrier gas velocity is shown in Figure 18a. Using benzene in the calculations for the Van-Deemter plot of HETP versus $\bar{u}$, shown in Figure 18b, gave a maximum of 3900 theoretical plates for the column. This corresponded to a carrier gas flow rate of 11.2ml min^{-1} which gave a complete analysis time of 23.76 minutes with a resolution of 0.96 for ethyl benzene and meta-xylene. To decrease analysis time the column was operated near the practical optimum gas velocity and the resultant chromatogram is shown in Figure 19. This gave an analysis time of 15.36 minutes with a resolution of 1.03 for ethyl benzene and meta-xylene. Further work showed that para-xylene co-eluted with its meta isomer. The high selectivity of this column for the separation of aliphatic and aromatic hydrocarbons is demonstrated with decane being eluted prior to benzene. Examination of the Rohrschneider system[277] of column classification shows that of all the stationary phases examined TCEP exhibits the highest x value at 6.00. The x term represents the degree of retardation of aromatic substances on the stationary phase. This column has been used in the remaining part of this investigations at the following operating conditions.

Column temperature 80 °C

Injector temperature 180 °C

Detector temperature 250 °C

Carrier gas flow rate 18ml min^{-1}

b) Sampling tube evaluation

Table 25 shows the efficiency of desorption of the standard mixture from the Tenax GC sampling tubes at different heater block temperatures. At heater block temperatures of 300 and 350 °C good recoveries and chromatographic peak shapes were obtained for all the components in the standard mixture. The temperature dependence of the sampling tube centre with time at each heater block temperature was similar to the charcoal tubes shown in Figure 15. Heater block temperatures of 300 and 350 °C corresponded to adsorbent bed temperatures of 225 and 290 °C respectively after 60 seconds. On one occasion a heater block temperature of 400 °C was used but the Tenax GC became discoloured and it was considered that some degree of decomposition must have occurred, therefore the tube was discarded. Brown and Purnell[256] studied the performance of Tenax GC for the collection and desorption of a number of organic vapours. For the compounds studied quantitative recoveries were obtained with desorption temperatures in the range 100-150° C in a desorption volume of 50ml. However, in practice higher temperatures are required to rapidly sweep the sample from the sampling tube with carrier gas on to the analytical column in a small plug and prevent peak broadening on analysis.

Using a heater block temperature of 350°C and heating period of 60 seconds prior to desorption sampling tubes loaded with different sample volumes in the range 500-2500ml were analysed and the percentage recoveries of each component are shown in Table 26. At the maximum sample volume examined the sampling tubes were capable of quantitatively collecting all the components present except benzene which gave low recoveries at sample volumes greater than 1500ml. Breakthrough of benzene at higher sample volumes was confirmed by analysis of the back-up tubes with no evidence of the remaining components. Previous investigators using similar Tenax GC sampling tubes[256,257] studied the safe sampling volume of benzene saturated with water vapour at 20°C.

Brown and Purnell[256] calculated the safe sampling volume of benzene at flow rates in the range 5-600ml min^{-1} at 20°C to be four litres, which is in reasonable agreement with Clark et al[257] who gives a value of three litres at a flow rate of 200ml min^{-1}. The higher ambient temperature used in this work would account for the lower safe sampling volume found for benzene. In addition to the quantitative collection of aromatic hydrocarbons the results in Table 25 show that the Tenax GC sampling tubes can also be utilised for the quantitative sampling of octane, nonane and decane. To remain within the safe sampling limit of benzene the maximum sample volume was restricted to one litre corresponding to ten strokes using the Draeger hand pump. Again a sampling flow rate of 200ml min^{-1} was set by inserting a crimped orifice into

the Draeger pump inlet. It was observed that after desorbing the same sampling tube a number of times the Tenax GC showed signs of shrinkage. The adsorbent was reconsolidated and no adverse effects were observed on the tubes performance.

The collection efficiency of the sampling tubes was found to be unaffected in the presence of a high concentration of methane. This can be accounted for by the low affinity of the Tenax GC to adsorb methane. An expression derived to predict the safe sampling volume of n-alkanes on Tenax GC [275] gives a value of 1.3ml for methane at 35°C.

Figures 20 and 21 show chromatograms obtained for desorption of sampling tubes loaded with one litre samples of the standard mixture diluted by one and three orders of magnitude to give nominal component concentrations of 1ppm and 0.01 ppm. Peak area measurements from the flame ionisation detector gave a linear relationship for each component on dilution. With a one litre sample the limit of detection of 1,3,5, trimethylbenzene was calculated to be equivalent to 0.005 ppm.

Results from analysis of ten one litre samples of the standard mixture loaded under identical conditions on to separate sampling tubes and desorbed in the same manner each time are shown in Table 27. The components present in the standard mixture gave similar mean percentage recoveries varying in the range 95.4-97.1 for octane and 1,3,5 trimethylbenzene respectively with a meta-xylene exhibiting the highest relative standard deviation at $\pm$4.28%.

The times and conditions of storage employed with the charcoal tubes (Section 2.1.2 c) were used to study sample stability on the Tenax GC sampling tubes. Desorption and analysis of one litre samples of the standard mixture loaded on to each of the sampling tubes showed that regardless of the storage method quantitative recoveries of all the components in the standard mixture were obtained up to 72 hours, the maximum period studied. Pellizzari[271] has shown that desorption and analysis of a standard mixture stored on Tenax GC for a three week period gave recoveries in the range 80-95%. Desorption and analysis of an unsampled tube after 72 hours showed no indication of background contamination present above the limit of detection.

2.2.3 Low Molecular Weight Sulphur Compounds

a) Chromatographic analysis

Three columns packed with Tenax GC, Porapak QC and acetone washed Porapak QS were each evaluated for separation of low molecular weight sulphur compounds. A chromatogram obtained from a mixture containing hydrogen sulphide, carbonyl sulphide and sulphur dioxide prepared in a Tedlar bag and injected on to the Tenax GC column is shown in Figure 22. Although the peaks in the chromatogram show good separation and little tendency to tail it was only obtained after repeated injections. The effect of a series of replicate injections of a similar mixture on to the same column after an overnight break is shown in Figure 23. Carbonyl sulphide gave a reasonably constant response throughout, whilst hydrogen sulphide required up

to nine separate injections before repeatable results were obtained and sulphur dioxide was completely adsorbed, requiring a minimum of twenty injections before a constant level was achieved. Walker,[264] using a similar column packed with Tenax GC for the analysis of low molecular weight sulphur compounds observed that at low concentrations some gas was initially adsorbed but after the injection of several samples a constant response was observed. To try and overcome this problem pure samples of hydrogen sulphide and sulphur dioxide were purchased (B.D.H. Ltd) and injected on to the column, however, this proved unsuccessful for long term conditioning and further work with this column was discontinued.

The Porapak QS treated and untreated columns separated a similar mixture to that used above when operated isothermally at 40°C over the range of carrier gas flow rates studied. Using carbonyl sulphide in the calculations a plot of HETP versus $\bar{u}$ for the treated Porapak QS column gave the Van-Deemter curve shown in Figure 24a which resulted in a maximum of 285 theoretical plates. The curve minimum relates to a carrier gas flow rate of 3.1ml min^{-1} giving a complete analysis time of 14.71 minutes. A chromatographic trace obtained under these conditions is given in Figure 24b. Figure 25 shows a chromatogram obtained by operating the column above the practical optimum gas velocity at 8.0ml min^{-1}. This resulted in an analysis time of 5.97 minutes with complete baseline separation for all three components and no indication of tailing. Figure 26 shows the chromatogram

produced from injection of a similar mixture on to the untreated Porapak QS column operated under identical conditions to above. Baseline separation was achieved for each component in a total analysis time of 6.19 minutes, however, sulphur dioxide exhibited a slight degree of tailing.

To reduce the retention times of higher sulphur containing compounds, including carbon disulphide, temperature programming was carried out on the treated Porapak QS column. It was found that this caused the column to adsorb sulphur dioxide leading to non-quantitative results and for this reason isothermal operation was preferred. The column temperature was increased to 100° C for the injection of a mixture of carbon disulphide, hydrogen sulphide, carbonyl sulphide and sulphur dioxide and the chromatogram obtained is shown in Figure 27. Under these conditions the separation between hydrogen sulphide, carbonyl sulphide and sulphur dioxide was almost completely lost, however, carbon disulphide eluted without tailing in 4.32 minutes.

After operating at this temperature it was found necessary at the lower operating temperature of 40°C to condition the column with two injections of sulphur dioxide before a constant response was obtained.

Because of the known chemical reactivity of sulphur containing compounds[249] an assessment of the repeatability of replicate injections of hydrogen sulphide, carbonyl sulphide and sulphur dioxide was undertaken on the treated Porapak QS column operated at

40° C with a carrier gas flow rate of 8.0ml min^{-1}. Carbon disulphide was examined with the column temperature increased to 100 °C at the same flow rate. The retention times and repeatability of response obtained for each standard are shown in Table 28. This indicates that the repeatability of direct injection is very good with a maximum relative standard deviation of ±3.13% for sulphur dioxide. As the flame photometric detector responds to total sulphur it would be expected that the response to equal concentrations of hydrogen sulphide, carbonyl sulphide and sulphur dioxide would be identical. The higher integrator count obtained for sulphur dioxide is ascribed to the slight tailing of the peak.

The response from the flame photometric detector to sulphur compounds approximately obeys a square law. From experimental evidence[249] it is known that the exponent is not normally two but lies between 1.80 and 1.88. The Pye 304 chromatographic system used in this work had an exponent control included in the amplifier control that could be adjusted until a linear relationship was obtained between response and component concentration. Serial dilution of the 20 ppm standards with purified oxygen free nitrogen showed that a linear relationship was achieved for each standard between 0.25 ppm and 20 ppm using a control setting of 1.82. A summary of the chromatographic operating conditions used in the remainder of the work are shown below:

Chromatographic column	50 cm x 3 mm o.d. PTFE packed with 30 cm of treated Porapak QS.
Column temperature	1. 100°C (for analysis of carbon disulphide). 2. 40 °C (for analysis of remaining components).
Injector temperature	100°C
Detector temperature	150°C
Carrier gas flow rate	8.0ml min^{-1}

b) Sampling tube evaluation

Sampling tubes packed with Molecular sieve 5A, Porapak Q and the treated Porapak QS were examined for the quantitative collection and desorption of the four sulphur containing standards.

Hydrogen sulphide was used to determine the optimum desorption temperature and using heater block temperatures in the range 150-300°C with the normal heating period of sixty seconds prior to injection low recoveries (60-71%) were obtained from the Molecular sieve 5A sampling tubes. Decreasing the heating period resulted in improved recoveries even though the heater block remained in position after injection, with a ten second period giving maximum recoveries, as shown in Table 29. Temperature measurements taken at the centre of selected tubes, versus time, at different heater block temperatures gave similar profiles to those obtained from the charcoal sampling tubes shown in Figure 15. Heater block temperatures of 250°C and 300°C corresponded to mean adsorbent bed

temperatures of 50° and 60° C respectively at the sampling tube centre after ten seconds and 225° and 260°C after three minutes. The low recoveries found with the longer heating period can only be attributed to reaction between the Molecular sieve and hydrogen sulphide and confirms the suggestion made by Bertoni[274] that longer heating periods normally play a more important role in the possibility of decomposition than higher temperatures.

Consistently low recoveries were obtained from both types of Porapak sampling tubes over the range of heater block temperatures studied and repeated attempts to improve recoveries including varying the heating period proved unsuccessful. The results obtained using a ten second heating period are also shown in Table 29. The low recoveries can either be accounted for by the adsorbent having insufficient capacity for the quantitative collection of hydrogen sulphide or from decomposition on the material. In either case both materials are inappropriate as quantitative collection mediums and no further work was undertaken.

Two methods of sample loading were employed to evaluate the collection efficiency of the Molecular sieve 5A sampling tubes. Firstly, the results obtained from introducing known volumes of each standard gas mixture separately, diluted with purified oxygen free nitrogen, on to two sampling tubes in series are given in Table 30. The percentage recoveries of each component were determined from desorption and analysis of the front tubes using a heater block temperature of 300°C with a ten

second heating period prior to injection.

Typical chromatograms resulting from analysis of duplicate 100ml samples containing 0.1 ppm carbonyl sulphide are shown in Figure 28. For each component studied recoveries greater than 78% were observed over the range of sample volumes examined (100-1000ml) and a negative analysis of the back-up tubes confirmed that the safe sampling volume had not been exceeded for any component at the maximum sample volume collected. Black [265] determined the breakthrough volume, which he defined as the volume of gas required to elute fifty per cent of an adsorbed compound, of hydrogen sulphide and sulphur dioxide to be 22.5 and greater than 25 l/g on Molecular sieve 5A at 25°C. From this estimation it should be possible with our tubes to quantitatively collect larger samples, however, 'grab samples' might have to be taken and using the Draeger hand pump the sampling time of approximately six minutes for a one litre sample was considered limiting.

Since it was not possible to study the effect of water vapour on collection efficiency directly with the water bubbler arrangement (Figure 7) the second method of sample loading was used to indirectly introduce water vapour on to the sampling tube. An initial 100ml of a standard mixture containing hydrogen sulphide, carbonyl sulphide and sulphur dioxide was sampled, followed by the introduction of water vapour by the addition of known volumes of clean laboratory air. Carbon disulphide was studied separately using this procedure. The percentage recoveries of each compound were determined and the

results obtained are shown in Table 31. Satisfactory recoveries were only obtained when a sample was taken direct without the addition of air. The increasing addition of clean laboratory air led to progressively poorer recoveries. Since Molecular sieve 5A is a well known drying agent it was suspected that when air was introduced on to the sampling tube water vapour may become trapped within the molecular sieve internal cavities and come into contact with trapped sulphur compounds. Figure 29 shows a chromatogram resulting from desorption of a sampling tube loaded with a 100ml of the standard mixture followed by an additional 100ml of clean laboratory air. In addition to the low recoveries obtained for each component, sulphur dioxide exhibited excessive tailing. To overcome these problems the effectiveness of using a short drying pre-tube containing 0.5g of phosphorous pentoxide was investigated. It was found that when using the pre-tube drier quantitative recoveries of all components were achieved up to maximum diluent volume of 900ml. Figure 30 shows a chromatogram obtained when using the pre-tube drier with identical sample loading conditions to above. Comparing this chromatogram with Figure 29 shows that improved recoveries were obtained and the excessive tailing of sulphur dioxide is greatly reduced. In all future work a new pre-tube drier was used for each sampling tube during sample loading. It was further considered important to condition sampling tubes overnight prior to use, as described earlier, to remove any traces of water vapour. Following these precautions

carefully quantitative recoveries and acceptable peak shapes were obtained for each component on analysis.

A high concentration of methane was found to have no effect on the collection efficiency of the Molecular sieve 5A with desorption and analysis of sampling tubes giving good recoveries. Although Molecular sieve 5A is a strong adsorbent any displacement effect due to the presence of a high concentration of methane has been found to be insignificant due to the relatively small sample volume collected and the labile nature of methane. Possible interferences on the response of the flame photometric detector due to the presence of high concentration of hydrocarbons having the same retention times as sulphur containing compounds have been suggested by Mangani[278] as follows. If high concentrations of hydrocarbons are injected the effect at high detector sensitivity produces a positive peak from the flame photometric detector and the signal is additive at low concentrations of sulphur compounds. At higher sulphur component concentration the additive hydrocarbon effect becomes negligible and a "quenching" effect takes place. It was found that with the flame photometric detector amplifier set on a sensitive range direct injections of a mixture containing a nominal 5% methane produce a positive disturbance on the integrator baseline eighteen seconds after injection. The peak area measurement recorded was equivalent to 0.75 ppm hydrogen sulphide. However, the selectivity of the analytical column was high enough to eliminate any problems in the determination of the standard sulphur

compounds in the presence of a high concentration of methane.

Calibration of each sulphur gas was performed using the flowmeter dilution arrangement to generate concentrations in the range 0.002 ppm - 20 ppm. Desorption and analysis of sampling tubes loaded at each dilution stage with known sample volumes produced acceptable calibration curves that were linear for all sulphur compounds in the range 0.005 - 20 ppm using an exponent control setting of 1.82. At lower concentrations great difficulties were experienced in reproducing results. It was considered that this variation arose solely from the flowmeters which were at the bottom of their usable range and consequently flows were difficult to reproduce and maintain. Although adequate for the purpose of this application it is recommended that for more critical measurements due regard be given to the provision of high quality flow controllers, pressure regulators and temperature control. The reproducibility of the method is demonstrated in Table 32. Mean percentage recoveries varied in the range 90.0-95.5% for sulphur dioxide and carbonyl sulphide respectively with carbon disulphide giving the highest relative standard deviation at $\pm$9.0%. Taking into account the reactivity of sulphur compounds and the low concentrations examined the variations found in sample recoveries are considered adequate for this work.

The results of the storage tests showed that no significant losses occurred from sampling tubes after 36 hours. However desorption of the sampling tube stored on

the laboratory bench after 48 hours gave only 72% recovery of hydrogen sulphide. After 72 hours the recovery of hydrogen sulphide had decreased to 61% with carbonyl sulphide also showing losses giving 79% recovery. Sulphur dioxide showed no significant losses during this period. Sampling tubes stored in the refrigerator gave good recoveries for all compounds up to the maximum period studied. Analysis of an unsampled tube after 72 hours storage on the bench showed no signs of background contamination present using the most sensitive detector amplifier setting.

2.2.4 Aldehydes and Ketones

a) Chromatographic Analysis

Figure 31 shows an early chromatogram which confirmed that the 2,4 DNPH derivatives could be separated and detected at both 350 and 254 nm in a complete analysis time of twenty-four minutes. The resolution of propionaldehyde-2,4 DNPH and acetone 2,4 DNPH was poor, however, it was found after removing the packing from the inlet end of the ODS column and repacking with new material a repeat injection of the standard mixture gave a chromatogram as shown in Figure 32. Two features emerged, firstly, an improvement in resolution of the 2,4 DNPH derivatives of all the carbonyl compounds and secondly the column was able to separate the syn and anti forms of the acetaldehyde 2,4 dinitrophenylhydrazones.

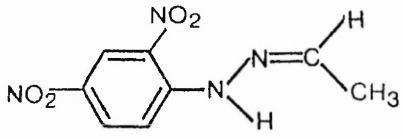

Syn-derivative

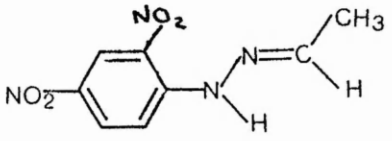

Anti-derivative

Calibration curves of detector response versus concentration were constructed for each compound in the range 2.5 µg-800 µg of pure derivative in 10ml of acetonitrile with triplicate injections performed at each dilution to give an assessment of calibration reproducibility. Over the concentration range studied acetone 2,4 DNPH derivative gave a linear response with a reproducibility of better than ±2.5% between 40-800 µg derivative, however, at 5 µg this figure had increased to ±6.0% and at 2.5 µg reproducibility was almost completely lost at ±26%. These variations were found to be typical for the remaining derivatives. Improvements in reproducibility at low concentrations could possibly have been achieved by thermostatically controlling the column temperature, however, lack of time prevented this avenue being investigated.

b) Sampling tube evaluation

A blank analysis of the impregnated support used to pack the first batch of sampling tubes is shown in Figure 33. Acetone was found to be the major contaminant being present at a concentration of 18 µg 2,4-DNPH derivative with acetaldehyde and formaldehyde also present as minor contaminants. Systematic tests were therefore carried

out on all the solvents and reagents and the following sources of contamination were identified. The 2,4 DNPH starting reagent contained the acetone 2,4 DNPH derivative, however, recrystallisation in ethanol allowed the pure material to be obtained. Preparation of the 2,4 DNPH-HCL from the pure base also showed the presence of the acetone derivative. Extraction of this material with dichloromethane (Aldrich Chemical Co. Ltd.) a solvent in which the acetone derivative is very soluble produced no improvement, even after recrystallisation from acetonitrile. It was found that injection of a 10 µl aliquot of a solution of 2,4 DNPH-HCL in acetonitrile always gave the same integrated area for the acetone derivative irrespective of whether 1.5g of material was dissolved in 10, 20 or 30ml of acetonitrile. This proved that acetone was present in the HPLC grade acetonitrile and that the derivative was produced at the same concentration. Therefore, a sample of 2,4 DNPH-HCL that had previously been washed with dichloromethane was prepared into a saturated solution in dichloromethane. Injection of a 10 µl aliquot of this solution produced no acetone 2,4 DNPH derivative on analysis. Redistillation of 500ml acetonitrile gave a fraction boiling at 80°C that showed no acetone derivative on analysis using 16mg of 2,4 DNPH-HCL in 10ml of the re-purified acetonitrile. Identification of the source of contamination and its means of removal has thus allowed a method for the preparation of blank sampling tubes as follows:

The 2,4 DNPH-HCL adsorbed on silica-gel was prepared as

described previously, but, a final washing with dichloromethane was required to obtain a blank impregnated support. Desorption of this material was then performed in 10ml of redistilled acetonitrile. A chromatogram resulting from desorption of a blank sampling tube prepared following this procedure is shown in Figure 34. Results from the experiments performed to determine sampling tube desorption efficiency and its reproducibility gave mean percentage recoveries of better than 95 $\pm$ 5% for all the compounds examined. Figures 35 and 36 show chromatograms resulting from entrapment and desorption of 100 µl of acetaldehyde gas and 0.07 µl of acetone liquid, which corresponds to 16.7 and 3.9 ppm respectively in six litres of sampled air. Comparison with standard calibration graphs gave recoveries of 96% and 98% for acetaldehyde and acetone respectively. The increase in length of colour change along the impregnated support, noted in the experimental section, suggests direct reaction of the carbonyl compound with the 2,4 DNPH and not adsorption on the silica gel followed by reaction. The desorption efficiency of formaldehyde was not examined because of difficulties in generating accurate concentrations. Bubbling or diffusion methods are little used for several reasons, such as the presence of stabilisers in manufactured aqueous solutions and the formation of formaldehyde hydrates, which are not well characterised.[279] If the determination of precise concentrations were important a number of descriptions of formaldehyde generation are reported based on the thermal

degradation of trioxane or polyoxymethylene.[280,281]

Tests were performed on sampling tubes prepared with the impregnated support split 1.0 : 0.5g in order to investigate the maximum sample volume that could be collected without breakthrough of any compound of interest. A negative analysis of the back-up portion from each tube confirmed that no significant loss occurred from the 1.0g front section even after sampling thirty litres, the maximum examined. Although larger samples may be collected it was considered that 30 litres would give sufficient sensitivity. For example, if acetone 2,4 DNPH was detected at 5 µg/10ml acetonitrile this would give an equivalent concentration of 0.016 ppm acetone from a thirty litre sample.

The stability of acetaldehyde and acetone collected on to sampling tubes was studied over a 72 hour period. Desorption and analysis of each set of sampling tubes showed that once formed the 2,4 DNPH derivatives were stable on the impregnated support for the maximum period studied. Desorbed solutions kept in a refrigerator for one week remained perfectly stable. Analysis of an unsampled tube after 72 hours showed no background interferences present, although it was considered pertinent to store tubes in an area free of organic contaminants.

2.3 Summary

A number of adsorbent packed sampling tubes have been examined for the quantitative collection of selected groups of gases and vapours, namely aliphatic and aromatic

hydrocarbons, sulphur containing compounds and carbonyl containing species. The collection efficiencies of suitable adsorbents have been studied under conditions likely to be encountered underground and the maximum sample volume that can be quantitatively collected has been determined. To overcome problems associated with using electrically powered sampling pumps underground, a Draeger hand pump has been employed to provide a simple yet reliable method of drawing known sample volumes through the sampling tubes.

The analytical system has been based on chromatographic techniques. A number of column packing materials have been evaluated and suitable systems developed to provide a good separation of selected components from each group of gases and vapours. Techniques have been developed for rapidly desorbing collected samples from the sampling tubes on to the analytical system. Using standard mixtures optimum conditions of transferences have been established and desorption efficiencies determined for each sampling tube.

In the past, one of the major problems with sample collection underground has been losses of components on the sampling vessel walls. Sample storage experiments have been conducted to test the feasibility of collecting samples underground and returning them to the laboratory. Standard mixtures loaded on to the sampling tubes have been shown to be stable for periods up to seven days.

Techniques for the collection and measurement of other gases and vapours have also been examined to provide a wide range of analytical procedures for the collection and analysis of gases and vapours that are of interest in coal mines.

CHAPTER 3

GENERATION AND IDENTIFICATION OF COMBUSTION PRODUCTS

Samples of coal for the combustion studies were collected from three seams known to be susceptible to spontaneous combustion; namely the Top Hard, Yard/Blackshale and Cockshead. Each coal sample was prepared and characterised following recommended British Coal procedures. A suitable experimental combustion apparatus was developed to enable the combustion products from each coal to be generated under carefully controlled and reproducible conditions. In the underground environment coal is likely to undergo heating in both aerobic and oxygen deficient conditions. Therefore investigations were performed in air and nitrogen to study the products evolved from each coal sample under the extremes of combustion atmospheres.

A parallel programme of work was also undertaken to identify products evolved from heated coal in the underground environment in order to provide basic information about the nature of combustion products present and to determine those gases peculiar to spontaneous combustion.

3.1 Experimental

3.1.1 Coals

Three collieries which were working coal seams known to be prone to spontaneous combustion were chosen for this study. Samples were taken underground from each seam following the standard procedures recommended in NCB

Report SNT/20/67[282] and then returned immediately to the laboratory for preparation. Initially this involved dividing each sample into subsections according to the quality of the coal. The thickness of each subsection was measured and subsequently broken into 75mm-25mm lumps prior to sample reduction and crushing to give <6 B.S mesh and <72 B.S mesh fractions. A composite sample was prepared from each of these fractions which represented the clean coal of the whole seam. Laboratory analysis was performed on the <72 mesh samples, whereas the larger sized fraction composite samples were retained for the combustion experiments. From previous experiments it has been shown that different size fractions of coal did not produced differences in the rate or pattern of evolution of combustion products.[100]

The samples were stored under nitrogen in air tight bottles to prevent ambient oxidation of the coal occurring. Details of the coal samples and results obtained from laboratory analysis are given on the following page.

3.1.2 Apparatus and Procedure for Generation of Combustion Products

Many of the previous studies undertaken to determine the combustion products evolved from heated coal have used a large sample mass and low combustion gas flow rate.[100,103] This combination was employed to overcome the analytical limits of detection. However, when using air as the combustion gas at elevated coal temperatures this led to insufficient oxygen to satisfy the adsorbent

Colliery	Seam	Coal Rank Code (CRC)	Ash Content % (w/w)	Volatile Matter % (w/w)	Sulphur % (w/w)				Chlorine % (w/w)
					Pyritic	Organic	Sulphate	Total	
Thoresby	Top Hard	702	4.4	32.4	0.14	0.37	0.41	0.92	0.72
Hucknall	Yard/ Blackshale	702	6.7	34.4	0.09	0.54	0.14	0.77	0.60
Wolstanton	Cockshead	502	5.3	33.7	0.10	0.42	0.38	0.90	0.83

characteristics of the coal. Thus, the products evolved were not truly oxidation products. At the other extreme of experimental conditions the apparent disappearance of products at increasing coal temperatures may be due to exhaustion of the original sample as much as to a change in the pattern of decomposition. Bearing these considerations in mind the experimental protocol adopted was as follows:

5g $\pm$ 1.0 mg of sample was placed into a 60cm long x 1.5 cm i.d. pyrex glass tube and held in place with silanised glass wool. A Pye Unicam Series 104 programmable gas chromatographic oven had a 2.0 cm diameter hole drilled in each side to hold the glass sample tube horizontally. The coal bed was then positioned in the middle of the oven allowing 5 cm of the tube to project from the oven outlet. The coal was heated at 4 ^{o}C min^{-1} up to a maximum temperature of 300^{o} C in a flow of 500 ml min^{-1} combustion gas, either oxygen free nitrogen or air, which had previously passed through traps containing activated charcoal and Molecular sieve 5A to remove contaminants. The combustion gas was preheated by flowing through a 2m long x 6mm o.d. coil inside the chromatographic oven. Flow rates were monitored using a 60-500 ml min^{-1} flowmeter (Platon type GTV), controlled with a fine needle valve, the flow being checked before each experiment using a soap film meter. Prior to carrying out experiments in nitrogen the system was flushed with the gas for ten minutes at 200 ml min^{-1} to remove any adsorbed oxygen from the coal surface. Two Chrome/Alumel thermocouples were

placed in the inlet and outlet of the sample to monitor the actual coal temperature during heating. During a number of experiments performed with air the coal temperature monitored by the inlet thermocouple exceeded the oven temperature above 270 °C, therefore these tests were discontinued at 250 °C.

Complementary experiments were performed to study the effect of different forms of sulphur in the coal on the combustion products evolved. Samples of the combustion products were collected for analysis at different temperatures using the techniques described in Section 2.1.

A parallel underground sampling programme was also established involving collieries where there was a reasonably high probability of an incident of spontaneous combustion occurring. This part of the study was performed as follows:

a) Samples were collected at selected collieries from within areas not substantially diluted by the general body mine atmosphere (pack pipe samples).

b) Control points were established at a number of underground locations to monitor the general body mine atmosphere.

c) The exhaust fumes produced from diesel locomotives during different operating conditions were investigated and the products evolved from several shotfiring events examined.

3.2 Results and Discussion

The experimental work has enabled a detailed examination to be undertaken of the products evolved from the three selected coals when heated in air and nitrogen under carefully controlled laboratory conditions. Furthermore, samples were collected underground from various locations during normal and abnormal activity and from other legitimate mining operations.

3.2.1 Hydrocarbons and permanent gases produced from coal heated in the laboratory

Samples of effluent gas were collected on to Charcoal and Tenax GC sampling tubes at regular intervals and analysed chromatographically as described earlier. The concentration of each component was calculated from its mean percentage recovery from the sampling tube and the chromatogram. At each temperature, a pressure capsule sample was taken for the analysis of carbon dioxide, carbon monoxide, methane and oxygen. The permanent gases, in particular the production of carbon monoxide and consumption of oxygen, were determined not only in this series of experiments but were also monitored during subsequent experimental tests to give an assessment of the repeatability of combustion conditions.

The concentration of each product identified at coal temperatures ranging from 50° C up to a maximum of 300°C are given in Tables 33-38. This temperature range was considered to be the critical range in the early stages of spontaneous combustion. With air as the combustion gas,

the coal temperature monitored by the inlet thermocouple exceeded the oven temperature above 270°C and the Thoresby and Hucknall coals self ignited before the maximum temperature of each run was reached.

The current method of assessing spontaneous combustion activity underground utilises the concentration of carbon monoxide and the $\frac{\text{carbon monoxide}}{\text{oxygen deficiency}} \times 100$ ratio (oxidation ratio) of samples taken in the general body of air. With coals heated in the laboratory in air, Chamberlain[100] found three distinct patterns of carbon monoxide production, viz. Coals having a C.R.C. 602-902 showed a rapid increase in carbon monoxide production below 100°C, with coals of C.R.C. 402-502 having slower rates initially but giving similar rates to the previous group above 100°C and finally coals having C.R.C. 101-401 gave the slowest rates of production initially. To compare the production of carbon monoxide from the three coals heated in air (Tables 33-35) with the results obtained by other workers all the data have been converted to rates of carbon monoxide evolution as follows:

Rate (mls of pure gas per g. of coal per min.) = $\frac{F \times C}{M \times 10^6}$ 3.1

where F is the flow rate of air (ml min^{-1}), C is the concentration of carbon monoxide evolved (ppm) and M is the mass of coal (g).

The results given in Table 39 show that up to coal temperatures of 150° C there is reasonable agreement between the rates of carbon monoxide evolution obtained

from the Thoresby, Hucknall and Wolstanton coals compared with those found by Chamberlain[100] and by Street,[103] bearing in mind the widely differing masses of coal and airflows employed. The lower evolution rates obtained by Chamberlain at higher temperatures can be explained by the experimental conditions the author used. For example, at a coal temperature of 150°C the oxygen concentration in the effluent gas had decreased to 14.75% and at 248°C had been almost completely consumed at 0.03%.

The dependence of carbon monoxide production on oxygen availability is clearly demonstrated from the experiments conducted in nitrogen (Tables 36-38), where much lower concentrations of carbon monoxide were observed than at the corresponding temperatures in air. The production of carbon monoxide from coal heated in nitrogen must result either from destruction of oxygen complexes from within the coal structure or from oxygen adsorbed by the coal substances during sample preparation and storage.

Any alternative method of assessing spontaneous combustion of equal or superior value to carbon monoxide might therefore be expected to relate closely or more sensitively to the pattern of evolution of carbon monoxide with temperature. Examination of Tables 33-38 shows that a number of hydrocarbons appear to give similar patterns of production to carbon monoxide.

To compare directly the rate of rise of these alternative indicators namely ethene, propene, benzene, toluene and methylcyclohexane and to give an appreciation of the temperature at which each can first be detected their

production as a function of temperature have been plotted and are shown graphically in Figures 37a-c and 38a-c. The maximum concentration of each indicator has been normalised to 100 units. When the three coals were heated in air (Figures 37a-c) the relative rate of rise of proposed indicators followed similar patterns to that of carbon monoxide except for the production of methylcyclohexane from the Thoresby and Hucknall coals. Methylcyclohexane production increased before a rapid rise in carbon monoxide and rose steadily up to the self ignition temperature. Generally, the proposed indicators showed significant increases in production above 150 °C. In nitrogen (Figures 37a-c) methylcyclohexane production again preceded carbon monoxide from the Thoresby coal but reached a maximum at 250° C. This peak in production was also observed for benzene and toluene and occurred from all three coals. Carbon monoxide, ethene and propene production rose steadily from 100° C up to the maximum temperature studied.

One unusual feature observed from the Thoresby coal was the significant increase in concentrations of higher molecular weight alkanes particularly at higher temperatures. This has also been observed by Vahrman et al[111] who identified alkanes in the range hexane to pentacosane, from a coal sample also from Thoresby Colliery, heated at 300 °C. The authors suggested that even these high molecular weight alkanes were held within the coals pore structure and were released on heating. However, geological data have shown that both samples were

taken from a coal seam associated with oil-bearing strata and this might account for the unusual pattern of high molecular weight alkanes observed.

A wider ranging analysis of the products evolved from the three test coals was undertaken using gas chromatography linked mass spectrometry. As in the previous study 5g of coal was heated in a tube furnace in an air flow of 500 ml min^{-1}. 100 ml samples of the effluent were collected using commercially available Tenax GC sampling tubes from each coal at 100 and 200°C. The complete analyses, in the form of reconstructed chromatograms, obtained from the total ion current, are shown in Figures 39a - 41a for the products evolved at 100°C, and Figures 42a - 44a for those evolved at 200° C. Figures 39b - 44b show expanded sections of the first 130 scans in more detail with peak identification given in Table 40.

It can be seen by examination of Figures 39b - 44b that, in contrast to the Thoresby coal, both Wolstanton and Hucknall coals produce relatively simple traces at both 100°C and 200 °C with the major products appearing in the first 130 scans. Although absolute quantification is difficult, it can be seen that for these two coals, benzene and toluene appear in the evolved products at both temperatures, and at the higher temperature they yield the largest peaks. The range of products evolved from the Thoresby coal is far more complex at both temperatures. Although benzene and toluene are still present as major products at 100 °C a large number of alkanes are also evolved, with production centred around tridecane. At

200°C an abundance of high molecular weight products are evolved with straight chain alkanes yielding major peaks. Other compounds present in significant quantities at this temperature included benzene, toluene and a number of substituted cycloalkanes.

The evolution patterns of hydrocarbons from heated coal can be explained if we assume that the products fall into three categories:

(i) The first group consists of alkanes which are held within the coal pore structure and emerge on heating primarily as desorption products. The effect of temperature on rate of desorption from the Hucknall coal heated in nitrogen can be seen from Table 37 where the maximum rates of desorption of ethane, propane, butanes and pentanes occurred at increasing temperatures. This trend can also be observed from the results of Chamberlain[100] shown in Table 3. Girling[106] also studied the rates of evolution of alkanes in the range butane to decane and found maximum rates of evolution occurred in two temperature ranges around 200°C and 400°C. Although alkanes are considered primarily to be desorption products the additional increase in concentrations found when the three test coals were heated in air must be attributed to their formation from coal oxidation.

(ii) The second group of products consists of aromatics and methylcyclohexane which are produced mainly from coal oxidation reaction mechanisms and to a

lesser extent from simple desorption. When the Hucknall coal was heated in nitrogen (Table 37) benzene, toluene and methylcyclohexane showed maximum rates of desorption at 250 ℃ producing concentrations of 1.86, 1.91 and 1.89 ppm respectively. When the coal was heated in air to 250 ℃, benzene, toluene and methylcyclohexane showed significant additional increase in production giving concentrations of 27.56, 31.73 and 9.71 ppm.

(iii) Finally, the third group of products includes ethene and propene, whose evolution patterns are similar to carbon monoxide, which are formed almost entirely from oxidation processes. In nitrogen their production from all three coals was minimal, rising slowly to the maximum temperature studied. However, in air, all three products showed significant increase in production particularly above 150°C.

Chamberlain[100] studied the production of ethene and propene in air and nitrogen (Table 3). In air, both products were detected at similar temperatures, giving similar rates of increase up to 233°C. Only ethene was observed in nitrogen at the maximum coal temperature examined. Any apparent discrepancies with the results obtained in this work can be attributed to the analytical detection limits of Chamberlain which for ethene and propene were 0.5 and 1.5 ppm respectively.

Of the hydrocarbons evolved from heated coal, ethene, propene, methylcyclohexane, benzene, toluene and higher aromatics have shown similar patterns of evolution to

carbon monoxide and therefore have the potential as alternative indicators for assessing spontaneous combustion activity underground.

3.2.2 Underground sampling programme

An underground sampling programme was undertaken involving collieries where there was a reasonably high probability of an incident of spontaneous combustion occurring. The results obtained from three collieries are given below:

a) Wolstanton Colliery

The district surveyed, 557's was an advancing coal face in the Cockshead seam. A diagram of the district and sampling points is shown in Figure 45. Twenty sets of samples were collected at regular intervals over a six month period and the results obtained are shown in Tables 41 and 42. Figures 46 and 47 show the products considered likely to be significant for intake and return respectively.

During this period, activity indicative of spontaneous combustion was discovered by monitoring a pack pipe, (a steel pipe 3m long which passed through the return roadside pack edge into the waste area) and this was therefore investigated from sample twelve onwards with the products of interest shown in Figure 48. Once again, the main results are given in Table 32.

Examination of Figure 46 indicates that the intake results give low concentrations of carbon monoxide and hydrocarbons which are considered to be normal background levels expected in a colliery intake.

The pack pipe results (Figure 48) show a reasonably constant level of carbon monoxide at 4000 ppm for samples twelve to sixteen followed by a decreasing trend for samples seventeen to twenty. This decrease is clearly reflected by a sharp fall in the benzene + toluene concentrations but this fall is less marked for methylcyclohexane and even less for ethene + propene except for sample twenty. An explanation for these trends is that the spontaneous combustion is cooling, with a consequent initial decrease in production of the higher molecular weight aromatic products followed by methylcyclohexane and finally ethene + propene. The fall in the oxidation ratio supports the explanation that activity is decreasing. The anomously low levels of ethene + propene and methylcyclohexane for sample fifteen can only be attributed to faulty charcoal tube sampling.

In the return (Figure 27) the carbon monoxide, after a small increase in concentration centred on sample two, showed a steady increase, from 10 ppm for sample five to 19 ppm for sample sixteen. The subsequent decrease, to 8 ppm for sample twenty reflects decreased activity in the pack pipe. The initial rise in carbon monoxide centred on sample two is also observed in ethene + propene and benzene + toluene and to a lesser extent in methylcyclohexane. The high carbon monoxide concentration in sample thirteen, thought to be due to short term colliery activity is not associated with spontaneous combustion, is also reflected in both

ethene + propene and methylcyclohexane concentrations but not in the benzene + toluene figure. This is probably caused by a difference in time of sampling. The decreasing trend in carbon monoxide concentrations for samples seventeen to twenty is reflected in the ethene + propene and in the benzene + toluene concentrations but not in the methylcyclohexane concentration.

The current method of assessing spontaneous combustion activity is based upon the concentration of carbon monoxide and the oxidation ratio

$$\text{oxidation ratio} = \frac{\text{carbon monoxide}}{\text{oxygen deficiency}} \times 100 \quad \ldots\ldots\ldots 3.2$$

An alternative method of indication of equal or superior utility might therefore be expected to relate to carbon monoxide.

The degree of association existing between carbon monoxide and each selected hydrocarbon has been estimated from its corresponding correlation coefficient (r). This measure has been calculated from the independent variables using the following expression.

$$r = \frac{1}{n} \frac{\Sigma(x - \bar{x})(y - \bar{y})}{SD_{(x)} \quad SD_{(y)}} \quad \ldots\ldots\ldots\ldots\ldots 3.3$$

where n is the number of data sets, x and $\bar{x}$ are the concentrations of carbon monoxide in ppm and the mean value respectively and y and $\bar{y}$ are the corresponding values of the component of interest, and SD is the respective standard deviation.

For computation purposes this expression was rewritten

as follows:

$$r = \frac{\Sigma(x - \bar{x})\,(y - \bar{y})}{\sqrt{\Sigma(x - \bar{x})^2\ \Sigma(y - \bar{y})^2}} \qquad \text{.....3.4}$$

A value approaching to plus 1 indicates a high positive correlation.

The values obtained from the return outbye end and pack pipe samples (Tables 42 and 43) are given below:

First factor	Second factor	Correlation coefficient	
		Return	Pack pipe
Carbon monoxide	Ethene+propene	0.876	0.693
Carbon monoxide	Benzene+toluene	0.131	0.795
Carbon monoxide	Methylcyclohexane	0.280	0.754

The results for ethene + propene and methylcyclohexane from the pack pipe, sample fifteen, were inexplicably low and have been attributed to faulty sampling. By omitting these figures ethene + propene and methylcyclohexane gave improved correlation coefficients of 0.740 and 0.852 respectively.

b) Thoresby Colliery

The district surveyed was 200's, an advancing coal face working in the Top Hard seam. A lay-out of the district and sampling points are shown in Figure 49. It was known that this district was heavily contaminated by ingress of natural mineral oil, and it was found on analysis that the relatively high concentrations of high molecular weight alkanes interfered with the quantitative measurement of aromatic products and it is therefore not possible to quote accurate concentrations of these compounds.

Shortly after the survey was undertaken an incident of spontaneous combustion occurred and a rapid deterioration of the situation necessitated abandoning the working area and completely sealing off the district.

The results obtained for the seven surveys undertaken prior to sealing off the district are given in Table 44 and Figure 50, and show an increasing trend in the concentration of carbon monoxide from 28 ppm to 59 ppm which was also reflected by an increasing oxidation ratio. This trend was also followed by ethene + propene which increased from 0.43 ppm up to a maximum of 2.06 ppm, however, methylcyclohexane showed no such trend and actually decreased during the first half of the monitoring programme. No explanation can be found for this behaviour. Because of the increasing trend in carbon monoxide production the district was sealed off, but regular sampling of the gas behind the return stopping continued for a further six week period and the results obtained are shown in Table 45 and Figure 51. Figure 51 shows that the concentrations of ethene + propene and methylcyclohexane closely follow the pattern of carbon monoxide production during this period. This is clearly illustrated by the dramatic increase shown in production of all compounds of interest and the oxidation ratio from the samples taken thirty days after sealing off. This has been attributed to an increase in the activity behind the sealed area. Whilst carbon monoxide and methylcyclohexane showed approximately

three fold increases in concentration ethene + propene exhibited a five fold increase. The correlation coefficients between the selected indicators and carbon monoxide before and after sealing off are shown below:

First factor	Second factor	Correlation coefficient	
		Before sealing	After sealing
Carbon monoxide	Ethene+propene	0.976	0.974
Carbon monoxide	Methylcyclohexane	-0.410	0.971

c) Daw Mill Colliery

The district studied was 62's an advancing coal face working in the Warwickshire Thick seam. Fifteen sets of samples were collected at regular intervals in the general body of the return air.

The results obtained are shown in Table 46 and Figure 52. Delays at the colliery meant that for the first three samples the coal face was not in full production and this is reflected by the low concentrations of carbon monoxide and hydrocarbons found. Following the start of full production (Sample 4), carbon monoxide showed an increase in concentration from 3 to 7 ppm and remained at the higher concentration throughout the survey. Although this rise is attributed to increased coal oxidation the situation was considered normal as indicated by the oxidation ratio. Ethene + propene and benzene + toluene also showed increases in concentration at the start of production although initially were less marked than carbon monoxide. Methylcyclohexane showed no such increase in concentration until sample six after

which time it closely followed the pattern of carbon monoxide production. A possible explanation for the above trends is that as the coal temperature rises due to increased oxidation, carbon monoxide is initially evolved and as the coal temperature increases further, ethene + propene and benzene + toluene are produced, followed by methylcyclohexane. The correlation coefficients between carbon monoxide and the selected indicators are shown below:

First factor	Second factor	Correlation coefficient
Carbon monoxide	Ethene+propene	0.802
Carbon monoxide	Benzene+toluene	0.838
Carbon monoxide	Methylcyclohexane	0.828

d) Investigation of diesel exhaust and shotfiring fumes

Investigations of the composition of diesel exhaust and shotfiring fumes were carried out underground to determine whether selected hydrocarbons could have a role in differentiating between carbon monoxide produced by spontaneous combustion and carbon monoxide from these other legitimate mining operations.

A joint survey of diesel and shotfiring fumes was undertaken at Linby Colliery. The diesel locomotive was powered by a 28 H.P. Hunslet engine operating in the High Hazles seam and the locomotive garage. Shotfiring was undertaken in 19's intake using 5 Kg of Penobel explosive (type P4/5), and sampling of the fumes was performed in 19's return. Background samples were collected to give an indication of normal ambient

concentrations.

The results obtained from the diesel exhaust survey (Table 47) show clearly the expected increase in carbon monoxide production and oxidation ratio during diesel operations. These increases can lead to false alarms in the detection of spontaneous combustion by conventional monitoring methods. Unfortunately the increase in ethene + propene and methylcyclohexane was of the same order as that produced during spontaneous combustion (cf Thoresby colliery incident, Table 44). Therefore in this case, the use of these gases to differentiate between carbon monoxide produced during spontaneous combustion and carbon monoxide from diesel exhaust fumes would not be feasible. High molecular weight alkanes were found to be present on the chromatographic trace which due to co-elution interfered with the quantitative measurement of aromatic products and it is therefore not possible to quote accurate concentrations for these compounds.

As with the diesel engine exhaust fumes the results obtained from the shotfiring exercise, (Table 47) illustrated the increase in carbon monoxide production which occurred. There was again a significant increase in ethene + propene concentrations of the same order to that in the diesel fume investigation, with benzene + toluene showing a smaller increase. However, the concentration of methylcyclohexane did not increase significantly during shotfiring and therefore it might be useful for characterising this source of underground

contamination.

In conjunction with the surveys described above, further samples were collected one metre from the diesel exhaust delivery and shotfiring fumes were sampled for analysis using gas chromatography linked mass spectrometry. The results are given in Tables 48 and 49 and the reconstructed ion chromatograms are shown in Figures 53 and 54.

The diesel exhaust sample (Figure 53) produced a very complex trace with the major feature being the production of normal alkanes in the range C_{10} -C_{18}, which are presumed to originate from the incomplete combustion of diesel fuel. A wide range of branched aliphatic hydrocarbons and aromatic species were also identified with benzene and toluene present as the main aromatic constituents of diesel exhaust fumes.

The trace shown in Figure 53, when compared with Figure 54, shows clearly the difference between diesel and shotfiring fumes and illustrates for shotfiring fumes, the complete absence of high molecular weight compounds. The only class of compounds which appear to be peculiar to shotfiring fumes are alcohols (peak numbers 1, 2, 5 and 7) the source of which is likely to be explosive rather than any locally heated coal.

3.2.3 Low molecular weight sulphur compounds produced from coal heated in the laboratory

The test coals and heating regime used were identical to that described in Section 3.1. Samples of effluent gas

from the combustion apparatus were collected on to Molecular sieve 5A sampling tubes for the analysis of hydrogen sulphide, carbonyl sulphide, sulphur dioxide and carbon disulphide. At each temperature a pressure capsule sample was also taken for the analysis of carbon dioxide, carbon monoxide, methane and oxygen. The results from this series of experiments are shown in Tables 50 and 51, and to give an appreciation of the temperature of appearance and relative rate of rise of each compound their production against temperature are shown graphically in Figures 55-56a-c where the maximum concentration of each compound is normalised to 100 units.

A brief summary of the chemistry of the selected sulphur compounds and their stability may help explain their patterns of production from heated coal.[283,284]

When carbon is heated with sulphur it forms the sulphide, carbon disulphide, (CS_2) additionally whenever carbon, oxygen and sulphur, or their compounds such as carbon monoxide, carbon disulphide and sulphur dioxide are brought together at elevated temperatures carbonyl sulphide (COS) is formed.

The subsequent reactions are determined by the equilibria

$$COS \longrightarrow CO + S \quad \text{and} \quad 2COS \longrightarrow CO_2 + CS_2$$

The quantities present in the equilibrium mixture at atmospheric pressure are as follows:

Temperature C	100	200	300	400
CO + S	-	-	-	-
CO_2 + CS_2	19	27	34	39
Unchanged COS	81	73	66	61

The physical properties of COS are intermediate between CS_2 and CO_2. It is an odourless gas unlike CS_2 which in the presence of moisture acquires its well known musty odour. Sulphur dioxide can be formed by heating sulphur or certain sulphides for example pyrites, in air. It is a reactive gas that can be readily adsorbed on to activated charcoal and its solubility in water at 30° C is 26.8 volumes per volume of water. It is a well known irritant gas producing lachrymatory irritation with an odour threshold of 0.5 ppm.[129]

Hydrogen sulphide can be produced by passing steam over heated iron sulphide, or when organic compounds rich in hydrogen, such as paraffins, naphthalenes and resins, are heated in the presence of sulphur. The gas has the characteristic smell observed during the putrefaction of eggs and has an odour threshold of less than 0.01 ppm.[129] As with sulphur dioxide it can be adsorbed by activated charcoal and is soluble in water (2.3 volumes per volume of water at 30°C).

The experimental results show that below 150° C all the sulphur compounds identified were present at concentrations below 1 ppm. Above this temperature, increases in concentrations were observed. For example, when the Thoresby coal was heated in air (Table 50) carbonyl sulphide and carbon disulphide exhibited a 150

and 50 fold increase in concentration respectively between 150°C and 250°C and sulphur dioxide gave a 140 fold increase between 175°C and 250°C. The production of sulphur dioxide below 175 °C may be masked due to its reaction with water, which was being evolved simultaneously. Hydrogen sulphide was not produced in significant quantities at any temperature being present in less than 1 ppm at the maximum temperature studied.

Figures 55a-c show that the pattern of carbonyl sulphide and carbon disulphide production from the three coals heated in air were very similar to carbon monoxide whilst the relative production of sulphur dioxide increased more rapidly above 200°C. When the three coals were heated in nitrogen (Table 51) the production of hydrogen sulphide and sulphur dioxide increased significantly above 250°C being present as major products at 300° C. Again carbonyl sulphide and carbon disulphide showed similar patterns of evolution to carbon monoxide (Figures 56a-c) rising steadily with increasing temperature, being present at lower concentrations than at the corresponding temperatures in air.

Two further coals were investigated to determine whether the patterns of sulphur compound production were affected by the relative proportions of pyritic sulphur present. Pyritic sulphur was chosen because of its wide variability in bituminous coal.

i. Mansfield Colliery, Deep Soft seam, with a total sulphur content of 0.86%, containing 0.09% pyritic and 0.73% organic sulphur.

ii. Harworth Colliery, Deep Soft seam, with a total sulphur content of 2.38%, containing 1.40% pyritic and 0.95% organic sulphur.

The balance in each case was inorganic sulphur.

The results given in Tables 52 and 53 show that both coals gave similar patterns of evolution to the three test coals with sulphur dioxide and carbonyl sulphide being the major sulphur-containing products evolved in air, with hydrogen sulphide production being highest in oxygen deficient conditions. At the highest temperature studied the production of sulphur dioxide from the Mansfield coal in both air and nitrogen was significant, reaching 7.7% and 39.0% of the carbon monoxide concentration respectively. The concentrations of products evolved from both coals were similar which would suggest that their production was not influenced by the pyritic sulphur content, but probably resulted from decomposition of the organic sulphur.

Of the sulphur products evolved from heated coal carbonyl sulphide and carbon disulphide have exhibited similar patterns of evolution to carbon monoxide whilst sulphur dioxide was produced in significant concentrations in both air and nitrogen atmospheres. Therefore, these products have the potential as alternative indicators for assessing spontaneous combustion activity underground.

3.2.4 Underground sampling programme

a) Bentinck Colliery

An incident of spontaneous combustion occurred in the

face start line area of K50's district, in the Blackshale seam and the production of sulphur containing compounds was assessed in addition to the normal analysis for the permanent gases. The incident was detected by the increasing concentration of carbon monoxide monitored in a steel pack pipe located into the face start line area. Initially samples were collected underground, however, the pack pipe was connected to the colliery tube bundle monitoring system allowing samples to be collected more conveniently on the colliery surface. The results obtained over a thirty six day period are shown in Table 54. Analysis of samples collected underground on to Molecular sieve 5A sampling tubes confirmed that carbonyl sulphide and carbon disulphide were the only sulphur containing species present as products of combustion from the incident. Although the laboratory studies indicated that sulphur dioxide would be useful as a spontaneous combustion indicator being produced at concentrations much greater than any other sulphur compound its absence in the underground environment is considered to be due to its high reactivity and solubility in water, making its long term survival in the mining environment extremely unlikely. Sulphur dioxide is a known irritant, producing lachrymatory irritation at concentrations below 20 ppm,[283] however, no effects of this nature have ever been reported by personnel involved with spontaneous combustion incidents.

Once the pack pipe had been connected to the colliery

tube bundle system (Sample 6), samples could be collected more conveniently on the surface, although there was a delay time in excess of sixty minutes due to the distance the sample had to be pumped from underground. To ensure that no losses of carbonyl sulphide or carbon disulphide occurred in the pipework of the monitoring system a comparison of the concentrations found in samples collected underground with those taken through the monitoring system was periodically carried out during the survey and the results obtained showed good agreement (Table 54).

The concentrations of selected products and the oxidation ratio obtained over the thirty six day monitoring period are shown in Figure 57. The production of carbonyl sulphide showed a similar pattern to carbon monoxide rising throughout the survey with the concentration of carbonyl sulphide being present at approximately four orders of magnitude lower than carbon monoxide. This ratio was lower than that found in the laboratory from the Thoresby and Hucknall coals heated in air but was similar to that from the Wolstanton coal. Throughout the survey carbon monoxide rose more rapidly than carbonyl sulphide although the general trend was very similar giving a correlation coefficient of 0.958. Carbon disulphide concentrations, however, did not show a similar trend and remained reasonably constant in the range 0.31-0.65 ppm over the whole period. This finding is not in agreement with results obtained earlier from heated coal in the laboratory, but may be attributed to

the poor stability of carbon disulphide.

b) Warsop Colliery

A steel pack pipe located in the face start line area of U19's district in the Deep Soft seam was surveyed. Twenty one samples were collected for the analysis of the permanent gases and thirteen for the analysis of sulphur containing compounds. The main results obtained are shown in Table 55 and Figure 58. Abnormal activity was known to be occurring in the face start line area and this was confirmed by analysis of the first sample which gave a concentration of 10000 ppm carbon monoxide and an oxidation ratio of 5.55.

The following seven samples showed a general decrease in the concentration of carbon monoxide to 7800 ppm reflecting decreased activity within the area. However, this was followed by a rapid increase in intensity giving a maximum concentration of 14000 ppm and an oxidation ratio of 7.06 for sample thirteen. The subsequent decrease to 2000 ppm for samples eighteen to twenty-one indicated that the spontaneous combustion was cooling and the situation was under control.

Figure 58 shows that throughout the survey the concentrations of carbonyl sulphide closely followed the pattern of carbon monoxide production giving a maximum concentration of 1.355 ppm for sample thirteen with a correlation coefficient of 0.995. Once again the concentrations of carbonyl sulphide were approximately four orders of magnitude lower than carbon monoxide. In contrast to the previous survey the production of carbon

disulphide generally followed the same pattern as carbon monoxide, although the decreasing trend from day thirteen is less marked, giving a correlation coefficient of 0.943. Compared with the previous survey which showed only a gradual increase in activity, the increase in this incident was very rapid with the concentration of carbon monoxide rising from 7800 to 14000 ppm over two days. This may account for the differences in the pattern of production of carbon disulphide observed from the two surveys.

Many descriptions have been attributed to the odour produced during incidents of spontaneous combustion, including a musty or mercaptan like smell. In the past this odour has been thought to be associated with the evolution of hydrogen sulphide, however, the results from the above two surveys indicate that this odour is likely to result from the production of carbon disulphide.

c) General body mine environment

Two underground districts which were known to be in areas prone to spontaneous combustion were selected to study the fluctuations in carbonyl sulphide, carbon disulphide and carbon monoxide concentrations in the general body of the mine environment during normal mining operations. Colliery details and the range of results obtained over a twelve week period are given on the following page.

Samples collected at weekly intervals showed that the concentrations of carbon monoxide remained reasonably

Colliery	District	Seam	Carbonyl sulphide ppb	Carbon disulphide ppb	Methane %	Carbon monoxide ppm	Oxidation ratio
Thoresby	201's return	Top Hard	7-9	5	0.37-0.64	11-12	0.22-0.28
Shirebrook	15's return	Piper	10-15	5	0.32-0.95	12-15	0.21-0.32

constant with no indication of abnormal activity at either site. The concentrations of carbonyl sulphide were also reasonably constant being present in the general body of mine air at approximately three orders of magnitude lower than that of carbon monoxide. This ratio was higher than that found in the pack pipe surveys described earlier, although the two situations are not directly comparable, because abnormal activity was occurring in both pack pipes and the source of products were from confined areas. Carbon disulphide was not detected from any of the samples, from either site, therefore some doubt must be cast upon its long term stability in the general body of the mine environment.

d) Investigation of diesel exhaust and shotfiring fumes

A number of exercises were undertaken to investigate the presence of sulphur containing compounds from diesel exhaust and shotfiring fumes. Two diesel locomotives were studied, firstly a Hudwood No. 4 fitted with a 100 BHP direct fuel injection engine, operating in the locomotive garage at Linby colliery, and secondly a Clayton 150 BHP indirect fuel injection engine operating in the locomotive garage at Bevercotes colliery. Samples were collected from both diesel engines, directly from the exhaust before dilution and approximately one and five metres from the exhaust outlet. Shotfiring fumes were collected during two separate events at Rufford colliery.

The results from the diesel exhaust surveys are given in Table 56a. Two locomotives were studied, the first operating under both idling and load conditions. Carbonyl sulphide was the only sulphur compound detected and was present in the undiluted exhaust fumes under idling and load conditions at 0.10 and 0.18 ppm respectively with corresponding carbon monoxide concentrations of 550 and 1450 ppm. The laboratory experiments on heated coal showed the higher concentration of carbon monoxide could be associated with a carbonyl sulphide concentration of approximately 2 ppm (Table 50, Hucknall coal). In the samples collected one and five metres from the exhaust enclosure, the concentration of carbonyl sulphide had been diluted to the normal background level. The second diesel locomotive was studied under idling conditions only and as expected carbon monoxide was present at a high concentration in the fumes from the exhaust direct. In contrast the concentration of carbonyl sulphide was very low, especially when compared with the laboratory experiments on heated coal.

Both the above surveys indicate that carbonyl sulphide is a trace gas capable of differentiating between spontaneous combustion of coal and diesel fumes as the source of carbon monoxide production by virtue of the value of the CO/COS ratio.

The results from the two shotfiring surveys (Table 56b) show carbon monoxide present in significant quantities in the general body of mine air with an exceptionally

high concentration of 1450 ppm being measured on one occasion. In no case was there a significant increase in carbonyl sulphide concentrations above the ambient level.

This indicates that, as with diesel exhaust fumes, carbonyl sulphide is suitable as a means of differentiating this source of carbon monoxide production from that produced during spontaneous combustion.

3.2.5 Aldehydes and Ketones produced from coal heated in the laboratory

The laboratory combustion apparatus and heating regime described in Section 3.1 were employed to study the production of this range of compounds from the Hucknall coal heated in air only.

At 50 °C intervals, a one litre sample of the effluent gas was drawn through the DNPH/silica-gel sampling tubes at a rate of 600ml min^{-1}. At each temperature a pressure capsule sample was collected for the analysis of permanent gases. The results of this study are given in Table 57. Formaldehyde, acetaldehyde, crotonaldehyde and acetone were detected as combustion products evolved from the heated coal. The relative productions of these compounds as a function of coal temperature are plotted with carbon monoxide in Figure 59, with the maximum concentration of each normalised to 100%. Figure 59 shows that acetone production increased at a lower temperature than carbon monoxide and continued to rise giving a maximum

concentration of 11.7 ppm at 250° C. Formaldehyde, acetaldehyde and carbon monoxide exhibited rapid increases in production above 150 °C and crotonaldehyde above 200 °C, with acetaldehyde being the major carbonyl compound present at 250 ° C. Generally the concentrations of products produced at temperatures likely to be critical in the early stages of spontaneous combustion (up to 250° C) are one to two orders of magnitude lower than the corresponding carbon monoxide concentrations.

The production of this range of compounds from heated coal has been confirmed by recent work on the thermal and oxidation chemistry of coal at low temperatures.[247] A test coal was oxidised at 100°C and infra-red spectrophotometry indicated the formation of a wide range of carbonyl containing species, the most abundant being ketones, aldehydes, esters and ethers. The author suggested mechanisms based on hydro-peroxide decomposition reactions, which are postulated to occur in coal oxidised at low temperatures.

3.2.6 Underground sampling programme

a) Warsop and Bentinck collieries

No incidents of spontaneous combustion occurred during the sampling programme, however, samples were collected underground from pack pipes known to contain significantly different concentrations of carbon monoxide and oxygen. One pack pipe at Warsop colliery was surveyed and three separate pipes at Bentinck colliery. The main results are given in Table 58.

The results from the Warsop pack pipe show acetone to be the only carbonyl species detected being present at 0.12 ppm. Although the pack pipe had previously indicated abnormal activity, routine monitoring over an extended period had shown relatively constant carbon monoxide concentrations indicating that very little activity was then occurring. The low acetone/carbon monoxide ratio (2.9×10^{-5}) may therefore be due to the stagnant nature of this gas and thereby indicative of little coal oxidation activity.

In the Bentinck colliery samples the acetone figures ranged between 0.18 and 0.76 ppm with carbon monoxide concentrations significantly lower (57-470 ppm) than at Warsop colliery, producing acetone/carbon monoxide ratios in the range 1.6×10^{-3} - 3.2×10^{-3}. Taking into account the widely differing carbon monoxide and oxygen concentrations in the three Bentinck colliery pack pipes the acetone/carbon monoxide ratios are reasonably constant and therefore may provide useful information regarding the degree of coal oxidation occurring.

Additionally, acetaldehyde was detected in all three pack pipes, albeit at lower concentrations than acetone. From this limited number of samples the production of acetaldehyde appears to be related to the oxygen content present, increasing in concentration at higher oxygen levels. This relationship may again be indicative of the extent of coal oxidation taking place. Unfortunately, due to lack of time no further work could

be undertaken to provide more data.

b) General body mine environment

Two underground districts were selected for this study, however, during the survey period no abnormal activity occurred at either site. Colliery details and the range of results obtained over a four week period are given on the following page.

The results from Bentinck colliery show that whilst there is only a small increase in acetaldehyde concentrations between intake and return there is a significant increase for acetone, with a mean concentration of 0.01 ppm in the intake and 0.112 ppm in the return. This increase is similar to that of carbon monoxide which increased due to normal mining operations from 1 to 10 ppm. Acetone and acetaldehyde were also present in the Shirebrook colliery samples and from the limited amount of data collected there does appear to be some correlation between the small fluctuations in carbon monoxide concentration and those of acetone and acetaldehyde.

c) Investigation of diesel exhaust and shotfiring fumes

Studies were performed to investigate the presence of carbonyl containing species from diesel and shotfiring fumes. The diesel locomotive studied was again a Clayton 150 H.P. indirect fuel engine operating at idling speed in the locomotive garage at Bevercotes colliery. Samples were collected from a shotfiring plume at Linby colliery, South intake heading.

The results obtained from the diesel exhaust survey

Colliery	District	Seam	Acetone ppm	Acetaldehyde ppm	Methane %	Carbon monoxide ppm	Oxidation ratio
Bentinck	69's intake	Blackshale	0.008-0.012	0.003-0.006	0.02-0.04	1 - 2	0.15-0.21
	69's return	"	0.110-0.113	0.007-0.010	0.43-0.62	9 - 11	0.29-0.31
Shirebrook	15's return	Piper	0.018-0.120	0.012-0.053	0.74-1.03	8 - 15	0.30-0.35

(Table 59) show that the three major products evolved from heated coal, namely formaldehyde, acetaldehyde and acetone are also the major carbonyl containing species present in diesel exhaust fumes, albeit at much lower concentrations relative to carbon monoxide. In the sample collected 5 metres from the exhaust enclosure, the concentrations of all three carbonyl compounds had been diluted to the normal background level, whereas carbon monoxide was still present at a significantly higher concentration, than the background.

As with the diesel exhaust survey the results from the shotfiring survey (Table 59) shows that the resultant plume contained formaldehyde, acetaldehyde and acetone, the highest concentration of all three being associated with the highest carbon monoxide concentration, indicating that they are all products of shotfiring activity.

3.2.7 Other gases of interest produced from coal heated in the laboratory

The experimental conditions described in Section 3.1 were employed to study the production of hydrogen, methane, hydrogen chloride and oxides of nitrogen from the three test coals heated in air and nitrogen. At each temperature studied a pressure capsule sample was collected for the analysis of permanent gases. The main results are given in Tables 60 and 61.

The results show that the concentration of hydrogen chloride evolved from all three coals heated in air

increased rapidly above 150° C producing a maximum concentration of 220 ppm from the Thoresby coal at 250 °C (Table 60). This figure corresponds to approximately 7% of the associated carbon monoxide concentration.

In nitrogen, hydrogen chloride was not evolved until a coal temperature of 200 °C, with the production from all three coals being significantly lower than in air, giving a maximum concentration of 12 ppm at 300 °C from the Thoresby coal (Table 61). Pearce,[285] who studied the mode of occurrence of chlorine in British coal observed the chlorine loss as hydrogen chloride to be similar in air and nitrogen with a threshold temperature of 180° C. However, these findings are not in agreement with Edgecombe[286] who suggested that chlorine loss from coal involved oxidation reactions. This work confirms that of Edgecombe and supports suggestions that chlorine is present in coal in one form and the bonding is sufficiently labile to be evolved as hydrogen chloride at temperatures above 150 °C.

Hydrogen was first observed at coal temperatures of 175° C and 250 °C in air and nitrogen respectively and increased in concentration up to the maximum temperature studied. The production of hydrogen from all three coals was found to be significantly higher in air than at the corresponding temperature in nitrogen. The production of hydrogen from coal heated under oxidising and reducing atmospheres has been studied by other workers[100,103] who also noted its dependence upon temperature and oxygen availability. Studies by Clay et al[287] showed that the

ratios of hydrogen to carbon monoxide produced from a range of coals heated in air were 0.05 at temperatures below 400°C. However, it is known that at carbonisation temperatures, (800° C-1000° C) the production of hydrogen can be very significant.

The production of nitrogen dioxide and nitric oxide from the test coals was below the detection limit of the method employed. This is not unexpected, since these products are known to be combustion products of high temperature oxidation, however, their production was studied to ensure that neither product was being formed by catalytic reactions.

The production of methane was not studied in detail because of the unknown extent to which the gas may have naturally desorbed from the test coals during sample collection, preparation and storage. It is therefore difficult to draw any firm conclusions as to its true pattern of production. Chamberlain [100] was able to show that above 100° C the pattern of production was unpredictable with increased production due to oxidation processes in one case and in another methane evolution was identical in air and nitrogen. Methane is known to occur naturally underground and its concentration varies with many factors including ventilation quantity, barometric changes, rate of coal cutting and the influence of adjacent seams, therefore any small change in concentration arising from an incident of spontaneous combustion would be obscured by these other factors.

3.2.8 Underground Sampling Programme

a) Bentinck and Warsop Collieries

Surveys were undertaken in conjunction with the exercises described earlier on the pack pipes at Bentinck and Warsop collieries (Section 3.2.4 a), and the main results obtained are given in Table 62. The laboratory results indicated that at a coal temperature of 250 °C the concentration of hydrogen chloride from all three coals was approximately 7% of the associated carbon monoxide figure. If this ratio were to be found underground, hydrogen chloride would be detectable at its lower limit of detection (0.1 ppm) when the carbon monoxide concentration exceeded 1 ppm. The results from both surveys showed that hydrogen chloride was not detected, even in the Warsop pack pipe where the carbon monoxide concentration exceeded 10000 ppm. It would therefore seem reasonable to suggest that hydrogen chloride is not detectable in the underground environment for reasons which are similar to those already suggested for sulphur dioxide, namely its high reactivity and solubility in water.

In the laboratory, analysis was performed immediately after production, whereas underground there is a much greater opportunity for any reactive gas to disappear due to surface reactions and condensation.

Although oxides of nitrogen were not detected as combustion products from coal heated in the laboratory, their existence underground was investigated using

Draeger stain tubes, type 0.5A. The production from both pack pipes was below the limit of detection of 0.5 ppm during the whole survey.

Figure 60 shows the concentration of hydrogen, carbon monoxide and oxidation ratios obtained from the Bentinck colliery pack pipe. During the first fifteen days of the survey the carbon monoxide concentration and oxidation ratio increased significantly from 24 to 1550 ppm and 0.01 to 0.98 respectively, whereas the hydrogen concentration increased from only 5 to 30 ppm over the same period. This was followed by a rapid increase in hydrogen production producing a maximum concentration of 340 ppm on day twenty-two. Carbon monoxide also increased in concentration over this period, however, its rate of production was lower than hydrogen. The pattern of production of both gases during the remainder of the survey were similar, although the production of hydrogen fluctuated to a greater extent than carbon monoxide. Both gases gave a correlation coefficient of 0.925 for the whole survey. A possible explanation of the above trends is that during the early part of the survey the coal involved in the incident was at a temperature at which carbon monoxide was produced in significant quantities but not hydrogen. The laboratory studies showed that below coal temperatures of 175° C hydrogen production was negligible. As the incident progressed and the coal temperature increased the production of hydrogen becomes significant.

In conjunction with this investigation Davies[288] performed further work to study the concentration of hydrogen and carbon monoxide produced and oxygen consumed from coal samples heated under controlled laboratory conditions. Analysis of these gases has allowed an expression, the Temperature Estimation Coefficient (TEC) to be formulated which exhibited a linear relationship with coal temperature.

$$TEC = Log\left[\frac{Log\ ([CO] \times 10) \times log\ ([H_2] \times 10)}{Log\ ([O_2] \times 100)}\right] \quad ....3.3$$

where

CO = concentration of carbon monoxide in parts per million

H_2 = concentration of hydrogen in parts per million

O_2 = concentration of oxygen in parts per million

The form of the best fit straight line produced:

$$Y = 0.0038X - 0.531$$

In order to assess the applicability of the equation to larger scale combustion a gas analysis and associated temperature measurement was obtained from the Homefire Smokeless Fuel Plant, Coventry. This represented the composition of top gases from a fluidised bed retort (4m diameter by approximately 18m high) during the controlled combustion stage of the fuel manufacture. The temperature of the retort was maintained close to 420 °C during operation.

Reported analysis -

N_2 %	CO_2 %	CH_4 %	O_2 %	CO ppm	H_2
83.3	8.6	3.1	0.3	3000	2000

Application of the TEC to the analysis yielded an estimated temperature of 433 ° C. Therefore, the expression has been applied to the results from underground surveys to see whether it is capable of predicting the temperature of coal involved in underground incidents.

At the start of the survey the expression gave a predicted coal temperature of 220 ° C, thereafter increasing steadily up to 290 °C on day fifteen. The rapid increase in hydrogen concentration which followed this period is associated with a predicted increase in temperature of 50 °C up to 340 °C. For the remainder of the survey the coal temperature was estimated to fluctuate less than 10° C. These predictions indicate that hydrogen is a high temperature product of combustion whose production is extremely temperature dependent, for example, its concentration increased over ten fold for an increase in coal temperature from 290 °C to 340 °C.

The main results from the second survey performed on the pack pipe at Warsop colliery are shown in Figure 61. A general decrease in the production of both hydrogen, carbon monoxide and the oxidation ratio was observed during the first eleven days of the survey, which resulted in an overall decrease in the estimated

temperature from 390° C to 370° C. This period was followed by a rapid increase in intensity centred on day thirteen producing maximum concentrations of 14000 and 5200 ppm carbon monoxide and hydrogen respectively, corresponding to an increase in the predicted temperature from 370° C to 410 °C. As with the previous survey the rate of production of carbon monoxide during this latter period was lower than hydrogen. The subsequent decrease in concentration of both gases was associated with a reduction in the predicted temperature to a minimum of 360 °C at the end of the survey. The inter-relationship between the two gases resulted in a correlation coefficient of 0.925.

The above confirms suggestions made earlier that hydrogen is a high temperature product of combustion. At this stage it is not possible to judge how closely the temperature estimates from the underground surveys relate to the true coal temperature, although the one example from the Homefire Plant is encouraging, and it appears that the production of hydrogen can be related to the varying temperature during an incident. The need to assess coal temperature during spontaneous combustion is an important factor when considering the possible ignition or explosion hazards whilst work is continuing to consolidate the incident.

Methane is the principle constituent of firedamp which is found naturally occurring in coal mines. Its concentration is known to vary with the ventilation quantity, barometric changes, rate of coal cutting and

the influence of adjacent seams. Lower hydrocarbons are also present in association with the methane as minor constituents totalling approximately five per cent of the methane. Any small change in the concentration of methane or lower hydrocarbons arising from an incident of spontaneous combustion would be obscured by these other sources of production. The pattern of production of methane has been studied in all the exercises described in this section.

Tables 41-46 show how the lower hydrocarbons, ethane and propane varied with the methane during normal and abnormal activity. As suggested, no relationship between these gases and the degree of activity occurring could be established, although the percentage of ethane and propane found in association with methane was significantly higher than five per cent on many occasions. No further detailed study of these gases was made during this investigation.

b) General body mine environment

The production of hydrogen in particular was studied in parallel with the surveys described earlier at Thoresby and Shirebrook collieries (Section 3.2.4 c). Samples collected at weekly intervals showed that the concentration of carbon monoxide remained reasonably constant in the range 12-15 ppm with no indication of abnormal activity. Both the laboratory studies and underground surveys have indicated that under normal conditions hydrogen production should be negligible. Samples collected for the analysis of hydrogen confirm

the above, being present at less than 2.5 ppm during the whole survey period. Wynne[289] obtained some background information concerning the concentration of hydrogen present in British coal mines. The author found hydrogen present in the general body return air at two separate collieries, at a level of 1.35 and 1.50 ppm with corresponding carbon monoxide concentrations of 9.0 and 8.0 ppm respectively. Applying the expression suggested by Davies to predict coal temperature to these figures produces a temperature of approximately 90 °C at both sites. It is considered that the predicted temperature may be over-estimated since any oxidation occurring in an unaffected area would be expected to be taking place at a lower temperature in the region of 40°C.

c) Investigation of diesel exhaust and shotfiring fumes

Samples were collected for analysis during the previous diesel and shotfiring exercises described earlier at Bevercotes and Linby collieries (Section 3.2.6 c). The results show that both activities resulted in the production of hydrogen and oxides of nitrogen in association with the expected increase in concentration of carbon monoxide. When sampled directly from the diesel locomotive exhaust, hydrogen and oxides of nitrogen were present at 15 and 100 ppm respectively in association with 870 ppm carbon monoxide. The resultant shotfiring plume produced maximum concentrations of 25 and 50 ppm hydrogen and oxides of nitrogen with the highest carbon monoxide concentration of 235 ppm.

3.3 Summary

The combustion products evolved from three different coals heated in air and nitrogen have been studied under carefully controlled laboratory conditions. This has allowed information concerning the appearance temperatures and evolution patterns of products produced from heated coal to be established. Three distinct patterns of evolution have been observed and several products not previously considered to be present in the temperature range studied have been identified. A number of products have been identified that exhibit similar patterns of evolution to carbon monoxide and therefore, showed potential as alternative indicators of spontaneous combustion.

Underground studies have been carried out at selected collieries during normal and abnormal activity to determine the presence and evolution patterns of products identified in the laboratory studies of possible alternative indicators of spontaneous combustion. The existence underground of a number of the proposed indicators has been demonstrated, albeit at lower concentrations than carbon monoxide and their evolution patterns during incidents of spontaneous combustion have been investigated in detail. Many of these products were also found in association with carbon monoxide as products of combustion from diesel locomotive exhausts and shotfiring fumes, which precludes their immediate use as unambiguous indicators of spontaneous combustion. However, it has been shown that ratios of different products to carbon monoxide, particularly H_2/CO and to one another may reveal

more information about the degree of activity and extent of oxidation of individual incidents.

Other products, for example, sulphur dioxide and hydrogen chloride have been found in significant quantities from coal heated in the laboratory in concentrations that increase with temperature, but these have not been observed underground. It is considered that this is due to their reactivity which makes survival in the mining environment extremely unlikely.

Carbonyl sulphide has been found to be the only combustion product that produces a similar pattern of evolution to carbon monoxide from both coal heated in the laboratory and during incidents of spontaneous combustion but does not appear to increase significantly during diesel locomotive and shotfiring activities. Therefore, it would appear that carbonyl sulphide has the potential to be used as an unambiguous indicator of spontaneous combustion. The concentration present during incidents of spontaneous combustion is, however, four orders of magnitude lower than carbon monoxide.

The existence underground of methane with lower hydrocarbons (firedamp) is well known and its presence has been found to be largely unaffected during incidents of spontaneous combustion varying in concentration to a greater extent due to other factors. The presence of the minor constituents of firedamp have been found to vary considerably comprising approximately 3-20% of the methane.

CHAPTER 4

CHARACTERIZATION OF SEMICONDUCTOR GAS SENSORS

The experimental work performed in this part of the study was conducted to investigate the basic operating characteristics of a range of commercially available tin oxide semiconductor gas sensors, (Taguchi Gas Sensors).

The manufacturers claim high sensitivity to flammable gases, resistance to poisoning, reliable reproducible production processes and availability. Their small physical size, rugged construction, relatively low power consumption and low unit cost also make them attractive for incorporation into practical monitoring systems. Therefore, the gas sensors have potential for either detection of the products evolved during spontaneous combustion of coal or measurement of methane concentrations underground. Table 12 summarises the main features and potential applications of the different types of sensor. In particular, the type 711 was recommended by Taguchi for detection of carbon monoxide and the type 812 for measurement of a wider range of gases and vapours such as benzene, carbon monoxide and sulphur dioxide and therefore appear suitable for the detection of spontaneous combustion. The type 813 appeared most promising for the detection of methane being recommended for the measurement of lower hydrocarbons such as methane, ethane, propane and butane.

The basic characteristics of the sensors have been studied including, composition, surface morphology, working temperature, ambient atmosphere dependence and effect of varying oxygen concentration.

4.1 Experimental

4.1.1 Sensor Handling

a) Physical Construction

The sensors are all physically similar and are of the form shown in Plate 3. The active semiconductor material is deposited on the outside of a small (40mm x 10mm) ceramic tubular former, through which passes a 60 micron diameter coiled electric heating filament. Predeposited 80 micron noble metal wire electrodes carry the circuit voltage and are inserted into the semiconductor material near the ends of the cylinder. These, and the heater wires are spot-welded to the sensor pins which are arranged to fit a seven pin miniature valve socket. The base and cover of the sensor housing are constructed of nylon 6,6. This material is claimed to have deformation temperature in excess of 240° C. Gas samples are introduced to the sensing element through a double layer of 100 mesh stainless steel gauze which acts as a flameproof barrier.

b) Electrical Characterisation

As outlined earlier in Chapter 1, semiconductor gas sensors function via modulation of the electrical properties of a solid caused by interactions which take place at the gas-solid interface. The vast majority of studies undertaken have relied on measurement of the direct-current resistance to produce the detection signal. Alternating currents of various frequencies have been employed in fundamental studies to elucidate the conductivity mechanisms.[290,291] It was considered that such a detailed characterisation of the electrical properties

of the sensors was outside the scope of the work reported here.

The literature contains a considerable amount of information relating to the techniques available for measuring the electrical resistance of solids, although many of these methods are designed to improve the precision of measurements carried out on well defined materials, for example, single crystals. In contrast, the commercial and experimental data concerning semiconductor gas sensors suggest that absolute precision is not a primary concern. The variation in electrical properties between nominally identical sensors when exposed to a detectable gas are normally greater than the uncertainties inherent in any particular measuring system. Therefore, the simple electrical measurement circuit, as recommended by the manufacturer was used during all the experimental work and is shown in Figure 62. A summary of the recommended circuit values are shown below:

Heater voltage (Vh) volts	5.0 ± 0.2
Circuit voltage (Vc) volts	24.0 max
Load resistor (RL) ohms	3960 ± 5

Two stabilised dual variable power supplies (Weir Series 413D) were used to provide the sensor heater and circuit voltage requirements. The sensor working temperature was varied by operating the heater voltage at fixed values over the range 5.00 - 7.00 ± 0.01V. It is recommended that the current passing through the sensor be restricted to 0.5mA. Therefore the circuit voltage was set at 1.000 ± 0.001V, applied across the sensor and a 3.96KΩ load

resistor, giving a maximum possible oxide current of 0.25mA.

Sensor response was measured indirectly as a change in voltage appearing across the load resistor with the output fed directly to a chart recorder (Chessell system 3000) to produce a continuous record. Equilibrium voltages were measured using a digital multimeter (R.S. Components) to a resolution of 10μV. The unknown resistance of the sensor was then obtained as follows:

$$Rs = \frac{(Vc-Vo)}{Vo} R_L \quad \text{.....4.1}$$

Where R_L (ohms) is the known load resistance, Vc (volts) is the circuit voltage, and Vo (volts) is the voltage drop across R_L.

To check the integrity of the electrical measuring system nominal resistance values in the range (10Ω - 2430KΩ) were measured using a digital multimeter and substituted into each circuit in place of the sensor and the respective voltage drop, Vo, across the 3.96KΩ load resistor R_L was measured. Typical results are shown in Table 63. With a circuit voltage, Vc, of 1.004V the resistors were varied to produce values of Vo in the range 1.6mV to 1.001V. Substituting each value of Vo into equation 4.1. enabled the corresponding resistance to be calculated. Agreement between the known and calculated resistance were generally good at ± 2.0%, although at the extreme of Vo above 0.995V this value rose to a maximum of + 9.3% producing an overall correlation coefficient of 0.9999. The overall performance of the electrical

measuring system was therefore considered acceptable for the purpose of this work. In order to allow comparisons to be made between the findings of other workers and the data obtained in this study the results have been presented later as follows:

i) In resistance form as described previously.

ii) As inverse resistance or conductance, G, (Siemens). Measurements are normally presented in this form for convenience since n-type semiconductor materials exhibit increased conductance in the presence of reducing gases.

iii) A simple method of monitoring sensor output, in a practical instrument would be to measure Vo using the electrical measuring circuit employed in this work. In the presence of reducing gases n-type semiconductor materials produce an increase in Vo.

Obviously, if the electrical measurements were combined with sample dimensions the data could have been presented in terms of electrical conductivity, which is defined as

$$\sigma = \frac{GL}{A} = \frac{L}{RA} \quad \text{ohm.metres}^{-1} \qquad .....4.2.$$

where L is the length of the specimen (metres), A is the cross sectional area of the specimen (metres^2), G is the conductance (Siemens) and

$$R = \frac{I}{G} \qquad .....4.3.$$

is the resistance (ohms) of the sample.

With the sensors employed in this work it was difficult to perform dimensional measurements and since the sensors were physically similar it was considered that conversion to a dimensionally insensitive parameter would not alter the general conclusions.

c) Mounting and Gas flow arrangement.

Two forms of sensor enclosures were studied; individual brass holders and a rectangular cell, 15 cm x 10 cm x 4 cm constructed from 1.0 cm PTFE sheet (Dalau Ltd.). Up to nine sensors could be mounted inside the cell in a 3 x 3 array. The individual brass blocks were connected in series by short lengths of silicone rubber tubing. Diagrams of both enclosures are shown in Figures 63a and 63b. To prevent erroneous results great care was taken to ensure that after machining the brass blocks all contaminants were carefully removed. The cleaning procedure described in Section 2.1.2a for the brass sampling tube holders was employed.

Pure gases and gas mixtures were normally supplied to the sensors at 600 ml min^{-1} directly from high pressure cylinders after passing through a precalibrated gas blending system (Signal gas blender, Section 2.1.2c). All interconnections within the system were made using 6.0 mm o.d. PTFE tubing. The relative humidity (R.H.) of gases reaching the sensors was controlled by passing through either a magnesium perchlorate drying tube (zero R.H.) or by bubbling through two dreschel bottles containing triple deionized water bottles in series (approximately 90% R.H). The gas flow and sensor enclosure were thermostatically

controlled and the experimental arrangement is shown in Figure 64.

During the initial experiments commercial grade compressed air was used to feed the sensors. The specification for B.O.C., commercial grade compressed air allows for varying contaminants including low concentrations of hydrogen and carbon monoxide to be present. It has been shown that both these contaminants can be removed by passing the gas through a bed of commercially available platinised honeycomb catalyst (Johnson Matthey Ltd.).

The catalyst was packed into a 150 cm long 10 mm diameter electrically wound ceramic tube. The tube windings were then coated with a ceramic cement (Autostic) to provide electrical protection and thermal insulation. The coating was allowed to dry at room temperature for forty-eight hours, before baking at 180°C for a further twenty-four hours. A variable voltage supply (Cressall Torovolt Model 66ZP) was connected across the windings and the temperature of the catalyst was measured at increasing voltages using a Chrome Alumel thermocouple inserted into the centre of the catalyst bed. The catalyst efficiency was studied by passing a standard mixture containing 100 ppm hydrogen and 100 ppm carbon monoxide in air through the catalyst bed at 600 ml min^{-1} and feeding the effluent directly to an infra-red carbon monoxide analyser (Analytical Development Company). Samples were also periodically extracted from the system for hydrogen analysis, as described earlier (2.1.9.b). The analytical detection limit for each gas was 0.5 and 2.5 ppm

respectively. The catalyst temperature was increased slowly until both gases were below their respective detection limit. This corresponded to a catalyst bed temperature of 140° C, however, the detection limit of hydrogen was considered to be significantly high, therefore, the bed temperature was increased to 170°C in order to remove residual traces of the gas.

4.1.2 Basic Sensor Characterization

a) Analytical Examination

The combined techniques of scanning electron microscopy, SEM, (3-30ADP scanning electron microscope) and energy dispersive X-ray analysis, EDXA, (860 series I;EDXA system with solid state silicon/lithium detector and ZAF4/FLS software) were utilised in an attempt to obtain information concerning the surface of the sensors. The instrument was operated as recommended by the manufacturer.

To obtain an estimation of elemental composition the top covers of the sensors were removed and the exposed active material examined under identical conditions using the EDXA facility. Electron photomicrographs were produced using the SEM after the sensors had been coated with gold (Polaron sputter coater). The resolution of the instrument was quoted to be approximately 7nm. Specimens were gold coated prior to insertion into the SEM to produce a surface layer with a higher secondary electron yield than the original material and to overcome surface charge build-up.

b) Estimate of sensor operating temperatures

As the physical form of the different sensors appeared to be identical an estimate of the operating temperatures of each was undertaken as follows.

The first method utilised a differential infra-red scanner (Probeye, Hughes Aircraft Corporation). The instrument was not calibrated and in order to measure a temperature it was necessary to match the intensity of the image produced by infra-red radiation, as observed through the instrument, with that produced by another heat source whose temperature could be varied and measured. For this purpose a brass cylinder, 50mm long and 20mm diameter was used.

The brass cylinder was covered with asbestos paper and an electric heating element of nichrome wire wound around the brass covered cylinder. The windings were coated with a layer of ceramic cement (Autostic) to provide thermal insulation and produce a surface similar to the semiconductor sensors. The coating was conditioned as described earlier. A thermometer socket, approximately 40mm in depth, was drilled into one end of the block to provide an assessment of the block temperature. A variable voltage supply (Cressall Torovolt, Model 66ZP) was used to provide the heating element voltage.

With the sensor cap removed the heater voltage to the brass cylinder was increased until the intensities of the infra-red radiation from the sensor and brass block appeared to be exactly matched. At this point the temperature of the brass cylinder as indicated by the

thermometer was noted. The temperature of each sensor was assessed over a range of heater voltages, from 3.5-7.0V. The second method of assessing the temperature of each sensor as a function of heater voltage involved attaching a Chrome/Alumel thermocouple bead constructed from 0.1mm diameter wire to the semiconductor surface using gold paste (Hanovia A1644, Engelhard Ltd).

c) Ambient atmosphere studies

The effect of changes in atmospheric conditions on sensor response was studied using the experimental arrangement shown in Figure 64. The sensors were operated under the manufacturers recommended conditions and additionally at an increased heater voltage of 7.0V.

A high pressure cylinder containing commercial grade compressed air was connected via 6mm o.d. PTFE tubing to the Signal gas blender system at the recommended inlet pressure of 2bar. The blender outlet flow of 600 ml min^{-1} was passed through the heated catalyst and magnesium perchlorate tower to remove traces of hydrogen, carbon monoxide and moisture, before being fed to the sensors. The sensor manufacturers recommend an initial stabilization period of forty eight hours prior to measurements being taken. Depending on the history of the sensor it was found that at least seven days were required to obtain stabilized outputs. This was taken as a change of less than $\pm$ 2% in Vo. Additionally, when the heater voltage was changed response measurements were performed only after the sensors were operated at a fixed temperature for several days. These precautions were

necessary to obviate the transient and long term drift which resulted from these procedures. The sensor responses, measured by the voltage change appearing across the load resistor were monitored continuously on chart recorders. After the initial stabilization period the gas flow was subjected to the following sequence of procedures, also see pages 227 and 228:

A cylinder air passed through heated catalyst and magnesium perchlorate;

B heated catalyst removed;

C magnesium perchlorate removed and heated catalyst introduced;

D heated catalyst removed;

E heated catalyst and water bubblers introduced;

F heated catalyst removed;

G synthetic air (21% oxygen/79% nitrogen) fed directly to sensors after passing through magnesium perchlorate.

After each operation the test atmosphere was fed to the sensors and their responses monitored continuously until stabilized outputs were obtained. This required at least twenty-four hours, particularly after a change from 'dry' to 'wet' gas and vice versa.

d) Effect of varying oxygen concentration

The effect of varying the oxygen concentration on sensor behaviour was investigated using 'dry' gases only.

A cylinder of oxygen free nitrogen and pure oxygen were connected via length of PTFE tubing to the Signal gas blending system at an inlet pressure of 2bar. By varying

the blender control setting and using the calibration graph shown in Figure 8, known oxygen/nitrogen standard mixtures could be generated in the range 100% to 0.1% oxygen. The actual concentration reaching the sensors was confirmed to ± 1% by diverting the blender effluent to a commercial paramagnetic oxygen analyser (Servomex 580A analyser). The gas flow was directed to the sensors after passing through the magnesium perchlorate drying tower. After each change in concentration the sensor outputs were monitored continuously until stabilized readings were obtained. This series of experiments were performed at sensor heater voltages of 5.0 and 7.0V. Additionally, the role of nitrogen, if any, on sensor behaviour was studied by replacing with argon and repeating the procedure described above.

4.2 Results and Discussion

The experimental work described previously was undertaken to study the basic operating characteristics of a range of commercially available semiconductor gas sensors, TGS types 711, 812 and 813. Their properties and response behaviour were investigated and the results discussed in relation to previous findings concerning the sensors principle of operation.

For clarity and ease of interpretation of results the data from only one of the three sensors examined of each type has been presented and discussed, although if wide discrepancies were observed this has been indicated.

4.2.1 Analytical Examination

At the time of this study the SEM/EDXA system was unable to provide a full quantitative analysis of sensor composition, however, each sensor was examined under identical conditions and the following observations are made on the basis of the spectral plot of counts versus energy for each sensor, reproduced in Figures 65-67, inclusive. As might be expected tin was the major component identified in each case, assumed to be present as the oxide. No peaks were observed to indicate the presence of active metal catalysts such as platinum or palladium at the instrumental limit of detection of 0.5%. As discussed in detail earlier, these additives are normally incorporated into the metal oxide to alter its selectivity towards different gases. The spectra did confirm the presence of silica and alumina in varying proportions and it is considered that the primary purposes of these additives were to act as either binders or catalyst supports.

Examination of the sensor electrode wires produced spectra which indicated the presence of gold and palladium as shown in Figure 68. This appears to be an unusual choice of electrode material, due to its high catalytic activity, since the electrode wires are deposited within the oxide. In normal operation the sensors are operated at elevated temperature and this could lead to the possibility of migration of the electrode material.

Electron photomicrographs taken at X200 and X500 magnification are reproduced in Figures 69-74 inclusive.

Although the surface of the sensors appeared quite different the overall impression was of a porous structure with large numbers of granules of varying sizes. Figures 69 and 70 showed the surface of the type 711 sensor to be covered with a number of large fissures, however, closer examination also revealed a system of finer cracks with the material appearing to have undergone a certain amount of sintering producing smooth unbroken areas of irregular shape. Examination of the type 813 sensor showed a more porous less fissured surface, (Figure 71) which at higher magnifications, (Figure 72) appeared to be formed from a large number of granules of varying sizes above an open structure. Figures 73 and 74 showed the surface of the type 813 sensor to be particularly granular and porous and closer examination revealed a large number of voids and fine cracks with the material appearing to have undergone the least degree of sintering.

A number of authors have considered the reactions taking place at the surface in terms of catalytic activity. Therefore, any differences on surface quality, such as porosity, surface area, topography and presence of additives would be expected to lead to different adsorption and surface reaction rates, resulting in different gas sensing characteristics.[193] Control of surface quality is recognised as an important parameter, although this is a major problem in sintered materials, and it is generally agreed that in order to improve sensor performance it is essential to understand the chemistry of the gas-solid interface.

4.2.2 Sensor Operating Temperature

Figure 75 shows the mean estimated temperatures for each sensor operated at heater voltages varying from 3.5 to 7.0V using the infra-red scanner method of measurement. It can be seen that the sensors operate at different temperatures as a function of heater voltage. At the recommended heater voltage of 5.0V, mean operating temperatures of 227, 311 and 345° ± 10°C were observed for the 711, 812 and 813 respectively, whilst at 7.0V the maximum heater voltage studied mean temperatures of 287, 385 and 440° ± 15°C were recorded.

It was considered that the main advantages of this method of temperature assessment were the need for physical contact with the semiconductor surface, with consequent thermal loss, were eliminated and according to the manufacturers claims, temperature differences of only a few degrees Celsius could be easily distinguished.

The thermocouple bead method of temperature assessment gave consistently lower temperatures, for all these three sensors being up to 30° C below that of the infra-red scanner method. In this case it must be assumed that the thermocouple bead and associated leads act, to some degree, as a heat sink and thus the recorded temperature would be expected to be lower than the actual sensor operating temperature.

Since the physical construction of the sensors appeared identical it may be expected that the same dissipation of electrical energy would produce equal temperatures. Figure 76 shows the energy (watts) dissipated by each

sensor over a range of heater voltages. A power dissipation of 0.5W calculated from the sensor heater voltage and corresponding current consumed was found to be equivalent to heater voltages of 7.1, 4.4 and 3.8V for the 711, 812 and 813 sensors respectively. Figure 75 shows that for the calculated heater voltages good correlation existed between power dissipation and operating temperature with the three different sensors producing surface temperatures of 290 $\pm$ 5° C. However, the relatively large power consumption of the sensors may prove too high for incorporation into a small portable battery powered instrument for use underground.

Very little information is available in the literature concerning sensor operating temperatures and that appearing produces conflicting values. Clifford and Tuma claim that the type 812 sensor operated in air at a constant heater voltage of 5.0V yielded a surface temperature of 445 $\pm$ 5°C,[211] which is some 130°C higher than that found in this work. Wynne, using similar experimental measurement techniques to those employed in this work estimated the operating temperature of the 711 to be in the range 102 - 239°C at heater voltages varying from 5-10.0V, the 812 from 88-319° C at 3 to 8.0V and the 813 from 98-309°C at 3-7.0V.[289] Ihokura, whilst working for Figaro, showed an example of the extremes of the sensors operating temperature to be approximately 100-600°C, however, the corresponding heater voltages were not included.[198]

The true operating temperature of each sensor is considered to be an important parameter if direct comparisons of response between different types of sensor are to be made. The wide variations in operating temperatures obtained between different workers may be attributed to the conditions under which the measurements were taken.

4.2.3 Ambient atmosphere studies

The results of these studies are given in Table 64. Figure 77 a and b illustrates the effect of different ambient test atmospheres on sensor behaviour when opeated at heater voltages of 5.0 and 7.0V. Before discussing these results a brief explanation of the basic operating principles of n-type metal oxide semiconductor gas sensors is presented. The electrical conductance of polycrystalline metal oxides may be considered to be determined by the density of free electrons in the conduction band. However, the intrinsic band gap in tin oxide (3.6eV) is too large for electrons to be thermally excited from the valence to the conductance band, and the electrons available for conduction are those associated with donor levels in the oxide lattice. The donor levels are associated with an excess of metal probably in the form of lattice oxygen defects.

At elevated temperatures in air it is generally accepted that the oxide surface may be populated by a number of physisorbed and chemisorbed species such as H_2O, OH^-, O_2, O_2^-, O^- and O^{2-}. It is not intended to suggest that all these species are present at any one particular

temperature. The electrical conductance of the oxide can be affected by these groups, due to their effect upon the density of conduction band electrons. If we consider that the formation of a bond between the oxide surface and adsorbed species results in the localisation of one or more electrons which were previously free to move within the conduction band, then such a process will result in a decrease in the density of conduction band electrons, ie will result in a decrease in conductance in tin oxide. Any reactions modulating these surface groups will give rise to a change in conductance although the exact form of the interactions are far more complex this simple explanation is considered adequate for present purposes.

The dependence of sensor response on ambient atmosphere composition may be explained if we consider the changes resulting from treatment of the test atmosphere as given in the procedures below:

A removal of hydrogen, carbon monoxide and residual water vapour from air test atmosphere,

B as A but test atmosphere contains hydrogen and carbon monoxide,

C test atmosphere contains residual water vapour, but impurity free,

D test atmosphere contains residual water vapour, hydrogen and carbon monoxide,

E test atmosphere saturated with water vapour, but impurity free,

F test atmosphere remains saturated but contains hydrogen and carbon monoxide,

G assumed to be water vapour and impurity free.

In an attempt to interpret the electrical conductance changes taking place under different test atmospheres it is convenient to first consider the sensors behaviour under an atmosphere containing no major impurities (procedure A). In the presence of clean dry air the available surface sites are assumed to be occupied by adsorbed oxygen species only and a fixed temperature equilibrium is eventually attained where the rate of adsorption is equal to the rate of desorption.

Several adsorbed oxygen species have been postulated, but is is now generally accepted that O_2^- groups dominate at low temperatures, which dissociate to O^- as the temperature is increased and O^{2-} predominates at higher temperatures. Figure 78 summarises possible routes for the formation of adsorbed oxygen species on the oxide surface. Water, which would be present on the sensor surface at the start of the experiment is considered to be removed by operating the sensors for an 'extended' period at their working temperature. Even so it is recognised that the oxide surface will not be completely free from water, however any remaining will be tightly bound. The equilibrium conductance established by the sensors under procedure A is considered to be their baseline conductance in 'clean dry air'.

Earlier studies indicated that at a fixed heater voltage the sensors operating temperature increased in the order type 711< 812<813. On a given surface the oxygen coverage would be expected to diminish with increasing temperature due to increased desorption of adsorbed species from the surface. This effect would produce an increase in conductance due to injection of electrons back into the conduction band. Positive temperature coefficients of conductance were exhibited by the sensors, which is consistent with semiconductor behaviour. At a fixed heater voltage the type 711 sensor exhibited the lowest conductance and the type 813 the highest with the type 812 intermediate.

If we next consider the effect of removing the magnesium perchlorate drying tower from the gas flow (procedure C) we can observe an increase in conductance of all three sensors at both heater voltages, as shown in Figures 77. If it is assumed that this increase is related to residual moisture in the cylinder air the effect would be expected to be greater when air saturated with water vapour was passed over the sensors (procedure E). Figures 77 demonstrates the sensor conductance in the presence of air saturated with water vapour. During both these procedures the heated catalyst remained in the gas flow.

The effect of gases and water vapour on the conductance of the sensors may be expressed as follows:

$$\%\Delta G = \frac{G_{gas} - G_{air}}{G_{air}} \times 100\% \quad \ldots\ldots\ldots\ldots 4.4$$

Where G_{gas} is the sensor conductance measured in the presence of contaminant, and G_{air} is the sensor conductance measured in air.

This expression, the percentage conductance change, $\%\Delta G$, corrects for different baseline levels and therefore allows comparison of sensor sensitivity. The values of $\%\Delta G$ given in Table 65 were calculated from the relevant data in Table 64. The effect of water vapour on $\%\Delta G$ is clearly demonstrated being most notable on the type 711 sensor, which functions at the lowest operating temperature. When operated at 5.0V heater voltage in the presence of air containing residual moisture and air saturated with water vapour, a 630% and 2080% change in sensor conductance was observed respectively. At increased sensor operating temperature (increased heater voltage) significantly lower values of $\%\Delta G$ were observed being 101% and 540% under corresponding test gas conditions. The increases in $\%\Delta G$ due to water vapour were less marked for the types 812 and 813 sensors although the overall pattern of decreased $\%\Delta G$ values at increasing temperature was exhibited.

The increase in conductance of tin oxide in the presence of water vapour has been noted by a number of workers[187,207] although, few have attempted to explain the mechanisms possible. Boyle and Jones[207] hypothesised that the increase in conductance in the presence of air containing water vapour was due to the accumulation of electrons near the surface of the oxide due to the dipole attraction of the polar water molecules. At increased sensor operating

temperatures when water is thermally desorbed the number of accumulated electrons, and therefore the conductance, will decrease. If the effect of thermally removing water is greater than the effect of thermally removing oxygen the net effect will be a decrease in conductance. The authors suggested that polar water molecules tend to be physisorbed instead of chemisorbed and therefore are bound less tightly to the surface. Willet studied the nature of surface species and electrical conductance effects on tin oxide gels when exposed to atmospheres containing different contaminants.[292] In the presence of atmospheric water vapour the author postulated that the increase in conductance observed could be attributed to the action of water in 'blocking' oxygen adsorption sites which would otherwise be available for oxygen adsorption, thereby increasing the conduction band population. It was tentatively suggested that physisorbed water could be responsible for this effect.

A further possible route for the observed increase in conductance would be to propose that the water vapour reacts directly with adsorbed oxygen species. If this process resulted in donation of electrons to the conduction band it would lead to an increase in conductance. The product gas subsequently desorbs as outlined below:

$$H_2O + O^-_{ads} \longrightarrow \text{Product} + e^-_{bulk} \quad \ldots\ldots\ldots\ldots 4.5$$

From the data obtained in this work it is not possible to draw any firm mechanistic conclusions concerning the

effect of water vapour on sensor conductance. However, it seems plausible to suggest that in the presence of air containing water vapour both physisorbed water and chemisorbed OH^- would be present on the sensor surface under the experimental conditions employed here.

The formation of OH^- might be expected to have the same effect on sensor conductance as the chemisorption of singly charged oxygen species, although occupation of OH^- instead of O^{2-} would lead to a net increase in sensor conductance. However, at lower sensor operating temperatures physisorbed water might be expected to predominate which would result in an increase in sensor conductance as outlined above. Programmed thermal desorption experiments have been performed in tin oxide exposed to water vapour.[183,293] In the temperature range 50-250 °C the surface species has been attributed to physisorbed water whilst at higher temperatures (300-500 °C) the surface species has been assigned to hydroxyl groups.[293]

The working temperature of the type 711 sensor at heater voltages of 5.0 and 7.0V were estimated earlier to be 227 and 287 °C respectively and therefore physisorbed water might be expected to predominate on the sensor surface without localisation of conduction band electrons leading to an increase in conductance. However, the type 812 and 813 sensors operate at temperatures above 300 °C and hydroxyl groups are considered to be the principle water derived species.

We can now consider the effect of removing the heated catalyst from the test gas flow (procedures B, D and F).

Reference to pages 227 and 228 shows that under the latter procedure the atmosphere was saturated with water vapour and trace concentrations of hydrogen and carbon monoxide were assumed to be present. Procedures D and B whilst not removing the trace impurities resulted in atmospheres containing residual moisture and dry gas respectively. Figure 77 and Table 65 shows that when using dry air containing trace impurities as the test atmosphere only relatively small increases in sensor conductance and $\%\Delta G$ were observed for all three types of sensor. However, when the test atmosphere was saturated with water vapour there was a significant increase in conductance reflected by the calculated values of $\%\Delta G$. This effect was particularly pronounced on the type 711 sensor which produced a 14000% increase in sensor conductance at the lower working temperature. The results obtained with residual water vapour present were intermediate. At this stage it is not possible to comment in detail on the effects produced by the trace impurities because of their assumed nature. Even so, it is worth noting that the test atmosphere saturated with water vapour containing trace impurities (F-A) produced the largest relative increase in conductance, $\%\Delta G$, however, this effect cannot be explained solely by summation of the responses attributed to the contaminants in dry air (B-A) and saturated water vapour (E-A) individually. This anomaly can only be explained if it is assumed that there is a synergistic effect in the presence of both contaminants and water vapour.

Finally, when dry synthetic air was used as the test gas atmosphere the sensor conductance returned to the baseline level in clean air as shown in Figure 77.

The data from this series of experiments may be summarised by noting that the sensor conductance is highly dependent upon the ambient atmosphere. It may be that this dependence on ambient atmosphere has led many researchers to consider the response of the sensor to lack reproducibility. However, provided measurements are made with careful regard to the condition of the ambient atmosphere these characteristics may be prevented. It is also worth noting at this stage that this series of experiments were performed using the PTFE sensor enclosure. When the test atmospheres were passed over the sensors held in individual brass holders, increased sensor conductances were observed. The only suggestion that can be put forward to explain this effect is that the brass blocks were 'outgassing', even after careful pretreatment. This also emphasises the importance of using a clean inert experimental arrangement to prevent erroneous and misleading results.

From the viewpoint of a practical underground sensor it is considered that the dependence of the sensor on ambient atmospheric compositions may lead to difficulties in obtaining a true baseline level.

4.2.4 Effect of varying oxygen concentration

The effect of varying the oxygen concentration over a wide range of oxygen/nitrogen ratios was studied using clean dry gases at sensor heater voltages of 5.0 and 7.0V.

Representative measurements of the voltage drop appearing across the load resistor, Vo, versus oxygen concentration are given in Table 66 and shown in Figure 79. All the sensors exhibited similar behaviour with, Vo, being relatively constant above approximately 10% oxygen but increasing sharply at lower oxygen concentrations. An increase in Vo represents an increase in sensor conductance ie an increase in the population of conduction band electrons. It is known that oxygen is strongly adsorbed on tin oxide, therefore, only small variations in sensor conductance occur at high oxygen concentration. Since Vo is relatively constant above 10% oxygen the effect of oxygen deficiency may be disregarded for sensor applications in coal mines.

If the results are presented as sensor resistance versus oxygen concentration in logarithmic form a linear relationship exists over the concentration range studied, as shown in Figure 80. Jones et al proposed a simple model to describe the adsorption of oxygen on n-type oxides.[217] The relationship was represented by a power law expression as follows:

$$\sigma = \text{Constant } P_{O_2}^{-a/x} \qquad \ldots\ldots\ldots\ldots 4.6$$

Where σ is the oxide conductance, P_{O_2} is the partial pressure of oxygen and a and x could take the following values in oxygen adsorption.

i) If oxygen is strongly bonded at the temperature of observation a = 0 and is independent of oxygen concentration.

ii) If oxygen is weakly bonded a = 1 or 1½; ie. a = 1 if oxygen is adsorbed as molecules and a = 1½ if oxygen is adsorbed dissociatively.

iii) x = 1 or 2 depending on whether the adsorbed species carry 1 or 2 electrons.

The authors suggested that an exponent value of $^{a}/_{x} = 0$ could be indicative of strongly adsorbed oxygen, a value of 0.5 may denote the presence of O_2^{2-} or O^- and a value of 0.25 may signify the presence of O^{2-}. Thus the exponent, that is the $^{a}/_{x}$ ratio, expresses the stoichiometry of the controlling reaction.

Clifford and Tuma who studied the steady state gas sensing characteristics of type 812 sensor suggested a similar expression, but with a totally different interpretation of the influencing factors on the exponent, to describe the power law nature of the resistance response as follows:[211]

$$R = RoP_{O_2}^{\beta} \qquad \text{.....4.7}$$

Where Ro represents the sensor resistance in air, P_{O_2} is the relative oxygen partial pressure and β is the power law exponent.

The authors concluded that in oxygen the power law exponent, β, could not be expressed as a single ratio of integers and was specific to the sensor varying in the range 0.25 - 0.55.

When operated at 5.0V heater voltage all three types of sensor produced exponent values of 0.39, within experimental error, and at the higher heater voltage the exponent value increased to 0.47. The results from the complete set of sensors studied showed an insignificant intersensor variation on the exponent. This may suggest that the sensor behaviour could be represented by integral ratio laws with values approximating to 0.5, however, these values also fall within the range 0.25 - 0.55 found by Clifford and therefore it is not possible to favour either approach.

Finally, in all the measurements when nitrogen was replaced by argon as ambient gas no effect on sensor resistance was observed. It is concluded that both nitrogen and argon are inert with respect to the sensors behaviour and is consistent with oxygen controlling sensor resistance.

4.3 Summary

The basic operating characteristics of the semiconductor gas sensors studied have been characterised in detail under carefully controlled conditions.

The oxide material, tin, has been confirmed, although no active catalyst materials could be detected. Examination of the sensor surface showed a non uniform surface covered with cracks and fissures of varying sizes with the material appearing to have undergone sintering to varying degrees. Independent techniques were employed to assess the working temperature of the sensors and at constant heater voltage the

working temperature increased in the order 711<812<813.

The response behaviour of the sensors to different ambient atmospheres have been studied in detail. The results indicate that when the measurements are performed under well defined conditions the sensors exhibit consistent characteristics. The sensors behaviour in varying oxygen concentrations is consistent with the operating principle of n-type semiconductors. The power law nature of the response exhibited exponents which were comparable to other studies performed on similar materials. It was also shown that oxygen plays a contributing role in governing sensor behaviour.

Overall the results indicate that the sensors behaviour are characteristic of state of the art semiconductor gas sensors.

CHAPTER 5

THE EFFECT OF GASES EVOLVED FROM HEATED COAL ON SEMICONDUCTOR GAS SENSORS

The final part of the experimental work was conducted in order to evaluate the potential of semiconductor gas sensors for either the detection of gaseous products of combustion which are evolved from coal during spontaneous combustion or the measurement of methane concentrations underground.

In any gaseous mixture the overall response of any gas sensor will be determined by its relative sensitivity to the individual components and the concentration at which those are present. The effects of the products of combustion evolved from heated coal on the behaviour of type 711, 812 and 813 Taguchi semiconductor gas sensors have been studied, both as individual components and as total "products of combustion".

The relative sensitivities of the sensors to a number of individual coal combustion products, identified earlier, have been determined over a range of sensor heater voltages. The potential of the type 711 and 812 sensors for the detection of spontaneous combustion has been examined by exposing the sensors to the total combustion products evolved from coal heated in air and nitrogen. Finally, the type 813 sensor has been evaluated for the measurement of methane in the presence of associated hydrocarbons (as in firedamp).

5.1 Experimental

5.1.1 The Effect of Individual Products on Sensor Response

Studies described earlier in Chapter 3 were undertaken to identify the gaseous products evolved from coal heated in the laboratory and from samples collected underground. A number of combustion products, for example, carbonyl sulphide, unsaturated aliphatics, aromatic hydrocarbons, methylcyclohexane, carbonyl containing species and hydrogen were identified as having potential as alternative indicators to carbon monoxide for the detection of spontaneous combustion of coal. In addition to carbon monoxide eight individual components listed below, were selected as being typical of the different classes of products of interest.

i. Hydrogen
ii. Ethene
iii. Propene
iv. Benzene
v. Toluene
vi. Methylcyclohexane
vii. Acetone
viii. Carbonyl sulphide

To study the effect of individual products on sensor response, standard mixture containing 1000 ppm of each product (ultra high purity, hydrogen free) were obtained from BOC Special Gases.

A second series of standard gas mixtures listed below were also obtained in order to determine sensor sensitivity in the presence of methane and associated hydrocarbons.

i.	Methane	1.0 % (v/v) 10,000ppm
ii.	Ethane	1000 ppm
iii.	Propane	1000 ppm
iv.	Synthetic firedamp containing:	
	Methane	1.0 % (v/v) 10,000ppm.
	Ethane	300 ppm
	Propane	50 ppm

Using the experimental arrangement shown in Figure 64 individual standard mixtures were passed to the sensors at approximately 600 ml min^{-1} either directly or after dilution with synthetic air. The gas was maintained at either zero humidity or was saturated with water vapour by passing through a magnesium perchlorate drying tower or water bubblers respectively before reaching the sensors. The effects of individual products on sensor response were initially studied at a heater voltage of 5.0V. Further studies were also undertaken to investigate sensor temperature dependence on the response to each gas. Responses were measured at sensor operating temperatures corresponding to heater voltages of 5.5, 6.0, 6.5 and 7.0V. During this series of experiments an estimation of variation of sensor response times was also undertaken. After changing the heater voltage it was found important in order to achieve repeatable measurements to allow sufficient time for the sensors to stabilise. Generally, this required at least twenty-four hours and only after

this time were gas response measurements undertaken. Each exposure was repeated at least twice to check the validity of the results.

5.1.2 Response of Gas Sensors to Total Products Evolved from Heated Coal

The apparatus, test coals and experimental conditions described in Chapter 3, in section 3.1.2, for the generation of combustion products from heated coal were adopted in this series of experiments. The procedure followed for combustion product evolution using either synthetic air or oxygen free nitrogen as combustion gases was as follows:

Synthetic air was passed at 500 ml min^{-1} over 5 $\pm$ 0.001g of coal at room temperature to the sensor enclosure which was connected directly to the generation apparatus. When oxygen free nitrogen was used as the combustion gas it was passed over the coal sample at 400 ml min^{-1} and pure oxygen at 100 ml min^{-1} fed into a tee-piece connected between the generation apparatus outlet and sensor enclosure inlet. This allowed responses to be measured in a nominally atmospheric air background, which the sensors require for normal operation, whilst maintaining an inert atmosphere over the coal sample. The combustion products were transferred to the sensors in either dry or wet condition. This was achieved by either passing the outlet flow from the combustion apparatus through a magnesium perchlorate drying tube, or by passing the

air/nitrogen through two water bubblers in series on the inlet side of the combustion apparatus with the outlet fed directly to the sensors.

The temperature of the coal sample was increased at $4\,^{o}C\ min^{-1}$ up to a maximum temperature of 300 °C and the sensor responses measured continuously. In this way profiles were obtained of the variation in sensor responses as the combustion products evolved at increasing coal temperature. Responses were measured at sensor operating temperatures corresponding to heater voltages of 5.0 and 7.0V.

5.2 Results and Discussion

The experimental approach described was undertaken to identify the products evolved from heated coal which make the major contributions to the overall response of each semiconductor gas sensor. It should also be possible to explain the main features of the total sensor response to either the combustion products evolved from heated coal or from methane and its associated hydrocarbons in terms of product appearance temperatures, concentration versus product temperature profiles and relative gas sensitivities.

Thus, the application of the sensors in underground monitoring systems should be assessed.

5.2.1 Sensitivity of Gas Sensors to Individual Products from Heated Coal

The effect of individual coal combustion products on sensor response was studied over a range of sensor heater

voltages and the experimental data are shown in Table 67. The date from each stage in the gas exposure cycle are presented in terms of absolute sensor conductance, G, whilst the arithmetic difference in absolute conductance, ΔG, as been used to represent the resultant sensor response; e.g. response to test gas dry, test gas saturated with water vapour and air saturated with water vapour. Although ΔG may be used to express sensor sensitivity, it is generally agreed that percentage conductance change, $\% \Delta G$, gives a better indication of the significance of the change, since it represents a measure of the effect of a test atmosphere on the sensitivity of a practical gas sensor. Therefore, the experimental data in Table 67 has also been presented in this form, whilst Figures 81-92 illustrate the variation of $\% \Delta G$ for each gas studied as a function of heater voltage. From a mechanistic viewpoint Willett has suggested that ΔG is effectively a measure of the number of surface oxygen groups removed from the sensor surface, whereas $\% \Delta G$ represents the significance of these groups in the conduction process.[292]

Before discussing the results it is worth noting the following points, although the plots for each exposure stage in the gas cycle consisted of only five points for one sensor from each type, they are still considered relevant because the general trends observed were similar to the other sensors studied. This study was not directed towards attempting to explain the mechanisms controlling sensor behaviour in the presence of a wide range of gases,

it is more concerned with characterizing sensor behaviour from the viewpoint of a practical gas sensor. However, a number of workers have attempted to elucidate the mechanisms controlling the gas sensing process. A common feature of the mechanisms proposed by the authors is the depletion of surface electron density by chemisorbed oxygen (O^{2-} , O^{-}). Subsequent reaction with and removal of these charged groups by the test gas is invariably assumed to be the important source of the sensor response, ie conductance change. The majority of mechanistic studies have concentrated on the changes in sensor behaviour during exposure to atmospheres containing carbon monoxide and oxygen. It is generally assumed that adsorbed carbon monoxide reacts with chemisorbed oxygen (O^{2-} O^{-}) on the sensor surface to form chemisorbed CO_2^{-} which then returns an electron to the conduction band. The resultant neutral carbon dioxide is subsequently desorbed, leaving a vacant site for re-occupation by oxygen from the atmosphere. The interaction may be broadly summarized by the reaction.

$$CO + O^{-} \text{ (or } O^{2-}) \longrightarrow CO_{2\ gas} + e \text{ (or } 2e^{-})$$

It is worth noting that the understanding of sensor mechanisms is at an early stage, even for the simplest case above, but such an explanation may be used to satisfactorily explain sensor behaviour without a more detailed knowledge of the surface chemistry involved.

The results presented in Figures 81-92 represent the sensors percentage conductance change, related to dry air, resulting from exposure to the test gas dry, test gas saturated with water vapour and air saturated with water vapour. Figures 81-92 illustrate that the sensors' response to water vapour discussed in Chapter 4, were evident over the range of heater voltages studied, although, in general reduced $\%\Delta G$ values were observed at increasing sensor operating temperatures. In addition to the sensors' independent sensitivity to water vapour, additional increases in sensitivity were observed in the presence of the test gases saturated with water vapour compared with the dry test gases.

A number of workers have noted this phenomenon, particularly in the presence of carbon monoxide, however, a coherent understanding of the processes involved has not yet been established. Boyle and Jones, suggested that carbon monoxide reacted with adsorbed oxygen to form carbon dioxide, which was catalysed by the presence of adsorbed water, whilst, Nitta has reported enhanced reaction rates due to the removal of hydroxyl groups.[207,196]

It has been suggested that the water gas reaction may be responsible for the enhanced sensitivity

$$CO + H_2O \longrightarrow CO_2 + H_2 \quad \text{.....5.1}$$

The hydrogen or intermediate products of the reaction might interact with the sensor surface with a higher efficiency than carbon monoxide.[182] More recently,

Willett has suggested that the reaction of carbon monoxide on tin oxide is an extremely complex process, highly dependent upon the precise nature of the surface and a single reaction pathway is unlikely to provide a satisfactory explanation of sensor behaviour.

It was tentatively suggested in Chapter 4 that physisorbed water may predominate on the surface of the 711 sensor due to its relatively low operating temperature, whereas, hydroxyl groups may be the principle water derived species on the 812 and 813 sensors due to their increasingly higher operating temperatures. Figures 81-92 show that the 'enhancement effects' on sensitivity due to the presence of water vapour were generally most noticeable on the 711 sensor with increases in sensitivity of up to several orders of magnitude being observed. Similar effects were also evident on the 812 and 813 sensors, albeit to a lesser extent. From the limited amount of experimental data it is not possible to predict the effect that water vapour may have on sensor sensitivity, however, it appears that the presence of an unsaturated system, for instance in ethene and propene, produces greater sensitivity than their saturated analogues ethane and propane. Further studies into this area might provide useful information as to the role water vapour plays in the reaction process.

The experimental data confirms the previously noted interaction of carbon monoxide and water vapour and the resultant enhancement effect was the most significant of the test gas studied. These findings are consistent with the suggestion that physisorbed water may be responsible for the observed increases, although it is not possible to

draw conclusions as to the actual role it plays in the reaction process. The increased sensitivity associated with the presence of water vapour would normally be of great importance in a practical gas sensor as a consequence of the variable water vapour concentration in ambient air. The detection of a gas in high humidity ambient air would be expected to differ from that in dry ambient air. However, for underground applications this problem may not arise, since at fixed points underground the ambient temperature and humidity are high although relatively constant.

Figures 81-92 also illustrate the variations in sensor sensitivity in the presence of the test gases as a function of heater voltage. A number of workers have shown that the change in sensitivity produced by a test gas increases with sensor operating temperature, up to a maximum, thereafter decreasing with increasing temperature.[179] Whilst the attainment of a maximum appears to be general, it occurs at different temperatures for different gases, normally in the range 100-600°C. Several workers have utilized this feature to determine the presence of carbon monoxide in a mixture containing methane.[177,209] Whilst the sensors used in this work exhibited variations in sensitivity as a function of heater voltage, no maxima were evident and generally the variations in sensitivity were insufficient to produce a high degree of specificity towards any particular gas. This is not unexpected considering the number of gases studied and the relatively narrow sensor temperature ranges examined.

From the viewpoint of a practical gas sensor the lack of selectivity may pose severe problems in the measurement of specific gas concentrations without some form of filtering system. However, the considerable increases in sensitivity, up to five orders of magnitude, observed in the presence of the test gases may prove advantageous for the early detection of the wide range of products evolved during the low temperature heating of coal.

During each gas exposure cycle, estimates of the sensors' response and recovery times were undertaken. Measurements were made manually from the response curves and recorder chart speed with no adjustments being allowed for the delay time due to dead volume in the valves and associated pipework. Response and recovery times could only be estimated to the nearest 30 seconds. Table 69 shows the values obtained for hydrogen, whilst some differences were observed for other gases they were not considered important in this work since in general they followed a similar pattern. At a fixed heater voltage, response times decreased in the order 711>812>813 (ie. order of increasing sensor temperature), whilst at increasing heater voltages, all the sensors exhibited decreased response times. The corresponding recovery times were somewhat longer, although the same general trends still applied. Increased response and recovery times were exhibited in the presence of water vapour at all the heater voltages studied. The response and recovery times exihibited by the sensors would appear adequate for applications where slowly moving trends were being

monitored, but in cases where sudden fluctuation in gas concentrations occur they may be impractical.

The study to date has been confined to the increases in sensitivity exhibited by the sensors in the presence of fixed gas concentrations. Obviously their behaviour as a function of gas concentration is of significant interest for practical applications. Three gases, hydrogen, carbon monoxide and methane were selected for this study. The effect of hydrogen was investigated because of the high sensitivities exhibited by the sensors, whilst carbon monoxide is an important product of combustion from heated coal and methane is present naturally underground at concentrations not normally exceeding 1.0%. The results of this study are illustrated in Figures 93-98 where the response of the sensors at 5.0 and 7.0V heater voltage have been given in terms of the voltage change appearing across the series load resistor in the electrical measuring circuit. Presenting the results in this manner clearly demonstrates the highly curvilinear nature of the voltage output at increasing gas concentrations. The shape of the calibration curves results to some extent from the mode of operation of the electrical measuring circuit. Whilst it is recognised that the voltage output does not truly represent the actual sensitivity of the sensor in terms of the change in sensor conductance,

ΔG, or percentage change, $\% \Delta G$, which increases approximately logarithmically with gas concentration it offers a practical compromise to translate this phenomenon into simple electrical circuitry for underground

applications. Therefore, the implications of using the load resistor measuring circuit in a practical system would be a large increase in voltage output at low gas concentrations but the disadvantage of poor discrimination at high concentrations. However, this may be advantageous for the early detection of the wide range of combustion products evolved from coal at low temperatures, although difficulties may be encountered with the measurement of a wide range of gas concentrations.

To conclude this part of the study it may be worthwhile to refer to the work performed in Chapter 4 on the sensors dependence on the ambient atmosphere. It was tentatively suggested that the observed increases in sensitivity in the presence of cylinder air saturated with water vapour compared with 'clean dry air' may be associated with contamination from low concentrations of hydrogen and carbon monoxide. The percentage increase in conductance resulting from exposure to 10 ppm of each gas calculated from the voltage output data in Figures 93 - 96, and the cylinder air data are shown below:

Heater voltage	5.0V			7.0V		
Sensor	711	812	813	711	812	813
Hydrogen dry	1290	1360	119	853	102	<10
Hydrogen wet	5230	1800	105	5510	115	<10
Carbon monoxide dry	<10	<10	<10	<10	<10	<10
Carbon monoxide wet	4100	128	19	1220	37	<10
Cylinder air dry	24	29	31	17	<10	<10
Cylinder air wet	11800	999	188	2160	57	15

It would appear that the increases resulting from exposure to cylinder air may be related to some extent to contamination with adventitious carbon monoxide. Significant increases in sensitivity to carbon monoxide were observed in the presence of water vapour. However, the increases cannot be totally accounted for by the presence of 10 ppm carbon monoxide. It seems unlikely that higher concentrations would have been present in the cylinder air, although this cannot be completely ruled out. The possibility of synergistic interaction between other contaminating gases cannot be discounted.

The increases in sensitivity due to the presence of contaminants at low concentrations in cylinder air clearly demonstrates the extreme sensitivity of the sensors, particularly the 711, and emphasises the need for well defined experimental conditions and calibration gases to prevent misleading results.

5.2.2 Response of Gas Sensors to Products Evolved from Heated Coal

The work described in Chapter 3, Generation and Identification of Combustion Products, identified the appearance temperatures and evolution patterns of a wide range of products evolved from coal heated in air and nitrogen. The effects of individual products on the behaviour of the 711, 812 and 813 gas sensors have been studied in the preceding section. The final part of this study described the effects of the total products of combustion from heated coal on the response of the 711 and 812 sensors and assesses the potential of the 813 sensor

for the measurement of methane concentrations. To demonstrate the effects on an underground instrument the response of the sensors have again been measured in terms of voltage change apearing across the series load resistor as a function of the combustion products evolved at increasing coal temperature. Therefore, from the response patterns observed here and information already established an explanation of the main features of the response of each sensor has been attempted. No attempt has been made to quantitatively explain the individual contributions of each product in terms of their effects on the total increase in response. It is considered that such a treatment would be extremely complex taking into account the wide range of gases present. Clifford suggested that the sensors exhibit both competitive and synergistic inter action when several gases are detected simultaneously, and Zaromb and Stetter have pointed out that its applicability would be very limited for semiconductor sensors which exhibit complex variations of response with the concentrations of different gases.(211,294)

5.2.3 Detection of the Total Products of Combustion Evolved from Heated Coal

The effect of the total products of combustion evolved from the Wolstanton, Hucknall and Thoresby test coals heated in air and nitrogen on the responses of the 711 and 812 sensors were studied. It was considered that the products evolved in air and nitrogen would 'envelope' the situation underground where coal may undergo heating in

both aerobic and oxygen deficient atmospheres. The response patterns observed were similar for each coal although the products evolved from the Thoresby coal produced the largest increases and the Wolstanton coal the smallest. Therefore, to simplify the discussion the results from only the Thoresby coal are presented, nevertheless it is considered that similar conclusions could be drawn for the other coals. The relevant data for the Thoresby coal are shown in Figures 37a, 38a, 55a and 56a and Tables 33, 36, 50, 51, 60 and 61. Whilst no information is available on the production of carbonyl containing products the data for the Hucknall coal, shown in Figure 59 and Table 57 are considered to be applicable for the purpose of this discussion.

Figures 99 - 100 show total response curves both dry and wet for the 711 and 812 sensors, operated at heater voltages of 5.0 and 7.0V for the Thoresby coal heated in air, whilst Figures 101 - 102 illustrate the corresponding curves in nitrogen.

We can now examine the main aspects of the response curves in terms of the appearance temperatures and concentration/temperature profiles of the combustion products evolved in air and nitrogen, identified in Chapter 3, and the sensitivities of the sensors to individual products determined in this part of the study. Although no undertaking has been made to quantitatively describe the individual contribution of each product to the response curves the sensitivity data has been interpreted to give an indication of the products that may play important roles.

If we first consider the dry response curves resulting from exposure of the sensors to the total products evolved in nitrogen. The response curves reflected the concentration/temperature profiles of the evolved products which exhibited appearance temperatures of approximately 100°C and increased in concentrations only gradually with increasing coal temperature. It was suggested in Chapter 3 that the products evolved in nitrogen were held within the coal pore structure and emerged at increasing temperatures as desorption products producing similar concentrations in nitrogen and air. The sensitivity data indicates that the sensors are likely to respond to the full range of evolved products and any differences in the magnitude of the response curves results from the relative sensitivities of the sensors. The increased dry response curves observed on exposure of the sensors to the total products evolved in air can be attributed directly to the increase in concentrations of products due to oxidation reactions. The products considered to be primarily responsible for the increased response include, carbon monoxide, ethene, propene, aromatic hydrocarbons, methyl-cyclohexane, carbonyl sulphide, carbonyl containing species, hydrogen chloride and hydrogen. All the products, except hydrogen, exhibited appearance temperatures in the range 100-150°C, which correlates well with initial responses of the sensors, thereafter the products showed significant increases in production with coal temperature. Hydrogen is considered to be a high temperature oxidation product, however, the extreme sensitivities exhibited by

the sensors to this gas suggests that it may make a significant contribution to the response curves above a coal temperature of approximately 200°C. Significant differences in the response curves were observed in the presence of the combustion products wet. The initial response of the sensors to the products evolved in air occurred at approximately 100°C. Above this temperature the sensors exhibited different behaviour with the response of the 711 sensors, at first increasing rapidly with rising coal temperature; however, at elevated coal temperatures when the products were being generated at higher concentrations the response increased only gradually. The tendency to 'saturation' results to some extent from the characteristics of the electrical measuring circuit so that changes in response due to variations in combustion product concentrations were less marked. It is worth noting that the actual change in sensor conductance, ΔG, or percentage conductance change, $\% \Delta G$, increase approximately logarithmically with the products evolved at increasing coal temperature. The response of the 812 sensor increased steadily above approximately 100 °C, with increasing coal temperature up to the maximum studied. The wet response curves resulting from exposure of the sensor to the total products evolved in nitrogen, also exhibited increased output compared with the corresponding dry response curves although the magnitude of the responses were less marked than with air as the combustion gas. It was shown earlier that the sensors exhibited significant increases in sensitivity on

exposure to a number of the individual products saturated with water vapour compared with the products dry. Therefore, it seems reasonable to suggest that the catalytic effect, associated with the presence of water vapour, may be responsible for the differences in the total response curves wet and dry. However it has been noted that the sensors exhibit both competitive and synergistic interaction when several gases are detected simultaneously. Nevertheless the increases in sensitivity exhibited by the sensors on exposure to carbon monoxide saturated with water vapour and the temperature/ concentration profile of the product from heated coal would suggest that this gas may make a significant contribution to the total response curves wet.

With the exception of hydrogen chloride, all the products considered to be primarily responsible for the observed increases in sensor responses have been shown, in Chapter 3, to be present underground, increasing in concentration during incidents of spontaneous combustion. Although, both sensors exhibited increased responses on exposure to the products evolved from heated coal in both air and nitrogen from the viewpoint of a practical underground instrument it is considered that the initial rapid increase in response of the 711 may be advantageous for the early detection of the products evolved at low concentrations during the initial stages of spontaneous combustion.

5.2.4 Measurement of Methane Concentration

The 813 sensor was investigated to assess its potential for the measurement of methane concentration underground. Two standard mixtures; one containing 1.0% methane in air and the other 1% methane, 300 ppm ethane and 50 ppm propane in air were used to investigate the response characteristics of the sensor. The former mixture enabled the actual response to methane to be established whilst the latter represented a synthetic firedamp mixture. The mixtures were serially diluted and the resultant responses at each concentration were noted. Table 69 and Figures 103-104 illustrate the sensor responses at 5.0 and 7.0V heater voltage in terms of the output voltage across the series load resistor as a function of methane concentration.

Compared with the sensor response to methane, significant increases in response were observed on exposure to the synthetic firedamp mixture. Due to the highly non-linear response characteristics of the sensor it is difficult to relate directly the individual contributions of ethane and propane to the increased responses, however, the sensitivity data does indicate that whilst only present in the gas mixture as minor constituents they might be expected to make significant contributions to the increased responses.

From the viewpoint of a practical gas sensor, many of the gases present underground that might interfere with the measurement of methane concentrations could be eliminated, with the exception of hydrogen and carbon monoxide, by operating the sensor behind a charcoal cloth. The

sensitivity data suggests that the sensor would exhibit highest sensitivity to methane at 5.0V heater voltage. However, it is considered that the non-linearity of the response would lead to severe discrimination problems at high methane concentrations. Measurements made earlier of the sensor response and recovery times indicated that they may be inadequate where sudden fluctuations in gas concentration may occur, such as methane outbursts. Taking into account the overall response behaviour of the sensor it appears unlikely that the sensor has the potential to replace the pellistor for the measurement of methane concentrations underground.

5.3 Summary

The final part of this study was undertaken in order to investigate the potential of the type 711 and 812 gas sensors for the detection of spontaneous combustion of coal and the type 813 sensor for the measurement of methane concentrations. The discussion concentrated on the operation of the sensors from the viewpoint of practical underground systems.

The sensor responses were initially studied in the presence of the individual combustion products of coal. This approach made it possible to characterize the behaviour of each sensor in terms of sensitivity, selectivity, and response and recovery times, under carefully controlled conditions.

By using this information in conjunction with the appearance temperatures and concentration/temperature

profiles of the combustion products, identified in Chapter 3, it has been possible to explain qualitatively the main features of the overall response curves of the 711 and 812 sensors resulting from exposure to the total products evolved from coal heated in air and nitrogen. A similar approach was adopted to describe the response of the 813 sensor in the presence of methane and associated hydrocarbons (firedamp).

It has been suggested that the 711 and 812 sensors may form the basis of a highly sensitive practical underground monitoring system for the early detection of the products evolved during the low temperature heating of coal, however, the characteristics of the 813 sensor appeared less amenable to the design of a simple instrument for the direct measurement of methane concentrations.

CHAPTER 6

C O N C L U S I O N S

The main object of this study has been the identification of the low temperature products of combustion from heated coal and their detection using metal oxide semi-conductors.

A wide range of analytical procedures were developed for the quantitative collection and analysis of selected groups of gases and vapours evolved from heated coal that were considered to be of interest, namely aliphatic and aromatic hydrocarbons, sulphur containing compounds and carbonyl species. The range of gases were specified and suitable collection techniques were identified and examined under conditions that were likely to be encountered underground. A number of chromatographic procedures were developed for the separation and detection of the individual class of gases and vapours. Techniques for the measurement of other gases and vapours were also studied and finally GC/MS facilities were used to provide an extended analysis.

The combustion products evolved from three different coals heated in air and nitrogen were examined under carefully controlled laboratory conditions. This enabled information concerning appearance, temperatures and evolution patterns of the products to be established. Three distinct patterns of evolution were identified and several combustion products not previously considered to be present in the temperature range studied were identified. In the coal mining industry carbon monoxide is currently used as an

indicator of the onset of spontaneous combustion of coal, however, a number of other combustion products were identified in this work that may have potential as alternative indicators.

Studies were carried out at selected collieries to establish whether the combustion products identified in the laboratory were also present in the underground environment. The existence of a number of the products was demonstrated and their evolution patterns during incidents of spontaneous combustion were studied in detail in relation to the production of carbon monoxide. Many of the products were also detected in association with carbon monoxide from other legitimate mining activities, such as diesel locomotive exhausts and shotfiring fumes which would preclude their immediate use as unambiguous indicators of spontaneous combustion of coal. However, it was suggested that the ratios of different products to carbon monoxide and to one another may reveal more information concerning the degree and extent of activity of incidents of spontaneous combustion. A relationship between carbon monoxide, hydrogen, and oxygen was applied with encouraging results to a number of incidents to predict the varying temperature of coal during spontaneous combustion. The requirement to assess coal temperature during spontaneous combustion was considered important taking into account the potential ignition or explosion hazard. Several products were found in significant quantities from coal heated in the laboratory, however, they were not observed in the mining environment and it was suggested that this was due to their reactivity.

Carbonyl sulphide appeared to be the only combustion product that produced a similar evolution pattern to carbon monoxide from both coal heated in the laboratory and during incidents of spontaneous combustion, but did not seem to increase significantly from other legitimate mining activities. It was therefore suggested that carbonyl sulphide may have the potential to be used as an unambiguous indicator of spontaneous combustion.

The presence of methane in association with lower aliphatic hydrocarbons (firedamp) underground was largely unaffected during incidents of spontaneous combustion varying to a greater extent from other factors such as ventilation quantity, barometric pressure changes, rate of coal extraction and the influence of adjacent coal seams. In the general mining environment the concentrations of methane were normally less than 1.0% with the presence of the minor constituents of firedamp comprising approximately 3-20% of the methane concentration.

Three commercially available tin oxide based semiconductor gas sensors, namely the Taguchi, TGS, type 711, 812 and 813 were selected to investigate their performance for the detection of the products evolved from heated coal. In particular the type 711 and 812 gas sensors were chosen for the detection of spontaneous combustion and the type 813 sensor for the measurement of methane concentrations.

The basic characteristics of the sensors were studied, including composition, surface morphology, working temperature, ambient atmosphere dependence, and effect of varying oxygen concentration. It was concluded that if

measurements were performed under well defined conditions the sensors exhibited consistent behaviour, characteristic of state of the art semiconductor gas sensors.

The effect of the products of combustion from heated coal on the sensors response were studied both as individual and total products. This approach made it possible to identify the range of products which made significant contributions to the total responses.

Although the sensors exhibited high sensitivity to the individual products they lacked a high degree of selectivity towards any particular product which precluded their immediate use as specific gas detectors. However, this feature was considered advantageous for the detection of the wide range of products evolved at low concentrations during the initial stages of spontaneous combustion. In addition to the independent sensitivity of the sensors to water vapour, enhanced effects on sensitivity were observed on exposure to the individual products saturated with water vapour compared with the products dry. For underground applications this behaviour does not present a major problem since the ambient humidity at fixed locations underground whilst high is relatively constant. It is considered that this dependence on the ambient environment has led many workers to consider the response of the sensors to lack reproducibility.

The main features of the overall response curves of 711 and 812 sensors resulting from exposure to the total products of combustion evolved from coal heated in air and nitrogen were qualitatively explained in terms of the individual sensitivity data, and the products appearance

temperatures and concentration/temperature profiles. A similar approach was adopted to describe the response of the 813 sensor in the presence of methane and associated hydrocarbons.

The work described suggests that for the early detection of spontaneous combustion the type 711 and 812 sensors have potential to form the basis of a highly sensitive practical underground monitoring system indicating the presence of combustion products evolved during the low temperature heating of coal. However, the response characteristics of the 813 sensor suggests that it is unlikely that the sensor could find immediate application underground for the measurement of methane concentrations.

"What, frighted with false fire?"

HAMLET, Act III, Scene 2.

CHAPTER 7

F U T U R E W O R K

This work has formed a comprehensive study of the combustion products evolved from heated coal. A number of the products identified in the laboratory studies have been shown to be present, increasing in concentration, with increasing activity during incidents of spontaneous combustion. It has been suggested that the ratios of these products to carbon monoxide or to one another may lead to a greater understanding of the degree and extent of activity of particular incidents. Whilst semiconductor gas sensors have been shown to be extremely sensitive to the individual combustion products, they lack the selectivity for immediate use as specific gas detectors. However, it was considered that the sensors might form the basis of an underground system for monitoring the total combustion products evolved during the initial stages of spontaneous combustion. An alternative approach would be to employ the sensors as gas chromatographic detectors : Wynne carried out preliminary studies on the performance of the 711 sensor as a GC detector and found lower limits of detection of approximately 0.002 ppm hydrogen and 0.01 ppm for low molecular weight hydrocarbons. It might, therefore, be possible to incorporate the sensors into a programmed portable GC system to monitor, either in situ or from a number of remote sites underground with each sample fed sequentially to a centrally sited instrument. Such applications could either monitor

specified compounds and detect thresholds or observe the changing ratio of two or more components and issue appropriate warnings.

It has been shown that the response of the sensors to carbon monoxide in particular can be significantly influenced by the simultaneous presence of water vapour. This feature has been noted by a number of other workers; however, no clear understanding of the chemical processes involved has yet been established. Studies have been performed using infra red absorption spectroscopy to provide information into the chemical species present on the surface of tin-oxide gels operated at near ambient temperatures. Although this work has provided valuable insights into the reaction processes, its relevance to commercial sensors is rather questionable. The application of fourier transform infra red operated in the reflective mode might overcome some of the previous problems and allow the chemical species formed on the surface of actual sensors to be studied.

REFERENCES

1. **L. Grainger, J. Gibson,** Coal Utilisation: Technology, Economics and Policy. Graham and Trotman, 1981.
2. National Coal Board, Report and Accounts 1985/6.
3. **D.W. van Krevelen,** Coal: Typology, Chemistry and Physics, Elsevier, 1961.
4. World Energy Resources 1985-2020. World Energy Conference, IPC, 1978.
5. Survey of Energy Resources. World Energy Conference, Munich, 1980.
6. **W. Francis,** Coal: Its Formation and Composition, 2nd Edn, Arnold; 1961.
7. **J.S.S. Brame, J.G. King,** Fuel, 5th Edn. Arnold, 1955.
8. **J. Gibson,** J. Inst. Fuel 51, 67, 1978.
9. **J.B. Caldwell,** Colliery Guardian 213, 489, 1966.
10. **C.R. Kinney, E.I. Doucette,** Nature 182, 785, 1958.
11. **P.H. Given,** EPA-650/2-74-118, St. Louis, 1974.
12. **G.H. Ashley,** Pa.Geol Survey, 4th Series, Bull.M6, Pt.1., 1928.
13. **D.J. Allardice, D.G. Evans,** Analytical Methods for Coal and Coal Products, Vol. 1, Academic Press.
14. **T.A. Kukharenko,** Proc. Symp. on the Nature of Coal. Central Fuel Res. Inst., Jealgora, India, 185, 1959.
15. **L. Blom,** Thesis, Delft, 1960.
16. **A. Halleux, S. Delavarenne, H. Tschameler,** Fuel 40, 74, 1961.
17. **B.C. Gerstein, L.M. Ryan, P.D. Murphy,** A.C.S. 24(1), 90, 1979.

18. **A.W. Scaroni, R.H. Essenhigh,** A.C.S. Divn. of Fuel Chemistry. 23(4), 124, 1978.

19. **M. Teichmuller, R. Teichmuller,** Adv. in Chem. Ser. A.C.S. No. 55, 133, 1966.

20. **M. Teichmuller, R. Teichmuller,** Geological Aspects of Coal Metamorphism, ed by D. Murchison, T.S. Westall, 233, Elsevier, 1968.

21. **R. Hayatsu, R.E. Winans, R.G Scott, L.P. Moore, M.H. Studier,** Nature, 275(5676), 116, 1978.

22. Ibid, A.C.S. (71) 108, 1978.

23. **A. Attar, F. Dupuis,** A.C.S. 24(1), 166, 1979.

24. **J.N. Chakrabarti,** Analytical Methods for Coal and Coal Products, Vol. 1, Academic Press.

25. **L.J. Edgcombe,** Fuel, 34, 429, 1955.

26. **G.N. Daybell, W.J.S. Pringle,** Fuel 37, 283, 1958.

27. **J.A. Cox, A.E. Larson, R.H. Carlson,** Fuel, 63, 1334, 1984.

28. **J.N. Chakrabarti, H.N. Dasgupta,** J. Indian Chem. Soc. 28, 664, 1951.

29. **P.H. Given,** Fuel 39, 147, 1960.

30. **G.J. Pitt,** Coal and Modern Coal Processing, Academic Press, 1979.

31. **S.K. Chakrabarty, N. Berkowitz,** Fuel, 53(4), 240; 1974.

32. **G.R. Hill, L.B. Lyon,** Ind. Eng. Chem. 54, 36, 1962.

33. **P.R. Solomon,** New Approaches in Coal Chemistry, 1981.

34. **P.R. Solomon, D.G. Hamblen,** Presented at Conf. on Chemistry and Physics of Coal Utilisation, West Virginia, 1980.

35. **P.R. Solomon,** Fuel (69), 3, 1981.

36. **B. Gerstein,** Awaiting publication.

37. **B.K. Mazumdar,** Fuel 51, 284, 1972.

38. **R. Bent, W.K. Joy, W.R. Ladner,** Fuel 43, 5, 1964.

39. **A.K. Chatterjie, B.K. Mazumdar,** Fuel 47, 93, 1968.

40. **I.G.C. Dryden,** Fuel 41, 301, 1962.

41. **I.G.C. Dryden,** Fuel 41, 55, 1962.

42. **J.K. Brown, W.R. Ladner,** Fuel 39, 87, 1960.

43. **J.F.M. Oth, H. Tschamler,** Fuel 42, 467, 1963.

44. **P.R. Solomon,** The Evolution of Pollutants during the Rapid Devolatilisation of Coal. Report NSF/RA-770422, NTIS, PB278496/AS.

45. **P.R. Solomon, M.B. Colket,** Fuel 57, 749, 1978.

46. **D.H. Bangham,** Ann. Rep. Chem. Soc. 40, 29, 1943.

47. **M.W. Travers,** Fuel 30, 223, 1957.

48. Coal Directorate of the C.E.C. Firedamp Drainage Handbook, 1983

49. **E. Berl,** Bull. Am. Assoc. Petrol. Geol. Vol. 24, 1865, 1940.

50. **I.G.C. Dryden,** J. Inst. Fuel Vol. 30, No. 195, 193, 1957.

51. **G. Eglinton, M.T.J. Murphy,** Organic Geochemistry, 699, Springer-Verlay, New York, 1969.

52. **M. Teichmuller, R. Teichmuller,** Diagenesis in Sediments, ed by G. Lerson and G.V. Chilinger. Elsevier, New York, 1967.

53. Health and Safety, Mines and Quarries, 1970.

54. " " " 1971.

55. " " " 1972.

56. " " " 1973.

57. " " " 1974.

58. Health and Safety, Mines and Quarries, 1975.
59. " " " 1976.
60. " " " 1977.
61. " " " 1978.
62. " " " 1979.
63. Health and Safety, Mines, 1980.
64. " " 1981.
65. " " 1982.
66. Health and Safety, Mines, 1983.
67. **W. Highton, J.M. Cooper,** Min. Engr., 43, July 1982.
68. **J.N. Williams,** Power and Works Engineering, 333, 1960.
69. **S.B. Lord,** Presented to Inst. Min. Engrs. Nov. 1983.
70. **H.S. Eisner, P.B. Smith,** S.M.R.E. R.R. 130, 1956.
71. **K.J. Linacre, D.H. Jones,** Safety in Mines Research Establishment Res. Rep. No. 179, 1959.
72. **J.C. Chugh,** Seminar on Combating Mine Fires, Silver Jubilee Vol. C.M.R.S. Dhanbad, India, 1980.
73. **R. Gosh,** Fuel 65, 1042, 1986.
74. **R. Plot,** Spontaneous combustion in Heaps, History of Staffordshire, 1686.
75. **P.C. Boives,** Ind. Chem. 30, 12.
76. **I. Miyagawa,** J. Soc. Chem. Ind. 50, 325, 1931.
77. National Coal Board, Library Archives.
78. National Coal Board, Library Archives.
79. **J.S. Haldane, F.G. Meachem,** Trans. Inst. Min. Engrs. 16, 457, 1898.
80. **R.V. Wheeler,** J. Chem. Soc. 113, 945.
81. **J.D. Davis, J.F. Byrne,** Ind. Eng. Chem. 17, 125, 1925

82. **L.D. Schmidt,** Chemistry of Coal Utilisation, Vol.1 Wiley, 1945.

83. **W. Oplinsk, P. Gobays, T. Paulikowski, J. Roemus,** Chem. Abs. 43, 4603, 1954.

84. **G.H. Yohe, C.A. Harman,** J. Am. Soc. 63, 555, 1941.

85. **R.E. Jones, D.T.A. Townsend,** Trans. Faraday Soc. 42, 297, 1946.

86. **B.H. Chalizhazar, C.E. Spooner,** Fuel 36, 127, 1957.

87. **G.H. Yohe,** Illinois State Geological Survey Report of Investigations, 207, 1958.

88. **P.G. Sevenster,** Fuel 40, 7, 18, 1961.

89. **D.W. van Krevelen, J. Schuyer,** Coal Science. Aspects of Coal Constitution. Elsevier, 1957.

90. **I. Graham,** Trans. Inst. Min. Engrs. 48, 1914-1915.

91. **W.A. Frey,** Olukohle 39, 603, 1943.

92. **M. Guney,** C.I.M. Bulletin, March, 138, 1971.

93. **H.F. Coward,** Research Report, Safety in Mines, No. 142, 1957.

94. **T.F. Windmill,** Trans. Inst. Min. Engrs. 48, 535, 1914-1915.

95. **D. Humphreys,** Masters Eng. Sc. Degree Thesis, Queensland Univ.

96. **L.D. Schmidt, J.L. Elder,** Ind. Eng. Chem. 32, 249, 1940.

97. **T.F. Windmill,** Trans. Inst. Min. Engrs. 51, 493, 1914-1915.

98. **G.S. Scott,** U.S.B.M. 455, 1944.

99. **S.J. Criddle,** Coll. Guardian, 202, 664, 1961.

100. **E.A.C. Chamberlain, D.A. Hall, J.T. Thirlaway,** Min. Engr. 130, 121, 1970.

101. **N.W. Hurst, T.A. Jones, B. Mann, R.L. van Ewyk, P. Walden,** Fire and Materials, Vol.0. No.0. 1984.

102. **J. Tashiro, M. Kono, I. Takakuwa,** J. Min. and Met. Inst. of Japan 87, 395, 1971.

103. **P.J. Street, J. Smalley, A.T.S. Cunningham,** Fuel 57, 217, 1976.

104. **W.A. Bone, G.W. Himus,** Coal, its Constitution and Uses, Longmans, Green and Co. 1936.

105. **H.C. Howard,** Chemistry of Coal Utilisation, Vol.1 Wiley and Sons Inc. 761, 1945.

106. **G.W. Girling,** Benzole Producers Ltd., Research Paper 3, 1962.

107. **H.W. Holden, J.C. Robb,** Fuel 39, 39, 1960.

108. **D. Fitzgerald, D.W. van Krevelen,** Fuel 38, 17, 1959.

109. **A.G. Kim,** U.S.B.M. Research Report 7965, 1964.

110. **Z. Weber, P. Kusy,** Presented at 20th Int. Conf. of Safety in Mines Research Inst. Sheffield 1983.

111. **M. Vahrman, R.H. Watts,** Fuel 51, 235, 1972.

112. **L.F. Whiting, P.W. Langvardt,** Anal. Chem. 56, 1755, 1984.

113. **A.A. Herod, N.J. Hodges, E. Pritchard, C.A. Smith,** Coal Research Est. Internal Report 1982.

114. **A.A. Herod, C.A. Smith,** Fuel 64, 281, 1985.

115. **B.A. Pursall, S.K. Gosh,** Min. Engr. 511, 1965.

116. **T. Kitagawa,** Presented at 10th Int. Conf. of Safety in Mines Research, Pittsburgh 1959.

117. **G.H.R. Gwatkin, N. Wood,** N.C.B. Internal Report, 1969

118. **E.A.C. Chamberlain, G. Barrass, J.T. Thirlaway,** Fuel 53, 217, 1976.

119. **M. Hartzberg, C.D. Litton, R. Garloff,** U.S.B.M., R1 8206, 1977.

120. **R.M. Statcham,** U.S.B.M. Progress Report, 1974.

121. **C.J. Fauconnier, J.D.R. Beukes,** Journal of Mine Vent Soc. of South Africa, 57, 1978.

122. N.C.B. Internal Report, Scottish Area Scientific Department, May 1984.

123. **N. Harrison,** Presented at Int. Mine Vent. Cong. South Africa, 1975.

124. Tube Bundle Techniques. N.C.B. Booklet 1972.

125. **E.A.C. Chamberlain, G.H.R. Gwatkin,** Presented at 16th Int. Conf. of Safety in Mines Research, U.S.A. 1975.

126. **J.E. Wood, G.H.R. Gwatkin, T.H. Whitelam,** Min. Engr. 134, 383, 1975.

127. Mine Safety Appliances, Data Sheet, 07G-07-01, 1982.

128. SCO1 Carbon Monoxide Detector Manual, No. 08500M-1200, 1983.

129. Draeger Detector Tube Handbook, 1986.

130. **J.G. Beeley, P.E. Harrison,** N.C.B. Internal Report SML/442, 1978.

131. **M. Kennedy,** J. Applied Phys. 16, 109, 1965.

132. N.C.B. Ionising Radiations Regulations, - Fire Detection, 1985.

133. N.C.B. Notes of Guidance on Installation, North Derbyshire Area, 1968.

134. Ventilation in Coal Mines N.C.B. Mining Dept. 1979.

135. **D.P. Creedy,** Ph.D. Thesis. University of Wales, 1985

136. **F. Baron, H. Duckam,** Great Pit Disasters in Great Britain, 1700 to present day. David and Charles, 1973

137. Act for the Inspection of Coal Mines, 1850.

138. Mines and Quarries Act, 1954.

139. **M.J. McPherson,** Int. Jnl. of Min. Engrs. Vol.2, No. 3 Oct. 1984.

140. **R. Williams, I.H. Morris,** Symp. on Environmental Engineering in Coal Mining, Harrogate 1972.

141. Ministry of Technology, Testing Memorandum No.71, 1970

142. Mine Safety Appliances, Instrument Division, Technical Note.

143. **S.J. Gentry, P.T. Walsh,** Sensors and Actuators 5, 239, 1984.

144. **W.H. King,** Anal. Chem. 36, 1735, 1964.

145. **J.F. Alder, J.J. McCallum,** Analyst. 108, 1169, 1983.

146. **A. Kindlund, H. Sundgren, I. Lundstrom,** Sensors and Actuators, 6, 1, 1984.

147. **H.M. Ho, G.G. Guilbault, E.P. Schiede,** Anal. Chem. 54, 1998, 1982.

148. ibid, Anal. Chem. 52, 1489, 1980.

149. **W.H. King,** Jr. Environ. Sci. Technol. 4, 1136, 1970.

150. **J. Hlavay, G.G. Guilbault,** Anal. Chem. 50, 1044, 1978

151. **W.H. King,** Jr. Anal. Chem. 9, 36, 1735, 1964.

152. **K.H. Karmarker, L.M. Webber, G.G. Guilbault,** Anal. Chem. Acta, 81, 265, 1976.

153. **S.M. Fraser, T.E. Edmonds, T.S. West,** Analyst 111, 10, 1986.

154. **H. Wohltjen, R.E. Dessy,** Anal. Chem. 51, 1458, 1979.

155. **A. Bryant, D.L. Lee, J.F. Vetelino,** Ultrasonics Symp. Proc. 1981.

156. **A.J. Ricco, S.J. Martin, T.E. Zipperian,** Sensors and Actuators, 8, 319, 1985.

157. **A. D'Amico,** Appl. Phys. Lett, 41, 300, 1982.

158. **A. Venema, E. Nieuwkoop, M.J. Vellekoop, M.S. Nieuwenhuizen, A.W. Barendsz,** Sensors and Actuators, 10, 47, 1986.

159. **F.W. Karasek,** U.S. Patent No. 3538744, 1970.

160. **J.B. Angell, S.C. Terry, P.W. Barth,** Sci. Am., 248 44, 1983.

161. **A.A. Saaman, P. Bergveld,** Sensors and Actuators, 7, 75, 1985.

162. **P. Bergveld,** Sensors and Actuators, 8, 109, 1985.

163. **J.N. Zemel, B. Keramati, C.W. Spivak,** Sensors and Actuators, 1, 427, 1981.

164. **S.J. Fonash, H. Huston, S. Ashjok,** Sensors and Actuators, 2, 363, 1982.

165. **J.N. Zemel, J.J. Young, H. Rahnamai,** Crit. Rev. Solid State Sci. 1, 1, 1975.

166. **M.C. Steele, B.A. MacIver,** Appl. Phys. Lett, 28, 687, 1976.

167. **M. Yamamoto, S. Tonamura, T. Matsuoka, H. Tsubomura,** Surf. Sci. 92, 400, 1980.

168. **D.K. Burns, P.N. Kember, S. Taylor, E.W. Williams,** Environ. Tech. Lett. 1, 259, 1980.

169. **I. Lundstrom,** Sensors and Actuators 1, 403, 1981.

170. **J.P. Couput, B. Cornut, C. Chambu,** Proc. of the Int. Meeting on Chemical Sensors, Fukuoka, Japan, 1983.

171. **A. Spetz, F. Winquist, C. Nylander, I. Lundstrom,** Proc. of the Int. Meeting on Chemical Sensors, Fukuoka, Japan, 1983.

172. **K. Dobos, D. Krey, G. Zimmer,** Proc. of the Inst. Meeting on Chemical Sensors, Fukuoka, Japan, 1983.

173. **S.R. Morrison,** The Chemical Physics of Surfaces, Plenum Press, New York, 1978.

174. **P.T. Moseley, B.C. Tofield,** Materials Science and Technology Vol. 1, 505, 1985.

175. **H.P. Hubnar, E. Obermeier,** Technisches Messen. tm 52 Jahrgang Heft 2/1985.

176. **W.E. Garner,** Chemistry of the Solid State, Butterworths, London, 1955.

177. **G. Heiland,** Sensors and Actuators, 2, 343, 1982.

178. **T. Seiyama, A. Kato, K. Fujiishi, M. Nagatani,** Anal. Chem. 34, 10, 1962.

179. **J.G. Firth, A. Jones, T.A. Jones,** Ann. Occup. Hyg. Vol. 18, 63, 1975.

180. **Z.M. Jarzebski,** Oxide Semiconductors Pergamon Press, 1973.

181. **P. Mark,** Surface Science, 25, 192, 1971.

182. **S.R. Morrison,** Sensors and Actuators 2, 329, 1982.

183. **S.C. Chang,** Proc. Int. Meeting Chem. Sensors, Fukuoka, Japan, 1983.

184. **A. Clark,** The Chemisorptive Bond, Academic Press, New York, 1977.

185. **H. Windischmann, P. Mark,** J. Electrochem Soc. 126, 627, 1979.

186. **M. Egashira, Y. Yoshida, S. Kawasumi,** Sensors and Actuators, 9, 147, 1986.

187. **J.F. McAleer, P.T. Moseley, B.C. Tofield, D.E. Williams,** Material Science and Tech. Vol.1, 1985.

188. **Y. Morooka, A. Ozaki,** J. of Catalysis 5, 116, 1966.

189. **G.N. Advani, L. Nanis,** Sensors and Actuators 2, 201, 1981/82.

190. **J.G. Firth, A. Jones, T.A. Jones,** Proc. of the Joint Conf. on Environ. Sensors and Applications, London, 1974.

191. **R.J. Stetter,** J. of Colloid and Interface Sci. 65, 3, 432, 1978.

192. **P.K. Clifford,** Proc. of the Int. Meeting on Chemical Sensors, Fukuoka, Japan, 1983.

193. **S.J. Gentry, T.A. Jones,** Sensors and Actuators, 10, 141, 1986.

194. **A. Jones, B. Mann,** Section Technical Report, 1980.

195. **G.S.V. Coles, K.J. Gallagher, J. Watson,** Sensors and Actuators, 7, 89, 1985.

196. **M. Nitta, M. Haradome,** J. of Electronic Materials, Vol.8, No. 5, 571, 1979.

197. **Y. Okayama, K. Fukaya, H. Kojima, Y. Terásawa, T. Handa,** Proc. of Int. Meeting on Chemical Sensors, Fukuoka, Japan, 1983.

198. **K. Ihokura,** Presented at A.C.S./C.S.J. Chemical Congress, Hawaii, U.S.A. 1979.

199. **H. Wako,** J. of Electrochem. Soc. of Japan, Vol. 48, No. 5, 284, 1980.

200. **P. Li, C.J. Wang,** Proc. of Int. Meeting on Chemikcal Sensors, Fukuoka, Japan, 1983.

201. **M. Yamazoe, Y. Kurokawa, T. Seiyama,** Proc. of Int. Meeting on Chemical Sensors, Fukuoka, Japan, 1983.

202. **R. Lalauze, C. Pijolat,** Sensors and Actuators, 6, 119, 1984.

203. **M. Nitta, S. Kanefusa, M. Haradome,** J. Electrochem. Soc. 125, 1676, 1978.

204. **Bott** et al United States Patent, 3, 865, 550, 1975.

205. **K. Shiratori, M. Katsura, T. Tsuchiya,** Proc. of Int. Meeting on Chemical Sensors, Fukuoka, Japan, 1983.

206. **M.J. Gibson,** N.C.B. Internal Report No. 82/7, 1982.

207. **J.F. Boyle, K.A. Jones,** J. of Electronic Materials, Vol. 6, No. 6, 717, 1977.

208. **J. Watson,** Sensors and Actuators 5, 29, 1984.

209. **B. Bott, T.A. Jones, B. Mann,** Sensors and Actuators 5, 65, 1984.

210. **E.D. Thornton, P.G. Harrison,** J. Chem. Soc. Faraday Trans. 71, 461, 1975.

211. **P.K. Clifford, D.T. Tuma,** Sensors and Actuators, 3, 233, 1982/83.

212. **T. Oyabu,** J. Appl. Phys. 53, 4, 2785, 1982.

213. **T. Oyabu, T. Osawa, T. Kurobe,** J. Appl. Phys. 53, 11, 7125, 1982.

214. **H. Ogawa, A. Abe, M. Nishikawa, S. Hayakawa,** J. Elec. Soc. 128, 3, 685, 1981.

215. **K. Murakami, S. Yasunaga, S. Sunakara, K. Ihokura,** Proc. of Int. Meeting on Chemical Sensors, Fukuoka, Japan, 1983.

216. **S. Sakai,** European Patent EP-0-115-182-A2, 1984.

217. **A. Jones, T.A. Jones, B. Mann, J.G. Firth,** Sensors and Actuators 5, 75, 1984.

218. **B. Bott, J.G. Firth, A. Jones, T.A. Jones,** Brit Patent 1374575, 1974.

219. **S.C. Kashyap,** J. Appl. Phys. 44, 10, 4381, 1973.

220. Figaro T.G.S. Gas Sensor, General Catalogue.

221. **N. Taguchi,** Brit. Patent, 1 257 155, 1971.

222. **N. Taguchi,** Brit. Patent, 1 259 566, 1972.

223. **N. Taguchi,** Brit. Patent, 1 280 809, 1972.

224. **N. Taguchi,** Brit. Patent, 1 282 993, 1972.

225. **N. Taguchi,** Brit. Patent, 1 288 009, 1972.

226. **N. Taguchi,** Brit. Patent, 1 288 539, 1972.

227. **J. Watson, D. Tanner,** Radio and Elec. Eng. 44, 85, 1974.

228. **J. Watson, R.A. Yates,** Elec. Eng. 47, May, 1985.

229. **K. Persaud, G. Dodd,** Nature, Vol. 299, No. 5881, 352, 1982.

230. **J.P. Wagner, A. Fookson, M. May,** J. Fire and Flame, Vol. 7, 71, 1976.

231. **W.E. Burnett,** Environ. Sci. Technol. 3, 744, 1969.

232. **T. Kato,** U.S. Nat. Tech. Inform. Ser. P.B. Report N4-11933/TR-289-73.

233. **I.M. Williams,** Anal. Chem. 37, 1723, 1965.

234. **R.D. Barnes, L. Maria Law, A.J. Macleod,** Analyst 106, 412, 1981.

235. **S.O. Farwell, S.J. Gluck,** Anal. Chem. 51, 609, 1979.

236. **F. Bruner, P. Ciccioli, F. DiNardo,** J. Chromatogr. 99, 661, 1974.

237. National Institute of Occupational Safety and Health, Manual of Sampling Data Sheets, Dept. of Health, Education and Welfare, (N10SH) Publ. 77-159, Cincinnati, 1977.

238. **K. Grob, G. Grob,** J. Chromatogr. 1, 62, 1971.

239. **F.R. Cropper, S. Kaminsky,** Anal. Chem. 35, 735, 1963.

240. **F.X. Mueller, J.A. Miller,** Int. Lab. 34, 1974.

241. **F.W. Williams, M.E. Umstead,** Anal. Chem. 40, 2232, 1968.

242. **R. Perry, J.D. Twibell,** Atmos. Environ. 7, 929, 1973.

243. **B.I. Brookes, S.M. Jickells, R.S. Nicolson,** J. Assoc. Publ. Analysts 16, 101, 1978.

244. **J.W. Russell, L.A. Shadoff,** J. Chromatogr. 134, 375, 1977.

245. **H. Peterson,** Anal. Chem. 50, 2152, 1978.

246. **J.E. Scott,** Analyst, 102, 614, 1977.

247. **J.S. Gethner,** Fuel (64), 1985.

248. Supelco International Cat. 1984.

249. **C.J. Cowper, A.J. Derose,** The Analysis of Gases by Chromatography, Pergamon Series, Vol. 7, 1983.

250. Phase Separations Ltd., G.C and HPLC Catalogue, 1986/87.

251. **R. Mindrup,** Jnl. Chromat. Sci. Vol.16, 380, 1978.

252. **J.H. Purnell,** Progress in Gas Chromatography, Wiley Interscience, 1968.

253. **D. Ambrose,** Gas Chromatography, Butterworths, 1971.

254. **J.J. Van Deemter, F.J. Zuiderweg, A. Klinkenberg,** Chem. Sci. 5, 271, 1956.

255. Handbook of Physics and Chemistry 54th edition CRC press, 1973/74.

256. **R.H. Brown, C.J. Purnell,** J. Chromatogr. 178, 79, 1979.

257. **A.I. Clark, A.E. McIntyre, J.N. Lester, R. Perry,** J. Chromatogr. 252, 147, 1982.

258. **A. Dravnieks, B.K. Krotoszynski, J. Whitfield, A. O'Donnell, T. Burgwald,** Environ. Sci. Technol. 5, 1221, 1971.

259. **J. DeGreef, M. DeProft, G.S. Neff,** Anal. Chem. 48, 38, 1976.

260. **A. Zlatkis, H.A. Lichtenstein, A. Tishbee,** Chromatographia, 6, 67, 1973.

261. **J.S. Parsons, S. Mitzner,** Environ. Sci. Technol. 9, 1053, 1975.

262. **R.K. Koppe, D.F. Adams,** Environ. Sci. Technol. 1, 479, 1967.

263. **T.L.C. deSouza, D.C. Lane, S.P. Bhatia,** Anal. Chem. 47, 3, 543, 1975.

264. **D.S. Walker,** Analyst, 397, April, 1978.

265. **M.S. Black, R. Herbst, D.R. Hitchcock,** Anal. Chem. 50, 848, 1978.

266. **L. Torres, M. Frikha, J. Mathieu, M.L. Riba,** Int. J. Environ. Anal. Chem. 13, 155, 1983.

267. **A.B. Roe,** J. Inst. Water Engrs. Sci. 36, 2, 118, 1982

268. **F. Bruner, P. Ciccioli, G. Bertoni,** J. Chromatogr. 120, 200, 1976.

269. **J.P. Guenier, P. Simon, J. Delcourt, M.R. Didierjean, C. Lefevre, J. Muller,** Chromatogr. 18, 3, 1984.

270. Air Analysis in the Mining Industry, Vol. 1, 1973.

271. **E.D. Pellizzari, J.E. Bunch, R.E. Berkley, J. McRae,** Anal. Lett. 9, 45, 1976.

272. **A. Braithwaite, F.J. Smith,** Chromatographic Methods, Chapman and Hall, London, 1985.

273. **W.R. Supina,** The Packed Column in Gas Chromatography, Supelco Ltd. Bellefonte, Pa, 1974.

274. **G. Bertoni, F. Bruner, A. Liberti, C. Perrino,** J. Chromatogr. 203, 263, 1981.

275. **D.T. Coker, A.M. McDougall,** IE and S. News, 7, March, 1984.

276. **A. Wehrli, E. Kovats,** Helv. Chim. Acta. 42, 2709, 1959.

277. **L. Rohrschneider,** J. Chromatogr. 22, 6, 1966.

278. **F. Mangani, F. Bruner,** Anal.Chem. 55, 2193, 1983.

279. **R.K. Beasley, C.E. Hoffmann, M.L. Ruepell, J.W. Worley,** Anal.Chem. 52, 1110, 1980.

280. **E.R. Kennedy, R.H. Hill,** Anal. Chem. 54, 1739, 1982.

281. **K.L. Gelsling, R.R. Miksch,** Anal. Chem. 54, 140, 1982.

282. N.C.B. Internal Report. SNT/20/67.

283. The Analytical Chemistry of Industrial Poisons, Hazards and Solvents. Second edn M.B. Jacobs, Interscience, New York.

284. Inorganic Chemistry, Fifth edn. P.C.L. Thorne, E.R. Roberts, Gurney and Jackson, London.

285. **W.C. Pearce,** Ph.D. Thesis. Sheffield Polytechnic 1984.

286. **L.T. Edgcombe,** Fuel 35, 38, 1956.

287. **R.C.S. Clay, S. Gibson, A. Wynne,** N.C.B. Internal Report, EMRL/108/76.

288. **H.P. Davies, D.W. Holdom,** N.C.B. Internal Report, EMRL/32/85.

289. **A. Wynne,** M.Phil Thesis, Sheffield Polytechnic, 1981.

290. **J.F. McAleer, P.T. Moseley, J.O.W. Norris, D.E. Williams,** J. Chem. Soc., Faraday Trans. 1, 83, 1323, 1987.

291. **J. Maier,** Berichte-Bunsenges. Phys. Chemie, 90, 1, 26, 1986.

292. **M.J. Willett,** Ph.D. Thesis, Nottingham University 1987.

293. **Y. Matsuura, K. Takahata, K. Ihokura,** Sensors and Actuators, 14, 223, 1988.

294. **S. Zaromb, J.R. Stetter,** Sensors and Actuators, 6, 225, 1984.

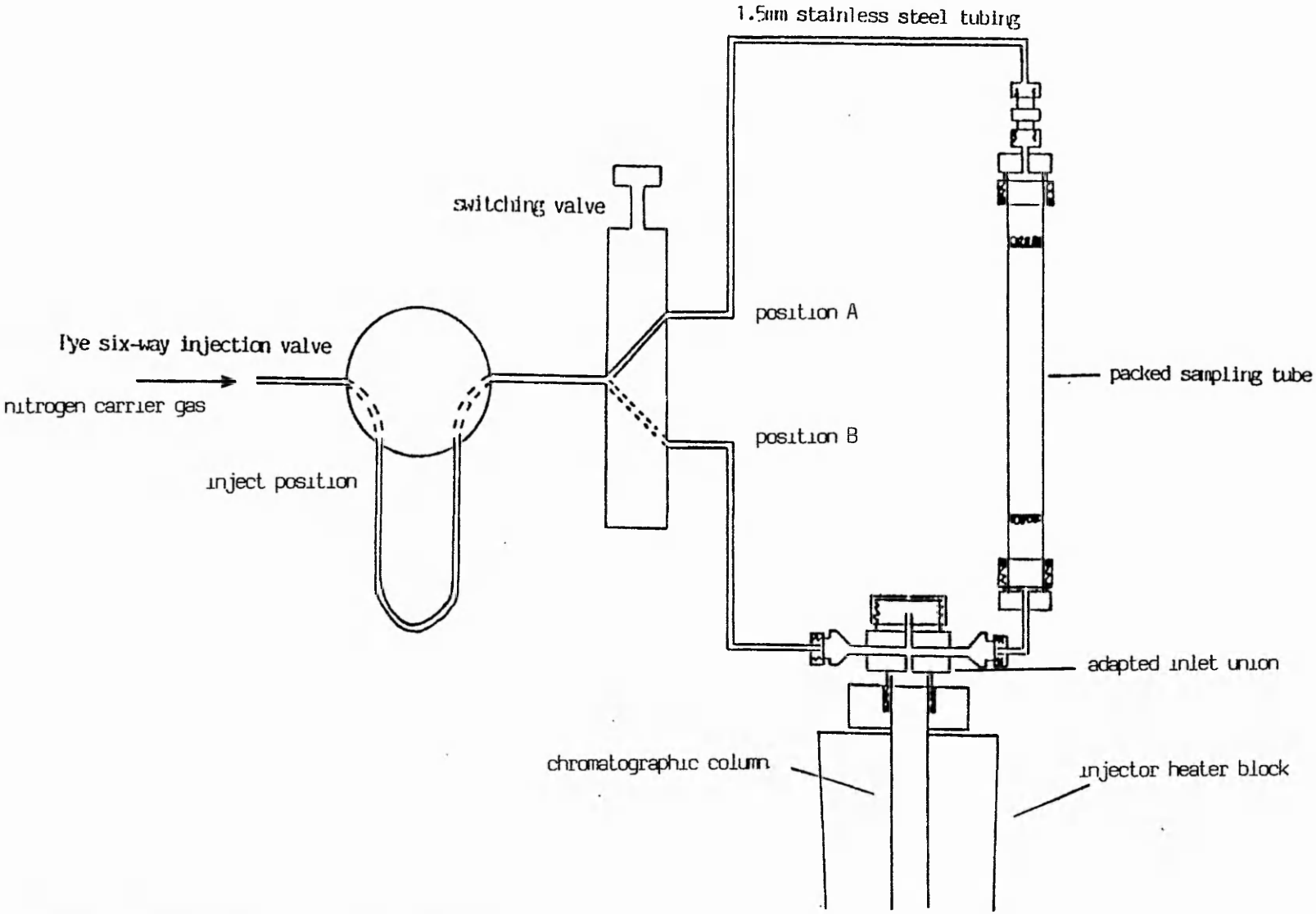

Figure 6 Schematic diagram of desorption system

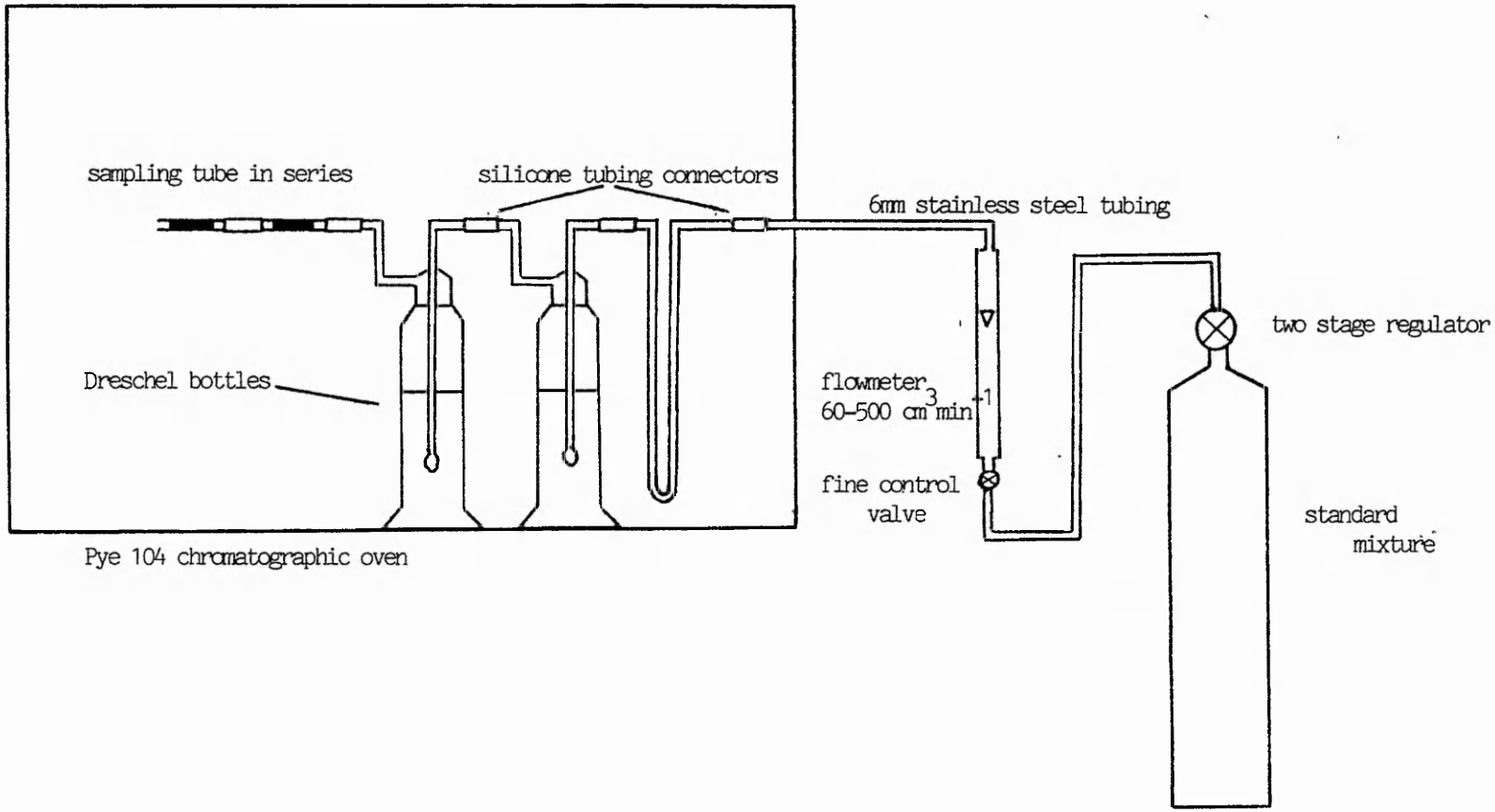

Figure 7. Schematic diagram of apparatus used in determination of the safe sampling volume.

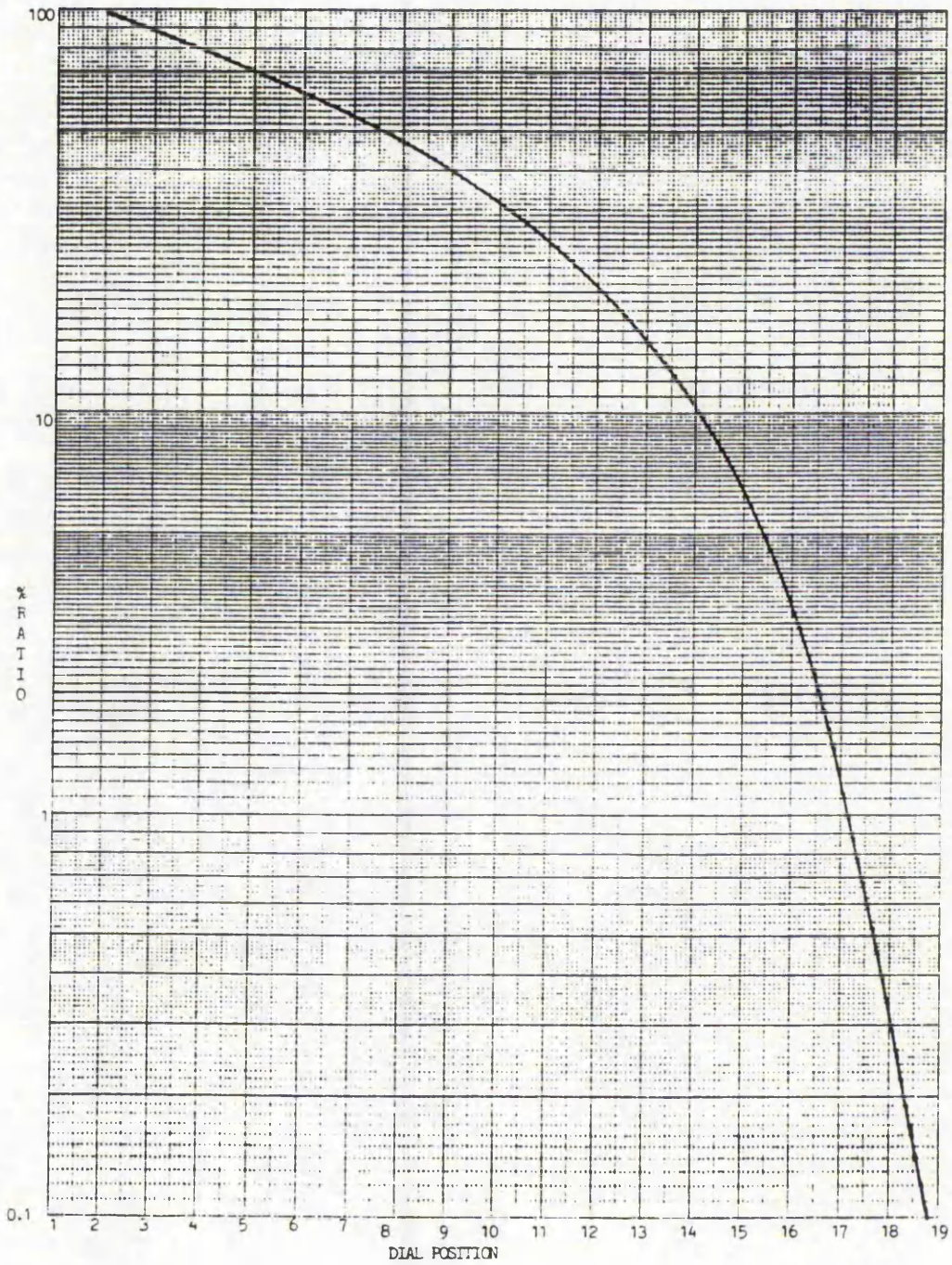

Figure 8. Calibration graph showing dial position versus ratio of blend of calibration gases.

Chromatographic Conditions

Column	Molecular sieve 13X, 40-60 mesh 2m x 6mm o.d.
Column temperature	50°C
Injector temperature	75°C
Detector temperature	110°C
Sample volume	5ml
Bridge current	100 mA
Dectector sensitivity	Trace A x 5 Trace B x 1
Chart speed	5mm min^{-1}

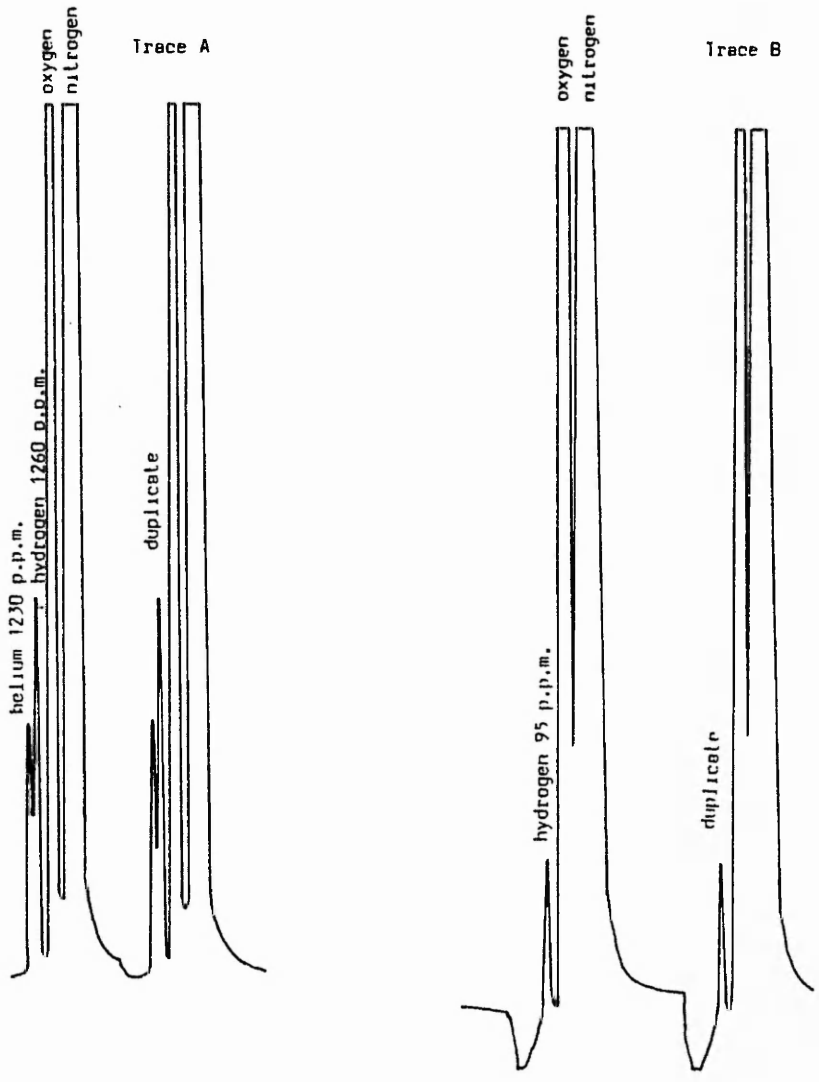

Figure 9. Chromatograms of standard mixtures containing hydrogen separated on Molecular sieve 13X (traces reduced from A4-A3).

Chromatographic conditions.

Column	Porapak Q, 80-100 mesh 2m x 3mm o.d.
Column temperature	30°C
Injector temperature	110°C
Detector temperature	150°C
Carrier gas flow rate	12.5 ml min^{-1}
Sample volume	2 ml
Detector sensitivity	10^{-12} x16
Integrator attn	x8
Chart speed	5mm min^{-1}

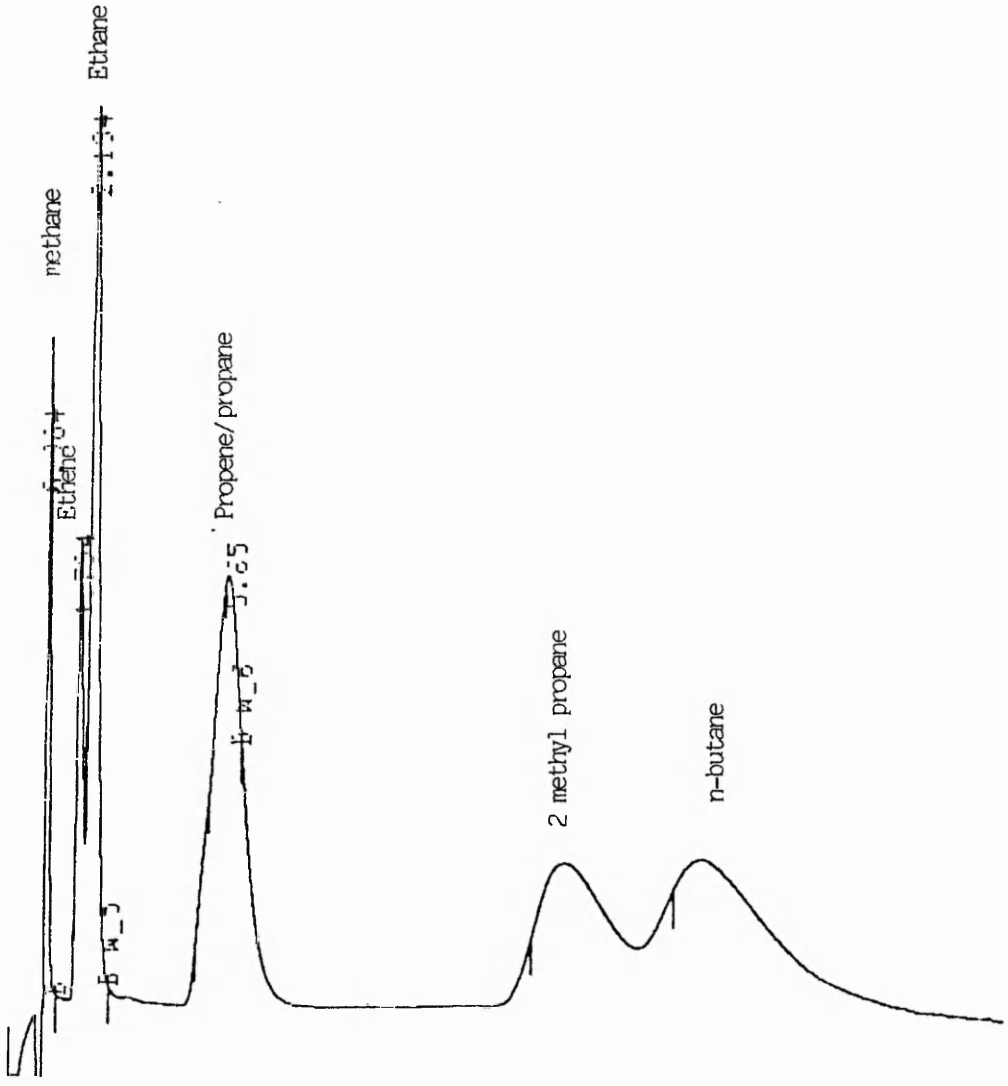

Figure 10. Chromatogram of C_1-C_4 hydrocarbon standard mixture on Porapak Q.

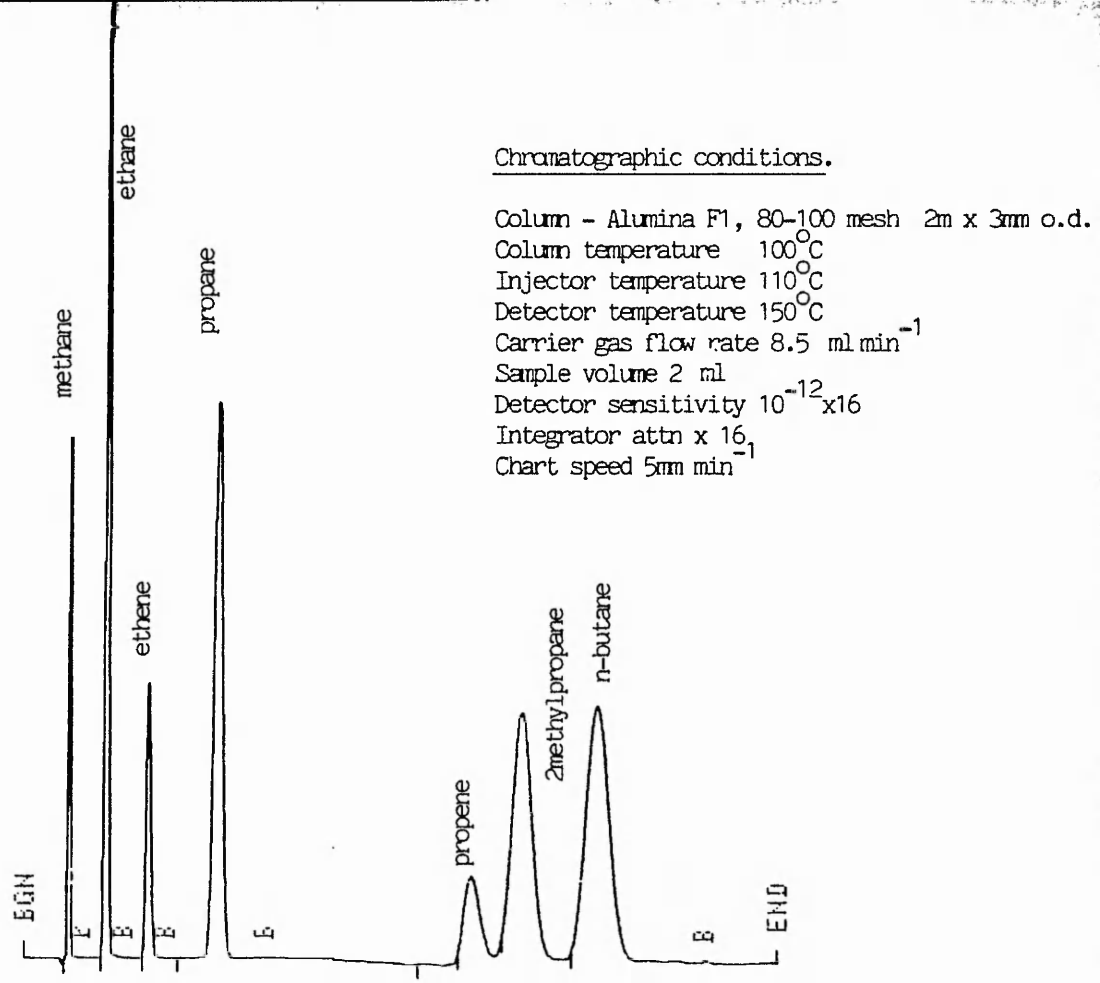

Figure 11a. Chromatogram of C_1–C_4 hydrocarbon standard mixture at optimum carrier gas velocity.

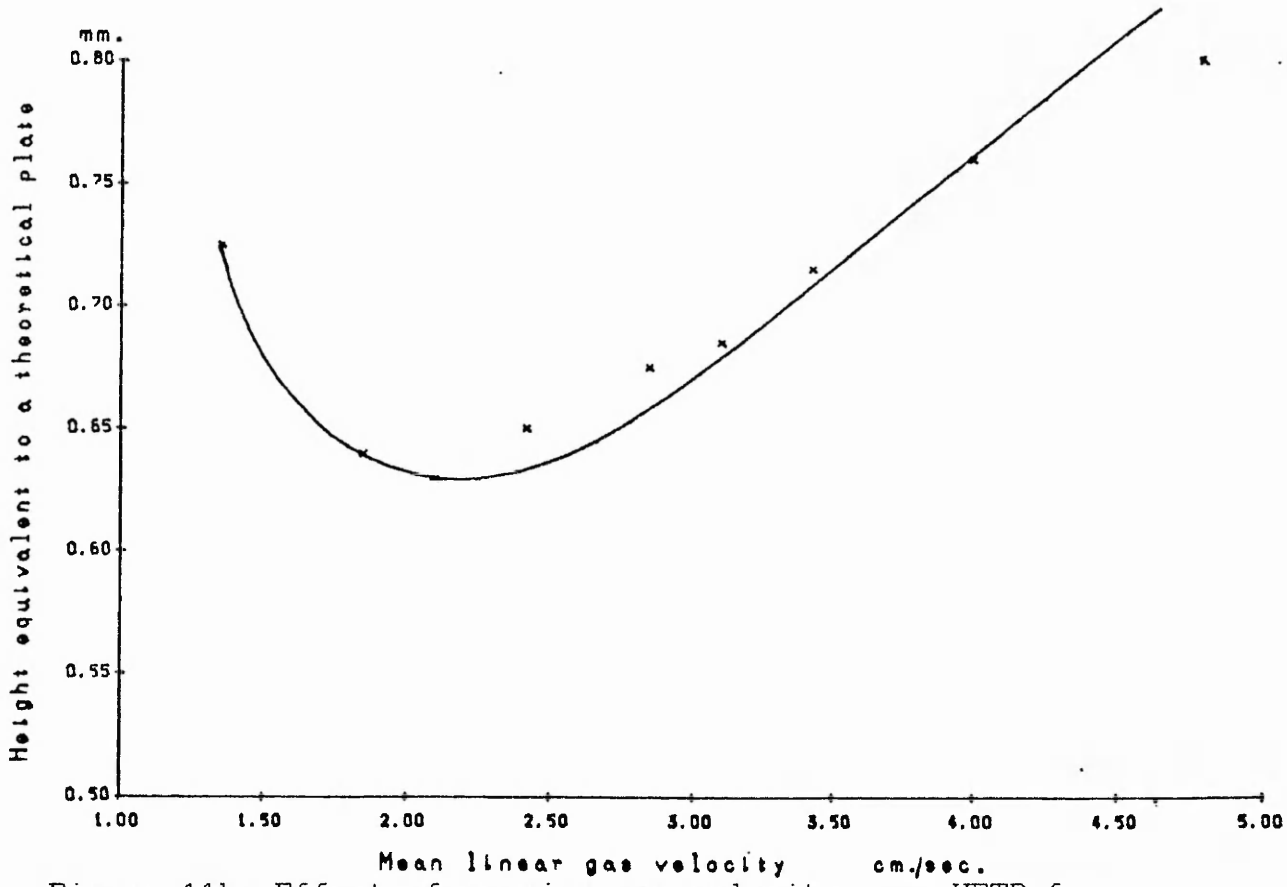

Figure 11b. Effect of carrier gas velocity upon HETP for 2 methyl propane at 100°C on alumina F1.

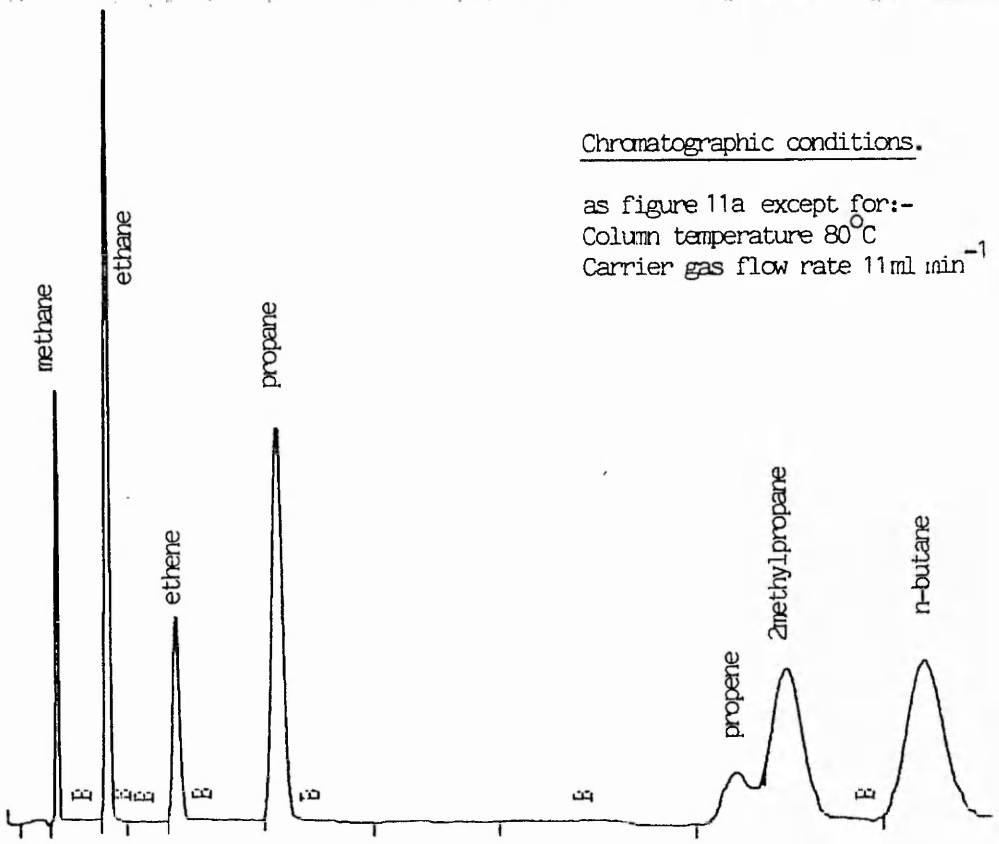

Figure 12a. Chromatogram of C_1-C_4 hydrocarbon standard mixture at optimum carrier gas velocity.

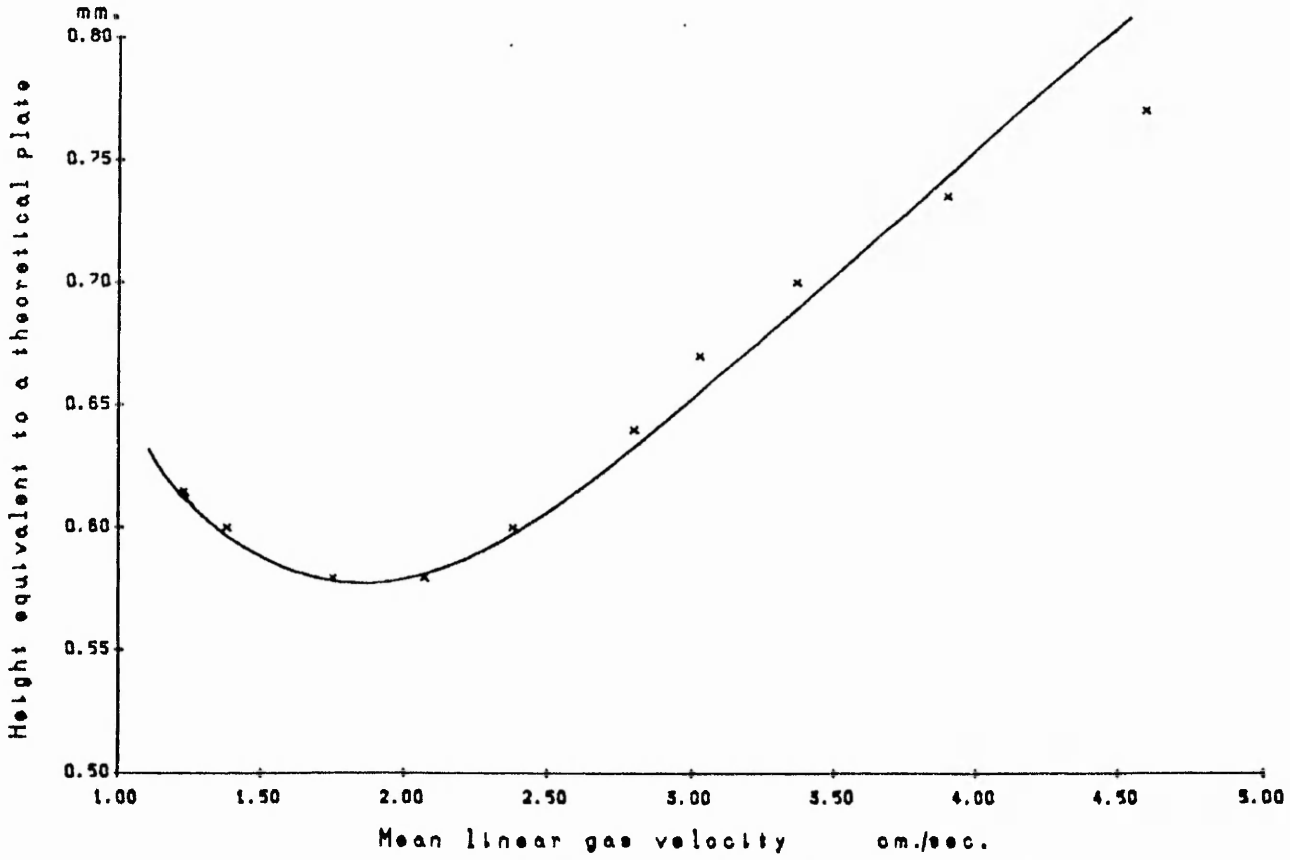

Figure 12a. Effect of carrier gas velocity upon HETP for 2-methylpropane at 80°C on alumina F1.

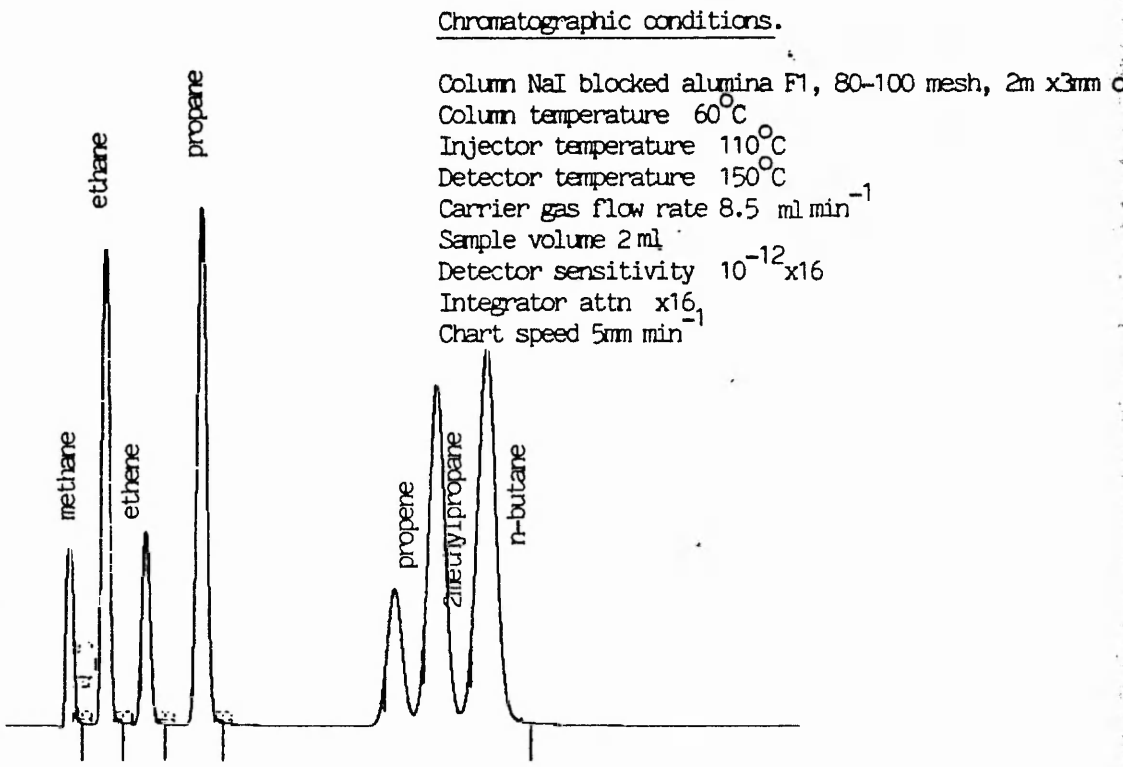

Figure 13a. Chromatogram of C_1-C_4 hydrocarbon standard mixture at optimum carrier gas velocity.

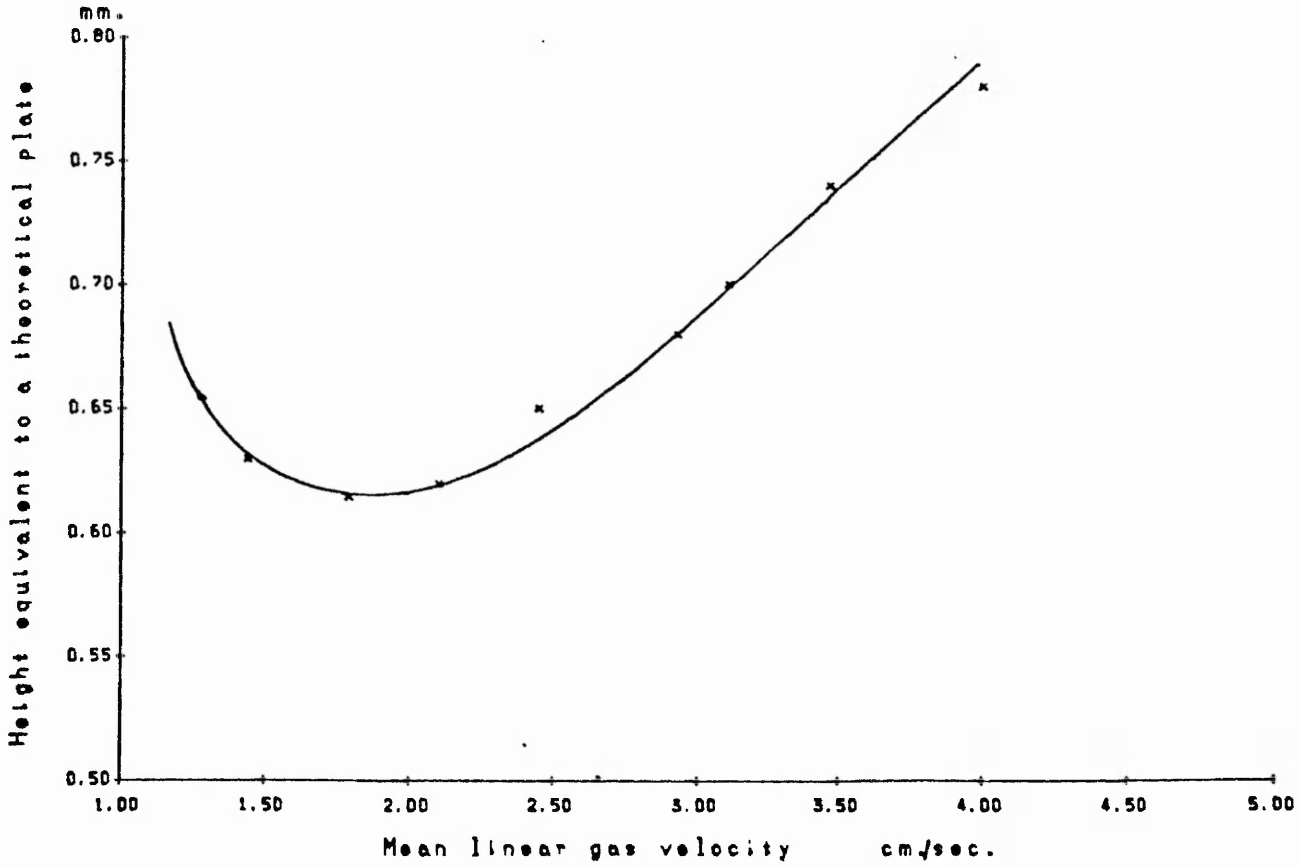

Figure 13b. Effect of carrier gas velocity upon HETP at 60°C on NaI modified alumina.

Chromatographic conditions.

Column NaÏ blocked alumina F1, 80-100 mesh,
2m x 3mm o.d.
Column temperature 50-220°C at 8°min^{-1}, hold
Injector temperature 110°C
Detector temperature 250°C
Carrier gas flow rate 15 ml min^{-1}
Sample volume 2 ml
Detector sensitivity 10^{12}x16 , x4
Integrator attn x16
Chart speed 5mm min^{-1}

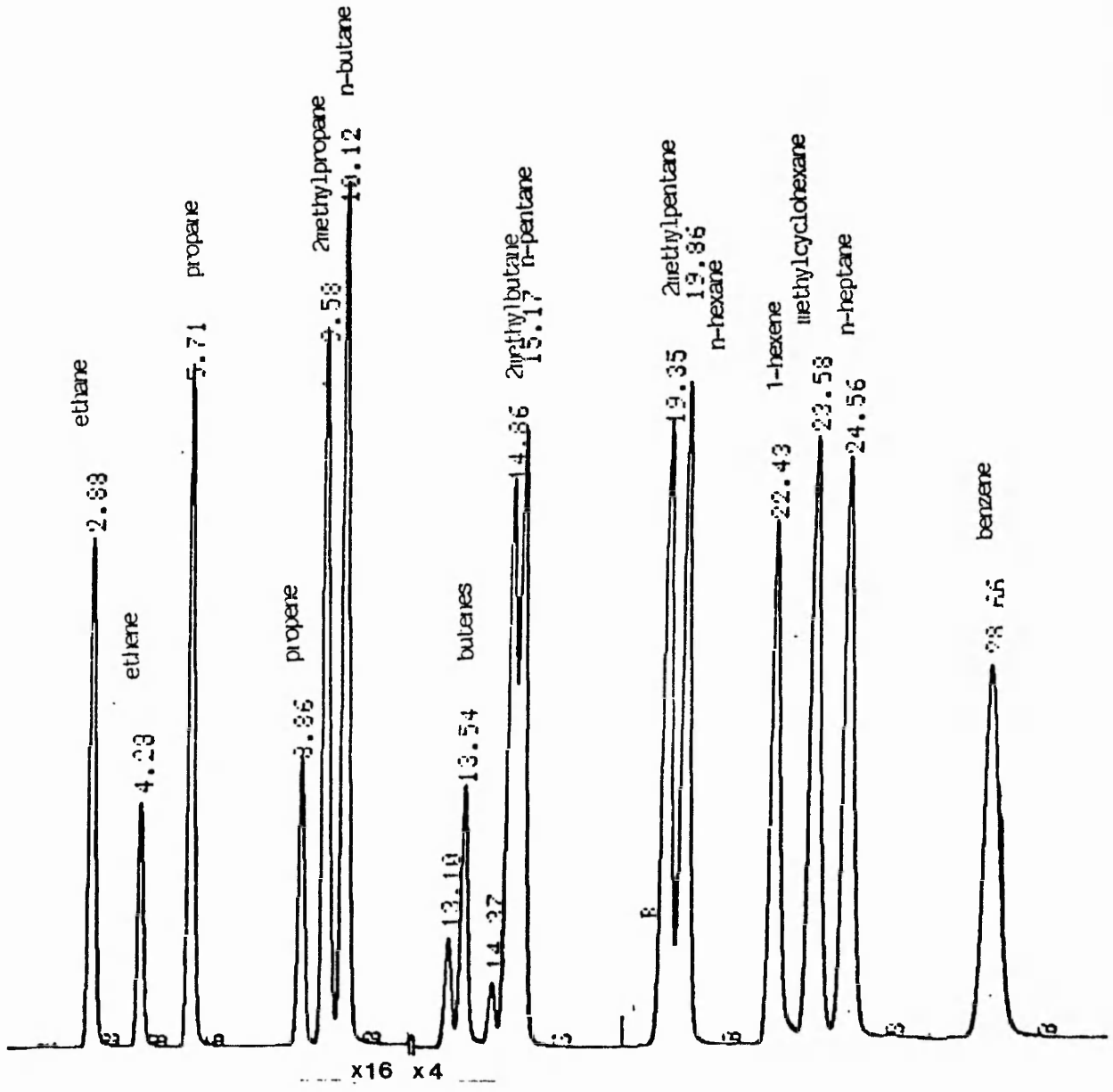

Figure 14. Chromatogram of C_2-C_7 hydrocarbons.

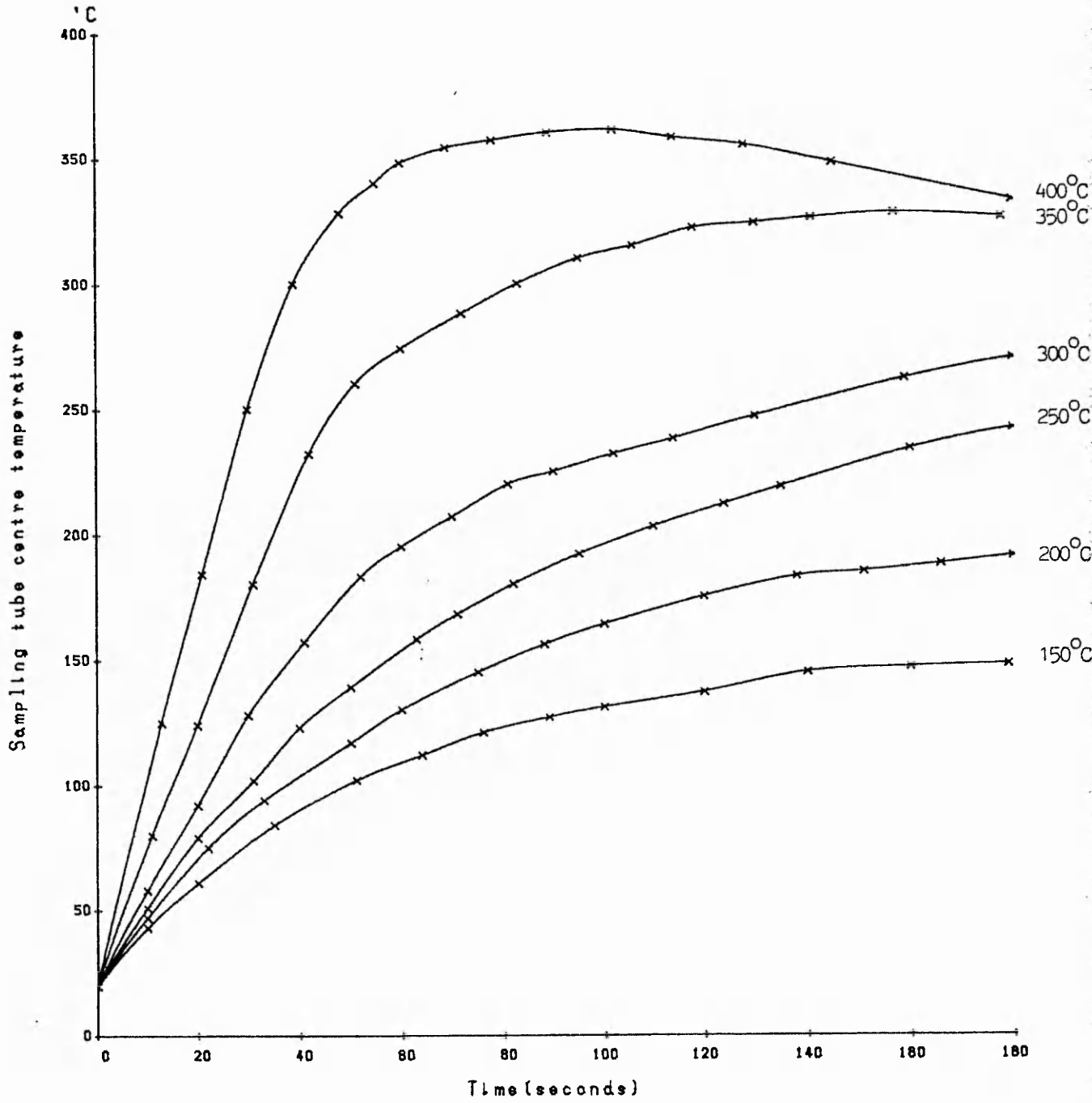

Figure 15. Mean adsorbent temperature at sampling tube centre versus time at different heater block temperatures.

Chromatographic conditions.

Column NaT blocked alumina F1, 80-100 mesh, 2m x 3mm o.d.
Column temperature 50-220°C at 8°C min^{-1}, hold
Injector temperature 110°C
Detector temperature 250°C
Carrier gas flow rate 15 ml min^{-1}
Sample volume 100 ml
Desorption conditions Heater block 350°C for 60 seconds
Detector sensitivity as shown
Integrator attn x64
Chart speed 10 mm min^{-1}

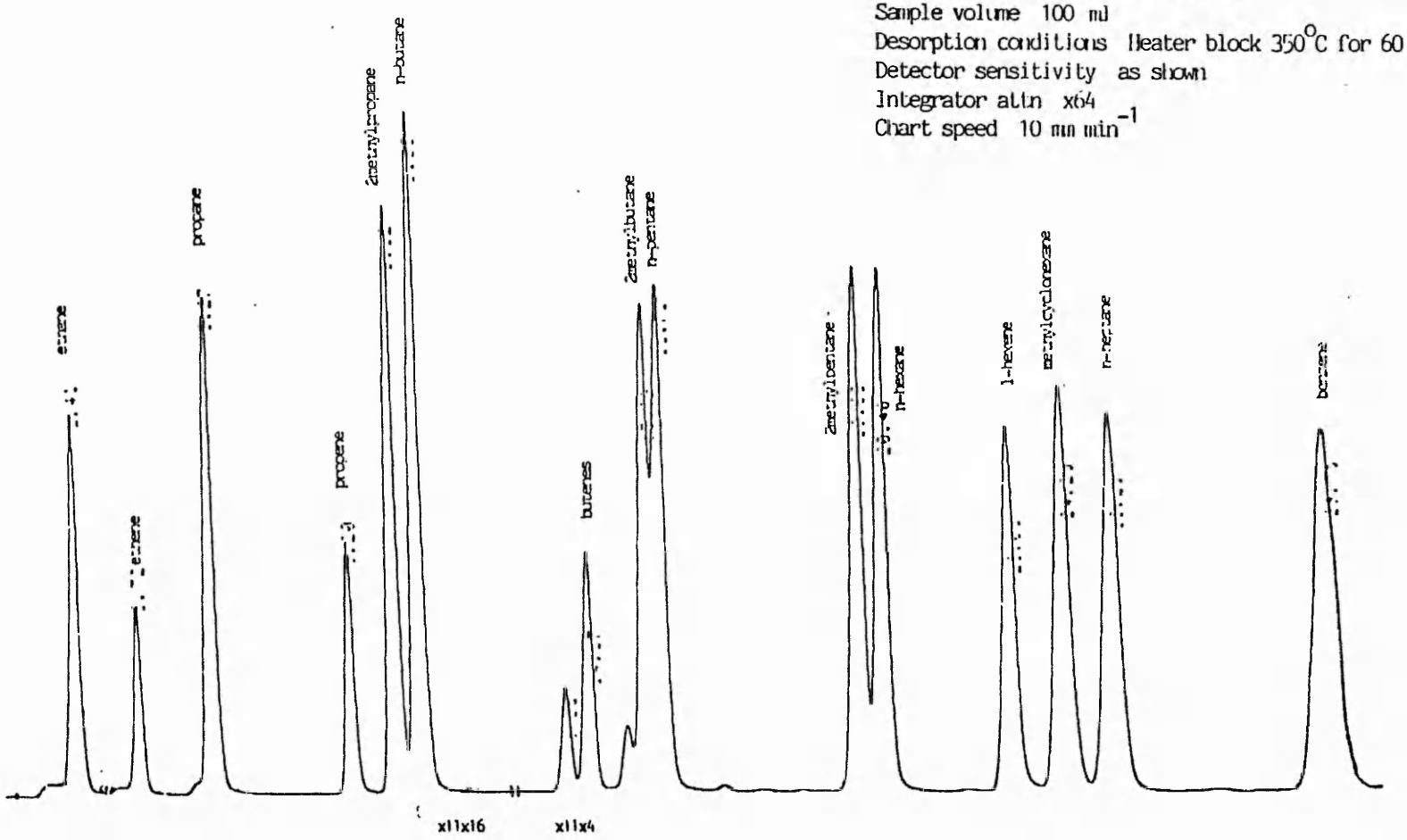

Figure 16. Desorption of a 100 ml sample of the C_2-C_7 hydrocarbon standard mixture. (Trace reduced from A4 - A3)

Chromatographic conditions.

Column Tenax G.C. 80-100 mesh, 1m x 3mm o.d.
Column temperature 150°C
Injector temperature 180°C
Detector temperature 200°C
Carrier gas flow rate 15 ml min^{-1}
Sample volume 1 ml
Detector sensitivity $10x10^{2}$
Integrator attn x1
Chart speed 5mm min^{-1}

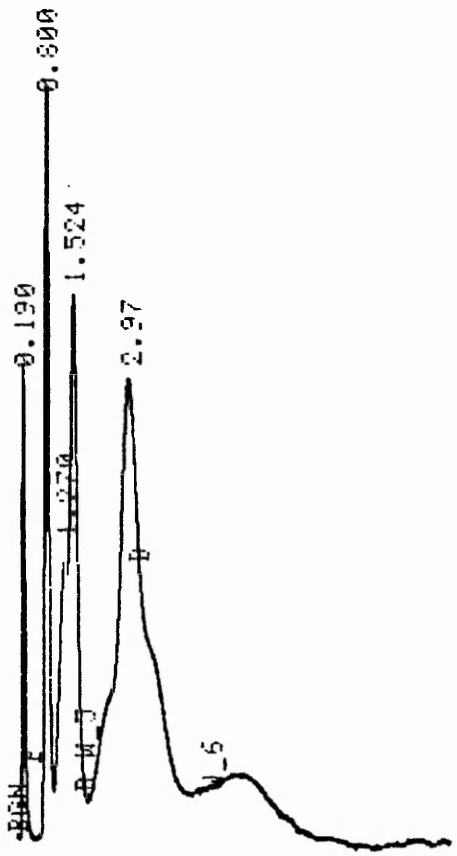

Figure 17. Chromatogram of aliphatic and aromatic hydrocarbon standard mixture on Tenax GC.

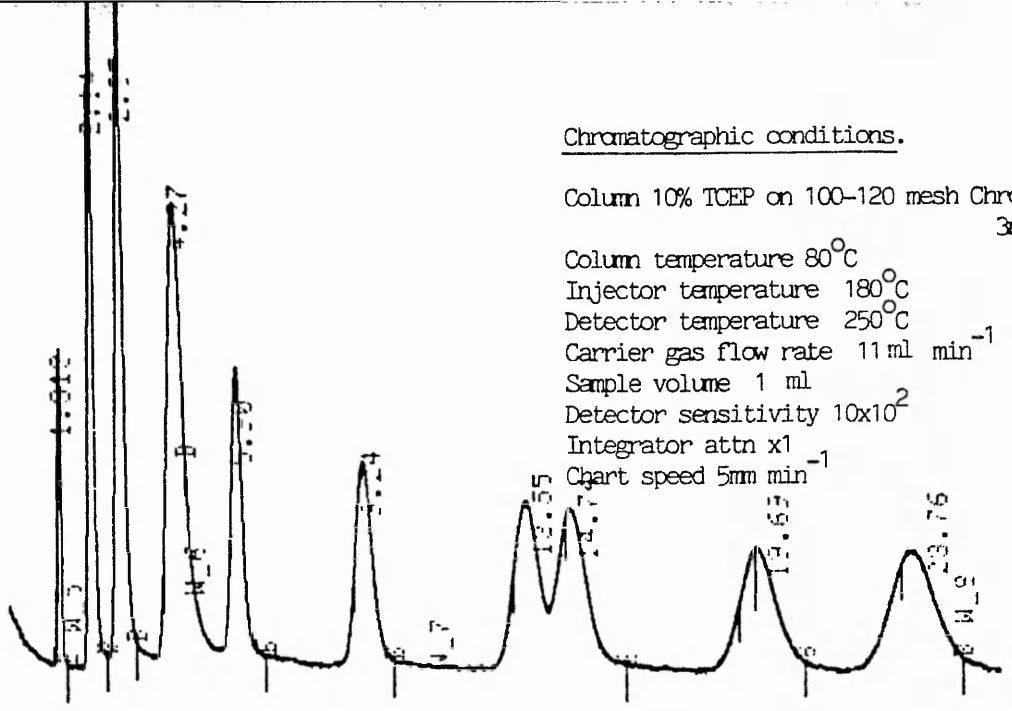

Figure 18a. Chromatogram of aliphatic and aromatic hydrocarbon standard mixture at optimum carrier gas velocity.

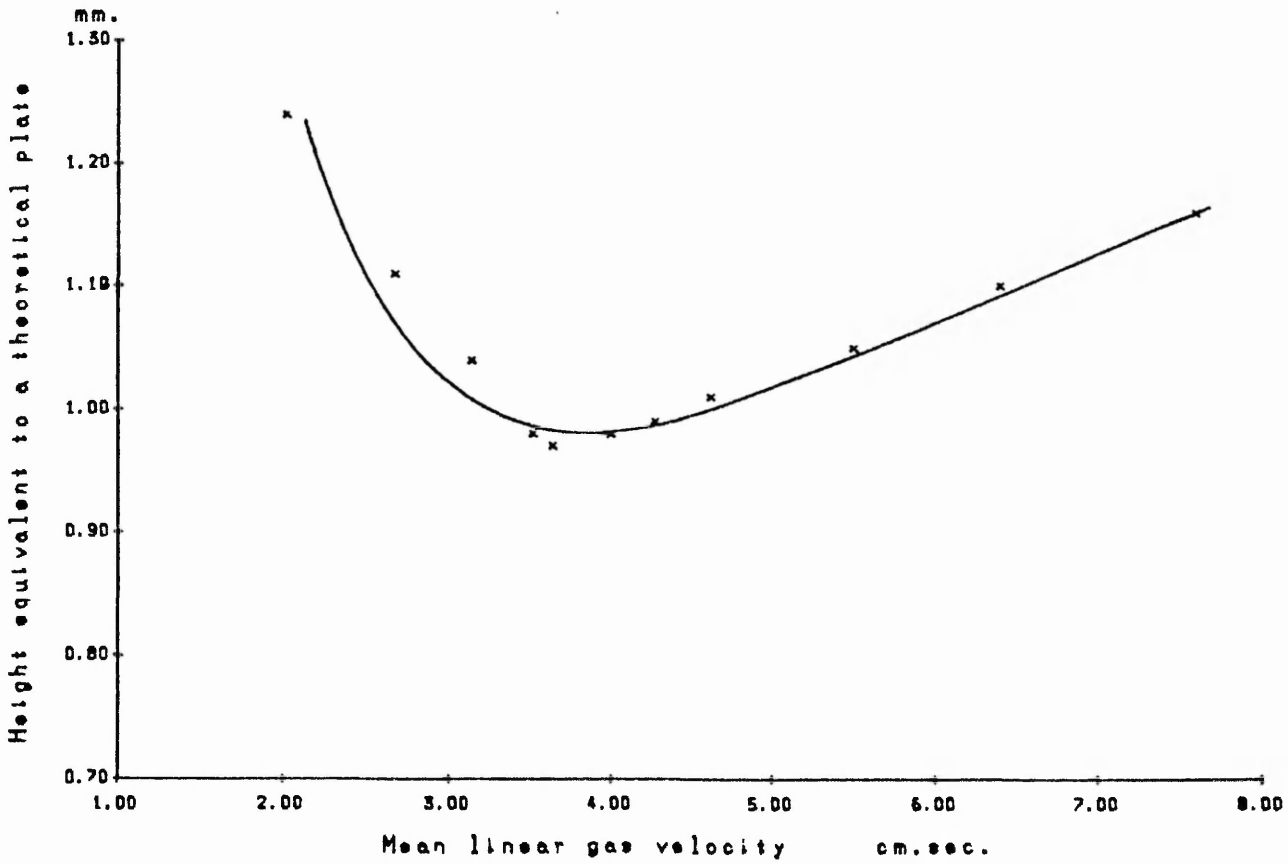

Figure 18b. Effect of carrier gas velocity upon HETP for benzene at 80°C on TCEP.

Chromatographic conditions.

Identical to Figure 18a except for:-
Carrier gas flow rate 18 ml min^{-1}

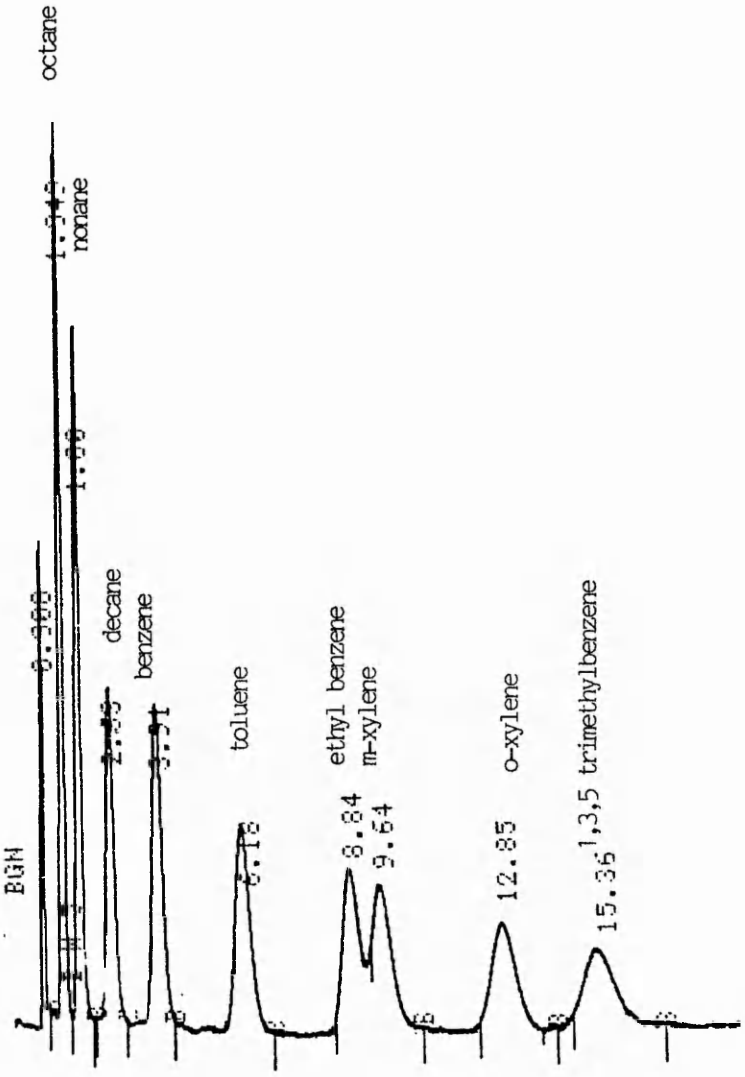

Figure 19. Chromatogram of aliphatic and aromatic hydrocarbon standard mixture at practical optimum carrier gas velocity.

Chromatographic conditions.

Identical to Figure 19 except for:-
Desorption conditions Heater block 350°C for 60 secs.
Sample volume 1000 ml
Detector sensitivity $10x10^2$
Integrator attn x128

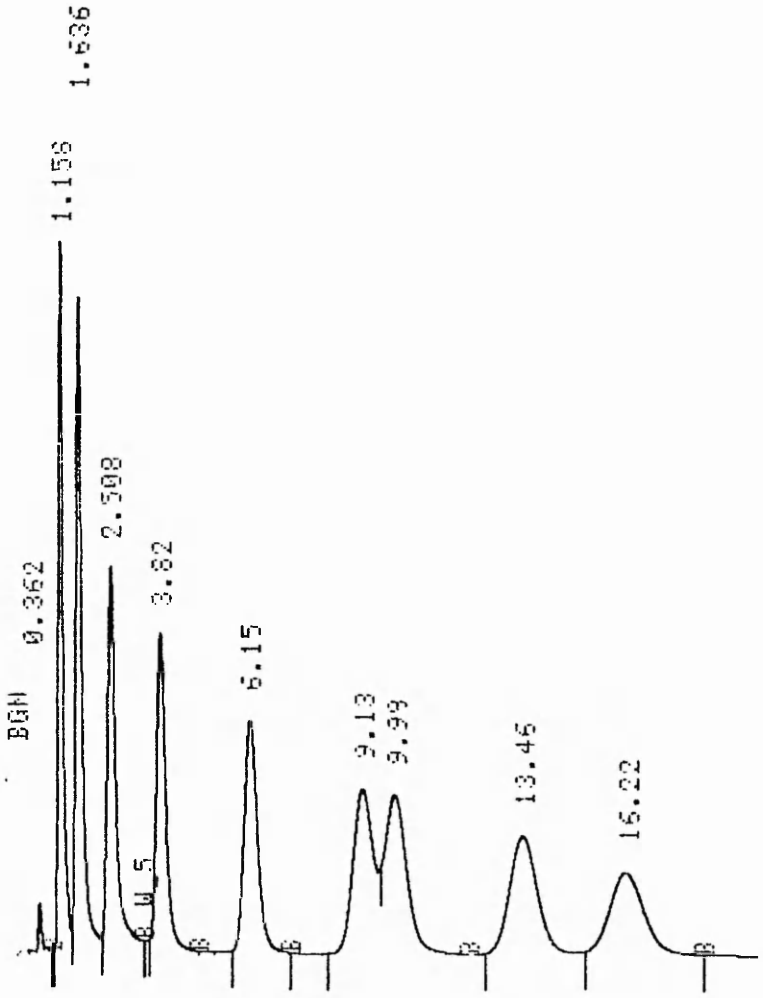

Figure 20. Desorption of a one litre sample of the aliphatic and aromatic hydrocarbon standard diluted ten fold.

Chromatographic conditions.

Identical to Figure 19 except for:-
Desorption conditions Heater block 350°C for 60 secs.
Sample volume 1000 ml
Detector sensitivity 10×10^2
Integrator attn x1

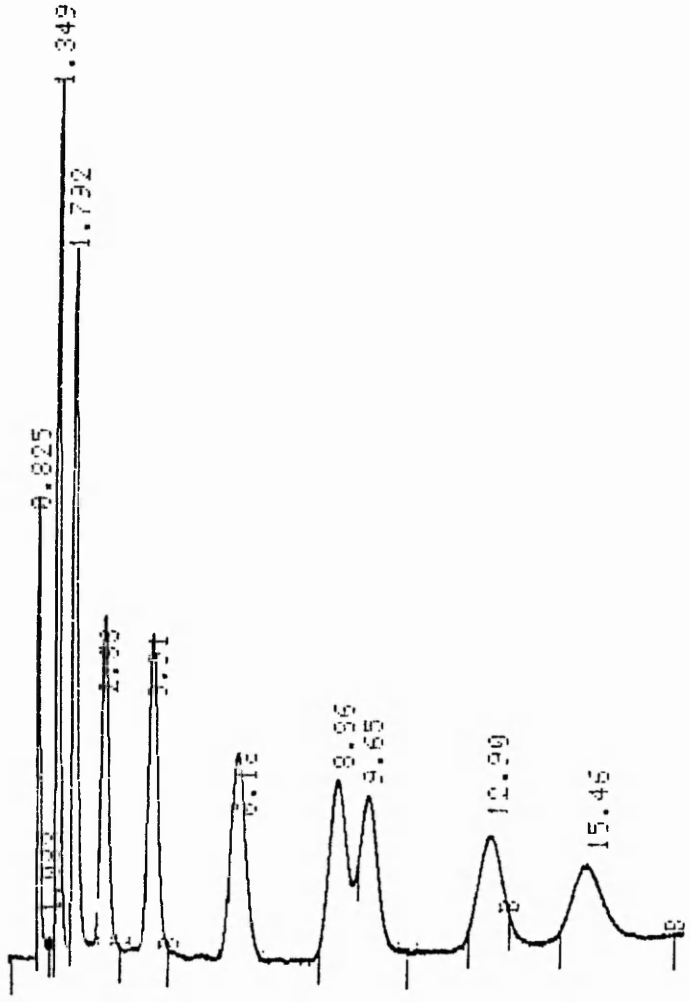

Figure 21. Desorption of a one litre sample of the aliphatic and aromatic hydrocarbon standard mixture diluted by three orders of magnitude.

Chromatographic conditions.

Column Tenax G.C. 80-100 mesh 1mx3mm o.d.
Column temperature 40°C
Injector temperature 100°C
Detector temperature 150°C
Carrier gas flow rate 6.0ml min^{-1}
Sample volume 2.5 ml
Detector sensitivity x256
Integrator attn x4
Chart speed 5mm min^{-1}

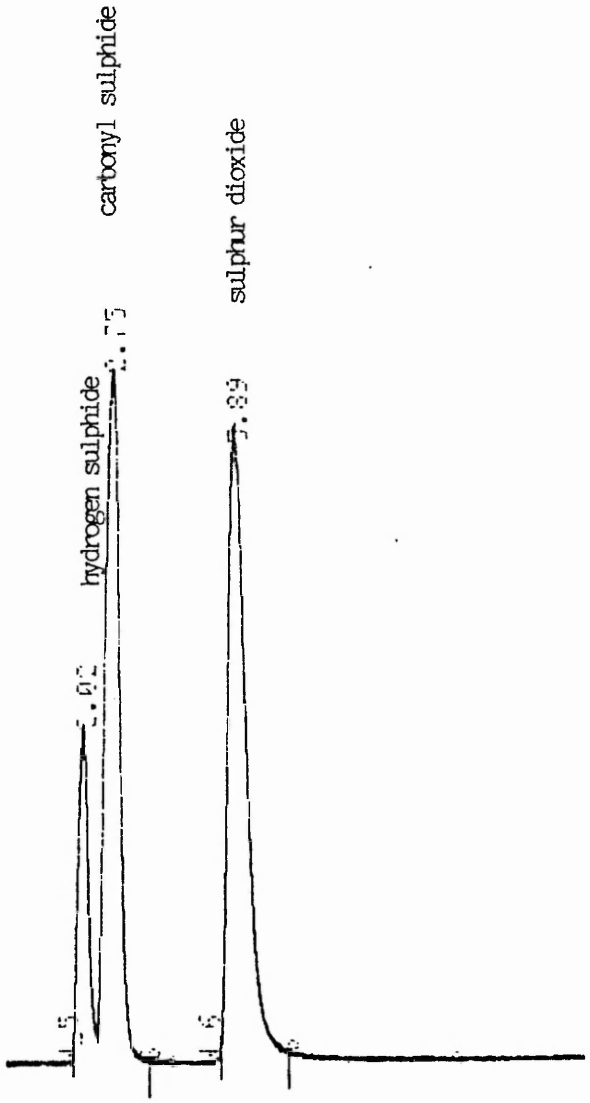

Figure 22. Chromatogram of sulphur compounds on Tenax G.C.

Chromatographic conditions.

Identical to Figure 21, except the column left overnight.

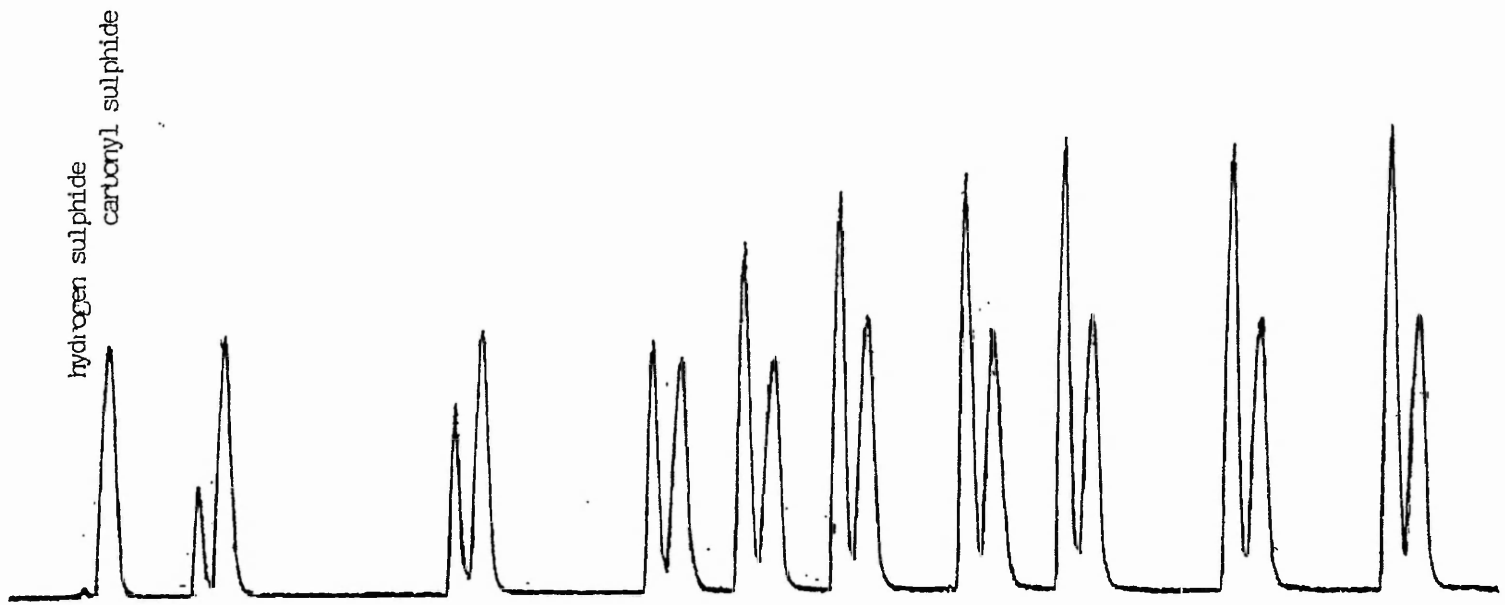

Figure 23. Replicate injections of a mixture containing hydrogen sulphide, carbonyl sulphide and sulphur dioxide on Tenax G.C.

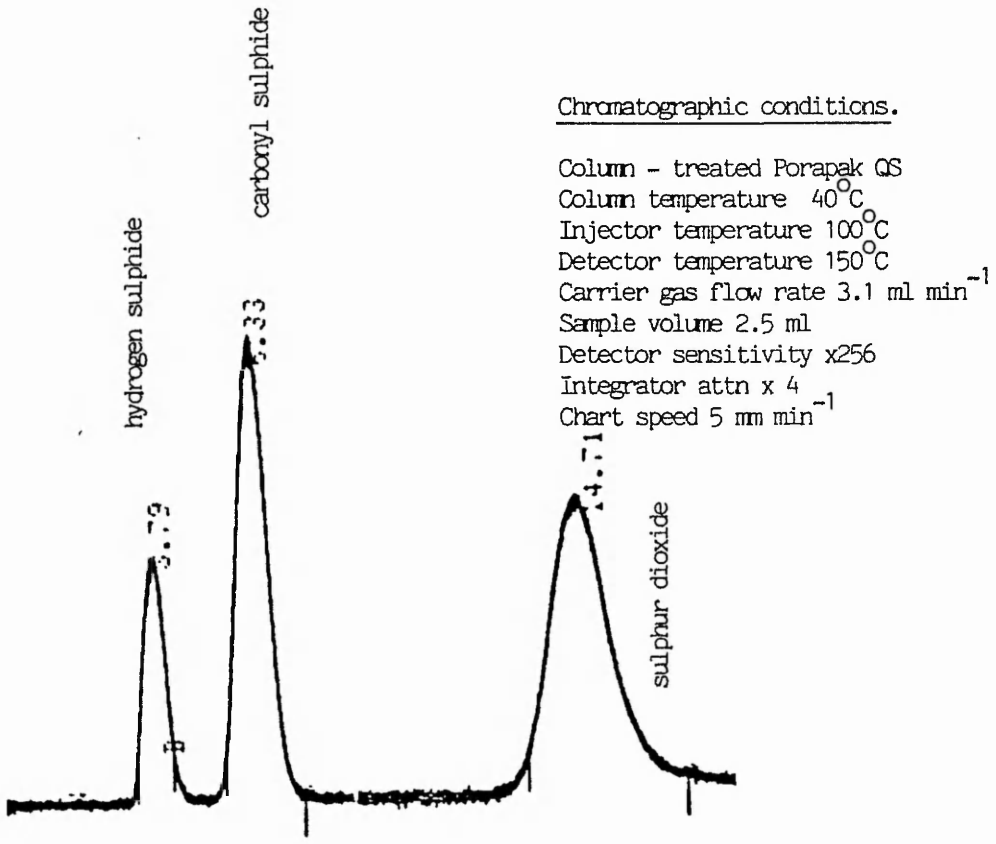

Figure 24a. Chromatogram of sulphur gases at optimum carrier gas velocity.

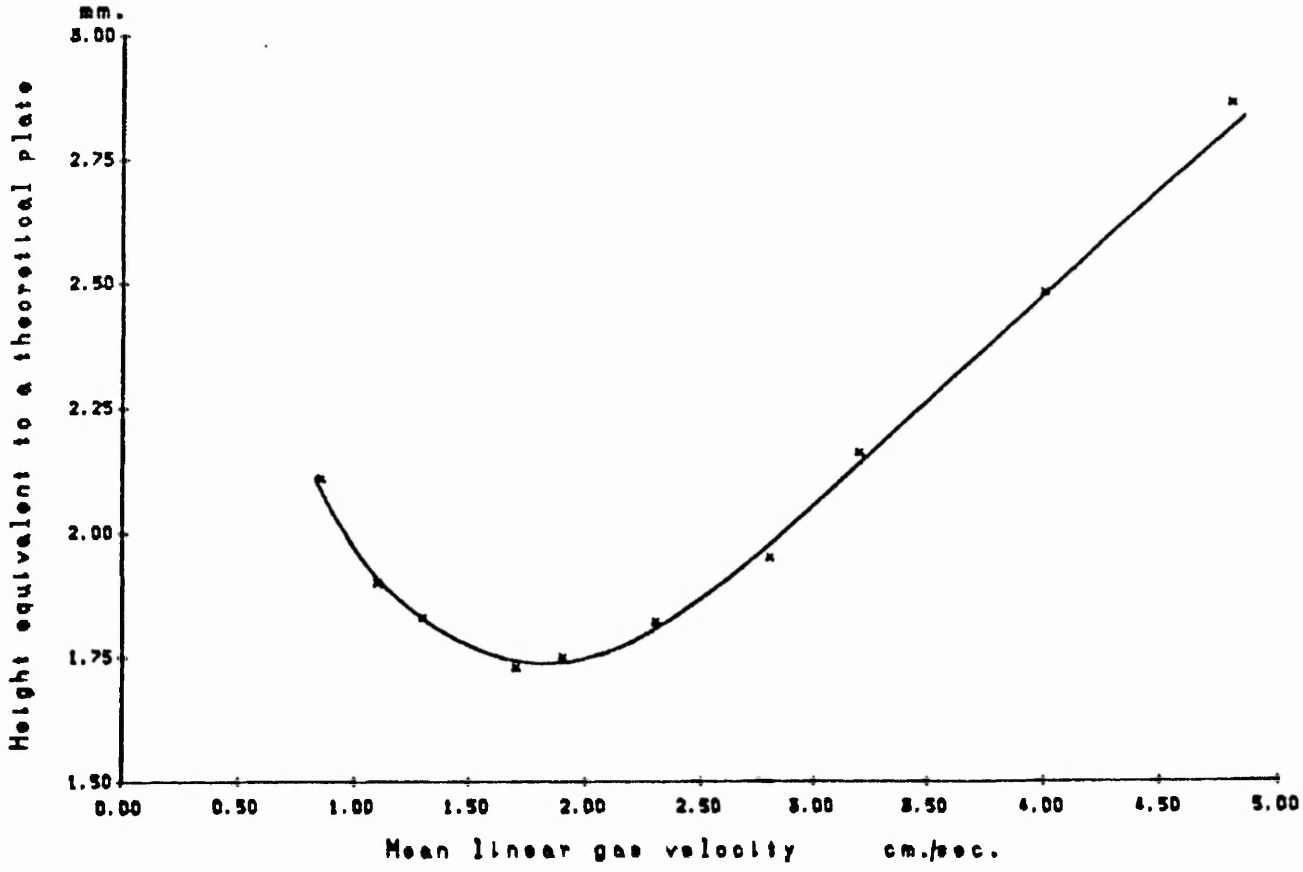

Figure 24b. Effect of carrier gas velocity upon HETP for carbonyl sulphide at 40°C on treated Porapak QS.

Chromatographic conditions.

Column - treated Porapak QS
Column temperature 40°C
Injector temperature 100°C
Detector temperature 150°C
Carrier gas flow rate 8.0 ml min^{-1}
Sample volume 2.5 ml
Detector sensitivity x256
Integrator attn x 4
Chart speed 5 mm min^{-1}

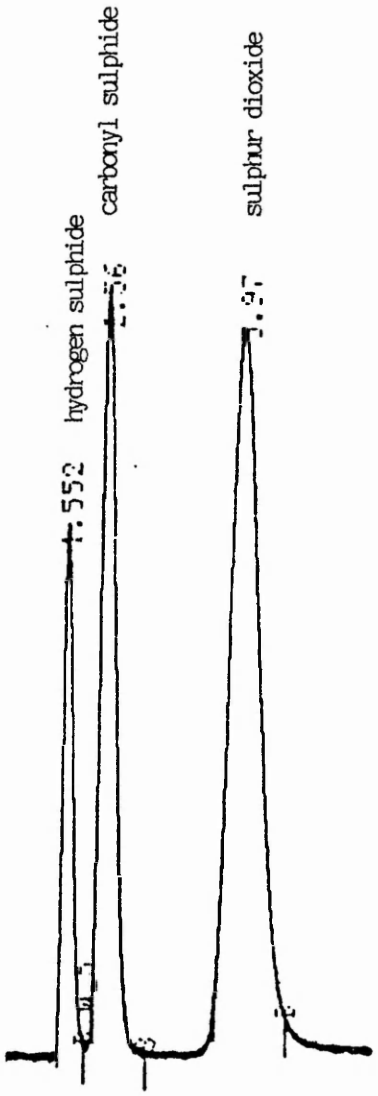

Figure 25. Chromatogram of sulphur gases at practical optimum carrier gas velocity.

Chromatographic conditions.

Identical to Figure 25.

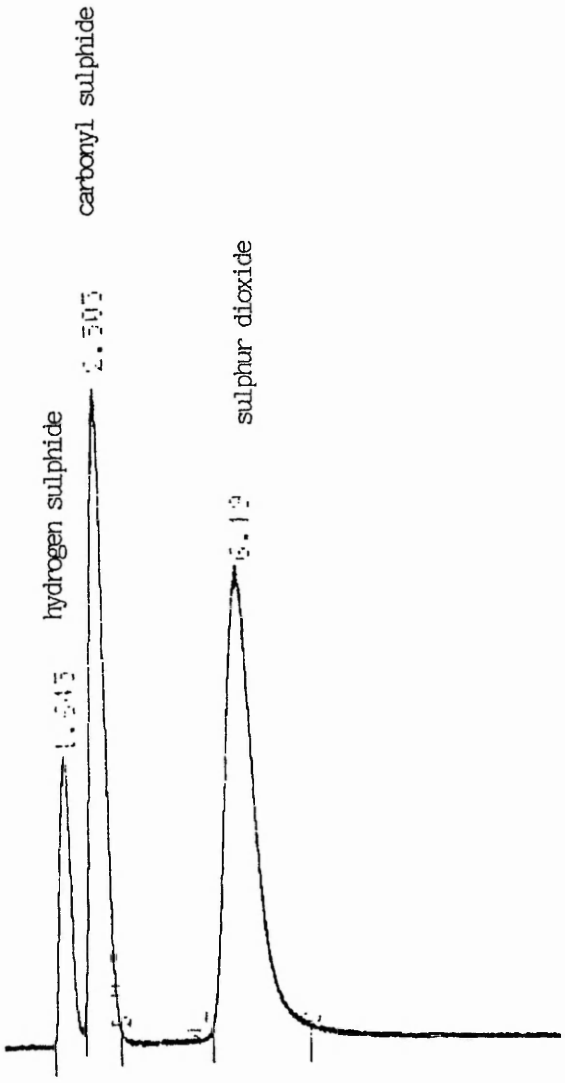

Figure 26. Chromatogram of sulphur gases on untreated Porapak QS.

Chromatographic conditions.

Identical to Figure 25 except for:-
Column temperature 100°C

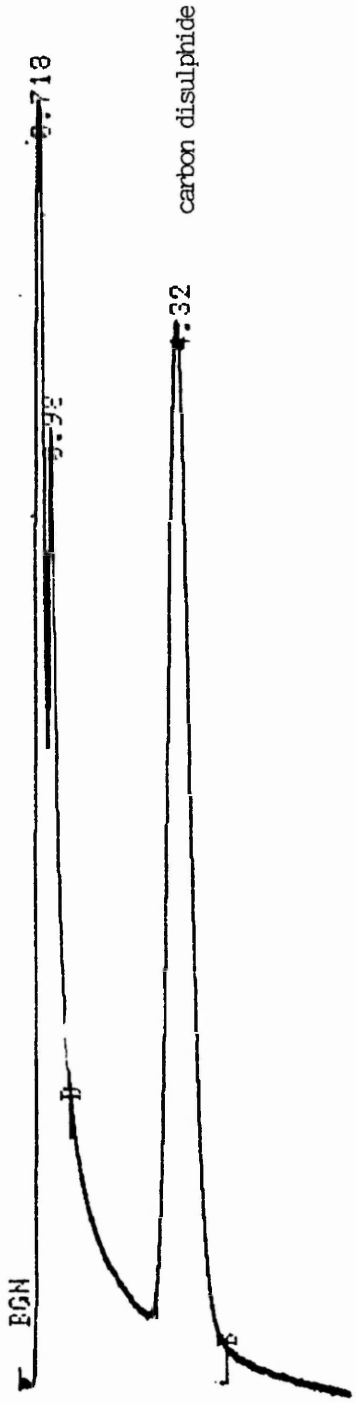

Figure 27. Chromatogram of sulphur gases on treated Porapak QS.

Chromatographic conditions.

Identical to Figure 25 except:-
Desorption conditions - Heater block
300°C for 10 secs.
Sample volume 100 ml
Detector sensitivity x256
Integrator attn x4

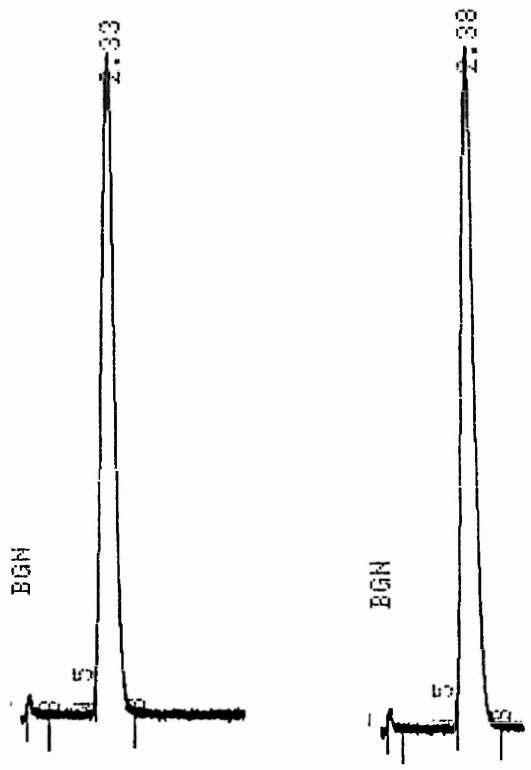

Figure 28. Desorption of 100ml of 0.1ppm carbonyl sulphide.

Chromatographic conditions.

Identical to Figure 25 except:-
Desorption conditions - Heater block 300°C
for 10 secs.
Sample volume 100ml
Detector sensitivity 1024
Integrator attn x16

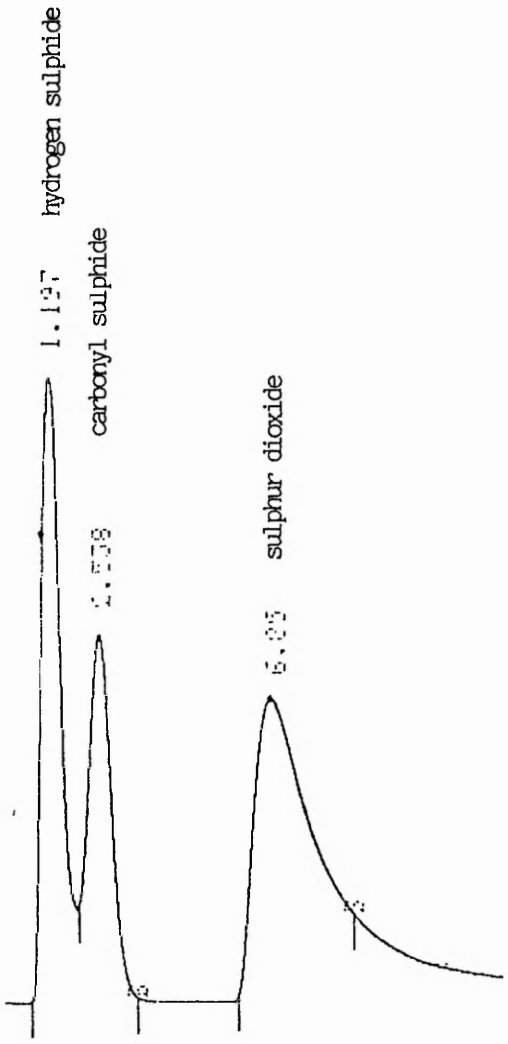

Figure 29. Desorption of 100ml sample of sulphur compounds plus 100ml of clean laboratory air.

Chromatographic conditions.

Identical to Figure 25 except:-
Desorption conditions - Heater block 300°C
for 10 secs.
Sample volume 100ml + 100ml laboratory air
Detector sensitivity 1024
Integrator attn x16

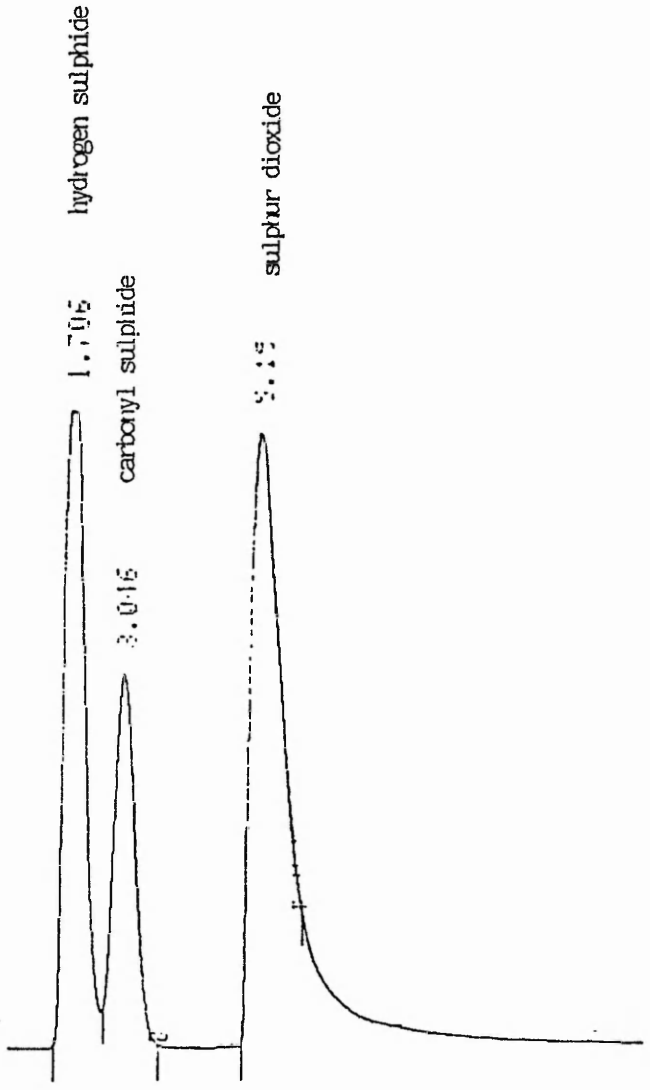

Figure 30. Desorption of 100ml sample of sulphur compounds plus 100ml dry clean laboratory air.

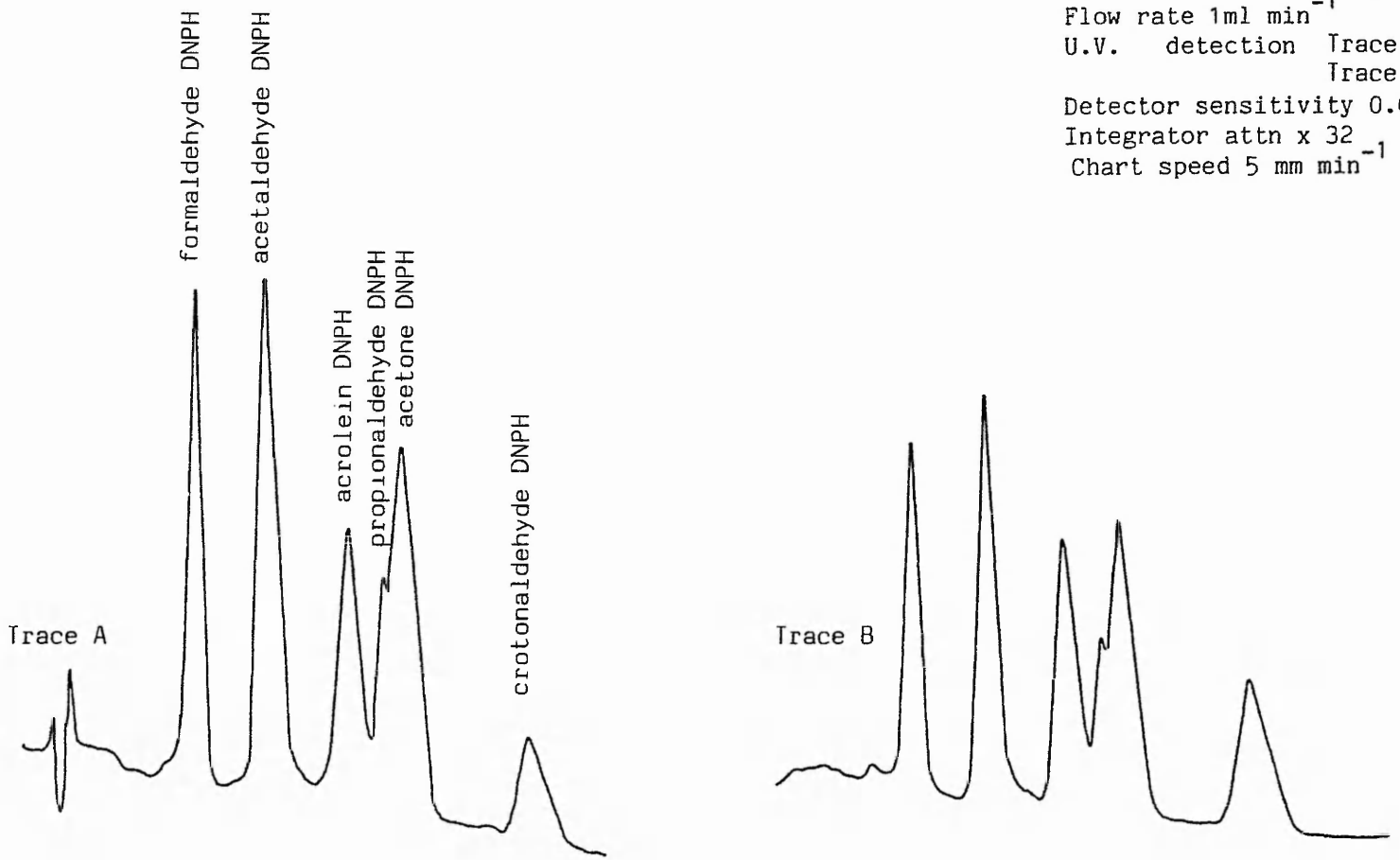

Chromatographic conditions.

Column C_{18} bonded silica column
5u, 25cm x 6mm i.d.
Eluent methanol 65% water 35%
Flow rate 1ml min^{-1}
U.V. detection Trace A 350 nm
Trace B 254 nm
Detector sensitivity 0.08 A.U.F.S.
Integrator attn x 32
Chart speed 5 mm min^{-1}

Figure 31. Chromatograms of synthetic mixture of DNPH derivatives.

Chromatographic conditions.

Column	C_{18} bonded silica column 5.0, 25cm x 6mm id
Eluent	Methanol 65%, water 35%
Flow rate	1 ml min^{-1}
U.V. detection	350 nm
Detector sensitivity	0.08 AUFS
Integrator attenuation	x 32
Chart speed	5mm min^{-1}

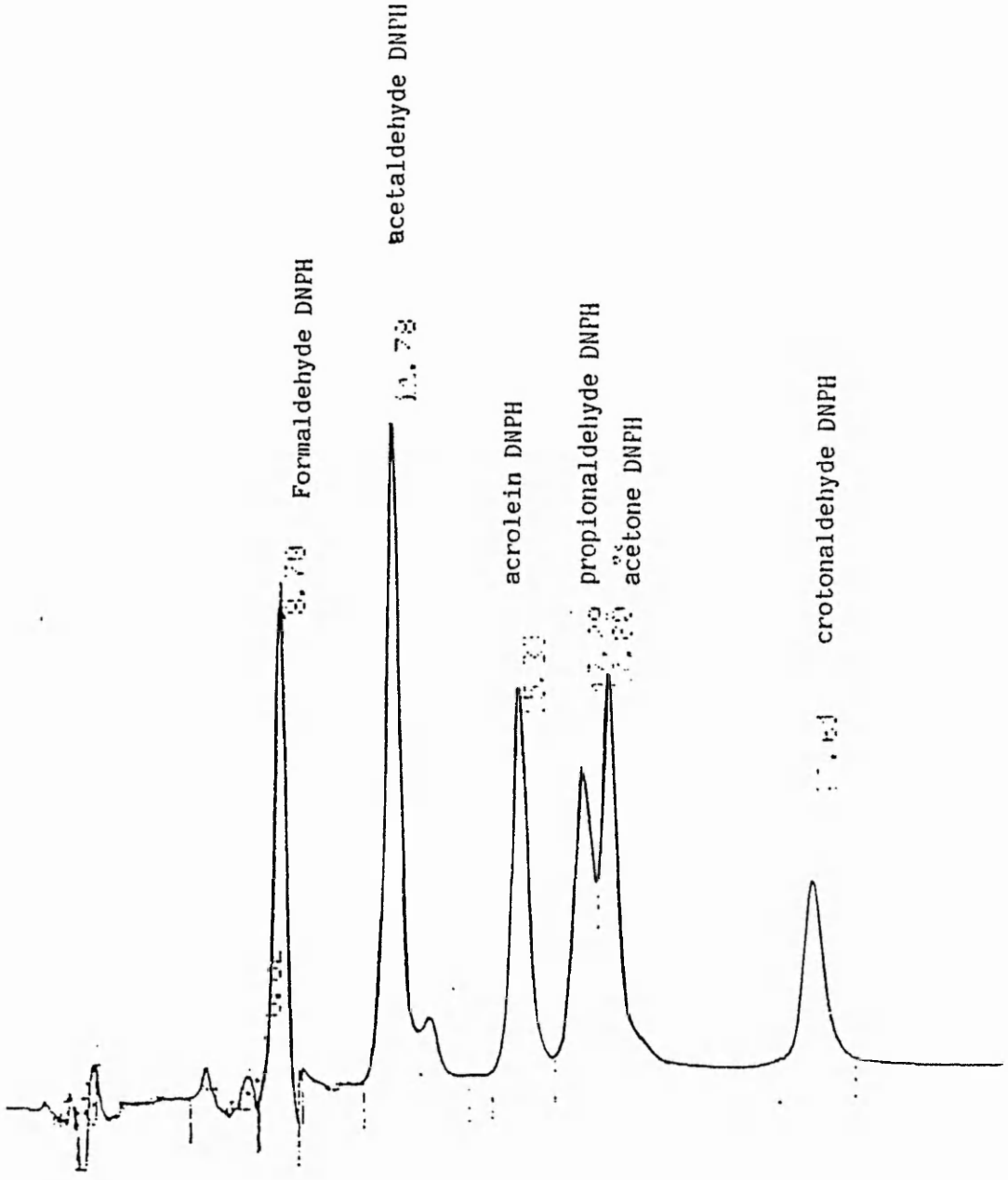

Figure 32. Chromatogram of synthetic mixture of DNPH derivatives

Chromatographic conditions.

Identical to Figure 32

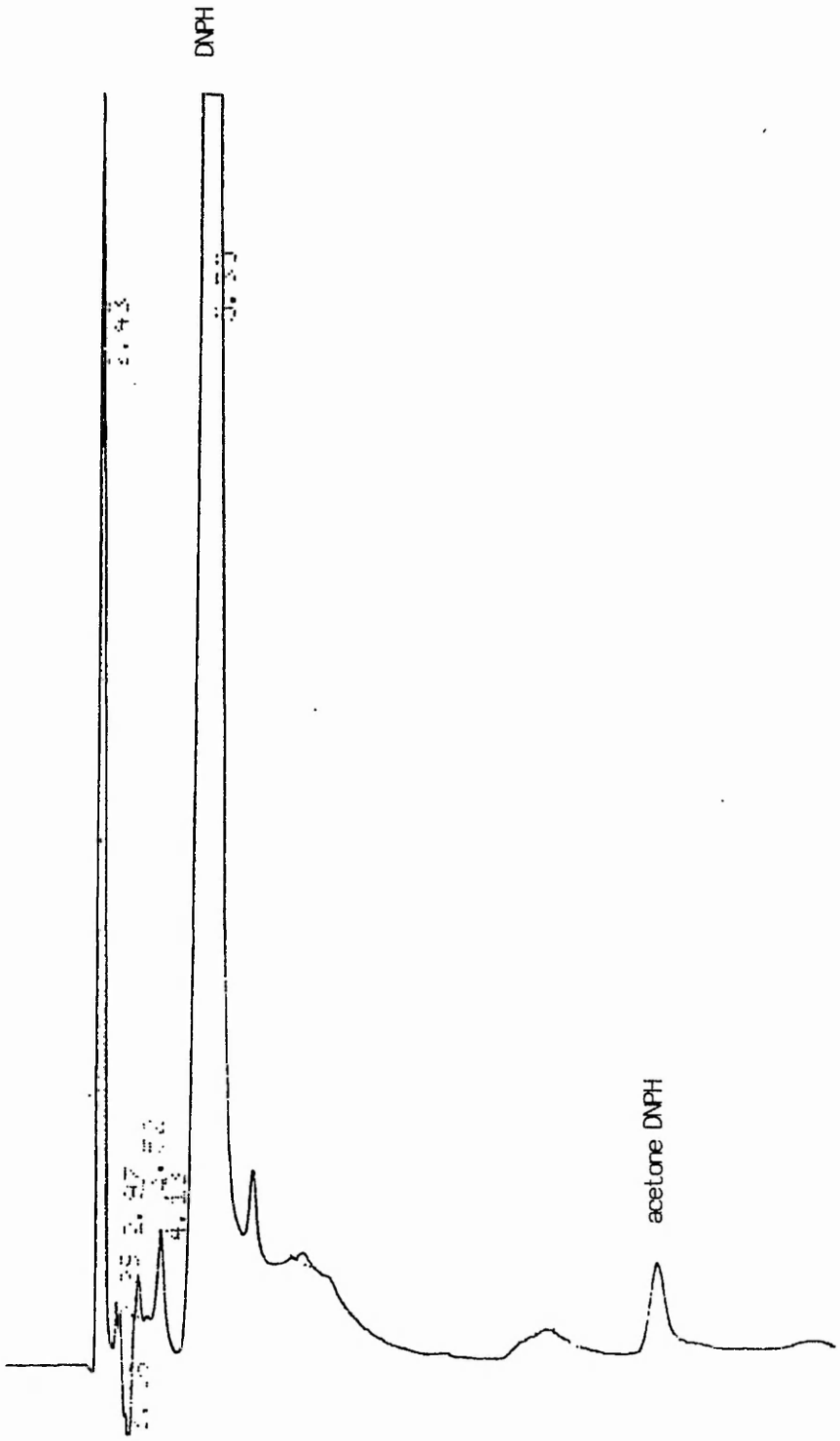

Figure 33. Chromatogram of an unsampled tube desorbed into acetonitrile.

Chromatographic conditions.

Identical to Figure 32

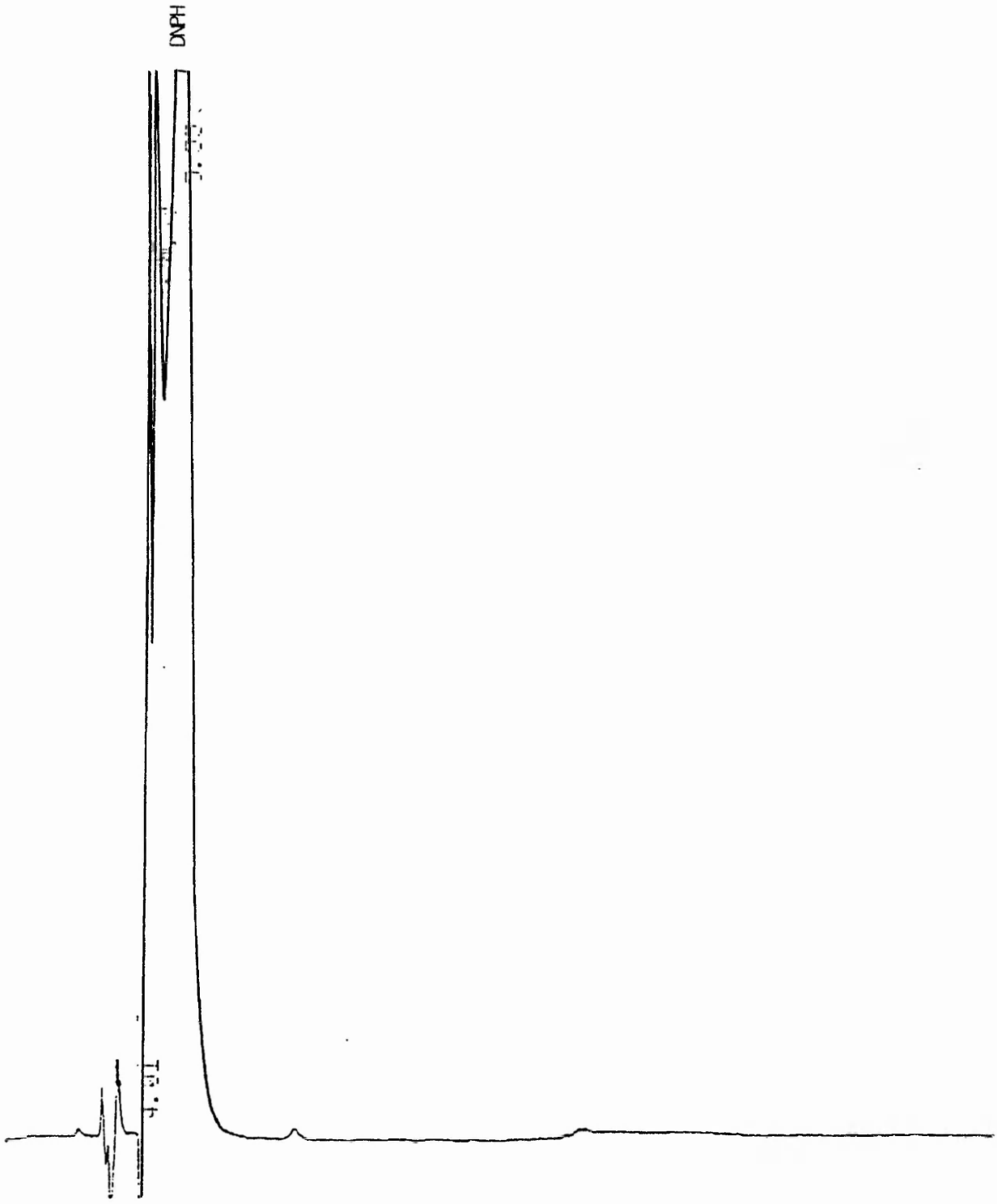

Figure 34. Chromatogram of an unsampled tube desorbed into acetonitrile.

Chromatographic conditions.

Identical to Figure 32

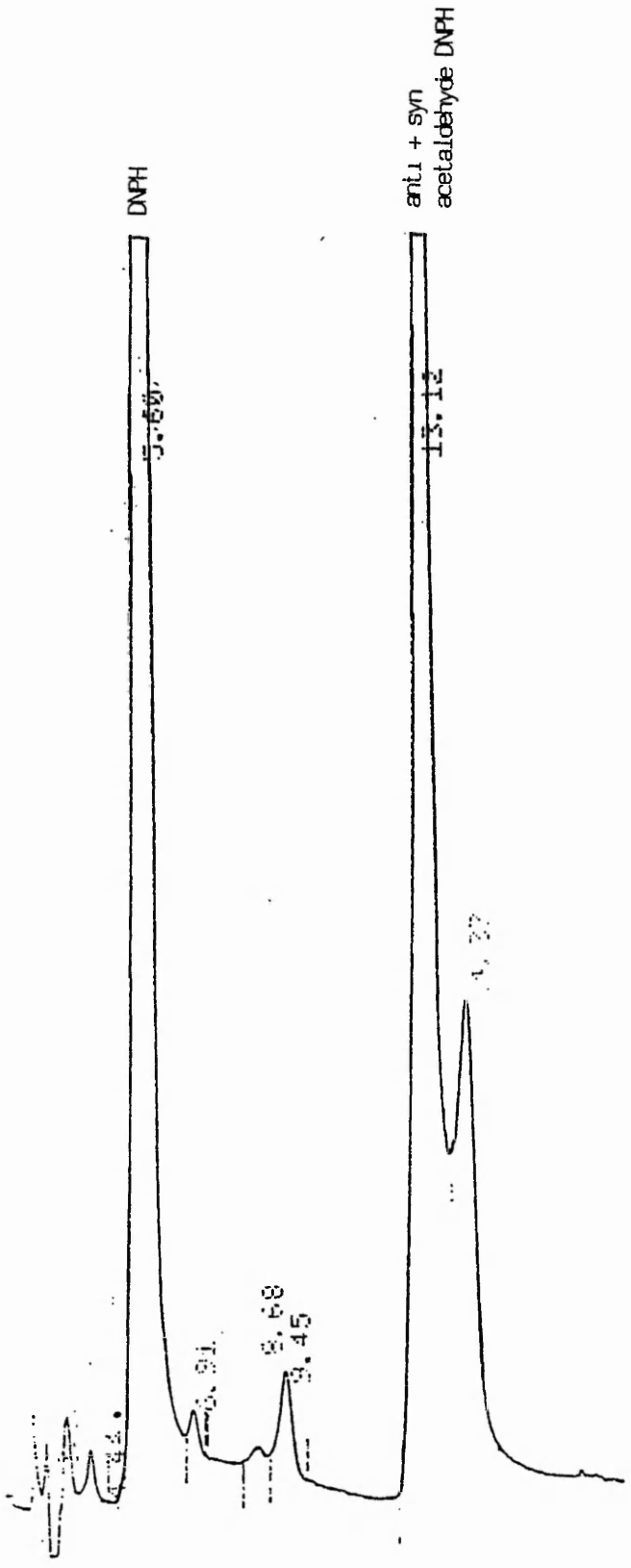

Figure 35. Chromatogram of acetaldehyde DNPH derivatives resulting from entrapment and desorption of 100ul acetaldehyde gas.

Chromatographic conditions.

Identical to Figure 32 except for:-
Integrator attn x16

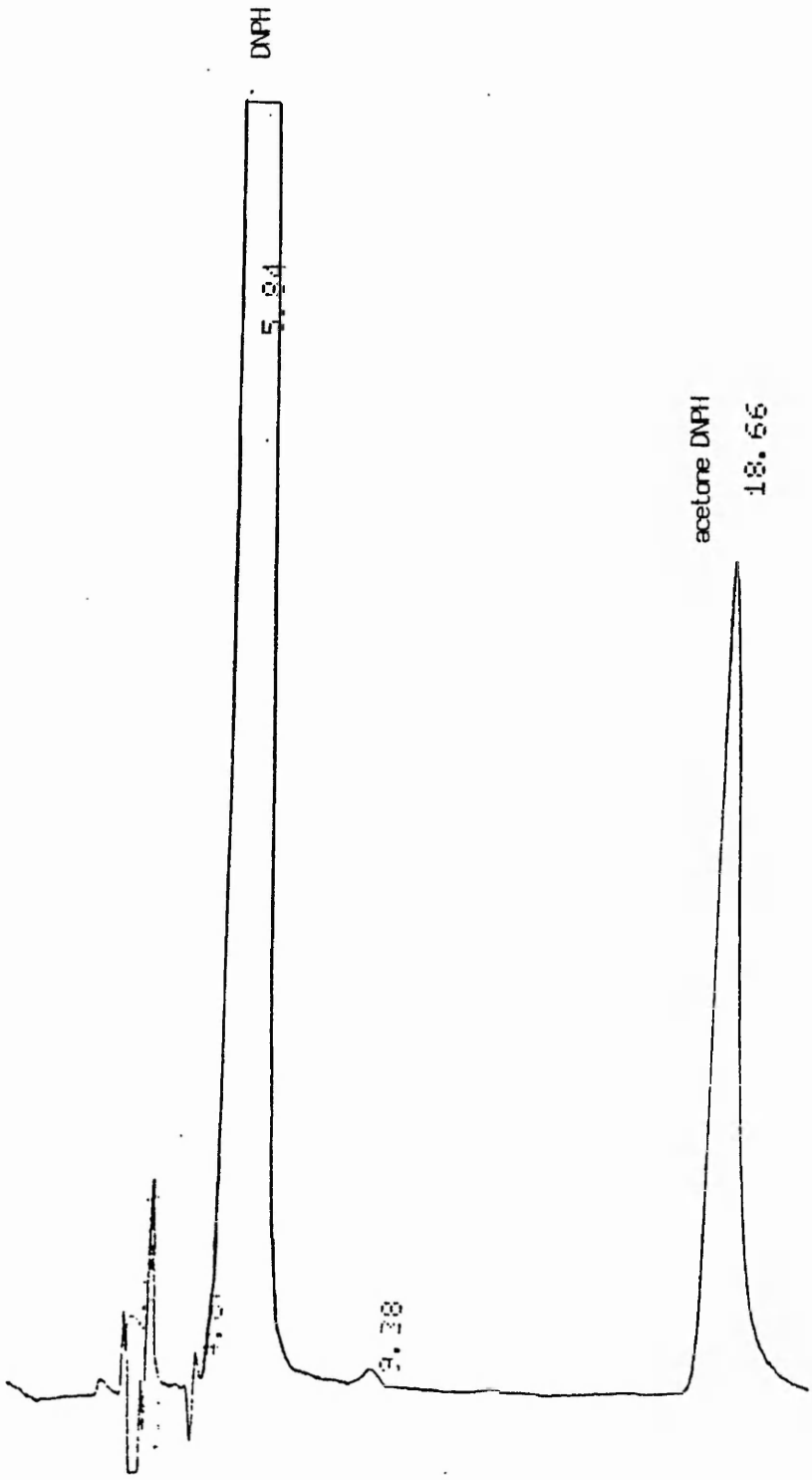

Figure 36. Chromatogram of acetone DNPH derivative resulting from entrapment and desorption of 0.07ul acetone liquid.

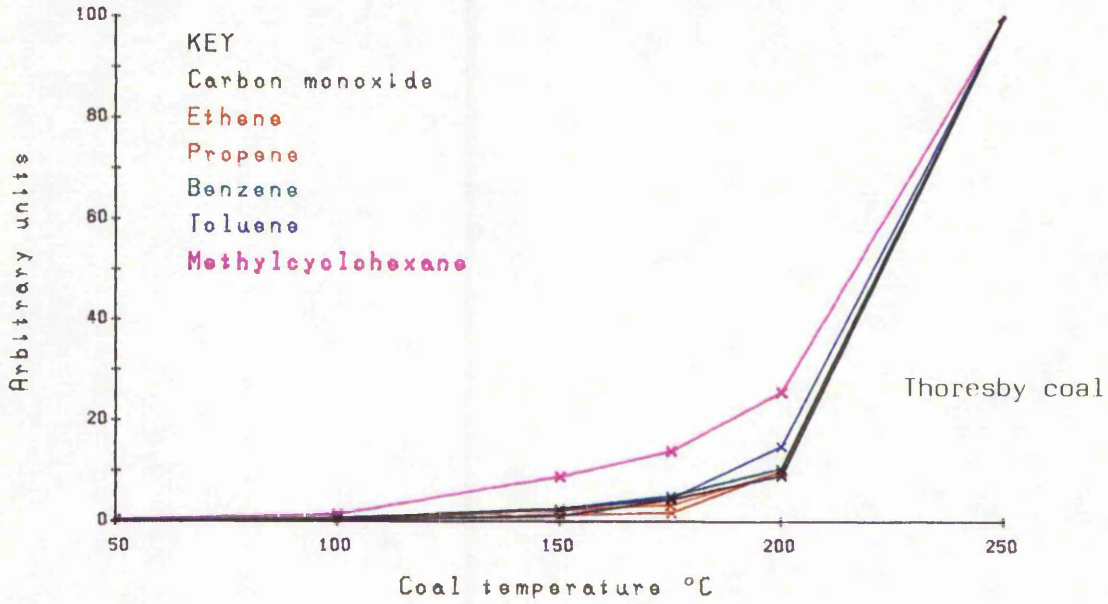

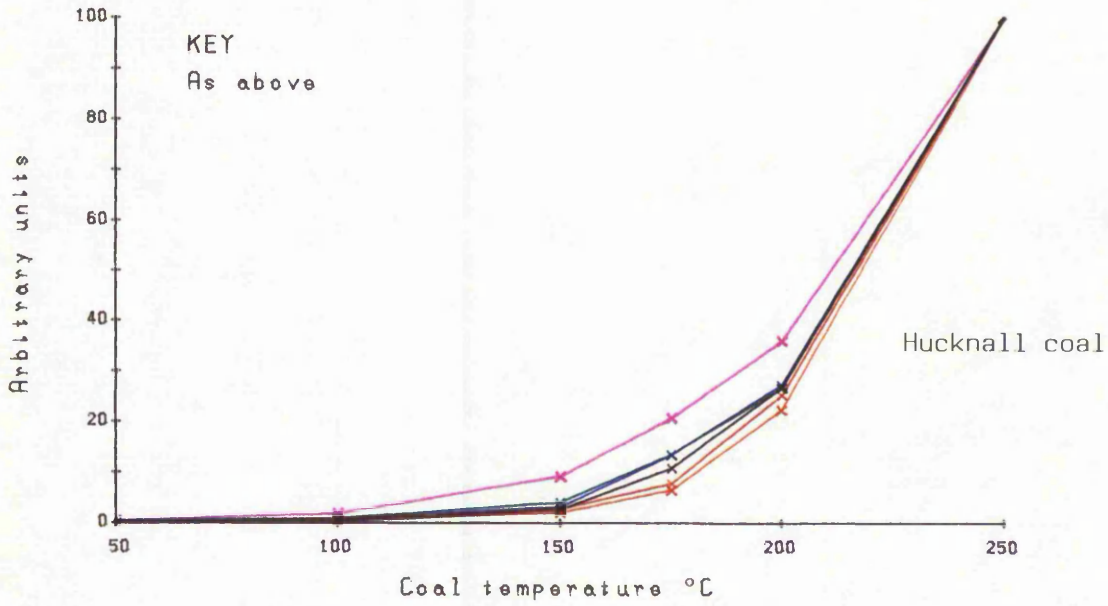

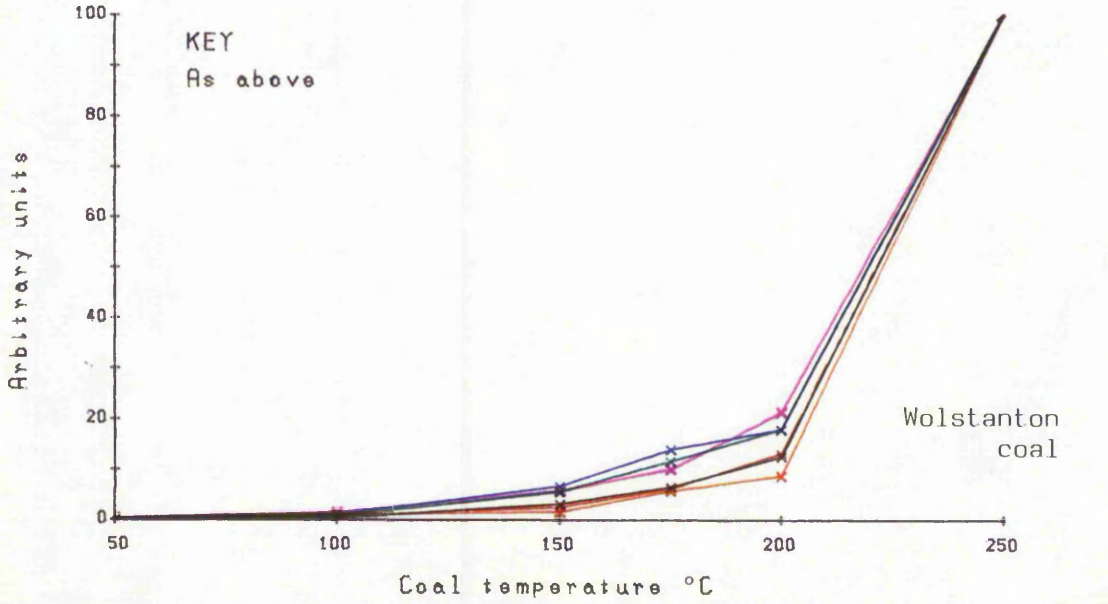

Figs 37a-c. Evolution pattern from test coals heated in air.

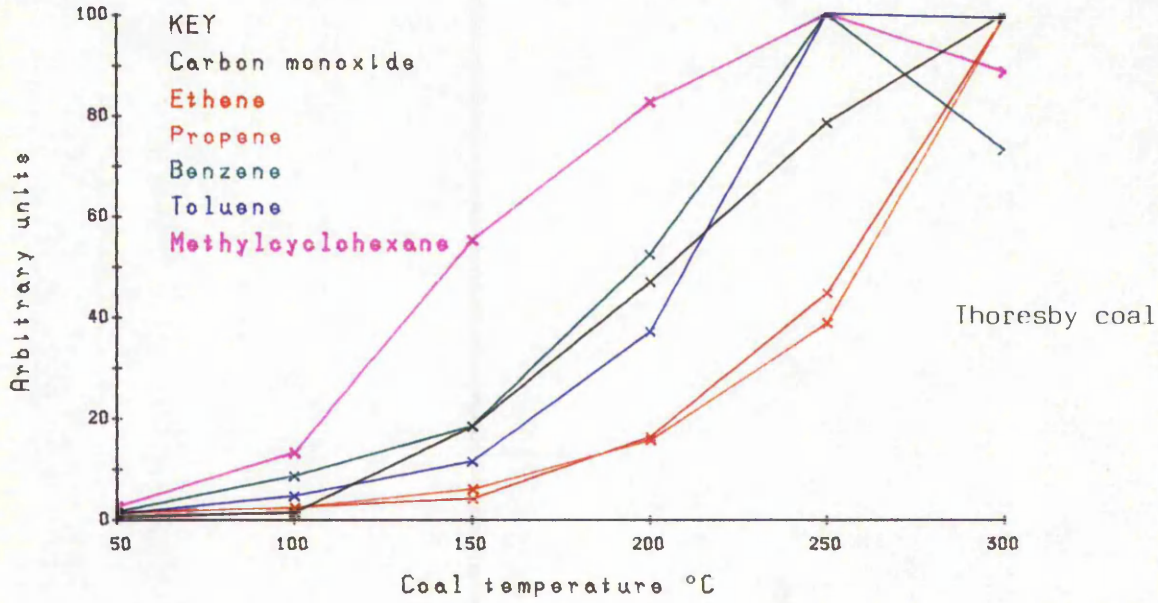

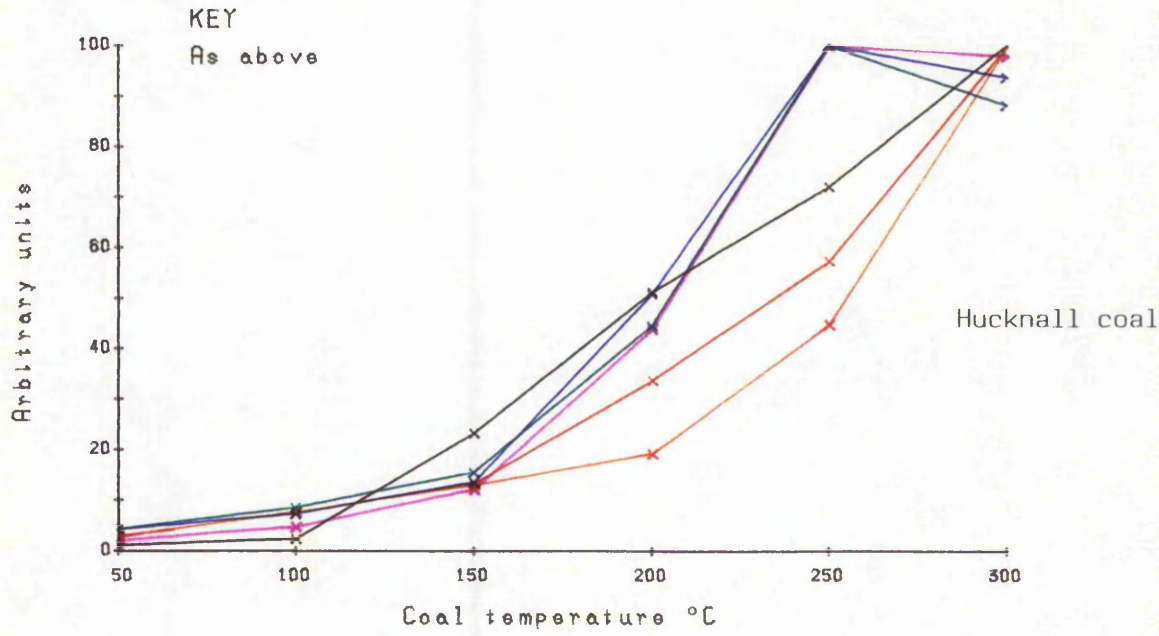

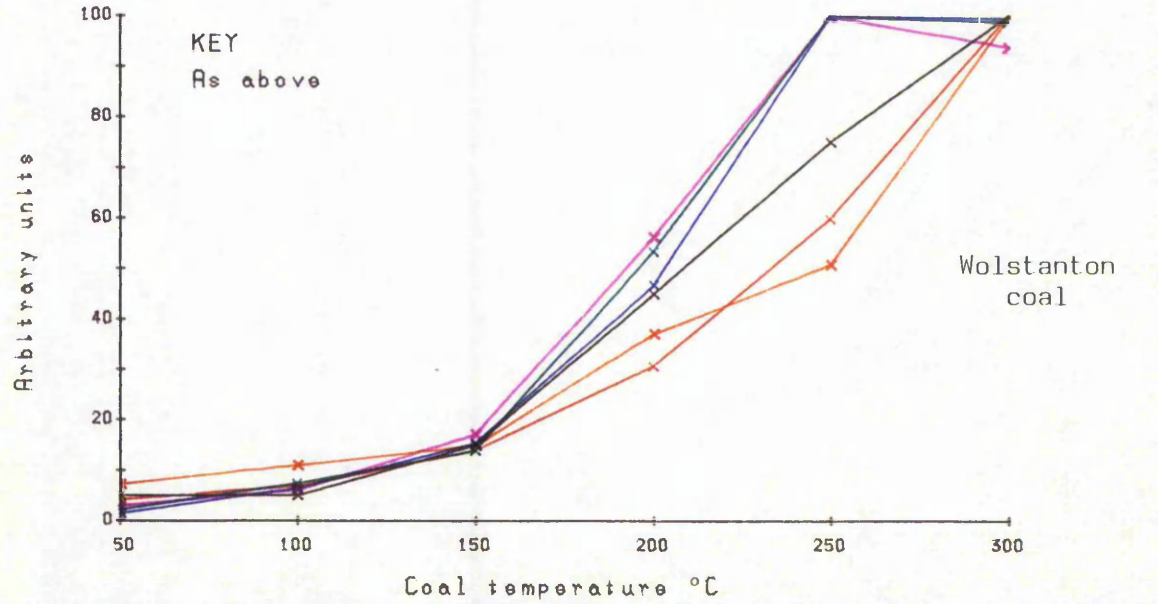

Figs 38a-c. Evolution pattern from test coals heated in nitrogen

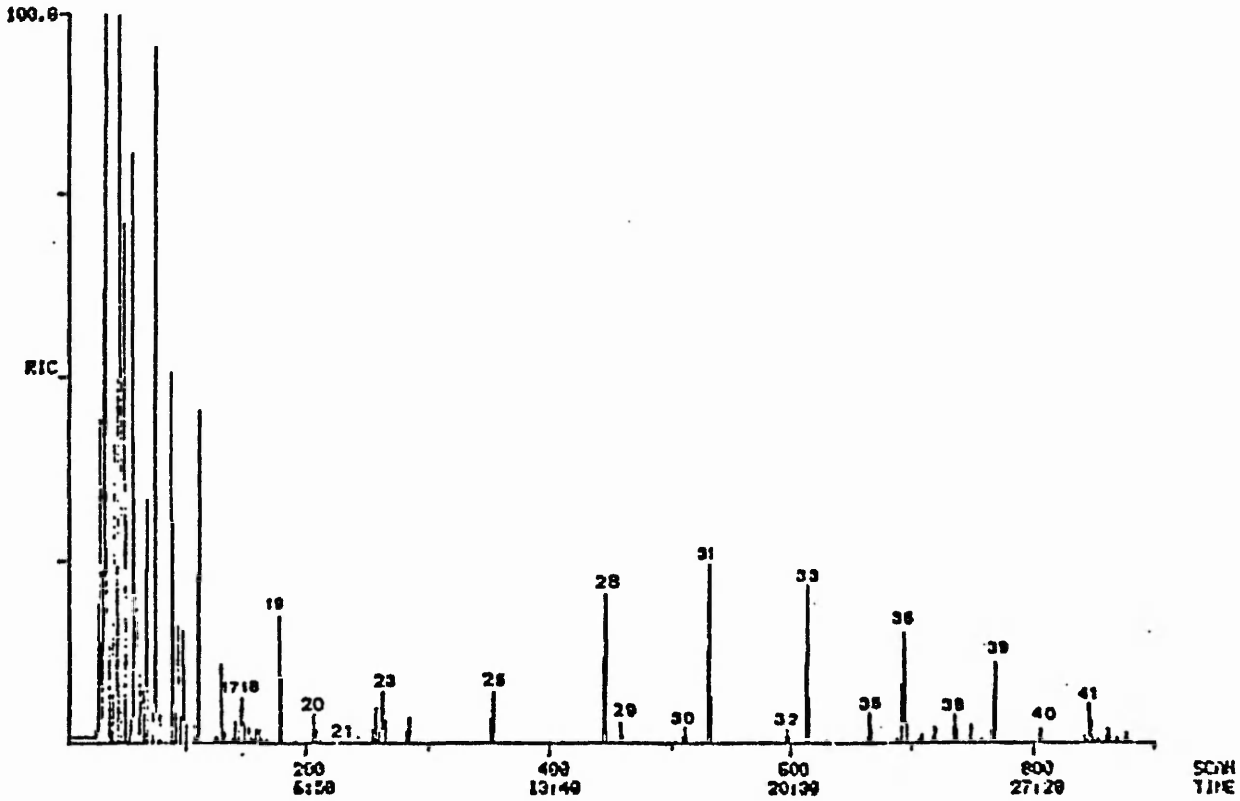

Figure 39a. GC/MS reconstructed ion chromatogram produced from Thoresby coal heated in air at 100°C.

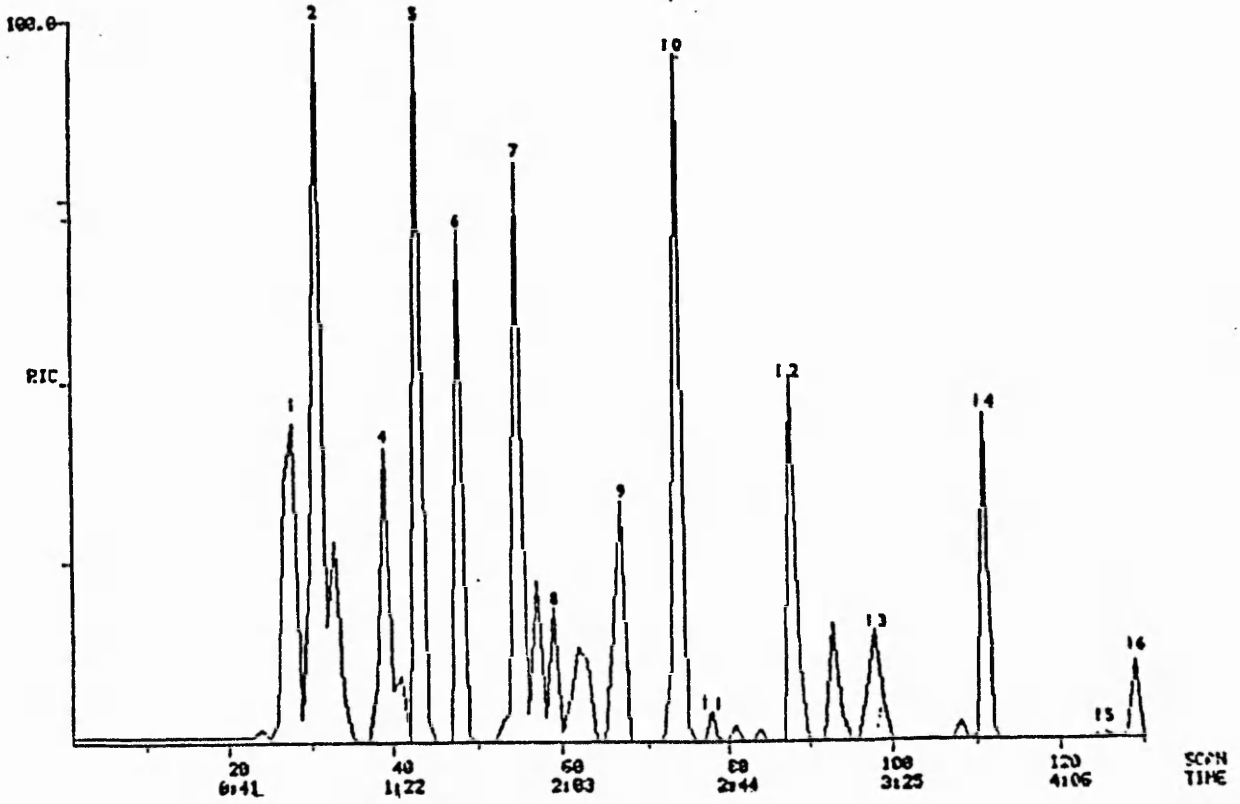

Figure 39b. Expanded section of scans 0-130 from GC/MS reconstructed ion chromatogram.

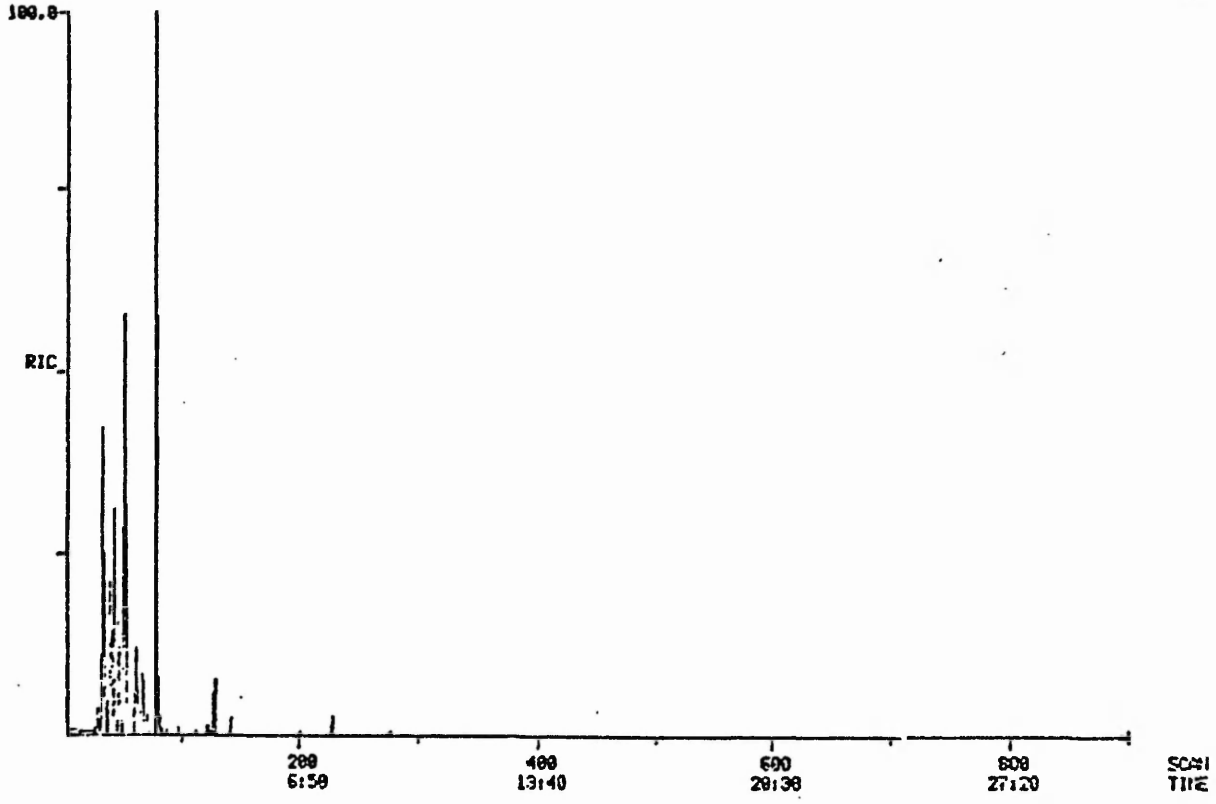

Figure 40a. GC/MS reconstructed ion chromatogram produced from Hucknall coal heated in air at 100°C.

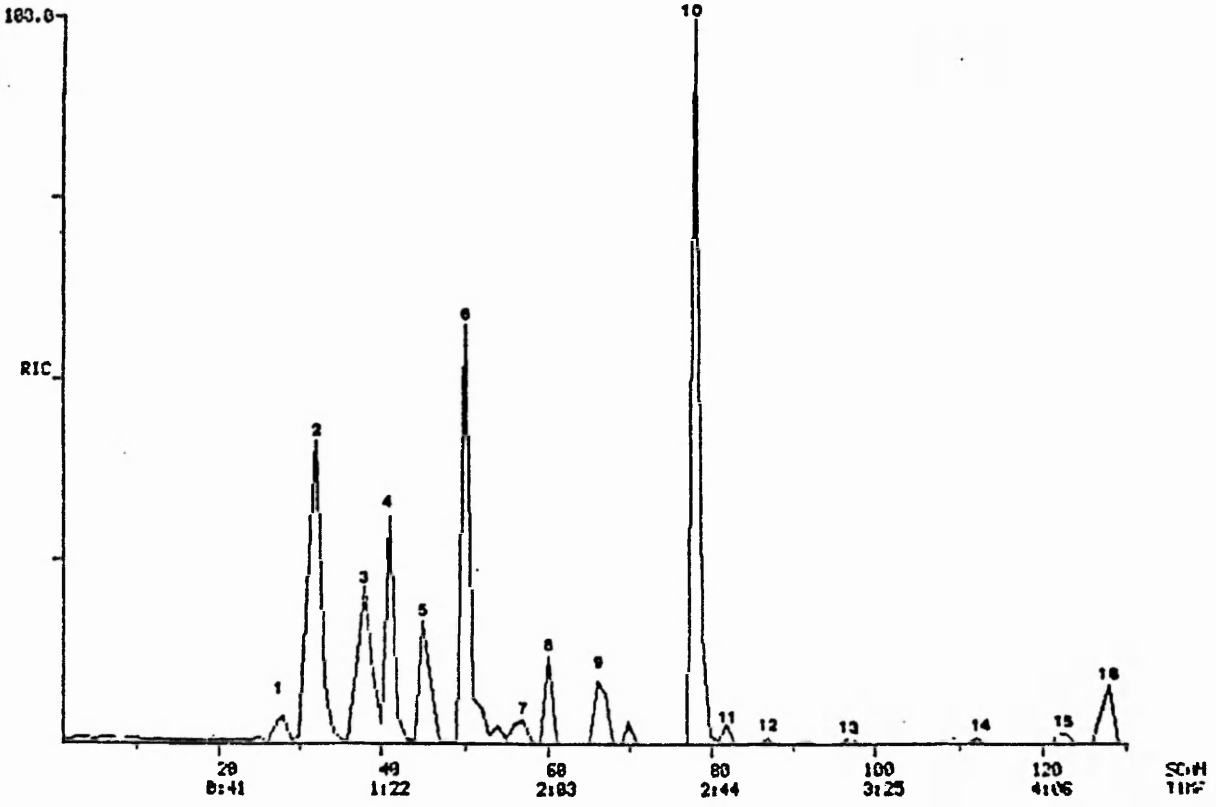

Figure 40b. Expanded section of scans 0-130 from GC/MS reconstructed ion chromatogram.

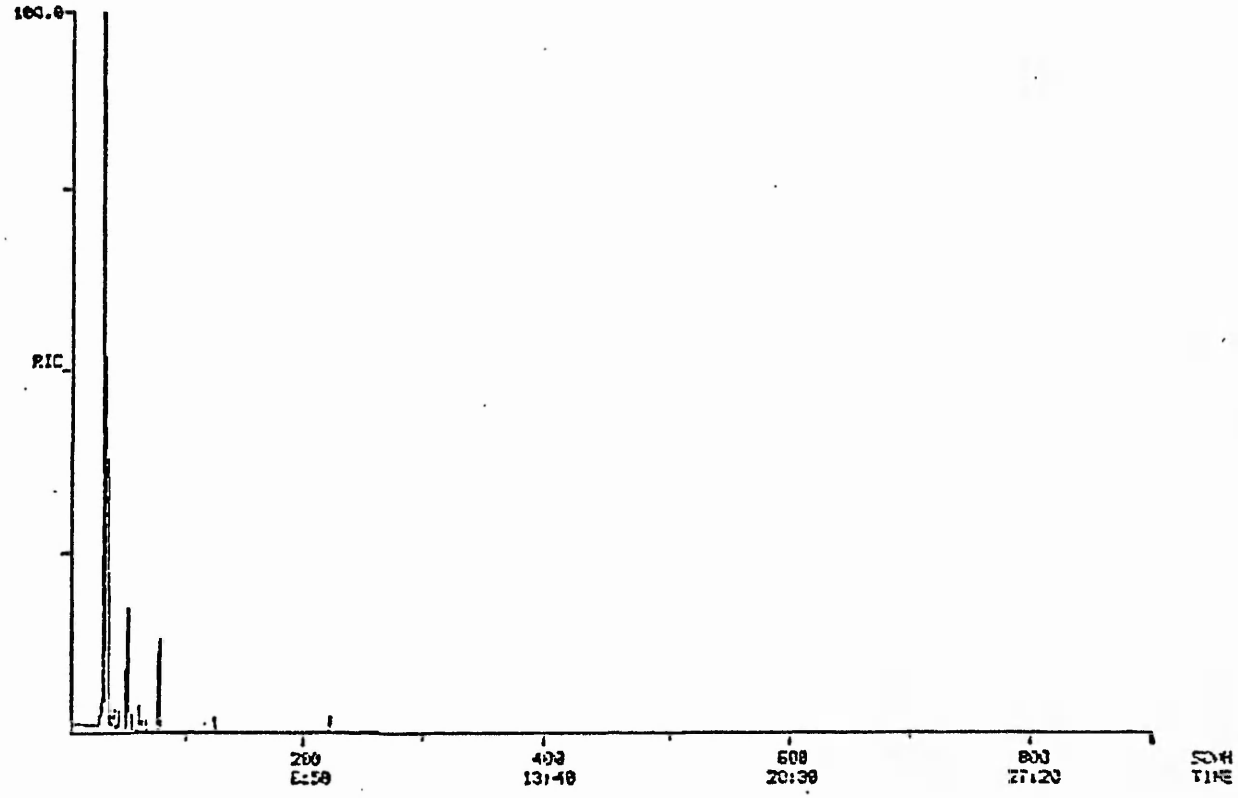

Figure 41a. GC/MS reconstructed ion chromatogram produced from Wolstanton coal heated in air at 100°C.

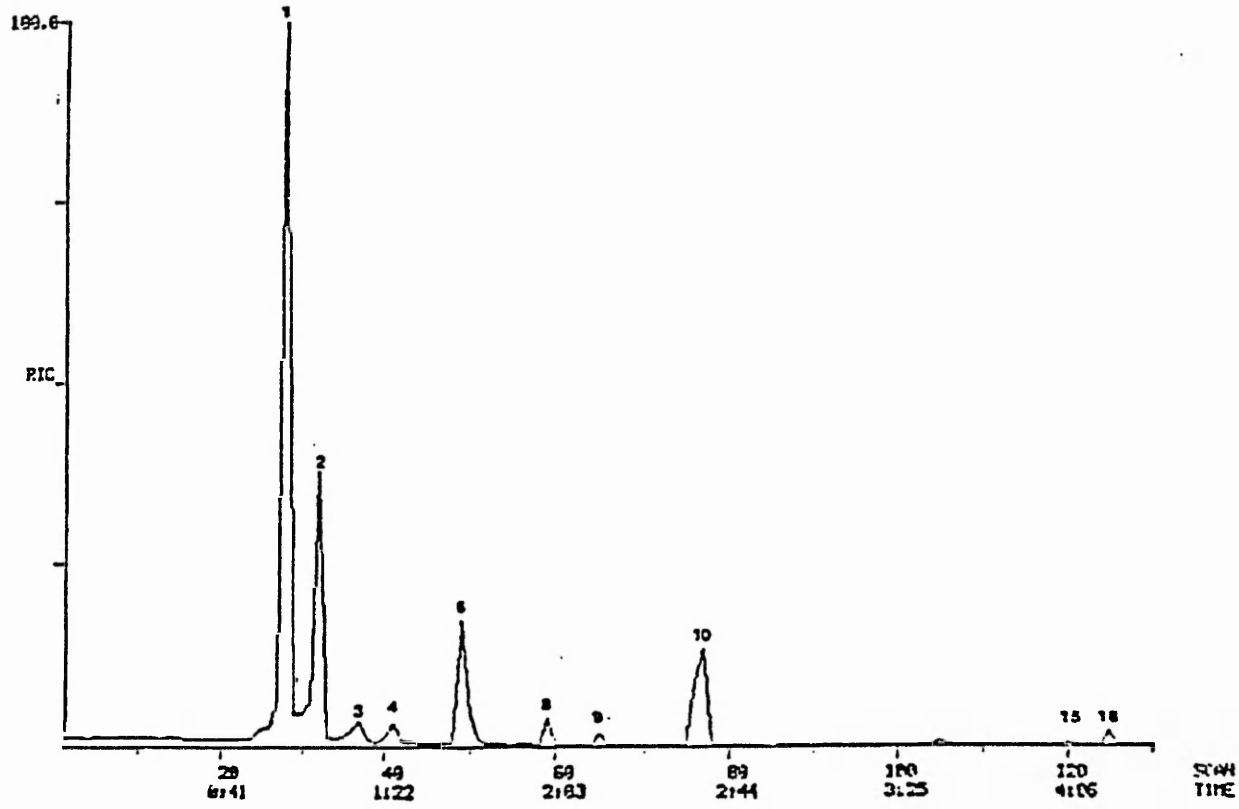

Figure 41b. Expanded section of scans 0-130 from GC/MS reconstructed ion chromatogram.

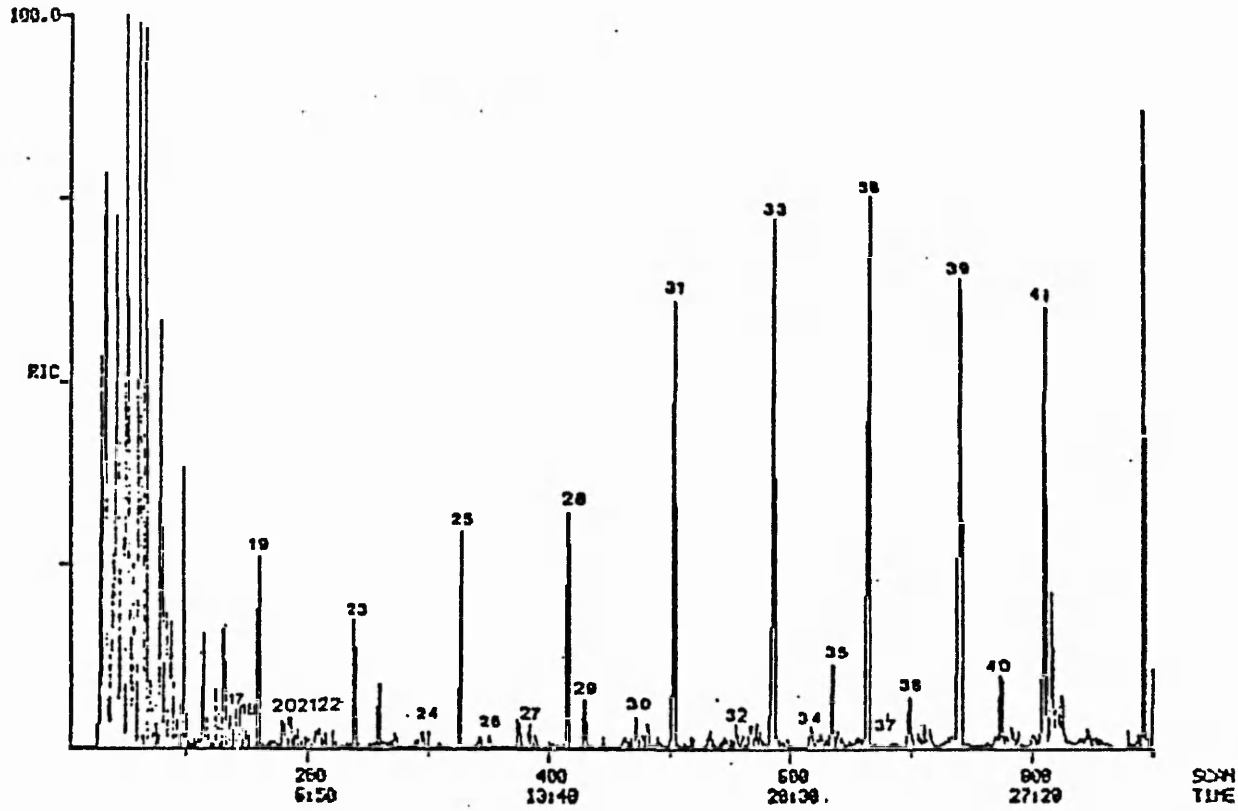

Figure 42a. GC/MS reconstucted ion chromatogram produced from Thoresby coal heated in air at 200°C.

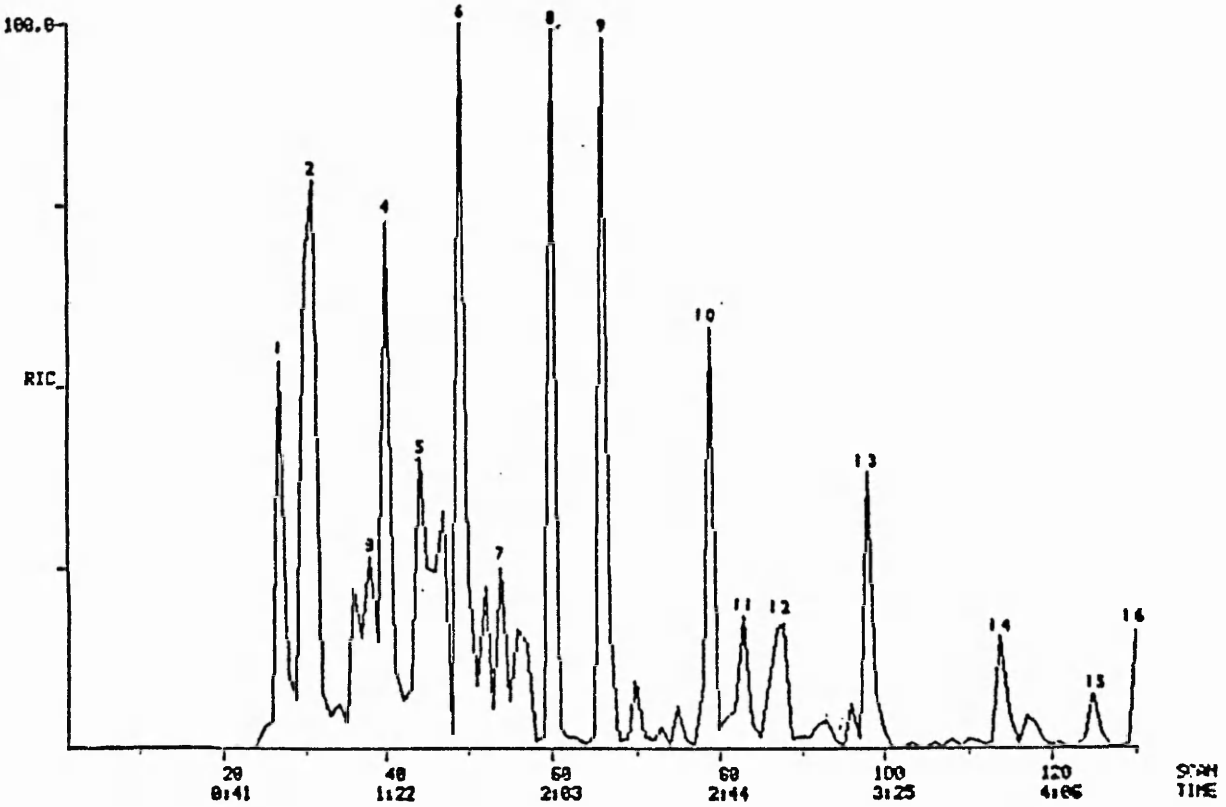

Figure 42b. Expanded section of scans 0-130 from GC/MS reconstructed ion chromatogram.

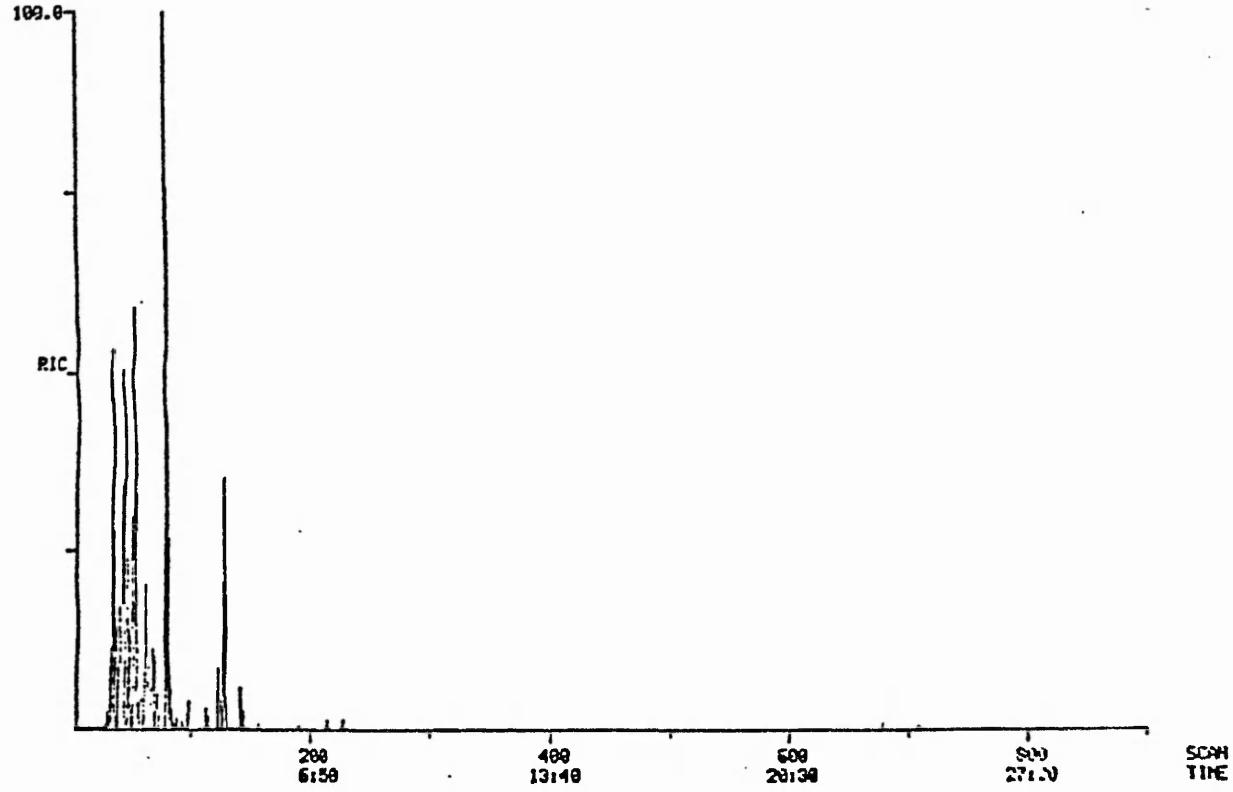

Figure 43a. GC/MS reconstructed ion chromatogram produced from Hucknall coal heated in air at 200°C.

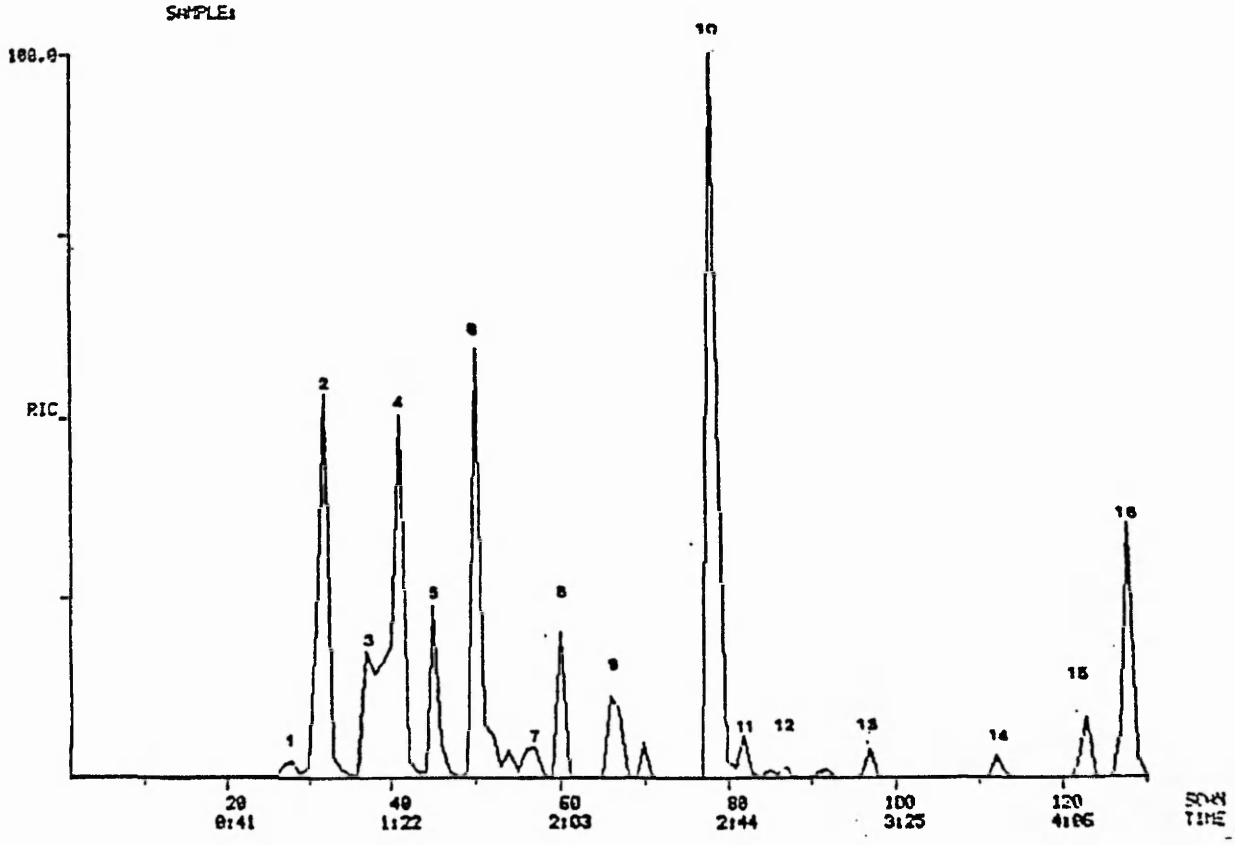

Figure 43b. Expanded section of scans 0-130 from GC/MS reconstructed ion chromatogram.

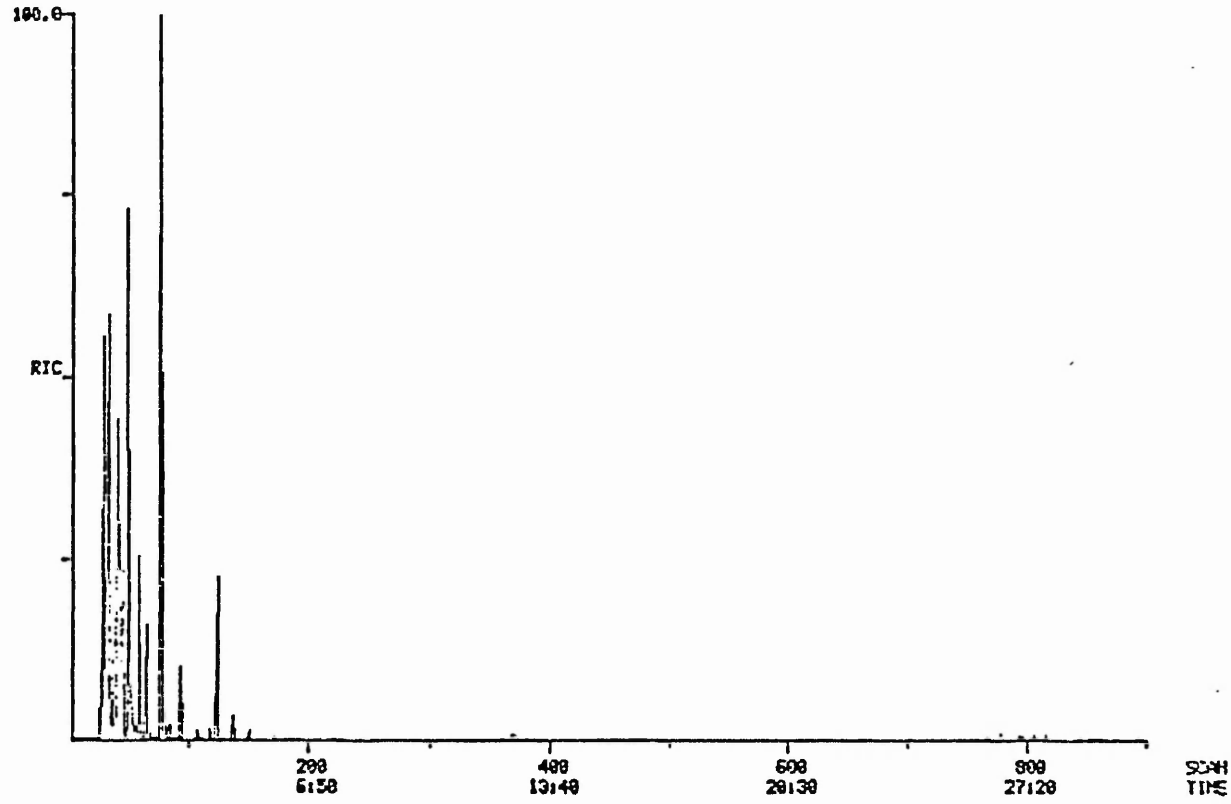

Figure 44a. GC/MS reconstructed ion chromatogram produced from Wolstanton coal heated in air at 200°C.

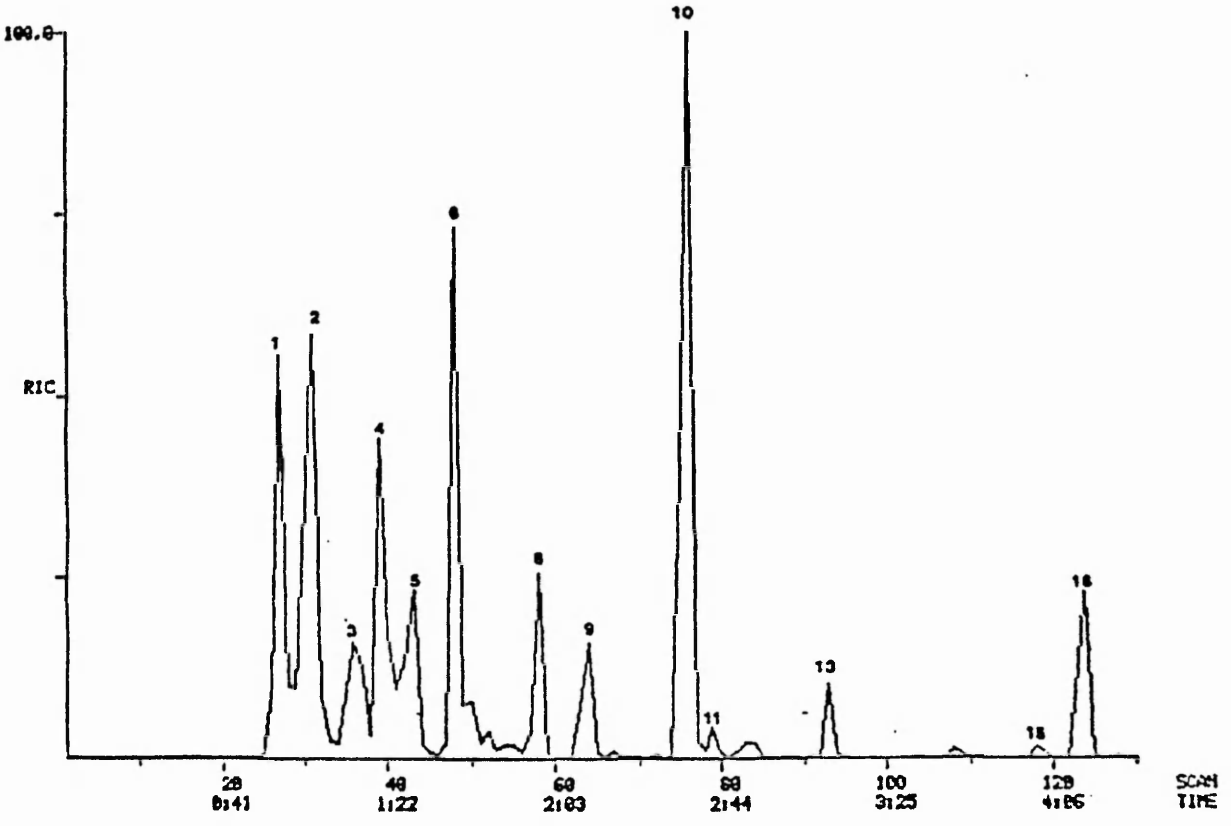

Figure 44b. Expanded section of scans 0-130 from GC/MS reconstructed ion chromatogram.

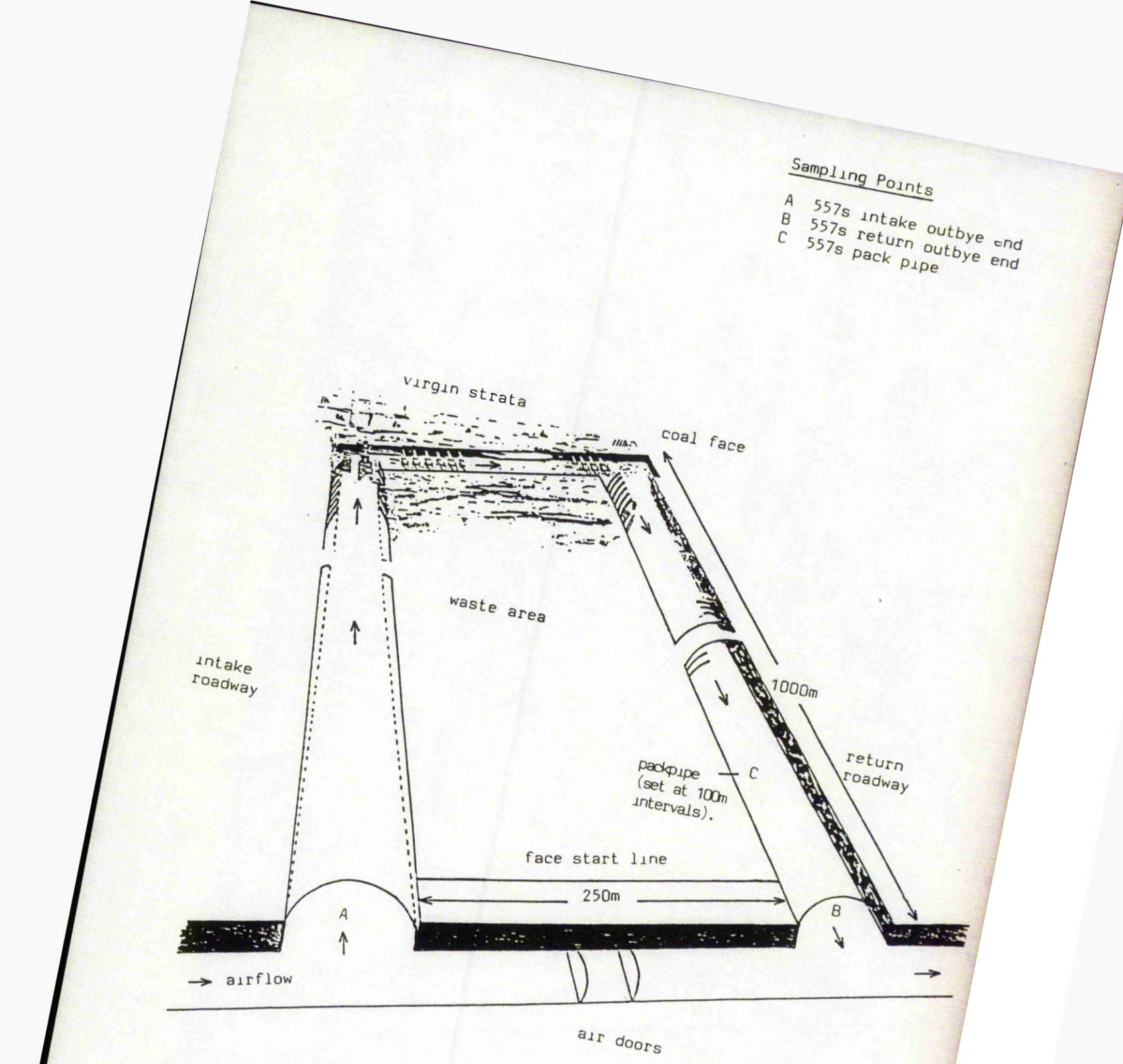

Figure 45. Schematic diagram of 557s distict and sampling points.

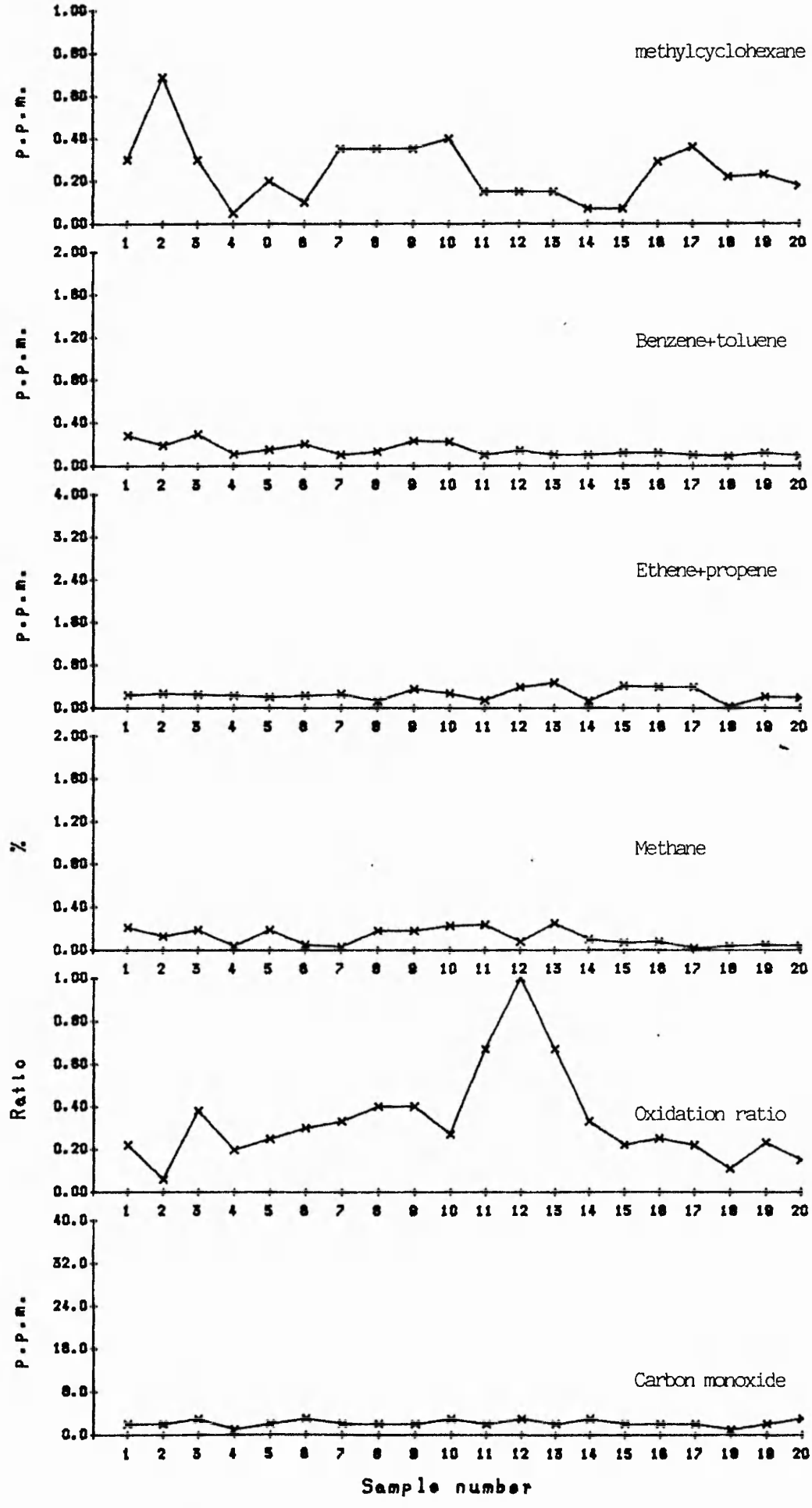

Figure 46. Wolstanton colliery 557s intake outbye end.

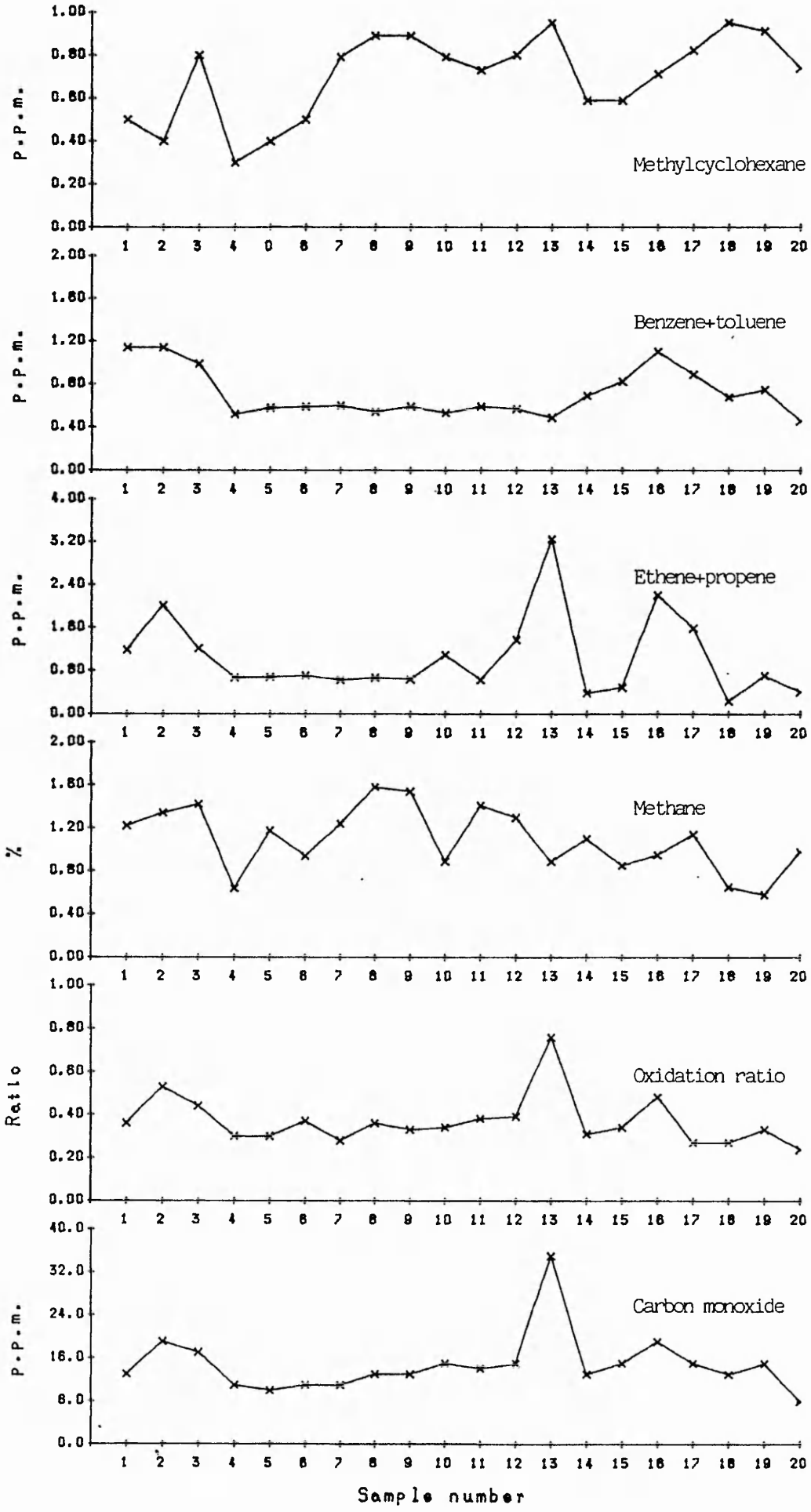

Figure 47. Wolstanton colliery 557s return outbye end.

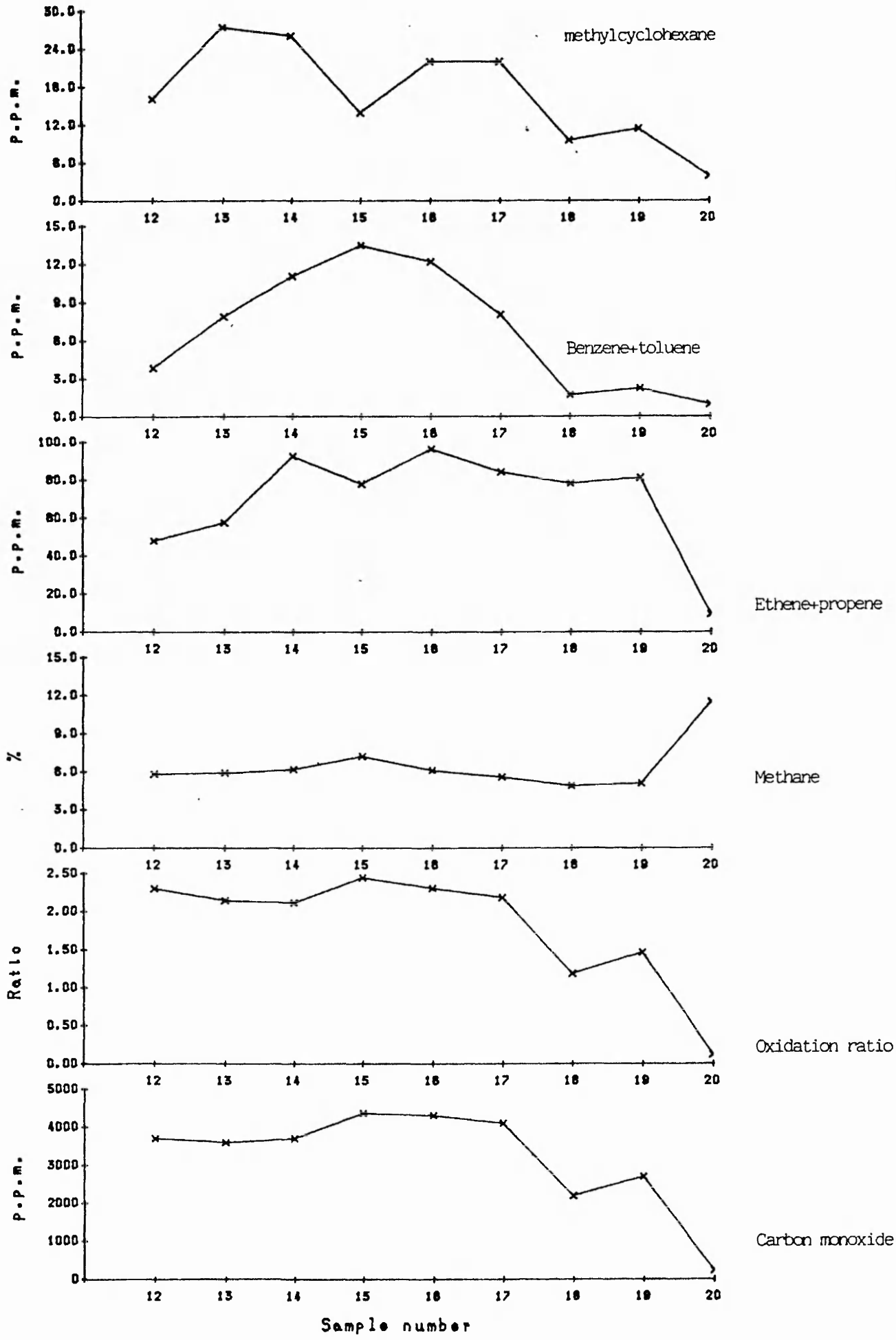

Figure 48. Wolstanton colliery, 557s district, pack pipe.

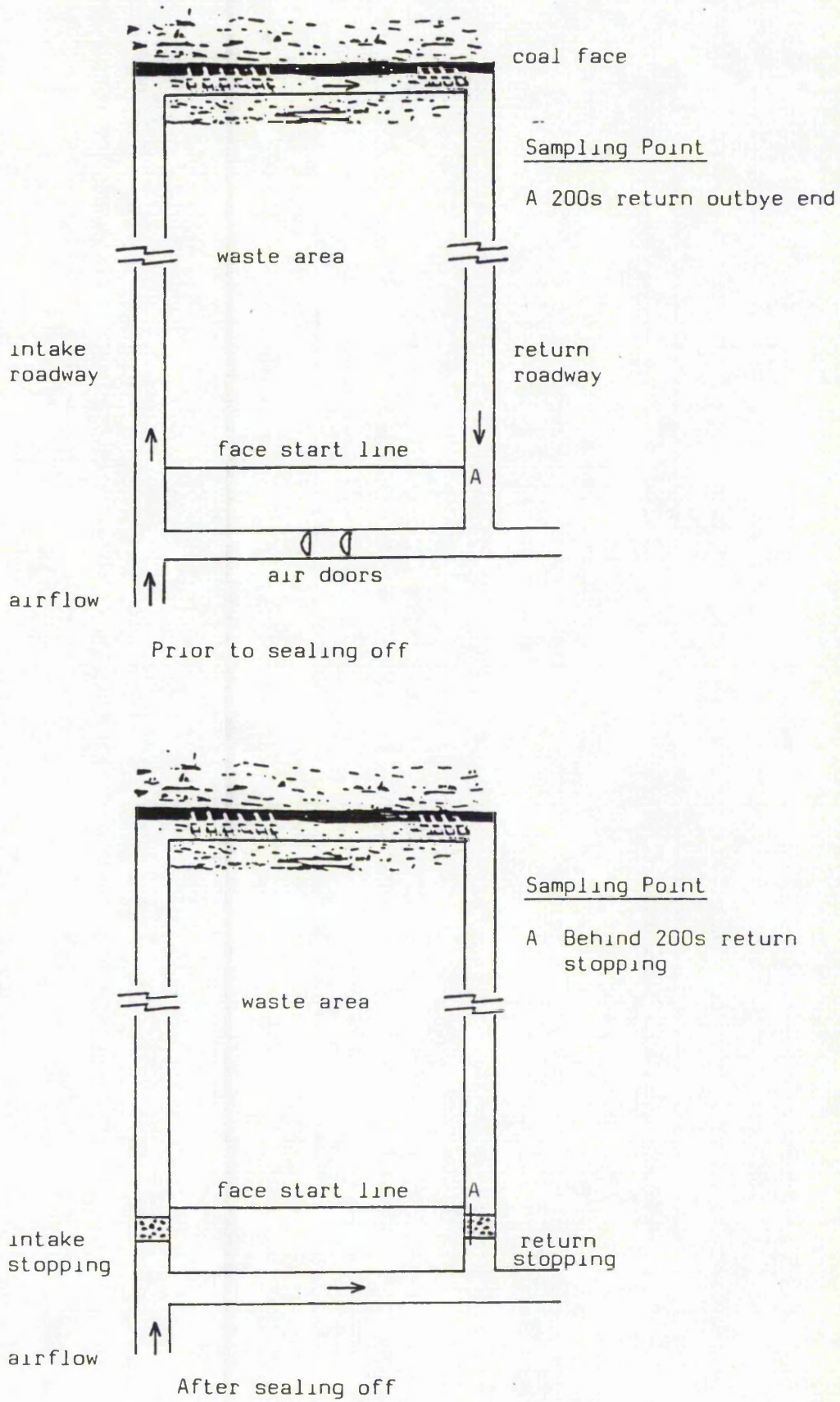

Figure 49. General view 200s district and sampling points.

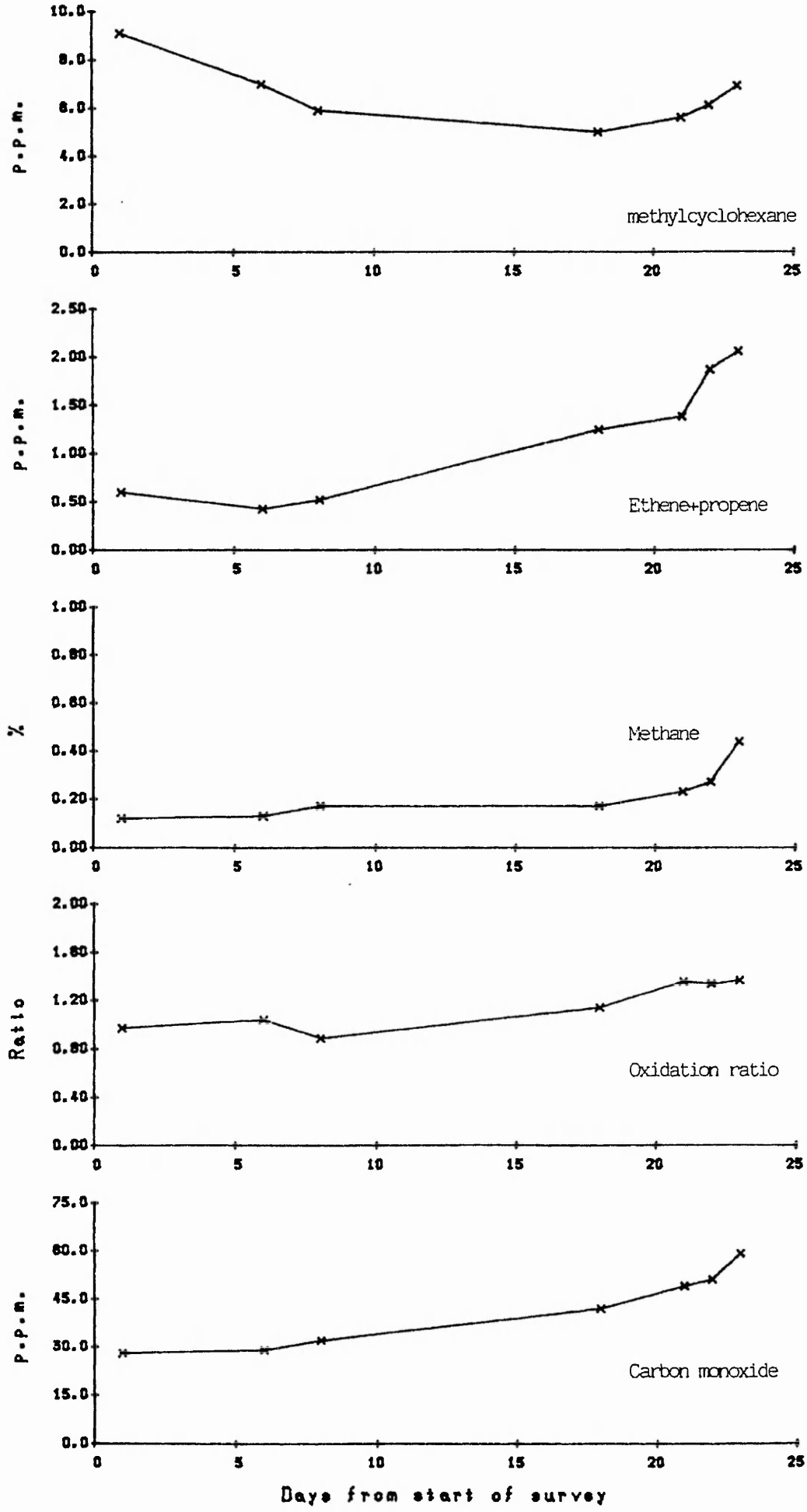

Figure 50. Thoresby colliery 200s return outbye end - prior to sealing off.

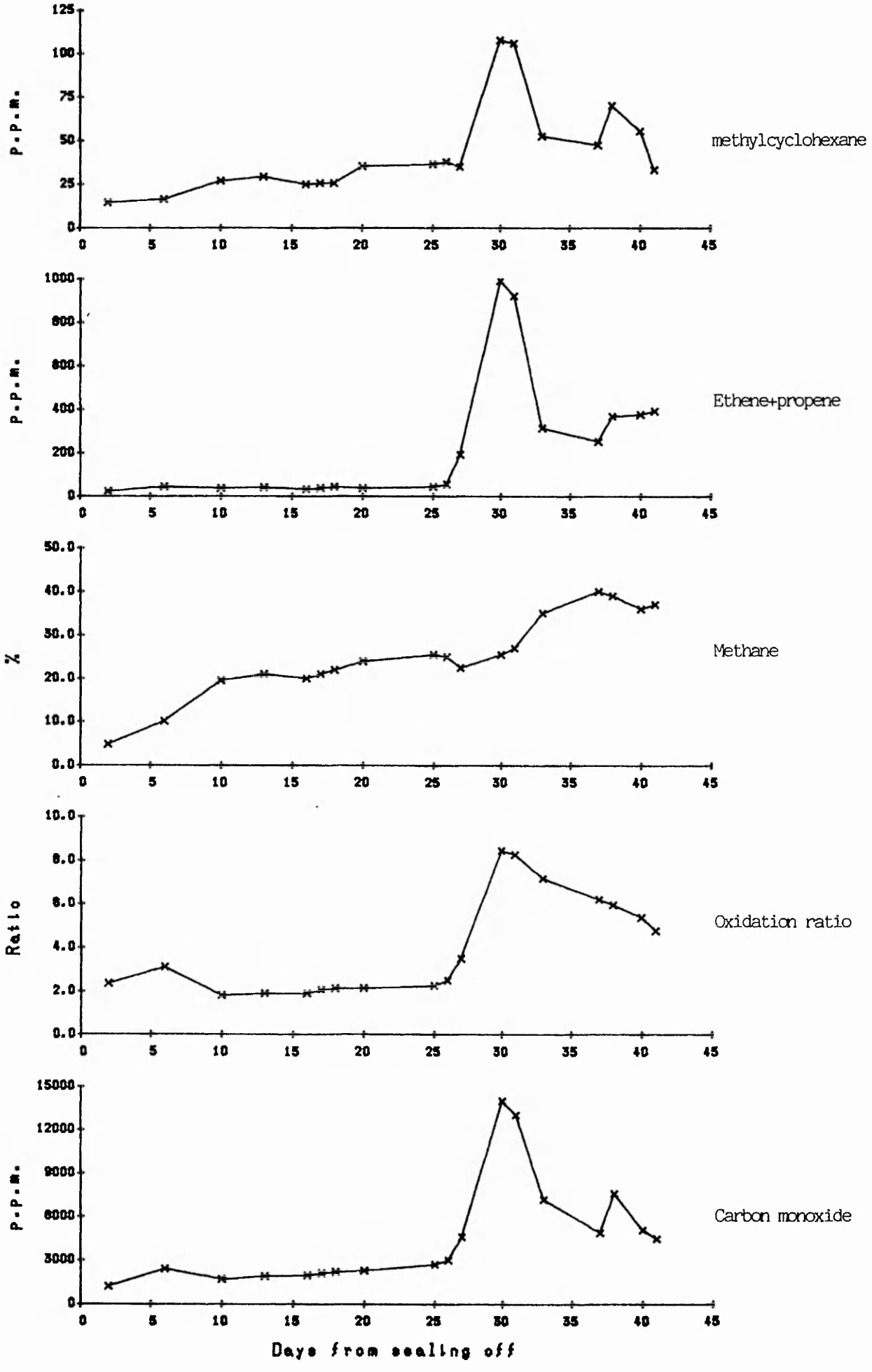

Figure 51. Thoresby colliery 200s return - after sealing off.

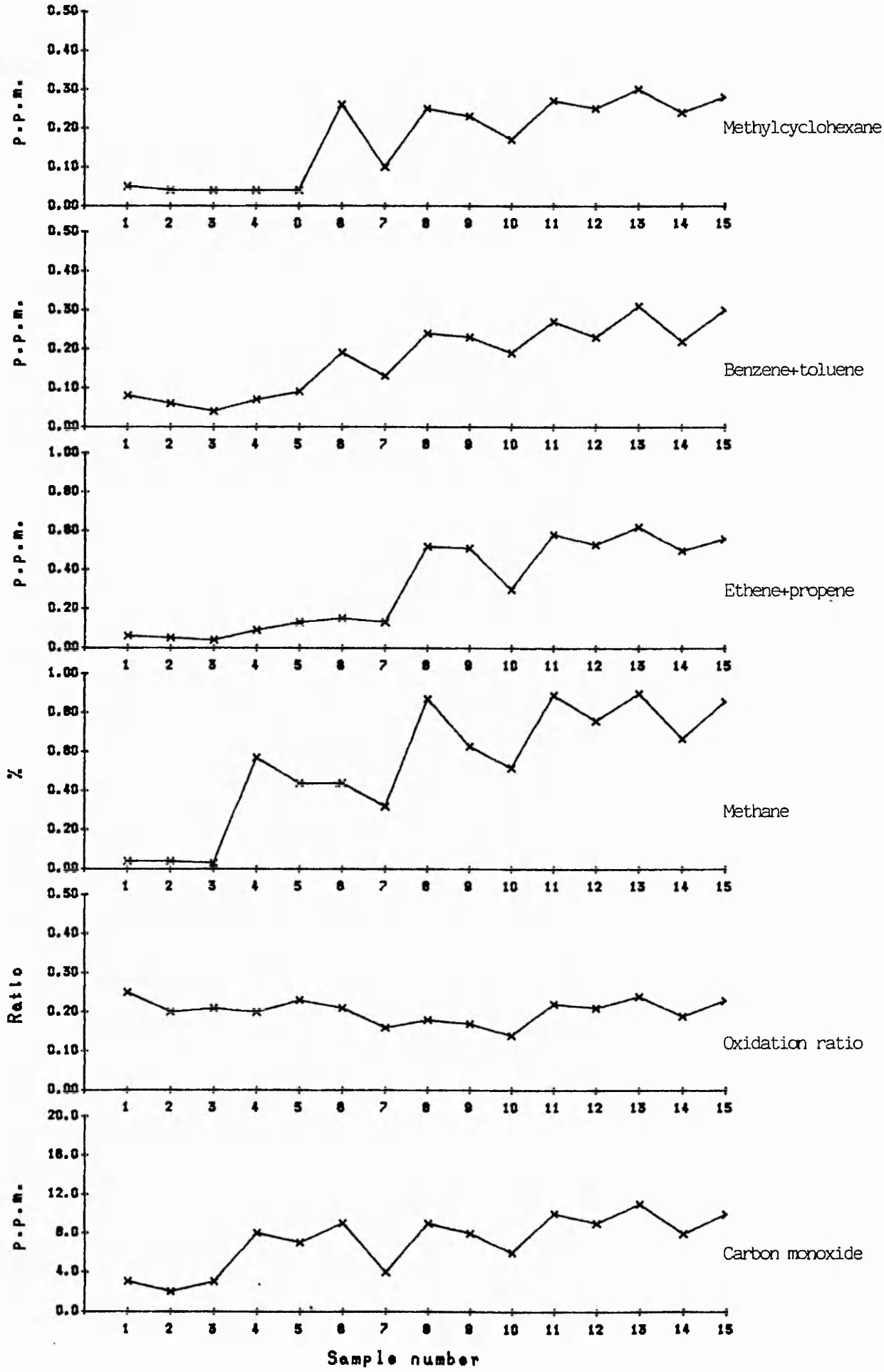

Figure 52. Daw Mill colliery 62s return outbye end.

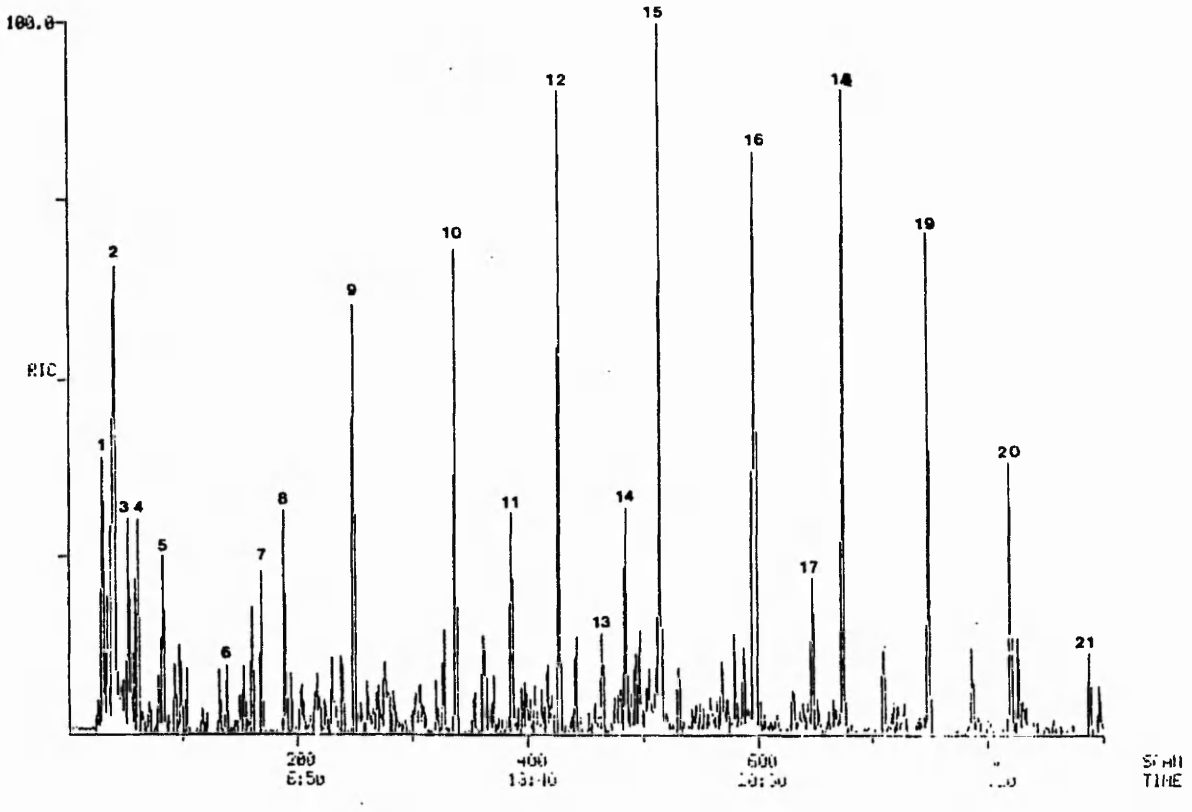

Figure 53. GC/MS reconstructed ion chromatogram of diesel fumes taken one metre from exhaust.

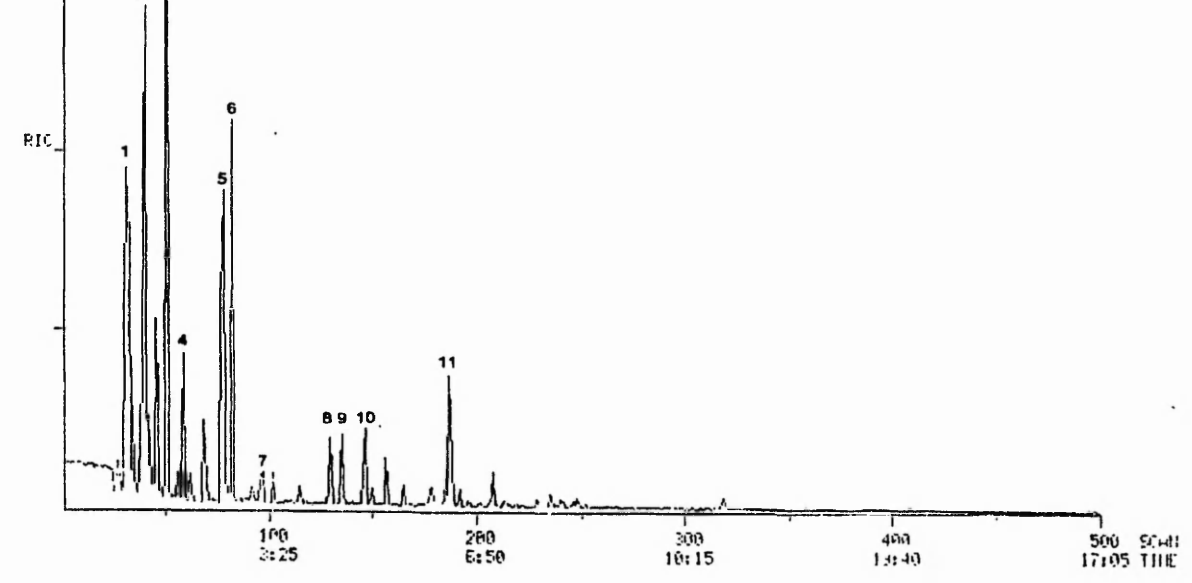

Figure 54. GC/MS reconstructed ion chromatogram of shotfiring fumes.

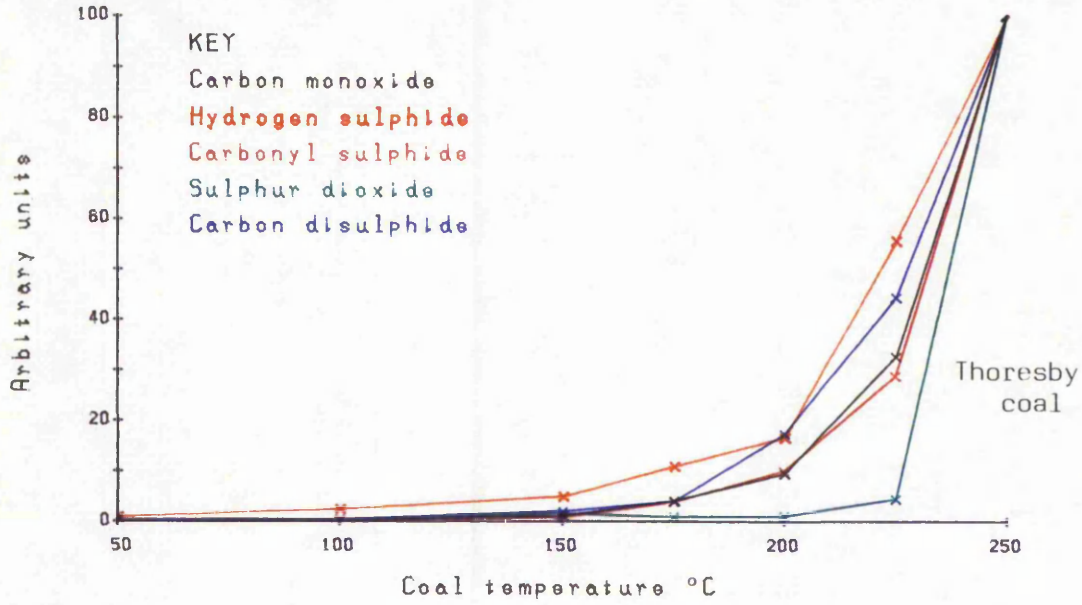

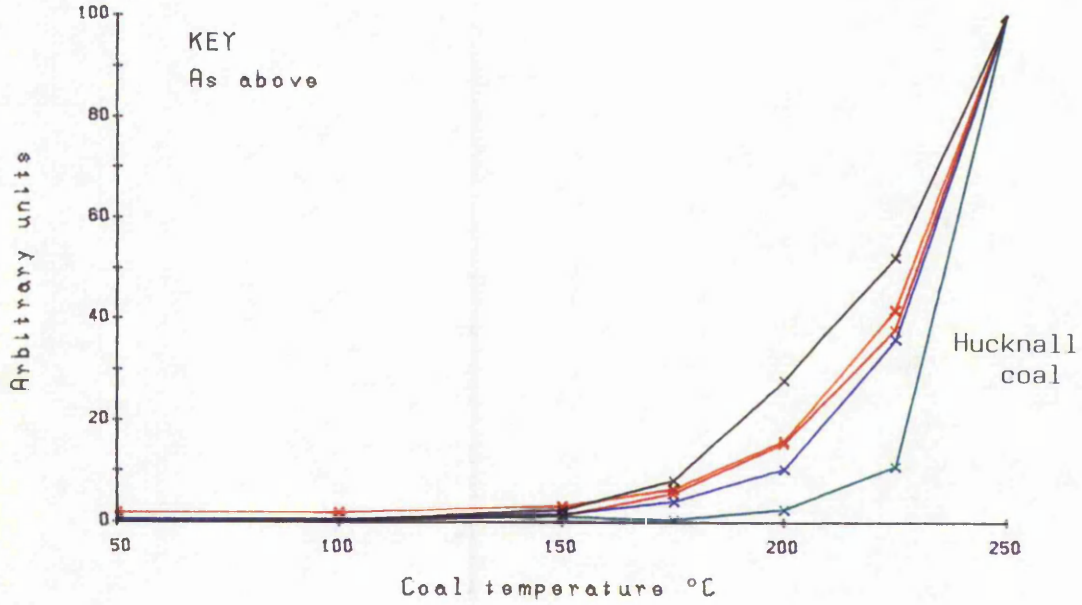

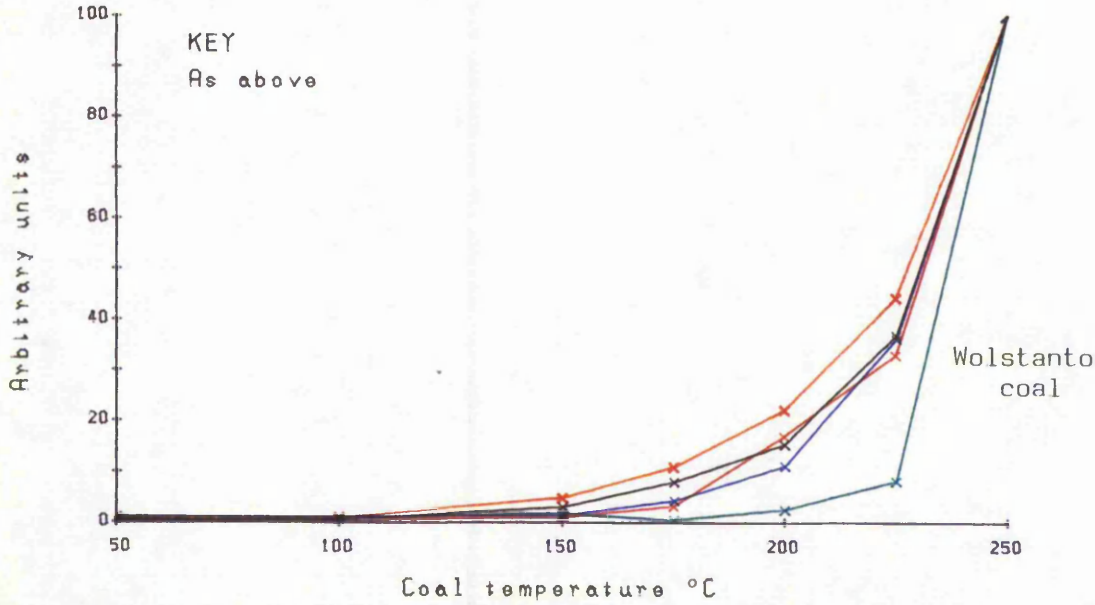

Figs 55a-c. Evolution pattern from test coals heated in air.

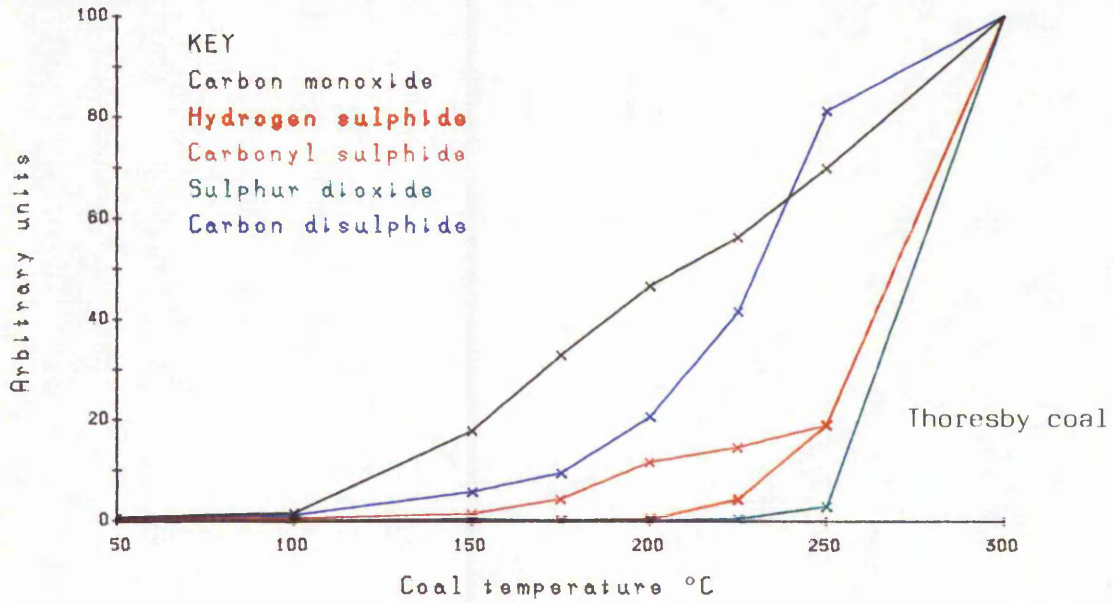

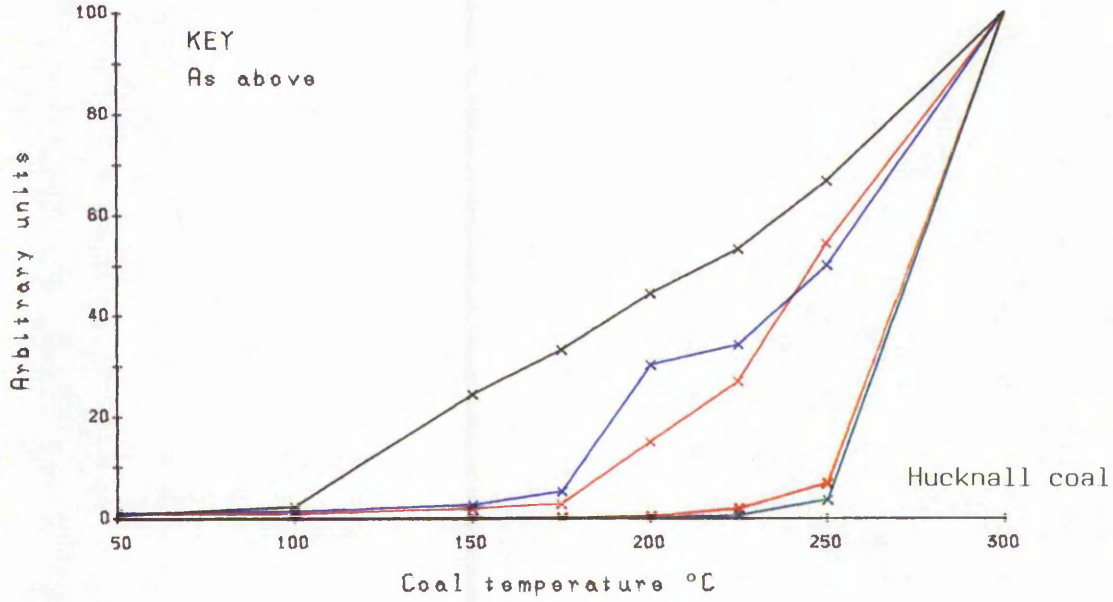

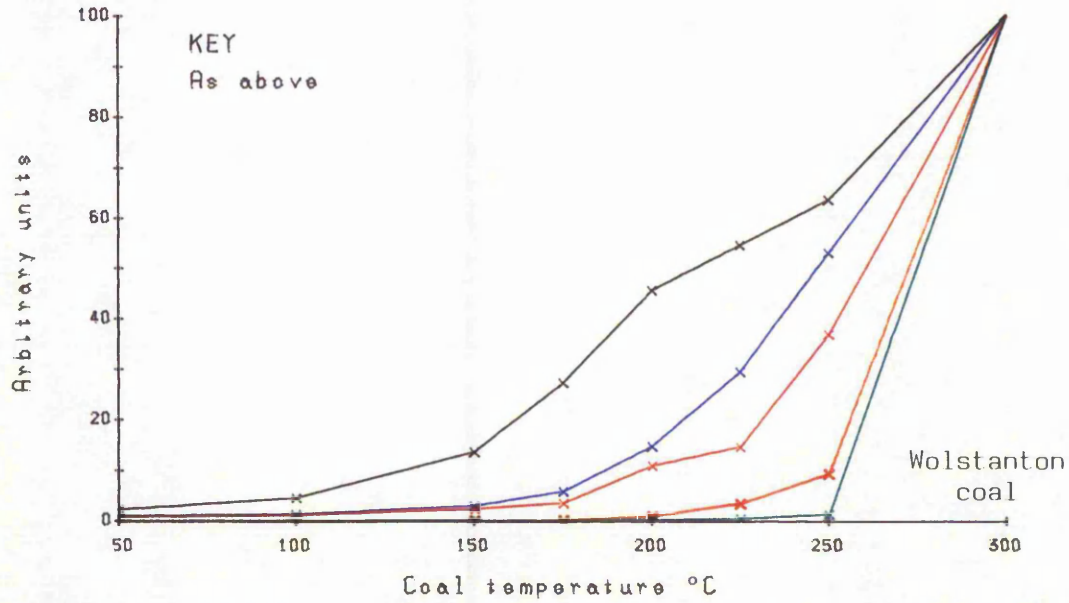

Figs 56a-c. Evolution pattern from test coals heated in nitrogen

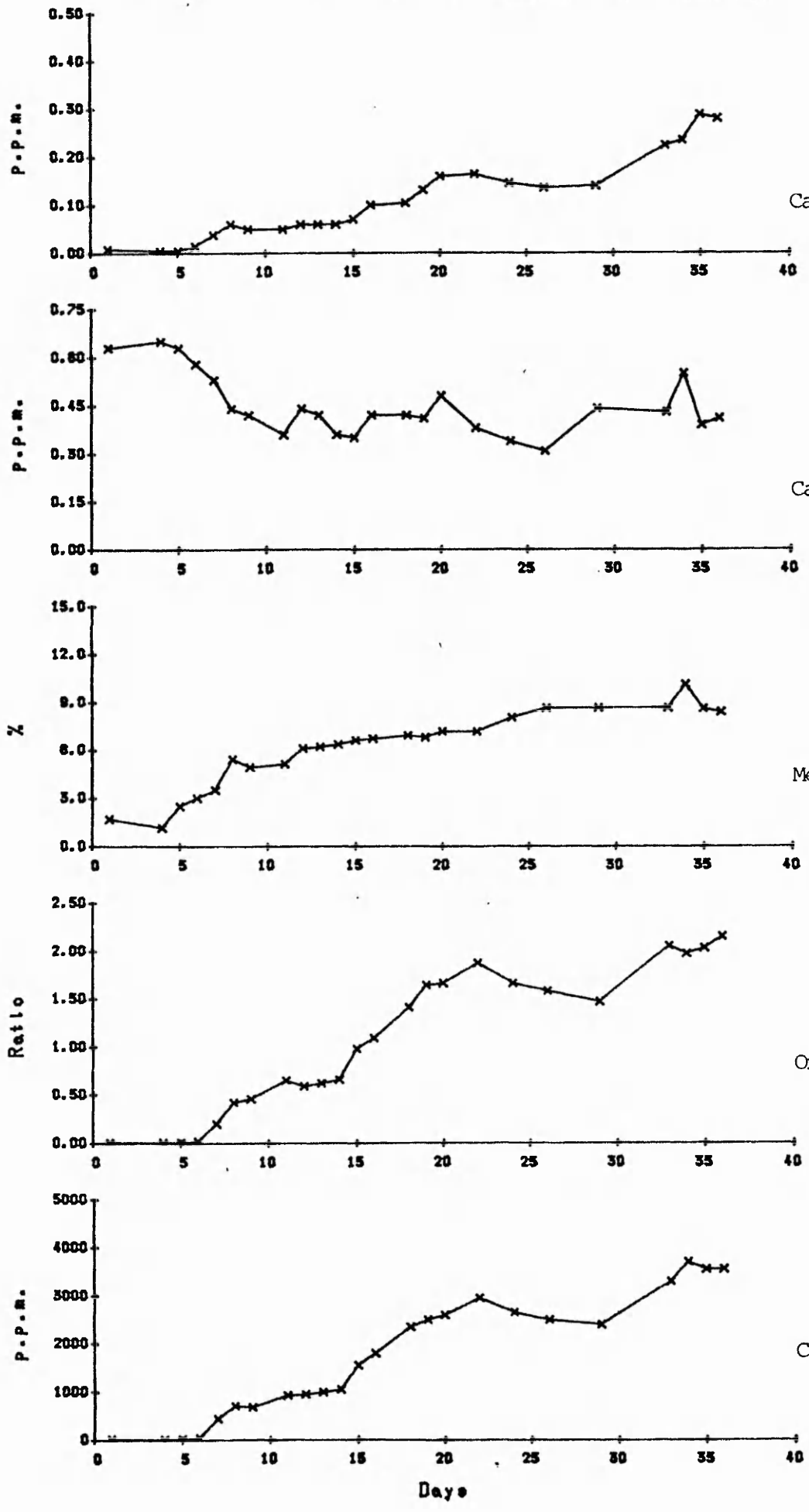

Figure 57. Bentinck colliery K50s return pack pipe.

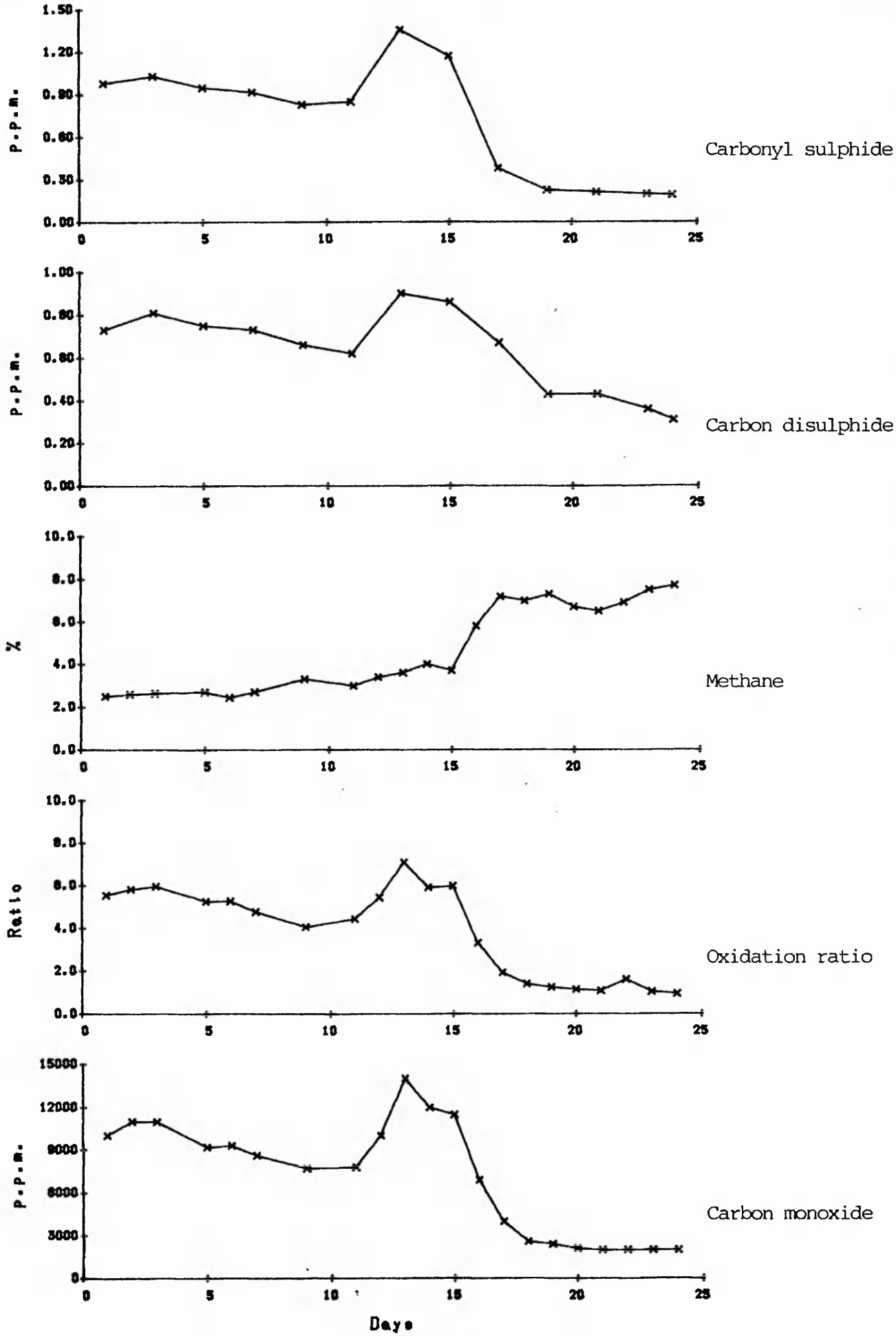

Figure 58. Warsop colliery U19s return pack pipe.

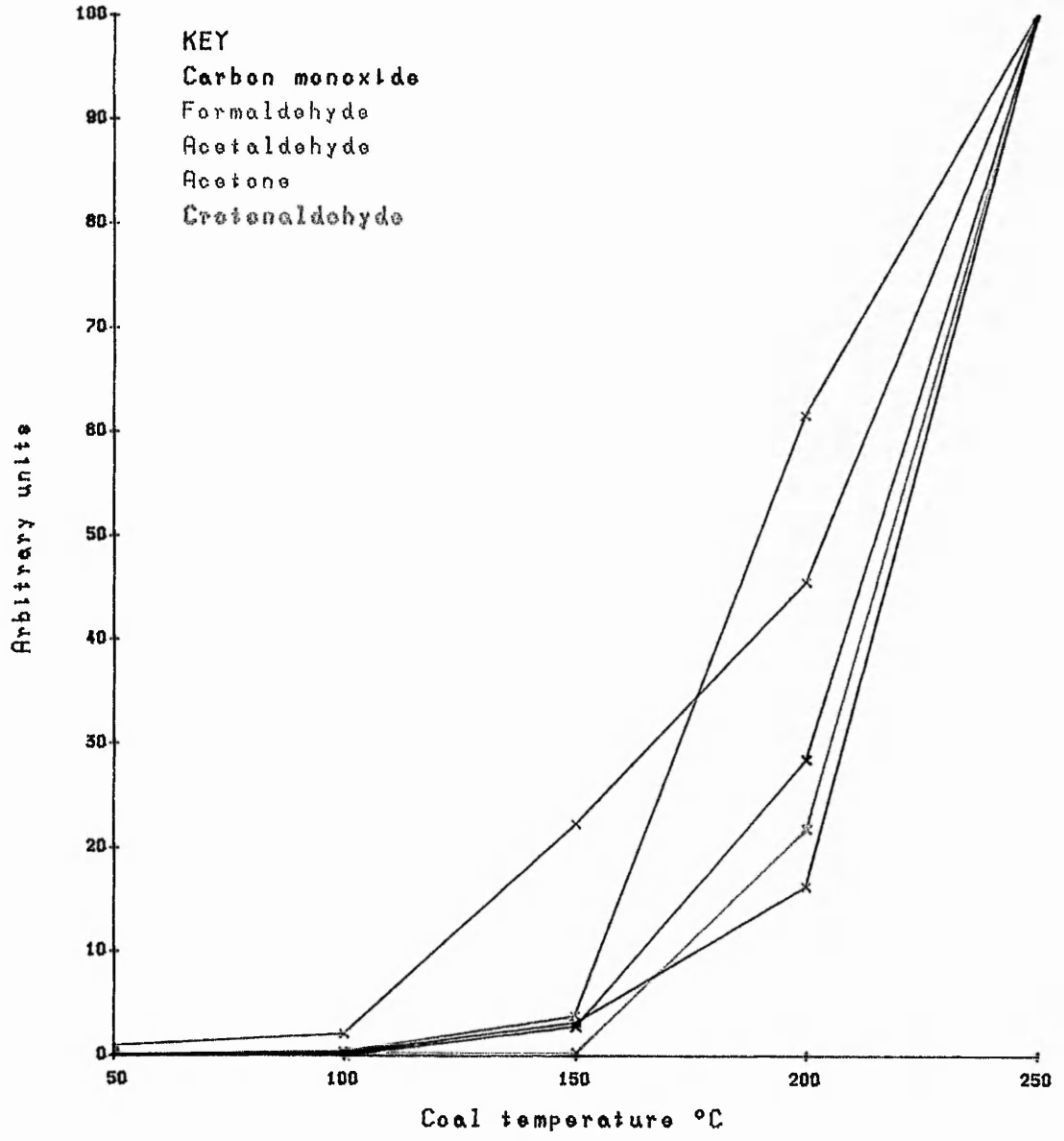

Figure 59. Evolution pattern of carbonyl compounds from Hucknall coal heated in air.

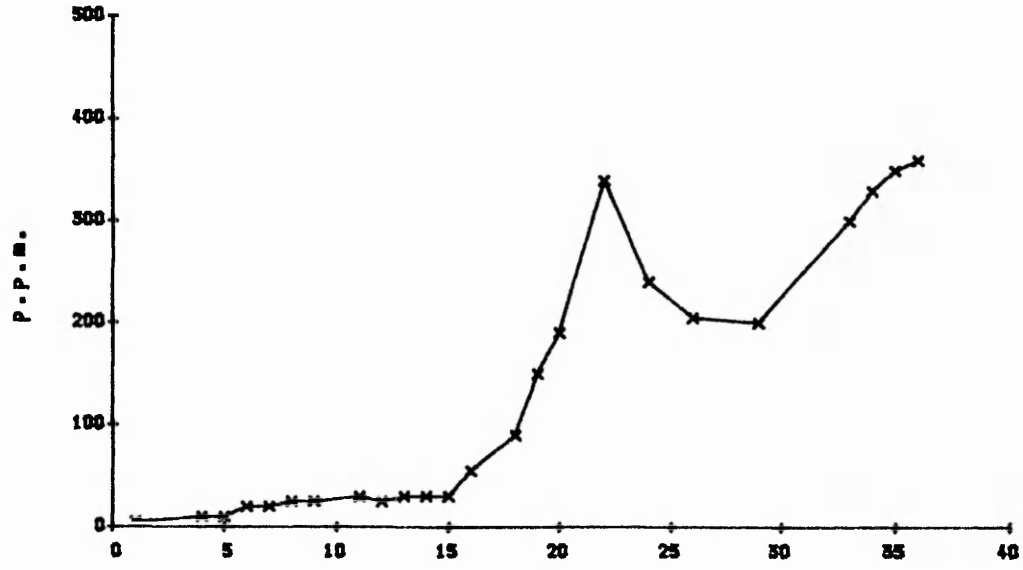

Hydrogen

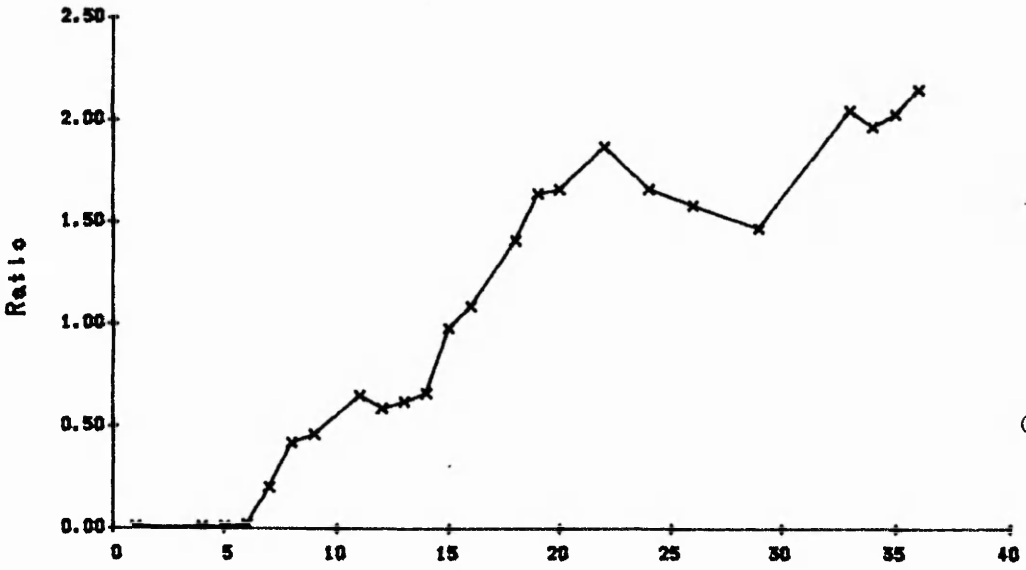

Oxidation ratio

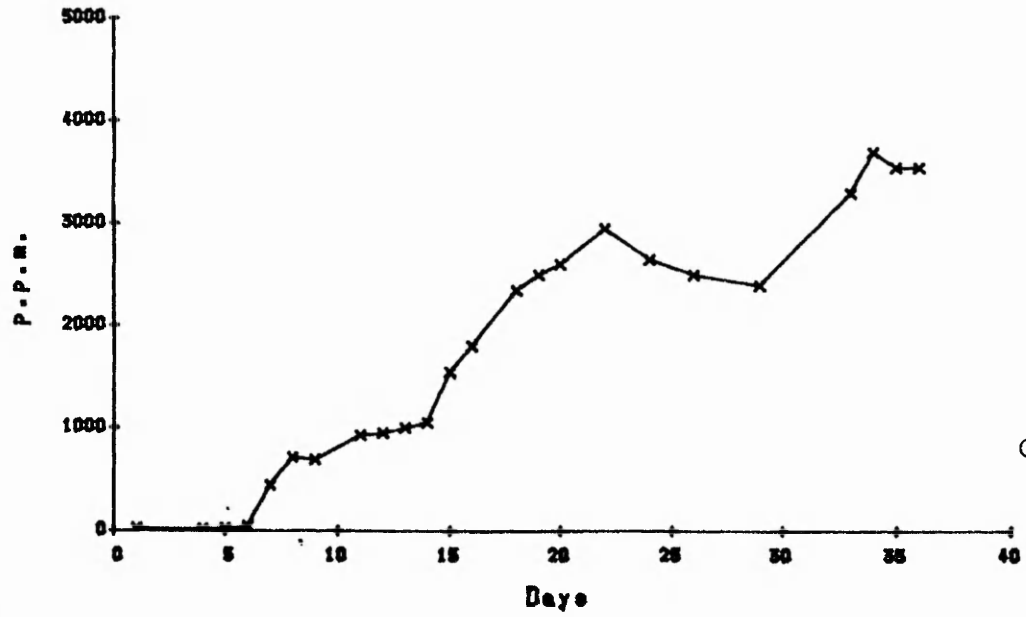

Carbon monoxide

Figure 60. Bentinck colliery K50s return pack pipe.

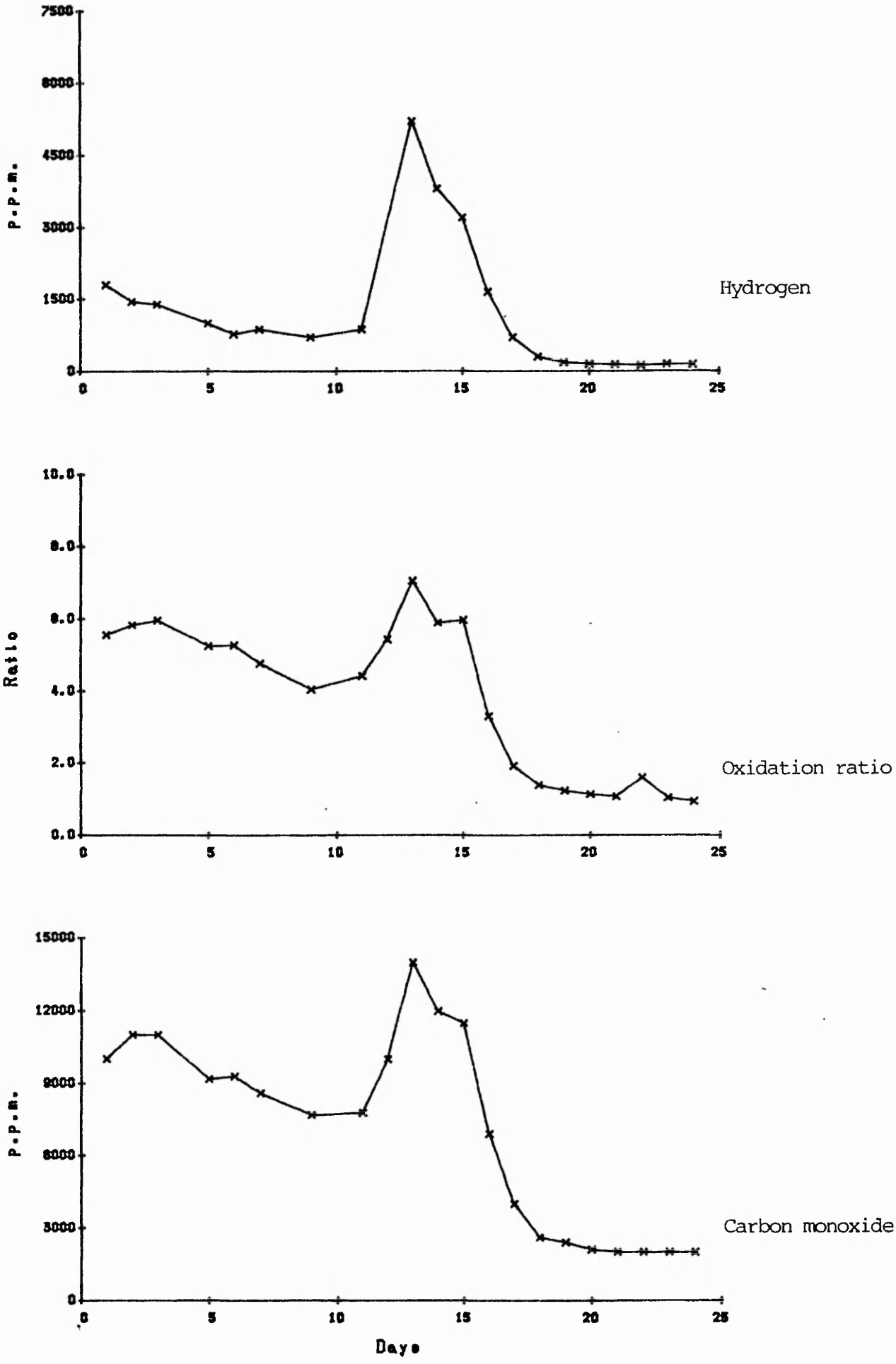

Figure 61. Warsop colliery U19s return pack pipe.

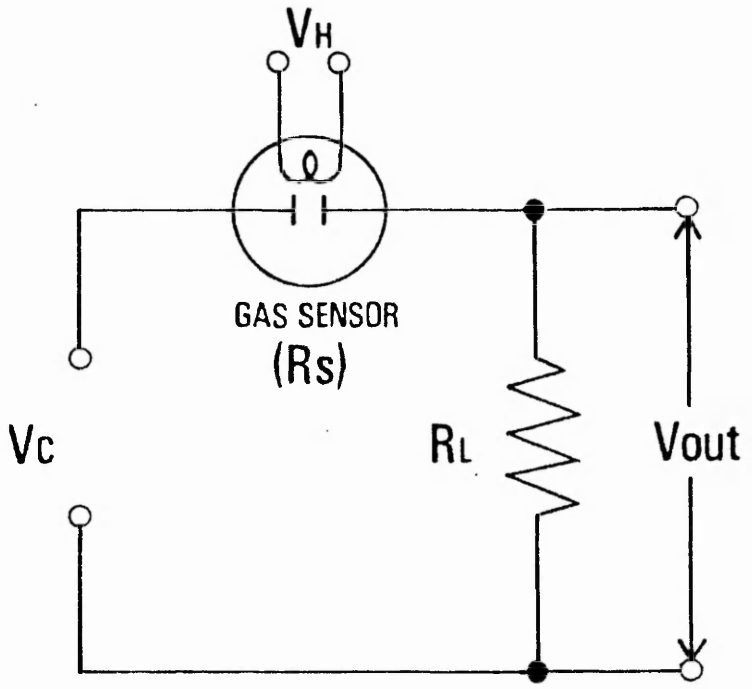

V_H – Heater voltage

V_c – Circuit voltage

R_L – Load resistor

V_{out} – Voltage change across RL

Figure 62. Electrical measuring circuit employed in sensor studies.

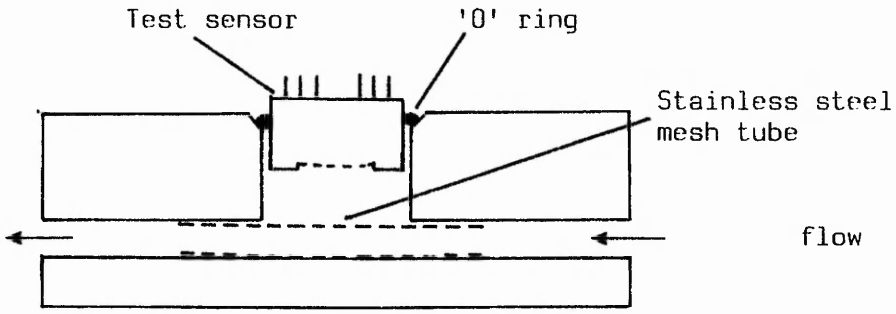

Figure 63a. Schematic diagram of brass test block.

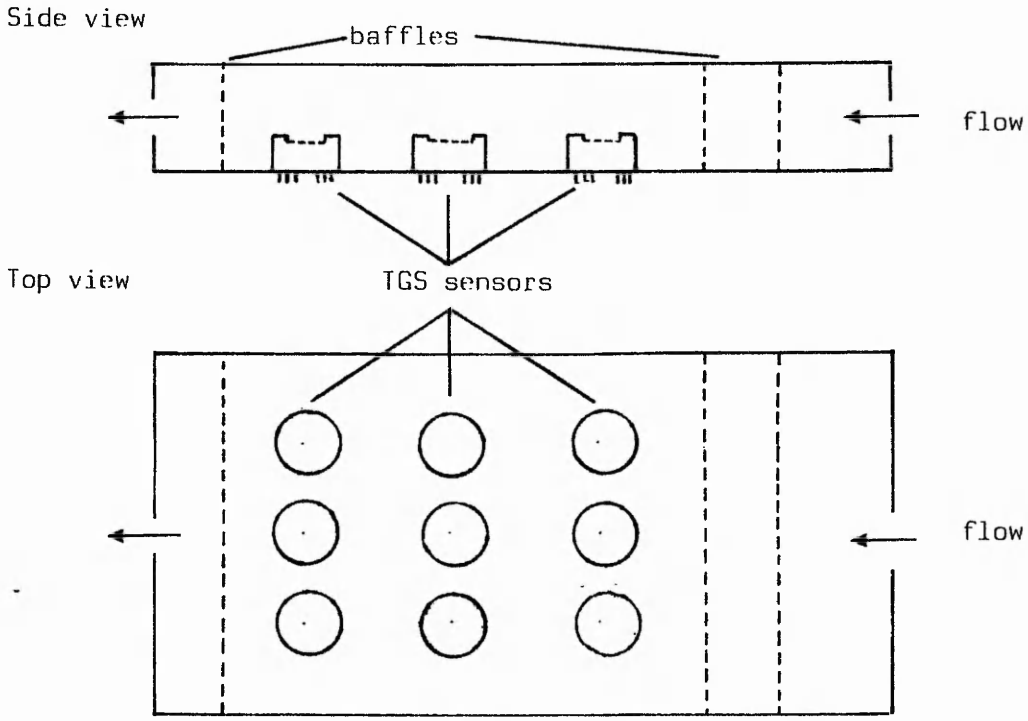

Figure 63b. Schematic diagram of PTFE test cell.

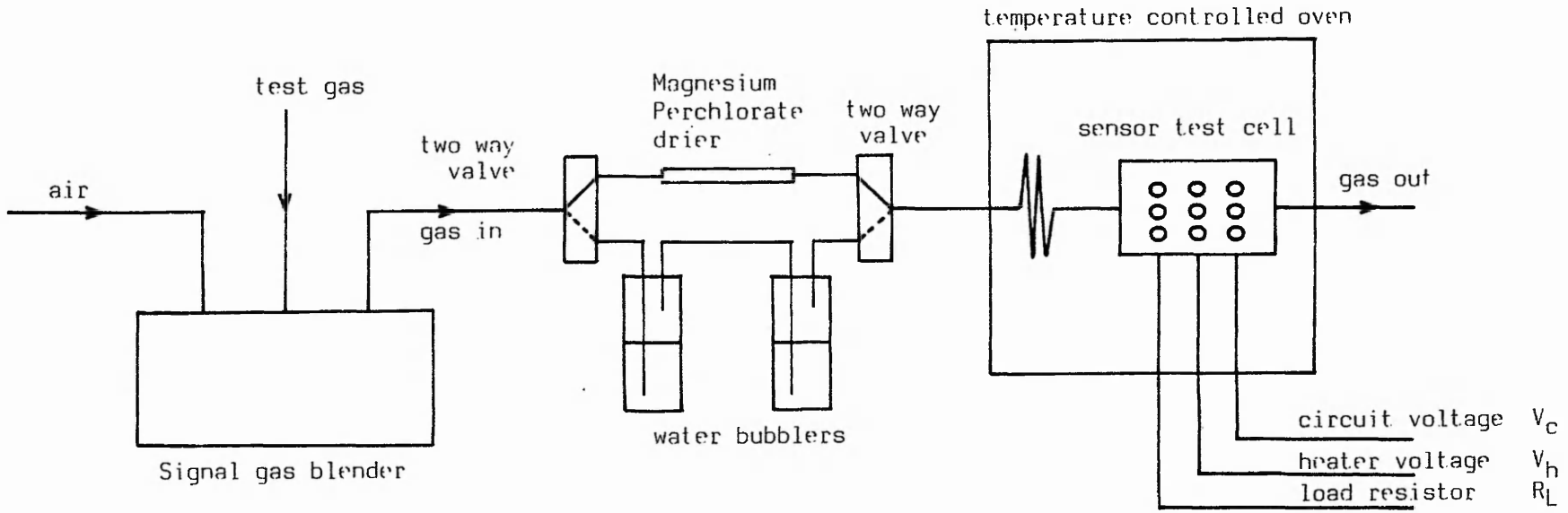

Figure 64 Schematic diagram of experimental arrangement for sensor studies

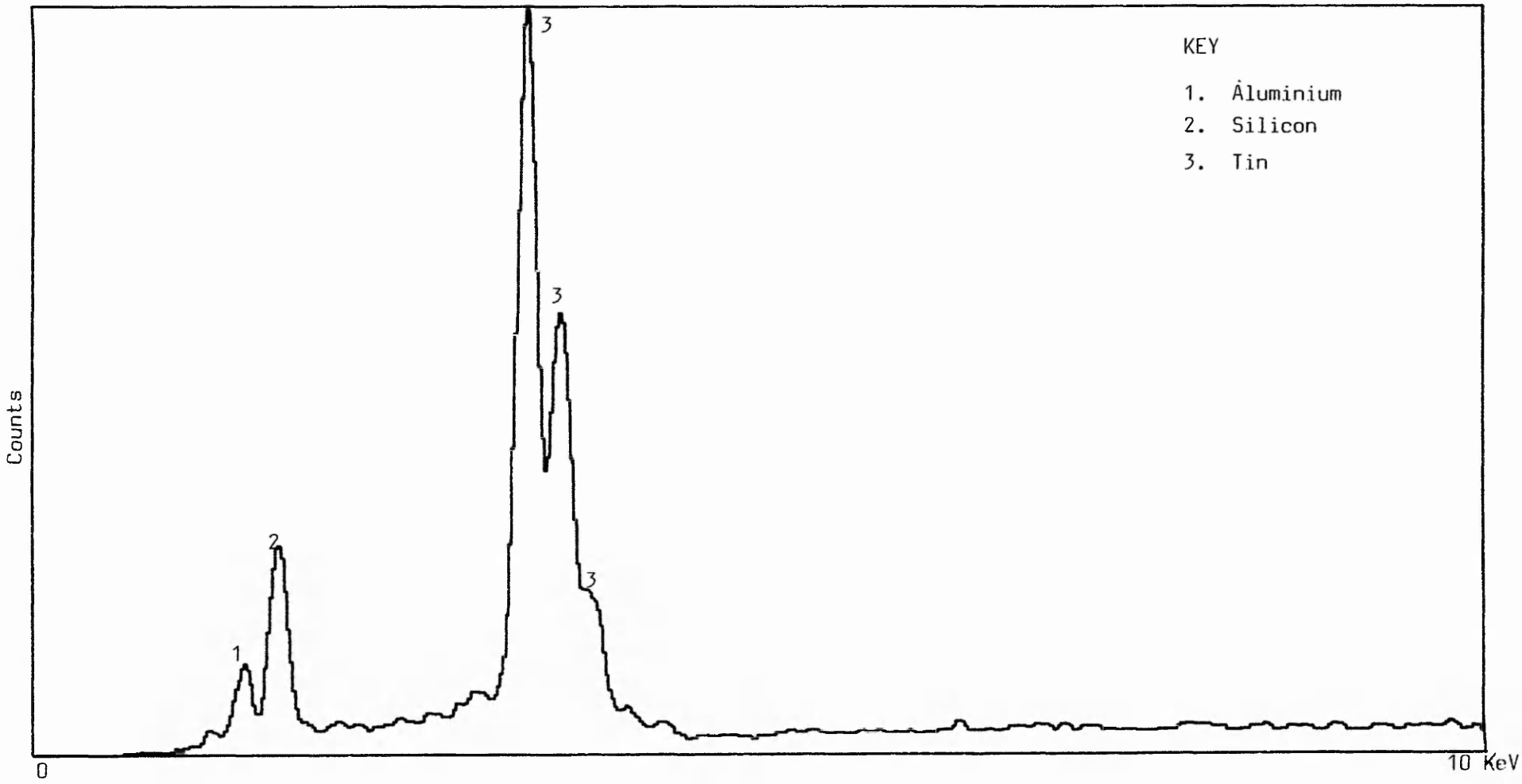

Figure 65 Energy dispersive X-ray analysis spectrum of 711 sensor surface

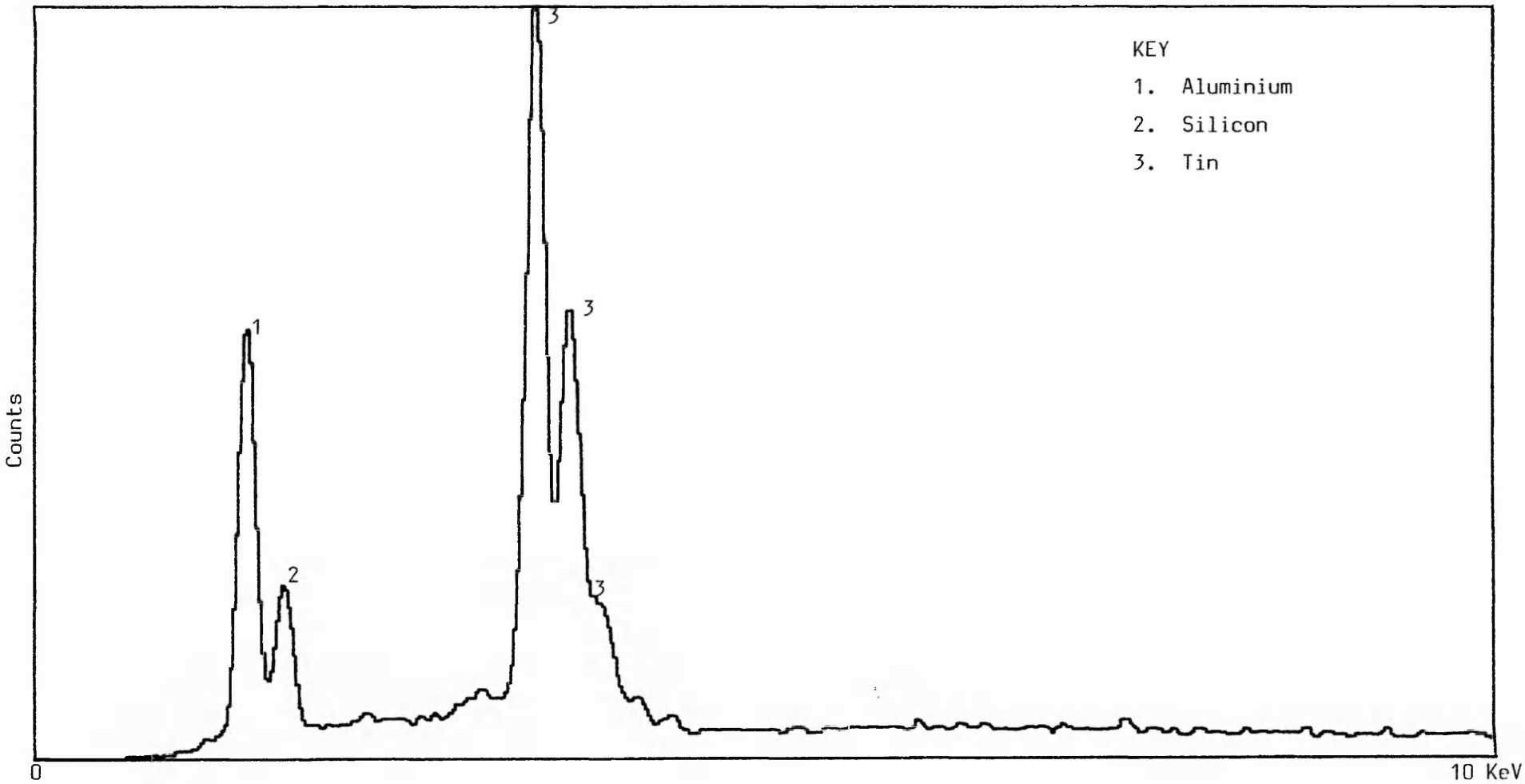

Figure 66 Energy dispersive X-ray analysis spectrum of 812 sensor surface

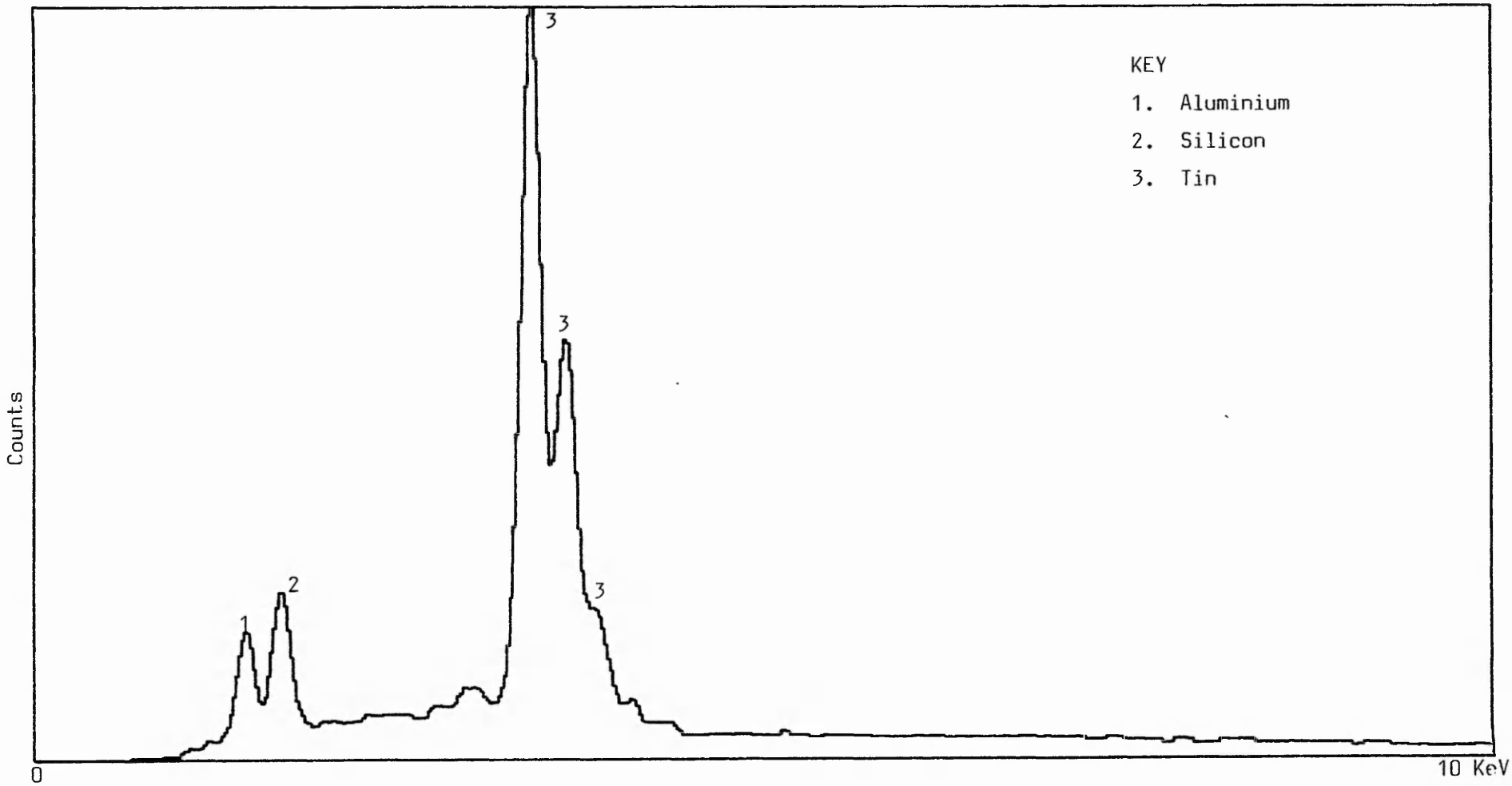

Figure 67 Energy dispersive X-ray analysis spectrum of 813 sensor surface

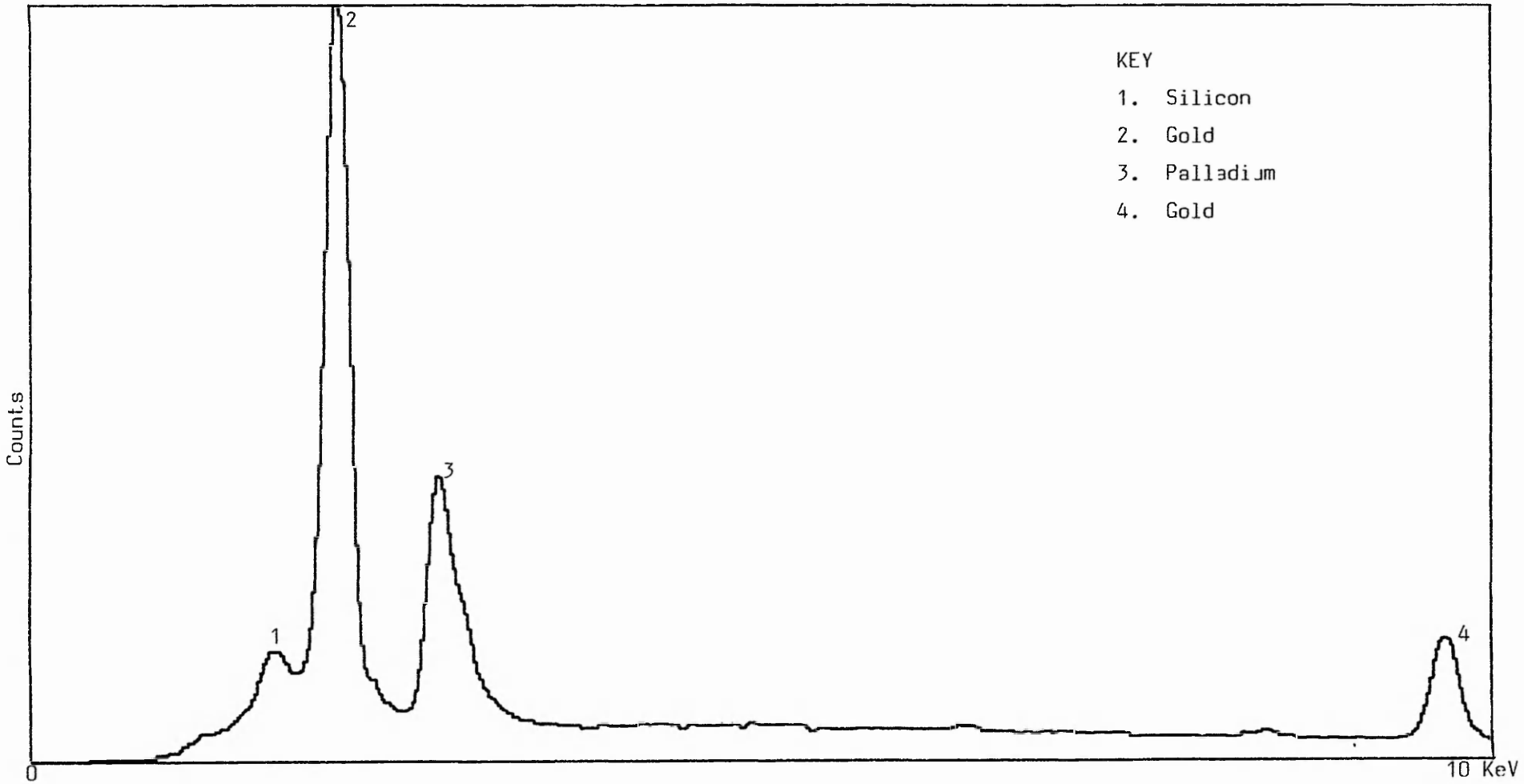

Figure 68 A typical energy dispersive X-ray analysis spectrum of the sensors electrode wires

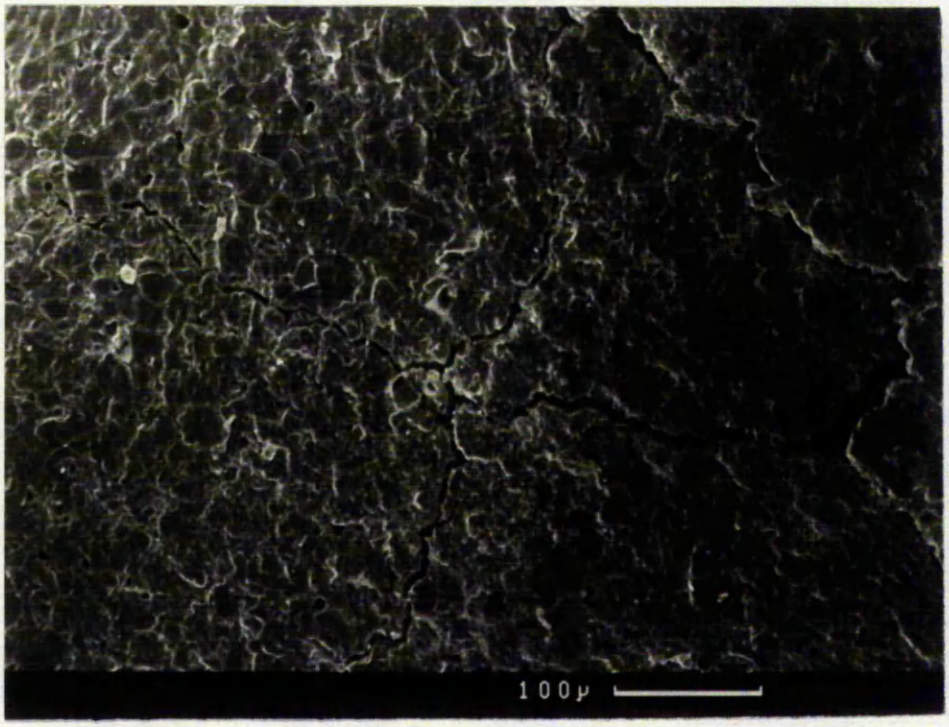

Figure 69. Scanning electron photomicrograph of 711 surface
Magnification x200

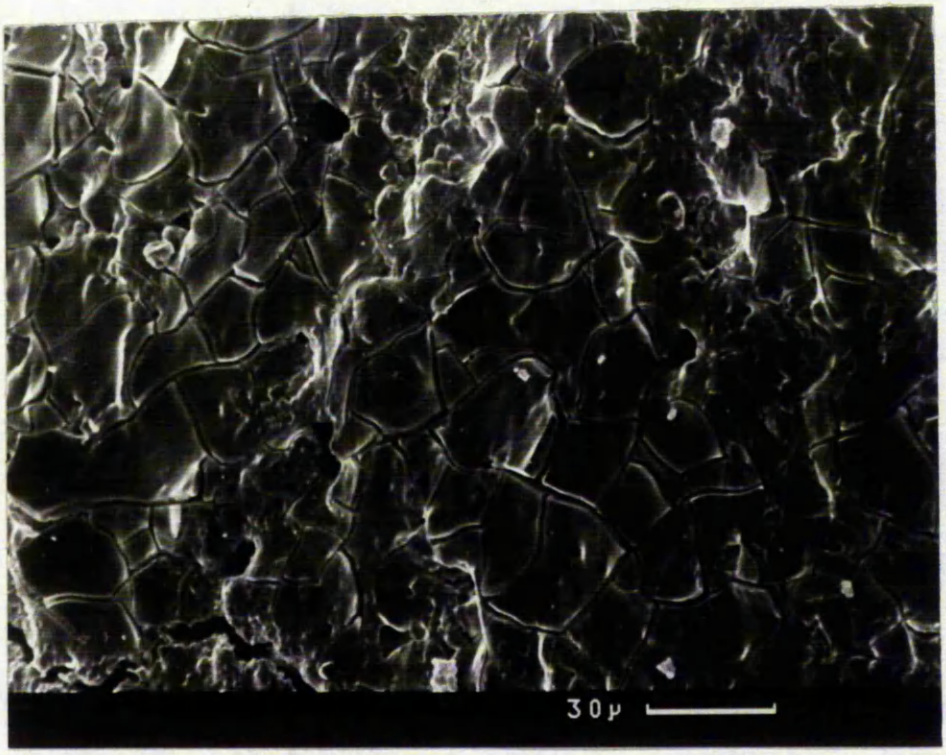

Figure 70. Scanning electron photomicrograph of 711 surface
Magnification x500

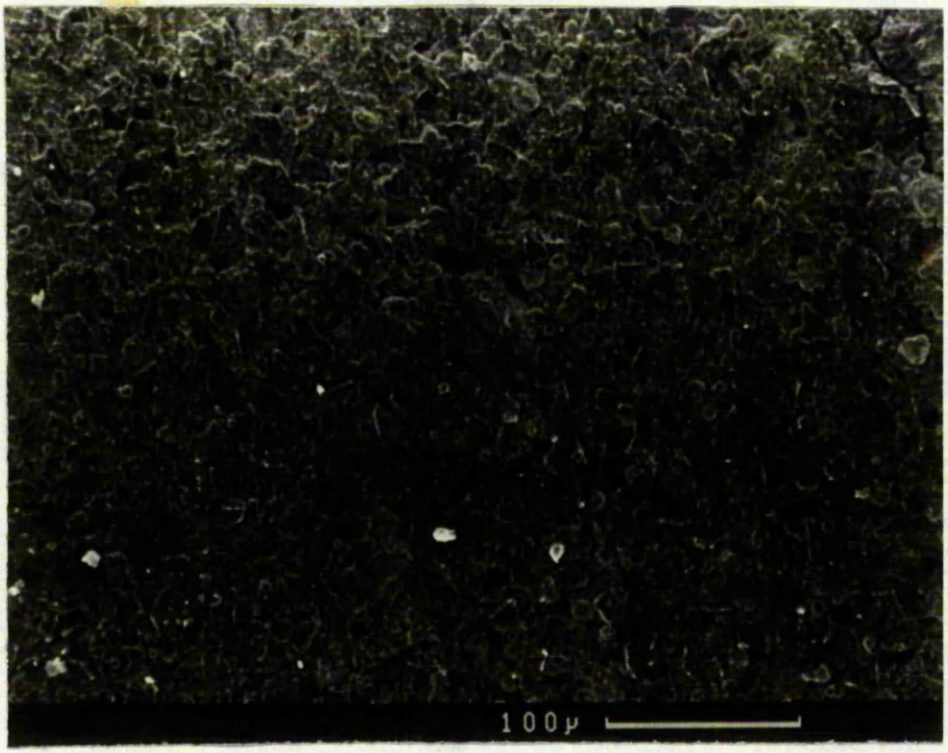

Figure 71. Scanning electron photomicrograph of 812 surface
Magnification x200

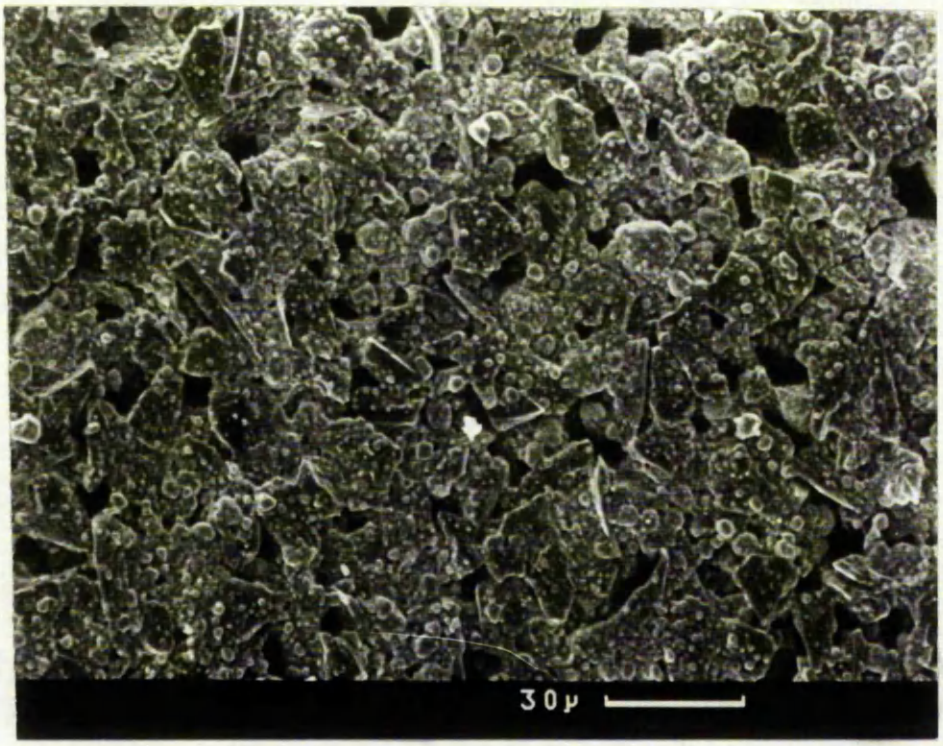

Figure 72. Scanning electron photomicrograph of 812 surface
Magnification x500

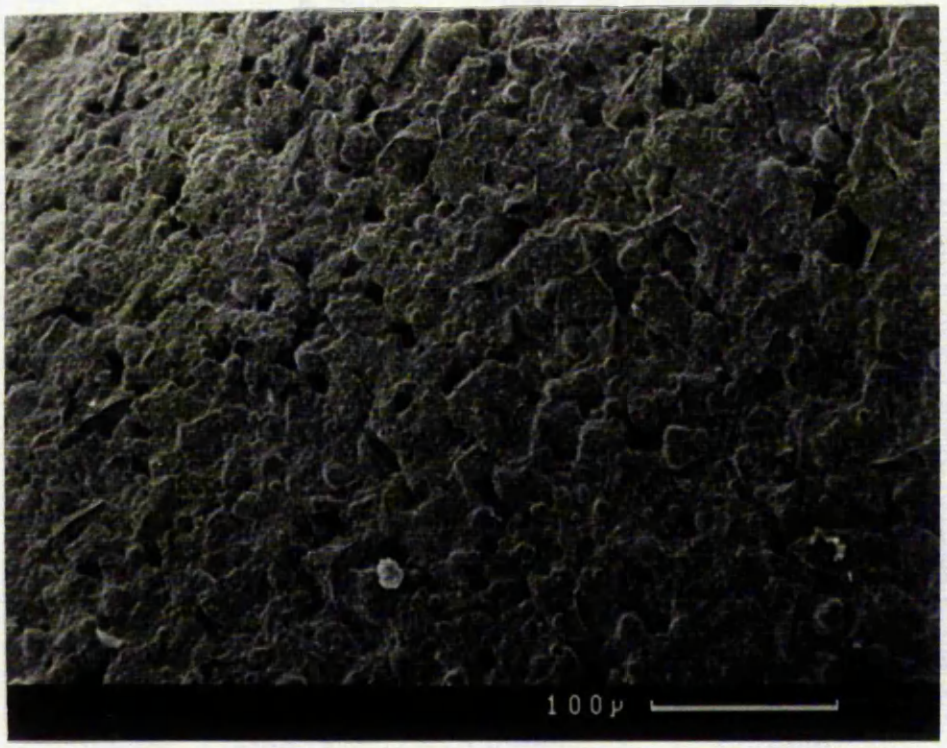

Figure 73. Scanning electron photomicrograph of 813 surface
Magnification x200

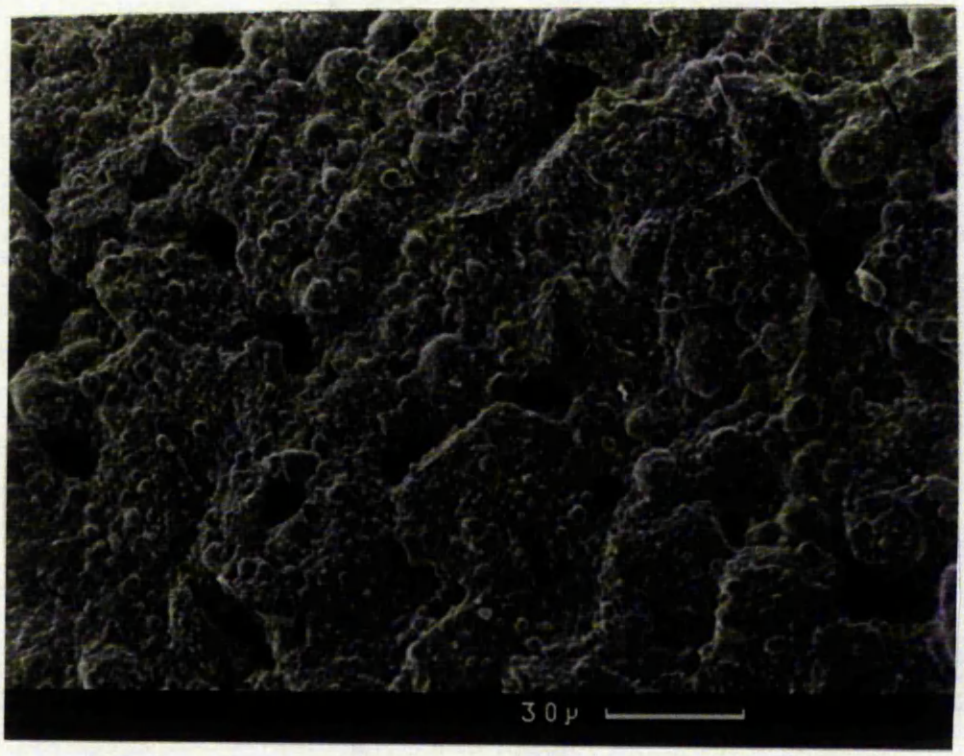

Figure 74. Scanning electron photomicrograph of 813 surface
Magnification x500

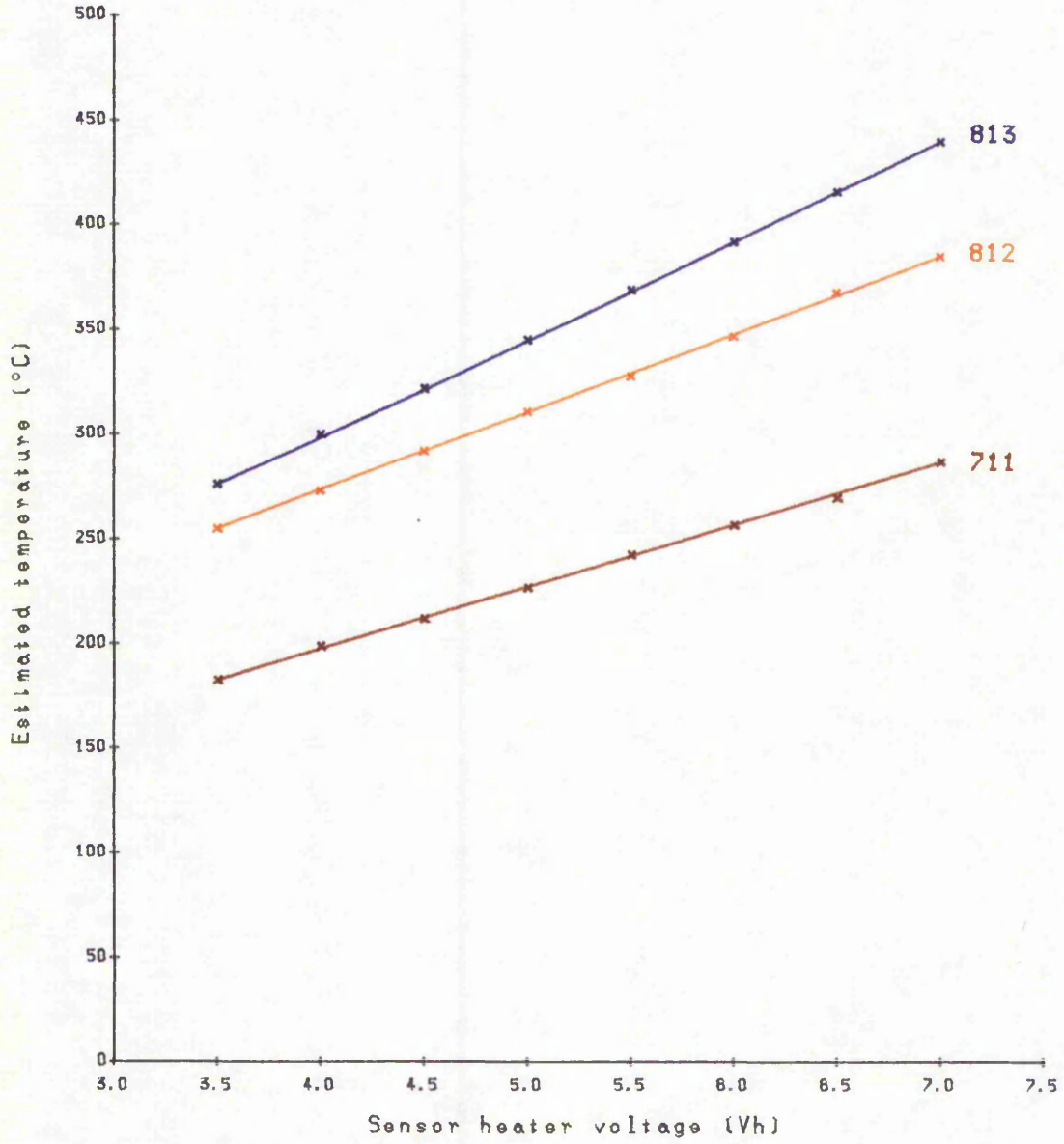

Figure 75. Variation in sensor operating temperature over a range of heater voltages.

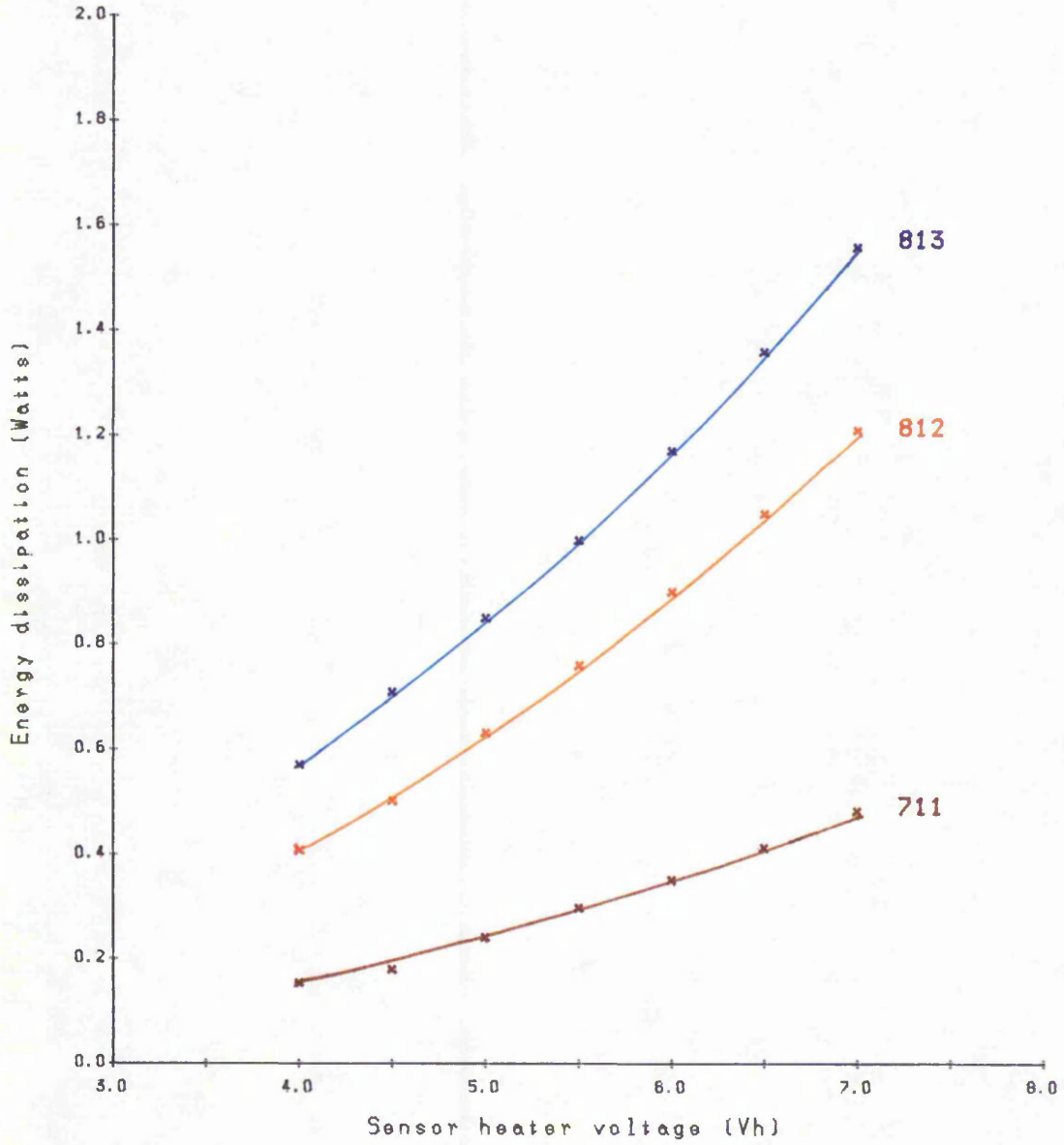

Figure 76. Variation in energy dissipated by each sensor over a range of heater voltages.

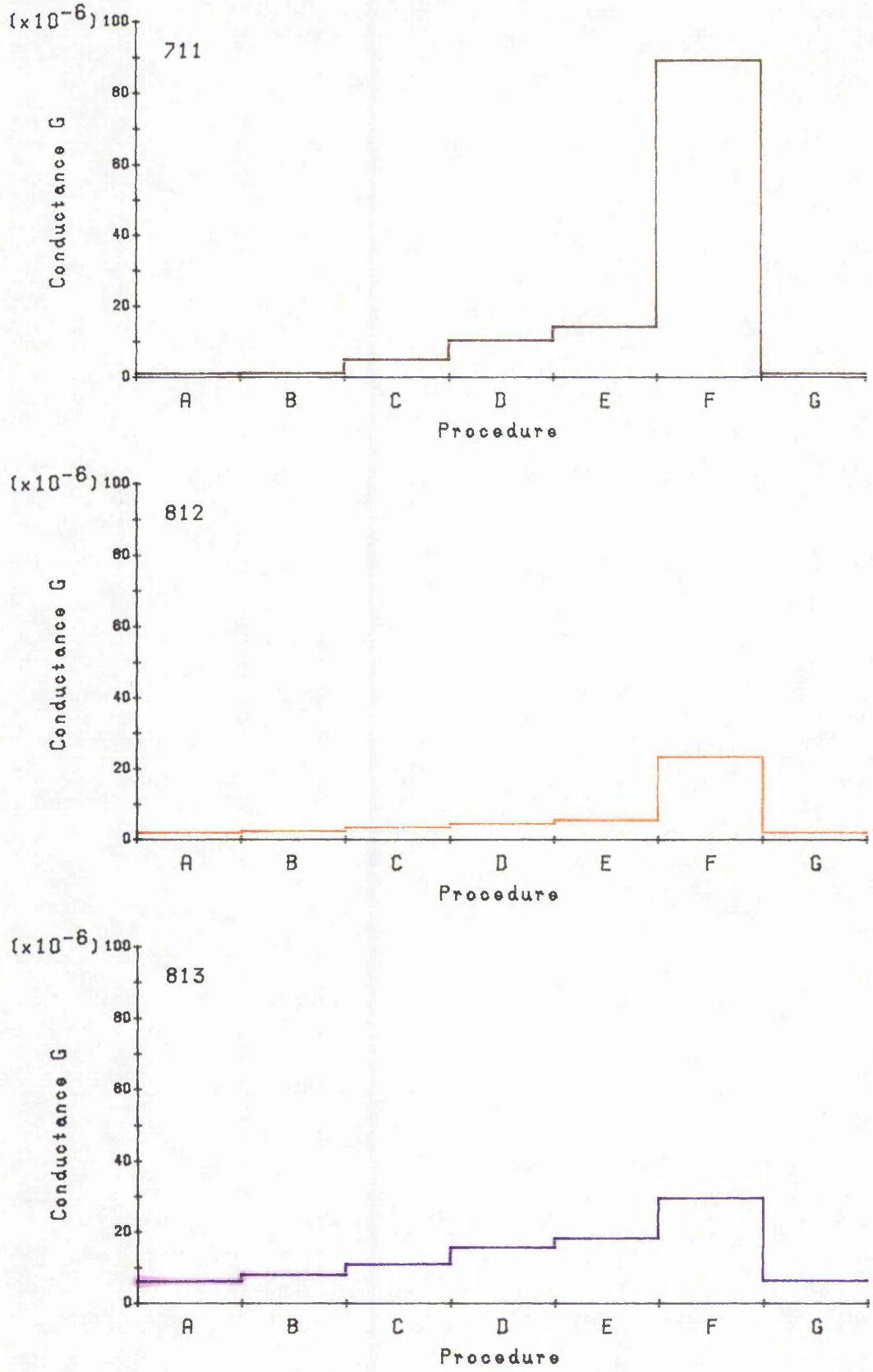

See pages 220 and 226 for an explanation of Procedures A-G.

Figure 77a. The effect of different ambient test atmospheres on sensor behaviour when operated at 5.0V heater voltage.

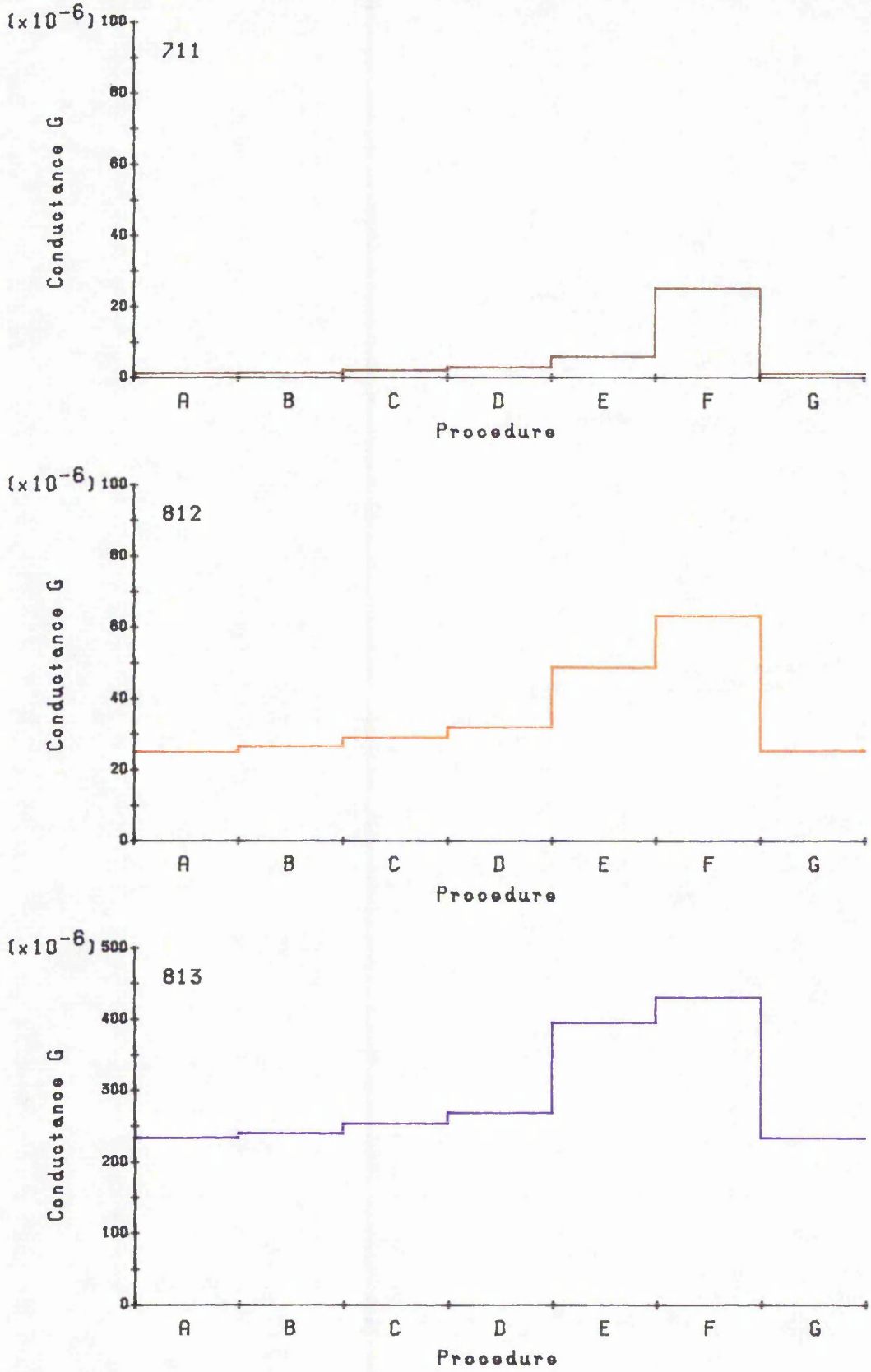

See pages 220 and 226 for an explanation of Procedures A-G.

Figure 77b. The effect of different ambient test atmospheres on sensor behaviour when operated at 7.0V heater voltage.

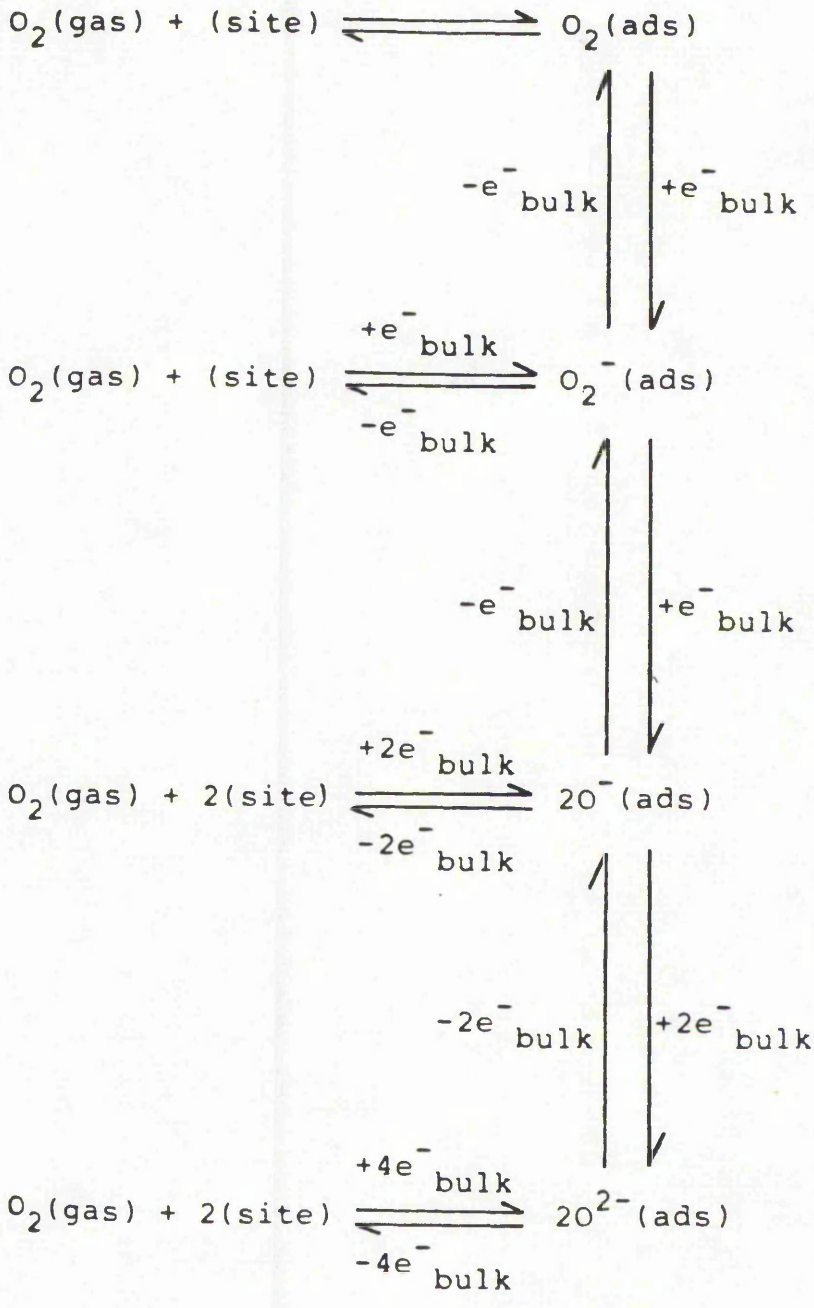

Figure 78. Summary of possible routes for the formation of adsorbed oxygen species on tin oxide surfaces.

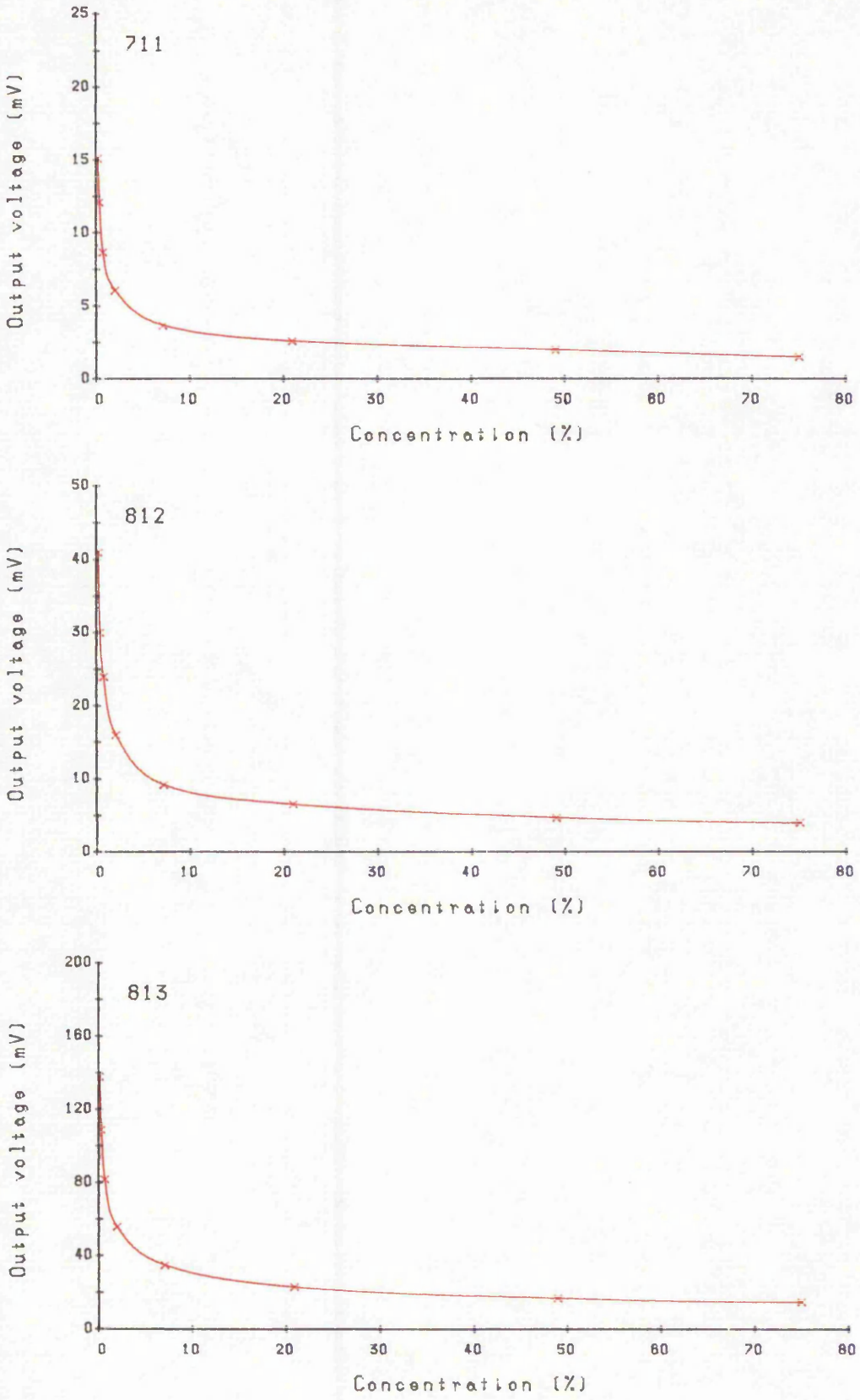

Figure 79a. Variation in voltage appearing across series load resistor versus oxygen concentration at a sensor heater voltage of 5.0V.

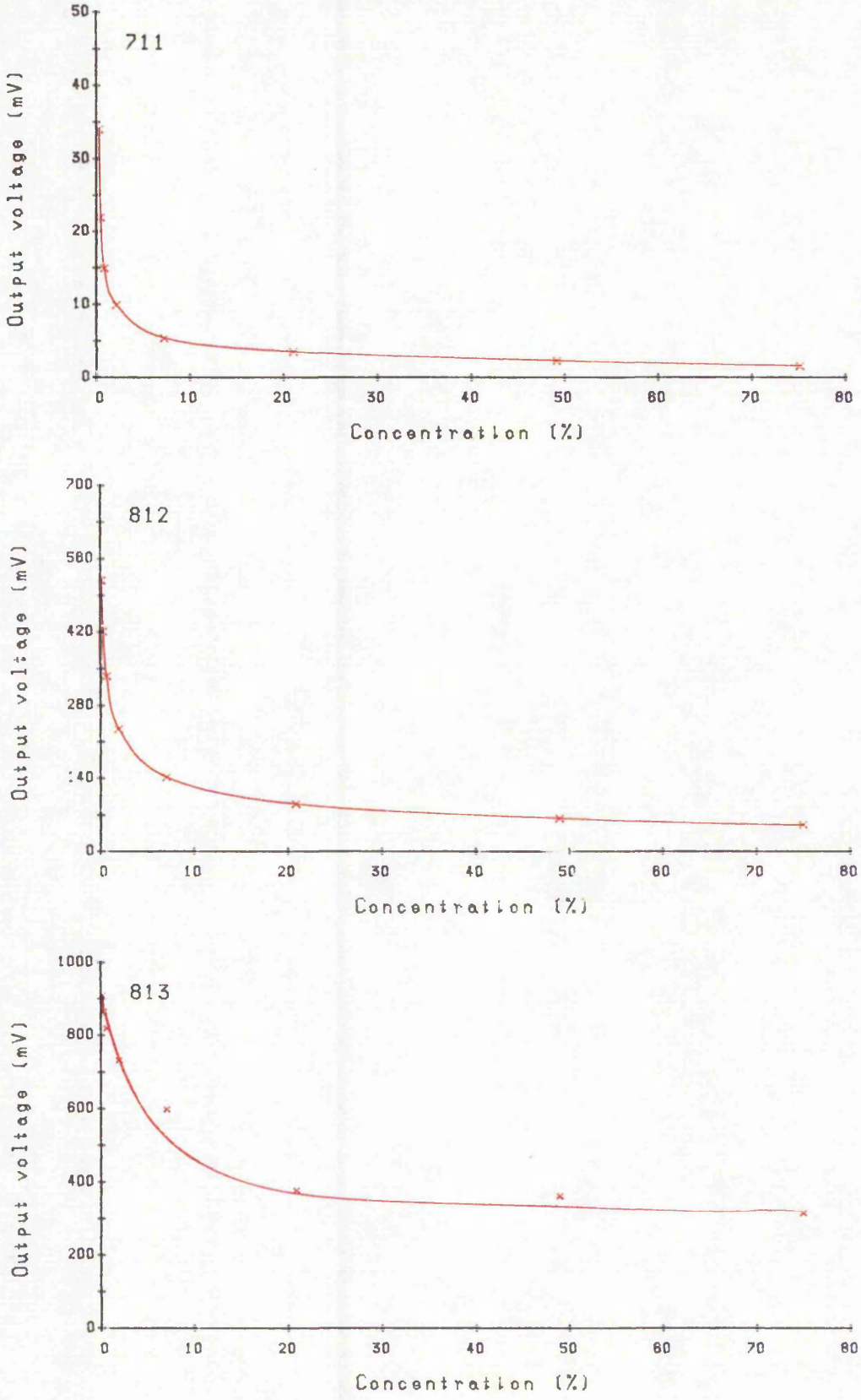

Figure 79b. Variation in voltage appearing across series load resistor versus oxygen concentration at a sensor heater voltage of 7.0V.

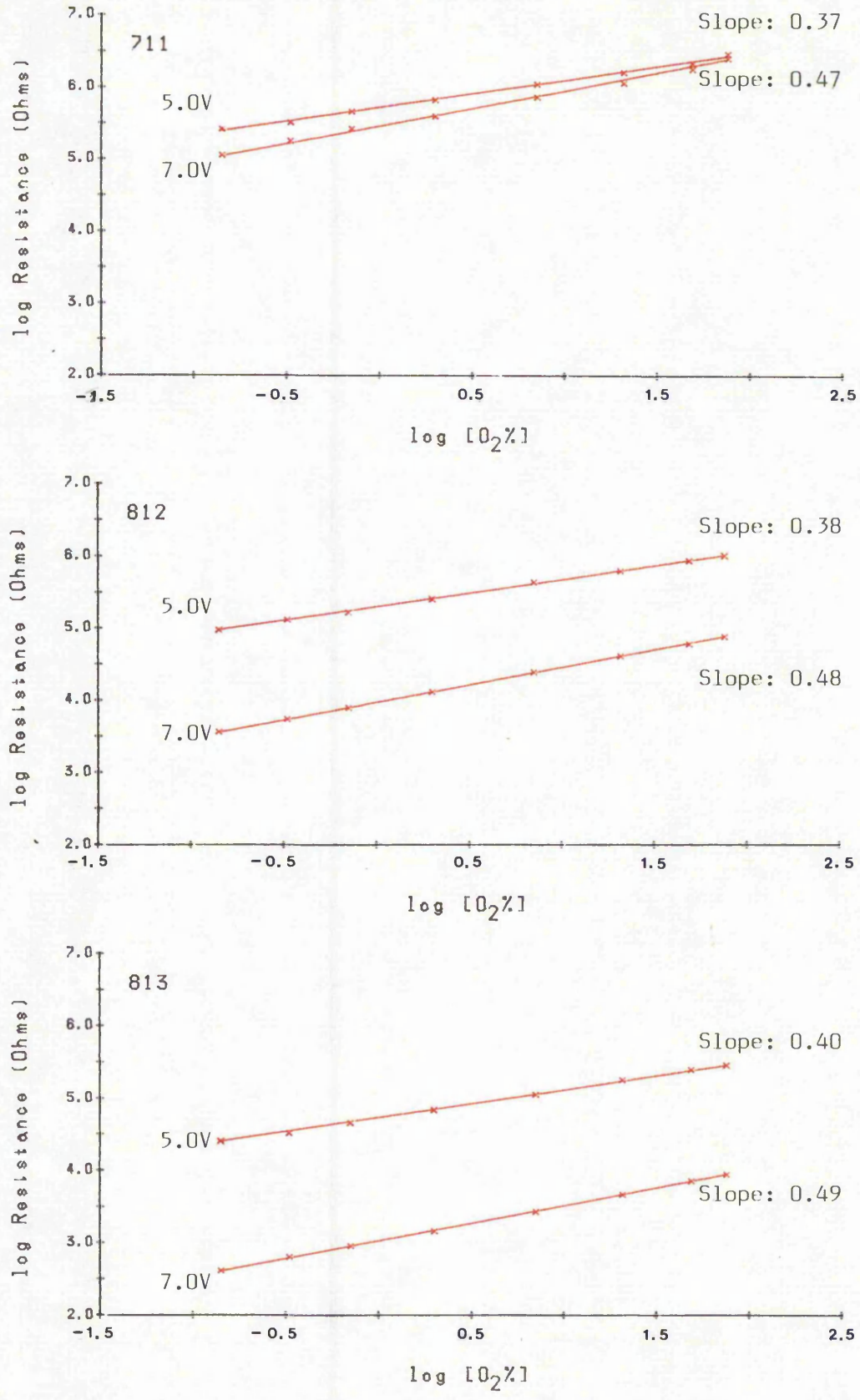

Oxygen (dry)

Best straight line fitted by least squares method.

Figure 80. Sensor resistance at 5.0 and 7.0V heater voltage as a function of oxygen concentration.

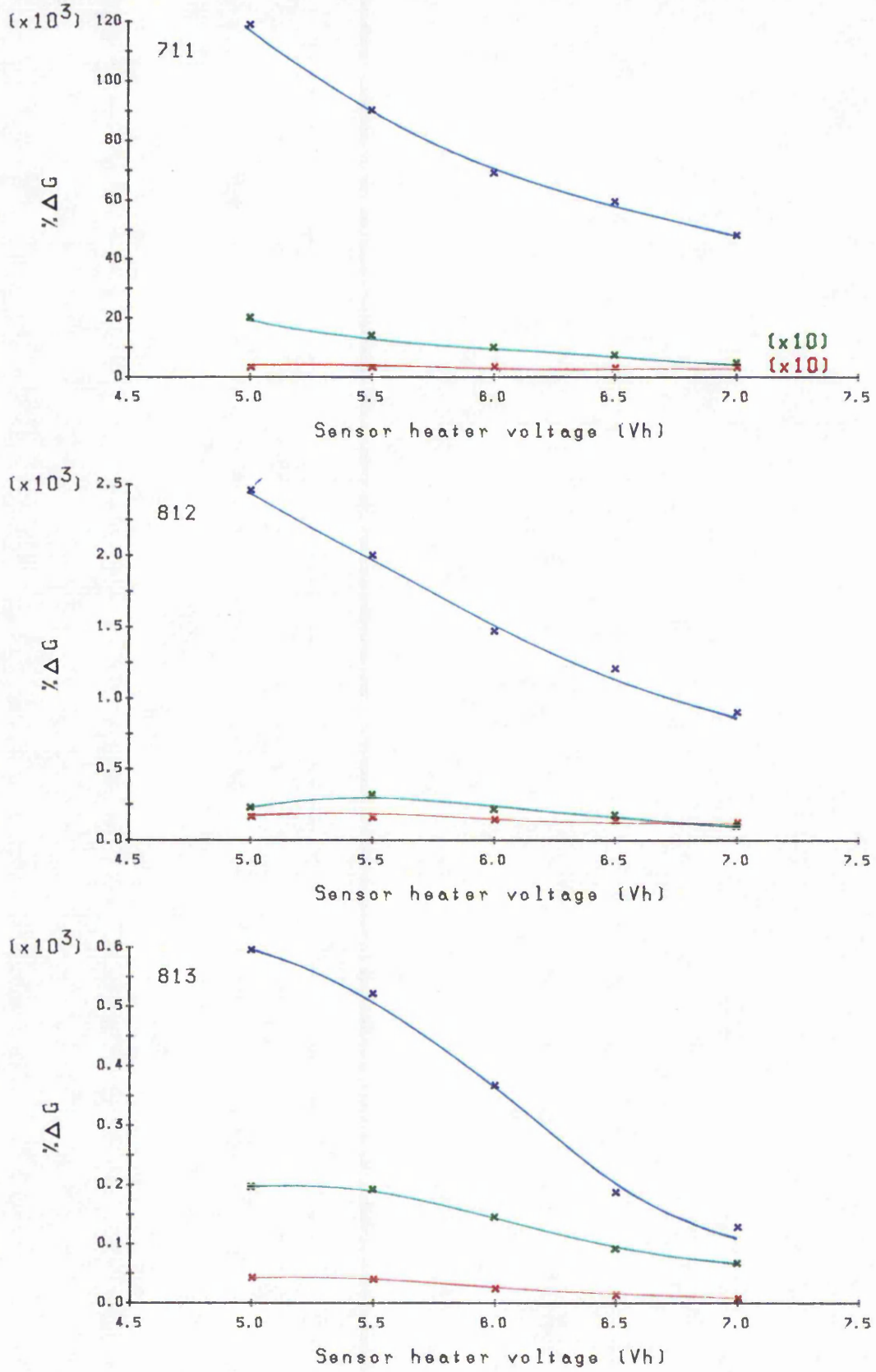

Figure 81. Variation in sensor sensitivity to carbon monoxide as a function of heater voltage.

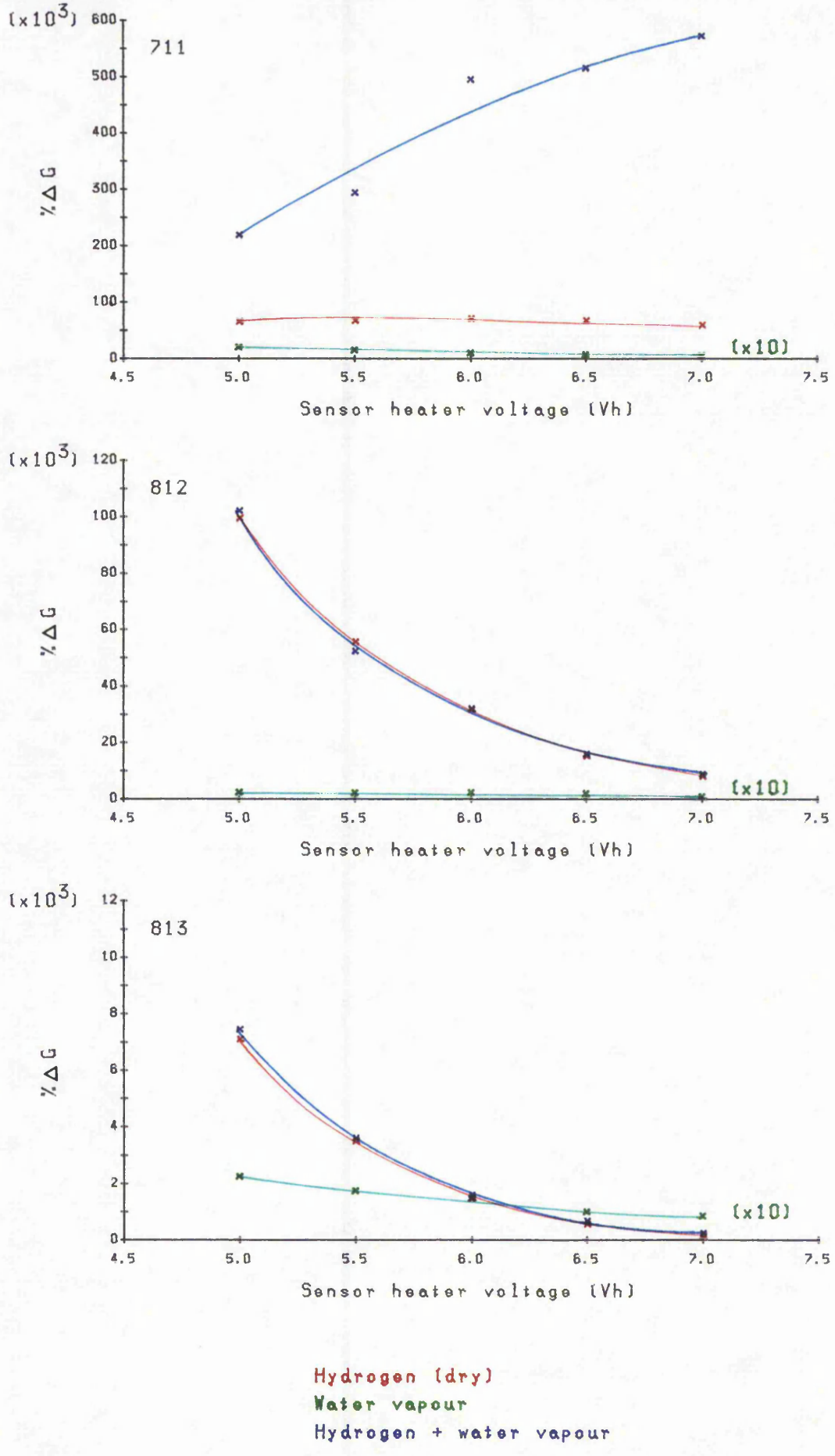

Figure 82. Variation in sensor sensitivity to hydrogen as a function of heater voltage.

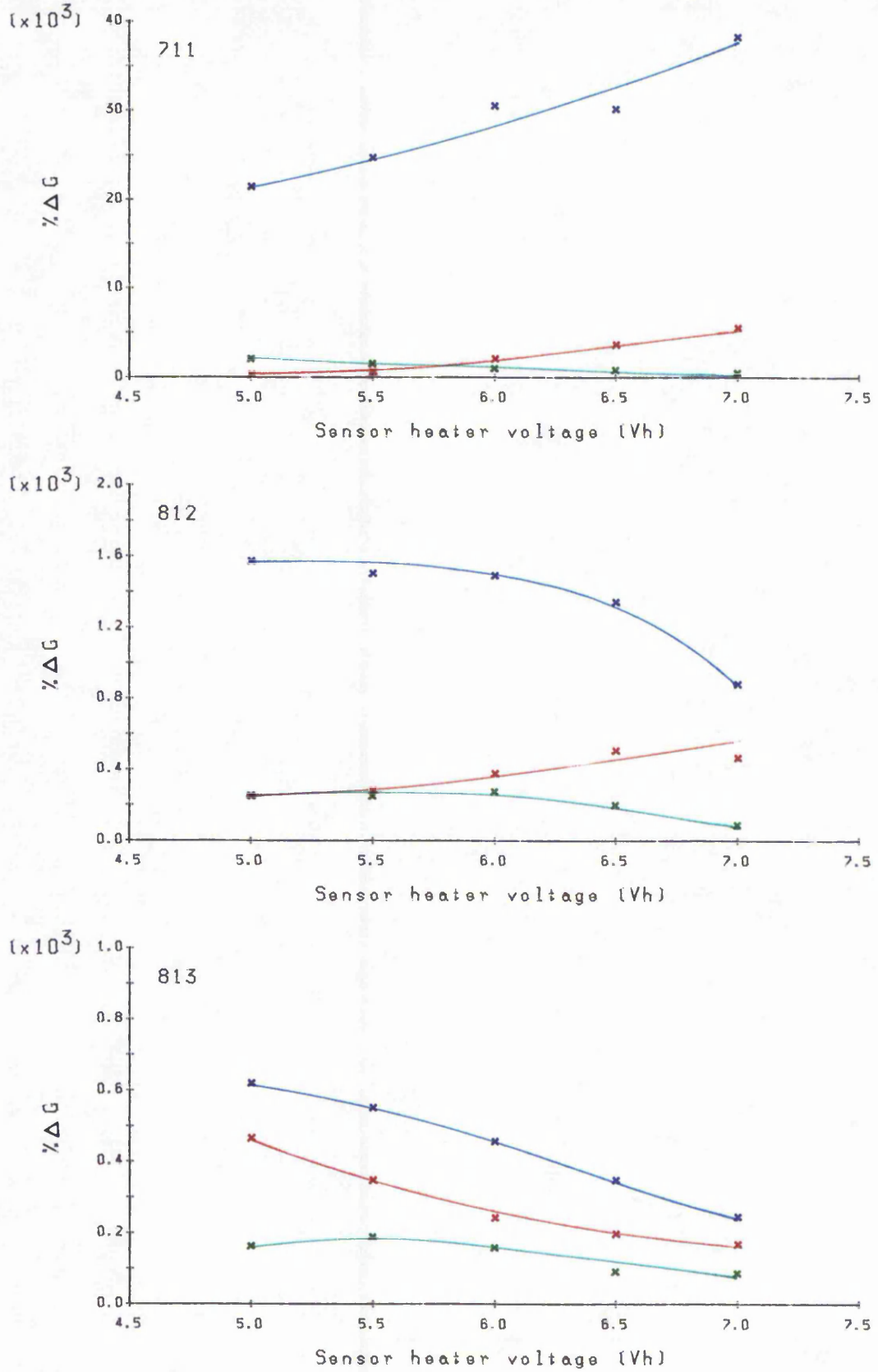

Figure 83. Variation in sensor sensitivity to ethene as a function of heater voltage.

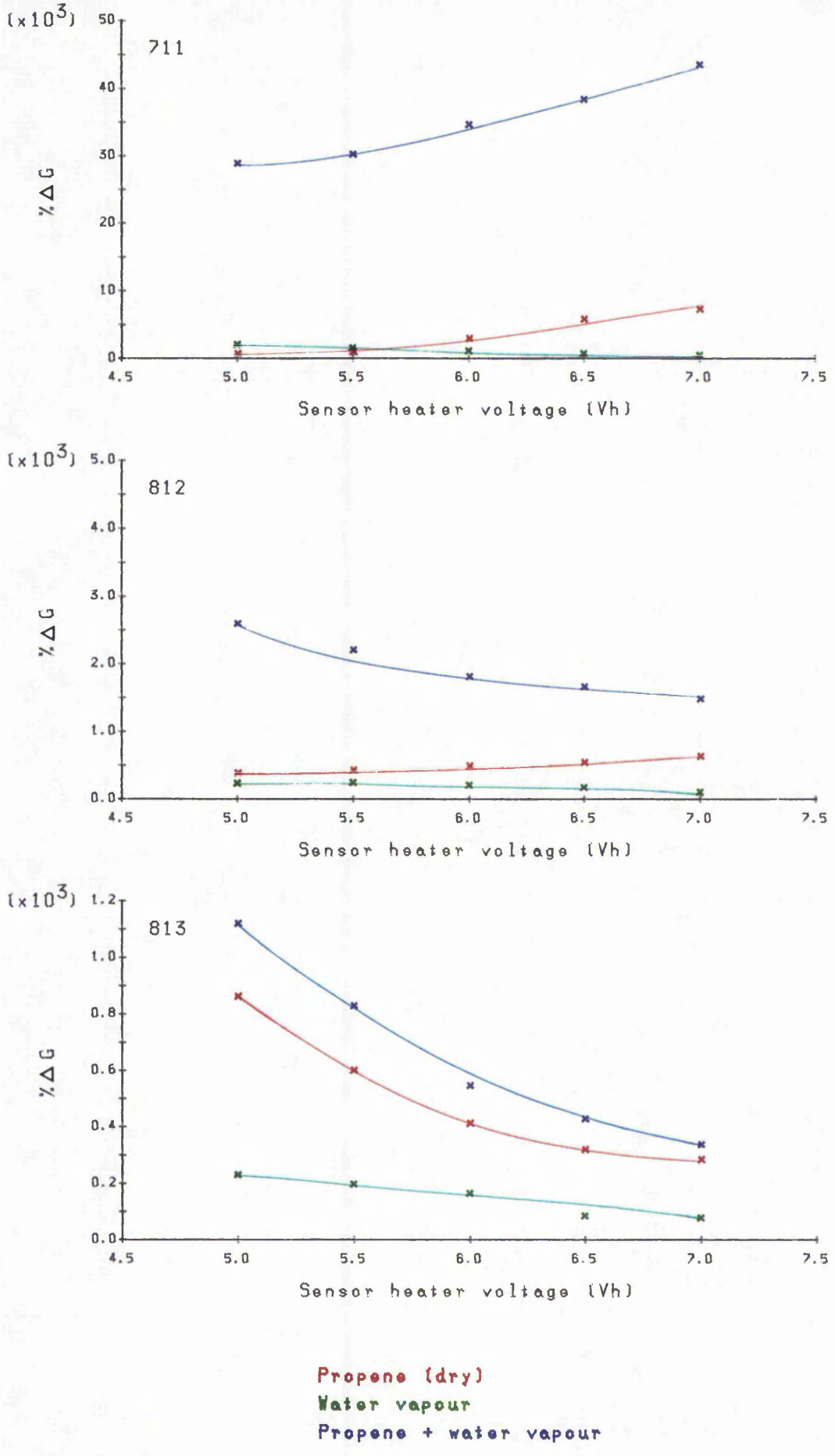

Figure 84. Variation in sensor sensitivity to propene as a function of heater voltage.

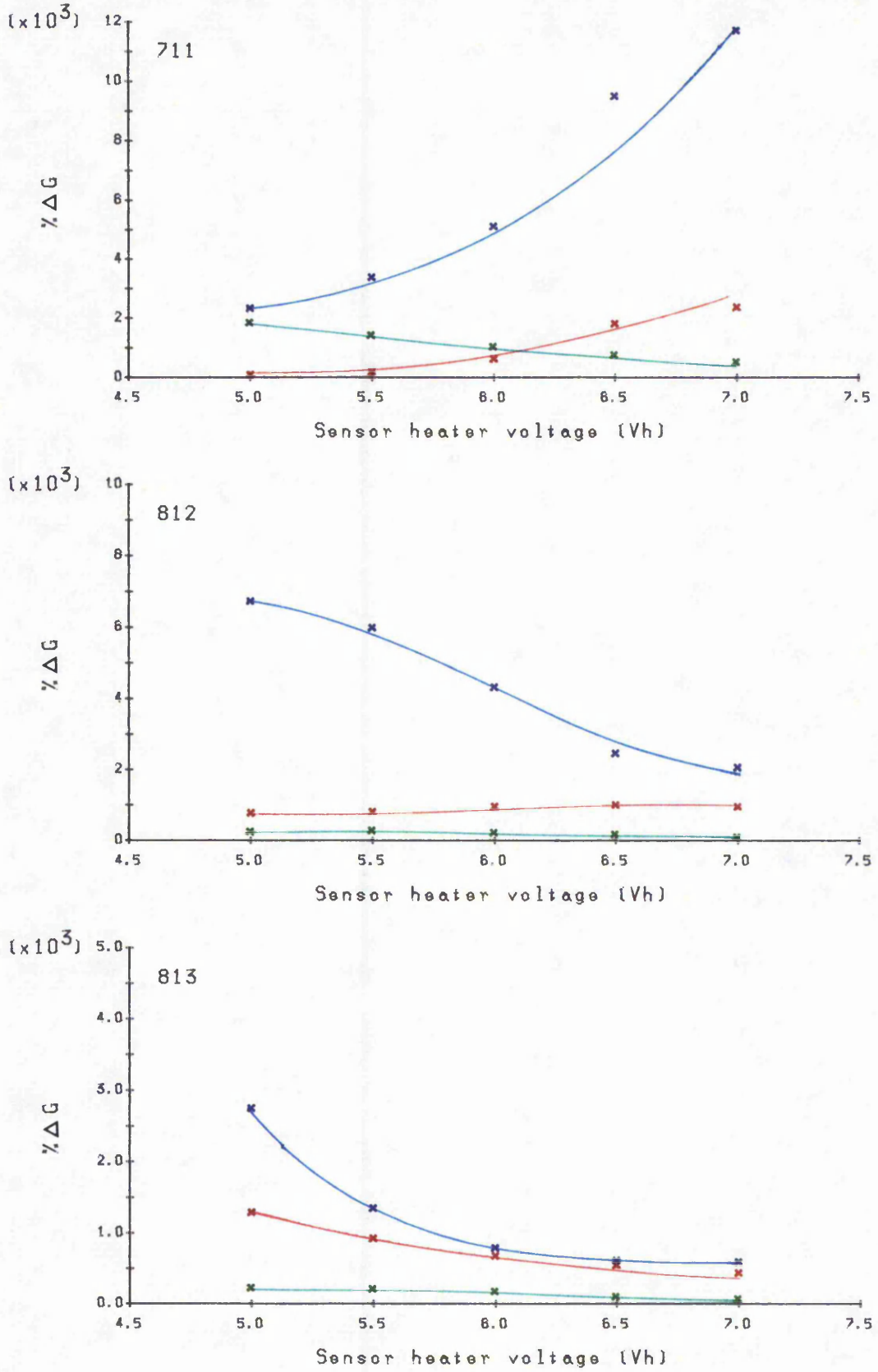

Figure 85. Variation in sensor sensitivity to benzene as a function of heater voltage.

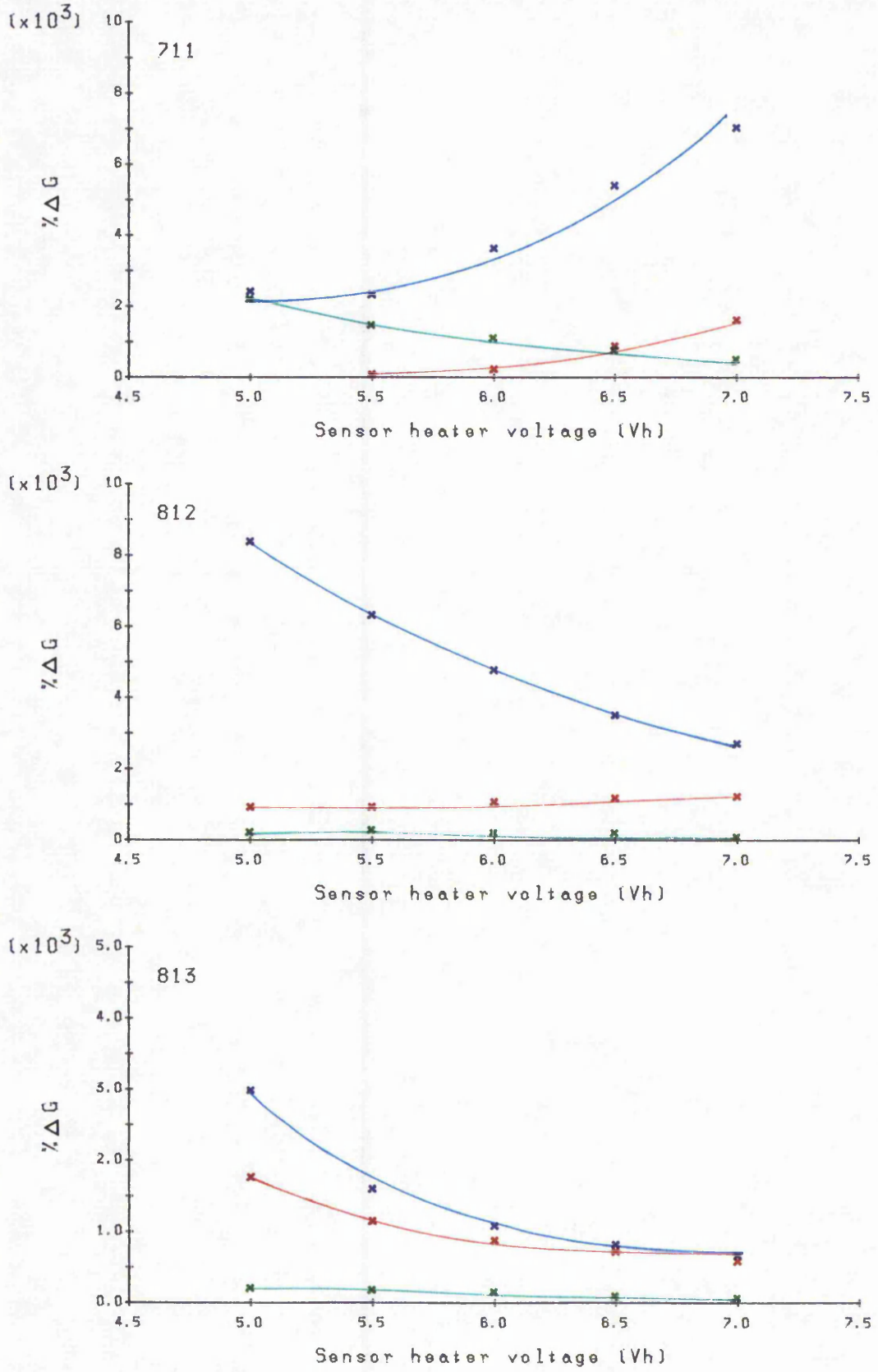

Figure 86. Variation in sensor sensitivity to toluene as a function of heater voltage.

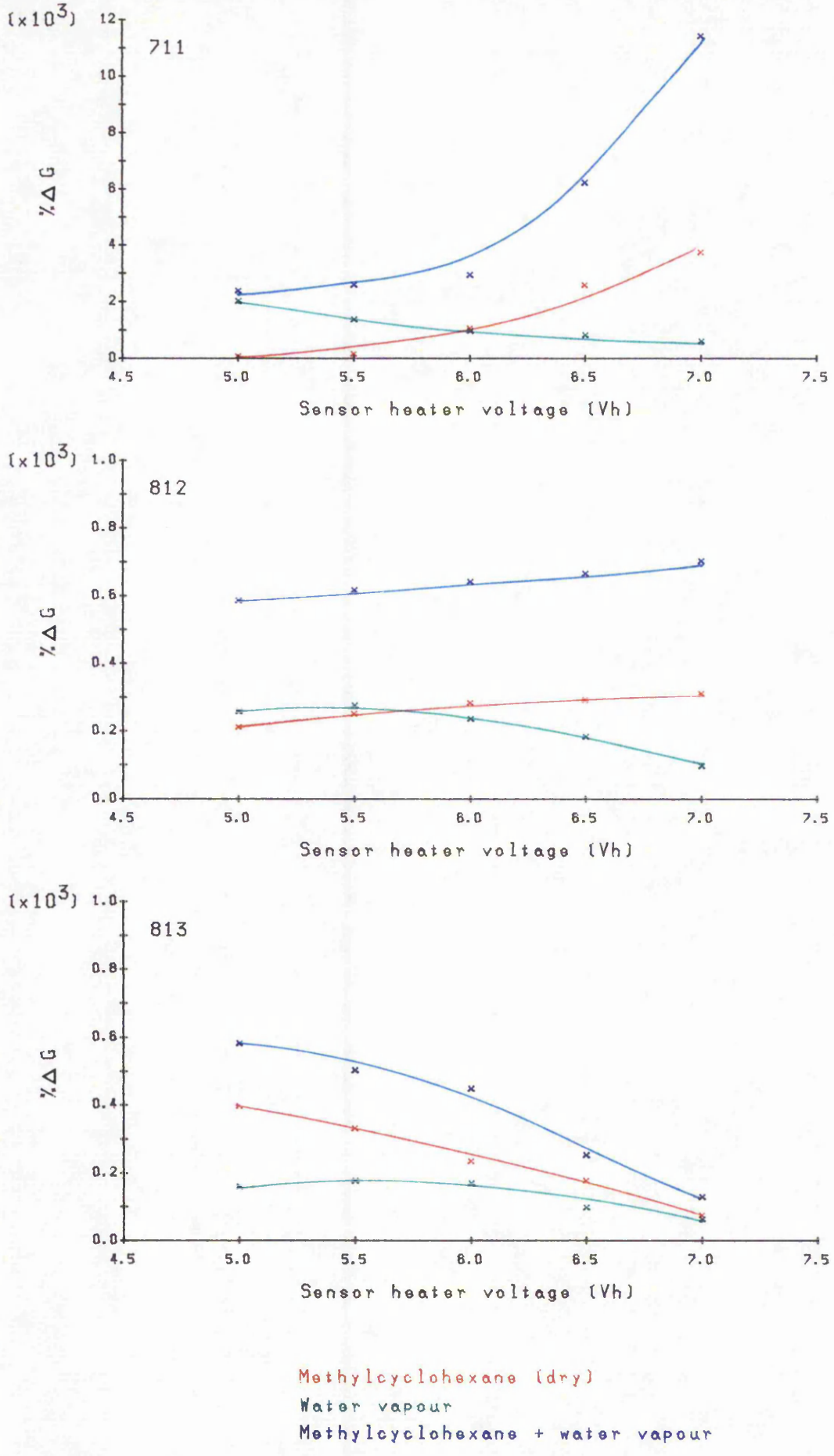

Figure 87. Variation in sensor sensitivity to methylcyclohexane as a function of heater voltage.

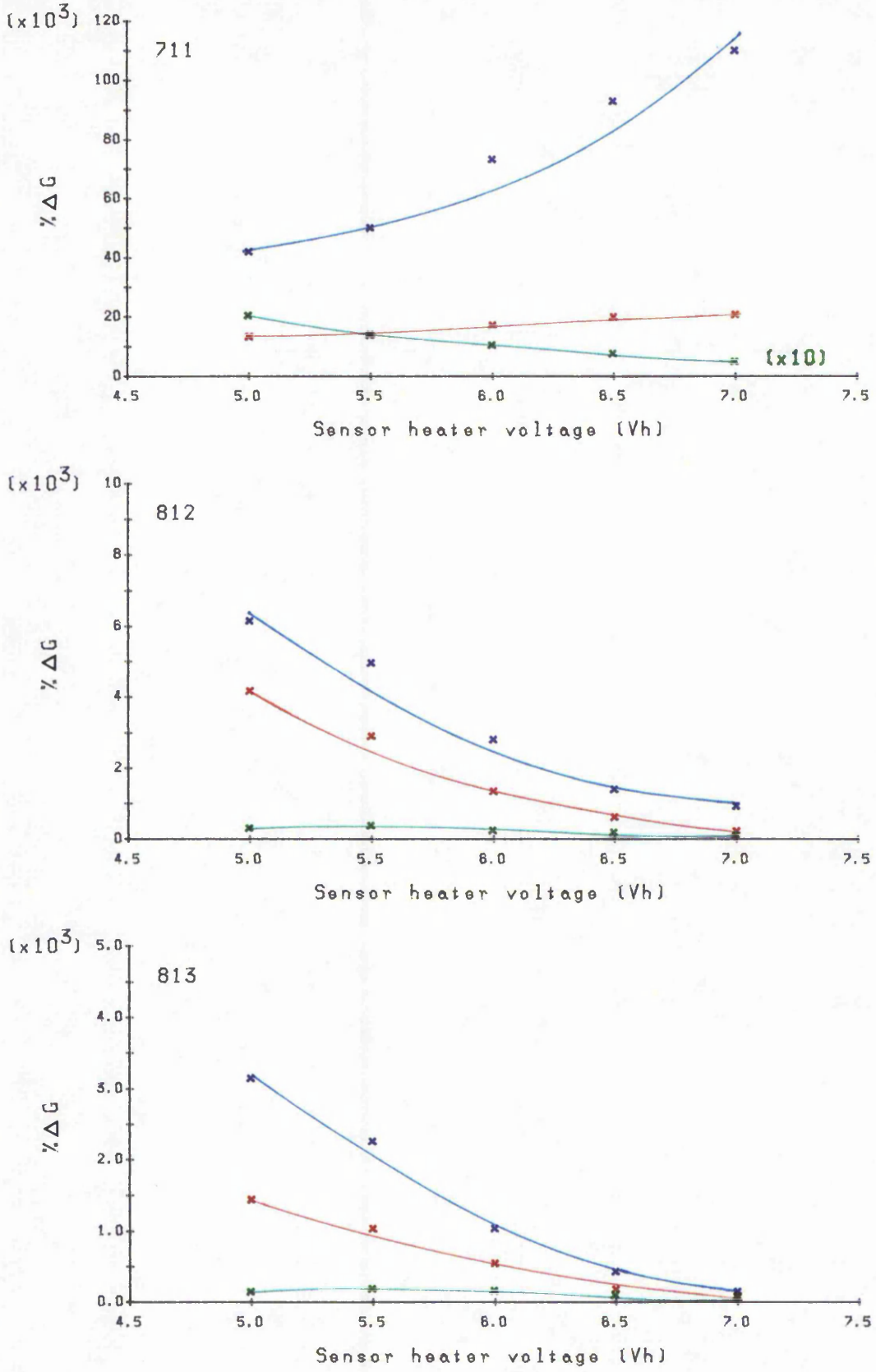

Figure 88. Variation in sensor sensitivity to carbonyl sulphide as a function of heater voltage.

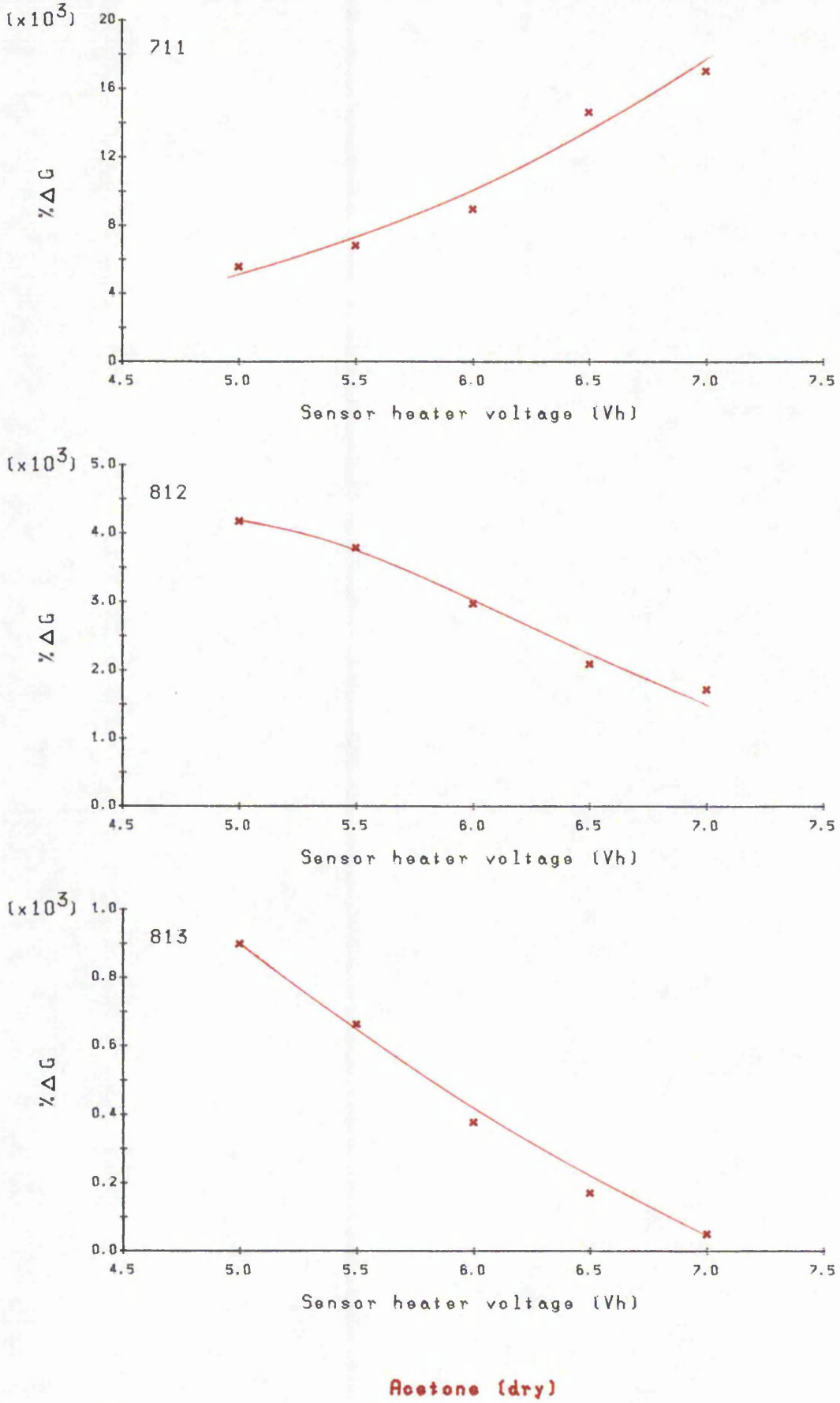

Figure 89. Variation in sensor sensitivity to acetone as a function of heater voltage.

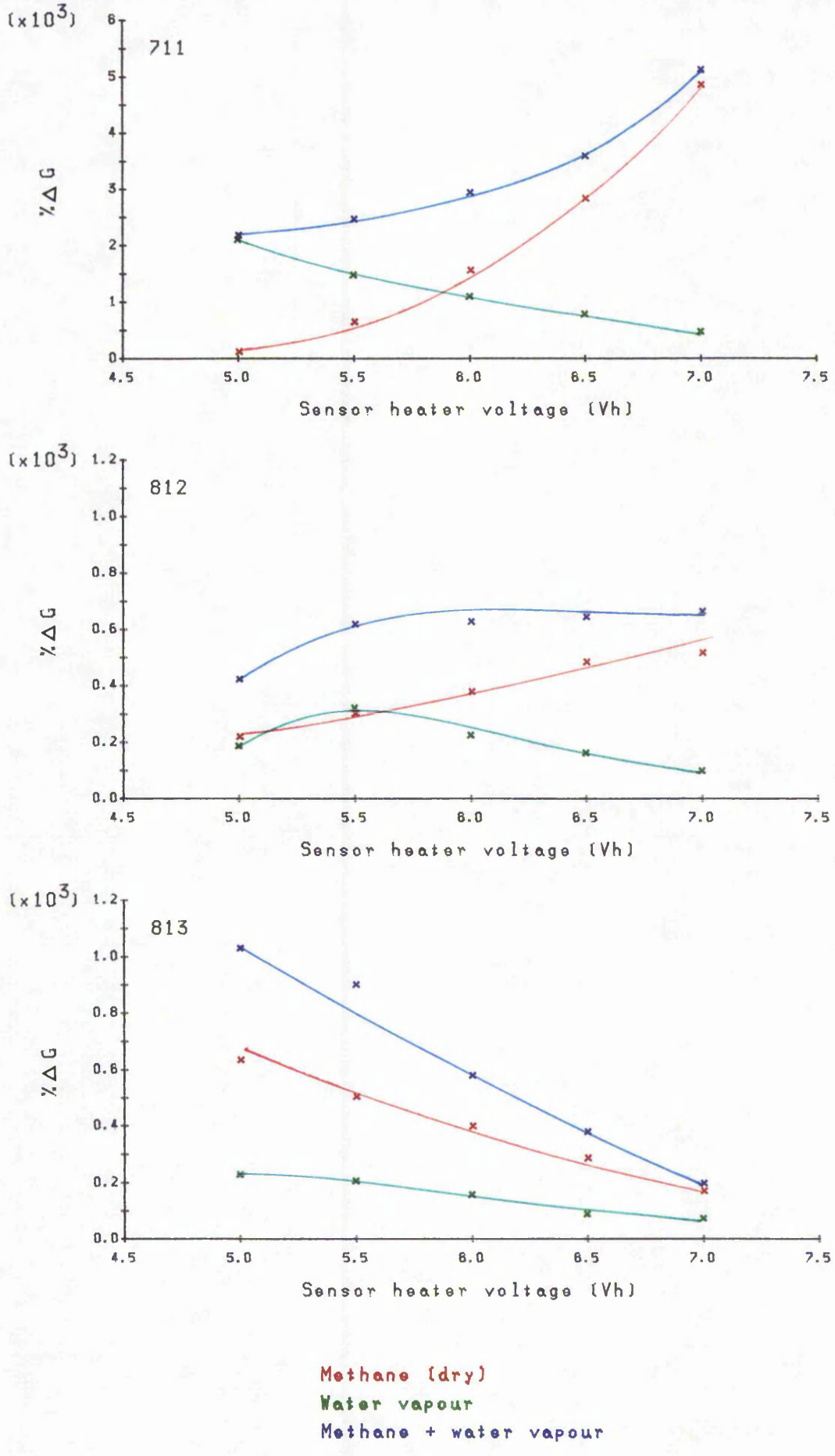

Figure 90. Variation in sensor sensitivity to methane as a function of heater voltage.

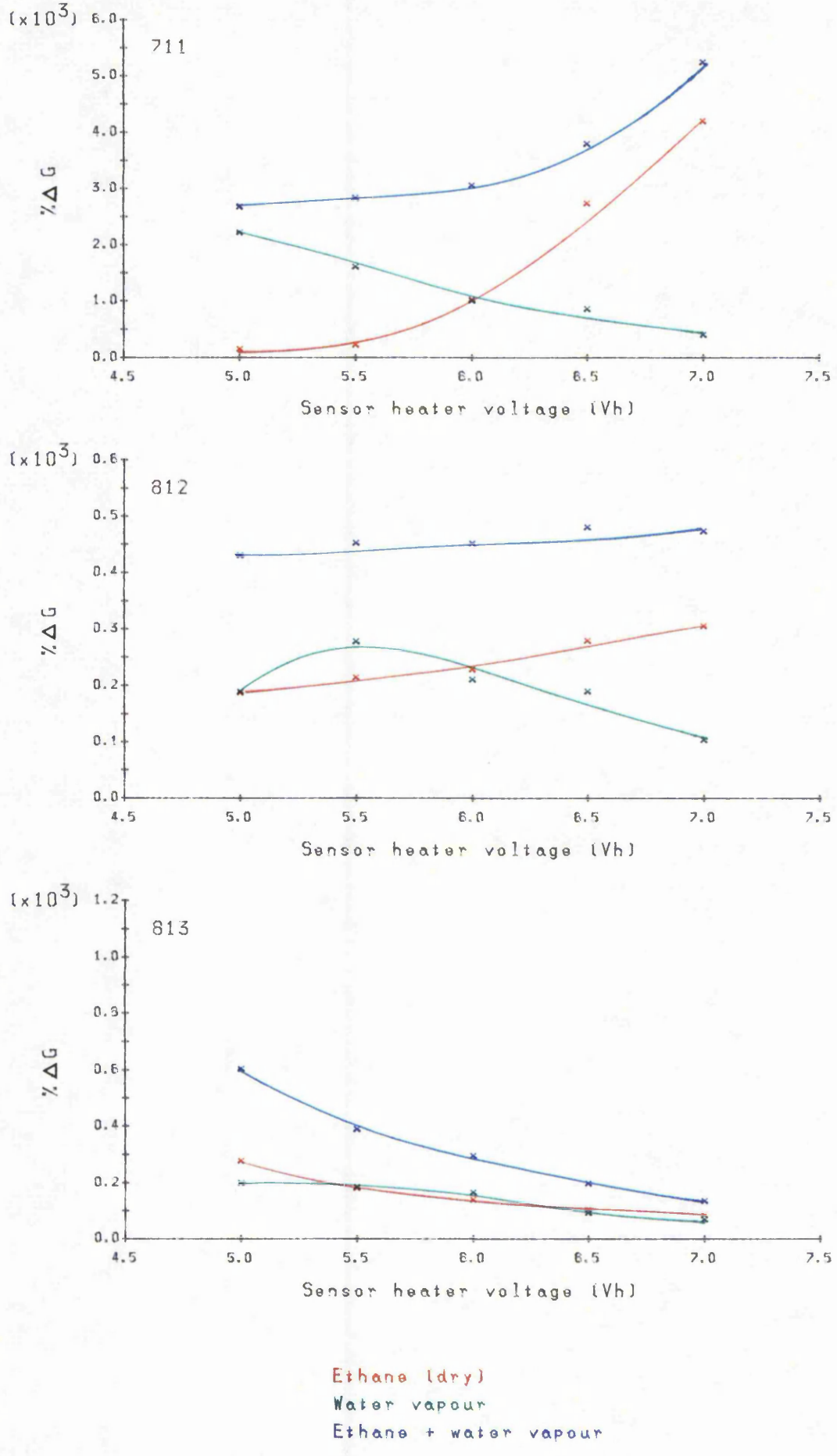

Figure 91. Variation in sensor sensitivity to ethane as a function of heater voltage.

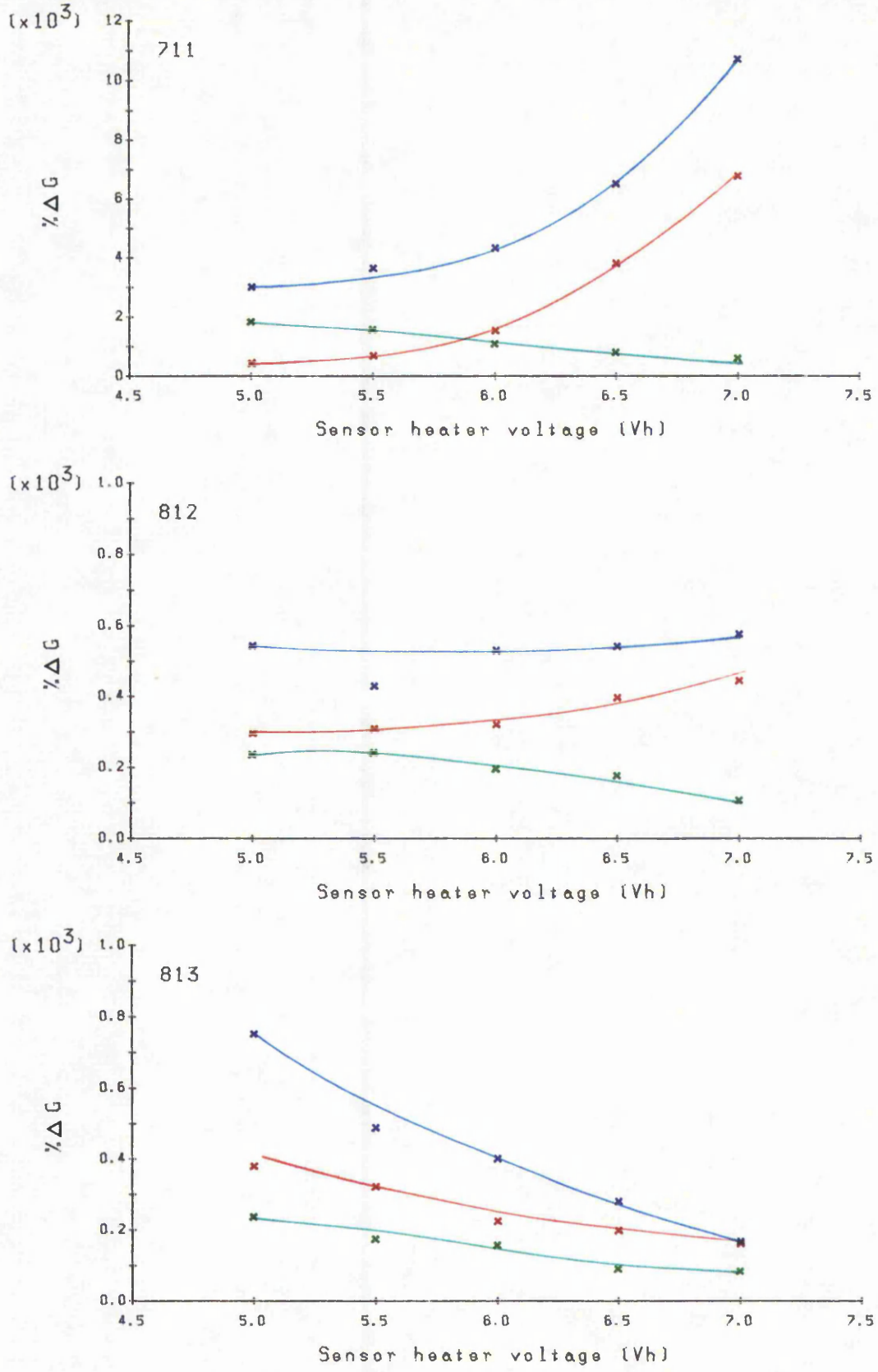

Figure 92. Variation in sensor sensitivity to propane as a function of heater voltage.

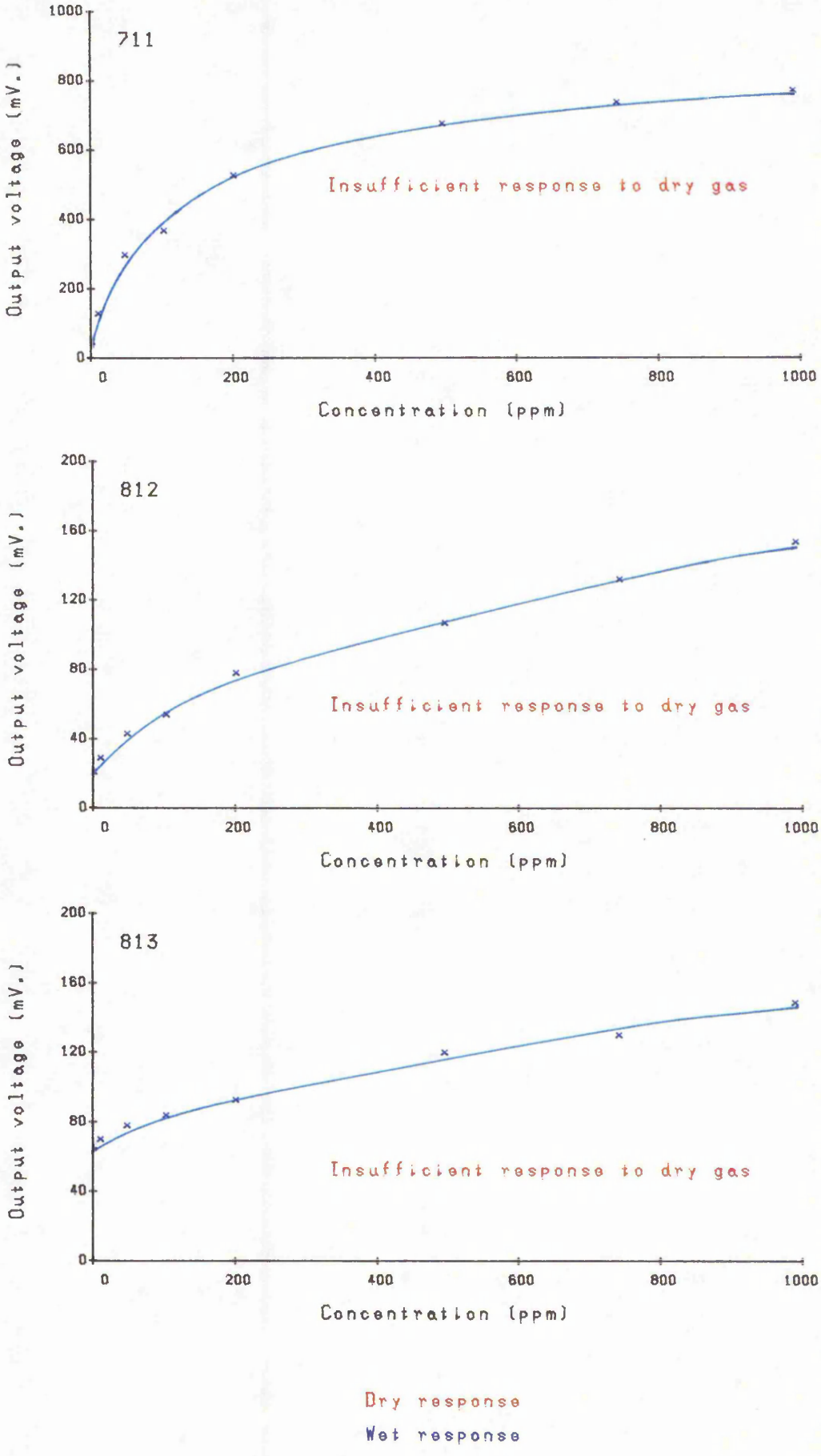

Figure 93. Variation in output voltage as a function of carbon monoxide concentration at 5.0V heater voltage.

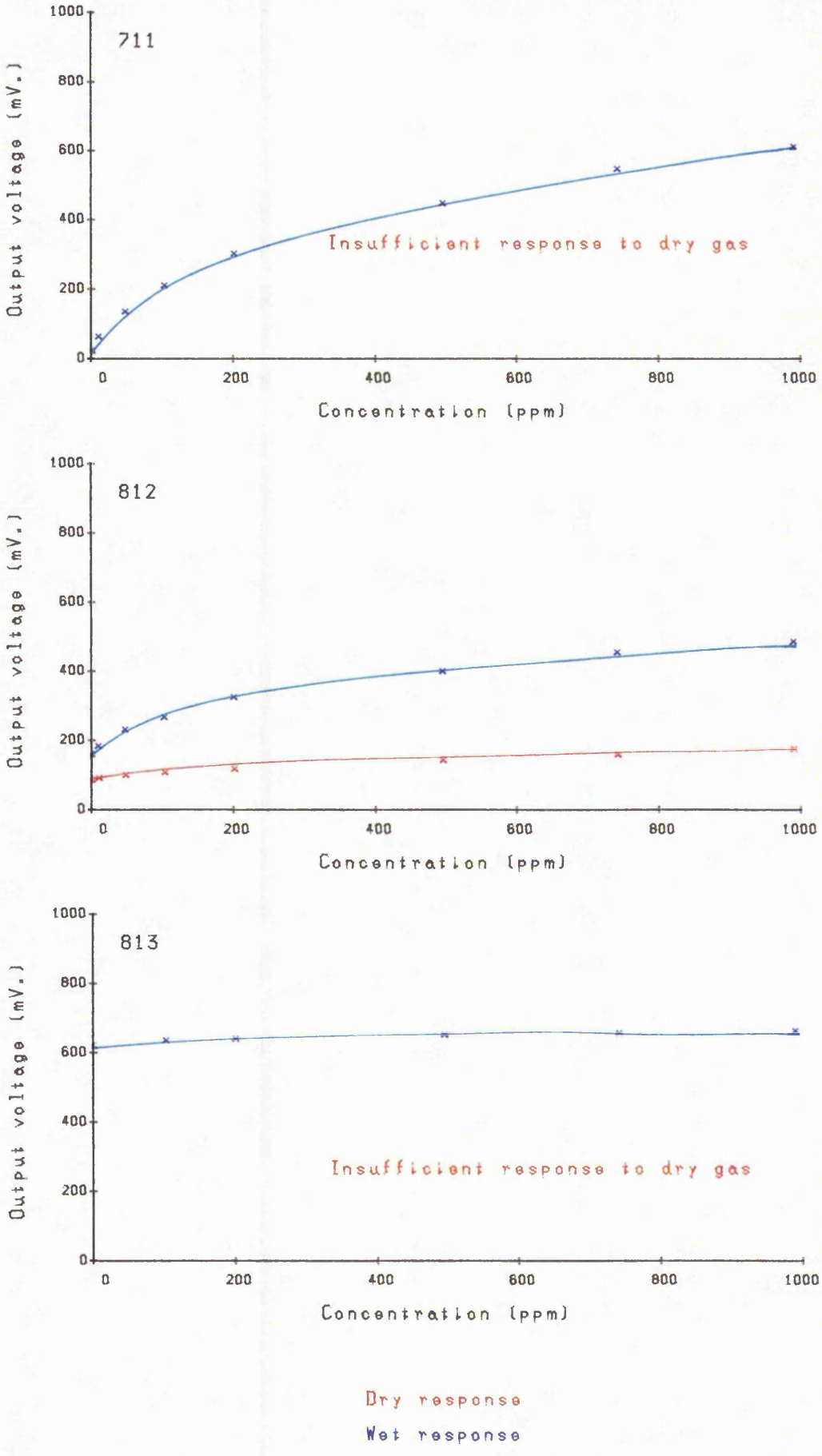

Figure 94. Variation in output voltage as a function of carbon monoxide concentration at 7.0V heater voltage.

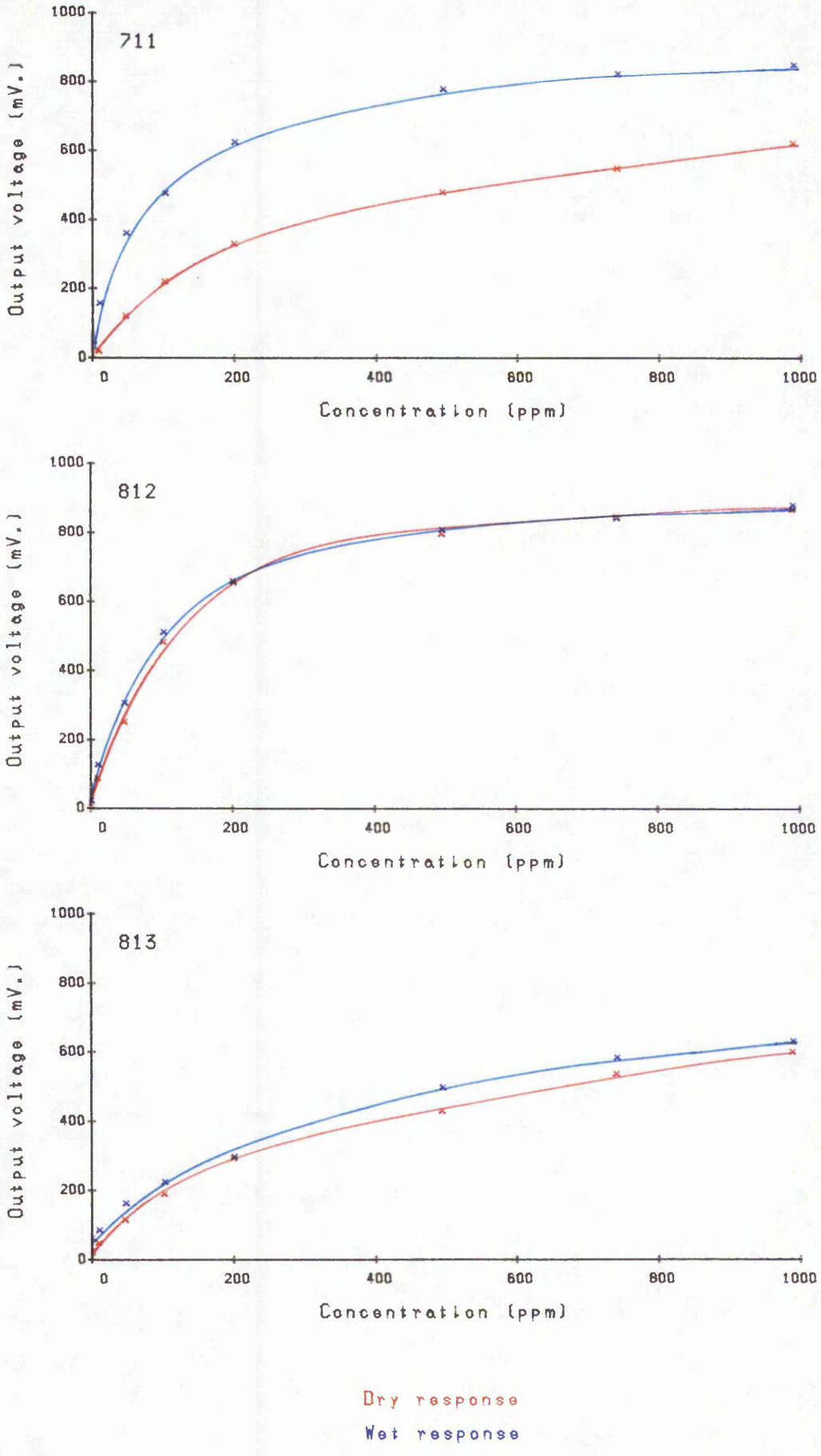

Figure 95. Variation in output voltage as a function of hydrogen concentration at 5.0V heater voltage.

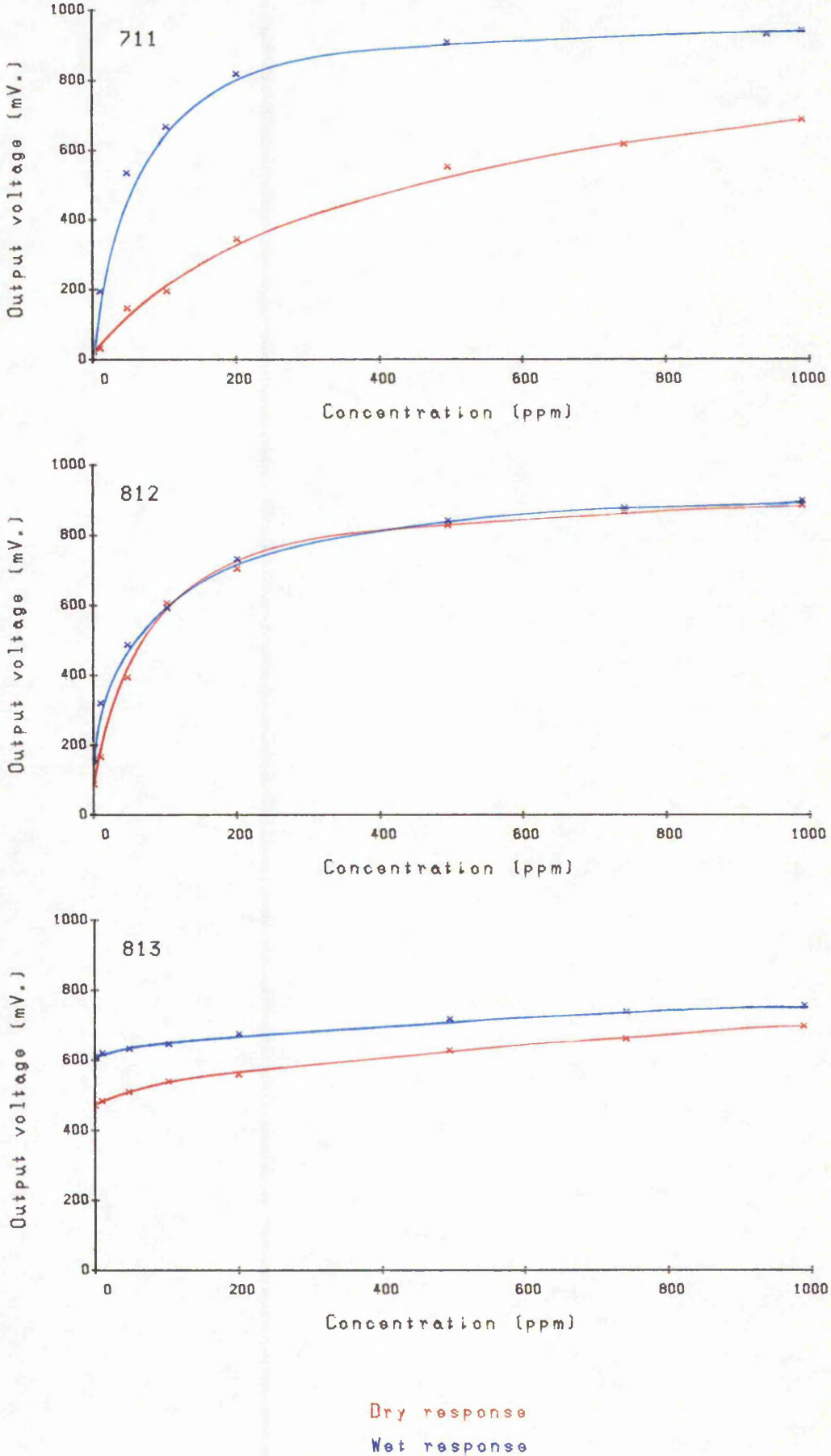

Figure 96. Variation in output voltage as a function of hydrogen concentration at 7.0V heater voltage.

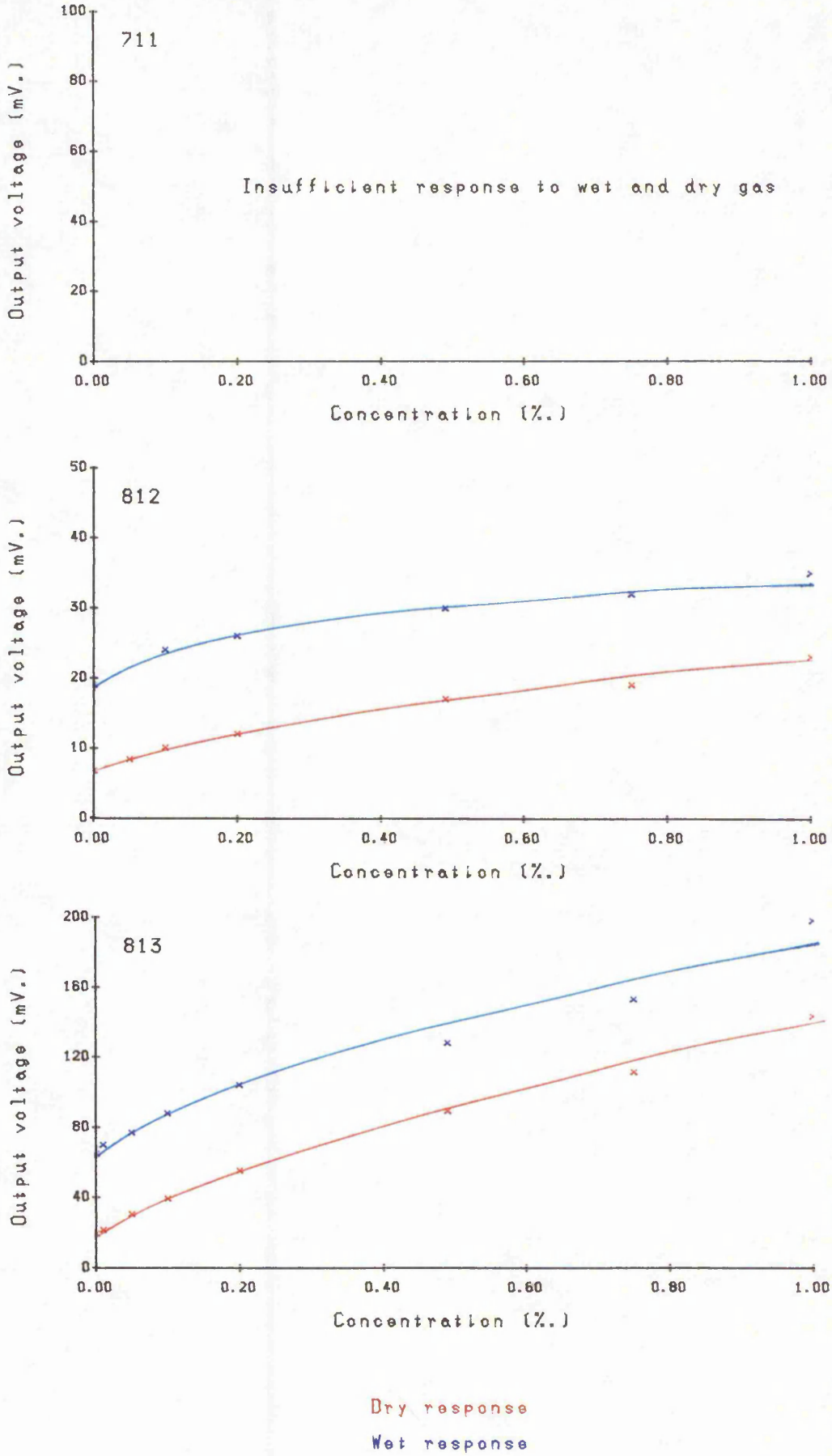

Figure 97. Variation in output voltage as a function of methane concentration at 5.0V heater voltage.

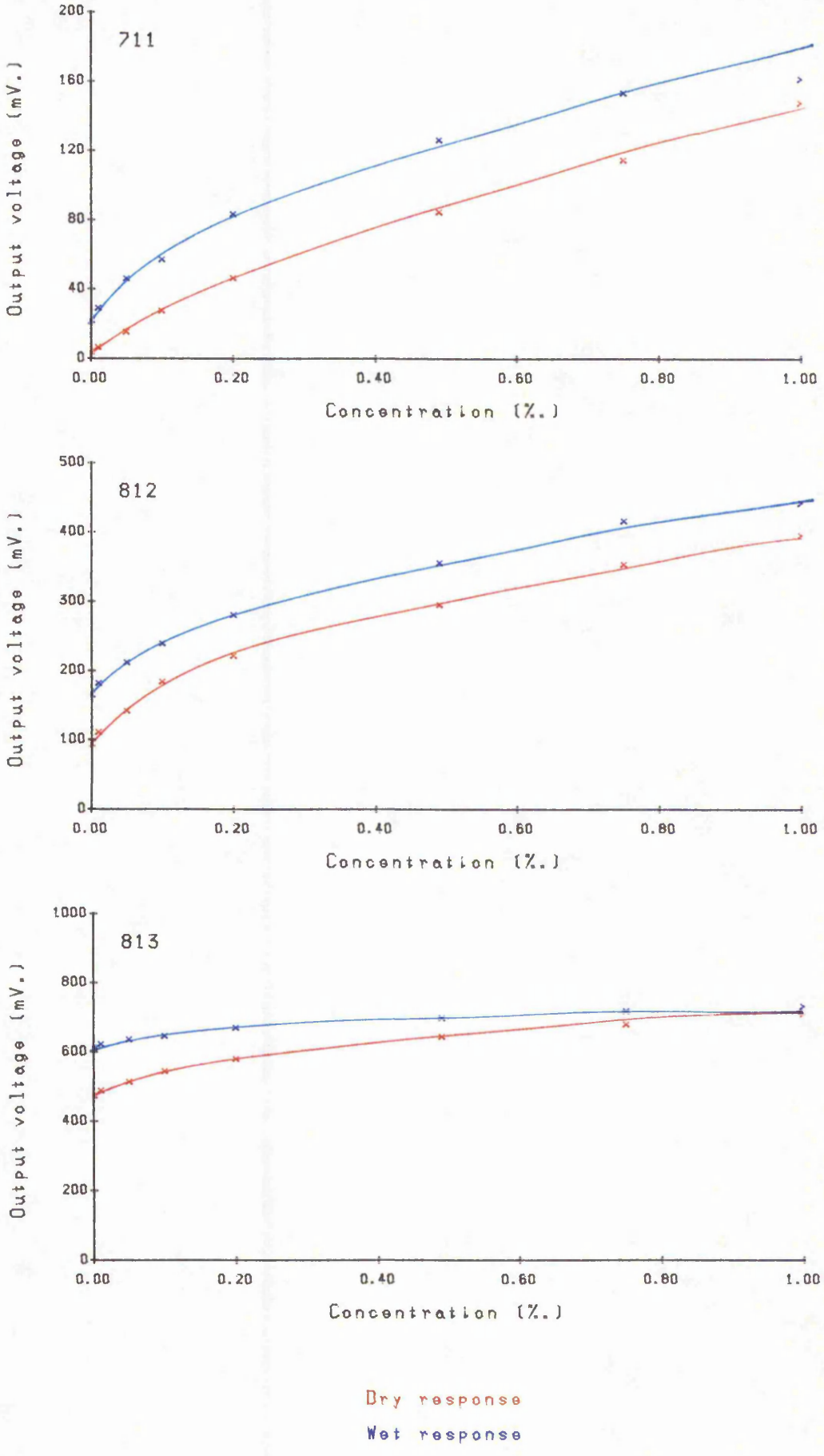

Figure 98. Variation in output voltage as a function of methane concentration at 7.0V heater voltage.

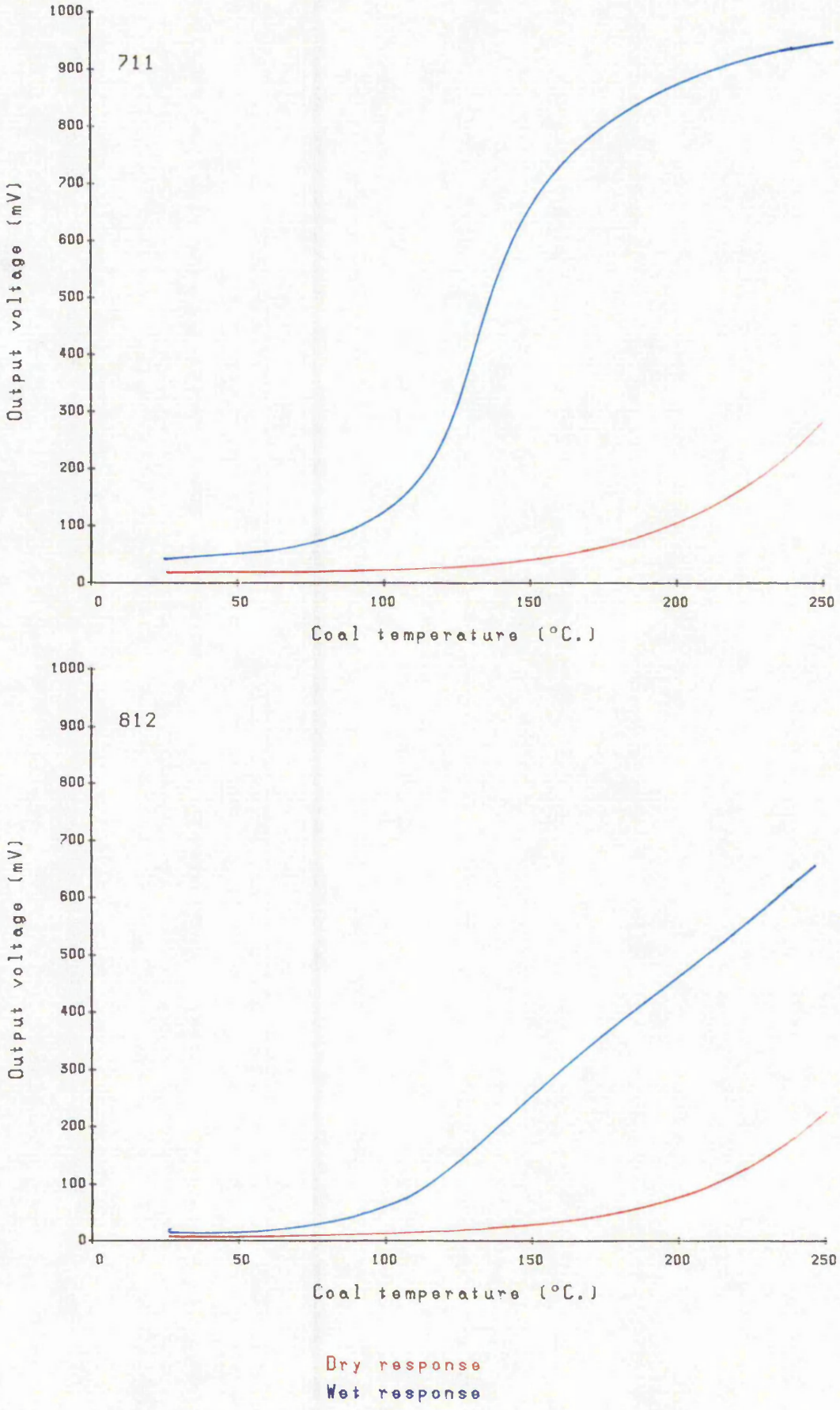

Figure 99. Total sensor responses at 5.0V heater voltage as a function of temperature for coal heated in air.

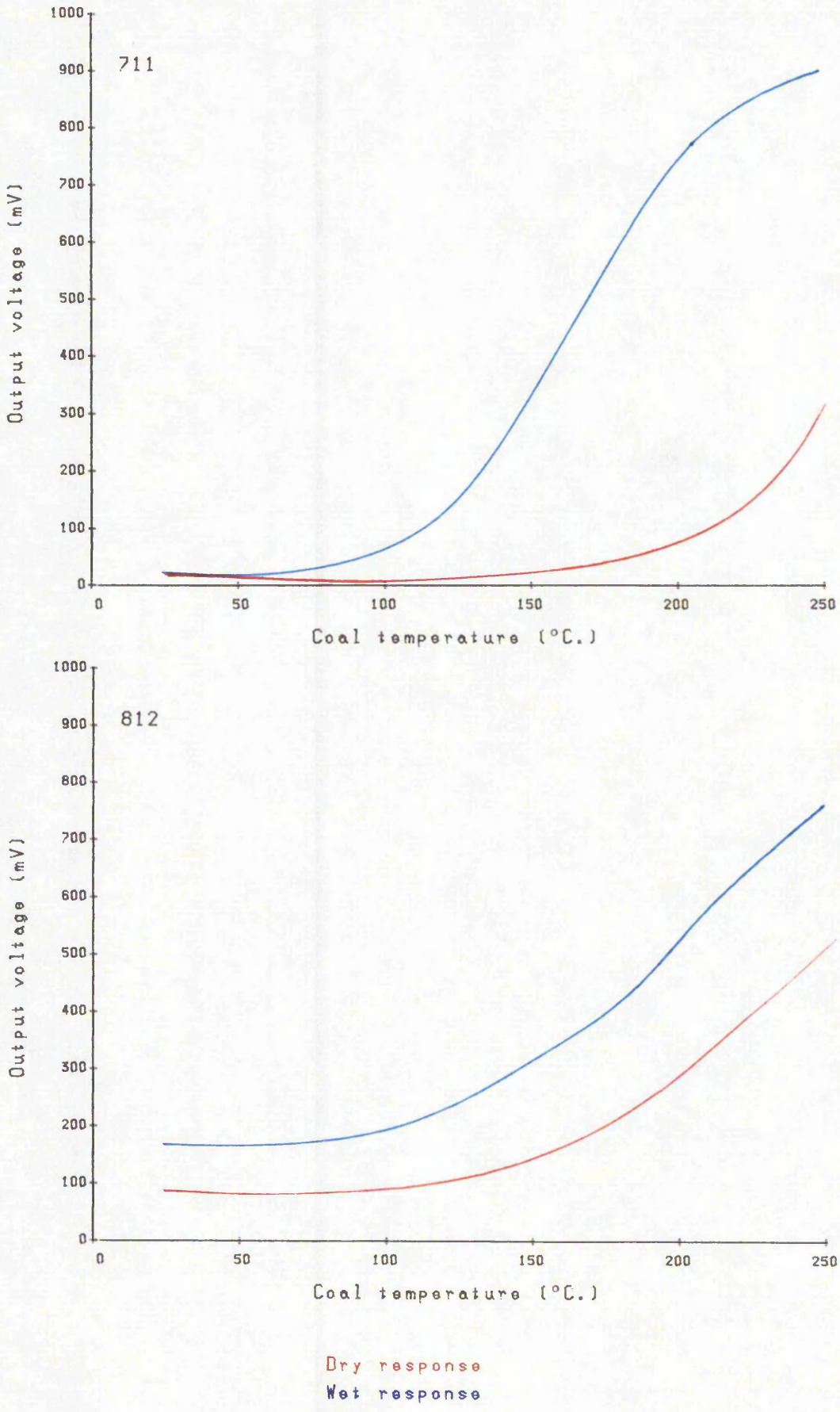

Figure 100. Total sensor responses at 7.0V heater voltage as a function of temperature for coal heated in air.

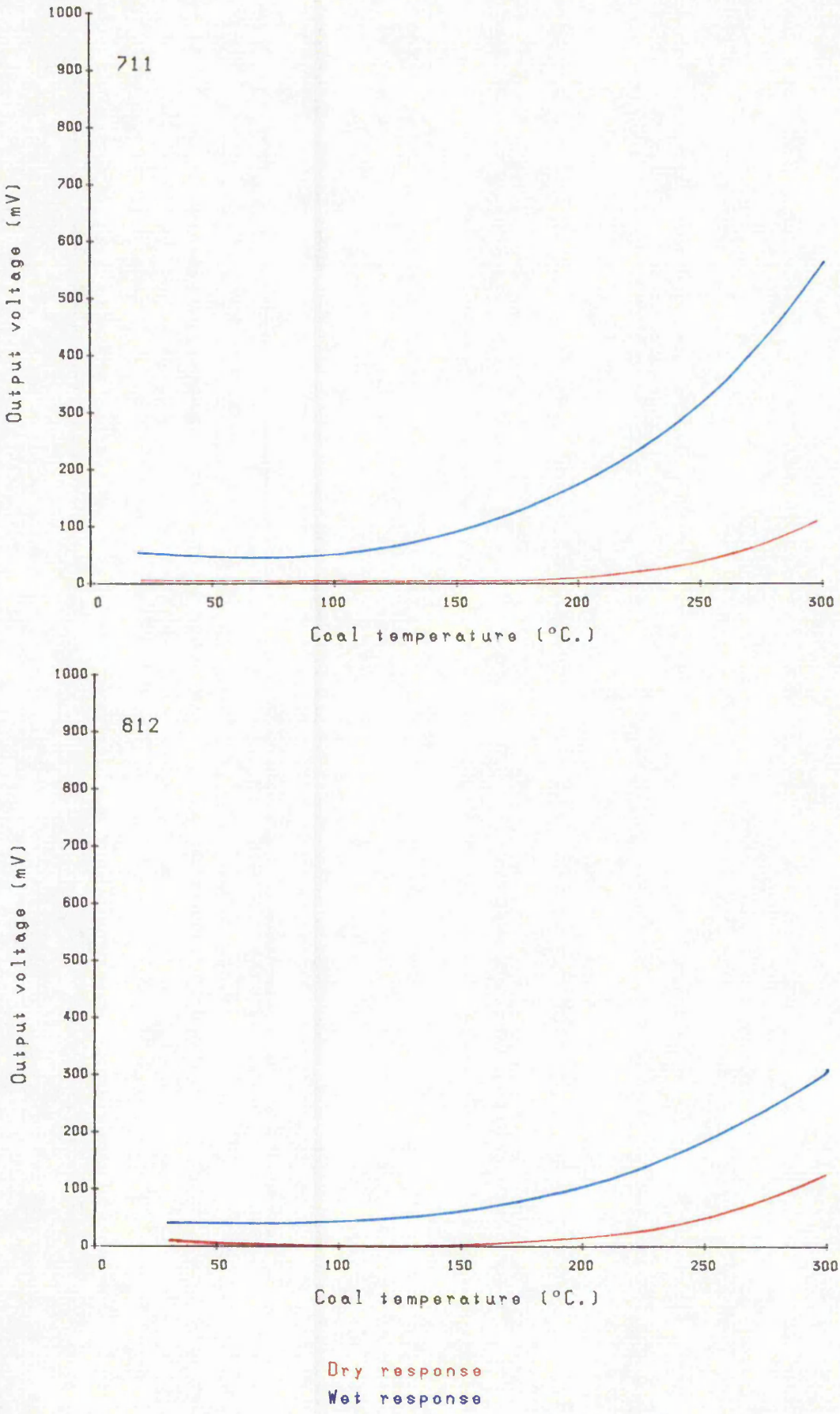

Figure 101. Total sensor responses at 5.0V heater voltage as a function of temperature for coal heated in nitrogen.

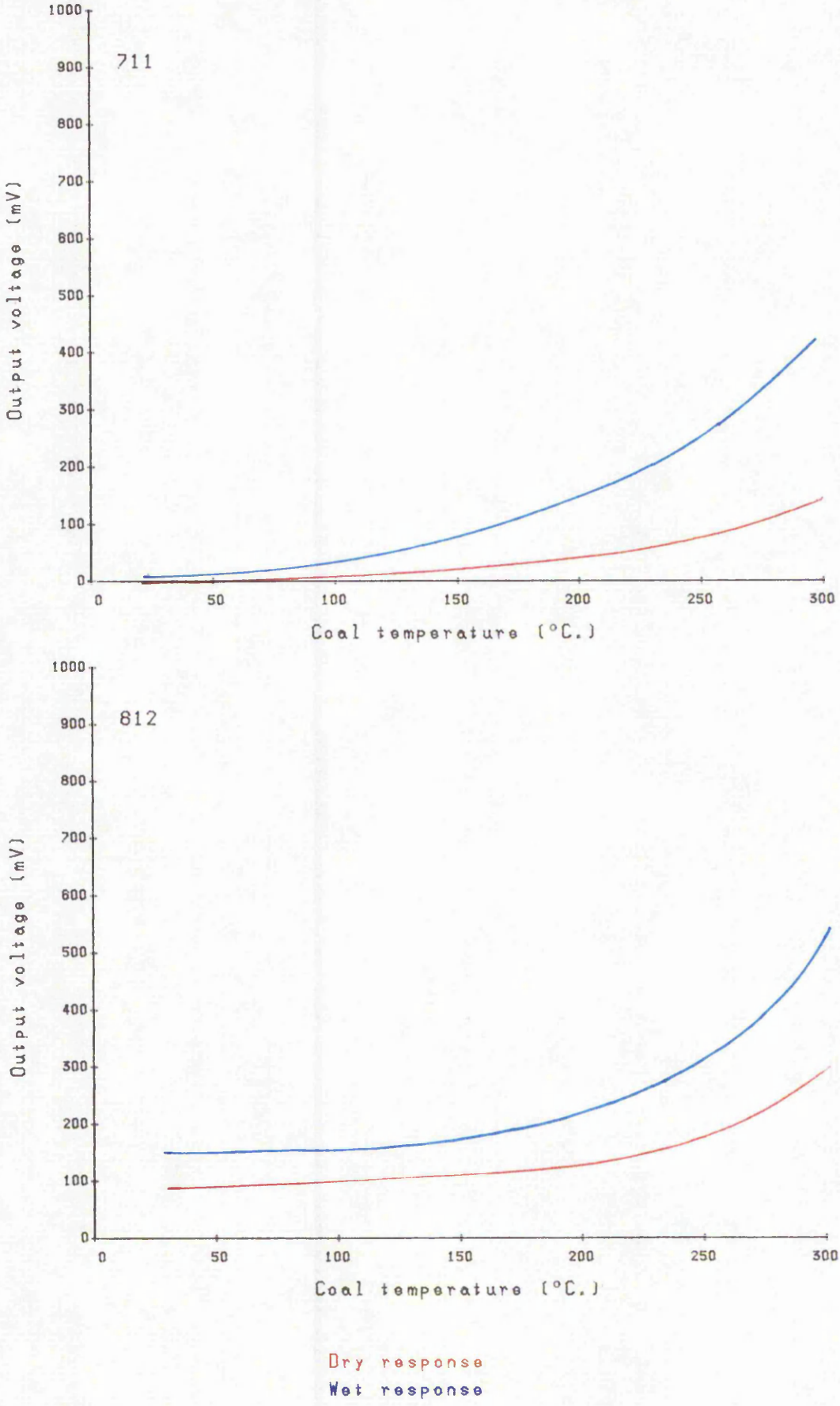

Figure 102. Total sensor responses at 7.0V heater voltage as a function of temperature for coal heated in nitrogen.

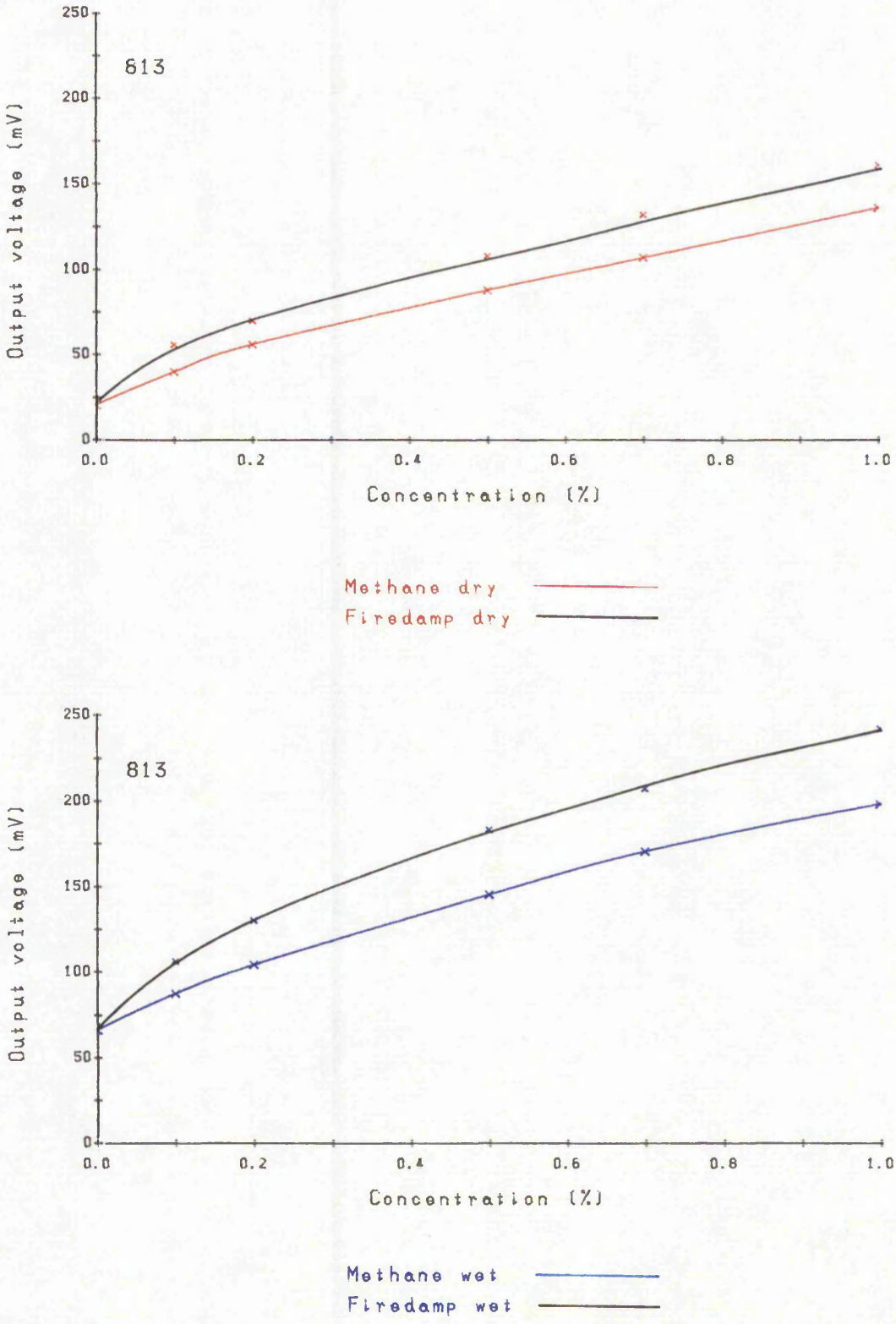

Figure 103. Variation in voltage appearing across series load resistor versus concentration at a sensor heater voltage of 5.0V

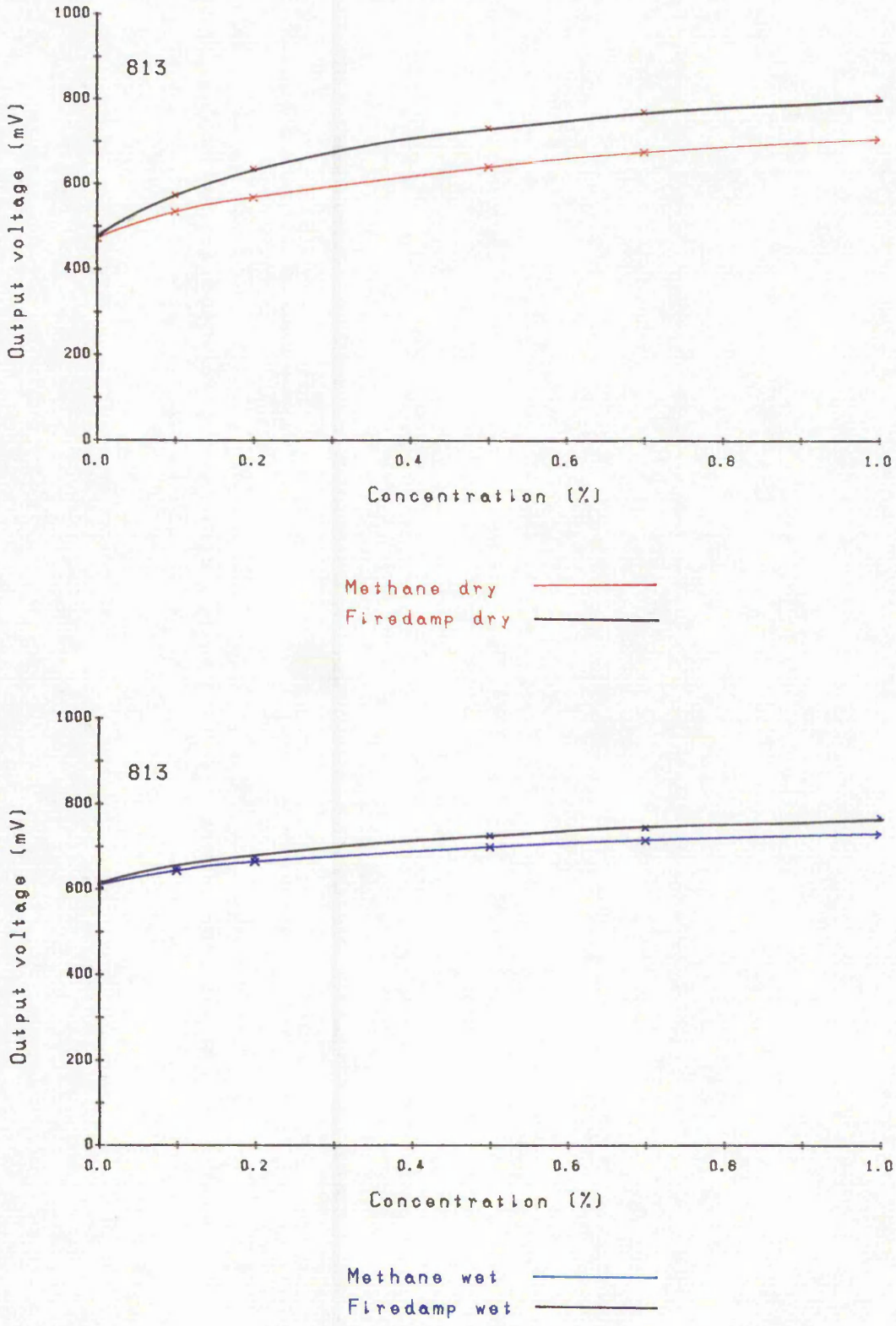

Figure 104. Variation in voltage appearing across series load resistor versus concentration at a sensor heater voltage of 7.0V

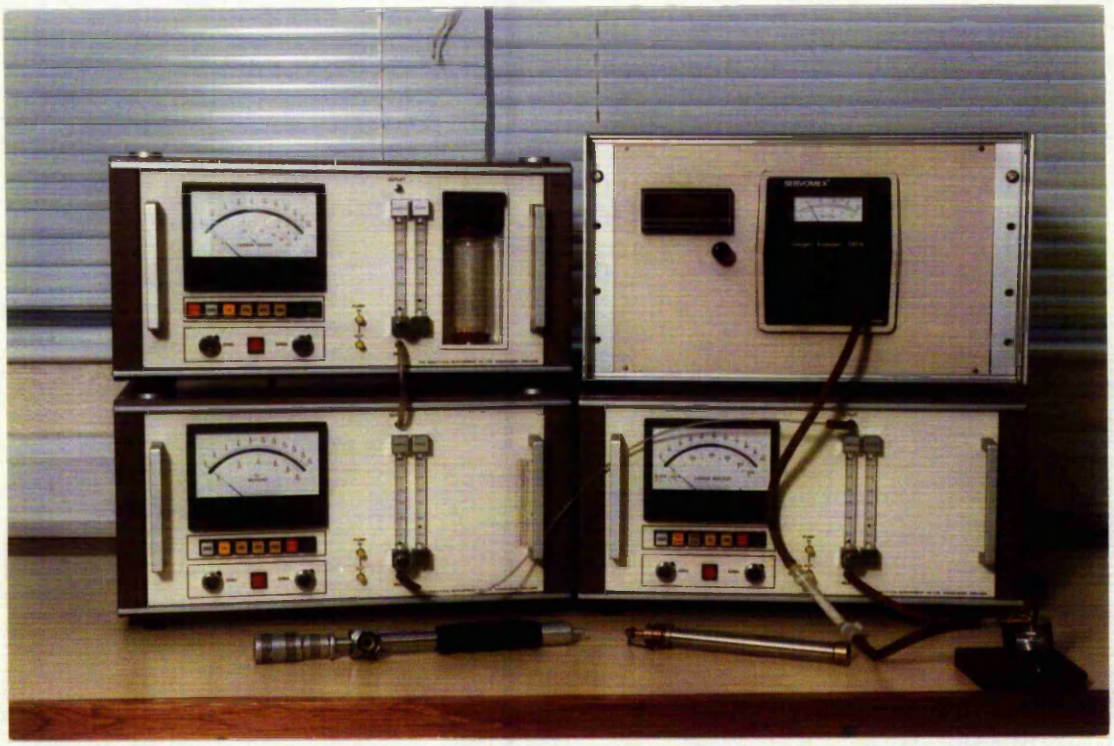

Top left	Infra-red carbon dioxide analyser
Top right	Paramagnetic oxygen analyser
Bottom right	Infra-red carbon monoxide analyser
Bottom left	Infra-red methane analyser
Foreground	Sampling equipment

Plate 1. View of instrument arrangement and sampling equipment

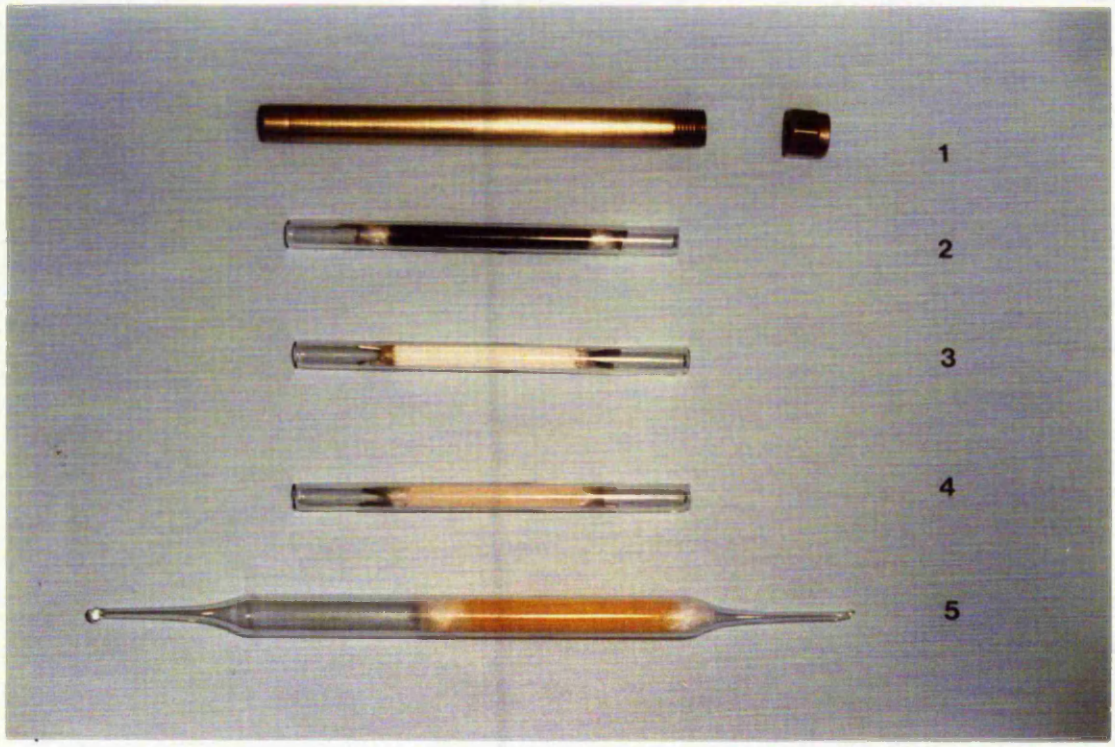

1. Sampling tube holder and cap
2. Charcoal packed sampling tube
3. Tenax packed sampling tube
4. Molecular sieve 5A packed sampling tube
5. 1% DNPH on silica gel packed sampling tube

Plate 2. View of the sampling tubes and holder developed for collection of the products evolved from heated coal.

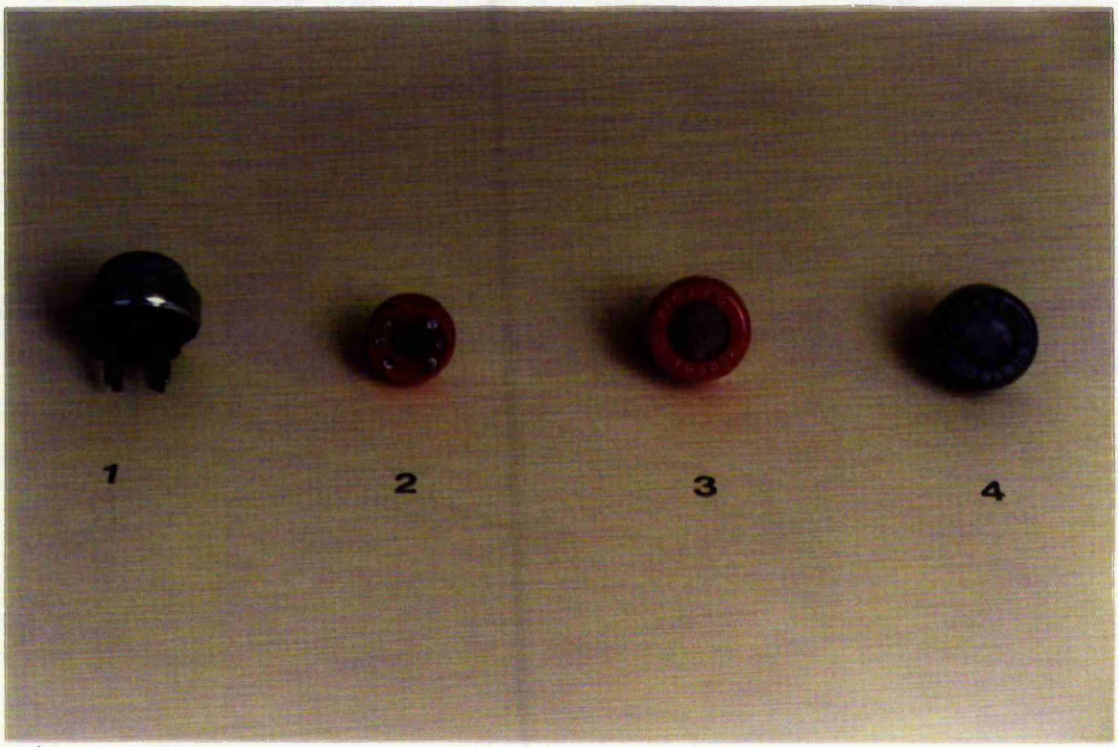

1. TGS 711
2. TGS 812 with top cover removed
3. TGS 812
4. TGS 813

Plate 3. View of the Taguchi Gas Sensors

Table 13 Chromatographic Materials and Operating Conditions

Chromatographic packing material	Column parameters	Carrier gas flow rate ml min^{-1}
Alumina F.1 80-100 B.S. mesh	2m x 3mm o.d. stainless steel column. Temperature, isothermal at 100°C	5-20
Porapak Q 80-100 B.S. mesh	2m x 3mm o.d. stainless steel column. Temperature, isothermal at 30°C	15.0
40% sodium iodide modified Alumina F.1 80-100 B.S. mesh	2m x 3mm o.d. stainless steel column. Temperature, isothermal at 50,60 and 70°C	5-20

Table 14 Chromatographic Materials and Operating Conditions

Chromatographic packing material	Column parameters	Carrier gas flow rate ml min^{-1}
10% 1,2,3 tris(2 cyanoethoxy) propane TCEP on 100-120 B.S. mesh Chromosorb P.AW.	3m x 3mm o.d. stainless steel column. Temperature, isothermal at 80°C	5-40
Tenax GC 80-100 B.S. mesh	1m x 3mm o.d. stainless steel column. Temperature, isothermal at 150°C	15

Table 15 Chromatographic Materials and Operating Conditions

Chromatographic packing material	Column parameters	Carrier gas flow rate ml min^{-1}
Tenax GC 80-100 B.S. mesh	1m x 3mm o.d. PTFE column. Temperature, isothermal at 40°C	15
Porapak QS 80-100 B.S. mesh	45cm x 3mm o.d. PTFE column packed to a length of 30cm. 1. Temperature isothermal at 40°C 2. Temperature isothermal at 100°C	2-20

Table 16 Melting points of 2,4-Dinitrophenylhydrazine derivatives

DNPH Derivative	Melting point °C	
	As determined	Quoted *
Formaldehyde	165	166
Acetaldehyde	168	168
Propionaldehyde	154.5	155
Acrolein	164	165
Crotonaldehyde	190	190
Acetone	127	128

* Taken from Handbook of Physics and Chemistry CRC press 1973/74

Table 17 Manufacturers instrument specification

Gas	Ranges	Accuracy	Cross sensitivity
Carbon dioxide	0-0.2% 0-10.0% 0-20.0% 0-100%	±2.0% off full scale deflection over the whole scale	10% carbon monoxide = 20 ppm 2% water vapour = negligible 100% methane = negligible
Carbon monoxide	0-100 ppm 100-1000 ppm 0-1.0% 1.0-10%	as above	100% carbon dioxide = 75 ppm 2% water vapour = 2 ppm 20% methane = 2ppm
Methane	0-0.2% 0-10.0% 0-20.0% 0-100%	as above	100% carbon dioxide = negligible 2% water vapour = 220 ppm 10% carbon monoxide = 30 ppm
Oxygen	0-10.0% 0-25.0% 0-100%	±1.0% of full scale deflection over the whole scale	Only common gases having comparable paramagnetic susceptibility are nitric oxide and nitrogen dioxide

Table 18 Percentage component recovery from Niosh activated charcoal at different heater block temperatures

Component	Heater block temperature °C			
	250	300	350	400
	%	%	%	%
Ethane	80.8	86.0	92.7	95.9
Ethene	89.1	90.8	94.7	97.7
Propane	91.3	93.3	94.0	96.9
Propene	90.9	91.7	95.2	97.8
Methylpropane	87.0	94.1	96.3	96.8
N-butane	85.2	91.5	95.5	97.1
But-1-ene	85.1	90.0	93.8	97.4
2-Methylbutane	82.6	90.4	95.6	96.9
N-pentane	77.3	85.8	96.0	97.7
2-Methylpentane	76.3	83.5	94.8	95.3
N-hexane	74.6	85.1	94.1	95.8
Hex-1-ene	77.1*	83.4	87.6	96.1
Methylcyclohexane	77.8*	83.4	94.0	97.0
N-heptane	71.5*	81.0*	96.6	97.0
Benzene	72.8	80.5*	95.3	103.1

* Denotes peak broadening on analysis

Table 19 Percentage component recovery from Porapak Q at different heater block temperatures

Component	Heater block temperature °C			
	150	200	250	300
	%	%	%	%
Ethane	36.6	35.7	36.5	33.4
Ethene	34.0	33.8	35.1	31.6
Propane	82.3	84.4	83.7	85.3
Propene	81.1	89.9	86.8	88.4
Methylpropane	79.0	87.6	97.6	98.1
N-butane	78.9	87.0	98.0	95.3
But-1-ene	78.6	86.0	97.3	96.5
2-Methylbutane	78.1	83.5	97.6	96.8
N-pentane	78.0	84.7	98.2	97.0
2-Methylpentane	70.7*	84.0	95.8	96.7
N-hexane	67.3*	85.0	96.7	94.8
Hex-1-ene	60.2*	83.2*	96.1	95.1
Methylcyclohexane	58.5*	82.3*	97.8	96.2
N-heptane	56.2*	81.3*	96.9	95.0
Benzene	53.8*	80.7*	95.2	94.9

* Denotes peak broadening on analysis

Table 20 Percentage component recovery from activated charcoal type 208 C at different heater block temperatures

Component	Heater block temperature °C			
	250	300	350	400
	%	%	%	%
Ethane	84.1	88.7	93.6	96.8
Ethene	90.4	93.7	94.9	97.2
Propane	92.0	94.0	95.1	98.1
Propene	91.3	92.9	94.9	97.2
Methylpropane	86.8	94.5	95.8	97.0
N-butane	87.2	94.6	97.4	97.8
But-1-ene	85.0	95.1	96.9	97.3
2-Methylbutane	83.7	91.2	96.2	96.5
N-pentane	79.9	86.9	98.8	99.6
2-Methylpentane	78.8	86.8	96.9	95.8
N-hexane	74.5	85.7	97.2	97.0
Hex-1-ene	76.8*	79.7	87.8	95.0
Methylcyclohexane	79.0*	84.9	95.2	96.8
N-heptane	73.0*	84.3	98.4	98.1
Benzene	76.3*	84.0	97.1	102.3

* Denotes peak broadening on analysis

Table 21 The effect of sample volume on the safe sampling volume of Porapak Q

Component	Sample volume ml						
	50	100	150	200	300	400	500
	%	%	%	%	%	%	%
Ethane	65.8	34.3	30.2	28.6	27.8	23.6	22.0
Ethene	60.2	31.1	28.6	26.3	24.6	21.1	20.1
Propane	98.0	86.3	87.0	83.4	82.1	82.3	79.2
Propene	97.2	85.8	84.2	81.2	80.2	78.8	77.4
Methylpropane	97.6	98.6	97.1	96.8	90.7	89.6	82.1
N-butane	96.9	98.3	95.7	97.1	93.6	91.8	90.9
But-1-ene	97.8	96.2	98.0	95.4	96.3	94.7	93.4
2-Methylbutane	96.3	96.6	97.8	96.8	95.7	98.0	97.2
N-pentane	97.7	97.0	97.3	96.3	98.2	95.7	96.9
2-Methylpentane	96.8	97.3	98.1	95.9	97.6	98.0	97.3
N-hexane	97.1	96.3	97.4	98.0	97.7	97.2	95.8
Hex-1-ene	97.0	97.7	95.7	96.7	99.3	97.4	96.3
Methylcyclohexane	98.1	96.3	97.7	98.0	96.6	99.1	95.6
N-heptane	97.5	96.8	97.4	95.8	96.7	98.2	98.1
Benzene	97.0	97.8	98.3	96.3	95.2	97.8	96.8

All figures are expressed in terms of percentage sample recovery

Table 22 The effect of sample volume on the safe sampling volume of Niosh activated charcoal

Component	Sample volume ml						
	50	100	150	200	300	400	500
	%	%	%	%	%	%	%
Ethane	98.0	97.2	97.0	90.0	87.8	85.2	83.8
Ethene	98.1	97.0	95.1	83.7	81.3	77.4	76.2
Propane	97.1	96.4	97.2	96.8	95.6	98.0	96.8
Propene	95.2	97.7	96.8	98.1	95.8	97.3	95.4
Methylpropane	96.7	95.6	97.0	94.2	97.3	96.9	96.0
N-butane	95.6	97.4	95.8	93.6	98.0	97.7	96.4
But-1-ene	95.0	98.2	98.1	97.4	95.8	96.0	95.8
2-Methylbutane	96.3	95.8	97.8	95.6	96.2	95.3	96.1
N-pentane	97.4	95.6	96.7	97.0	96.8	98.0	97.0
2-Methylpentane	96.2	97.8	98.0	96.9	97.3	96.3	96.7
N-hexane	95.9	95.2	97.4	94.8	96.6	99.1	96.3
Hex-1-ene	97.7	97.4	95.6	94.4	96.0	95.9	95.9
Methylcyclohexane	96.8	95.2	97.1	96.1	97.1	96.0	96.2
N-heptane	97.0	97.8	95.2	94.2	96.4	95.8	95.6
Benzene	96.5	97.1	95.5	95.3	97.8	97.1	97.4

All figures are expressed in terms of percentage sample recovery

Table 23 The effect of sample volume on the safe sampling volume of activated charcoal type 208C

Component	Sample volume ml						
	50	100	150	200	300	400	500
	%	%	%	%	%	%	%
Ethane	97.9	98.0	98.0	92.2	90.2	87.3	84.6
Ethene	97.7	97.8	97.3	86.6	82.6	78.8	76.3
Propane	96.3	95.0	98.9	97.9	95.9	98.3	97.3
Propene	97.4	96.1	97.3	98.4	96.2	97.2	98.1
Methylpropane	97.9	95.7	96.7	95.4	97.0	96.5	97.9
N-butane	96.0	97.3	97.0	95.3	97.1	96.7	97.3
But-1-ene	97.1	96.4	95.2	97.4	98.6	96.1	97.9
2-Methylbutane	96.3	97.8	97.1	96.7	97.0	96.9	98.0
N-pentane	98.3	98.0	97.1	99.6	98.1	97.4	98.3
2-Methylpentane	95.9	96.4	96.8	97.4	98.0	96.5	97.1
N-hexane	97.4	97.3	96.7	97.0	98.2	97.8	98.1
Hex-1-ene	94.2	97.1	95.7	97.2	95.3	96.0	95.3
Methylcyclohexane	96.0	95.3	95.7	97.3	98.1	97.3	96.9
N-heptane	95.6	96.3	97.4	95.7	96.2	93.9	97.5
Benzene	97.5	98.5	96.6	95.3	98.0	95.9	97.3

All figures are expressed in terms of percentage component recovery

Table 24 Reproducibility of Sampling Tube Preparation

Component	Sampling Tube Number										Mean Recovery	Relative Standard Deviation
	1	2	3	4	5	6	7	8	9	10		
	%	%	%	%	%	%	%	%	%	%	%	%
Ethane	91.3	98.8	92.4	97.6	95.3	90.4	92.7	97.3	93.9	95.0	94.5	2.99
Ethene	92.4	99.4	93.6	98.6	97.3	96.0	95.7	97.8	97.1	94.3	96.2	2.34
Propane	102.3	96.4	97.3	93.8	95.7	97.0	95.8	98.4	95.4	99.1	96.9	2.49
Propene	97.4	97.6	91.2	93.6	95.4	91.8	96.6	97.1	94.8	95.0	95.0	2.40
Methylpropane	93.6	98.9	91.2	97.5	98.3	95.1	92.9	94.6	93.8	97.9	95.7	2.51
N-butane	99.6	95.6	92.3	94.3	95.6	96.0	94.4	97.3	93.2	97.5	95.6	2.27
2 methylbutane	99.3	91.4	93.2	98.4	95.8	96.4	94.9	97.0	95.1	96.7	95.7	2.57
N-pentane	97.4	98.6	91.2	94.3	98.1	93.6	91.9	98.8	96.4	97.0	95.8	2.74
2 methylpentane	99.7	95.3	94.1	93.0	98.4	95.8	96.1	93.8	98.1	92.3	95.7	2.57
N-hexane	92.6	98.6	97.4	93.1	92.8	97.1	96.6	97.4	95.3	97.0	95.8	2.30
1 hexane	91.0	97.8	98.8	93.7	92.1	94.6	95.3	91.4	92.3	94.1	94.1	2.78
Methylcyclohexane	91.4	94.8	92.4	96.6	97.8	97.4	92.3	96.1	93.2	94.4	94.6	2.41
N-heptane	97.4	92.3	98.4	97.1	97.2	95.3	98.4	92.8	96.4	98.1	96.3	2.29
Benzene	94.8	91.8	96.4	90.2	98.3	92.4	97.1	96.3	92.4	94.6	94.4	2.80

All figures expressed in terms of percentage component recovery

Table 25 Percentage recovery from Tenax GC at different heater block temperatures

Component	Heater block temperature °C			
	200	250	300	350
	%	%	%	%
Octane	97.3	93.4	98.2	90.4
Nonane	93.1*	97.4	104.3	103.6
Decane	92.7*	94.0*	99.2	98.6
Benzene	95.2	98.6	103.1	99.6
Toluene	93.6	102.4	96.5	98.0
Ethyl benzene	94.3	96.1	102.8	101.5
Meta-xylene	97.5	93.7	100.2	98.4
Ortho-xylene	93.4	96.9	95.6	102.4
1,3,5 Trimethylbenzene	92.5*	95.1*	98.7	105.3

* Denotes peak broadening on analysis

Table 26 The effect of sample volume on the safe sampling volume of Tenax GC

Component	Sample volume ml				
	500	1000	1500	2000	2500
	%	%	%	%	%
Octane	93.2	98.6	102.3	96.5	96.8
Nonane	96.3	100.6	92.3	97.8	102.3
Decane	94.3	101.1	97.3	94.7	97.3
Benzene	97.4	100.3	92.6	90.6	77.4
Toluene	98.6	95.9	103.2	100.6	97.6
Ethyl benzene	100.8	92.1	91.3	98.2	96.5
Meta xylene	93.3	95.8	101.7	94.6	104.3
Ortho xylene	103.6	96.5	95.4	94.9	98.3
1,3,5 Trimethylbenzene	91.6	99.4	97.6	95.1	100.8

All figures are expressed in terms of percentage sample recovery

Table 27 Reproducibility of Sampling Tube Preparation

Component	Sampling Tube Number										Mean Recovery	Relative Standard Deviation
	1	2	3	4	5	6	7	8	9	10		
	%	%	%	%	%	%	%	%	%	%	%	%
Octane	92.7	96.3	93.2	97.6	91.0	98.3	101.2	96.4	95.1	92.2	95.4	3.17
Nonane	103.2	93.6	93.1	92.7	94.3	100.8	97.2	93.4	99.2	96.1	96.6	3.50
Decane	95.4	101.8	96.4	99.8	93.7	97.6	92.6	95.7	92.5	96.1	96.2	2.98
Benzene	98.3	93.4	101.6	95.1	97.2	94.0	100.5	94.7	96.8	98.1	97.0	2.73
Toluene	97.4	94.2	95.2	99.2	93.8	98.6	91.9	98.6	99.0	97.3	96.6	2.55
Ethyl benzene	94.5	102.8	92.1	99.4	103.6	94.2	91.8	96.4	93.8	97.5	96.6	4.18
Meta-xylene	99.5	91.8	99.4	91.2	93.4	99.1	103.6	93.8	100.8	94.3	96.7	4.28
Ortho xylene	92.9	97.4	99.5	94.2	101.8	93.7	98.0	96.1	94.5	97.6	96.6	2.82
1,3,5 Trimethyl-benzene	100.9	92.6	101.3	98.2	99.1	92.3	97.7	96.1	98.3	94.7	97.1	3.15

All figures expressed in terms of percentage component recovery

Table 28 Repeatability of Direct Injections of Different Sulphur Gases

20 ppm Hydrogen sulphide		20 ppm Carbonyl sulphide		20 ppm Sulphur dioxide		20 ppm Carbon disulphide	
Retention time (secs)	Integrator counts (K)	Retention time (secs)	Integrator counts (K)	Retention time (secs)	Integrator counts (K)	Retention time (secs)	Integrator counts (K)
93	283	154	274	358	323	259	604
93	274	153	268	355	300	263	612
93	270	153	280	366	314	257	638
93	289	154	274	358	302	261	586
93	270	154	283	356	316	260	616
Mean	277		276		311		611
Relative Standard Deviation	3.06		2.12		3.13		3.09

Table 29 Percentage recovery of 1 ppm hydrogen sulphide at different heater block temperatures

Heater block temperature °C	Percentage recovery		
	Molecular sieve 5A	Porapak Q	Porapak QS
	%	%	%
150	80.2*	13.2	12.4
200	82.3	10.6	10.8
250	92.7	16.7	9.6
300	89.6	11.3	13.1

* Denotes peak broadening on analysis

Table 30 The effect of sample volume on the safe sampling volume of molecular sieve 5A

Component	Sample volume ml			
	100	200	500	1000
	%	%	%	%
Hydrogen sulphide	86.4	90.6	94.8	88.2
Carbonyl sulphide	102.4	91.1	96.7	105.3
Sulphur dioxde	91.4	84.3	86.8	85.3
Carbon disulphide	82.3	78.8	89.0	86.2

Component concentration nominally 0.1 ppm
All figures are expressed in terms of percentage component recovery.

Table 31 The effect of dilution on recovery for 100 ml sample volume

Diluent air quantity	Percentage recovery equivalent			
	Hydrogen sulphide	Carbonyl sulphide	Sulphur dioxide	Carbon disulphide
	%	%	%	%
0	94.0	97.6	90.4	89.5
100	88.6	89.2	81.2	83.2
200	70.3	73.8	60.5	78.5
400	54.7	50.3	41.7	70.1
900	39.1	36.4	28.6	62.3

All figures are expressed in terms of percentage component recovery

Table 32 Reproducibility of Sampling Tube Preparation

Component	Sampling Tube Number										Mean Recovery	Relative Standard Deviation
	1	2	3	4	5	6	7	8	9	10		
	%	%	%	%	%	%	%	%	%	%	%	%
Hydrogen sulphide	85.6	110.2	96.2	87.4	107.8	93.0	89.6	91.7	86.5	90.3	93.8	8.6
Carbonyl sulphide	93.6	86.1	107.4	92.4	85.8	105.6	89.5	95.0	102.3	97.4	95.5	7.6
Sulphur dioxide	86.1	98.3	83.7	99.4	80.7	89.5	98.3	81.7	93.6	88.4	90.0	7.1
Carbon disulphide	94.5	106.3	80.7	86.3	102.4	82.5	98.3	84.0	93.2	83.9	91.2	9.0

All figures expressed in terms of percentage component recovery

Table 33 Analysis of products evolved from Thoresby coal as a function of temperature in air

Concentration (ppm) unless stated	Mean temperature of coal bed °C					
	50	100	150	175	200	250
Oxygen (%)	20.93	20.90	20.86	20.60	20.24	18.01
Carbon dioxide (%)	<0.01	0.01	0.02	0.04	0.06	0.76
Carbon monoxide	<1.0	3.0	30	140	290	3250
Methane (%)	<0.01	<0.01	0.01	0.03	0.02	0.01
Oxidation ratio	-	0.75	2.14	3.41	3.52	9.68
Ethane	0.34	6.94	17.34	13.38	10.05	3.80
Propane	0.19	0.48	3.43	6.32	12.32	15.41
Methylpropane	0.10	0.32	1.16	4.11	12.41	22.20
Butane	0.08	0.17	0.68	1.83	4.61	11.62
Cyclo+2 methylbutane	0.03	0.06	1.02	2.49	5.31	6.91
Pentane	0.40	0.10	0.73	1.83	3.43	5.41
Cyclo+2 methypentane	0.04	0.22	2.34	3.80	5.13	7.85
Hexane	0.03	0.22	1.43	2.48	3.74	4.16
Methylcyclohexane	0.07	0.21	1.36	2.16	3.94	15.36
Heptane	0.02	0.12	0.82	1.87	3.14	7.22
Octane	0.01	0.16	1.34	2.56	6.02	11.12
Nonane	0.01	0.14	1.21	2.97	6.41	14.82
Decane	0.01	0.13	0.84	3.14	7.12	18.13
Ethene	0.03	0.06	0.31	0.44	1.27	12.85
Propene	0.03	0.07	0.23	0.30	1.61	15.62
Benzene	0.05	0.18	0.95	1.98	4.07	39.20
Toluene	0.07	0.19	0.91	1.83	6.03	40.60
Ethylbenzene	0.02	0.07	0.41	0.80	1.52	8.07
Meta+paraxylene	0.03	0.10	0.33	0.50	0.83	4.21
Orthoxylene	0.02	0.04	0.14	0.39	0.63	3.46
1,3,5 trimethylbenzene	0.01	0.03	0.09	0.14	0.20	0.78

Table 34 Analysis of products evolved from Hucknall coal as a function of temperature in air

Concentration (ppm) unless stated	Mean temperature of coal bed °C					
	50	100	150	175	200	250
Oxygen (%)	20.93	20.90	20.75	20.47	19.82	18.53
Carbon dioxide (%)	<0.01	0.01	0.01	0.04	0.10	0.82
Carbon monoxide	<1.0	3.0	49	210	520	1950
Methane (%)	<0.01	<0.01	0.01	0.03	0.02	0.01
Oxidation ratio	-	0.75	1.88	3.57	3.68	7.22
Ethane	0.38	7.28	19.28	18.56	12.27	4.17
Propane	0.21	1.66	8.30	17.70	33.29	40.72
Methylpropane	0.13	1.06	7.54	17.86	35.71	50.32
Butane	0.20	1.19	5.69	12.20	19.65	30.74
Cyclo+2 methylbutane	0.08	0.40	3.34	5.89	12.74	17.76
Pentane	0.13	0.37	1.98	3.74	6.24	10.26
Cyclo+2 methypentane	0.06	0.33	1.84	3.84	7.26	13.14
Hexane	0.04	0.24	0.72	1.44	2.20	3.47
Methylcyclohexane	0.05	0.18	0.90	2.03	3.51	9.71
Heptane	0.02	0.05	0.57	1.02	2.86	3.84
Octane	0.01	0.03	0.28	0.58	1.40	2.34
Nonane	0.01	0.03	0.23	0.42	1.08	2.02
Decane	<0.01	0.02	0.13	0.26	1.37	2.31
Ethene	0.04	0.08	0.29	0.87	2.95	13.05
Propene	0.04	0.08	0.30	0.82	2.59	10.13
Benzene	0.10	0.24	1.13	3.74	7.35	27.56
Toluene	0.09	0.23	0.97	4.26	8.66	31.73
Ethylbenzene	0.02	0.06	0.42	1.43	2.96	7.41
Meta+paraxylene	0.02	0.09	0.24	1.03	2.00	6.36
Orthoxylene	0.01	0.06	0.21	0.75	1.42	2.94
1,3,5 trimethylbenzene	<0.01	0.03	0.11	0.19	0.39	1.27

Table 35 Analysis of products evolved from Wolstanton coal as a function of temperature in air

Concentration (ppm) unless stated	Mean temperature of coal bed °C					
	50	100	150	175	200	250
Oxygen (%)	20.93	20.92	20.87	20.84	20.81	20.13
Carbon dioxide (%)	<0.01	<0.01	<0.01	0.01	0.02	0.07
Carbon monoxide	<1.0	1.0	13	28	55	440
Methane (%)	<0.01	<0.01	0.01	0.04	0.03	0.02
Oxidation ratio	-	-	1.63	2.80	3.93	4.08
Ethane	0.12	0.30	1.89	8.83	17.07	17.68
Propane	0.07	0.38	1.28	5.34	8.05	17.82
Methylpropane	0.02	0.16	1.32	4.07	7.61	18.52
Butane	0.07	0.25	4.07	10.87	13.39	24.05
Cyclo+2 methylbutane	0.02	0.04	0.40	1.78	2.32	5.94
Pentane	0.02	0.09	1.09	2.38	5.82	14.03
Cyclo+2 methypentane	0.02	0.04	0.25	0.62	1.34	3.80
Hexane	0.02	0.06	0.34	1.80	2.20	5.94
Methylcyclohexane	0.02	0.07	0.26	0.46	0.97	4.51
Heptane	0.02	0.04	0.14	0.44	0.85	2.70
Octane	0.01	0.02	0.10	0.36	0.83	3.85
Nonane	<0.01	0.02	0.06	0.10	0.45	2.34
Decane	<0.01	0.01	0.03	0.05	0.37	2.04
Ethene	0.04	0.08	0.12	0.27	0.61	6.88
Propene	0.04	0.11	0.33	0.77	1.63	12.04
Benzene	0.04	0.14	1.03	2.20	3.38	18.82
Toluene	0.04	0.18	1.29	2.74	3.52	19.63
Ethylbenzene	0.01	0.03	0.18	0.32	0.48	3.71
Meta+paraxylene	0.02	0.08	0.39	0.56	0.83	4.42
Orthoxylene	<0.01	0.02	0.07	0.17	0.36	0.83
1,3,5 trimethylbenzene	<0.01	0.01	0.03	0.05	0.12	0.29

Table 36 Analysis of products evolved from Thoresby coal as a function of temperature in nitrogen

Concentration (ppm) unless stated	Mean temperature of coal bed °C					
	50	100	150	200	250	300
Oxygen (%)	N.D	N.D	N.D	N.D	N.D	N.D
Carbon dioxide (%)	<0.01	<0.01	<0.01	0.01	0.02	0.03
Carbon monoxide	<1.0	1.0	13	33	55	70
Methane (%)	<0.01	<0.01	<0.01	0.01	0.02	0.01
Ethane	0.34	6.03	14.87	8.12	3.04	0.52
Propane	0.17	0.44	2.83	8.47	5.06	3.42
Methylpropane	0.09	0.27	0.96	8.61	16.41	10.78
Butane	0.07	0.18	0.51	3.66	7.07	5.12
Cyclo+2 methylbutane	0.04	0.08	0.89	4.43	5.66	3.40
Pentane	0.03	0.06	0.51	2.14	3.12	2.78
Cyclo+2 methylpentane	0.04	0.20	1.81	4.02	5.37	5.01
Hexane	0.03	0.15	1.07	2.86	3.63	2.97
Methylcyclohexane	0.05	0.25	1.03	1.54	1.86	1.65
Heptane	0.03	0.10	0.63	2.53	5.42	8.12
Octane	0.02	0.15	0.99	5.71	8.95	11.36
Nonane	0.01	0.13	0.83	6.35	13.12	19.30
Decane	0.01	0.12	0.60	7.03	16.15	25.74
Ethene	0.03	0.05	0.12	0.31	0.75	1.92
Propene	0.04	0.06	0.10	0.38	1.02	2.26
Benzene	0.03	0.16	0.34	0.96	1.83	1.34
Toluene	0.04	0.17	0.42	1.35	3.63	3.60
Ethylbenzene	0.02	0.06	0.19	0.62	1.76	1.98
Meta+paraxylene	0.03	0.08	0.13	0.21	0.88	1.41
Orthoxylene	0.02	0.03	0.12	0.19	0.74	1.20
1,3,5 trimethylbenzene	0.01	0.02	0.07	0.12	0.20	0.35

N.D. Indicates not detected

Table 37 Analysis of products evolved from Hucknall coal as a function of temperature in nitrogen

Concentration (ppm) unless stated	Mean temperature of coal bed °C					
	50	100	150	200	250	300
Oxygen (%)	N.D	N.D	N.D	N.D	N.D	N.D
Carbon dioxide (%)	<0.01	<0.01	<0.01	0.01	0.02	0.03
Carbon monoxide	<1.0	1.0	10	22	31	43
Methane (%)	<0.01	<0.01	<0.01	0.03	0.02	0.01
Ethane	0.42	8.94	15.39	6.16	1.46	0.71
Propane	0.20	1.09	5.82	20.12	28.36	5.40
Methylpropane	0.11	0.99	5.83	22.49	26.46	13.23
Butane	0.23	1.03	3.94	14.57	18.84	12.42
Cyclo+2 methylbutane	0.07	0.35	2.03	7.70	9.96	6.57
Pentane	0.11	0.32	1.86	4.57	5.96	4.08
Cyclo+2 methylpentane	0.06	0.31	1.44	4.47	6.92	6.03
Hexane	0.04	0.20	0.52	1.54	2.89	3.09
Methylcyclohexane	0.04	0.09	0.23	0.83	1.89	1.85
Heptane	0.02	0.05	0.38	1.81	3.13	5.12
Octane	0.01	0.03	0.22	0.72	1.81	5.01
Nonane	0.01	0.02	0.19	0.56	1.23	1.64
Decane	<0.01	0.01	0.08	0.37	1.72	2.40
Ethene	0.04	0.10	0.17	0.25	0.58	1.29
Propene	0.03	0.08	0.14	0.35	0.60	1.03
Benzene	0.08	0.16	0.29	0.83	1.86	1.64
Toluene	0.08	0.14	0.26	0.97	1.91	1.79
Ethylbenzene	0.02	0.06	0.15	0.43	1.02	1.23
Meta+paraxylene	0.03	0.08	0.18	0.33	0.56	0.80
Orthoxylene	0.01	0.05	0.16	0.31	0.60	0.87
1,3,5 trimethylbenzene	<0.01	0.02	0.10	0.18	0.29	0.48

N.D. indicates not detected

Table 38 Analysis of products evolved from Wolstanton coal as a function of temperature in nitrogen

Concentration (ppm) unless stated	Mean temperature of coal bed °C					
	50	100	150	200	250	300
Oxygen (%)	N.D	N.D	N.D	N.D	N.D	N.D
Carbon dioxide (%)	<0.01	<0.01	<0.01	<0.01	0.01	0.02
Carbon monoxide	<1.0	1.0	3.0	9.0	15	20
Methane (%)	<0.01	<0.01	0.01	0:02	0.02	0.01
Ethane	0.11	0.28	1.77	16.85	15.64	4.42
Propane	0.07	0.34	1.25	7.01	17.00	8.34
Methylpropane	0.02	0.14	1.26	7.28	16.25	14.33
Butane	0.06	0.23	3.63	11.71	22.56	22.05
Cyclo+2 methylbutane	0.02	0.04	0.35	2.02	4.49	18.26
Pentane	0.02	0.08	0.94	4.27	11.59	19.67
Cyclo+2 methylpentane	0.02	0.03	0.18	1.11	3.07	6.84
Hexane	0.02	0.05	0.35	1.62	4.95	6.61
Methylcyclohexane	0.02	0.04	0.11	0.36	0.64	0.60
Heptane	0.01	0.02	0.13	0.23	0.38	0.58
Octane	0.01	0.02	0.05	0.16	0.24	0.47
Nonane	<0.01	<0.01	0.04	0.14	0.17	0.31
Decane	<0.01	<0.01	0.02	0.06	0.14	0.19
Ethene	0.04	0.06	0.08	0.20	0.27	0.53
Propene	0.03	0.05	0.10	0.22	0.43	0.72
Benzene	0.04	0.13	0.24	0.92	1.72	1.70
Toluene	0.03	0.13	0.31	0.94	2.01	2.00
Ethylbenzene	0.01	0.02	0.08	0.13	0.26	0.68
Meta+paraxylene	0.02	0.04	0.11	0.27	0.51	0.96
Orthoxylene	<0.10	0.02	0.04	0.07	0.16	0.29
1,3,5 trimethylbenzene	<0.01	0.01	0.01	0.02	0.03	0.07

N.D. indicates not detected

Table 39 Comparison of Carbon monoxide Evolution Rates from different Coals heated in Air

Coal Temperature °C	CRC 502 (100)	CRC 702 (100)	CRC 902 (100)	CRC 502 (101)	CRC 902 (103)	Thoresby coal CRC 702	Hucknall coal CRC 702	Wolstanton coal CRC 502
50	0.032×10^{-4}		0.16×10^{-4}		0.5×10^{-4}	$<1.0 \times 10^{-4}$	$<1.0 \times 10^{-4}$	$<1.0 \times 10^{-4}$
100	0.8×10^{-4}	2.8×10^{-4}	5.6×10^{-4}	8.6×10^{-4}	2.8×10^{-4}	3.0×10^{-4}	3.0×10^{-4}	1.0×10^{-4}
150	14.4×10^{-4}	28.9×10^{-4}		114×10^{-4}		30×10^{-4}	49×10^{-4}	13×10^{-4}
175	56×10^{-4}					140×10^{-4}	210×10^{-4}	28×10^{-4}
200	136×10^{-4}					290×10^{-4}	520×10^{-4}	55×10^{-4}
250	312×10^{-4}					3250×10^{-4}	1950×10^{-4}	440×10^{-4}

Rates of evolution given in $mlg^{-1}min^{-1}$

Table 40 Extended mass spectrometer analysis of products evolved from heated coal

Peak number	Identification	Peak number	Identification
1	butanes	22	trimethylbenzene
2	pentanes	23	decanes
3	2 methylpentane + acetone	24	methyldecane
4	hexane	25	undecane
5	methylcyclopentane + 2 methylhexane	26	naphthalene
		27	methylundecane
6	benzene + cyclohexane	28	dodecane
7	dimethylcyclopentane	29	methylnaphthalene
8	heptane	30	methyldodecane
9	methylcyclohexane	31	tridecane
10	toluene	32	methyltridecane
11	methylheptane	33	tetradecane
12	1,3 dimethylcyclohexane	34	2,6 or 2,7 dimethyl-naphthalene
13	octane		
14	1 ethyl-3 methylcyclo-pentane	35	methyltetradecane
		36	pentadecane
15	ethyl benzene	37	trimethylnaphthalene
16	ortho + paraxylene	38	methylpentadecane
17	methyloctane	39	hexadecane
18	metaxylene	40	methylhexadecane
19	nonane	41	heptadecane
20	1 methylethylbenzene		
21	methylnonane		

Table 41 Analysis from Wolstanton colliery 557s intake outbye end

Sample number	Carbon monoxide ppm	Oxidation Ratio	Methane %	Ethane ppm	Propane ppm	Ethene ppm	Propene ppm	Benzene ppm	Toluene ppm	Methyl cyclohexane ppm
1	2	0.22	0.21	230	35	0.12	0.12	0.14	0.14	0.30
2	2	0.06	0.13	105	18	0.06	0.21	0.07	0.12	0.69
3	3	0.38	0.19	153	24	0.12	0.13	0.12	0.17	0.30
4	1	0.20	0.04	45	9	0.12	0.11	0.04	0.07	0.05
5	2	0.25	0.19	150	22	0.06	0.14	0.05	0.10	0.20
6	3	0.30	0.05	118	18	0.12	0.11	0.09	0.11	0.10
7	2	0.33	0.03	88	12	0.12	0.14	0.04	0.06	0.35
8	2	0.40	0.18	165	22	0.06	0.07	0.06	0.07	0.35
9	2	0.40	0.18	153	24	0.06	0.29	0.07	0.16	0.35
10	3	0.27	0.23	165	26	0.06	0.21	0.08	0.14	0.40
11	2	0.67	0.24	176	26	0.04	0.11	0.04	0.06	0.15
12	3	1.00	0.08	116	25	0.17	0.22	0.05	0.09	-
13	2	0.67	0.25	589	118	0.25	0.22	0.06	0.04	0.15
14	3	0.33	0.10	187	22	0.08	0.05	0.05	0.05	0.07
15	2	0.22	0.07	177	19	0.25	0.16	0.05	0.07	0.07
16	2	0.25	0.08	150	25	0.17	0.22	0.06	0.06	0.29
17	2	0.22	0.02	100	21	0.17	0.22	0.05	0.05	0.36
18	1	0.11	0.04	49	10	0.02	0.01	0.03	0.06	0.22
19	2	0.23	0.05	80	31	0.12	0.09	0.05	0.07	0.23
20	3	0.15	0.04	53	17	0.11	0.08	0.04	0.05	0.18

- indicates no data

Table 42 Analysis from Wolstanton colliery 557s return outbye end

Sample number	Carbon monoxide ppm	Oxidation Ratio	Methane %	Ethane ppm	Propane ppm	Ethene ppm	Propene ppm	Benzene ppm	Toluene ppm	Methyl cyclohexane ppm
1	13	0.36	1.22	1539	243	0.82	0.36	0.38	0.76	0.50
2	19	0.53	1.34	1065	157	1.27	0.74	0.50	0.64	0.42
3	17	0.44	1.42	1243	164	0.88	0.33	0.40	0.59	0.81
4	11	0.30	0.64	532	92	0.35	0.32	0.22	0.30	0.32
5	10	0.30	1.18	-	-	-	-	0.26	0.32	-
6	11	0.37	0.94	947	121	0.47	0.24	-	-	0.48
7	11	0.28	1.24	1065	164	0.35	0.28	0.28	0.32	0.79
8	13	0.36	1.58	1243	167	0.35	0.32	0.24	0.32	0.89
9	13	0.33	1.54	1065	150	0.35	0.29	0.24	0.35	0.89
10	15	0.34	0.89	769	136	0.59	0.50	0.23	0.30	0.79
11	14	0.38	1.41	736	145	0.17	0.46	0.30	0.29	0.73
12	15	0.39	1.30	982	208	0.83	0.54	0.31	0.26	-
13	35	0.76	0.89	1277	159	1.67	1.58	0.24	0.25	0.95
14	13	0.31	1.10	1198	242	0.17	0.22	0.33	0.36	0.59
15	15	0.34	0.85	690	167	0.33	0.16	0.42	0.40	0.59
16	19	0.48	0.95	1060	194	0.58	1.63	0.53	0.57	-
17	15	0.27	1.14	933	208	0.50	1.09	0.44	0.45	-
18	13	0.27	0.65	589	138	0.08	0.16	0.42	0.26	0.95
19	15	0.33	0.58	633	120	0.37	0.34	0.47	0.28	0.91
20	8	0.24	0.98	948	188	0.28	0.13	0.23	0.23	0.74

- indicates no data

Table 43 Analysis from Wolstanton colliery 557s return packpipe

Sample number	Carbon monoxide ppm	Oxidation Ratio	Methane %	Ethane ppm	Propane ppm	Ethene ppm	Propene ppm	Benzene ppm	Toluene ppm	Methyl cyclohexane ppm
12	3700	2.30	5.80	4910	1526	12.5	35.3	0.77	3.04	16.1
13	3600	2.14	5.90	6875	1664	25.0	32.6	3.46	4.41	27.4
14	3700	2.11	6.20	7857	2080	51.7	40.7	4.62	6.43	26.0
15	4350	2.44	7.20	7270	1805	31.7	46.2	5.13	8.33	13.9
16	4300	2.30	6.10	6875	1630	48.3	47.8	2.44	9.76	21.9
17	4100	2.18	5.60	6875	2080	30.0	54.3	1.99	6.07	21.9
18	2200	1.18	4.90	8348	2843	37.5	40.7	0.92	0.77	9.5
19	2700	1.46	5.10	5214	1580	27.5	43.5	1.09	1.13	11.3
20	230	0.12	11.50	9071	3774	4.2	5.1	0.44	0.53	3.9

Table 44 Analysis from Thoresby colliery 200s return outbye end, prior to sealing off

Days	Carbon monoxide ppm	Oxidation Ratio	Methane %	Ethane ppm	Propane ppm	Ethene ppm	Propene ppm	Methyl cyclohexane ppm
1	28	0.97	0.12	78.6	43.7	0.33	0.27	9.1
6	29	1.04	0.13	68.7	37.5	0.21	0.22	7.0
8	32	0.89	0.17	70.7	41.6	0.25	0.27	5.9
18	42	1.14	0.17	118	49.9	0.75	0.49	5.0
21	49	1.36	0.23	108	58.3	0.67	0.71	5.6
22	51	1.34	0.27	125	63.1	1.00	0.87	6.1
23	59	1.37	0.44	157	77.7	1.08	0.98	6.9

Table 45 Analysis from Thoresby colliery 200s return, after sealing off

Days	Carbon monoxide ppm	Oxidation Ratio	Methane %	Ethane ppm	Propane ppm	Ethene ppm	Propene ppm	Methyl cyclohexane ppm
2	1200	2.35	4.8	1870	830	11.7	11.4	14.6
6	2400	3.09	10.1	2700	1160	26.7	18.5	16.5
10	1700	1.81	19.5	3830	1940	20.0	17.4	27.1
13	1900	1.89	21.0	4050	2085	23.2	18.0	29.4
16	1950	1.88	20.0	4520	2045	18.3	13.0	24.9
17	2100	2.03	21.0	4665	2045	24.6	13.6	25.6
18	2200	2.12	22.0	4620	2045	28.3	15.2	25.6
20	2300	2.13	24.0	5110	2220	17.5	20.6	35.3
25	2700	2.25	25.5	5300	2360	20.0	25.0	36.6
26	3000	2.48	25.0	5600	2500	30.0	25.5	38.0
27	4600	3.48	22.5	5305	2360	153	39.4	35.1
30	14000	8.44	25.5	5695	2565	866	125	108
31	13000	8.26	27.0	5890	2500	812	109	106
33	7200	7.17	35.0	4910	1735	258	57	52.7
37	4900	6.20	40.0	4515	1665	208	46	47.7
38	7600	5.95	39.0	4990	2705	291	77	70.2
40	5100	5.36	36.0	5305	1940	316	61	55.6
41	4500	4.75	37.0	5890	2150	333	59	33.4

Table 46 Analysis from Daw Mill 62s return outbye end

Sample number	Carbon monoxide ppm	Oxidation Ratio	Methane %	Ethane ppm	Propane ppm	Ethene ppm	Propene ppm	Benzene ppm	Toluene ppm	Methyl cyclohexane ppm
1	3.0	0.25	0.04	12.4	1.7	0.03	0.03	0.04	0.04	0.05
2	2.0	0.20	0.04	12.0	1.5	0.02	0.03	0.03	0.03	0.04
3	3.0	0.21	0.03	7.0	1.0	0.01	0.03	0.02	0.02	0.04
4	8.0	0.20	0.57	186	30.0	0.04	0.05	0.04	0.03	0.04
5	7.0	0.23	0.44	82	13.0	0.08	0.05	0.05	0.04	0.04
6	9.0	0.21	0.44	75	15.3	0.12	0.03	0.09	0.10	0.26
7	4.0	0.16	0.32	63	10.8	0.10	0.03	0.08	0.05	0.10
8	9.0	0.18	0.87	255	38.0	0.25	0.27	0.11	0.13	0.25
9	8.0	0.17	0.63	177	22.7	0.33	0.18	0.11	0.12	0.23
10	6.0	0.14	0.52	170	22.3	0.21	0.09	0.10	0.09	0.17
11	10.0	0.22	0.89	250	35.1	0.36	0.22	0.14	0.13	0.27
12	9.0	0.21	0.76	210	27.6	0.28	0.25	0.12	0.11	0.25
13	11.0	0.24	0.90	253	34.4	0.36	0.26	0.16	0.15	0.30
14	8.0	0.19	0.67	194	25.8	0.30	0.20	0.11	0.11	0.24
15	10.0	0.23	0.86	221	29.0	0.31	0.25	0.16	0.14	0.28

Table 47 Analysis fof diesel and shotfiring fumes

Component (ppm) unless stated	Diesel exhaust survey				Shotfiring fumes survey		
	Locomotive garage		High Hazles seam		19s return 100m outbye face		
	No diesel operating	Diesel idling sample 5m from exhaust	No diesel operating	Diesel idling sample 1m from exhaust	Prior to shotfiring	5 mins after shotfiring	8 mins after shotfiring
Carbon monoxide	3.0	39	5.0	340	5.0	45	80
Oxidation ratio	0.14	1.11	0.26	1.05	0.26	2.14	3.64
Methane %	0.04	0.04	0.16	0.18	0.16	0.17	0.16
Ethane	3.63	3.93	19.64	26.52	19.64	26.52	28.31
Propane	0.42	0.62	2.84	4.51	2.84	3.47	3.63
Ethene	0.13	0.50	0.17	8.10	0.17	1.75	3.14
Propene	0.08	0.33	0.05	1.69	0.05	0.33	0.70
Benzene	0.01	-	0.01	-	0.01	0.03	0.03
Toluene	0.01	-	0.01	-	0.01	0.02	0.03
Methyl-cyclohexane	0.02	0.04	0.07	0.22	0.07	0.07	0.09

- indicates presence of interferring compounds

Table 48 Extended mass spectrometer analysis of diesel fumes taken one metre from exhaust

Peak number	Identification
1	pentanes
2	hexanes + acetic acid
3	benzene + cyclohexane
4	heptane
5	toluene
6	meta+para xylene
7	nonane
8	benzaldehyde
9	decane
10	undecane
11	naphthalene
12	dodecane
13	methyltetrahydronaphthalene
14	methylnaphthalene
15	tridecane
16	tetradecane
17	branched aliphatic hydrocarbon
18	pentadecane
19	hexadecane
20	heptadecane
21	octadecane

Table 49 Extended mass spectrometer analysis of shotfiring fumes

Peak number	Identification
1	pentanes + pentanol
2	hexanes + hexanol
3	benzene + cyclohexane
4	heptane
5	methylpentanol + methylcyclohexane
6	toluene
7	alcohol
8	ethyl benzene
9	meta+para xylene
10	styrene

Table 50 Production of sulphur compounds from test coals as a function of temperature in air

Test coal	Component (ppm) unless stated	Mean temperature of coal bed °C						
		50	100	150	175	200	225	250
Thoresby	Oxygen (%)	20.91	20.89	20.80	20.31	20.11	19.14	18.12
	Carbon monoxide	1.0	3.0	30	125	290	1010	3100
	Hydrogen sulphide	<0.005	<0.005	0.01	0.02	0.03	0.10	0.18
	Carbonyl sulphide	<0.005	0.01	0.04	0.23	0.60	1.73	6.03
	Sulphur dioxide	< 0.01	< 0.01	0.14	0.08	0.09	0.38	8.45
	Carbon disulphide	< 0.01	< 0.01	0.06	0.12	0.53	1.36	3.07
Hucknall	Oxygen (%)	20.92	20.86	20.71	20.27	19.67	19.08	18.66
	Carbon monoxide	< 1.0	3.0	46	160	560	1050	2010
	Hydrogen sulphide	<0.005	<0.005	0.01	0.02	0.05	0.13	0.31
	Carbonyl sulphide	<0.005	0.02	0.06	0.27	0.74	1.82	4.80
	Sulphur dioxide	< 0.01	< 0.01	0.07	0.03	0.14	0.59	5.37
	Carbon disulphide	< 0.01	< 0.01	0.03	0.08	0.21	0.73	2.03
Wolstanton	Oxygen (%)	20.93	20.88	20.82	20.75	20.69	20.32	20.19
	Carbon monoxide	< 1.0	1.0	11	30	58	140	400
	Hydrogen sulphide	<0.005	<0.005	<0.005	0.01	0.02	0.04	0.09
	Carbonyl sulphide	<0.005	<0.005	0.01	0.03	0.16	0.31	0.94
	Sulphur dioxide	< 0.01	< 0.01	0.03	< 0.01	0.04	0.13	1.56
	Carbon disulphide	< 0.01	< 0.01	< 0.01	0.03	0.08	0.26	0.72

Table 51 Production of sulphur compounds from test coals as a function of temperature in nitrogen

Test coal	Component (ppm) unless stated	Mean temperature of coal bed °C							
		50	100	150	175	200	225	250	300
Thoresby	Carbon monoxide	< 1.0	< 1.0	13	24	34	41	51	73
	Hydrogen sulphide	<0.005	<0.005	0.01	0.03	0.08	0.76	3.23	16.84
	Carbonyl sulphide	<0.005	<0.005	<0.005	0.03	0.08	0.10	0.13	0.68
	Sulphur dioxide	< 0.01	< 0.01	0.13	0.06	0.06	0.16	0.86	28.30
	Carbon disulphide	< 0.01	< 0.01	0.03	0.05	0.11	0.22	0.43	0.53
Hucknall	Carbon monoxide	< 1.0	< 1.0	11	15	20	24	30	45
	Hydrogen sulphide	<0.005	<0.005	0.02	0.05	0.11	0.38	1.28	18.21
	Carbonyl sulphide	<0.005	<0.005	<0.005	0.01	0.05	0.09	0.18	0.33
	Sulphur dioxide	< 0.01	< 0.01	0.09	0.05	0.06	0.29	1.45	39.60
	Carbon disulphide	< 0.01	< 0.01	0.02	0.04	0.23	0.26	0.38	0.76
Wolstanton	Carbon monoxide	< 1.0	< 1.0	3.0	6.0	10	12	14	22
	Hydrogen sulphide	<0.005	<0.005	0.01	0.02	0.06	0.19	0.49	5.21
	Carbonyl sulphide	<0.005	<0.005	<0.005	0.01	0.03	0.04	0.10	0.27
	Sulphur dioxide	< 0.01	< 0.01	0.02	<0.01	0.03	0.06	0.13	9.37
	Carbon disulphide	< 0.01	< 0.01	<0.01	0.02	0.05	0.10	0.18	0.34

Table 52 Production of sulphur components from coals containing low and high pyritic sulphur heated in air

Test coal	Component (ppm) unless stated	Mean temperature of coal bed °C					
		150	175	200	250	250	300
Mansfield	Oxygen (%)	20.78	20.54	20.26	19.62	18.60	18.70
0.09% pyritic	Carbon monoxide	19	135	490	1450	3100	4750
sulphur	Hydrogen sulphide	<0.005	0.01	0.03	0.15	0.22	0.05
	Carbonyl sulphide	0.05	0.48	1.37	3.71	6.85	11.70
	Sulphur dioxide	0.22	0.03	0.03	0.11	7.40	365
	Carbon disulphide	0.02	0.07	0.13	0.41	2.31	4.76
Harworth	Oxygen (%)	20.84	20.70	20.63	20.21	20.05	19.71
1.40% pyritic	Carbon monoxide	16	48	200	640	900	2300
sulphur	Hydrogen sulphide	0.10	0.20	0.26	0.38	0.31	0.04
	Carbonyl sulphide	0.02	0.03	0.45	1.83	4.89	11.12
	Sulphur dioxide	0.18	0.16	0.51	0.84	8.40	136
	Carbon disulphide	0.03	0.11	0.16	0.48	1.66	3.57

Table 53 Production of sulphur compounds from coals containing low and high pyritic sulphur heated in nitrogen

Test coal	Component (ppm) unless stated	Mean temperature of coal bed °C					
		150	175	200	225	250	300
Mansfield 0.09% pyritic sulphur	Carbon monoxide	6.0	12	16	24	33	49
	Hydrogen sulphide	0.02	0.04	0.07	0.53	2.86	14.30
	Carbonyl sulphide	<0.005	<0.005	0.02	0.05	0.15	0.47
	Sulphur dioxide	0.22	0.02	0.03	0.08	0.26	19.10
	Cardon disulphide	< 0.01	0.02	0.05	0.12	0.20	0.48
Harworth 1.40% pyritic sulphur	Carbon monoxide	3.0	7.0	12	16	25	34
	Hydrogen sulphide	0.03	0.06	0.12	0.70	1.63	7.08
	Carbonyl sulphide	0.01	0.02	0.03	0.07	0.13	0.62
	Sulphur dioxide	0.10	0.05	0.12	0.15	0.24	12.60
	Carbon disulphide	< 0.01	0.03	0.05	0.13	0.19	0.37

Table 54 Analysis from Bentinck colliery K50s return packpipe

Day	Carbonyl sulphide ppm	Carbon disulphide ppm	Methane %	Oxygen %	Carbon monoxide ppm	Oxidation ratio
1*	0.009	0.63	1.70	0.94	24	< 0.01
4*	0.005	0.65	1.17	0.12	17	< 0.01
5*	0.005	0.63	2.50	0.42	25	0.01
6	0.015	0.58	3.00	0.30	43	0.02
7*	0.038	0.47	3.90	5.00	440	0.23
7	0.038	0.53	3.50	5.56	370	0.20
8	0.060	0.44	5.40	6.26	710	0.42
9	0.050	0.42	4.90	7.71	690	0.46
11	0.050	0.36	5.10	8.10	930	0.65
12	0.060	0.44	6.10	6.42	950	0.59
13*	0.060	0.42	6.10	6.65	940	0.59
13	0.060	0.42	6.20	6.45	1000	0.62
14	0.060	0.36	6.35	6.45	1050	0.66
15	0.070	0.35	6.60	6.27	1550	0.98
16	0.100	0.42	6.70	5.66	1800	1.09
18	0.104	0.42	6.90	5.31	2350	1.41
19*	0.135	0.45	6.75	6.48	2450	1.58
19	0.132	0.41	6.80	6.48	2500	1.64
20	0.160	0.48	7.15	6.05	2600	1.66
22	0.164	0.38	7.15	5.77	2950	1.87
24	0.146	0.34	8.05	5.30	2650	1.66
26	0.136	0.31	8.65	5.05	2500	1.58
29	0.140	0.44	8.65	4.70	2400	1.47
33	0.224	0.43	8.65	4.72	3300	2.05
34*	0.232	0.53	10.00	2.06	3700	1.98
34	0.235	0.55	10.10	2.04	3700	1.97
35	0.288	0.39	8.60	3.68	3550	2.03
36	0.280	0.41	8.40	4.52	3550	2.15
37	Sampling pipe blocked					

* Samples collected underground

Table 55 Analysis from Warsop colliery U19s return packpipe

Day	Carbonyl sulphide ppm	Carbon disulphide ppm	Methane %	Oxygen %	Carbon monoxide ppm	Oxidation ratio
1	0.98	0.73	2.50	3.80	10000	5.55
2	-	-	2.60	2.90	11000	5.82
3	1.03	0.81	2.65	3.36	11000	5.96
5	0.95	0.75	2.70	4.20	9200	5.26
6	-	-	2.45	4.08	9300	5.27
7	0.915	0.73	2.70	3.80	8600	4.77
9	0.83	0.66	3.30	2.90	7700	4.06
11	0.85	0.62	3.00	4.10	7800	4.43
12	-	-	3.40	3.40	10000	5.43
13	1.355	0.90	3.60	2.01	14000	7.06
14	-	-	4.00	1.55	12000	5.89
15	1.17	0.86	3.70	2.44	11500	5.97
16	-	-	5.80	1.32	6900	3.30
17	0.38	0.67	7.20	1.22	4000	1.92
18	-	-	7.00	2.70	2600	1.40
19	0.225	0.43	7.30	1.90	2400	1.24
20	-	-	6.70	3.00	2100	1.14
21	0.21	0.43	6.50	3.00	2000	1.08
22	-	-	6.90	1.70	2000	1.60
23	0.195	0.36	7.50	0.77	2000	1.04
24	0.19	0.31	7.70	1.03	2000	0.94

- indicates no sample

Table 56a Analysis of diesel and shotfiring fumes

Locomotive	Operating details	Sampling point	Carbonyl sulphide ppm	Carbon disulphide ppm	Methane %	Carbon monoxide ppm	Oxidation ratio
Hudwood 100BPH	-	No diesel operating	<0.005	<0.01	0.03	3.0	0.26
diesel engine	Idling	1m from exhaust	<0.005	<0.01	0.03	9.0	0.66
	Idling	Exhaust direct	<0.010	<0.01	0.03	550	1.61
	Load	5m from exhaust	<0.005	<0.01	0.03	4.0	0.30
	Load	1m from exhaust	<0.005	<0.01	0.03	15	0.97
	Load	Exhaust direct	<0.018	<0.01	0.03	1450	1.93
Clayton 150	-	No diesel operating	<0.005	<0.01	0.01	1.0	0.20
BPH diesel	Idling	5m from exhaust	<0.005	<0.01	0.01	6.0	0.35
	Idling	1m from exhaust	<0.005	<0.01	0.01	92	0.78
	Idling	Exhaust direct	0.005	<0.01	0.01	930	1.25

Table 56b Shotfiring fumes

Shotfiring details	Sampling details	Carbonyl sulphide ppm	Carbon disulphide ppm	Methane %	Carbon monoxide ppm	Oxidation ratio
42 kg of Penobel	Prior to shotfiring	<0.005	<0.01	0.02	1.0	0.17
P4/P5	5 mins after shotfiring	<0.005	<0.01	0.03	7.0	0.88
	8 mins after shotfiring	<0.005	<0.01	0.03	54	5.40
38 kg of Penobel	Prior to shotfiring	<0.005	<0.01	0.02	1.0	0.25
P4/P5	10 mins after shotfiring	<0.005	<0.01	0.04	1200	150
	13 mins after shotfiring	<0.005	<0.01	0.05	1450	242

Table 57 Production of carbonyl compounds from Hucknall coal as a function of temperature in air

Component (ppm) unless stated	Mean temperature of coal bed °C				
	50	100	150	200	250
Oxygen	20.90	20.85	20.69	20.18	18.21
Carbon monoxide	< 1.0	2.0	53	540	1890
Formaldehyde	<0.01	0.12	1.14	18.30	29.70
Acetaldehyde	<0.01	0.11	1.07	5.35	32.80
Acetone	0.12	0.25	2.61	5.33	11.70
Crotonaldehyde	<0.01	<0.01	<0.01	0.32	1.46

Table 58 Analysis of return packpipe samples

Component (ppm) unless stated	Return packpipe samples			
	Warsop	Bentinck 1	Bentinck 2	Bentinck 3
Methane %	10.30	2.75	34.00	13.60
Oxygen %	0.93	18.30	0.12	3.36
Carbon monoxide	4100	57	64	470
Oxidation ratio	2.02	0.24	0.04	0.26
Acetaldehyde	<0.01	0.08	0.04	0.05
Acetone	1.25	0.18	0.23	0.76

Table 59 Analysis of diesel and shotfiring fumes

Component (ppm) unless stated	Diesel exhaust survey				Shotfiring fumes survey		
	Clayton 150 BHP diesel engine				15 kg of Penobel P4/P5		
	No diesel operating	Diesel idling 5m from exhaust	Diesel idling 1m from exhaust	Diesel idling exhaust direct	Prior to shotfiring	5 minutes after shotfiring	10 minutes after shotfiring
Carbon monoxide	1.0	5.0	106	870	2.0	62	235
Oxidation ratio	0.18	0.30	0.82	1.13	0.21	4.83	7.96
Methane %	0.01	0.01	0.01	0.01	0.02	0.02	0.02
Formaldehyde	<0.01	<0.01	1.14	6.50	<0.01	0.15	1.20
Acetaldehyde	<0.01	<0.01	0.43	2.46	<0.01	0.02	0.08
Acetone	<0.01	<0.01	0.10	1.31	<0.01	0.05	0.15
Crotonaldehyde	<0.01	<0.01	<0.01	0.11	<0.01	<0.01	<0.01

Table 60 Production of other gases of interest from test coals as a function of temperature in air

Test coal	Component (ppm) unless stated	Mean temperature of coal bed °C						
		50	100	150	175	200	225	250
Thoresby	Oxygen %	20.91	20.88	20.82	20.39	20.16	19.08	18.02
	Carbon monoxide	1.0	3.0	33	132	275	1025	3150
	Methane %	<0.01	<0.01	0.01	0.03	0.02	0.01	0.01
	Hydrogen	< 2.5	< 2.5	< 2.5	< 2.5	2.5	7.5	20
	Hydrogen chloride	< 0.1	< 0.1	3.0	10	25	103	220
	Nitrogen dioxide	<0.10	<0.10	<0.10	<0.10	<0.10	<0.10	<0.10
	Nitric oxide	<0.50	<0.50	< .50	<0.50	<0.50	<0.50	<0.50
Hucknall	Oxygen %	20.91	20.87	20.73	20.35	19.73	19.14	18.59
	Carbon monoxide	< 1.0	3.0	52	185	510	1000	1910
	Methane %	<0.01	<0.01	0.01	0.03	0.02	0.02	0.01
	Hydrogen	< 2.5	< 2.5	< 2.5	2.5	5.0	7.5	15
	Hydrogen chloride	<0.10	<0.10	1.5	2.5	15	60	140
	Nitrogen dioxide	<0.10	<0.10	<0.10	<0.10	<0.10	<0.10	<0.10
	Nitric oxide	<0.50	<0.50	<0.50	<0.50	<0.50	<0.50	<0.50
Wolstanton	Oxygen %	20.93	20.91	20.83	20.76	20.70	20.28	20.10
	Carbon monoxide	< 1.0	1.0	12	30	56	160	410
	Methane %	<0.01	<0.01	0.01	0.04	0.03	0.02	0.02
	Hydrogen	< 2.5	< 2.5	< 2.5	< 2.5	< 2.5	< 2.5	2.5
	Hydrogen chloride	<0.10	<0.10	0.5	5	6	14	28
	Nitrogen dioxide	<0.10	<0.10	<0.10	<0.10	<0.10	<0.10	<0.10
	Nitric oxide	<0.50	<0.50	<0.50	<0.50	<0.50	<0.50	<0.50

Table 61 Production of other gases of interest from three test coals as a function of temperature in nitrogen

Test coal	Component (ppm) unless stated	Mean temperature of coal bed °C							
		50	100	150	175	200	225	250	300
Thoresby	Carbon monoxide	< 1.0	1.0	12	23	36	42	53	74
	Methane %	<0.01	<0.01	<0.01	0.01	0.01	0.02	0.02	0.01
	Hydrogen	< 2.5	< 2.5	< 2.5	< 2.5	< 2.5	< 2.5	5.0	10
	Hydrogen chloride	<0.10	<0.10	<0.10	<0.10	1.0	3.0	7.0	12
	Nitrogen dioxide	<0.10	<0.10	<0.10	<0.10	<0.10	<0.10	<0.10	<0.10
	Nitric oxide	<0.50	<0.50	<0.50	<0.50	<0.50	<0.50	<0.50	<0.50
Hucknall	Carbon monoxide	< 1.0	1.0	10	16	23	27	33	46
	Methane %	<0.01	<0.01	<0.01	0.02	0.03	0.03	0.02	0.01
	Hydrogen	< 2.5	< 2.5	< 2.5	< 2.5	< 2.5	< 2.5	2.5	7.5
	Hydrogen chloride	<0.10	<0.10	<0.10	<0.10	1.00	2.0	4.0	9.0
	Nitrogen dioxide	<0.10	<0.10	<0.10	<0.10	<0.10	<0.10	<0.10	<0.10
	Nitric oxide	<0.50	<0.50	<0.50	<0.50	<0.50	<0.50	<0.50	<0.50
Wolstanton	Carbon monoxide	< 1.0	1.0	2.0	5.0	10	13	15	23
	Methane %	<0.01	<0.01	0.01	0.01	0.01	0.02	0.02	0.01
	Hydrogen	< 2.5	< 2.5	< 2.5	< 2.5	< 2.5	< 2.5	< 2.5	5.0
	Hydrogen chloride	<0.10	<0.10	<0.10	<0.10	<0.10	1.0	2.0	4.0
	Nitrogen dioxide	<0.10	<0.10	<0.10	<0.10	<0.10	<0.10	<0.10	< 0.10
	Nitric oxide	<0.50	<0.50	<0.50	<0.50	<0.50	<0.50	<0.50	< 0.50

Table 62 Analysis from Bentinck and Warsop colliery return packpipes

Bentinck colliery K50s return packpipe				Warsop colliery U19s return packpipe			
Day	Hydrogen ppm	Carbon monoxide ppm	Oxidation ratio	Day	Hydrogen ppm	Carbon monoxide ppm	Oxidation ratio
1*	5	24	< 0.01	1	1800	10000	5.55
4*	10	17	< 0.01	2	1450	11000	5.82
5*	10	25	0.01	3	1400	11000	5.96
6	20	43	0.02	5	1000	9200	5.26
7*	20	440	0.23	6	770	9300	5.27
7	20	370	0.20	7	870	8600	4.77
8	25	710	0.42	9	700	7700	4.06
9	25	690	0.46	11	860	7800	4.43
11	30	930	0.65	13	5200	14000	7.06
12	25	950	0.59	14	3800	12000	5.89
13*	30	940	0.59	15	3200	11500	5.97
13	30	1000	0.62	16	1650	6900	3.30
14	30	1050	0.66	17	700	4000	1.92
15	30	1550	0.98	18	300	2600	1.40
16	55	1800	1.09	19	180	2400	1.24
18	90	2350	1.41	20	150	2100	1.14
19*	110	2450	1.58	21	140	2000	1.08
19	150	2500	1.64	22	120	2000	1.60
20	190	2600	1.66	23	145	2000	1.04
22	340	2950	1.87	24	140	2000	0.94
24	240	2650	1.66				
26	205	2500	1.58				
29	200	2400	1.47				
33	300	3300	2.05				
34*	330	3700	1.98				
34	330	3700	1.97				
35	350	3550	2.03				
36	360	3550	2.15				

* Underground sample

Table 63 Integrity check on measuring circuit

Known resistance value (KΩ)	Output across load resistor Vo (volts)	Calculated resistance (KΩ)
0.0108	1.001	0.0118
0.0153	1.000	0.0158
0.0335	0.996	0.0318
0.0684	0.986	0.0723
0.201	0.956	0.201
0.686	0.856	0.685
0.971	0.807	0.967
2.20	0.647	2.185
3.30	0.547	3.308
4.70	0.459	4.702
6.80	0.368	6.844
9.92	0.286	9.942
14.70	0.211	14.88
22.60	0.151	22.37
32.80	0.109	32.52
47.00	0.077	47.67
100.3	0.0380	100.7
324	0.0122	322.0
682	0.0058	681.5
1010	0.0039	1010
1164	0.0034	1165
1570	0.0025	1586
2430	0.0016	2481

Fixed circuit supply voltage Vc = 1.004 ± 0.001 volts

Load resistor R_L = 3.96 KΩ

Table 64 Variation in sensor conductance on exposure to different ambient test atmospheres

Test procedure	Heater voltage 5.0V			Heater voltage 7.0V		
	711	812	813	711	812	813
	Sensor conductance G (siemens)					
Through magnesium perchlorate and heated catalyst A.	6.33×10^{-7}	1.78×10^{-6}	5.94×10^{-6}	8.87×10^{-7}	2.50×10^{-5}	2.33×10^{-4}
Heated catalyst removed B.	7.85×10^{-7}	2.29×10^{-6}	7.81×10^{-6}	1.04×10^{-6}	2.65×10^{-5}	2.39×10^{-4}
Magnesium perchlorate removed and heated catalyst introduced C.	4.62×10^{-6}	3.32×10^{-6}	1.08×10^{-5}	1.78×10^{-6}	2.90×10^{-5}	2.53×10^{-4}
Heated catalyst removed D.	9.98×10^{-6}	4.37×10^{-6}	1.55×10^{-5}	2.55×10^{-6}	3.19×10^{-5}	2.68×10^{-4}
Water bubblers and heated catalyst introduced E.	1.38×10^{-5}	5.41×10^{-6}	1.81×10^{-5}	5.68×10^{-6}	4.88×10^{-5}	3.95×10^{-4}
Heated catalyst removed F.	8.87×10^{-5}	2.32×10^{-5}	2.93×10^{-5}	2.48×10^{-5}	6.31×10^{-5}	4.30×10^{-4}
Synthetic air introduced G.	6.58×10^{-7}	1.91×10^{-6}	6.21×10^{-6}	9.12×10^{-7}	2.53×10^{-5}	2.33×10^{-4}

Table 65 Effect of different ambient test atmospheres on percentage conductance change

Atmosphere dependence	Heater voltage 5.0V			Heater voltage 7.0V		
	711	812	813	711	812	813
	Percentage conductance change (%ΔG)					
Response to residual water vapour (C-A/A)x100%	630	87	82	101	16	9
Response to saturated water vapour (E-A/A)x100%	2080	204	205	540	95	70
Response to contaminants in dry air (B-A/A)x100%	24	29	31	17	6	3
Response to contaminants and residual water vapour (D-A/A)x100%	1477	146	161	187	28	15
Response to contaminants and saturated water vapour (F-A/A)x100%	13918	1203	393	2696	152	85

Table 66 Measurements of voltage drop across sensor load resistor at different oxygen concentrations

Oxygen concentration (%)	Heater voltage 5.0V			Heater voltage 7.0V		
	711	812	813	711	812	813
	Voltage drop (mV)					
0.14	15	41	137	34	519	906
0.33	12	30	108	22	421	862
0.71	8.6	24	81	15	336	817
2.01	6.0	16	55	10	235	730
7.10	3.6	9.2	34	5.4	142	595
20.90	2.5	6.5	22	3.5	90	374
49.00	1.9	4.7	16	2.3	63	359
75.00	1.4	4.0	14	1.6	51	312

Table 67 Effect of individual coal combustion products on sensor sensitivity as a function of heater voltage

(i)

Test gas	Type 711					Type 812					Type 813				
Heater voltage(Vh)	5.0	5.5	6.0	6.5	7.0	5.0	5.5	6.0	6.5	7.0	5.0	5.5	6.0	6.5	7.0
Carbon monoxide															
G; Dry air	6.33×10^{-7}	6.84×10^{-7}	7.34×10^{-7}	7.85×10^{-7}	8.87×10^{-7}	1.65×10^{-6}	3.33×10^{-6}	6.48×10^{-6}	1.38×10^{-5}	2.38×10^{-5}	6.21×10^{-6}	1.36×10^{-5}	3.64×10^{-5}	9.20×10^{-5}	2.15×10^{-4}
G; Dry air/ 1000ppm CO	2.81×10^{-6}	3.07×10^{-6}	3.33×10^{-6}	3.33×10^{-6}	3.85×10^{-6}	4.37×10^{-6}	8.62×10^{-6}	1.58×10^{-5}	3.25×10^{-5}	5.36×10^{-5}	8.88×10^{-6}	1.90×10^{-5}	4.52×10^{-5}	1.04×10^{-5}	2.34×10^{-4}
ΔG	2.18×10^{-6}	2.39×10^{-6}	2.60×10^{-6}	2.55×10^{-6}	2.96×10^{-6}	2.72×10^{-6}	5.29×10^{-6}	9.32×10^{-6}	1.87×10^{-5}	2.29×10^{-5}	2.67×10^{-6}	5.40×10^{-6}	8.80×10^{-6}	1.20×10^{-5}	1.90×10^{-5}
%ΔG	3.44×10^{2}	3.49×10^{2}	3.54×10^{2}	3.25×10^{2}	3.34×10^{2}	1.65×10^{2}	1.59×10^{2}	1.44×10^{2}	1.36×10^{2}	1.25×10^{2}	4.30×10^{1}	3.97×10^{1}	2.42×10^{1}	1.30×10^{1}	8.84
G; Wet air	1.33×10^{-5}	1.03×10^{-5}	8.08×10^{-6}	6.74×10^{-6}	5.15×10^{-6}	5.42×10^{-6}	1.39×10^{-5}	2.05×10^{-5}	3.81×10^{-5}	4.81×10^{-5}	1.84×10^{-5}	3.97×10^{-5}	8.92×10^{-5}	1.76×10^{-4}	3.98×10^{-4}
ΔG	1.27×10^{-5}	9.57×10^{-6}	7.35×10^{-6}	5.96×10^{-6}	4.26×10^{-6}	3.77×10^{-6}	1.06×10^{-5}	1.40×10^{-5}	2.43×10^{-5}	2.43×10^{-5}	1.22×10^{-5}	2.61×10^{-5}	5.28×10^{-5}	8.40×10^{-5}	1.83×10^{-4}
%ΔG	2.01×10^{3}	1.40×10^{3}	1.00×10^{3}	7.59×10^{2}	4.80×10^{2}	2.28×20^{2}	3.18×10^{2}	2.16×10^{2}	1.76×10^{2}	1.02×10^{2}	1.96×10^{2}	1.92×10^{2}	1.45×10^{2}	9.13×10^{1}	8.51×10^{1}
G; Wet air/ 1000ppm CO	7.57×10^{-4}	6.18×10^{-4}	5.08×10^{-4}	4.67×10^{-4}	4.26×10^{-4}	4.60×10^{-5}	7.00×10^{-5}	1.02×10^{-4}	1.81×10^{-4}	2.39×10^{-4}	4.32×10^{-5}	8.46×10^{-5}	1.70×10^{-4}	2.65×10^{-4}	4.92×10^{-4}
ΔG	7.56×10^{-4}	6.17×10^{-4}	5.07×10^{-4}	4.66×10^{-4}	4.25×10^{-4}	4.43×10^{-5}	6.67×10^{-5}	9.55×10^{-5}	1.67×10^{-4}	2.15×10^{-4}	3.70×10^{-5}	7.10×10^{-5}	1.34×10^{-4}	1.73×10^{-4}	2.77×10^{-4}
%ΔG	1.19×10^{5}	9.02×10^{4}	6.91×10^{4}	5.94×10^{4}	4.79×10^{4}	2.68×10^{3}	2.00×10^{3}	1.47×10^{3}	1.21×10^{3}	9.04×10^{2}	5.96×10^{2}	5.22×10^{2}	3.68×10^{2}	1.88×10^{2}	1.29×10^{2}
Hydrogen															
G; Dry air	6.58×10^{-7}	7.09×10^{-7}	7.60×10^{-7}	8.11×10^{-7}	9.38×10^{-7}	1.75×10^{-6}	3.33×10^{-6}	5.94×10^{-5}	1.30×10^{-5}	2.50×10^{-5}	5.68×10^{-6}	1.47×10^{-5}	3.57×10^{-5}	8.92×10^{-5}	2.25×10^{-4}
G; Dry air/ 1000ppm H_2	4.37×10^{-4}	4.86×10^{-4}	5.47×10^{-4}	5.57×10^{-4}	5.72×10^{-4}	1.74×10^{-3}	1.85×10^{-3}	1.89×10^{-3}	2.00×10^{-3}	2.09×10^{-3}	4.10×10^{-4}	5.31×10^{-4}	5.65×10^{-4}	5.98×10^{-4}	6.09×10^{-4}
ΔG	4.36×10^{-4}	4.85×10^{-7}	5.46×10^{-4}	5.56×10^{-4}	5.71×10^{-3}	1.74×10^{-3}	1.85×10^{-3}	1.88×10^{-3}	1.99×10^{-3}	2.07×10^{-3}	4.04×10^{-4}	5.16×10^{-4}	5.29×10^{-4}	5.09×10^{-4}	3.84×10^{-4}
%ΔG	6.63×10^{4}	6.84×10^{4}	7.18×10^{4}	6.86×10^{4}	6.08×10^{4}	9.94×10^{4}	5.56×10^{4}	3.17×10^{4}	1.53×10^{4}	8.28×10^{3}	7.11×10^{3}	3.51×10^{3}	1.48×10^{3}	5.71×10^{2}	1.71×10^{2}
G; Wet air	1.39×10^{-5}	1.13×10^{-5}	8.62×10^{-6}	7.01×10^{-6}	5.68×10^{-6}	5.94×10^{-6}	1.08×10^{-5}	1.96×10^{-5}	3.91×10^{-5}	4.99×10^{-5}	1.84×10^{-5}	4.04×10^{-5}	8.78×10^{-5}	1.78×10^{-4}	4.14×10^{-4}
ΔG	1.32×10^{-5}	1.06×10^{-5}	7.86×10^{-6}	6.20×10^{-6}	4.74×10^{-6}	4.19×10^{-6}	7.47×10^{-6}	1.37×10^{-5}	2.61×10^{-5}	2.24×10^{-5}	1.27×10^{-5}	2.57×10^{-5}	5.21×10^{-5}	8.88×10^{-5}	1.89×10^{-5}
%ΔG	2.01×10^{3}	1.50×10^{3}	1.03×10^{3}	7.64×10^{2}	5.05×10^{2}	2.39×10^{2}	2.24×10^{2}	2.31×10^{2}	2.01×10^{2}	9.96×10^{1}	2.24×10^{2}	1.74×10^{2}	1.46×10^{2}	9.95×10^{1}	8.40×10^{1}
G; Wet air/ 1000ppm H_2	1.44×10^{-3}	2.09×10^{-3}	3.76×10^{-3}	4.18×10^{-3}	5.36×10^{-3}	1.78×10^{-3}	1.74×10^{-3}	1.92×10^{-3}	2.09×10^{-3}	2.25×10^{-3}	4.30×10^{-4}	5.47×10^{-4}	6.21×10^{-4}	6.76×10^{-4}	8.04×10^{-4}
ΔG	1.44×10^{-3}	2.09×10^{-3}	3.76×10^{-3}	4.18×10^{-3}	5.36×10^{-3}	1.78×10^{-3}	1.74×10^{-3}	1.91×10^{-3}	2.08×10^{-3}	2.23×10^{-5}	4.24×10^{-4}	5.32×10^{-4}	5.68×10^{-4}	5.87×10^{-4}	5.79×10^{-4}
%ΔG	2.19×10^{5}	2.94×10^{5}	4.95×10^{5}	5.15×10^{5}	5.71×10^{5}	1.02×10^{5}	5.23×10^{4}	3.21×10^{4}	1.60×10^{4}	8.92×10^{3}	7.46×10^{3}	3.61×10^{3}	1.59×10^{3}	6.58×10^{2}	2.57×10^{2}

Table 67 Effect of individual coal combustion products on sensor sensitivity as a function of heater voltage

(ii)

Test gas	Type 711					Type 812					Type 813				
Heater voltage(Vh)	5.0	5.5	6.0	6.5	7.0	5.0	5.5	6.0	6.5	7.0	5.0	5.5	6.0	6.5	7.0
Ethene															
G; Dry air	6.58×10^{-7}	6.84×10^{-7}	7.34×10^{-7}	8.36×10^{-7}	9.12×10^{-7}	1.70×10^{-6}	3.59×10^{-6}	5.42×10^{-6}	1.27×10^{-5}	2.59×10^{-5}	6.48×10^{-6}	1.44×10^{-5}	3.44×10^{-5}	9.20×10^{-5}	2.19×10^{-4}
G; Dry air/ 1000ppm C_2H_4	2.81×10^{-6}	5.15×10^{-6}	1.64×10^{-5}	3.15×10^{-5}	5.17×10^{-5}	5.94×10^{-6}	1.36×10^{-5}	2.59×10^{-5}	7.71×10^{-5}	1.47×10^{-4}	3.97×10^{-5}	6.43×10^{-5}	1.18×10^{-4}	2.74×10^{-4}	5.89×10^{-4}
ΔG	2.15×10^{-6}	4.47×10^{-6}	1.57×10^{-5}	3.07×10^{-5}	5.08×10^{-5}	4.24×10^{-6}	1.00×10^{-5}	2.05×10^{-5}	6.44×10^{-5}	1.21×10^{-4}	3.32×10^{-5}	4.99×10^{-5}	8.36×10^{-5}	1.82×10^{-4}	3.70×10^{-4}
$\%\Delta G$	3.27×10^{2}	6.53×10^{2}	2.14×10^{3}	3.67×10^{3}	5.57×10^{3}	2.49×10^{2}	2.79×10^{2}	3.78×10^{2}	5.07×10^{2}	4.67×10^{2}	5.12×10^{2}	3.47×10^{2}	2.43×10^{2}	1.98×10^{2}	1.69×10^{2}
G; Wet air	1.41×10^{-5}	1.11×10^{-5}	8.08×10^{-6}	7.54×10^{-6}	5.68×10^{-6}	5.94×10^{-6}	1.25×10^{-5}	2.02×10^{-5}	3.77×10^{-5}	4.85×10^{-5}	1.70×10^{-5}	4.15×10^{-5}	8.87×10^{-5}	1.75×10^{-4}	4.07×10^{-4}
ΔG	1.34×10^{-5}	1.04×10^{-5}	7.35×10^{-6}	6.70×10^{-6}	4.77×10^{-6}	4.24×10^{-6}	8.91×10^{-6}	1.48×10^{-5}	2.50×10^{-5}	2.26×10^{-5}	1.05×10^{-5}	2.71×10^{-5}	5.43×10^{-5}	8.30×10^{-5}	1.88×10^{-4}
$\%\Delta G$	2.04×10^{3}	1.52×10^{3}	1.00×10^{3}	8.01×10^{2}	5.23×10^{2}	2.49×10^{2}	2.48×10^{2}	2.73×10^{2}	1.97×10^{2}	8.72×10^{1}	1.62×10^{2}	1.88×10^{2}	1.58×10^{2}	9.02×10^{1}	8.58×10^{1}
G; Wet air/ 1000ppm C_2H_4	1.42×10^{-4}	1.70×10^{-4}	2.25×10^{-4}	2.53×10^{-4}	3.49×10^{-4}	2.84×10^{-5}	5.73×10^{-5}	8.60×10^{-5}	1.83×10^{-4}	2.54×10^{-4}	4.67×10^{-5}	9.38×10^{-5}	1.91×10^{-4}	4.12×10^{-4}	7.58×10^{-4}
ΔG	1.41×10^{-4}	1.69×10^{-4}	2.24×10^{-4}	2.52×10^{-4}	3.48×10^{-4}	2.67×10^{-5}	5.37×10^{-5}	8.06×10^{-5}	1.70×10^{-4}	2.28×10^{-4}	4.02×10^{-5}	7.94×10^{-5}	1.57×10^{-4}	3.20×10^{-4}	5.39×10^{-4}
$\%\Delta G$	2.14×10^{4}	2.47×10^{4}	3.05×10^{4}	3.01×10^{4}	3.82×10^{4}	1.57×10^{3}	1.50×10^{3}	1.49×10^{3}	1.34×10^{3}	8.80×10^{2}	6.20×10^{2}	5.51×10^{2}	4.56×10^{2}	3.48×10^{2}	2.46×10^{2}
Propene															
G; Dry air	6.33×10^{-7}	7.09×10^{-7}	7.34×10^{-7}	8.11×10^{-7}	9.12×10^{-7}	1.83×10^{-6}	3.59×10^{-6}	6.48×10^{-6}	1.44×10^{-5}	2.50×10^{-5}	5.42×10^{-6}	1.41×10^{-5}	3.41×10^{-5}	9.43×10^{-5}	2.24×10^{-4}
G; Dry air/ 1000ppm C_3H_6	5.15×10^{-6}	7.81×10^{-6}	2.26×10^{-5}	4.81×10^{-5}	6.71×10^{-5}	8.81×10^{-6}	1.90×10^{-5}	3.81×10^{-5}	9.25×10^{-5}	1.83×10^{-4}	5.21×10^{-5}	9.87×10^{-5}	1.75×10^{-4}	3.95×10^{-4}	8.60×10^{-4}
ΔG	4.52×10^{-6}	7.10×10^{-6}	2.18×10^{-5}	4.73×10^{-5}	6.62×10^{-5}	6.98×10^{-6}	1.54×10^{-5}	3.16×10^{-5}	7.81×10^{-5}	1.58×10^{-4}	4.67×10^{-5}	8.46×10^{-5}	1.40×10^{-4}	3.01×10^{-4}	6.36×10^{-4}
$\%\Delta G$	7.14×10^{2}	1.00×10^{3}	2.97×10^{3}	5.83×10^{3}	7.25×10^{3}	3.81×10^{2}	4.29×10^{2}	4.88×10^{2}	5.42×10^{2}	6.32×10^{2}	8.62×10^{2}	6.00×10^{2}	4.12×10^{2}	3.19×10^{2}	2.84×10^{2}
G; Wet air	1.33×10^{-5}	1.16×10^{-5}	8.89×10^{-6}	6.47×10^{-6}	5.42×10^{-6}	5.94×10^{-6}	1.22×10^{-5}	1.96×10^{-5}	3.87×10^{-5}	5.10×10^{-5}	1.78×10^{-5}	4.18×10^{-5}	8.97×10^{-5}	1.73×10^{-4}	3.95×10^{-4}
ΔG	1.27×10^{-5}	1.09×10^{-5}	8.16×10^{-6}	5.66×10^{-6}	4.51×10^{-6}	4.11×10^{-6}	8.61×10^{-6}	1.31×10^{-5}	2.43×10^{-5}	2.60×10^{-5}	1.24×10^{-5}	2.77×10^{-5}	5.56×10^{-5}	7.87×10^{-5}	1.71×10^{-4}
$\%\Delta G$	2.01×10^{3}	1.54×10^{3}	1.11×10^{3}	6.98×10^{2}	4.95×10^{2}	2.25×10^{2}	2.40×10^{2}	2.02×10^{2}	1.69×10^{2}	1.04×10^{2}	2.29×10^{2}	1.96×10^{2}	1.63×10^{2}	8.35×10^{1}	7.63×10^{1}
G; Wet air/ 1000ppm C_3H_6	1.83×10^{-4}	2.15×10^{-4}	2.55×10^{-4}	3.12×10^{-4}	3.97×10^{-4}	4.92×10^{-5}	8.24×10^{-5}	1.24×10^{-4}	2.53×10^{-4}	3.95×10^{-4}	6.59×10^{-5}	1.31×10^{-4}	2.20×10^{-4}	4.97×10^{-4}	9.79×10^{-4}
ΔG	1.82×10^{-4}	2.14×10^{-4}	2.54×10^{-4}	3.11×10^{-4}	3.96×10^{-4}	4.74×10^{-5}	7.88×10^{-5}	1.17×10^{-4}	2.39×10^{-4}	3.70×10^{-4}	6.05×10^{-5}	1.17×10^{-4}	1.86×10^{-4}	4.03×10^{-4}	7.55×10^{-4}
$\%\Delta G$	2.88×10^{4}	3.02×10^{4}	3.46×10^{4}	3.83×10^{4}	4.34×10^{4}	2.59×10^{3}	2.20×10^{3}	1.81×10^{3}	1.66×10^{3}	1.48×10^{3}	1.12×10^{3}	8.29×10^{2}	5.45×10^{2}	4.27×10^{2}	3.37×10^{2}

these sensors have been shown by Kennedy to be exceptionally limited.[131] He reported that, at a wind speed of 2 m sec^{-1} the maximum height of the 60°C contour from a fire producing 27kw to be only 14 inches and this was reached three feet downwind of the fire. The sensors are usually installed near the roof of a roadway and are regarded to be more of a strategic defence against open fire than a spontaneous combustion detection system.

1.6.3 Smoke Detection[132,133]

The first smoke detectors were introduced underground in 1962, their method of operation is as follows:

The detector consists of two electrodes connected to a D.C. source. The air between the electrodes is ionised by alpha particles emitted from an Americium radioactive source, (Am 241). The ions thus produced travel towards their respective electrodes with a velocity determined by their mass and the electrostatic field present. When particulate combustion products enter the detector they collide with the ions to produce a heavier charged species, their drift velocity is reduced and thus the ionisation current decreases.

The early detectors were found in practice to be very sensitive to high humidity and dusty atmospheres which resulted in instability and false alarms. Design modifications to improve performance resulted in the introduction of a new model in 1975. This overcame many of the earlier problems but it was shown to be unreliable under certain conditions and has therefore been used mainly as a warning type device.

Table 7

References in Legislation to Specific Concentration of Firedamp

Authority	Amount of Gas	Requirement
Ventilation Reg. 2	0-0.25% firedamp	Every intake airway the air of which has not ventilated another working place shall normally be kept free from inflammable gas up to within 300 feet of the first working place.
Loco. Reg. 14(1) (b) (i)	0.2% firedamp	Locomotive roadways ventilated with fresh air and containing not more than 0.2% firedamp over a period of thirty consecutive days need only be sampled at intervals not exceeding thirty days.
Vent. Reg. 2(2)	0.25% firedamp	If six samples taken by an inspector at not less than fortnightly intervals in the general body of the air in an intake airway up to 300 feet from the first working place average not more than 0.25% firedamp the roadway may be classified "free from inflammable gas".
Vent. Reg.13	0.5% firedamp	If the last six statutory determinations in a return airway 30 feet from the face exceed this level, a specified proportion of the firedamp detectors required by Ventilation Reg. 12(1) must be automatic detectors.
Loco. Reg. 14(1) (b) (ii) Vent. Reg. 7(1) (b)	0.6% firedamp	Locomotive roadways (other than those ventilated with fresh air), and also places sampled because either electricity is in use or because shots are fired, need be sampled only every thirty days if every result obtained in the previous thirty days is not more than 0.6%. Weekly sampling must be recommenced when any figure exceeds 0.6%.
Loco. Reg.14(1) (a) Vent. Reg. 7(1) (a)	0.8% firedamp	If any sample taken by virtue of the Locomotive Regulations or of the Ventilation Regulations relating to the use of either shot firing or electricity shows more than 0.8% samples must be taken at intervals not exceeding 24 hours for the next seven following working days.
Vent. Reg. 8(2)	1.0% firedamp	The Manager must inform the Inspector of any occasion other than when determinations are made at junctions in return airways in accordance with Vent. Reg. 7(A), when this concentration of firedamp if found to be exceeded unless the Inspector has otherwise directed or the excess was due to a temporary derangement of the ventilation.
Section 68(1) Elec. Reg. 6(1) and (3) (as amended 1967) Exp. Reg. 47(1) to (5) Loco. Reg. 16 Section 79(1) and (5)(b)	1.25% firedamp	(i) This is the upper limit that Regulations may prescribe as the concentration above which electricity must be cut off. (ii) Above 1.25% a person must either cut off the electricity from all electrical apparatus (other than telephone or signalling or any apparatus for detecting inflammable gas, including ancillary apparatus) or report to someone who is empowered to do so. Also, when the concentration falls to this level, the senior official on duty may restore the electricity supply. (iii) Shotfiring is prohibited on the return side of any point showing a greater firedamp content. (iv) Locomotive running must be discontinued if any determination of firedamp exceeds 1.25% until the Manager so directs. (v) In mines other than safety lamp mines men must be withdrawn from the affected area.
Section 79(5) (a) Firedamp drainage Reg. 13 (e)	2.0% firedamp	(i) In a safety lamp mine 2.0% is deemed to be "excessive concentration" and men must be withdrawn from the area. (ii) In an area where firedamp is vented from a drainage system into an underground roadway must be fenced.
Firedamp drainage Reg. 15 (c)	40.0% firedamp	Firedamp must not be discharged to a utilisation plant if it contains less than 40% flammable gas.

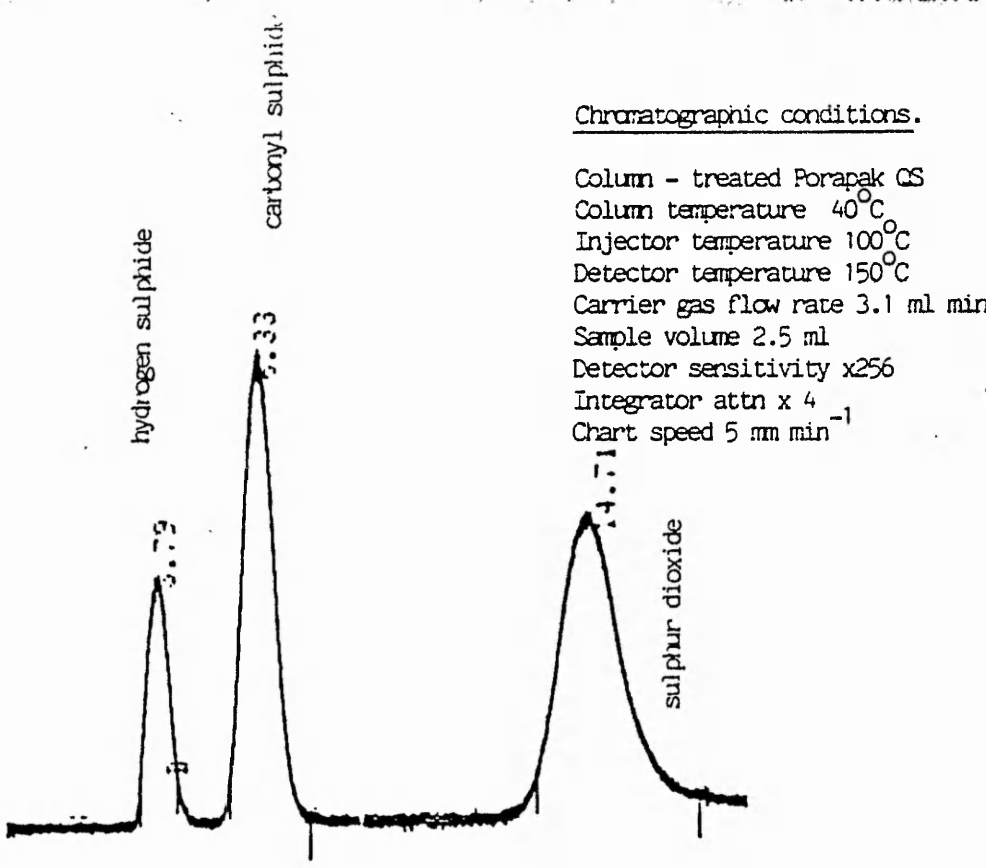

Figure 24a. Chromatogram of sulphur gases at optimum carrier ga velocity.

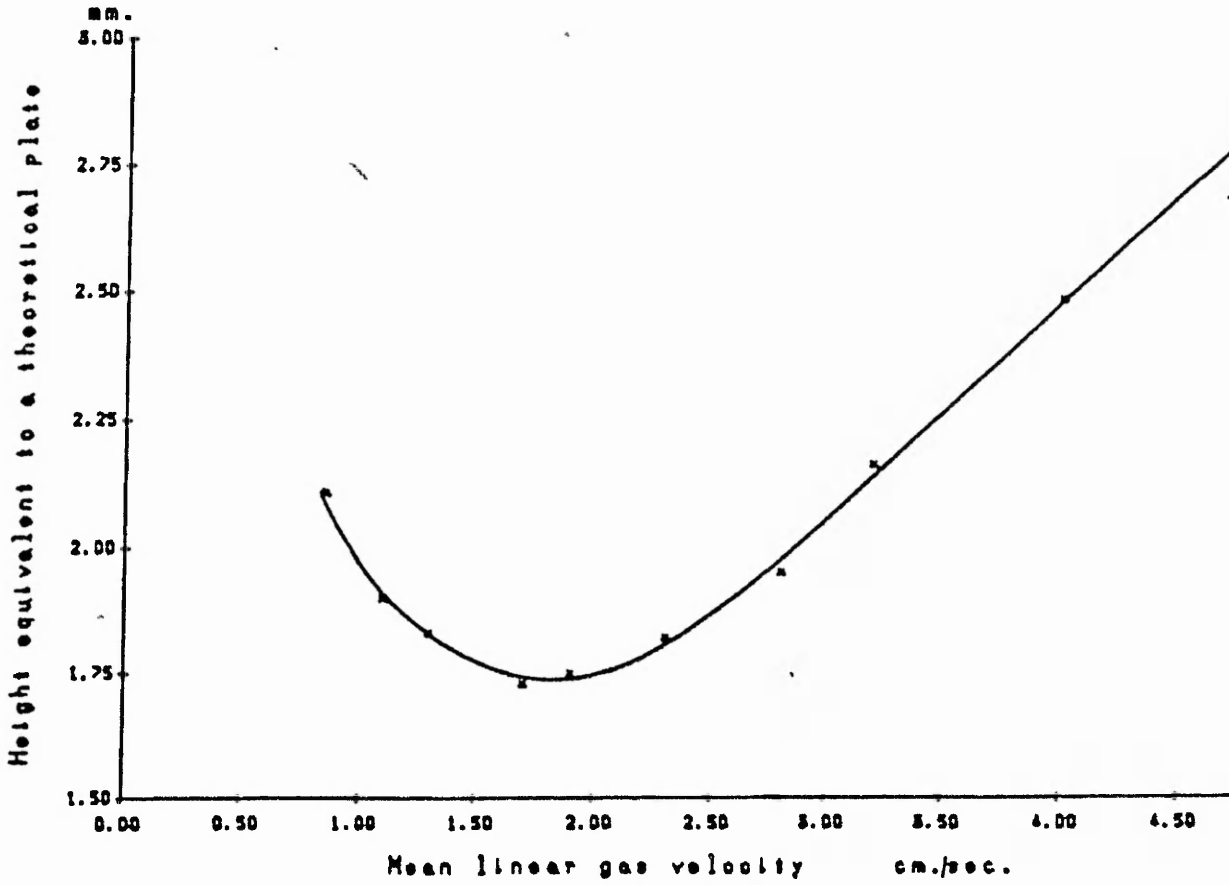

Figure 24b. Effect of carrier gas velocity upon HETP for carbonyl sulphide at 40°C on treated Porapak QS.

Table 67 Effect of individual coal combustion products on sensor sensitivity as a function of heater voltage

(iii)

Test gas	Type 711					Type 812					Type 813				
Heater voltage(Vh)	5.0	5.5	6.0	6.5	7.0	5.0	5.5	6.0	6.5	7.0	5.0	5.5	6.0	6.5	7.0
Benzene															
G; Dry air	6.84×10^{-7}	7.09×10^{-7}	7.60×10^{-7}	8.36×10^{-7}	9.12×10^{-7}	1.65×10^{-6}	3.07×10^{-6}	6.21×10^{-6}	1.33×10^{-5}	2.50×10^{-5}	5.68×10^{-6}	1.33×10^{-5}	3.38×10^{-5}	9.10×10^{-5}	2.28×10^{-4}
G; Dry air/ 1000ppm C_6H_6	1.32×10^{-6}	2.06×10^{-6}	5.68×10^{-6}	1.61×10^{-5}	2.26×10^{-5}	1.44×10^{-5}	2.81×10^{-5}	6.67×10^{-5}	1.47×10^{-4}	2.65×10^{-4}	7.89×10^{-5}	1.36×10^{-4}	2.65×10^{-4}	5.89×10^{-4}	1.23×10^{-3}
ΔG	6.36×10^{-7}	1.35×10^{-6}	4.92×10^{-6}	1.52×10^{-5}	2.17×10^{-5}	1.28×10^{-5}	2.50×10^{-5}	6.05×10^{-5}	1.34×10^{-4}	2.40×10^{-4}	7.32×10^{-5}	1.23×10^{-4}	2.31×10^{-4}	4.98×10^{-4}	1.00×10^{-3}
$\%\Delta G$	9.30×10^{1}	1.90×10^{2}	6.47×10^{2}	1.82×10^{3}	2.38×10^{3}	7.76×10^{2}	8.14×10^{2}	9.74×10^{2}	1.01×10^{3}	9.60×10^{2}	1.29×10^{3}	9.25×10^{2}	6.83×10^{2}	5.47×10^{2}	4.39×10^{2}
G; Wet air	1.33×10^{-5}	1.08×10^{-5}	8.62×10^{-6}	7.27×10^{-6}	5.68×10^{-6}	5.68×10^{-6}	1.16×10^{-5}	1.99×10^{-5}	3.74×10^{-5}	4.92×10^{-5}	1.84×10^{-5}	4.08×10^{-5}	9.15×10^{-5}	1.81×10^{-4}	3.88×10^{-4}
ΔG	1.26×10^{-5}	1.01×10^{-5}	7.86×10^{-6}	6.43×10^{-6}	4.77×10^{-6}	4.03×10^{-6}	8.53×10^{-6}	1.37×10^{-5}	2.41×10^{-5}	2.42×10^{-5}	1.27×10^{-5}	2.75×10^{-5}	5.77×10^{-5}	9.00×10^{-5}	1.60×10^{-4}
$\%\Delta G$	1.84×10^{3}	1.42×10^{3}	1.03×10^{3}	7.69×10^{2}	5.23×10^{2}	2.44×10^{2}	2.78×10^{2}	2.21×10^{2}	1.81×10^{2}	9.68×10^{1}	2.24×10^{2}	2.07×10^{2}	1.71×10^{2}	9.89×10^{1}	7.02×10^{1}
G; Wet air/ 1000ppm C_6H_6	1.64×10^{-5}	2.47×10^{-5}	3.97×10^{-5}	8.02×10^{-5}	1.08×10^{-4}	1.13×10^{-4}	1.87×10^{-4}	2.74×10^{-4}	3.42×10^{-4}	5.42×10^{-4}	1.62×10^{-4}	1.92×10^{-4}	3.02×10^{-4}	6.49×10^{-4}	1.59×10^{-3}
ΔG	1.60×10^{-5}	2.40×10^{-5}	3.89×10^{-5}	7.94×10^{-5}	1.07×10^{-4}	1.11×10^{-4}	1.84×10^{-4}	2.68×10^{-4}	3.29×10^{-4}	5.17×10^{-4}	1.56×10^{-4}	1.79×10^{-4}	2.68×10^{-4}	5.58×10^{-4}	1.36×10^{-3}
$\%\Delta G$	2.34×10^{3}	3.39×10^{3}	5.12×10^{3}	9.50×10^{3}	1.17×10^{4}	6.73×10^{3}	5.99×10^{3}	4.32×10^{3}	2.47×10^{3}	2.07×10^{3}	2.75×10^{3}	1.35×10^{3}	7.93×10^{2}	6.13×10^{2}	5.96×10^{2}
Toluene															
G; Dry air	6.07×10^{-7}	6.58×10^{-7}	7.34×10^{-7}	8.11×10^{-7}	9.12×10^{-7}	1.68×10^{-7}	3.07×10^{-6}	6.21×10^{-6}	1.30×10^{-5}	2.50×10^{-5}	5.68×10^{-6}	1.44×10^{-5}	3.51×10^{-5}	9.01×10^{-5}	2.33×10^{3}
G; Dry air/ 1000ppm C_7H_8	*	1.22×10^{-6}	2.55×10^{-6}	8.08×10^{-6}	1.58×10^{-5}	1.73×10^{-5}	3.19×10^{-5}	7.33×10^{-5}	1.68×10^{-4}	3.36×10^{-4}	1.06×10^{-4}	1.79×10^{-4}	3.42×10^{-4}	7.42×10^{-4}	1.59×10^{-3}
ΔG	*	5.62×10^{-7}	1.86×10^{-6}	7.27×10^{-6}	1.49×10^{-5}	1.56×10^{-5}	2.88×10^{-5}	6.71×10^{-5}	1.55×10^{-4}	3.11×10^{-4}	1.00×10^{-4}	1.65×10^{-4}	3.07×10^{-4}	6.52×10^{-4}	1.36×10^{-3}
$\%\Delta G$	*	8.54×10^{1}	2.48×10^{2}	8.96×10^{2}	1.63×10^{3}	9.29×10^{2}	9.38×10^{2}	1.08×10^{3}	1.19×10^{3}	1.24×10^{3}	1.76×10^{3}	1.15×10^{3}	8.75×10^{2}	7.24×10^{2}	5.84×10^{2}
G; Wet air	1.39×10^{-5}	1.03×10^{-5}	8.89×10^{-6}	7.01×10^{-6}	5.68×10^{-6}	5.42×10^{-6}	1.16×10^{-5}	1.93×10^{-5}	3.91×10^{-5}	4.88×10^{-5}	1.73×10^{-5}	3.97×10^{-5}	8.78×10^{-5}	1.75×10^{-4}	3.95×10^{-4}
ΔG	1.33×10^{-5}	9.64×10^{-6}	8.16×10^{-6}	6.20×10^{-6}	4.77×10^{-6}	3.74×10^{-6}	8.53×10^{-6}	1.31×10^{-5}	2.61×10^{-5}	2.38×10^{-5}	1.16×10^{-6}	2.53×10^{-5}	5.36×10^{-5}	8.49×10^{-5}	1.62×10^{-4}
$\%\Delta G$	2.19×10^{3}	1.47×10^{3}	1.11×10^{3}	7.64×10^{2}	5.23×10^{2}	2.23×10^{2}	2.78×10^{2}	2.11×10^{2}	2.01×10^{2}	9.52×10^{1}	2.04×10^{2}	1.76×10^{2}	1.53×10^{2}	9.42×10^{1}	6.95×10^{1}
G; Wet air/ 1000ppm C_7H_8	1.47×10^{-5}	1.61×10^{-5}	2.74×10^{-5}	4.39×10^{-5}	6.51×10^{-5}	1.43×10^{-4}	2.25×10^{-4}	3.02×10^{-4}	4.69×10^{-4}	7.04×10^{-4}	1.76×10^{-4}	2.44×10^{-4}	4.14×10^{-4}	8.31×10^{-4}	1.78×10^{-3}
ΔG	1.41×10^{-5}	1.54×10^{-5}	2.67×10^{-5}	4.31×10^{-5}	6.42×10^{-5}	1.41×10^{-4}	2.22×10^{-4}	2.96×10^{-4}	4.56×10^{-4}	6.79×10^{-4}	1.70×10^{-4}	2.30×10^{-4}	3.79×10^{-4}	7.41×10^{-4}	1.55×10^{-4}
$\%\Delta G$	2.42×10^{3}	2.34×10^{3}	3.64×10^{3}	5.41×10^{3}	7.04×10^{3}	8.39×10^{3}	7.23×10^{3}	4.77×10^{3}	3.51×10^{3}	2.72×10^{3}	2.99×10^{3}	1.60×10^{3}	1.08×10^{3}	8.22×10^{2}	6.65×10^{2}

Table 67 Effect of individual coal combustion products on sensor sensitivity as a function of heater voltage

(iv)

Test gas	Type 711					Type 812					Type 813				
Heater voltage(Vh)	5.0	5.5	6.0	6.5	7.0	5.0	5.5	6.0	6.5	7.0	5.0	5.5	6.0	6.5	7.0
Methylcyclohexane															
G; Dry air	6.07×10^{-7}	6.84×10^{-7}	7.34×10^{-7}	7.60×10^{-7}	8.11×10^{-7}	1.65×10^{-6}	3.07×10^{-6}	5.68×10^{-6}	1.36×10^{-5}	2.59×10^{-5}	6.74×10^{-6}	1.55×10^{-5}	3.28×10^{-5}	9.06×10^{-5}	2.34×10^{-4}
G; Dry air/ 1000ppm C_7H_{14}	1.17×10^{-6}	1.88×10^{-6}	8.62×10^{-6}	2.05×10^{-5}	3.12×10^{-5}	5.15×10^{-6}	1.08×10^{-5}	2.19×10^{-5}	5.36×10^{-5}	1.07×10^{-4}	3.35×10^{-5}	6.71×10^{-5}	1.10×10^{-4}	2.53×10^{-4}	4.09×10^{-4}
ΔG	5.63×10^{-7}	1.20×10^{-6}	7.89×10^{-6}	1.97×10^{-5}	3.04×10^{-5}	3.50×10^{-6}	7.73×10^{-6}	1.62×10^{-5}	4.00×10^{-5}	8.11×10^{-5}	2.68×10^{-5}	5.16×10^{-5}	7.72×10^{-5}	1.62×10^{-4}	1.75×10^{-4}
%ΔG	9.28×10^{1}	1.75×10^{2}	1.07×10^{3}	2.59×10^{3}	3.75×10^{3}	2.12×10^{2}	2.52×10^{2}	2.85×10^{2}	2.94×10^{2}	3.13×10^{2}	3.97×10^{2}	3.33×10^{2}	2.35×10^{2}	1.78×10^{2}	7.48×10^{1}
G; Wet air	1.30×10^{-5}	1.03×10^{-5}	8.08×10^{-6}	7.27×10^{-6}	5.94×10^{-6}	5.94×10^{-6}	1.16×10^{-5}	1.93×10^{-5}	3.87×10^{-5}	5.14×10^{-5}	1.76×10^{-5}	4.32×10^{-5}	8.92×10^{-5}	1.81×10^{-4}	3.85×10^{-4}
ΔG	1.24×10^{-5}	9.57×10^{-6}	7.35×10^{-6}	6.51×10^{-6}	5.13×10^{-6}	4.29×10^{-6}	8.53×10^{-6}	1.36×10^{-5}	2.51×10^{-5}	2.55×10^{-5}	1.09×10^{-5}	2.77×10^{-5}	5.64×10^{-5}	9.04×10^{-5}	1.51×10^{-4}
%ΔG	2.04×10^{3}	1.40×10^{3}	1.00×10^{3}	8.57×10^{2}	6.33×10^{2}	2.60×10^{2}	2.78×10^{2}	2.39×10^{2}	1.85×10^{2}	9.84×10^{1}	1.62×10^{2}	1.79×10^{2}	1.72×10^{2}	9.98×10^{1}	6.45×10^{1}
G; Wet air/ 1000ppm C_7H_{14}	1.50×10^{-5}	1.84×10^{-5}	2.23×10^{-5}	4.81×10^{-5}	9.34×10^{-5}	1.13×10^{-5}	2.20×10^{-5}	4.21×10^{-5}	1.04×10^{-4}	2.08×10^{-4}	4.60×10^{-5}	9.34×10^{-5}	1.80×10^{-4}	3.21×10^{-4}	5.37×10^{-4}
ΔG	1.44×10^{-5}	1.77×10^{-5}	2.16×10^{-5}	4.73×10^{-5}	9.26×10^{-5}	9.65×10^{-6}	1.89×10^{-6}	3.64×10^{-5}	9.04×10^{-5}	1.82×10^{-4}	3.93×10^{-5}	7.79×10^{-5}	1.47×10^{-4}	2.30×10^{-4}	3.03×10^{-4}
%ΔG	2.37×10^{3}	2.59×10^{3}	2.94×10^{3}	6.22×10^{3}	1.14×10^{4}	5.85×10^{2}	6.16×10^{2}	6.41×10^{2}	6.65×10^{2}	7.02×10^{2}	5.83×10^{2}	5.03×10^{2}	4.48×10^{2}	2.53×10^{2}	1.29×10^{2}
Carbonyl sulphide															
G; Dry air	6.07×10^{-7}	7.09×10^{-7}	7.34×10^{-7}	8.36×10^{-7}	9.12×10^{-7}	1.57×10^{-6}	2.81×10^{-6}	6.21×10^{-6}	1.36×10^{-5}	2.53×20^{-5}	6.74×10^{-6}	1.41×10^{-5}	3.48×10^{-5}	9.10×10^{-5}	2.25×10^{-4}
G; Dry air/ 1000ppm COS	8.19×10^{-5}	9.97×10^{-5}	1.27×10^{-4}	1.68×10^{-4}	1.91×10^{-4}	6.71×10^{-5}	8.42×10^{-5}	9.01×10^{-5}	9.77×10^{-5}	1.02×10^{-4}	1.04×10^{-4}	1.61×10^{-4}	2.25×10^{-4}	2.57×10^{-4}	3.79×10^{-4}
ΔG	8.13×10^{-5}	9.90×10^{-5}	1.26×10^{-4}	1.67×10^{-4}	1.90×10^{-4}	6.55×10^{-5}	8.14×10^{-5}	8.39×10^{-5}	8.41×10^{-5}	7.67×10^{-4}	9.73×10^{-5}	1.47×10^{-4}	1.90×10^{-4}	1.66×10^{-4}	1.54×10^{-4}
%ΔG	1.34×10^{4}	1.40×10^{4}	1.72×10^{4}	2.00×10^{4}	2.08×10^{4}	4.17×10^{3}	2.90×10^{3}	1.35×10^{3}	6.18×10^{2}	9.88×10^{1}	1.44×10^{3}	1.04×10^{3}	5.46×10^{2}	1.82×10^{2}	6.84×10^{1}
G; Wet air	1.30×10^{-5}	1.05×10^{-5}	8.35×10^{-6}	7.27×10^{-6}	5.42×10^{-6}	6.21×10^{-6}	1.33×10^{-5}	2.08×10^{-5}	3.94×10^{-5}	5.03×10^{-5}	1.64×10^{-5}	4.01×10^{-5}	9.06×10^{-5}	1.76×10^{-4}	3.97×10^{-4}
ΔG	1.24×10^{-5}	9.79×10^{-6}	7.62×10^{-6}	6.43×10^{-6}	4.51×10^{-6}	4.64×10^{-6}	1.05×10^{-5}	1.46×10^{-5}	2.58×10^{-5}	2.50×10^{-5}	9.66×10^{-6}	2.60×10^{-5}	5.58×10^{-5}	8.50×10^{-5}	1.72×10^{-5}
%ΔG	2.04×10^{3}	1.38×10^{3}	1.04×10^{3}	7.69×10^{2}	4.95×10^{2}	2.96×10^{2}	3.74×10^{2}	2.35×10^{2}	1.90×10^{2}	9.88×10^{1}	1.43×10^{2}	1.84×10^{2}	1.60×10^{2}	9.34×10^{1}	7.64×10^{1}
G; Wet air/ 1000ppm COS	2.56×10^{-4}	3.56×10^{-4}	5.39×10^{-4}	7.78×10^{-4}	1.01×10^{-3}	9.82×10^{-5}	1.42×10^{-4}	1.80×10^{-4}	2.05×10^{-4}	2.63×10^{-4}	2.19×10^{-4}	3.33×10^{-4}	3.97×10^{-4}	4.82×10^{-4}	5.67×10^{-4}
ΔG	2.55×10^{-4}	3.55×10^{-4}	5.38×10^{-4}	7.77×10^{-4}	1.01×10^{-3}	9.66×10^{-5}	1.39×10^{-4}	1.74×10^{-4}	1.91×10^{-4}	2.37×10^{-4}	2.12×10^{-4}	3.19×10^{-4}	3.62×10^{-4}	3.91×10^{-4}	3.42×10^{-4}
%ΔG	4.20×10^{4}	5.01×10^{4}	7.33×10^{4}	9.29×10^{4}	1.10×10^{5}	6.15×10^{3}	4.95×10^{3}	2.80×10^{3}	1.40×10^{3}	9.37×10^{2}	3.15×10^{3}	2.26×10^{3}	1.04×10^{3}	4.30×10^{2}	1.52×10^{2}

Table 67 Effect of individual coal combustion products on sensor sensitivity as a function of heater voltage

Test gas	Heater voltage (Vh) (v)	Type 711					Type 812					Type 813				
		5.0	5.5	6.0	6.5	7.0	5.0	5.5	6.0	6.5	7.0	5.0	5.5	6.0	6.5	7.0
Acetone																
G; Dry air		6.07×10^{-7}	6.58×10^{-7}	7.34×10^{-7}	7.60×10^{-7}	8.36×10^{-7}	1.75×10^{-6}	3.07×10^{-6}	6.74×10^{-6}	1.39×10^{-5}	2.47×10^{-5}	5.15×10^{-6}	1.39×10^{-5}	3.71×10^{-5}	9.34×10^{-5}	2.22×10^{-4}
G; Dry air/ 1000ppm C_3H_6O		3.44×10^{-5}	4.56×10^{-5}	6.59×10^{-5}	1.12×10^{-4}	1.42×10^{-4}	7.46×10^{-5}	1.19×10^{-4}	2.07×10^{-4}	3.05×10^{-4}	4.49×10^{-4}	5.14×10^{-5}	1.06×10^{-4}	1.77×10^{-4}	2.53×10^{-4}	3.33×10^{-4}
ΔG		3.38×10^{-5}	4.49×10^{-5}	6.52×10^{-5}	1.11×10^{-4}	1.41×10^{-4}	7.29×10^{-5}	1.16×10^{-4}	2.00×10^{-4}	2.91×10^{-4}	4.24×10^{-4}	4.63×10^{-5}	9.21×10^{-5}	$1.40\times^{2}0^{-4}$	1.60×10^{-4}	1.11×10^{-4}
%ΔG		5.57×10^{3}	6.82×10^{3}	8.88×10^{3}	1.46×10^{4}	1.69×10^{4}	4.17×10^{3}	3.78×10^{3}	2.97×10^{3}	2.09×10^{3}	1.72×10^{3}	8.99×10^{2}	6.63×10^{2}	3.77×10^{2}	1.71×10^{2}	5.00×10^{1}
G; Wet air																
ΔG																
%ΔG																
G; Wet air/ 1000ppm C_3H_6O																
ΔG																
%ΔG																
Methane																
G; Dry air		6.33×10^{-7}	6.84×10^{-7}	7.34×10^{-7}	7.85×10^{-7}	8.87×10^{-7}	1.70×10^{-6}	2.81×10^{-6}	5.94×10^{-6}	1.41×10^{-5}	2.56×10^{-5}	5.42×10^{-6}	1.44×10^{-5}	3.54×10^{-5}	9.10×10^{-5}	2.28×10^{-4}
G; Dry air/ 1.0% CH_4		1.32×10^{-6}	5.51×10^{-6}	1.22×10^{-5}	2.29×10^{-5}	4.39×10^{-5}	5.42×10^{-6}	1.13×10^{-5}	2.84×10^{-5}	8.24×10^{-5}	1.58×10^{-4}	3.97×10^{-5}	8.69×10^{-5}	1.76×10^{-4}	1.72×10^{-4}	6.15×10^{-4}
ΔG		6.87×10^{-7}	4.47×10^{-6}	1.15×10^{-6}	2.21×10^{-5}	4.30×10^{-5}	3.72×10^{-6}	8.49×10^{-6}	2.44×10^{-5}	6.83×10^{-5}	1.32×10^{-4}	3.43×10^{-5}	7.25×10^{-5}	1.41×10^{-4}	2.61×10^{-4}	3.87×10^{-4}
%ΔG		1.09×10^{2}	6.54×10^{2}	1.56×10^{3}	2.82×10^{2}	4.85×10^{3}	2.19×10^{2}	3.02×10^{2}	3.79×10^{2}	4.84×10^{2}	5.16×10^{2}	6.33×10^{2}	5.03×10^{2}	3.98×10^{2}	2.86×10^{2}	1.70×10^{2}
G; Wet air		1.39×10^{-5}	1.08×10^{-5}	8.89×10^{-6}	7.01×10^{-6}	5.15×10^{-6}	4.89×10^{-6}	1.19×10^{-5}	1.93×10^{-5}	3.71×10^{-5}	5.09×10^{-5}	1.78×10^{-5}	4.42×10^{-5}	9.15×10^{-5}	1.72×10^{-4}	3.95×10^{-4}
ΔG		1.33×10^{-5}	1.01×10^{-5}	8.16×10^{-6}	6.23×10^{-6}	4.26×10^{-6}	3.19×10^{-6}	9.09×10^{-6}	1.34×10^{-5}	2.30×10^{-5}	2.53×10^{-5}	1.24×10^{-5}	2.98×10^{-5}	5.61×10^{-5}	8.10×10^{-5}	1.67×10^{-5}
%ΔG		2.10×10^{3}	1.48×10^{3}	1.11×10^{3}	7.93×10^{2}	4.80×10^{2}	1.87×10^{2}	3.23×10^{2}	2.26×10^{2}	1.63×10^{2}	9.88×10^{1}	2.29×10^{2}	2.07×10^{2}	1.58×10^{2}	8.90×10^{1}	7.32×10^{1}
G; Wet air/ 1.0% CH_4		1.44×10^{-5}	1.76×10^{-5}	2.23×10^{-5}	2.90×10^{-5}	4.63×10^{-5}	8.89×10^{-6}	2.02×10^{-5}	4.32×10^{-5}	1.05×10^{-4}	1.96×10^{-4}	6.12×10^{-5}	1.44×10^{-4}	2.40×10^{-4}	4.36×10^{-4}	6.79×10^{-4}
ΔG		1.38×10^{-5}	1.69×10^{-5}	2.16×10^{-5}	2.82×10^{-5}	4.54×10^{-5}	7.19×10^{-6}	1.74×10^{-6}	3.73×10^{-5}	9.09×10^{-5}	1.70×10^{-4}	5.58×10^{-5}	1.30×10^{-4}	2.05×10^{-4}	3.45×10^{-4}	4.51×10^{-4}
%ΔG		2.18×10^{3}	2.47×10^{3}	2.94×10^{3}	3.59×10^{3}	5.12×10^{3}	4.23×10^{2}	6.19×10^{2}	6.28×10^{2}	6.45×10^{2}	6.64×10^{2}	1.03×10^{3}	9.02×10^{2}	5.79×10^{2}	3.79×10^{2}	1.98×10^{2}

Table 67 Effect of individual coal combustion products on sensor sensitivity as a function of heater voltage

(vi)

Test gas	Type 711					Type 812					Type 813				
Heater voltage(Vh)	5.0	5.5	6.0	6.5	7.0	5.0	5.5	6.0	6.5	7.0	5.0	5.5	6.0	6.5	7.0
Ethane															
G; Dry air	5.57×10^{-7}	6.58×10^{-7}	7.09×10^{-7}	7.60×10^{-7}	9.63×10^{-7}	1.78×10^{-6}	3.07×10^{-6}	6.48×10^{-6}	1.30×10^{-5}	2.41×10^{-5}	5.94×10^{-6}	1.47×10^{-5}	3.48×10^{-5}	9.01×10^{-5}	2.32×10^{-4}
G; Dry air/ 1000ppm C_2H_6	1.52×10^{-6}	2.29×10^{-6}	8.08×10^{-6}	2.17×10^{-5}	4.15×10^{-5}	5.15×10^{-6}	9.70×10^{-6}	2.14×10^{-5}	4.95×10^{-5}	9.82×10^{-5}	2.26×10^{-5}	4.21×10^{-5}	8.46×10^{-5}	1.88×10^{-4}	4.37×10^{-4}
Δ G	9.63×10^{-7}	1.63×10^{-6}	7.37×10^{-6}	2.09×10^{-5}	4.05×10^{-5}	3.37×10^{-6}	6.63×10^{-6}	1.49×10^{-5}	3.65×10^{-5}	7.41×10^{-5}	1.67×10^{-5}	2.74×10^{-5}	4.98×10^{-5}	9.79×10^{-5}	2.05×10^{-4}
%ΔG	1.73×10^{2}	2.48×10^{2}	1.04×10^{3}	2.75×10^{3}	4.21×10^{3}	1.89×10^{2}	2.16×10^{2}	2.30×10^{2}	2.81×10^{2}	3.07×10^{2}	2.81×10^{2}	1.86×10^{2}	1.43×10^{2}	1.09×10^{2}	8.84×10^{1}
G; Wet air	1.30×10^{-5}	1.13×10^{-5}	7.81×10^{-6}	7.27×10^{-6}	4.89×10^{-6}	5.15×10^{-6}	1.16×10^{-5}	2.02×10^{-5}	3.77×10^{-5}	4.92×10^{-5}	1.78×10^{-5}	4.21×10^{-5}	9.25×10^{-5}	1.74×10^{-4}	3.92×10^{-4}
Δ G	1.24×10^{-5}	1.06×10^{-5}	7.10×10^{-6}	6.51×10^{-6}	3.93×10^{-6}	3.37×10^{-6}	8.53×10^{-6}	1.37×10^{-5}	2.47×10^{-5}	2.51×10^{-5}	1.19×10^{-5}	2.74×10^{-5}	5.77×10^{-5}	8.39×10^{-5}	1.60×10^{-4}
%ΔG	2.22×10^{3}	1.61×10^{3}	1.00×10^{3}	8.57×10^{2}	4.08×10^{2}	1.89×10^{2}	2.78×10^{2}	2.11×10^{2}	1.90×10^{2}	1.04×10^{2}	2.00×10^{2}	1.86×10^{2}	1.66×10^{2}	9.31×10^{1}	6.90×10^{1}
G; Wet air/ 1000ppm C_2H_6	1.55×10^{-5}	1.93×10^{-5}	2.23×10^{-5}	2.96×10^{-5}	5.14×10^{-5}	9.43×10^{-6}	1.70×10^{-5}	3.57×10^{-5}	7.54×10^{-5}	1.38×10^{-4}	4.18×10^{-5}	7.21×10^{-5}	1.38×10^{-4}	2.69×10^{-4}	5.47×10^{-4}
Δ G	1.49×10^{-5}	1.86×10^{-5}	2.16×10^{-5}	2.88×10^{-5}	5.04×10^{-5}	7.65×10^{-6}	1.39×10^{-5}	2.92×10^{-5}	6.24×10^{-5}	1.14×10^{-4}	3.59×10^{-5}	5.74×10^{-5}	1.03×10^{-4}	1.79×10^{-4}	3.15×10^{-4}
%ΔG	2.67×10^{3}	2.83×10^{3}	3.05×10^{3}	3.79×10^{3}	5.23×10^{3}	4.30×10^{2}	4.53×10^{2}	4.51×10^{2}	4.80×10^{2}	4.73×10^{2}	6.04×10^{2}	3.90×10^{2}	2.96×10^{2}	1.99×10^{2}	1.36×10^{2}
Propane															
G; Dry air	6.58×10^{-7}	6.84×10^{-7}	7.34×10^{-7}	7.85×10^{-7}	8.61×10^{-7}	1.63×10^{-6}	3.59×10^{-6}	6.74×10^{-6}	1.44×10^{-5}	2.38×10^{-5}	5.15×10^{-6}	1.50×10^{-5}	3.38×10^{-5}	9.39×10^{-5}	2.19×10^{-4}
G; Dry air/ 1000ppm C_3H_8	3.59×10^{-6}	5.42×10^{-6}	1.19×10^{-5}	3.06×10^{-5}	5.92×10^{-5}	6.48×10^{-6}	1.47×10^{-5}	2.84×10^{-5}	7.04×10^{-5}	1.30×10^{-4}	2.47×10^{-5}	6.31×10^{-5}	1.10×10^{-4}	2.81×10^{-4}	5.75×10^{-4}
Δ G	2.93×10^{-6}	4.74×10^{-6}	1.12×10^{-5}	2.98×10^{-5}	5.83×10^{-5}	4.85×10^{-6}	1.11×10^{-5}	2.17×10^{-5}	5.70×10^{-5}	1.06×10^{-4}	1.96×10^{-5}	4.81×10^{-5}	7.62×10^{-5}	1.87×10^{-4}	3.56×10^{-4}
%ΔG	4.45×10^{2}	6.93×10^{2}	1.53×10^{3}	3.80×10^{3}	6.77×10^{3}	2.96×10^{2}	3.09×10^{2}	3.21×10^{2}	3.96×10^{2}	4.45×10^{2}	3.80×10^{2}	3.21×10^{2}	2.25×10^{2}	1.99×10^{2}	1.62×10^{2}
G; Wet air	1.27×10^{-5}	1.13×10^{-5}	8.62×10^{-6}	7.01×10^{-6}	5.94×10^{-6}	5.42×10^{-6}	1.22×10^{-5}	1.99×10^{-5}	3.97×10^{-5}	4.92×10^{-5}	1.73×10^{-5}	4.11×10^{-5}	8.69×10^{-5}	1.79×10^{-4}	4.03×10^{-4}
Δ G	1.20×10^{-5}	1.06×10^{-7}	7.89×10^{-6}	6.23×10^{-6}	5.08×10^{-6}	3.79×10^{-6}	8.61×10^{-6}	1.32×10^{-5}	2.53×10^{-5}	2.54×10^{-5}	1.22×10^{-5}	2.61×10^{-5}	5.31×10^{-5}	8.51×10^{-5}	1.84×10^{-4}
%ΔG	1.82×10^{3}	1.55×10^{3}	1.07×10^{3}	7.94×10^{2}	5.90×10^{2}	2.35×10^{2}	2.40×10^{2}	1.95×10^{2}	1.76×10^{2}	1.07×10^{2}	2.37×10^{2}	1.74×10^{2}	1.57×10^{2}	9.06×10^{1}	8.40×10^{1}
G; Wet air/ 1000ppm C_3H_8	2.05×10^{-5}	2.56×10^{-5}	3.25×10^{-5}	5.10×10^{-5}	9.34×10^{-5}	1.05×10^{-5}	1.90×10^{-5}	4.25×10^{-5}	9.25×10^{-5}	1.61×10^{-4}	4.39×10^{-5}	8.83×10^{-5}	1.70×10^{-4}	3.57×10^{-4}	7.66×10^{-4}
Δ G	1.98×10^{-5}	2.49×10^{-5}	3.18×10^{-5}	5.02×10^{-5}	9.25×10^{-5}	8.87×10^{-6}	1.54×10^{-5}	3.58×10^{-5}	7.81×10^{-5}	1.37×10^{-4}	3.88×10^{-5}	7.33×10^{-5}	1.36×10^{-4}	2.63×10^{-4}	5.47×10^{-4}
%ΔG	3.01×10^{3}	3.64×10^{3}	4.33×10^{3}	6.50×10^{3}	1.07×10^{4}	5.44×10^{2}	4.29×10^{2}	5.31×10^{2}	5.42×10^{2}	5.76×10^{2}	7.53×10^{2}	4.89×10^{2}	4.02×10^{2}	2.80×10^{2}	2.50×10^{2}

Test gas concentrations 1000 ppm, except methane at 1.0%. All absolute conductance values and differences in siemens.

* Indicates unreliable data

Table 68 Sensor response and recovery times

Heater voltage V_h	Response time (mins) 90% of signal					
	711		812		813	
	Dry	Wet	Dry	Wet	Dry	Wet
5.0	4.5	6.5	3.5	4.5	2.5	3.5
5.5	3.5	5.0	2.5	3.0	1.5	2.0
6.0	3.0	4.0	2.0	2.5	1.0	1.5
6.5	2.0	2.5	1.0	1.5	0.5	1.0
7.0	1.5	2.0	0.5	1.0	0.5	0.5
	Recovery time (mins) 10% of signal					
5.0	5.5	7.5	4.5	6.0	3.0	4.5
5.5	5.0	6.5	3.5	4.0	2.0	2.5
6.0	4.0	5.5	2.5	3.5	1.0	2.0
6.5	3.0	3.5	1.5	2.0	0.5	1.5
7.0	1.5	2.5	1.0	1.5	0.5	1.0

Table 69 Response of 813 sensor as a function of gas concentration

	Heater Voltage 5.0V				Heater voltage 7.0V			
	Dry		Wet		Dry		Wet	
Concentration %	Methane	Firedamp	Methane	Firedamp	Methane	Firedamp	Methane	Firedamp
0	21	21	66	66	474	474	610	610
0.10	40	56	87	106	535	575	642	648
0.20	56	70	104	130	569	636	663	673
0.50	88	108	145	183	640	732	693	725
0.70	107	132	170	207	675	770	714	744
1.00	136	161	198	242	706	805	729	768

APPENDIX 1

CORROSION PROBLEMS IN MINE AIR SAMPLING TUBES

Mine air samples are routinely collected into pressurised anodised aluminium sampling tubes for the subsequent analysis of carbon dioxide, carbon monoxide, methane and oxygen. On certain occasions hydrogen determinations are also required on the same sample. During the course of this work, anomalous results were obtained for the analysis of hydrogen and carbon dioxide. Visual inspection of the internal surface of the suspect sampling tubes indicated corrosion with the formation of deep pits. An example of the effect is shown below:

	CO_2%	CH_4%	O_2%	CO%	H_2%
Unaffected tube	0.23	0.32	20.48	0.0006	< 0.0005
Suspect tube	<0.01	0.32	19.63	0.0009	2.5

When sampling underground it is possible for minewater to be drawn in an aerosol form into the sampling tube. The minewater can take the form of a concentrated solution of mainly sodium and calcium chlorides. It is considered that the corrosion processes are extremely complex, however a simplified explanation with respect to the observed changes is as follows.

When aluminium comes into contact with certain salts in solutions (sodium chloride in this case) the coherence of the protective film is destroyed and is then liable to attack from moist air.

$$H_2O + O_2 + Al \longrightarrow Al(OH)_3$$

The hydroxide formed is amphoteric and in the presence of acidic minewater produces a hydrolysed solution which yields sodium hydroxide.

$$3NaCl + Al(OH)_3 \longrightarrow NaOH$$

The sodium hydroxide can then attack the aluminium with the formation of hydrogen.

$$2NaOH + 3Al + 2H_2O \longrightarrow 2NaAlO_2 + 3H_2$$

In addition to chemical attack, electrochemical reaction may occur on the aluminium where it can act as both anode and cathode with minewater providing the electrolyte. Two possible reactions can occur.

i. With sodium chloride as electrolyte; at the anode aluminium chloride is produced and at the cathode sodium hydroxide is formed.

ii. With calcium chloride as electrolyte; at the anode aluminium chloride is formed and at the cathode calcium oxide is formed.

It is concluded that the second reaction takes place predominantly. The calcium oxide formed will react with moist air to form calcium carbonate.

$$CaO + H_2O + CO_2 \longrightarrow CaCO_3$$

The calcium carbonate can then react further with air to form calcium bicarbonate which is soluble.

$$CaCO_3 + H_2O + O_2 \longrightarrow Ca(HCO_2)$$

These reactions will account for the disappearance of carbon dioxide.

Discussions were held with the sampling tube manufacturers in an attempt to overcome the corrosion processes. The only apparent solution, although impractical, appeared to prevent minewater coming into contact with the aluminium surface. As a practical means of overcoming the problem the manufacturers suggested replacing the aluminium with stainless steel. Sampling tubes constructed from stainless steel have been used successfully during the course of this work for the subsequent analysis of hydrogen and carbon dioxide.